Theory Manual Version 3.6

Last Updated: February 17, 2022

Contributors
Steve Maas (steve.maas@utah.edu)
Michael Herron (michael.herron@utah.edu)
Dr. Jeffrey Weiss (jeff.weiss@utah.edu)
Dr. Gerard Ateshian (ateshian@columbia.edu)

Contact address
Musculoskeletal Research Laboratories, University of Utah
72 S. Central Campus Drive, Room 2646
Salt Lake City, Utah

Website
MRL: `http://mrl.sci.utah.edu`
FEBio: `http://febio.org`

Forum
`https://forums.febio.org/index.php`

Acknowledgments
Development of the FEBio project is supported in part by a grant from the U.S. National Institutes of Health (R01GM083925).

Contents

Chapter 1

Introduction

1.1 Overview of FEBio

FEBio is an implicit, nonlinear finite element solver that is specifically designed for applications in biomechanics. It offers analyses, constitutive models and boundary conditions that are relevant for this particular field. This section describes briefly the available features of FEBio. A more detailed overview of features can be found in the *FEBio User's Manual*.

FEBio supports two analysis types, namely *quasi-static* and *quasi-static poroelastic*. In a *quasi-static* analysis the (quasi-) static response of the system is sought; inertial terms are ignored. In a *quasi-static poroelastic* analysis a coupled solid-fluid problem is solved. The latter analysis type is useful for modeling tissues that have high water content and the explicit modeling of fluid movement relative to the solid phase is important.

Several nonlinear constitutive models are available to allow the user to model the often complicated biological tissue behavior. Several isotropic constitutive models are supported such as Neo-Hookean, Mooney-Rivlin, Veronda-Westmann, Arruda-Boyce and Ogden. These models have a nonlinear stress-strain response. In addition to the isotropic models, there are several anisotropic models available. These materials show anisotropic behavior in at least one preferred direction and are useful for modeling biological tissues such as tendons, muscles and other tissues that contain fibers. FEBio also contains a *rigid body* material model, which can be used to model rigid structures whose deformation is negligible compared to the deformable geometry.

Biological tissues can interact in very complicated ways. Therefore FEBio supports a wide range of boundary conditions to model these interactions. These include prescribed displacements, nodal forces, and pressure forces. Deformable models can also be connected to rigid bodies so that the user can model prescribed rotations and torques. Rigid bodies can be connected with rigid joints. Even more complicated interactions can be modeled using FEBio's contact interfaces. The user can choose between different types of contact interfaces, such as sliding interfaces, tied interfaces and rigid wall interfaces. A sliding interface is defined between two surfaces that are allowed to separate and slide across each other but are not allowed to penetrate. The rigid wall interface is also similar to the sliding interface, except that one of the contacting surfaces is a movable rigid wall. As of version 1.2, there is an implementation of a sliding interface that allows for fluid flow crossing the contact interface. The tied interface is similar to the sliding interface, but in this case, the surfaces are not allowed to slide or separate. In addition, the user may specify a body force which can be used to model the effects of gravity or base acceleration.

1.2 About this document

This document is a part of a set of three manuals that accompany FEBio: the *FEBio User's Manual*, describing how to use FEBio, the *FEBio Developer's Manual* for users who wish to modify or add features to the code, and this manual, which describes the theory behind most of the FEBio algorithms.

The purpose of this manual is to provide theoretical background on many of the algorithms that are implemented in FEBio. In this way the user can develop a better understanding of how the program works and how it can be used to create well defined biomechanical simulations. The authors have tried to be as detailed as possible to make the text coherent and comprehensible, but due to the complexity of some of the topics, some descriptions only skim the surface. Many of the theoretical ideas discussed in this manual can and have filled entire bookshelves. The explanations contained herein should be sufficient to give the reader a basic understanding of the theoretical developments. References to textbooks and the primary literature are provided for further reading.

Chapter 2 starts with a brief overview of some of the important concepts in continuum mechanics. Readers who are already familiar with this field can skip this chapter, although the material may be useful to get familiar with the notation and terminology used in this manual.

Chapter 3 describes the nonlinear finite element method. It also explains the Newton-Raphson method, which is the basis for most implementations of the nonlinear finite element method. A more specialized version of this algorithm, the BFGS method, is described as well since it is used in FEBio.

In Chapter 4 the different element types that are available in FEBio are described in detail. FEBio currently supports 3D solid elements, such as the linear hexahedral, pentahedral and tetrahedral elements, as well as quadrilateral and triangular shell elements.

Chapter 5 contains a detailed description of the material models in FEBio. Most of these models are based on hyperelasticity, which is introduced in chapter 2. Several transversely isotropic materials are described as well. This also discusses the biphasic material and its implementation in FEBio.

Chapter 7 describes the basics of the theory of contact and coupling. In FEBio the user can connect the different parts of the geometry in a variety of ways. There are rigid interfaces where a deformable model is attached to a rigid model, rigid joints where two or more rigid bodies connect, and sliding interfaces where two surfaces are allowed to separate and slide across each other but are not allowed to penetrate. The various contact and coupling algorithms are discussed as well together with their implementation in FEBio.

Chapter 2

Continuum Mechanics

This chapter contains an overview of some of the important concepts from continuum mechanics and establishes some of the notation and terminology that will be used in the rest of this document. The section begins by introducing the important concepts of deformation, stress and strain. Next the concept of hyperelasticity is discussed. Finally the concept of virtual work is discussed. This concept will be used later to derive the nonlinear finite element equations. For a more thorough introduction to the mathematics needed for continuum mechanics, the user can consult [27].

2.1 Vectors and Tensors

It is assumed that the reader is familiar with the concepts of vectors and tensors. This section summarizes the notation and some useful relations that will be used throughout the manual.

Vectors are denoted by small, bold letters, e.g. **v**. Their components will be denoted by v_i, where, unless otherwise stated, Latin under scripts such as $i$or Iwill range from 1 to 3. In matrix form a vector will be represented as a column vector and its transpose as a row vector:

$$\mathbf{v} = \begin{pmatrix} v_1 \\ v_2 \\ v_3 \end{pmatrix}, \qquad \mathbf{v}^T = \begin{pmatrix} v_1, & v_2, & v_3 \end{pmatrix} . \tag{2.1.1}$$

The following products are defined between vectors. Assume **u**, **v** are vectors. Also note that the Einstein summation convention is used throughout this manual [61].

The *dot* or *scalar product*:

$$\mathbf{u} \cdot \mathbf{v} = u_i v_i \, . \tag{2.1.2}$$

The *cross product*:

$$\mathbf{u} \times \mathbf{v} = \begin{bmatrix} u_2 v_3 - u_3 v_2 \\ u_3 v_1 - u_1 v_3 \\ u_1 v_2 - u_2 v_1 \end{bmatrix} . \tag{2.1.3}$$

The *vector outer product*:

$$(\mathbf{u} \otimes \mathbf{v})_{ij} = u_i v_j \, . \tag{2.1.4}$$

Note that vectors are also known as first order tensors. Scalars are known as zero order tensors. The outer product, defined by equation (2.1.4), is a second order tensor.

Second order tensors are denoted by bold, capital letters, e.g. $\mathbf{A}$. Some exceptions will be made to remain consistent with the literature. For instance, the Cauchy stress tensor is denoted

by $\boldsymbol{\sigma}$. However, the nature of the objects will always be clear from the context. The following operations on tensors are defined. Assume $\mathbf{A}$ and $\mathbf{B}$ are second-order tensors.

The *double contraction* or *tensor inner product* is defined as:

$$\mathbf{A} : \mathbf{B} = A_{ij}B_{ij} \,. \tag{2.1.5}$$

The *trace* is defined as:

$$\operatorname{tr} \mathbf{A} = \mathbf{I} : \mathbf{A} = A_{ii} \,. \tag{2.1.6}$$

Here $\mathbf{I}$ is the second order identity tensor with components δ_{ij}.

In general the components of tensors will change under a change of coordinate system. Nevertheless, certain intrinsic quantities associated with them will remain invariant under such a transformation. The scalar product between two vectors is such an example. The double contraction between two second-order tensors is another example. The following set of invariants for second-order tensors is commonly used:

$$\begin{aligned} I_1 &= \operatorname{tr} \mathbf{A}, \\ I_2 &= \frac{1}{2}\left((\operatorname{tr} \mathbf{A})^2 - \operatorname{tr} \mathbf{A}^2 \right). \\ I_3 &= \det \mathbf{A}. \end{aligned} \tag{2.1.7}$$

A tensor $\mathbf{S}$ is called symmetric if it is equal to its transpose:

$$\mathbf{S} = \mathbf{S}^T \,. \tag{2.1.8}$$

A tensor $\mathbf{W}$ is called anti-symmetric if it is equal to the negative of its transpose:

$$\mathbf{W} = -\mathbf{W}^T \,. \tag{2.1.9}$$

Any second order tensor $\mathbf{A}$ can be written as the sum of a symmetric tensor $\mathbf{S}$ and an anti-symmetric tensor $\mathbf{W}$:

$$\mathbf{A} = \mathbf{S} + \mathbf{W}, \tag{2.1.10}$$

where

$$\mathbf{S} = \frac{1}{2}\left(\mathbf{A} + \mathbf{A}^T\right), \text{ and } \mathbf{W} = \frac{1}{2}\left(\mathbf{A} - \mathbf{A}^T\right). \tag{2.1.11}$$

Also note that for any tensor $\mathbf{B}$ the following holds:

$$\mathbf{B} : \mathbf{A} = \mathbf{B} : \mathbf{S}\,, \quad \mathbf{B} : \mathbf{W} = \mathbf{0}\,. \tag{2.1.12}$$

With any anti-symmetric tensor a dual vector $\mathbf{w}$ can be associated such that,

$$\hat{\mathbf{w}} \cdot \mathbf{u} = \mathbf{w} \times \mathbf{u}\,, \tag{2.1.13}$$

where the second order tensor $\hat{\mathbf{w}}$ is defined as,

$$\hat{\mathbf{w}} = \begin{bmatrix} 0 & -w_3 & w_2 \\ w_3 & 0 & -w_1 \\ -w_2 & w_1 & 0 \end{bmatrix}. \tag{2.1.14}$$

A second order $\mathbf{Q}$ tensor is called *orthogonal* if $\mathbf{Q}^{-1} = \mathbf{Q}^T$.

In the implementation of the FE method it is often convenient to write symmetric second-order tensors using *Voigt notation*. In this notation the components of a 2^{nd} order symmetric tensor $\mathbf{A}$ are arranged as a column vector:

$$[\mathbf{A}] = \begin{bmatrix} A_{11} \\ A_{22} \\ A_{33} \\ A_{12} \\ A_{23} \\ A_{13} \end{bmatrix} . \tag{2.1.15}$$

Higher order tensors will be denoted by bold, capital, script symbols, e.g. $\boldsymbol{\mathcal{A}}$. An example of a third-order tensor is the *permutation tensor* $\mathcal{E}_{ijk}$, whose components are 1 for an even permutation of $(1, 2, 3)$, -1 for an odd permutation of $(1, 2, 3)$ and zero otherwise. The permutation symbol is useful for expressing the cross-product of two vectors in index notation:

$$(\mathbf{u} \times \mathbf{v})_i = \mathcal{E}_{ijk} u_j v_k \, . \tag{2.1.16}$$

An example of a fourth-order tensor is the elasticity tensor $\boldsymbol{\mathcal{C}}$ which, in linear elasticity theory, relates the small strain tensor $\boldsymbol{\varepsilon}$ and the Cauchy stress tensor $\boldsymbol{\sigma} = \boldsymbol{\mathcal{C}} : \boldsymbol{\varepsilon}$.

Higher order tensors can be constructed from second order tensors in a similar way as second order tensors can be constructed from vectors. If $\mathbf{A}$ and $\mathbf{B}$ are second order tensors, then the following fourth order tensors can be defind by requiring that the following must hold for any second order tensor $\mathbf{X}$:

$$(\mathbf{A} \otimes \mathbf{B}) : \mathbf{X} = (\mathbf{B} : \mathbf{X})\, \mathbf{A} \, , \tag{2.1.17}$$

$$(\mathbf{A} \oslash \mathbf{B}) : \mathbf{X} = \mathbf{A} \cdot \mathbf{X} \cdot \mathbf{B}^T \, , \tag{2.1.18}$$

$$(\mathbf{A} \osl \mathbf{B}) : \mathbf{X} = \mathbf{A} \cdot \mathbf{X}^T \cdot \mathbf{B}^T \, , \tag{2.1.19}$$

$$(\mathbf{A} \odot \mathbf{B}) : \mathbf{X} = \frac{1}{2} \left(\mathbf{A} \cdot \mathbf{X} \cdot \mathbf{B}^T + \mathbf{A} \cdot \mathbf{X}^T \cdot \mathbf{B}^T \right) . \tag{2.1.20}$$

The Cartesian component forms of the operators $\otimes$, $\oslash$, $\osl$ and $\odot$ are defined as follows:

$$(\mathbf{A} \otimes \mathbf{B})_{ijkl} = \mathbf{A}_{ij} \mathbf{B}_{kl} \, , \tag{2.1.21}$$

$$(\mathbf{A} \oslash \mathbf{B})_{ijkl} = \mathbf{A}_{ik} \mathbf{B}_{jl} \, , \tag{2.1.22}$$

$$(\mathbf{A} \osl \mathbf{B})_{ijkl} = A_{il} B_{jk} \, , \tag{2.1.23}$$

$$(\mathbf{A} \odot \mathbf{B})_{ijkl} = \frac{1}{2} \left(A_{ik} B_{jl} + A_{il} B_{jk} \right) . \tag{2.1.24}$$

The fourth order identity tensors are defined as:

$$\begin{aligned} \mathbf{A} &= \underline{\mathcal{I}} : \mathbf{A} \, , \\ \mathbf{A}^T &= \overline{\mathcal{I}} : \mathbf{A} \, , \end{aligned} \tag{2.1.25}$$

where $\underline{\mathcal{I}} = \mathbf{I} \oslash \mathbf{I}$ and $\overline{\boldsymbol{\mathcal{I}}} = \mathbf{I} \osl \mathbf{I}$. The components are given by:

$$\begin{aligned} \underline{\mathcal{I}}_{ijkl} &= \delta_{ik} \delta_{jl} \, , \\ \overline{\mathcal{I}}_{ijkl} &= \delta_{il} \delta_{jk} \, . \end{aligned} \tag{2.1.26}$$

We may also define $\boldsymbol{\mathcal{I}} = \frac{1}{2} \left(\underline{\mathcal{I}} + \overline{\mathcal{I}} \right)$, such that $\boldsymbol{\mathcal{I}} : \mathbf{A} = \frac{1}{2} \left(\mathbf{A} + \mathbf{A}^T \right)$ returns the symmetric part of $\mathbf{A}$. In the special case when $\mathbf{A}$ is symmetric it follows that $\underline{\mathcal{I}} : \mathbf{A} = \boldsymbol{\mathcal{I}} : \mathbf{A} = \mathbf{A}$.

2.2 The Directional Derivative

In later sections the nonlinear finite element method will be formulated. Anticipating an iterative solution method to solve the nonlinear equations, it will be necessary to linearize the quantities involved. This linearization process will utilize a construction called the *directional derivative* [27].

The directional derivative of a function $f(\mathbf{x})$ is defined as follows:

$$Df(\mathbf{x})[\mathbf{u}] = \left.\frac{d}{d\varepsilon}\right|_{\varepsilon=0} f(\mathbf{x}+\varepsilon\mathbf{u}) \,. \tag{2.2.1}$$

The quantity $\mathbf{x}$ may be a scalar, a vector or even a vector of unknown functions. For instance, consider a scalar function $f(\mathbf{x})$, where $\mathbf{x}$ is the position vector in $\mathbb{R}^3$. In this case the directional derivative is given by:

$$\begin{aligned} Df(\mathbf{x})[\mathbf{u}] &= \left.\frac{d}{d\varepsilon}\right|_{\varepsilon=0} f(\mathbf{x}+\varepsilon\mathbf{u}) \\ &= \frac{\partial f}{\partial x_i} u_i \\ &= \nabla f \cdot \mathbf{u} \,. \end{aligned} \tag{2.2.2}$$

Here, the symbol ∇("nabla") depicts the gradient operator.

The linearization of a function implies that it is approximated by a linear function. Using the directional derivative, a function f can be linearized as follows:

$$f(\mathbf{x}+\mathbf{u}) \cong f(\mathbf{x}) + Df(\mathbf{x})[\mathbf{u}] \,. \tag{2.2.3}$$

The directional derivative obeys the usual properties for derivatives.

1. *sum rule*: If $f = f_1 + f_2$, then

$$Df(\mathbf{x})[\mathbf{u}] = Df_1(\mathbf{x})[\mathbf{u}] + Df_2(\mathbf{x})[\mathbf{u}] \,. \tag{2.2.4}$$

2. *product rule*: If $f = f_1 \cdot f_2$, then

$$Df(\mathbf{x})[\mathbf{u}] = f_1(\mathbf{x}) \cdot Df_2(\mathbf{x})[\mathbf{u}] + f_2 \cdot Df_1(\mathbf{x})[\mathbf{u}] \,. \tag{2.2.5}$$

3. *chain rule*: If $f = g(h(\mathbf{x}))$, then

$$Df(\mathbf{x})[\mathbf{u}] = Dg(h(\mathbf{x}))[Dh(\mathbf{x})[\mathbf{u}]] \,. \tag{2.2.6}$$

2.3 Deformation, Strain and Stress

2.3.1 The deformation gradient tensor

Consider the deformation of an object from an initial or *reference configuration* to a deformed or *current configuration*. The location of the material particles in the reference configuration are denoted by $\mathbf{X}$ and are known as the *material coordinates.* Their location in the current configuration is denoted by $\mathbf{x}$ and known as the *spatial coordinates*. The *deformation map* $\boldsymbol{\varphi}$, which is a mapping from $\mathbb{R}^3$to$\mathbb{R}^3$, maps the coordinates of a material point to the spatial configuration:

$$\mathbf{x} = \boldsymbol{\varphi}(\mathbf{X}) \,. \tag{2.3.1}$$

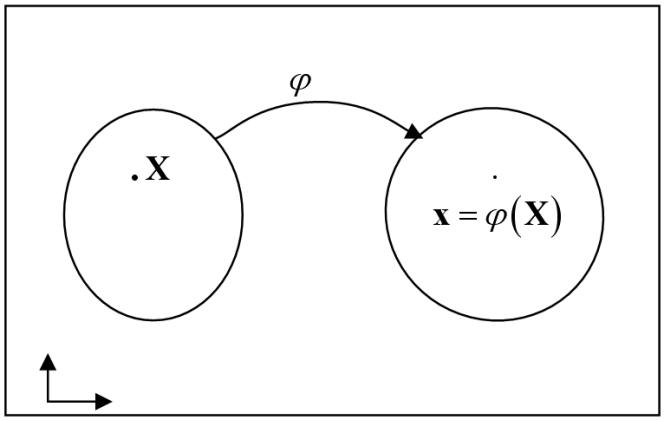

The deformation map

The displacement map $\mathbf{u}$ is defined as the difference between the spatial and material coordinates:

$$\mathbf{x} = \mathbf{X} + \mathbf{u}\left(\mathbf{X}\right) \,. \tag{2.3.2}$$

The *deformation gradient* is defined as

$$\mathbf{F} = \frac{\partial \boldsymbol{\varphi}}{\partial \mathbf{X}} \,. \tag{2.3.3}$$

The deformation gradient relates an infinitesimal vector in the reference configuration $d\mathbf{X}$ to the corresponding vector in the current configuration:

$$d\mathbf{x} = \mathbf{F} \cdot d\mathbf{X}. \tag{2.3.4}$$

The determinant of the deformation tensor $J = \det \mathbf{F}$ is called the *volume ratio*; it gives the volume change, or equivalently the change in density:

$$\rho_0 = \rho J \,. \tag{2.3.5}$$

Here ρ_0 is the density in the reference configuration and ρ is the current density.

When dealing with incompressible and nearly incompressible materials it will prove useful to separate the volumetric and the deviatoric (distortional) components of the deformation gradient. Such a separation must ensure that the deviatoric part of the deformation gradient, namely $\tilde{\mathbf{F}}$, does not produce any change in volume. Noting that the determinant of the deformation gradient gives the volume ratio, the determinant of $\tilde{\mathbf{F}}$ must therefore satisfy,

$$\det \tilde{\mathbf{F}} = 1 \,. \tag{2.3.6}$$

This condition can be achieved by choosing $\tilde{\mathbf{F}}$ as,

$$\tilde{\mathbf{F}} = J^{-1/3}\mathbf{F} \,. \tag{2.3.7}$$

Using the polar decomposition of a second order tensor, the deformation gradient can be written as a product of a positive definite symmetric tensor $\mathbf{V}$ (or $\mathbf{U}$) and a proper orthogonal tensor $\mathbf{R}$:

$$\mathbf{F} = \mathbf{V} \cdot \mathbf{R} = \mathbf{R} \cdot \mathbf{U} \,. \tag{2.3.8}$$

$\mathbf{V}$ is called the *left stretch tensor*, $\mathbf{U}$ is called the *right stretch tensor* and the orthogonal tensor $\mathbf{R}$ is called the *rotation*.

2.3.2 Strain

The *right Cauchy-Green deformation tensor* is defined as follows:

$$\mathbf{C} = \mathbf{F}^T \cdot \mathbf{F} \,. \tag{2.3.9}$$

This tensor is an example of a *material tensor* and is typically expressed a function of the material coordinates $\mathbf{X}$. The *left Cauchy-Green deformation tensor* is defined as follows:

$$\mathbf{b} = \mathbf{F} \cdot \mathbf{F}^T \,. \tag{2.3.10}$$

This tensor is an example of a *spatial tensor* and is typically expressed as a function of the spatial coordinates $\mathbf{x}$. The implementation of the updated Lagrangian finite element method used by FEBio is described in the spatial configuration.

The left and right deformation tensors can also be split into volumetric and deviatoric components. With the use of,(2.3.7) the deviatoric deformation tensors are:

$$\begin{aligned} \tilde{\mathbf{C}} &= \tilde{\mathbf{F}}^T \cdot \tilde{\mathbf{F}} = J^{-2/3}\mathbf{C} \,, \\ \tilde{\mathbf{b}} &= \tilde{\mathbf{F}} \cdot \tilde{\mathbf{F}}^T = J^{-2/3}\mathbf{b} \,. \end{aligned} \tag{2.3.11}$$

The deformation tensors defined above are not good candidates for strain measures since in the absence of strain they become the identity tensor $\mathbf{I}$. However, they can be used to define strain measures. The *Green-Lagrange strain tensor* is defined as:

$$\mathbf{E} = \frac{1}{2}\left(\mathbf{C} - \mathbf{I}\right) \,. \tag{2.3.12}$$

This tensor is a material tensor. Its spatial equivalent is known as the *Almansi strain tensor* and is defined as:

$$\mathbf{e} = \frac{1}{2}\left(\mathbf{I} - \mathbf{b}^{-1}\right) \,. \tag{2.3.13}$$

In the limit of small displacement gradients, the components of both strain tensors are identical, resulting in the *small strain tensor* or *infinitesimal strain tensor*:

$$\boldsymbol{\varepsilon} = \frac{1}{2}\left(\frac{\partial \mathbf{u}}{\partial \mathbf{x}} + \left(\frac{\partial \mathbf{u}}{\partial \mathbf{x}}\right)^T\right) \,. \tag{2.3.14}$$

Note that the small strain tensor is also the linearization of the Green Lagrange strain,

$$D\mathbf{E}\left[\mathbf{u}\right] = \mathbf{F}^T \cdot \boldsymbol{\varepsilon} \cdot \mathbf{F} \,. \tag{2.3.15}$$

2.3.3 Stress

The traction $\mathbf{t}$ on a plane bisecting the body is given by,

$$\mathbf{t} = \boldsymbol{\sigma} \cdot \mathbf{n}, \tag{2.3.16}$$

where $\boldsymbol{\sigma}$ is the *Cauchy stress tensor* and $\mathbf{n}$ is the outward unit normal vector to the plane. It can be shown that by the conservation of angular momentum that this tensor is symmetric ($\sigma_{ij} = \sigma_{ji}$) [99]. The Cauchy stress tensor, a spatial tensor, is the actual physical stress, that is, the force per unit deformed area. To simplify the equations of continuum mechanics, especially when working

in the material configuration, several other stress measures are often used. The *Kirchhoff stress tensor* is defined as

$$\boldsymbol{\tau} = J\boldsymbol{\sigma}\,. \tag{2.3.17}$$

The *first Piola-Kirchhoff stress tensor* is given as

$$\mathbf{P} = J\boldsymbol{\sigma}\cdot\mathbf{F}^{-T}\,. \tag{2.3.18}$$

Note that $\mathbf{P}$, like $\mathbf{F}$, is not symmetric. Also, like $\mathbf{F}$, $\mathbf{P}$ is known as a *two-point* tensor, meaning it is neither a material nor a spatial tensor. Since we have two strain tensors, one spatial and one material tensor, it would be useful to have similar stress measures. The Cauchy stress is a spatial tensor and the *second Piola-Kirchhoff (2^{nd} PK) stress tensor*, defined as

$$\mathbf{S} = J\mathbf{F}^{-1}\cdot\boldsymbol{\sigma}\cdot\mathbf{F}^{-T}\,, \tag{2.3.19}$$

is a material tensor. The inverse relations are:

$$\boldsymbol{\sigma} = \frac{1}{J}\boldsymbol{\tau}\,,\quad \boldsymbol{\sigma} = \frac{1}{J}\mathbf{P}\cdot\mathbf{F}^{T}\,,\quad \boldsymbol{\sigma} = \frac{1}{J}\mathbf{F}\cdot\mathbf{S}\cdot\mathbf{F}^{T}\,. \tag{2.3.20}$$

In many practical applications it is physically relevant to separate the hydrostatic stress and the deviatoric stress $\tilde{\boldsymbol{\sigma}}$ of the Cauchy stress tensor:

$$\boldsymbol{\sigma} = \tilde{\boldsymbol{\sigma}} + p\mathbf{I}\,. \tag{2.3.21}$$

Here, the pressure is defined as $p = \frac{1}{3}\operatorname{tr}\boldsymbol{\sigma}$. Note that the deviatoric Cauchy stress tensor satisfies $\operatorname{tr}\tilde{\boldsymbol{\sigma}} = 0$.

The directional derivative of the 2^{nd} PK stress tensor needs to be calculated for the linearization of the finite element equations. For a hyperelastic material, a linear relationship between the directional derivative of $\mathbf{S}$ and the linearized strain $D\mathbf{E}[\mathbf{u}]$ can be obtained:

$$D\mathbf{S}[\mathbf{u}] = \mathbb{C} : D\mathbf{E}[\mathbf{u}]\,. \tag{2.3.22}$$

Here, $\mathbb{C}$ is a fourth-order tensor known as the *material elasticity tensor*. Its components are given by

$$\begin{aligned}\mathbb{C}_{IJKL} &= \frac{\partial S_{IJ}}{\partial E_{KL}} = \frac{4\partial^2\Psi}{\partial C_{IJ}\partial C_{KL}}\,,\\ \mathbb{C} &= \frac{\partial\mathbf{S}}{\partial\mathbf{E}} = \frac{4\partial^2\Psi}{\partial\mathbf{C}\partial\mathbf{C}}\end{aligned} \tag{2.3.23}$$

where Ψ is the strain-energy density function for the hyperelastic material. The spatial equivalent – the *spatial elasticity tensor* $\boldsymbol{\mathcal{C}}$ – can be obtained from

$$\begin{aligned}\mathcal{C}_{ijkl} &= \frac{1}{J}F_{iI}F_{jJ}F_{kK}F_{lL}\mathbb{C}_{IJKL}\\ \boldsymbol{\mathcal{C}} &= \frac{1}{J}\left(\mathbf{F}\oslash\mathbf{F}\right) : \mathbb{C} : \left(\mathbf{F}^{T}\oslash\mathbf{F}^{T}\right)\end{aligned}\,. \tag{2.3.24}$$

2.4 Hyperelasticity

When the constitutive behavior is only a function of the current state of deformation, the material is *elastic*. In the special case when the work done by the stresses during a deformation is only

dependent on the initial state and the final state, the material is termed *hyperelastic* and its behavior is path-independent. As a consequence of the path-independence a *strain energy function* per unit undeformed volume can be defined as the work done by the stresses from the initial to the final configuration:

$$\Psi\left(\mathbf{F}\left(\mathbf{X}\right),\mathbf{X}\right)=\int_{t_0}^{t}\mathbf{P}\left(\mathbf{F}\left(\mathbf{X}\right),\mathbf{X}\right):\dot{\mathbf{F}}\,dt\,. \tag{2.4.1}$$

The rate of change of the potential is then given by

$$\dot{\Psi}\left(\mathbf{F}\left(\mathbf{X}\right),\mathbf{X}\right)=\mathbf{P}:\dot{\mathbf{F}}\,. \tag{2.4.2}$$

Or alternatively,

$$P_{iJ}=\sum_{i,J=1}^{3}\frac{\partial\Psi}{\partial F_{iJ}}\dot{F}_{iJ}\,. \tag{2.4.3}$$

Comparing (2.4.2) with (2.4.3) reveals that

$$\mathbf{P}\left(\mathbf{F}\left(\mathbf{X}\right),\mathbf{X}\right)=\frac{\partial\Psi\left(\mathbf{F}\left(\mathbf{X}\right),\mathbf{X}\right)}{\partial\mathbf{F}}. \tag{2.4.4}$$

This general constitutive equation can be further simplified by observing that, as a consequence of the objectivity requirement, Ψ may only depend on $\mathbf{F}$ through the stretch tensor $\mathbf{U}$ and must be independent of the rotation component $\mathbf{R}$. For convenience, however, $\Psi$is often expressed as a function of $\mathbf{C}=\mathbf{U}^2=\mathbf{F}^T\cdot\mathbf{F}$. Noting that $\frac{1}{2}\dot{\mathbf{C}}=\dot{\mathbf{E}}$ is work conjugate to the second Piola-Kirchhoff stress $\mathbf{S}$, establishes the following general relationships for hyperelastic materials:

$$\dot{\Psi}=\frac{\partial\Psi}{\partial\mathbf{C}}:\dot{\mathbf{C}}=\frac{1}{2}\mathbf{S}:\dot{\mathbf{C}},\quad\boxed{\mathbf{S}\left(\mathbf{C}\left(\mathbf{X}\right),\mathbf{X}\right)=2\frac{\partial\Psi}{\partial\mathbf{C}}=\frac{\partial\Psi}{\partial\mathbf{E}}}. \tag{2.4.5}$$

2.4.1 Isotropic Hyperelasticity

The hyperelastic constitutive equations discussed so far are unrestricted in their application. Isotropic material symmetry is defined by requiring the constitutive behavior to be independent of the material axis chosen and, consequently, Ψ must only be a function of the invariants of $\mathbf{C}$,

$$\Psi\left(\mathbf{C}\left(\mathbf{X}\right),\mathbf{X}\right)=\Psi\left(I_1,I_2,I_3,\mathbf{X}\right)\,, \tag{2.4.6}$$

where the invariants of **C** are defined here as,

$$I_1=\operatorname{tr}\mathbf{C}=\mathbf{C}:\mathbf{I},\;I_2=\frac{1}{2}\left[\left(\operatorname{tr}\mathbf{C}\right)^2-\operatorname{tr}\mathbf{C}^2\right],\;I_3=\det\mathbf{C}=J^2\,. \tag{2.4.7}$$

As a result of the isotropic restriction, the second Piola-Kirchhoff stress tensor can be written as,

$$\mathbf{S}=2\frac{\partial\Psi}{\partial\mathbf{C}}=2\frac{\partial\Psi}{\partial I_1}\frac{\partial I_1}{\partial\mathbf{C}}+2\frac{\partial\Psi}{\partial I_2}\frac{\partial I_2}{\partial\mathbf{C}}+2\frac{\partial\Psi}{\partial I_3}\frac{\partial I_3}{\partial\mathbf{C}}\,. \tag{2.4.8}$$

The second order tensors formed by the derivatives of the invariants with respect to **C** can be evaluated as follows:

$$\frac{\partial I_1}{\partial\mathbf{C}}=\mathbf{I}\,,\;\frac{\partial I_2}{\partial\mathbf{C}}=I_1\mathbf{I}-\mathbf{C}\,,\;\frac{\partial I_3}{\partial\mathbf{C}}=I_3\mathbf{C}^{-1}\,. \tag{2.4.9}$$

Introducing expressions (2.4.9) into equation (2.4.8) enables the second Piola-Kirchhoff stress to be evaluated as,

$$\mathbf{S} = 2\left\{\left(\Psi_1 + I_1\Psi_2 + I_2\Psi_3\right)\right)\mathbf{I} - \left(\Psi_2 + I_1\Psi_3\right)\mathbf{C}\} + \Psi_3\mathbf{C}^2\,, \tag{2.4.10}$$

where $\Psi_I = \partial\Psi/\partial I_1$, $\Psi_2 = \partial\Psi/\partial I_2$, and $\Psi_3 = \partial\Psi/\partial I_3$.

The Cauchy stresses can now be obtained from the second Piola-Kirchhoff stresses by using (2.3.20):

$$\boldsymbol{\sigma} = \frac{2}{J}\left\{\left(\Psi_1 + I_1\Psi_2 + I_2\Psi_3\right)\right)\mathbf{b} - \left(\Psi_2 + I_1\Psi_3\right)\mathbf{b}^2\right\} + \frac{1}{J}\Psi_3\mathbf{b}^3\,. \tag{2.4.11}$$

Note that in this equation Ψ_1, Ψ_2, and Ψ_3 still involve derivatives with respect to the invariants of $\mathbf{C}$. However, since the invariants of $\mathbf{b}$ are identical to those of $\mathbf{C}$, the quantitiesΨ_1, Ψ_2 and Ψ_3 may also be considered to be the derivatives with respect to the invariants of $\mathbf{b}$.

2.4.2 Isotropic Elasticity in Principal Directions

For isotropic materials, the principal directions of the strain and stress tensors are the same. Let the eigenvalues of $\mathbf{C}$ be denoted by λ_i^2 $(i = 1, 2, 3)$, then the strain energy density may be given as a function of these eigenvalues, $\Psi\left(\lambda_1^2, \lambda_2^2, \lambda_3^2\right)$. To derive the expression for the stress, recognize that

$$\frac{\partial\lambda_i^2}{\partial\mathbf{C}} = \mathbf{N}_i \otimes \mathbf{N}_i \equiv \mathbf{A}_i\,, \tag{2.4.12}$$

where the $\mathbf{N}_i$ are the eigenvectors of $\mathbf{C}$. It follows that the second Piola-Kirchhoff stress may be represented as

$$\mathbf{S} = \sum_{i=1}^{3} S_i\mathbf{A}_i\,, \tag{2.4.13}$$

where

$$S_i = 2\frac{\partial\Psi}{\partial\lambda_i^2}\,. \tag{2.4.14}$$

To evaluate the material elasticity tensor, recognize that

$$\frac{\partial\mathbf{A}_i}{\partial\mathbf{C}} = \frac{1}{\lambda_i^2 - \lambda_j^2}\left(\mathbf{A}_i \odot \mathbf{A}_j + \mathbf{A}_j \odot \mathbf{A}_i\right) + \frac{1}{\lambda_i^2 - \lambda_k^2}\left(\mathbf{A}_i \odot \mathbf{A}_k + \mathbf{A}_k \odot \mathbf{A}_i\right)\,, \tag{2.4.15}$$

where i, j, k form a permutation over $1, 2, 3$. Then it can be shown that the material elasticity tensor is given by

$$\begin{aligned}\mathbb{C} = &\sum_{i=1}^{3} 4\frac{\partial^2\Psi}{\partial\lambda_i^2\partial\lambda_i^2}\mathbf{A}_i \otimes \mathbf{A}_i \\ &+ \sum_{i=1}^{3}\sum_{j=i+1}^{3} 4\frac{\partial^2\Psi}{\partial\lambda_i^2\partial\lambda_j^2}\left(\mathbf{A}_i \otimes \mathbf{A}_j + \mathbf{A}_j \otimes \mathbf{A}_i\right)\,. \\ &+ \sum_{i=1}^{3}\sum_{j=i+1}^{3} 2\frac{S_i - S_j}{\lambda_i^2 - \lambda_j^2}\left(\mathbf{A}_i \odot \mathbf{A}_j + \mathbf{A}_j \odot \mathbf{A}_i\right)\end{aligned} \tag{2.4.16}$$

When eigenvalues coincide, L'Hospital's rule may be used to evalue the coefficient in the last term,

$$\lim_{\lambda_j^2 \to \lambda_i^2} 2\frac{S_i - S_j}{\lambda_i^2 - \lambda_j^2} = 4\left(\frac{\partial^2\Psi}{\partial\lambda_j^2\partial\lambda_j^2} - \frac{\partial^2\Psi}{\partial\lambda_i^2\partial\lambda_j^2}\right)\,. \tag{2.4.17}$$

The double summations in (2.4.16) are arranged such that the summands represent fourth-order tensors with major and minor symmetries.

In the spatial frame, the Cauchy stress is given by

$$\boldsymbol{\sigma} = \sum_{i=1}^{3} \sigma_i \mathbf{a}_i \,, \tag{2.4.18}$$

where

$$\mathbf{a}_i = \mathbf{n}_i \otimes \mathbf{n}_i \,, \tag{2.4.19}$$

and $\mathbf{n}_i = (\mathbf{F} \cdot \mathbf{N}_i) / \lambda_i$ are the eigenvectors of $\mathbf{b}$. The principal normal stresses are

$$\sigma_i = \frac{\lambda_i}{J} \frac{\partial \Psi}{\partial \lambda_i} \,. \tag{2.4.20}$$

The spatial elasticity tensor is given by

$$\begin{aligned} \boldsymbol{\mathcal{C}} = & \sum_{i=1}^{3} \left(J^{-1} \lambda_i^2 \frac{\partial^2 \Psi}{\partial \lambda_i^2} - \sigma_i \right) \mathbf{a}_i \otimes \mathbf{a}_i \\ & + \sum_{i=1}^{3} \sum_{j=i+1}^{3} J^{-1} \lambda_i \lambda_j \frac{\partial^2 \Psi}{\partial \lambda_i \partial \lambda_j} \left(\mathbf{a}_i \otimes \mathbf{a}_j + \mathbf{a}_j \otimes \mathbf{a}_i \right) . \\ & + \sum_{i=1}^{3} \sum_{j=i+1}^{3} 2 \frac{\lambda_j^2 \sigma_i - \lambda_i^2 \sigma_j}{\lambda_i^2 - \lambda_j^2} \left(\mathbf{a}_i \odot \mathbf{a}_j + \mathbf{a}_j \odot \mathbf{a}_i \right) \end{aligned} \tag{2.4.21}$$

2.4.3 Nearly-Incompressible Hyperelasticity

A material is considered incompressible if it shows no change in volume during deformation, or otherwise stated, if $J = 1$ holds throughout the entire body. It can be shown [27] that if the material is incompressible the hyperelastic constitutive equation becomes

$$\mathbf{S} = 2 \frac{\partial \tilde{\Psi}}{\partial \mathbf{C}} + p J \mathbf{C}^{-1} \,, \tag{2.4.22}$$

where $\tilde{\Psi} = \Psi \left(\tilde{\mathbf{C}} \right)$is the deviatoric strain energy function and p is the hydrostatic pressure. The presence of J may seem unnecessary, but retaining J has the advantage that equation (2.4.22) remains valid in the nearly incompressible case. Further, in practical terms, a finite element analysis rarely enforces $J = 1$ in a pointwise manner, and hence its retention may be important for the evaluation of stresses.

The process of defining constitutive equations in the case of nearly incompressible hyperelasticity is simplified by adding a volumetric energy component $U(J)$ to the distortional component $\tilde{\Psi}(\mathbf{C})$:

$$\Psi(\mathbf{C}) = \tilde{\Psi}(\mathbf{C}) + U(J) \,. \tag{2.4.23}$$

The second Piola-Kirchhoff tensor for a material defined by (2.4.23) is obtained in the standard manner with the help of equation (2.4.8).

$$\begin{aligned} \mathbf{S} &= 2 \frac{\partial \Psi}{\partial \mathbf{C}} \\ &= 2 \frac{\partial \tilde{\Psi}}{\partial \mathbf{C}} + 2 \frac{dU}{dJ} \frac{\partial J}{\partial C} \,, \\ &= 2 \frac{\partial \tilde{\Psi}}{\partial \mathbf{C}} + p J \mathbf{C}^{-1} \end{aligned} \tag{2.4.24}$$

where the pressure p is defined as

$$p = \frac{dU}{dJ}\,. \tag{2.4.25}$$

An example for U that will be used later in the definition of the constitutive models is

$$U\left(J\right) = \frac{1}{2}\kappa\left(\ln J\right)^2\,. \tag{2.4.26}$$

The parameter κ will be used later as a penalty factor that will enforce the (nearly-) incompressible constraint. However, κ can represent a true material coefficient, namely the bulk modulus, for a compressible material that happens to have a hyperelastic strain energy function in the form of (2.4.23). In the case where the dilatational energy is given by (2.4.26), the pressure is

$$p = \kappa\frac{\ln J}{J}\,. \tag{2.4.27}$$

Equation (2.4.24) can be further developed by applying the chain rule to the first term:

$$\mathbf{S} = pJ\mathbf{C}^{-1} + J^{-2/3}\,\mathrm{dev}\,\tilde{\mathbf{S}}\,, \tag{2.4.28}$$

where the *fictitious second Piola-Kirchoff* tensor [51] is defined by,

$$\tilde{\mathbf{S}} = 2\frac{\partial\tilde{\Psi}}{\partial\tilde{\mathbf{C}}}\,, \tag{2.4.29}$$

and Dev is the deviator operator in the reference frame:

$$\mathrm{Dev}\left(\cdot\right) = \left(\cdot\right) - \frac{1}{3}\left(\left(\cdot\right):\mathbf{C}\right)\mathbf{C}^{-1}. \tag{2.4.30}$$

The Cauchy stress can then be obtained from equation (2.3.20)$_3$:

$$\boldsymbol{\sigma} = p\mathbf{I} + \mathrm{dev}\,\tilde{\boldsymbol{\sigma}}\,, \tag{2.4.31}$$

where

$$\tilde{\boldsymbol{\sigma}} = \frac{2}{J}\tilde{\mathbf{F}}\cdot\frac{\partial\tilde{\Psi}}{\partial\tilde{\mathbf{C}}}\cdot\tilde{\mathbf{F}}^T\,. \tag{2.4.32}$$

The following expression will be useful in the following development.

$$\begin{aligned}\frac{d\tilde{C}_{IJ}}{dC_{KL}} &= J^{-2/3}\left(\frac{1}{2}\left(\delta_{IK}\delta_{JL}+\delta_{IL}\delta_{JK}\right) - \frac{1}{3}\tilde{C}_{IJ}\tilde{C}^{-1}_{KL}\right)\\ \frac{\partial\tilde{\mathbf{C}}}{\partial\mathbf{C}} &= J^{-2/3}\left(\mathbf{I}\odot\mathbf{I} - \frac{1}{3}\tilde{\mathbf{C}}\otimes\tilde{\mathbf{C}}^{-1}\right)\end{aligned}\,. \tag{2.4.33}$$

Notice that the contraction with a symmetric tensor $\mathbf{A}$ results in,

$$\begin{aligned}\frac{d\tilde{C}_{IJ}}{dC_{KL}}A_{IJ} &= J^{-2/3}\,\mathrm{Dev}\,A_{KL}\\ \mathbf{A}:\frac{\partial\tilde{\mathbf{C}}}{\partial\mathbf{C}} &= J^{-2/3}\,\mathrm{Dev}\,\mathbf{A}\end{aligned}\,. \tag{2.4.34}$$

The elasticity tensor, defined in (2.3.23), takes on the following form.

$$\begin{aligned}
\mathbb{C}_{IJKL} &= \left(J^2\frac{dp}{dJ}+Jp\right)C^{-1}_{IJ}C^{-1}_{KL} - 2pJ\mathcal{I}_{IJKL} \\
&\quad -\frac{2}{3}J^{-2/3}\left(\operatorname{Dev}\tilde{S}_{IJ}C^{-1}_{KL}+C^{-1}_{IJ}\operatorname{Dev}\tilde{S}_{KL}\right) \\
&\quad +\frac{2}{3}\tilde{S}_{RS}\tilde{C}_{RS}\left(\mathcal{I}_{IJKL}-\frac{1}{3}C^{-1}_{KL}C^{-1}_{IJ}\right)+J^{-4/3}\hat{\mathbb{C}}_{IJKL} \\
\mathbb{C} &= \left(J^2\frac{dp}{dJ}+Jp\right)\mathbf{C}^{-1}\otimes\mathbf{C}^{-1} - 2pJ\boldsymbol{\mathcal{I}} \\
&\quad -\frac{2}{3}J^{-2/3}\left(\operatorname{Dev}\tilde{\mathbf{S}}\otimes\mathbf{C}^{-1}+\mathbf{C}^{-1}\otimes\operatorname{Dev}\tilde{\mathbf{S}}\right) \\
&\quad +\frac{2}{3}\left(\tilde{\mathbf{S}}:\tilde{\mathbf{C}}\right)\left(\boldsymbol{\mathcal{I}}-\frac{1}{3}\mathbf{C}^{-1}\otimes\mathbf{C}^{-1}\right)+J^{-4/3}\hat{\mathbb{C}}
\end{aligned}, \tag{2.4.35}$$

where

$$\begin{aligned}
\hat{\mathbb{C}}_{IJKL} &= \tilde{\mathbb{C}}_{IJKL}-\frac{1}{3}\left(\tilde{\mathbb{C}}_{IJRS}\tilde{C}_{RS}\tilde{C}^{-1}_{KL}+\tilde{\mathbb{C}}_{RSKL}\tilde{C}_{RS}\tilde{C}^{-1}_{IJ}\right)+\frac{1}{9}\tilde{C}^{-1}_{IJ}\tilde{C}_{RS}\tilde{\mathbb{C}}_{RSMN}\tilde{C}_{MN}\tilde{C}^{-1}_{KL} \\
\hat{\mathbb{C}} &= \tilde{\mathbb{C}}-\frac{1}{3}\left(\tilde{\mathbb{C}}:\tilde{\mathbf{C}}\otimes\tilde{\mathbf{C}}^{-1}+\tilde{\mathbf{C}}^{-1}\otimes\tilde{\mathbf{C}}:\tilde{\mathbb{C}}\right)+\frac{1}{9}\tilde{\mathbf{C}}^{-1}\otimes\tilde{\mathbf{C}}:\tilde{\mathbb{C}}:\tilde{\mathbf{C}}\otimes\tilde{\mathbf{C}}^{-1}
\end{aligned}. \tag{2.4.36}$$

The spatial elasticity tensor follows from

$$\begin{aligned}
\boldsymbol{\mathcal{C}} &= \left(J\frac{dp}{dJ}+p\right)\mathbf{I}\otimes\mathbf{I}-2p\mathbf{I}\odot\mathbf{I} \\
&\quad -\frac{2}{3}\left(\operatorname{dev}\tilde{\boldsymbol{\sigma}}\otimes\mathbf{I}+\mathbf{I}\otimes\operatorname{dev}\tilde{\boldsymbol{\sigma}}\right) \\
&\quad +\frac{2}{3}\left(\tilde{\boldsymbol{\sigma}}:\mathbf{I}\right)\left(\mathbf{I}\odot\mathbf{I}-\frac{1}{3}\mathbf{I}\otimes\mathbf{I}\right)+\hat{\boldsymbol{C}}
\end{aligned}, \tag{2.4.37}$$

where

$$\begin{aligned}
\hat{\mathcal{C}}_{ijkl} &= \frac{1}{J}\tilde{F}_{iI}\tilde{F}_{jJ}\tilde{F}_{kK}\tilde{F}_{lL}\hat{\mathbb{C}}_{IJKL} \\
\hat{\boldsymbol{\mathcal{C}}} &= \frac{1}{J}\left(\tilde{\mathbf{F}}\oslash\tilde{\mathbf{F}}\right):\hat{\mathbb{C}}:\left(\tilde{\mathbf{F}}^T\oslash\tilde{\mathbf{F}}^T\right) \\
&= \tilde{\boldsymbol{\mathcal{C}}}-\frac{1}{3}\left(\mathbf{I}\otimes\mathbf{I}:\tilde{\boldsymbol{\mathcal{C}}}+\tilde{\boldsymbol{\mathcal{C}}}:\mathbf{I}\otimes\mathbf{I}\right)+\frac{1}{9}\left(\mathbf{I}:\tilde{\boldsymbol{\mathcal{C}}}:\mathbf{I}\right)\mathbf{I}\otimes\mathbf{I}
\end{aligned}. \tag{2.4.38}$$

2.4.4 Transversely Isotropic Hyperelasticity

Transverse isotropy can be introduced by adding a vector field representing the material preferred direction explicitly into the strain energy [108]. We require that the strain energy depends on a unit vector field $\mathbf{A}$, which describes the local fiber direction in the undeformed configuration. When the material undergoes deformation, the vector $\mathbf{A}(\mathbf{X})$ may be described by a unit vector field $\mathbf{a}(\boldsymbol{\varphi}(\mathbf{X}))$. In general, the fibers will also undergo length change. The fiber stretch, λ, can be determined in terms of the deformation gradient and the fiber direction in the undeformed configuration,

$$\lambda\mathbf{a} = \mathbf{F}\cdot\mathbf{A}\,. \tag{2.4.39}$$

Also, since $\mathbf{a}$ is a unit vector,

$$\lambda^2 = \mathbf{A}\cdot\mathbf{C}\cdot\mathbf{A}\,. \tag{2.4.40}$$

The strain energy function for a transversely isotropic material, $\Psi(\mathbf{C}, \mathbf{A}, \mathbf{X})$ is an isotropic function of $\mathbf{C}$ and $\mathbf{A} \otimes \mathbf{A}$. It can be shown [99] that the following set of invariants are sufficient to describe the material fully:

$$I_1 = \operatorname{tr} \mathbf{C}\,, \quad I_2 = \frac{1}{2}\left[(\operatorname{tr} \mathbf{C})^2 - \operatorname{tr} \mathbf{C}^2\right]\,, \quad I_3 = \det C = J^2\,, \tag{2.4.41}$$

$$I_4 = \mathbf{A} \cdot \mathbf{C} \cdot \mathbf{A}\,, \quad I_5 = \mathbf{A} \cdot \mathbf{C}^2 \cdot \mathbf{A}\,. \tag{2.4.42}$$

The strain energy function can be written in terms of these invariants such that

$$\Psi(\mathbf{C}, \mathbf{A}, \mathbf{X}) = \Psi\left(I_1(\mathbf{C}), I_2(\mathbf{C}), I_3(\mathbf{C}), I_4(\mathbf{C}, \mathbf{A}), I_5(\mathbf{C}, \mathbf{A})\right)\,. \tag{2.4.43}$$

The second Piola-Kirchhoff can now be obtained in the standard manner:

$$\mathbf{S} = 2\frac{\partial \Psi}{\partial \mathbf{C}} = 2\sum_{i=1}^{5} \frac{\partial \Psi}{\partial I_i}\frac{\partial I_i}{\partial \mathbf{C}}\,. \tag{2.4.44}$$

In the transversely isotropic constitutive models described in Chapter 5 it is further assumed that the strain energy function can be split into the following terms:

$$\Psi(\mathbf{C}, \mathbf{A}) = \Psi_1(I_1, I_2, I_3) + \Psi_2(I_4) + \Psi_3(I_1, I_2, I_3 I_4)\,. \tag{2.4.45}$$

The strain energy function Ψ_1 represents the material response of the isotropic ground substance matrix, Ψ_2 represents the contribution from the fiber family (e.g. collagen), and Ψ_3 is the contribution from interactions between the fibers and matrix. The form (2.4.45) generalizes many constitutive equations that have been successfully used in the past to describe biological soft tissues e.g. [52, 55, 56]. While this relation represents a large simplification when compared to the general case, it also embodies almost all of the material behavior that one would expect from transversely isotropic, large deformation matrix-fiber composites.

2.4.5 Tension-Bearing Fiber Materials

In biomechanics we often find it convenient to model fibrous or fibrillar materials using one-dimensional fibers that can only sustain tension. Typically, such fibers are represented with a strain energy density function

$$\Psi_r(\mathbf{C}) = H(I_n - 1)\,\Psi_n(I_n)\,, \quad I_n = \mathbf{n}_r \cdot \mathbf{C} \cdot \mathbf{n}_r \tag{2.4.46}$$

where $\mathbf{n}_r$ is the unit vector along the fiber in its reference configuration, and I_n is the square of the stretch ratio along the fiber. The Heaviside unit step function $H(I_n - 1)$ in eq.(2.4.46) ensures that the fiber contributes strain energy only when it is under tension ($I_n > 1$); thus, the constitutive model $\Psi_n(I_n)$ for the tensile response of the fiber must reduce to zero when $I_n = 1$.

Using the hyperelasticity relations presented above, the Cauchy stress in this fiber material can be evaluated as

$$\boldsymbol{\sigma} = H(I_n - 1)\,2J^{-1}\frac{d\Psi_n}{dI_n}(\mathbf{F} \cdot \mathbf{n}_r) \otimes (\mathbf{F} \cdot \mathbf{n}_r)\,, \tag{2.4.47}$$

and the spatial elasticity tensor is

$$\mathcal{C} = 4J^{-1}\frac{d^2\Psi_n}{dI_n^2}(\mathbf{F} \cdot \mathbf{n}_r) \otimes (\mathbf{F} \cdot \mathbf{n}_r) \otimes (\mathbf{F} \cdot \mathbf{n}_r) \otimes (\mathbf{F} \cdot \mathbf{n}_r)\,. \tag{2.4.48}$$

If we denote the unit vector along the fiber in the current configuration as $\mathbf{n} \equiv I_n^{-1/2}\mathbf{F}\cdot\mathbf{n}_r$, the above expressions may be rewritten as $\boldsymbol{\sigma} = H\left(I_n - 1\right) 2J^{-1} I_n \Psi_n'\left(I_n\right) \mathbf{n}\otimes\mathbf{n}$ and $\mathcal{C} = 4J^{-1} I_n^2 \Psi_n''\left(I_n\right) \mathbf{n}\otimes\mathbf{n}\otimes\mathbf{n}\otimes\mathbf{n}$. As explained in [4], these fiber models must be combined with a ground matrix in order to produce a stable material response. In FEBio this can be done by using a constrained mixture of solid constituents (for example, see Section 2.8.4).

In the classical fiber mechanics literature it was suggested that uncoupled fiber formulations could also be implemented, whereby

$$\Psi_r\left(\mathbf{C}\right) = H\left(\tilde{I}_n - 1\right)\tilde{\Psi}_n\left(\tilde{I}_n\right) + U\left(J\right)\,, \quad \tilde{I}_n = \mathbf{n}_r\cdot\tilde{\mathbf{C}}\cdot\mathbf{n}_r\,, \tag{2.4.49}$$

and the Cauchy stress $\boldsymbol{\sigma}$ is given by Eq.(2.4.31) where

$$\tilde{\boldsymbol{\sigma}} = H\left(\tilde{I}_n - 1\right) 2J^{-1}\frac{d\tilde{\Psi}_n}{d\tilde{I}_n}\left(\tilde{\mathbf{F}}\cdot\mathbf{n}_r\right)\otimes\left(\tilde{\mathbf{F}}\cdot\mathbf{n}_r\right)\,. \tag{2.4.50}$$

Uncoupled fiber formulations of this kind are available in FEBio. More recently however, several studies have demonstrated that using $H\left(\tilde{I}_n - 1\right)$ to detect whether a fiber is in tension or compression is non-physical, since $\tilde{I}_n \neq I_n$ and I_n is the sole true measure of the tensile stretch in the fiber [48, 49, 87]. Therefore, uncoupled fiber formulations have fallen out of favor, even though FEBio still allows users to employ these for historical reasons. It is now recommended to use the standard (unconstrained) fiber models, also available in FEBio, with the formulation given in Eqs.(2.4.46)-(2.4.48), even when the ground matrix uses an uncoupled formulation.

2.5 Biphasic Material

Biphasic materials may be used to model deformable porous media. A biphasic material represents a mixture of a porous permeable solid and an interstitial fluid. Each constituent is intrinsically incompressible, but the mixture may change volume as interstitial fluid is exchanged with the pore space of the solid. Biphasic materials require the explicit modeling of fluid that permeates the solid. The biphasic material model is useful to simulate materials that show flow-dependent viscoelastic behavior resulting from the frictional interactions of the fluid and solid. Several biological materials such as cartilage can be described more accurately this way.

2.5.1 Governing Equations

Consider a mixture consisting of a solid constituent and a fluid constituent. Both constituents are considered to be intrinsically incompressible, but the mixture can change volume when fluid enters or leaves the porous solid matrix [29, 75]. According to the kinematics of the continuum [102], each constituent α of a mixture ($\alpha = s$ for the solid and $\alpha = w$ for the fluid) has a separate motion $\boldsymbol{\chi}^{\alpha}(\mathbf{X}^{\alpha}, t)$ which places particles of each mixture constituent, originally located at $\mathbf{X}^{\alpha}$, in the current configuration $\mathbf{x}$ according to

$$\mathbf{x} = \boldsymbol{\chi}^{\alpha}(\mathbf{X}^{\alpha}, t) \; . \tag{2.5.1}$$

For the purpose of finite element analyses, the motion of the solid matrix, $\alpha = s$, is of particular interest.

The governing equations that enter into the statement of virtual work are the conservation of linear momentum and the conservation of mass, for the mixture as a whole. Under quasi-static conditions, the conservation of momentum reduces to

$$\operatorname{div} \boldsymbol{\sigma} + \rho \mathbf{b} = \mathbf{0} \, , \tag{2.5.2}$$

where σ is the Cauchy stress for the mixture, ρ is the mixture density and $\mathbf{b}$ is the external mixture body force per mass. Since the mixture is porous, this stress may also be written as

$$\boldsymbol{\sigma} = -p\mathbf{I} + \boldsymbol{\sigma}^{e} \, , \tag{2.5.3}$$

where p is the fluid pressure and σ^{e} is the effective or extra stress, resulting from the deformation of the solid matrix. Conservation of mass for the mixture requires that

$$\operatorname{div}(\mathbf{v}^{s} + \mathbf{w}) = 0 \, , \tag{2.5.4}$$

where $\mathbf{v}^{s} = \partial \boldsymbol{\chi}^{s} / \partial t$ is the solid matrix velocity and $\mathbf{w}$ is the flux of the fluid relative to the solid matrix. Let the solid matrix displacement be denoted by $\mathbf{u}$, then $\mathbf{v}^{s} = \dot{\mathbf{u}}$.

To relate the relative fluid flux $\mathbf{w}$ to the fluid pressure and solid deformation, it is necessary to employ the equation of conservation of linear momentum for the fluid,

$$-\varphi^{w} \operatorname{grad} p + \rho^{w} \mathbf{b}^{w} + \hat{\mathbf{p}}_{d}^{w} = \mathbf{0} \, , \tag{2.5.5}$$

where φ^{w} is the solid matrix porosity, $\rho^{w} = \varphi^{w} \rho_{T}^{w}$ is the apparent fluid density and ρ_{T}^{w} is the true fluid density, $\mathbf{b}^{w}$ is the external body force per mass acting on the fluid, and $\hat{\mathbf{p}}_{d}^{w}$ is the momentum exchange between the solid and fluid constituents, typically representing the frictional interaction between these constituents. This equation neglects the viscous stress of the fluid in comparison

to $\hat{\mathbf{p}}_d^w$. The most common constitutive relation is $\hat{\mathbf{p}}_d^w = -\varphi^w \mathbf{k}^{-1} \cdot \mathbf{w}$, where the second order, symmetric tensor $\mathbf{k}$ is the hydraulic permeability of the mixture. When combined with Eq.(2.5.5), it produces

$$\mathbf{w} = -\mathbf{k} \cdot (\operatorname{grad} p - \rho_T^w \mathbf{b}^w) \ , \tag{2.5.6}$$

which is equivalent to Darcy's law. In general, $\mathbf{k}$ may be a function of the deformation.

2.6 Biphasic-Solute Material

A biphasic-solute material is an extension of the biphasic material model that also includes transport and mechano-chemical effects of a neutral solute. Transport of a solute in a porous medium includes diffusion, resulting from gradients in the solute concentration, and convection of the solute by the solvent, as a result of fluid pressure gradients. Mechano-chemical effects describe phenomena such as osmotic pressurization and swelling.

2.6.1 Governing Equations

The governing equations adopted in this finite element implementation of neutral solute transport in deformable porous media are based on the framework of mixture theory [30, 102]. A single solute is considered in this presentation for notational simplicity, though the extension of equations to multiple solutes is straightforward. Various forms of the governing equations have been presented in the prior literature [6, 74], though a presentation that incorporates all the desired features of this implementation has not been reported previously and is thus detailed here.

The fundamental modeling assumptions adopted in this treatment are quasi-static conditions for momentum balance (negligible effects of inertia), intrinsic incompressibility of all constituents (invariant true densities), isothermal conditions, negligible volume fraction of solute relative to the solid and solvent, and negligible effects of solute and solvent viscosities (friction within constituents) relative to frictional interactions between constituents. These assumptions are often made in studies of biological tissues and cells. External body forces and chemical reactions are not considered.

The three constituents of the mixture are the porous-permeable solid matrix ($\alpha = s$), the solvent ($\alpha = w$), and the solute ($\alpha = u$). The motion of the solid matrix is described by the displacement vector $\mathbf{u}$, the pressure of the interstitial fluid (solvent+solute) is p, and the solute concentration (on a solution-volume basis) is c. The total (or mixture) stress may be described by the Cauchy stress tensor $\boldsymbol{\sigma} = -p\mathbf{I} + \boldsymbol{\sigma}^e$, where $\mathbf{I}$ is the identity tensor and $\boldsymbol{\sigma}^e$ is the stress arising from the strain in the porous solid matrix. Because it is porous, the solid matrix is compressible since the volume of pores changes as interstitial fluid enters or leaves the matrix. Under the conditions outlined above, the balance of linear momentum for the mixture reduces to

$$\operatorname{div} \boldsymbol{\sigma} = -\operatorname{grad} p + \operatorname{div} \boldsymbol{\sigma}^e = \mathbf{0}\,. \tag{2.6.1}$$

Similarly, the equations of balance of linear momentum for the solvent and solute are given by

$$\begin{aligned} \rho^w \operatorname{grad} \tilde{\mu}^w + \mathbf{f}^{ws} \cdot (\mathbf{v}^s - \mathbf{v}^w) + \mathbf{f}^{wu} \cdot (\mathbf{v}^u - \mathbf{v}^w) = \mathbf{0}\,, \\ -\rho^u \operatorname{grad} \tilde{\mu}^u + \mathbf{f}^{us} \cdot (\mathbf{v}^s - \mathbf{v}^u) + \mathbf{f}^{uw} \cdot (\mathbf{v}^w - \mathbf{v}^u) = \mathbf{0}\,, \end{aligned} \tag{2.6.2}$$

where ρ^α is the apparent density (mass of α per volume of the mixture), $\tilde{\mu}^\alpha$ is the mechano-chemical potential and $\mathbf{v}^\alpha$ is the velocity of constituent α. $\mathbf{f}^{\alpha\beta}$ is the diffusive drag tensor between constituents α and β representing momentum exchange via frictional interactions, which satisfies $\mathbf{f}^{\beta\alpha} = \mathbf{f}^{\alpha\beta}$. An important feature of these relations is the incorporation of momentum exchange term between the solute and solid matrix, $\mathbf{f}^{us} \cdot (\mathbf{v}^s - \mathbf{v}^u)$, which is often neglected in other treatments but plays an important role for describing solid-solute interactions [1, 2, 74]. These momentum equations show that the driving force for the transport of solvent or solute is the gradient in its mechano-chemical potential, which is resisted by frictional interactions with other constituents.

The mechano-chemical potential is the sum of the mechanical and chemical potentials. The chemical potential μ^α of α represents the rate at which the mixture free energy changes with

increasing mass of α. The mechanical potential represents the rate at which the mixture free energy density changes with increasing volumetric strain of α. In a mixture of intrinsically incompressible constituents, where the volumetric strain is idealized to be zero, this potential is given by $(p - p_0)/\rho_T^\alpha$, where ρ_T^α is the true density of α (mass of α per volume of α), which is invariant for incompressible constituents, and p_0 is some arbitrarily set reference pressure (e.g., ambient pressure).

From classical physical chemistry, the general form of a constitutive relation for the chemical potential is $\mu^\alpha = \mu_0^\alpha(\theta) + (R\theta/M^\alpha)\ln a^\alpha$ [101], where R is the universal gas constant, θ is the absolute temperature, M^α is the molecular weight (invariant) and a^α is the activity of constituent α (a non-dimensional quantity); $\mu_0^\alpha(\theta)$ is the chemical potential at some arbitrary reference state, at a given temperature. For solutes, physical chemistry treatments let $a^u = \gamma c/c_0$, where c_0 is the solute concentration in some standard reference state (an invariant, typically $c_0 = 1\,\mathrm{M}$), and γ is the non-dimensional activity coefficient, which generally depends on the current state (e.g., concentration) but reduces to unity under the assumption of ideal physico-chemical behavior [101]. Since this representation is strictly valid for free solutions only, whereas solutes may be partially excluded from some of the interstitial space of a porous solid matrix, Mauck et al. [74] extended this representation of the solute activity to let $a^u = \gamma c/\kappa c_0$, where the solubility κ represents the fraction of the pore space which is accessible to the solute ($0 < \kappa \leqslant 1$). In this extended form, it becomes clear that even under ideal behavior ($\gamma = 1$), the solute activity may be affected by the solubility. Indeed, for neutral solutes, the solubility also represents the partition coefficient of the solute between the tissue and external bath [63, 78].

When accounting for the fact that the solute volume fraction is negligible compared to the solvent volume fraction [5, 101], the general expressions for $\tilde{\mu}^w$ and $\tilde{\mu}^u$ take the form

$$\begin{aligned} \tilde{\mu}^w &= \mu_0^w(\theta) + \frac{1}{\rho_T^w}\left(p - p_0 - R\theta\,\Phi\,c\right), \\ \tilde{\mu}^u &= \mu_0^u(\theta) + \frac{R\theta}{M}\ln\frac{\gamma c}{\kappa c_0}, \end{aligned} \tag{2.6.3}$$

where Φ is the osmotic coefficient (a non-dimensional function of the state), which deviates from unity under non-ideal physico-chemical behavior. Therefore, a complete description of the physico-chemical state of solvent and solute requires constitutive relations for Φ and the effective solubility $\tilde{\kappa} = \kappa/\gamma$, which should generally depend on the solid matrix strain and the solute concentration.

It is also necessary to satisfy the balance of mass for each of the constituents. In the absence of chemical reactions, the statement of balance of mass for constituent α reduces to

$$\frac{\partial \rho^\alpha}{\partial t} + \operatorname{div}\left(\rho^\alpha \mathbf{v}^\alpha\right) = 0\,. \tag{2.6.4}$$

The apparent density may be related to the true density via $\rho^\alpha = \varphi^\alpha \rho_T^\alpha$, where φ^α is the volume fraction of α in the mixture. Due to mixture saturation (no voids), the volume fractions add up to unity. Since the volume fraction of solute is considered negligible ($\varphi^u \ll \varphi^s, \varphi^w$), it follows that $\sum_\alpha \varphi^\alpha \approx \varphi^s + \varphi^w = 1$. Since ρ_T^α of an incompressible constituent is invariant in space and time, these relations may be combined to produce the mixture balance of mass relation,

$$\operatorname{div}\left(\mathbf{v}^s + \mathbf{w}\right) = 0, \tag{2.6.5}$$

where $\mathbf{w} = \varphi^w\left(\mathbf{v}^w - \mathbf{v}^s\right)$ is the volumetric flux of solvent relative to the solid. The balance of mass for the solute may also be written as

$$\frac{\partial\left(\varphi^w c\right)}{\partial t} + \operatorname{div}\left(\mathbf{j} + \varphi^w c\,\mathbf{v}^s\right) = 0\,, \tag{2.6.6}$$

where $\mathbf{j} = \varphi^w c\,(\mathbf{v}^u - \mathbf{v}^s)$ is the molar flux of solute relative to the solid. This mass balance relation is obtained by recognizing that the solute apparent density (mass per mixture volume) is related to its concentration (moles per solution volume) via $\rho^u = (1-\varphi^s)\,Mc \approx \varphi^w Mc$. Finally, it can be shown via standard arguments that the mass balance for the solid matrix reduces to

$$\varphi^s = \frac{\varphi^s_r}{J}\,, \tag{2.6.7}$$

where φ^s_r is the solid volume fraction in the reference state, $J = \det \mathbf{F}$ and $\mathbf{F} = \mathbf{I} + \operatorname{grad}\mathbf{u}$ is the deformation gradient of the solid matrix.

Inverting the momentum balance equations in (2.6.2), it is now possible to relate the solvent and solute fluxes to the driving forces according to

$$\begin{aligned} \mathbf{w} &= -\tilde{\mathbf{k}}\cdot\left(\rho^w_T \operatorname{grad}\tilde{\mu}^w + Mc\frac{\mathbf{d}}{d_0}\operatorname{grad}\tilde{\mu}^u\right)\,, \\ \mathbf{j} &= \mathbf{d}\cdot\left(-\frac{M}{R\theta}\varphi^w c \operatorname{grad}\tilde{\mu}^u + \frac{c}{d_0}\mathbf{w}\right)\,, \end{aligned} \tag{2.6.8}$$

where $\mathbf{d}$ is the solute diffusivity tensor in the mixture (solid+solution), d_0 is its (isotropic) diffusivity in free solution; $\tilde{\mathbf{k}}$ is the hydraulic permeability tensor of the solution (solvent+solute) through the porous solid matrix, which depends explicitly on concentration according to

$$\tilde{\mathbf{k}} = \left[\mathbf{k}^{-1} + \frac{R\theta c}{\varphi^w d_0}\left(\mathbf{I} - \frac{\mathbf{d}}{d_0}\right)\right]^{-1}\,, \tag{2.6.9}$$

where $\mathbf{k}$ represents the hydraulic permeability tensor of the solvent through the solid matrix. The permeability and diffusivity tensors are related to the diffusive drag tensors appearing in (2.6.2) according to

$$\begin{aligned} \mathbf{k} &= (\varphi^w)^2\,(\mathbf{f}^{ws})^{-1}\,, \\ \mathbf{d}_0 &= R\theta\varphi^w c\,(\mathbf{f}^{uw})^{-1} \equiv d_0\mathbf{I}\,, \\ \mathbf{d} &= R\theta\varphi^w c\,(\mathbf{f}^{us} + \mathbf{f}^{uw})^{-1}\,, \end{aligned} \tag{2.6.10}$$

though these explicit relationships are not needed here since $\mathbf{k}$, $\mathbf{d}$ and d_0 may be directly specified in a particular analysis. Since the axiom of entropy inequality requires that the tensors $\mathbf{f}^{\alpha\beta}$ be positive semi-definite (see appendix of [9]), it follows that d_0 must be greater than or equal to the largest eigenvalue of $\mathbf{d}$. Constitutive relations are needed for these transport properties, which relate them to the solid matrix strain and solute concentration. Note that the relations in (2.6.10) represent generalizations of Darcy's law for fluid permeation through porous media, and Fick's law for solute diffusion in porous media or free solution.

2.6.2 Continuous Variables

In principle, the objective of the finite element analysis is to solve for the three unknowns, $\mathbf{u}$, p and c, using the partial differential equations that enforce mixture momentum balance in (2.6.1), mixture mass balance in (2.6.5), and solute mass balance in (2.6.6). The remaining solvent and solute momentum balances in (2.6.8), and solid mass balance in (2.6.7), have been reduced to relations that may be substituted into the three partial differential equations as needed. Solving these equations requires the application of suitable boundary conditions that are consistent with mass, momentum and energy balances across boundary surfaces or interfaces. When defining

boundaries or interfaces on the solid matrix (the conventional approach in solid mechanics), whose outward unit normal is $\mathbf{n}$, mass and momentum balance relations demonstrate that the mixture traction $\mathbf{t} = \boldsymbol{\sigma} \cdot \mathbf{n}$ and normal flux components $w_n = \mathbf{w} \cdot \mathbf{n}$ and $j_n = \mathbf{j} \cdot \mathbf{n}$ must be continuous across the interface [5, 38]. Therefore, $\mathbf{t}$, w_n and j_n may be prescribed as boundary conditions.

Combining momentum and energy balances across an interface also demonstrates that $\tilde{\mu}^w$ and $\tilde{\mu}^u$ must be continuous [5, 59], implying that these mechano-chemical potentials may be prescribed as boundary conditions. However, because of the arbitrariness of the reference states μ_0^w, μ_0^u, p_0 and c_0, and the ill-conditioning of the logarithm function in the limit of small solute concentration, the mechano-chemical potentials do not represent practical choices for primary variables in a finite element implementation. An examination of (2.6.3) also shows that continuity of these potentials across an interface does not imply continuity of the fluid pressure p or solute concentration c. Therefore, pressure and concentration are also unsuitable as nodal variables in a finite element analysis and they must be replaced by alternative choices. Based on the similar reasoning presented by Sun et al. [100], an examination of the expressions in (2.6.3) shows that continuity may be enforced by using

$$\begin{aligned} \tilde{p} &= p - R\theta\,\Phi\,c\,, \\ \tilde{c} &= \frac{c}{\tilde{\kappa}}\,, \end{aligned} \tag{2.6.11}$$

where $\tilde{p}$ is the effective fluid pressure and $\tilde{c}$ is the effective solute concentration in the mixture. Note that $\tilde{p}$ represents that part of the fluid pressure which does not result from osmotic effects (since the term $R\theta\,\Phi\,c$ may be viewed as the osmotic pressure contribution to p), and $\tilde{c}$ is a straightforward measure of the solute activity, since $a^u = \tilde{c}/c_0$. Therefore these alternative variables have clear physical meanings.

Since the unknowns are now given by $\mathbf{u}$, $\tilde{p}$ and $\tilde{c}$, the governing partial differential equations may be rewritten in the form

$$\begin{aligned} &\operatorname{grad}(\tilde{p} + R\theta\,\Phi\,\tilde{\kappa}\tilde{c}) + \operatorname{div}\boldsymbol{\sigma}^e = \mathbf{0}\,, \\ &\operatorname{div}(\mathbf{v}^s + \mathbf{w}) = 0\,, \\ &\frac{\partial(\varphi^w\tilde{\kappa}\tilde{c})}{\partial t} + \operatorname{div}(\mathbf{j} + \varphi^w\tilde{\kappa}\tilde{c}\,\mathbf{v}^s) = 0\,, \end{aligned} \tag{2.6.12}$$

where

$$\begin{aligned} \mathbf{w} &= -\tilde{\mathbf{k}} \cdot \left(\operatorname{grad}\tilde{p} + R\theta\frac{\tilde{\kappa}}{d_0}\mathbf{d} \cdot \operatorname{grad}\tilde{c} \right)\,, \\ \mathbf{j} &= \tilde{\kappa}\mathbf{d} \cdot \left(-\varphi^w \operatorname{grad}\tilde{c} + \frac{\tilde{c}}{d_0}\mathbf{w} \right)\,, \\ \tilde{\mathbf{k}} &= \left[\mathbf{k}^{-1} + \frac{R\theta}{\varphi^w}\frac{\tilde{\kappa}\tilde{c}}{d_0}\left(\mathbf{I} - \frac{\mathbf{d}}{d_0} \right) \right]^{-1}\,. \end{aligned} \tag{2.6.13}$$

Constitutive equations are needed to relate $\boldsymbol{\sigma}^e$, $\mathbf{k}$, $\mathbf{d}$, d_0, $\tilde{\kappa}$ and Φ to the solid matrix strain and effective solute concentration.

2.7 Triphasic and Multiphasic Materials

Multiphasic materials represent an extension of the biphasic-solute material, where the mixture may contain a multitude of solutes. These solutes may be either electrically charged (ionized) or neutral. Similarly, the solid matrix may either carry electrical charge (a fixed charge density) or be neutral. A triphasic material is a special case of a multiphasic material, having two solutes

that carry opposite charges. Triphasic and multiphasic materials may be used to model porous deformable biological tissues whose solid matrix may be charged and whose interstitial fluid may contain any number of charged or neutral solutes. When mixture constituents are electrically charged, the response of the tissue to various loading conditions may encompass a range of mechano-electrochemical phenomena, including permeation, diffusion, osmosis, streaming potentials and streaming currents. To better understand multiphasic materials, the reader is encouraged to review the descriptions of biphasic (Section 2.5) and biphasic-solute materials (Section 2.6).

2.7.1 Governing Equations

In multiphasic materials the solvent is assumed to be neutral, whereas the solid and solutes may carry charge. The mixture is isothermal and all constituents are considered to be intrinsically incompressible. Since the viscosity of the fluid constituents (solvent and solutes) is considered negligible relative to the frictional interactions among constituents, the stress tensor σ for the mixture includes only a contribution from the fluid pressure p and the stress $\boldsymbol{\sigma}^e$ in the solid,

$$\boldsymbol{\sigma} = -p\mathbf{I} + \boldsymbol{\sigma}^e \,. \tag{2.7.1}$$

The mechano-chemical potential of the solvent is given by

$$\tilde{\mu}^w = \mu_0^w\left(\theta\right) + \frac{1}{\rho_T^w}\left(p - p_0 - R\theta\Phi\sum_\alpha c^\alpha\right) , \tag{2.7.2}$$

where $\mu_0^w\left(\theta\right)$ is the solvent chemical potential in the solvent standard state, θ is the absolute temperature, ρ_T^w is the true density of the solvent (which is invariant since the solvent is assumed intrinsically incompressible), p is the fluid pressure, p_0 is the corresponding pressure in the standard state, R is the universal gas constant, Φ is the non-dimensional osmotic coefficient, and c^α is the solution volume-based concentration of solute α. The summation is taken over all solutes in the mixture. The mechano-electrochemical potential of each solute is similarly given by

$$\tilde{\mu}^\alpha = \mu_0^\alpha\left(\theta\right) + \frac{R\theta}{M^\alpha}\left(\frac{z^\alpha F_c}{R\theta}\left(\psi - \psi_0\right) + \ln\frac{\gamma^\alpha c^\alpha}{\kappa^\alpha c_0^\alpha}\right) , \tag{2.7.3}$$

where M^α is the molar mass of the solute, γ^α is its activity coefficient, κ^α is its solubility, z^α is its charge number, and c_0^α is its concentration in the solute standard state; F_c is Faraday's constant, ψ is the electrical potential of the mixture, and ψ_0 is the corresponding potential in the standard state.

In these relations, Φ and γ^α are functions of state that describe the deviation of the mixture from ideal physico-chemical behavior; κ^α represents the fraction of the pore volume which may be occupied by solute α. The standard state represents an arbitrary set of reference conditions for the physico-chemical state of each constituent. Therefore, the values of $\mu_0^w\left(\theta\right)$, p_0, ψ_0, $\mu_0^\alpha\left(\theta\right)$, and c_0^α, remain invariant over the entire domain of definition of an analysis. Since κ^α and γ^α appear together as a ratio, they may be combined into a single material function, $\hat{\kappa}^\alpha = \kappa^\alpha/\gamma^\alpha$, called the effective solubility.

In multiphasic mixtures, it is also assumed that electroneutrality is satisfied at every point in the continuum. Therefore, the net electrical charge summed over all constituents must reduce to zero, and no net charge accumulation may occur at any time. Denoting the fixed charge density of the solid by c^F (moles of equivalent charge per solution volume), and recognizing that the solvent is always considered neutral, the electroneutrality condition may be written as

$$c^F + \sum_\alpha z^\alpha c^\alpha = 0 \,. \tag{2.7.4}$$

This condition represents a constraint on a mixture of charged constituents. If none of the constituents are charged ($c^F = 0$ and $z^\alpha = 0$ for all α), the constraint disappears.

Each constituent of the mixture must satisfy the axiom of mass balance. In the absence of chemical reactions involving constituent α, its mass balance equation is

$$\frac{\partial \rho^\alpha}{\partial t} + \operatorname{div}\left(\rho^\alpha \mathbf{v}^\alpha\right) = 0\,, \tag{2.7.5}$$

where ρ^α is the apparent density and $\mathbf{v}^\alpha$ is the velocity of that constituent. For solutes, the apparent density is related to the concentration according to $\rho^\alpha = (1-\varphi^s)\, M^\alpha c^\alpha$, where φ^s is the volume fraction of the solid. When the solute volume fractions are negligible, it follows that $1-\varphi^s \approx \varphi^w$, where φ^w is the solvent volume fraction. The molar flux of the solute relative to the solid is given by $\mathbf{j}^\alpha = \varphi^w c^\alpha \left(\mathbf{v}^\alpha - \mathbf{v}^s\right)$, where $\mathbf{v}^\alpha$ is the solute velocity. Using these relations, the mass balance relation for the solute may be rewritten as

$$\frac{1}{J}\frac{D^s}{Dt}\left(J\varphi^w c^\alpha\right) + \operatorname{div}\mathbf{j}^\alpha = 0\,, \tag{2.7.6}$$

where $D^s\left(\cdot\right)/Dt$ represents the material time derivative in the spatial frame, following the solid; $J = \det\mathbf{F}$, where $\mathbf{F}$ is the deformation gradient of the solid. This form of the mass balance for the solute is convenient for a finite element formulation where the mesh is defined on the solid matrix.

The volume flux of solvent relative to the solid is given by $\mathbf{w} = \varphi^w\left(\mathbf{v}^w - \mathbf{v}^s\right)$, where $\mathbf{v}^w$ is the solvent velocity. When solute volume fractions are negligible, the mass balance equation for the mixture reduces to

$$\operatorname{div}\left(\mathbf{v}^s + \mathbf{w}\right) = 0\,. \tag{2.7.7}$$

Finally, the mass balance for the solid may be reduced to the form $D^s\left(J\varphi^s\right)/Dt = 0$, which may be integrated to produce the algebraic relation $\varphi^s = \varphi^s_r/J$, where φ^s_r is the solid volume fraction in the stress-free reference state of the solid.

Differentiating the electroneutrality condition in (2.7.4) using the material time derivative following the solid, and substituting the mass balance relations into the resulting expressions, produces a constraint on the solute fluxes:

$$\operatorname{div}\sum_{\alpha\neq s,w} z^\alpha \mathbf{j}^\alpha = 0\,. \tag{2.7.8}$$

Recognizing that $\mathbf{I}_e = F_c\sum_{\alpha\neq s,w} z^\alpha\mathbf{j}^\alpha$ is the current density in the mixture, with F_c representing Faraday's constant, the relation of (2.7.8) reduces to one of the Maxwell's equation, $\operatorname{div}\mathbf{I}_e = 0$, in the special case when there can be no charge accumulation (electroneutrality).

As described in Section 2.6.2, the fluid pressure p and solute concentrations c^α are not continuous across boundaries of a mixture, whereas $\tilde{\mu}^w$ and $\tilde{\mu}^\alpha$'s for the solutes do satisfy continuity. Therefore, in a finite element implementation, the following continuous variables are used as nodal degrees of freedom:

$$\tilde{p} = p - R\theta\Phi\sum_{\alpha\neq s,w} c^\alpha\,, \tag{2.7.9}$$

which represents the effective fluid pressure, and

$$\tilde{c}^\alpha = c^\alpha/\tilde{\kappa}^\alpha\,, \tag{2.7.10}$$

which represents the effective solute concentration. In the last expression, $\tilde{\kappa}^\alpha$ is the partition coefficient of the solute, which is related to the effective solubility and electric potential according to

$$\tilde{\kappa}^\alpha = \hat{\kappa}^\alpha \exp\left(-\frac{z^\alpha F_c\psi}{R\theta}\right)\,. \tag{2.7.11}$$

Physically, since $R\theta\,\Phi\sum_{\alpha\neq s,w} c^\alpha$ is the osmotic (chemical) contribution to the fluid pressure, $\tilde{p}$ may be interpreted as that part of the total (mechano-chemical) fluid pressure which does not result from osmotic effects; thus, it is the mechanical contribution to p. Similarly, the effective solute concentration $\tilde{c}^\alpha$ represents the true contribution of the molar solute content to its electrochemical potential.

When using these variables instead of mechano-electrochemical potentials, the momentum equations for the solvent and solutes may be inverted to produce the following flux relations:

$$\mathbf{w} = -\tilde{\mathbf{k}}\cdot\left(\mathrm{grad}\tilde{p} + R\theta\sum_{\beta\neq s,w}\frac{\tilde{\kappa}^\beta}{d_0^\beta}\mathbf{d}^\beta\cdot\mathrm{grad}\tilde{c}^\beta\right)\,, \tag{2.7.12}$$

and

$$\mathbf{j}^\alpha = \tilde{\kappa}^\alpha\mathbf{d}^\alpha\cdot\left(-\varphi^w\mathrm{grad}\tilde{c}^\alpha + \frac{\tilde{c}^\alpha}{d_0^\alpha}\mathbf{w}\right)\,, \tag{2.7.13}$$

where

$$\tilde{\mathbf{k}} = \left[\mathbf{k}^{-1} + \frac{R\theta}{\varphi^w}\sum_{\alpha\neq s,w}\frac{c^\alpha}{d_0^\alpha}\left(\mathbf{I} - \frac{\mathbf{d}^\alpha}{d_0^\alpha}\right)\right]^{-1} \tag{2.7.14}$$

is the effective hydraulic permeability of the solution (solvent+solutes) in the mixture. The momentum equation for the mixture is

$$\mathrm{div}\,\boldsymbol{\sigma} = \mathbf{0}\,. \tag{2.7.15}$$

2.8 Constrained Reactive Mixture of Solids

A solid material may consist of a heterogeneous mixture of various solid constituents that are constrained to move together. In this section we describe fundamental considerations for such constrained mixtures.

2.8.1 Mixture Kinematics

Consider a constrained mixture of multiple solid constituents σ. The motion of each constituent is given by $\boldsymbol{\chi}^\sigma\left(\mathbf{X}^\sigma, t\right)$, where $\mathbf{X}^\sigma$ denotes a material point in the reference configuration of that constituent. At the current time t, various constituents σ which occupy an elemental region with a spatial position $\mathbf{x}$ may have originated from distinct referential positions $\mathbf{X}^\sigma$. We often label a convenient constituent as the *master constituent* s (e.g., the oldest constituent in a reactive mixture with evolving composition) and call the reference configuration $\mathbf{X}^s$ the *master reference configuration*. All the referential mass densities and mass density supplies (see below) are evaluated relative to the master reference configuration $\mathbf{X}^s$. The kinematics of each constituent σ may be related to the kinematics of the master constituent s through

$$\mathbf{x} = \boldsymbol{\chi}^s\left(\mathbf{X}^s, t\right) = \boldsymbol{\chi}^\sigma\left(\mathbf{X}^\sigma, t\right)\,. \tag{2.8.1}$$

Taking the material time derivative of this relation in the material frame and recognizing that this relation must hold for all t in the case of a constrained mixture establishes that all constituents share the same velocity $\mathbf{v}^\sigma = \mathbf{v}^s$. However, as detailed previously [9, 76], constituents may have distinct deformation gradients $\mathbf{F}^\sigma = \partial\boldsymbol{\chi}^\sigma/\partial\mathbf{X}^\sigma$. When a reaction converts a reactant $\sigma = a$ into a product $\sigma = b$, these constituents may have distinct reference configurations. The deformation

gradient of the master constituent $\mathbf{F}^s$, which also serves as the total deformation gradient, may be related to the *relative deformation gradient* $\mathbf{F}^\sigma$ of constituent σ by applying the chain rule to Eq.(2.8.1), producing

$$\mathbf{F}^s\left(\mathbf{X}^s, t\right) = \frac{\partial \boldsymbol{\chi}^s\left(\mathbf{X}^s, t\right)}{\partial \mathbf{X}^\sigma} \cdot \frac{\partial \mathbf{X}^\sigma\left(\mathbf{X}^s\right)}{\partial \mathbf{X}^s} = \mathbf{F}^\sigma\left(\mathbf{X}^s, t\right) \cdot \mathbf{F}^{\sigma s}\left(\mathbf{X}^s\right) . \tag{2.8.2}$$

In this expression, $\mathbf{F}^{\sigma s}\left(\mathbf{X}^s\right)$ is the deformation gradient of σ relative to s, which must be *postulated by constitutive assumption*. The relationship between $\mathbf{X}^\sigma$ and $\mathbf{X}^s$ is time-invariant; consequently, $\mathbf{F}^{\sigma s}$ is a time-invariant spatial mapping. It follows that only one deformation gradient represents an independent state variable in a constrained mixture framework, whereas all others are related to it via Eq.(2.8.2); any of the $\mathbf{F}^\sigma$'s may be selected, based on convenience. In Eq.(2.8.2) the spatio-temporal arguments have been written explicitly for clarity. These dependencies are implied in the forthcoming sections and henceforth those arguments may be selectively suppressed. Taking the determinant of Eq.(2.8.2) produces a relation between the volume ratios $J^\sigma = \det \mathbf{F}^\sigma$ and $J^s = \det \mathbf{F}^s$,

$$J^s = J^\sigma J^{\sigma s} , \tag{2.8.3}$$

where $J^{\sigma s} = \det \mathbf{F}^{\sigma s}$.

2.8.2 Mixture Composition

Each constituent σ has an *apparent mass density* ρ^σ which may evolve due to deformation, or due to reactive processes which alter the mixture composition. Following [**? ?**], we define the *referential apparent mass density* ρ_r^σ of each constituent as

$$\rho_r^\sigma = J^s \rho^\sigma . \tag{2.8.4}$$

Equation (2.8.4) expresses the mass of constituent σ per referential volume of the master constituent s; thus ρ_r^σ may only evolve if the mass content changes via reactions, making it a suitable state variable for tracking composition in a reactive framework. The axiom of mass balance for each constituent σ may be written as

$$\dot{\rho}_r^\sigma = \hat{\rho}_r^\sigma , \tag{2.8.5}$$

where the dot operator represents the material time derivative and $\hat{\rho}_r^\sigma$ is the *referential mass supply density* for constituent σ, representing the rate at which mass (per referential volume) is added to σ due to reactions with all other mixture constituents [9, 76]. A constitutive relation must be provided for $\hat{\rho}_r^\sigma$ for various types of reactions. The mixture referential mass density ρ_r is given by

$$\rho_r = \sum_\sigma \rho_r^\sigma . \tag{2.8.6}$$

This summation is carried out over all constituents. When a constrained mixture of solid constituents represents a closed system, ρ_r remains constant over time. Taking the material time derivative of Eq.(2.8.6) and using Eq.(2.8.5) shows that the referential mass density supplies must satisfy

$$\sum_\sigma \hat{\rho}_r^\sigma = 0 . \tag{2.8.7}$$

2.8.3 Mixture Free Energy and Stress

The *referential free energy density* of the mixture is obtained as

$$\Psi_r = \rho_r \psi = \sum_\sigma \rho_r^\sigma \psi^\sigma \,, \tag{2.8.8}$$

where ψ^σ is the *specific free energy* of constituent σ and ψ is the specific free energy of the mixture. An important function of state which arises later in our treatment is the *chemical potential* of constituent σ, given by

$$\mu^\sigma = \frac{\partial \Psi_r}{\partial \rho_r^\sigma} \,. \tag{2.8.9}$$

The mixture Cauchy stress is given by

$$\boldsymbol{\sigma} = \frac{1}{J^s} \frac{\partial \Psi_r}{\partial \mathbf{F}^s} \cdot (\mathbf{F}^s)^T = \frac{2}{J^s} \mathbf{F}^s \cdot \frac{\partial \Psi_r}{\partial \mathbf{C}^s} \cdot (\mathbf{F}^s)^T \,, \tag{2.8.10}$$

where $\mathbf{C}^s = \mathbf{F}^s \cdot (\mathbf{F}^s)^T$ is the right Cauchy-Green tensor. The spatial elasticity tensor may be evaluated from

$$\boldsymbol{\mathcal{C}} = \frac{4}{J^s} (\mathbf{F}^s \oslash \mathbf{F}^s) : \frac{\partial^2 \Psi_r}{\partial \mathbf{C}^s \partial \mathbf{C}^s} : \left((\mathbf{F}^s)^T \oslash (\mathbf{F}^s)^T \right) \,. \tag{2.8.11}$$

In reactive frameworks where ρ_r^σ evolves according to Eq.(2.8.5), it may be convenient to define the mass fraction

$$w^\sigma = \frac{\rho_r^\sigma}{\rho_r} \,, \tag{2.8.12}$$

in which case we may rewrite Eq.(2.8.8) as $\Psi_r = \sum_\sigma w^\sigma \Psi_r^\sigma$ where $\Psi_r^\sigma \equiv \rho_r \psi^\sigma$ is the referential strain energy density of solid σ under the assumption that it is the sole mixture constituent, normalized by the referential volume of the master constituent s. Based on Eq.(2.8.6) the mass fractions satisfy $\sum_\sigma w^\sigma = 1$. In this case, when $\mathbf{X}^\sigma \neq \mathbf{X}^s$ and ψ^σ is most conveniently expressed as a function of $\mathbf{F}^\sigma$, we may use Eq.(2.8.2) to evaluate $\partial \mathbf{F}^s / \partial \mathbf{F}^\sigma = \mathbf{I} \oslash (\mathbf{F}^{\sigma s})^{-T}$ and calculate the mixture stress using the alternative form

$$\boldsymbol{\sigma} = \frac{1}{J^s} \sum_\sigma w^\sigma \frac{\partial \Psi_r^\sigma}{\partial \mathbf{F}^\sigma} \cdot (\mathbf{F}^\sigma)^T \,. \tag{2.8.13}$$

This expression shows that the mixture stress may evolve not only due to temporal changes in the state of strain but also due to reactive changes in the mass fractions w^σ.

In FEBio the referential strain energy density for any solid mixture constituent σ is evaluated from the same library of constitutive models used in single-constituent solids. In this library the calculation of the referential strain energy density is based on the assumption that the reference configuration corresponds to the configuration when the deformation gradient passed to those functions is equal to the identity tensor. Thus, passing $\mathbf{F}^s$ to those functions returns the correct Ψ_r^σ. However, when passing $\mathbf{F}^\sigma$ as an argument to those functions, the referential volume is based on the configuration $\mathbf{X}^\sigma$. Let the referential free energy density returned by FEBio for an argument $\mathbf{F}^\sigma$ be denoted by Ψ_0^σ. We may similarly denote the corresponding Cauchy stress and spatial elasticity tensors by $\boldsymbol{\sigma}_0^\sigma$ and $\boldsymbol{\mathcal{C}}_0^\sigma$. Here, the subscript 0 has two meanings: First it emphasizes that the corresponding function is evaluated using $\mathbf{F}^\sigma$ for the mixture constituent σ; second it emphasizes that the calculation returns the corresponding measure under the assumption that the mixture consists entirely of that constituent, so that its multiplication by the scale factor w^σ

returns the actual contribution of that measure to the entire mixture. Based on Eq.(2.8.3) we find that $\Psi_r^\sigma = J^{\sigma s}\Psi_0^\sigma$ so that the mixture free energy density may be evaluated from

$$\Psi_r = \sum_\sigma w^\sigma J^{\sigma s}\Psi_0^\sigma\left(\mathbf{F}^\sigma\right) , \tag{2.8.14}$$

whereas the mixture Cauchy stress and spatial elasticity are given by

$$\boldsymbol{\sigma} = \sum_\sigma w^\sigma \boldsymbol{\sigma}_0^\sigma , \quad \boldsymbol{\mathcal{C}} = \sum_\sigma w^\sigma \boldsymbol{\mathcal{C}}_0^\sigma , \tag{2.8.15}$$

where

$$\boldsymbol{\sigma}_0^\sigma = \frac{1}{J^\sigma}\frac{\partial \Psi_0^\sigma}{\partial \mathbf{F}^\sigma}\cdot\left(\mathbf{F}^\sigma\right)^T = \frac{1}{J^s}\frac{\partial \Psi_r^\sigma}{\partial \mathbf{F}^\sigma}\cdot\left(\mathbf{F}^\sigma\right)^T \tag{2.8.16}$$

and

$$\boldsymbol{\mathcal{C}}_0^\sigma = \frac{4}{J^\sigma}\left(\mathbf{F}^\sigma \oslash \mathbf{F}^\sigma\right) : \frac{\partial^2 \Psi_0^\sigma}{\partial \mathbf{C}^\sigma \partial \mathbf{C}^\sigma} : \left(\left(\mathbf{F}^\sigma\right)^T \oslash \left(\mathbf{F}^\sigma\right)^T\right) . \tag{2.8.17}$$

These relations show that the Cauchy stress and spatial elasticity tensor of constituent σ in Eq.(2.8.15) may be evaluated using existing FEBio functions without needing to adjust for the choice of reference configuration $\mathbf{X}^s$ or $\mathbf{X}^\sigma$, as evidenced by Eq.(2.8.16) in the case of the stress. However the referential strain energy density needs to be properly scaled by $J^{\sigma s}$ as shown in Eq.(2.8.14).

The calculation of the 2nd Piola-Kirchhoff stress $\mathbf{S}$ for each generation σ is more elaborate. When using the master reference configuration $\mathbf{X}^s$, this stress is given by

$$\mathbf{S}^\sigma\left(\mathbf{F}^s\right) = 2\frac{\partial \Psi_r^\sigma\left(\mathbf{F}^s\right)}{\partial \mathbf{C}^s} .$$

When using the reference configuration $\mathbf{X}^\sigma$, the stress is evaluated from a similar relation

$$\mathbf{S}_0^\sigma\left(\mathbf{F}^\sigma\right) = 2\frac{\partial \Psi_0^\sigma\left(\mathbf{F}^\sigma\right)}{\partial \mathbf{C}^\sigma} .$$

It can be shown that these stresses are related according to

$$\mathbf{S}^\sigma\left(\mathbf{F}^s\right) = J^{\sigma s}\left(\mathbf{F}^{\sigma s}\right)^{-1}\cdot\mathbf{S}_0^\sigma\left(\mathbf{F}^\sigma\right)\cdot\left(\mathbf{F}^{\sigma s}\right)^{-T} .$$

FEBio does not use this calculation for solid mixtures, as all internal calculations employ the Cauchy stress.

2.8.4 Simple Solid Mixtures

In the simplest type of non-reactive constrained mixtures of solids all constituents σ share the same reference configuration $\mathbf{X}^\sigma = \mathbf{X}^s$, in which case $\mathbf{F}^\sigma = \mathbf{F}^s$ and $J^{\sigma s} = 1$. For this type of mixture where ρ_r^σ does not evolve, it is convenient to set $w^\sigma = 1$ for all σ and scale the material properties of Ψ_r^σ to properly reflect the contribution of each constituent σ to the mixture. Thus, the relation of Eq.(2.8.15) reduces to

$$\boldsymbol{\sigma} = \sum_\sigma \boldsymbol{\sigma}_0^\sigma . \tag{2.8.18}$$

This type of non-reactive mixture of solids is represented in FEBio using the material "*solid mixture*".

When each constituent of a solid mixture is modeled using an uncoupled formulation to enforce nearly isochoric responses, the strain energy density of this type of mixture is given by

$$\Psi_r = U(J) + \sum_\sigma \tilde{\Psi}_r^\sigma \left(\tilde{\mathbf{F}}^s, \rho_r^\sigma\right) , \tag{2.8.19}$$

where $U(J)$ is the volumetric energy component, $\tilde{\Psi}_r = \sum_\sigma \tilde{\Psi}_r^\sigma$ is the distortional energy component, and $\tilde{\mathbf{F}}^s$ is the distortional part of the deformation gradient, as described in Section 2.4.3. This type of non-reactive mixture of uncoupled solids is represented in FEBio using the material "*uncoupled solid mixture*".

2.8.5 Multigenerational Interstitial Growth

Multigenerational interstitial growth mechanics may be modeled using a reactive mixture of constrained solids as described in [8]. In this framework it is assumed that a porous solid matrix may gain mass via interstitial growth, such that the porosity of the solid decreases with increasing solid mass content. The history of growth is discretized temporally into generations σ such that the mass added in the time interval $t^\sigma \leq t < t^{\sigma+1}$ has a reference configuration $\mathbf{X}^\sigma$. This model assumes that each generation σ gets deposited into the existing mixture in a stress-free state. This can be achieved by adopting the constitutive assumption that $\mathbf{X}^\sigma = \boldsymbol{\chi}^s(\mathbf{X}^s, t^\sigma)$. In other words, the reference configuration of generation σ is the current configuration of the solid mixture at time t^σ. An alternative form of this constitutive model is that $\mathbf{F}^\sigma(\mathbf{X}^s, t^\sigma) = \mathbf{I}$ while the new generation σ is being deposited, or equivalently $\mathbf{F}^{\sigma s}(\mathbf{X}^s) = \mathbf{F}^s(\mathbf{X}^s, t^\sigma)$ according to Eq.(2.8.2).

The underlying assumption of multigenerational growth is that $\mathbf{F}^s(\mathbf{X}^s, t^\sigma)$ evolves for each generation σ either due to load-induced deformations or deformations produced by swelling processes, such as cell growth or Donnan swelling.

This type of multigenerational growth material is implemented in FEBio as "*multigeneration*" for mixtures of elastic solids, and as "*multiphasic-multigeneration*" for reactive multiphasic mixtures whose solid constituent is a multigenerational growth material. In this type of material the user needs to prescribe the generation birth times t^σ and the properties of the material of each generation σ. The code automatically prescribes $\mathbf{F}^{\sigma s}$ based on the constitutive model given above, for each generation σ. For example, one may use a material model whose response depends on the evolving composition ρ_r^σ of that generation. The composition ρ_r^σ may evolve either due to chemical reactions modeled in a multiphasic framework, or by associating a user-defined load curve with ρ_r^σ. Thus, the material properties (and the stress response) of generation σ need not remain constant over the generation time interval $t^\sigma \leq t < t^{\sigma+1}$, even though $\mathbf{F}^{\sigma s}$ remains constant during that generation.

When the growth process is negative ($\hat{\rho}_r^\sigma < 0$), it implies that the solid constituent σ is losing mass (solid resorption); this loss of mass terminates when $\rho_r^\sigma = 0$. A material model that depends on ρ_r^σ may exhibit evolving material properties during this resorption process until that generation produces zero stress when $\rho_r^\sigma = 0$.

As a result of these evolving growth processes, this multigeneration mixture may exhibit residual stresses.

2.8.6 Prescribed Pre-Stretch

An alternative approach to multigenerational growth is to prescribe $\mathbf{F}^{\sigma s}$ as a user-defined function. For isotropic stretching we may define

$$\mathbf{F}^{\sigma s} = \lambda^{\sigma s}\mathbf{I} , \tag{2.8.20}$$

where $\lambda^{\sigma s} > 0$ is the stretch ratio. A value greater than unity causes swelling whereas a value less than unity causes contraction; $\lambda^{\sigma s} = 1$ produces $\mathbf{F}^{\sigma s} = \mathbf{I}$, which recovers the simple solid mixture described in Section 2.8.4. In FEBio a load curve may be associated with $\lambda^{\sigma s}$ to ramp up the prescribed deposition stretch.

For orthotropic stretching we define mutually orthogonal symmetry planes with unit normals $\mathbf{a}_i$ ($i = 1, 2, 3$ and $\mathbf{a}_i \cdot \mathbf{a}_j = \delta_{ij}$). Then,

$$\mathbf{F}^{\sigma s} = \sum_{i=1}^{3} \lambda_i^{\sigma s} \mathbf{a}_i \otimes \mathbf{a}_i \,, \tag{2.8.21}$$

where $\lambda_i^{\sigma s}$ is the stretch ratio for the prescribed stretch along $\mathbf{a}_i$; in general, $\lambda_1^{\sigma s} \neq \lambda_2^{\sigma s} \neq \lambda_3^{\sigma s}$, though this model can be specialized to transversely isotropic stretch by setting two of these stretch ratios equal to each other.

At lower symmetries the constitutive model for $\mathbf{F}^{\sigma s}$ must necessarily combine stretch and rotation. For monoclinic materials, deformations may be prescribed along three unit vectors $\mathbf{a}_i$ that satisfy $\mathbf{a}_1 \cdot \mathbf{a}_2 = 0$, $\mathbf{a}_1 \cdot \mathbf{a}_3 = 0$, and $\mathbf{a}_2 \cdot \mathbf{a}_3 \neq 0$, such that $\mathbf{a}_1$ defines the single plane of symmetry. In this case,

$$\begin{aligned} \mathbf{F}^{\sigma s} = \lambda_1^{\sigma s} \mathbf{a}_1 \otimes \mathbf{a}_1 + \frac{\lambda_2^{\sigma s}}{1-\alpha_{23}^2} \mathbf{a}_2 \otimes (\mathbf{a}_2 - \alpha_{23}\mathbf{a}_3) \\ + \frac{\lambda_3^{\sigma s}}{1-\alpha_{23}^2} \mathbf{a}_3 \otimes (\mathbf{a}_3 - \alpha_{23}\mathbf{a}_2) \end{aligned} \,, \tag{2.8.22}$$

where $\lambda_i^{\sigma s}$ is the stretch along $\mathbf{a}_i$ and $\alpha_{23} = \mathbf{a}_2 \cdot \mathbf{a}_3$. Under general conditions (i.e., when $\lambda_1^{\sigma s} \neq \lambda_2^{\sigma s} \neq \lambda_3^{\sigma s}$ and $\alpha_{23} \neq 0$), the polar decomposition theorem shows that this deformation gradient is not a pure stretch, as it also involves a rotation.

The deformation gradient for expansion of a triclinic material may be similarly constructed by finding $\mathbf{F}^{\sigma s}$ such that $\mathbf{F}^{\sigma s} \cdot \mathbf{a}_i = \lambda_i^{\sigma s} \mathbf{a}_i$ (no sum) for non-orthogonal and non-collinear unit vectors $\mathbf{a}_i$,

$$\begin{aligned} \mathbf{F}^{\sigma s} = \frac{\lambda_1^{\sigma s}}{d} \mathbf{a}_1 \otimes \left(\left(1-\alpha_{23}^2\right) \mathbf{a}_1 - \left(\alpha_{12} - \alpha_{13}\alpha_{23}\right) \mathbf{a}_2 - \left(\alpha_{13} - \alpha_{12}\alpha_{23}\right) \mathbf{a}_3 \right) \\ + \frac{\lambda_2^{\sigma s}}{d} \mathbf{a}_2 \otimes \left(-\left(\alpha_{12} - \alpha_{13}\alpha_{23}\right) \mathbf{a}_1 + \left(1-\alpha_{13}^2\right) \mathbf{a}_2 - \left(\alpha_{23} - \alpha_{12}\alpha_{13}\right) \mathbf{a}_3 \right) \\ + \frac{\lambda_3^{\sigma s}}{d} \mathbf{a}_3 \otimes \left(-\left(\alpha_{13} - \alpha_{12}\alpha_{23}\right) \mathbf{a}_1 - \left(\alpha_{23} - \alpha_{12}\alpha_{13}\right) \mathbf{a}_2 + \left(1-\alpha_{12}^2\right) \mathbf{a}_3 \right) \end{aligned} \tag{2.8.23}$$

where

$$d = 1 - \alpha_{12}^2 - \alpha_{13}^2 - \alpha_{23}^2 + 2\alpha_{23}\alpha_{13}\alpha_{12} \tag{2.8.24}$$

and $\alpha_{ij} = \mathbf{a}_i \cdot \mathbf{a}_j$ is the cosine of the angle between $\mathbf{a}_i$ and $\mathbf{a}_j$.

This type of elastic solid with prescribed pre-stretch is modeled in FEBio using the materials "*prestretch elastic*" and "*prestretch uncoupled elastic*". In the uncoupled version each solid constituent in the mixture has a deformation gradient $\mathbf{F}^{\sigma}$ which produces nearly isochoric responses ($J^{\sigma} = 1$), whereas no constraint is placed on the volumetric strain of the pre-stretch $\mathbf{F}^{\sigma s}$.

2.9 Equilibrium Swelling

When the interstitial fluid of a porous medium contains one or more solutes, an osmotic pressure may be produced in the fluid if the osmolarity of the interstitial fluid is non-uniform, or if it is different from that of the external bathing solution surrounding the porous medium. In general, since the osmolarity of the interstitial fluid may vary over time in transient problems, the analysis of such swelling effects may be addressed using, for example, the biphasic-solute material model described in Section 2.6. However, if we are only interested in the steady-state response for such types of materials, when solvent and solute fluxes have subsided, the analysis may be simplified considerably.

The Cauchy stress tensor for a mixture of a porous solid and interstitial fluid is given by

$$\boldsymbol{\sigma} = -p\mathbf{I} + \boldsymbol{\sigma}^e \,, \tag{2.9.1}$$

where p is he fluid pressure and $\boldsymbol{\sigma}^e$ is the stress in the solid matrix resulting from solid strain. When steady-state conditions are achieved, the fluid pressure p results exclusively from osmotic effects and ambient conditions (i.e., it does not depend on the loading history). Thus, in analogy to Eq.(2.6.11), $p = \tilde{p} + R\theta\Phi c$ where $\tilde{p}$ is the mechanical pressure resulting from ambient conditions and $R\theta\Phi c$ is the osmotic pressure resulting from the osmolarity c of the solution.

The osmotic pressure p may produce swelling of the solid matrix, which is opposed by the solid matrix stress. This becomes more apparent when considering, for example, the case of a traction-free body. The traction is given by $\mathbf{t} = \boldsymbol{\sigma} \cdot \mathbf{n}$, where $\mathbf{n}$ is the unit outward normal to the boundary. When $\mathbf{t} = \mathbf{0}$, the relation of Eq.(2.9.1) produces $p = \mathbf{n} \cdot \boldsymbol{\sigma}^e \cdot \mathbf{n}$, clearly showing that the osmotic pressure p is balanced by the swelling solid matrix.

The interstitial osmolarity (number of moles of solute per volume of interstitial fluid) may be related to the solute and solid content according to

$$c = \frac{c_r}{J - \varphi_r^s} \,, \tag{2.9.2}$$

where c_r is the number of moles of solute per volume of the mixture in the reference configuration, φ_r^s is the volume fraction of the solid in the reference configuration, and $J = \det \mathbf{F}$ is the volume ratio of the porous solid matrix. Neither c_r nor φ_r^s depend on the solid matrix deformation, thus Eq.(2.9.2) provides the explicit dependence of c on J. This relation shows that the osmolarity of the interstitial fluid is dependent on the relative change in volume of the solid matrix with deformation. Effectively, under equilibrium swelling conditions, the term $-p\mathbf{I}$ in Eq.(2.9.1) represents an elastic stress and may be treated in this manner when analyzing equilibrium swelling conditions.

Since p also depends on the osmotic coefficient, if we assume that Φ depends on the solid strain at most via a dependence on J, we may thus state generically that $p = p\,(J)$ under equilibrium swelling. It follows that the elasticity tensor for $\boldsymbol{\sigma}$ is

$$\boldsymbol{\mathcal{C}} = -\left(p + J\frac{dp}{dJ}\right)\mathbf{I}\otimes\mathbf{I} + 2p\mathbf{I}\,\overline{\otimes}\,\mathbf{I} + \boldsymbol{\mathcal{C}}^e \,, \tag{2.9.3}$$

where $\boldsymbol{\mathcal{C}}^e$ is the elasticity tensor of $\boldsymbol{\sigma}^e$.

2.9.1 Perfect Osmometer

Consider a porous medium with an interstitial fluid that consists of a solvent and one or more solutes, whose boundary is permeable to the solvent but not to the solutes (e.g., a biological cell).

Since solutes are trapped within such a medium, c_r is a constant in this type of problem. Since the boundary is permeable to the solvent, $\tilde{p}$ must be continuous across the boundary. Assuming ideal physicochemical conditions, $\Phi = 1$, and zero ambient pressure, this continuity requirement implies that $p = R\theta\,(c - c^*)$, where $c^*$is the osmolarity of the external environment. Using Eq.(2.9.2), it follows that

$$p = R\theta \left(\frac{c_r}{J - \varphi_r^s} - c^* \right) . \tag{2.9.4}$$

The reference configuration (the stress-free configuration of the solid) is achieved when $J = 1$ and $p = 0$, from which it follows that $c_r = (1 - \varphi_r^s)\, c_0^*$, where c_0^* is the value of c^* in the reference state. Therefore Eq.(2.9.4) may also be written as

$$p = R\theta c^* \left(\frac{1 - \varphi_r^s}{J - \varphi_r^s} \frac{c_0^*}{c^*} - 1 \right) , \tag{2.9.5}$$

and this expression may be substituted into Eq.(2.9.3) to evaluate the corresponding elasticity tensor.

A perfect osmometer is a porous material whose interstitial fluid behaves ideally and whose solid matrix exhibits negligible resistance to swelling ($\boldsymbol{\sigma}^e \approx \mathbf{0}$). In that case $p = 0$ and Eq.(2.9.5) may be rearranged to yield

$$J = (1 - \varphi_r^s)\, \frac{c_0^*}{c^*} + \varphi_r^s. \tag{2.9.6}$$

This equation is known as the Boyle-van't Hoff relation for a perfect osmometer. It predicts that variations in the relative volume of such as medium with changes in external osmolarity c^* is an affine function of c_0^*/c^*, with the intercept at the origin representing the solid volume fraction and the slope representing the fluid volume fraction, in the reference configuration.

FEBio implements the relation of Eq.(2.9.5) for the purpose of modeling equilibrium swelling even when solid matrix stresses are not negligible. The name "perfect osmometer" is adopted for this model because it reproduces the Boyle-van't Hoff response in the special case when $\boldsymbol{\sigma}^e = \mathbf{0}$.

2.9.2 Cell Growth

The growth of cells requires the active uptake of soluble mass to provide the building blocks for various intracellular structures, such as the cytoskeleton or chromosomes, and growth contributes to the osmolarity of the intracellular space. The resulting mechano-chemical gradient drives solvent into the cell as well, contributing to its volumetric growth.

Cell growth may be modeled using the "perfect osmometer" framework by simply increasing the mass of the intracellular solid matrix and membrane-impermeant solute. This is achieved by using Eq.(2.9.4) to model the osmotic pressure and allowing the parameters φ_r^s and c_r (normally constant) to increase over time as a result of growth. Since cell growth is often accompanied by cell division, and since daughter cells typically achieve the same solid and solute content as their parent, it may be convenient to assume that φ_r^s and c_r increase proportionally, though this is not an obligatory relationship. To ensure that the initial configuration is a stress-free reference configuration, let $c_r = (1 - \varphi_r^s)\, c^*$ in the initial state prior to growth.

2.9.3 Donnan Equilibrium Swelling

Consider a porous medium whose solid matrix holds a fixed electrical charge and whose interstitial fluid consists of a solvent and two monovalent counter-ions (such as Na^+ and Cl^-). The

boundaries of the medium are permeable to the solvent and ions. The fixed charge density is denoted by c^F; it is a measure of the number of fixed charges per volume of the interstitial fluid in the current configuration. This charge density may be either negative or positive, thereby producing an imbalance in the concentration of anions and cations in the interstitial fluid. To determine the osmolarity of the interstitial fluid, it is necessary to equate the mechano-chemical potential of the solvent and the mechano-electrochemical potential of the ions between the porous medium and its surrounding bath. When assuming ideal physicochemical behavior, the interstitial osmolarity (resulting from the interstitial ions) is given by

$$c = \sqrt{\left(c^F\right)^2 + \left(2c^*\right)^2}\,, \tag{2.9.7}$$

where c^* is the salt concentration in the bath. Alternatively, we note that the osmolarity of the bath is $\bar{c}^* = 2c^*$. Though this expression may be equated with Eq.(2.9.2), the resulting value of c_r is not constant in this case, since ions may transport into or out of the pore space; therefore that relation is not useful here.

However, since the number of charges fixed to the solid matrix is invariant, we may manipulate Eq.(2.9.2) to produce a relation between the fixed charge density in the current configuration, c^F, and the corresponding value in the reference configuration,c_r^F,

$$c^F = \frac{1-\varphi_r^s}{J-\varphi_r^s} c_r^F\,. \tag{2.9.8}$$

Now the osmotic pressure resulting from the difference in osmolarity between the porous medium and its surrounding bath is given by

$$p = R\theta\left(\sqrt{\left(\frac{1-\varphi_r^s}{J-\varphi_r^s}c_r^F\right)^2 + \left(\bar{c}^*\right)^2} - \bar{c}^*\right)\,. \tag{2.9.9}$$

This expression may be substituted into Eq.(2.9.3) to evaluate the corresponding elasticity tensor.

When the osmotic pressure results from an imbalance in osmolarity produced by a fixed charge density, it is called a Donnan osmotic pressure. The analysis associated with this relation is called Donnan equilibrium.

2.10 Chemical Reactions

Chemical reactions may be incorportated into a multiphasic mixture by adding a mass supply term to the equation of mass balance,

$$\frac{\partial \rho^\alpha}{\partial t} + \operatorname{div}\left(\rho^\alpha \mathbf{v}^\alpha\right) = \hat{\rho}^\alpha \,, \tag{2.10.1}$$

Where $\hat{\rho}^\alpha$ is the volume density of mass supply to α resulting from chemical reactions with all other mixture constitutents. Since mass must be conserved over all constituents, mass supply terms are constrained by

$$\sum_\alpha \hat{\rho}^\alpha = 0 \,. \tag{2.10.2}$$

In a mixture containing a solid constituent (denoted by $\alpha = s$), it is conveniemt to define the mixture domain (and thus the finite element mesh) on the solid and evaluate mass fluxes of constituents relative to the solid,

$$\mathbf{m}^\alpha = \rho^\alpha \left(\mathbf{v}^\alpha - \mathbf{v}^s\right) \,. \tag{2.10.3}$$

Substituting Eq.(2.10.3) into Eq.(2.10.1), the differential form of the mass balance may be rewritten as

$$\frac{D^s \rho_r^\alpha}{Dt} + J \operatorname{div} \mathbf{m}^\alpha = \hat{\rho}_r^\alpha \,, \tag{2.10.4}$$

Where $D^s\left(\cdot\right)/Dt$ represents the material time derivative in the spatial frame, following the solid, $J = \det \mathbf{F}$, where $\mathbf{F}$ is the deformation gradient of the solid matrix; ρ_r^α is the apparent density and $\hat{\rho}_r^\alpha$ is the volume density of mass supply to α normalized to the mixture volume in the reference configuration,

$$\rho_r^\alpha = J\rho^\alpha, \quad \hat{\rho}_r^\alpha = J\hat{\rho}^\alpha. \tag{2.10.5}$$

Since ρ_r^α is the mass of α in the current configuration per volume of the mixture in the reference configuration (an invariant quantity), this parameter represents a direct measure of the mass content of α in the mixture, which may thus be used as a state variable in a framework that accounts for chemical reactions. A distinction is now made between solid and solute species in the mixture, since they are often treated differential in an analysis.

2.10.1 Solid Matrix and Solid-Bound Molecular Constituents

For constituents constrained to move with the solid (denoted generically by $\alpha = \sigma$ and satisfying $\mathbf{v}^s = \mathbf{v}^\sigma$, $\forall\sigma$), the statement of mass balance in Eq.(2.10.4) reduces to the special form

$$D^s \rho_r^\sigma / Dt = \hat{\rho}_r^\sigma \,. \tag{2.10.6}$$

This representation makes it easy to see that alterations in ρ_r^σ can occur only as a result of chemical reactions (such as synthesis, degradation, or binding). In contrast, as seen in Eq.(2.10.4), alterations in ρ_r^α for solutes or solvent ($\alpha \neq \sigma$) may also occur as a result of mass transport into or out of the pore space of the solid matrix. Therefore, ρ_r^σ is the natural choice of state variable for describing the content of solid constituents in a reactive mixture.

When multiple solid species are present, the net solid mass content may be given by $\rho_r^s = \sum_\sigma \rho_r^\sigma$ whereas the net mass supply of solid is $\hat{\rho}_r^s = \sum_\sigma \hat{\rho}_r^\sigma$ such that $D^s \rho_r^s / Dt = \hat{\rho}_r^s$. The referential solid volume fraction, φ_r^s, may be evaluated from

$$\varphi_r^s = \varphi_0^s + \sum_\sigma \rho_r^\sigma / \rho_T^\sigma, \tag{2.10.7}$$

where ρ_T^σ is the true density of solid constituent σ (mass of σ per volume of σ) and φ_0^s is the referential solid volume fraction of solid constituents not explicitly modeled by solid-bound molecules (a user-defined parameter). According to Eq.(2.10.5), it follows that the solid volume fraction in the current configuration is given by $\varphi^s = \varphi_r^s/J$. Note that $0 \leqslant \varphi^s \leqslant 1$ under all circumstances, while $0 \leqslant \varphi_r^s \leqslant J$, implying that φ_r^s may exceed unity when solid growth occurs. In this study, it is assumed that all mixture constituents are intrinsically incompressible, implying that their true density is invariant.

The various constituents of the solid matrix may be electrically charged. Let z^σ be the charge number (equivalent charge per mole) of solid constituent σ, then the net referential fixed charge density of the solid matrix (equivalent charge per fluid volume in the referential configuration) is given by

$$c_r^F = \frac{1}{1-\varphi_r^s} \sum_\sigma \frac{z^\sigma \rho_r^\sigma}{M^\sigma} \,, \tag{2.10.8}$$

where M^σ is the molar mass of σ (an invariant quantity) and $1-\varphi_r^s$ represents the referential volume fraction of all fluid constituents (solvent + solutes) in a saturated mixture. Based on the kinematics of the continuum, the fixed charge density in the current configuration is

$$c^F = \frac{1-\varphi_r^s}{J-\varphi_r^s} c_r^F \,. \tag{2.10.9}$$

2.10.2 Solutes

Solutes are denoted generically by $\alpha = \iota$. In chemistry solute content is often represented in units of molar concentration (moles per fluid volume). It follows that solute molar concentration c^ι and molar supply $\hat{c}^\iota$ are related to ρ^ι and $\hat{\rho}^\iota$ via

$$c^\iota = \frac{\rho^\iota}{(1-\varphi^s)\, M^\iota}, \quad \hat{c}^\iota = \frac{\hat{\rho}^\iota}{(1-\varphi^s)\, M^\iota} \,. \tag{2.10.10}$$

The molar flux of constituent ι relative to the solid is given by

$$\mathbf{j}^\iota = (1-\varphi^s)\, c^\iota \left(\mathbf{v}^\iota - \mathbf{v}^s\right) \,, \tag{2.10.11}$$

where it may be noted that $\mathbf{m}^\iota = M^\iota \mathbf{j}^\iota$. Combining these relations with Eqs.(2.10.4)-(2.10.5) produces the desired form of the mass balance for the solutes,

$$\frac{1}{J} \frac{D^s \left[J\,(1-\varphi^s)\, c^\iota\right]}{Dt} + \mathrm{div}\mathbf{j}^\iota = (1-\varphi^s)\, \hat{c}^\iota \,. \tag{2.10.12}$$

This form is suitable for implementation in a finite element analysis where the mesh is defined on the solid matrix.

2.10.3 Mixture with Negligible Solute Volume Fraction

The volume fraction of each constituent is given by $\varphi^\alpha = \rho^\alpha/\rho_T^\alpha$. In a saturated mixture these volume fractions satisfy $\sum_\alpha \varphi^\alpha = 1$. Substituting $\rho^\alpha = \varphi^\alpha \rho_T^\alpha$ into Eq.(2.10.1), dividing across by ρ_T^α (invariant for intrinsically incompressible constituents), and taking the sum of the resulting expression over all constituents produces

$$\mathrm{div}\left(\sum_\alpha \varphi^\alpha \mathbf{v}^\alpha\right) = \sum_\alpha \frac{\hat{\rho}^\alpha}{\rho_T^\alpha} \,. \tag{2.10.13}$$

This mass balance relation for the mixture expresses the fact that the mixture volume will change as a result of chemical reactions where the true density of products is different from that of reactants. Indeed, assuming that ρ_T^α is the same for all α would nullify the right-hand-side of Eq.(2.10.13) based on Eq.(2.10.2). We now adopt the assumption that solutes occupy a negligible volume fraction of the mixture ($\varphi^\iota \ll 1$), from which it follows that $\varphi^s + \varphi^w \approx 1$ and $\sum_\alpha \varphi^\alpha \mathbf{v}^\alpha \approx \mathbf{v}^s + \mathbf{w}$, where $\mathbf{w} = \varphi^w (\mathbf{v}^w - \mathbf{v}^s)$ is the volumetrix flux of solvent relative to the solid. Thus, the mixture mass balance may be reduced to

$$\operatorname{div}(\mathbf{v}^s + \mathbf{w}) = \sum_\alpha \frac{\hat{\rho}^\alpha}{\rho_T^\alpha}. \tag{2.10.14}$$

In the special case of the solvent ($\alpha = w$), FEBio uses a solvent supply, $\hat{\varphi}^w = \hat{\rho}^w / \hat{\rho}_T^w$, which may be incorporated in Eq.(2.10.14) as

$$\operatorname{div}(\mathbf{v}^s + \mathbf{w}) = \hat{\varphi}^w + \sum_{\alpha \neq w} \frac{\hat{\rho}^\alpha}{\rho_T^\alpha}. \tag{2.10.15}$$

2.10.4 Chemical Kinetics

Productions rates are described by constitutive relations which are functions of the state variables. In a biological mixture under isothermal conditions, the minimum set of state variables needed to describe reactive mixtures that include a solid matrix are: the (uniform) temperature θ, the solid matrix deformation gradient $\mathbf{F}$ (or related strain measures), and the molar content c^α of the various constituents. This set differs from the classical treatment of chemical kinetics in fluid mixtures by the inclusion of $\mathbf{F}$ and the subset of constituents bound to the solid matrix. To maintain a consistent notation in this section, solid-bound molecular species are described by their molar concentrations and molar supplies which may be related to their referential mass density and referential mass supply according to

$$c^\sigma = \frac{\rho_r^\sigma}{(J - \varphi_r^s) M^\sigma}, \quad \hat{c}^\sigma = \frac{\hat{\rho}_r^\sigma}{(J - \varphi_r^s) M^\sigma}. \tag{2.10.16}$$

Consider a general chemical reaction,

$$\sum_\alpha \nu_R^\alpha \mathcal{E}^\alpha \rightarrow \sum_\alpha \nu_P^\alpha \mathcal{E}^\alpha, \tag{2.10.17}$$

where $\mathcal{E}^\alpha$ is the chemical species representing constituent α; ν_R^α and ν_P^α represent stoichiometric coefficients of the reactants and products, respectively. Since the molar supply of reactants and products is constrained by stoichiometry, it follows that all molar supplies $\hat{c}^\alpha$ in a specific chemical reaction may be related to a production rate $\hat{\zeta}$ according to

$$\hat{c}^\alpha = \nu^\alpha \hat{\zeta}, \tag{2.10.18}$$

where ν^α represents the net stoichiometric coefficient for $\mathcal{E}^\alpha$,

$$\nu^\alpha = \nu_P^\alpha - \nu_R^\alpha. \tag{2.10.19}$$

Thus, formulating constitutive relations for $\hat{c}^\alpha$ is equivalent to providing a single relation for $\hat{\zeta}(\theta, \mathbf{F}, c^\alpha)$. When the chemical reaction is reversible,

$$\sum_\alpha \nu_R^\alpha \mathcal{E}^\alpha \rightleftharpoons \sum_\alpha \nu_P^\alpha \mathcal{E}^\alpha, \tag{2.10.20}$$

the relations of Eqs.(2.10.18)-(2.10.19) still apply but the form of $\hat{\zeta}$ would be different.

Using the relations of Eqs.(2.10.10), (2.10.16) and (2.10.18), it follows in general that $\hat{\rho}^\alpha = (1-\varphi^s)\, M^\alpha \nu^\alpha \hat{\zeta}$, so that the constraint of Eq.(2.10.2) is equivalent to enforcing stoichiometry, namely,

$$\sum_\alpha \nu^\alpha M^\alpha = 0\,. \tag{2.10.21}$$

Thus, properly balancing a chemical reaction satisfies this constraint.

The mixture mass balance in Eq.(2.10.15) may now be rewritten as

$$\operatorname{div}\left(\mathbf{v}^s + \mathbf{w}^w\right) = \hat{\varphi}^w + (1-\varphi^s)\,\hat{\zeta}\overline{\mathcal{V}}\,, \tag{2.10.22}$$

where $\overline{\mathcal{V}} = \sum_{\alpha\neq w} \nu^\alpha \mathcal{V}^\alpha$ and $\mathcal{V}^\alpha = M^\alpha/\rho_T^\alpha$ is the molar volume of α. (Currently in FEBio, $\hat{\varphi}^w$ is specified independently of $\hat{\zeta}$, because users may choose to neglect the contribution from $\overline{\mathcal{V}}$ in Eq.(2.10.22); therefore, if one desires to model chemical reactions, Eq.(2.10.17) or Eq.(2.10.20), that involve the solvent, it is necessary to explicitly provide a solvent supply function compatible with the above relations, namely $\hat{\varphi}^w = (1-\varphi^s)\,\hat{\zeta}\nu^w\mathcal{V}^w$.) Similarly, the solute mass balance in Eq.(2.10.12) becomes

$$\frac{1}{J}\frac{D^s\left[J\,(1-\varphi^s)\,c^\iota\right]}{Dt} + \operatorname{div}\mathbf{j}^\iota = (1-\varphi^s)\,\nu^\iota\hat{\zeta}\,. \tag{2.10.23}$$

These mass balance equations reduce to those of non-reactive mixtures when $\hat{\zeta} = 0$.

2.11 Fluid Mechanics

2.11.1 Mass and Momentum Balance

In a spatial (Eulerian) frame, the momentum balance equation for a continuum is

$$\rho\mathbf{a} = \operatorname{div}\boldsymbol{\sigma} + \rho\mathbf{b}\,, \tag{2.11.1}$$

where ρ is the density, $\boldsymbol{\sigma}$ is the Cauchy stress, $\mathbf{b}$ is the body force per mass, and $\mathbf{a}$ is the acceleration, given by the material time derivative of the velocity $\mathbf{v}$ in the spatial frame,

$$\mathbf{a} = \dot{\mathbf{v}} = \frac{\partial\mathbf{v}}{\partial t} + \mathbf{L}\cdot\mathbf{v}\,, \tag{2.11.2}$$

where $\mathbf{L} = \operatorname{grad}\mathbf{v}$ is the spatial velocity gradient. The mass balance equation is

$$\dot{\rho} + \rho\operatorname{div}\mathbf{v} = 0\,, \tag{2.11.3}$$

where the material time derivative of the density in the spatial frame is

$$\dot{\rho} = \frac{\partial\rho}{\partial t} + \operatorname{grad}\rho\cdot\mathbf{v}\,. \tag{2.11.4}$$

Let $\mathbf{F}$ denote the deformation gradient (the gradient of the motion with respect to the material coordinate). The material time derivative of $\mathbf{F}$ is related to $\mathbf{L}$ via

$$\dot{\mathbf{F}} = \mathbf{L}\cdot\mathbf{F}\,. \tag{2.11.5}$$

Let $J = \det\mathbf{F}$ denote the Jacobian of the motion (the volume ratio, or ratio of current to referential volume, $J > 0$); then, the dilatation (relative change in volume between current and reference

configurations) is given by $e = J - 1$. Using the chain rule, J's material time derivative is $\dot{J} = J\mathbf{F}^{-T} : \dot{\mathbf{F}}$ which, when combined with Eq.(2.11.5), produces a kinematic constraint between $\dot{J}$ and $\operatorname{div}\mathbf{v}$,

$$\dot{J} = J \operatorname{div}\mathbf{v}\,. \tag{2.11.6}$$

Substituting this relation into the mass balance, eq.(2.11.3), produces $\overline{\dot{\rho J}} = 0$, which may be integrated directly to yield

$$\rho = \rho_r / J\,, \tag{2.11.7}$$

where ρ_r is the density in the reference configuration (when $J = 1$). Since ρ_r is obtained by integrating the above material time derivative of ρJ, it is an intrinsic material property that must be invariant in time and space.

The Cauchy stress is given by

$$\boldsymbol{\sigma} = -p\mathbf{I} + \boldsymbol{\tau}\,, \tag{2.11.8}$$

where $\mathbf{I}$ is the identity tensor, $\boldsymbol{\tau}$ is the viscous stress, p is the pressure arising from the elastic response,

$$p = -\frac{d\Psi_r(J)}{dJ}\,, \tag{2.11.9}$$

and Ψ_r is the free energy density of the fluid (free energy per volume of the continuum in the reference configuration). The axiom of entropy inequality dictates that Ψ_r cannot be a function of the rate of deformation $\mathbf{D} = \left(\mathbf{L} + \mathbf{L}^T\right)/2$. In contrast, the viscous stress $\boldsymbol{\tau}$ is generally a function of J and $\mathbf{D}$.

Boundary conditions may be derived by satisfying mass and momentum balance across a moving interface Γ. Let Γ divide the material domain V into subdomains V_+ and V_- and let the outward normal to V_+ on Γ be denoted by $\mathbf{n}$. The jump condition across Γ derived from the axiom of mass balance requires that

$$[[\rho\mathbf{u}_\Gamma]]\cdot\mathbf{n} = 0\,, \tag{2.11.10}$$

where $\mathbf{u}_\Gamma \equiv \mathbf{v} - \mathbf{v}_\Gamma$ on Γ and $\mathbf{v}_\Gamma$ is the velocity of the interface Γ. Thus, $\mathbf{u}_\Gamma$ represents the velocity of the fluid relative to Γ. The double bracket notation denotes $[[f]] = f_+ - f_-$, where f_+ and f_- represent the value of f on Γ in V_+ and V_-, respectively. This jump condition implies that the mass flux normal to Γ must be continuous. In particular, if V_+ is a fluid domain and V_- is a solid domain, and Γ denotes the solid boundary (e.g., a wall), we use $\rho_+ = \rho$, $\mathbf{v}_+ = \mathbf{v}$ for the fluid, and $\mathbf{v}_- = \mathbf{v}_\Gamma$ for the solid, such that Eq.(2.11.10) reduces to $\rho(\mathbf{v} - \mathbf{v}_\Gamma)\cdot\mathbf{n} = 0$. The jump condition derived from the axiom of linear momentum balance similarly requires that

$$[[\boldsymbol{\sigma} - \rho\mathbf{u}_\Gamma\otimes\mathbf{u}_\Gamma]]\cdot\mathbf{n} = \mathbf{0}\,. \tag{2.11.11}$$

This condition implies that the jump in the traction $\boldsymbol{\sigma}\cdot\mathbf{n}$ across Γ must be balanced by the jump in momentum flux normal to Γ. In addition to jump conditions dictated by axioms of conservation, viscous fluids require the satisfaction of the no-slip condition,

$$(\mathbf{I} - \mathbf{n}\otimes\mathbf{n})\cdot[[\mathbf{u}_\Gamma]] = \mathbf{0}\,, \tag{2.11.12}$$

which implies that the velocity component tangential to Γ is continuous across that interface.

In our finite element treatment we use $\mathbf{v}$ and J as nodal variables, implying that our formulation automatically enforces continuity of these variables across element boundaries, thus $[[\mathbf{v}]] = [[\mathbf{u}_\Gamma]] = \mathbf{0}$ and $[[J]] = 0$. Based on Eqs.(2.11.7) and (2.11.9), it follows that the density and elastic pressure are continuous across element boundaries in this formulation, $[[\rho]] = 0$ and $[[p]] = 0$. Thus, the mass jump in Eq.(2.11.10) is automatically satisfied, and the momentum jump in eq.(2.11.11) reduces to $[[\boldsymbol{\sigma}]]\cdot\mathbf{n} = \mathbf{0}$, requiring continuity of the traction, or more specifically according to (2.11.8), the continuity of the viscous traction $\boldsymbol{\tau}\cdot\mathbf{n}$, since p is automatically continuous.

2.11.2 Energy Balance

The energy balance for a continuum may be written in integral form over a control volume V as

$$\frac{d}{dt}\int_V \rho\left(\varepsilon+\frac{1}{2}\mathbf{v}\cdot\mathbf{v}\right)\,dV = -\int_S \rho\left(\varepsilon+\frac{1}{2}\mathbf{v}\cdot\mathbf{v}\right)(\mathbf{v}\cdot\mathbf{n})\,dS + \int_S \mathbf{t}\cdot\mathbf{v}\,dS + \int_V \rho\mathbf{b}\cdot\mathbf{v}\,dV \\ - \int_S \mathbf{q}\cdot\mathbf{n}\,dS + \int_V \rho r\,dV \quad , \tag{2.11.13}$$

where S is the control surface bounding V, ε is the specific internal energy, $\mathbf{q}$ is the heat flux across S, and r is the heat supply per mass to the material in V resulting from other sources. Bringing the time derivative inside the integral on the left-hand-side, and using the divergence theorem, this integral statement of the energy balance may be written as

$$\int_V \left[\rho\left(\dot{\varepsilon}+\mathbf{v}\cdot\mathbf{a}\right)+\rho\left(\varepsilon+\frac{1}{2}\mathbf{v}\cdot\mathbf{v}\right)\left(\operatorname{div}\mathbf{v}-\frac{\dot{J}}{J}\right)\right]\,dV \\ = \int_V \left[\boldsymbol{\sigma}:\mathbf{D}-\operatorname{div}\mathbf{q}+\rho r+\mathbf{v}\cdot\left(\operatorname{div}\boldsymbol{\sigma}+\rho\mathbf{b}\right)\right]\,dV \quad . \tag{2.11.14}$$

This statement must be valid for arbitrary control volumes and arbitrary processes, from which we conventionally derive the differential form of the axioms of mass, momentum and energy balance.

For the specialized conditions of a viscous fluid at constant temperature assumed in our treatment, the only state variables for the functions of state ε, $\boldsymbol{\sigma}$ and $\mathbf{q}$ are J and $\mathbf{D}$ (i.e., the temperature is not a state variable since it is assumed constant). Under these conditions the entropy inequality shows that the specific entropy η and the heat flux $\mathbf{q}$ must be zero, and the Cauchy stress $\boldsymbol{\sigma}$ must have the form of Eq.(2.11.8) where p is given by Eq.(2.11.9) as a function of J only, leaving the residual dissipation statement $\boldsymbol{\tau}:\mathbf{D}\geq 0$ as a constraint that must be satisfied by constitutive relations for $\boldsymbol{\tau}$. (For a Newtonian fluid, this constraint is satisfied when the viscosities μ and κ are positive.) From these thermodynamic restrictions we conclude that $\varepsilon=\psi$, where ψ is the specific (Helmholtz) free energy, with $\Psi_r=\rho_r\psi$.

For the conditions adopted here (isothermal viscous fluid), the axiom of energy balance reduces to $\rho\dot{\psi}=\boldsymbol{\sigma}:\mathbf{D}+\rho r$; since ψ is only a function of J, this expression may be further simplified using Eqs.(2.11.6)-(2.11.9) to produce $\boldsymbol{\tau}:\mathbf{D}+\rho r=0$. In other words, isothermal conditions may be maintained only if heat dissipated by the viscous stress is emitted in the form of a heat supply density $\rho r=-\boldsymbol{\tau}:\mathbf{D}$ (heat leaving the system). Now, the integral form of the energy balance in Eq.(2.11.14) simplifies to

$$\int_V \left[\mathbf{v}\cdot\left(\operatorname{div}\boldsymbol{\sigma}+\rho\left(\mathbf{b}-\mathbf{a}\right)\right)+\rho\left(\psi+\frac{1}{2}\mathbf{v}\cdot\mathbf{v}\right)\left(\frac{\dot{J}}{J}-\operatorname{div}\mathbf{v}\right)\right]\,dV=0\,. \tag{2.11.15}$$

A comparison of this statement with the statement of virtual work, presented below in Eq.(3.5.1), establishes a clear correspondence between the virtual velocity $\delta\mathbf{v}$ and $\mathbf{v}$, and between the virtual energy density δJ and $\rho\left(\psi+\frac{1}{2}\mathbf{v}\cdot\mathbf{v}\right)$, with the latter representing the sum of the internal (free) and kinetic energy densities.

2.12 Fluid-Structure Interactions

We model the fluid domain in an FSI analysis as a mixture of an isothermal compressible viscous fluid and a hyperelastic compressible solid, where the solid has zero apparent density, and

negligible (but non-zero) elasticity [90]. In a mixture framework, all mixture constituents coexist at every point in the continuum. For our FSI implementation, the finite element mesh is defined on the solid material, and the negligible (but non-zero) elasticity of the solid is intended to regularize the mesh deformation. The fluid flows through this mesh, unimpeded by the solid. In particular, in this FSI model there is no frictional interaction between the fluid and solid materials inside the mixture domain (i.e., no Darcy-Brinkman type of friction), but the no-slip boundary condition may be prescribed on boundaries of the mixture domain, where applicable.

2.12.1 FSI Governing Equations

The momentum balance for the fluid is

$$\rho^f \mathbf{a}^f = \operatorname{div} \boldsymbol{\sigma}^f + \rho^f \mathbf{b} \,, \tag{2.12.1}$$

where $\mathbf{b}$ is the external body force acting on the FSI domain, $\mathbf{a}^f$ is the fluid acceleration,

$$\mathbf{a}^f = \frac{\partial \mathbf{v}^f}{\partial t} + \mathbf{L}^f \cdot \mathbf{v}^f \,, \tag{2.12.2}$$

and $\mathbf{L}^f = \operatorname{grad} \mathbf{v}^f$ is the fluid velocity gradient. In principle, the same momentum equation may be used for the solid (substituting f with s); however, since we opted to let $\rho^s = 0$ (no solid mass), the momentum balance for the solid simply reduces to

$$\operatorname{div} \boldsymbol{\sigma}^s = \mathbf{0} \,. \tag{2.12.3}$$

We model the fluid as isothermal and compressible, consistent with our CFD implementation. Thus, the fluid stress may be separated into the elastic pressure $p\left(J^f\right)$, which only depends on the fluid volume ratio J^f, and the viscous stress $\boldsymbol{\tau}\left(J^f, \mathbf{L}^f\right)$, as

$$\boldsymbol{\sigma}^f = -p\mathbf{I} + \boldsymbol{\tau} \,. \tag{2.12.4}$$

Recall that there is no dependence on temperature in an isothermal formulation. As done in our previous study, we integrate the mass balance for the fluid to produce

$$\rho^f = \frac{\rho_r^f}{J^f} \,, \tag{2.12.5}$$

where ρ_r^f is the fluid density in the reference state (e.g., under ambient pressure) and $J^f = \det \mathbf{F}^f$, where $\mathbf{F}^f$ is the fluid deformation gradient. We also use the kinematic constraint

$$\frac{\partial J^f}{\partial t} + \operatorname{grad} J^f \cdot \mathbf{v}^f = J^f \operatorname{div} \mathbf{v}^f \,, \tag{2.12.6}$$

to relate the fluid volume ratio J^f to its velocity $\mathbf{v}^f$, in the spatial frame.

The mesh through which the fluid flows is defined on the solid component of the mixture. Therefore, we define the relative velocity between the fluid and solid as

$$\mathbf{w} = \mathbf{v}^f - \mathbf{v}^s \,. \tag{2.12.7}$$

Since the solid has zero volume fraction, this expression is the same as the flux of fluid relative to the solid. We choose to define the nodal degrees of freedom in the mixture domain to be the

relative fluid velocity $\mathbf{w}$, the fluid dilatation $e^f = J^f - 1$, and the solid displacement $\mathbf{u}^s$, which is related to the solid velocity via $\mathbf{v}^s = \dot{\mathbf{u}}^s$, with the dot operator denoting the material time derivative following the solid. (For notational convenience, we will continue using J^f in the equations below, instead of e^f). Now,

$$\mathbf{v}^f = \mathbf{w} + \mathbf{v}^s \,, \tag{2.12.8}$$

from which it follows that the fluid velocity gradient is

$$\mathbf{L}^f = \mathbf{L}^w + \mathbf{L}^s \,, \tag{2.12.9}$$

where $\mathbf{L}^w = \operatorname{grad} \mathbf{w}$ and $\mathbf{L}^s = \operatorname{grad} \mathbf{v}^s$. The fluid acceleration may now be rewritten in terms of the FEA degrees of freedom as

$$\mathbf{a}^f = \dot{\mathbf{w}} + \dot{\mathbf{v}}^s + (\mathbf{L}^w + \mathbf{L}^s) \cdot \mathbf{w} \,, \tag{2.12.10}$$

where

$$\begin{aligned} \dot{\mathbf{v}}^s &= \frac{\partial \mathbf{v}^s}{\partial t} + \mathbf{L}^s \cdot \mathbf{v}^s \\ \dot{\mathbf{w}} &= \frac{\partial \mathbf{w}}{\partial t} + \mathbf{L}^w \cdot \mathbf{v}^s \end{aligned} \tag{2.12.11}$$

are the material time derivatives of the solid and relative fluid velocities, in the frame following the solid. We conveniently use this material time derivative (instead of the material time derivative following the fluid) since we define the mixture domain mesh on the solid.

Similarly, the kinematic constraint relating J^f and $\mathbf{v}^f$ may be rewritten as

$$\dot{J}^f + \operatorname{grad} J^f \cdot \mathbf{w} = J^f \operatorname{div} (\mathbf{w} + \mathbf{v}^s) \,, \tag{2.12.12}$$

where

$$\dot{J}^f = \frac{\partial J^f}{\partial t} + \operatorname{grad} J^f \cdot \mathbf{v}^s \,. \tag{2.12.13}$$

Finally, as done routinely in our studies of biphasic and multiphasic materials, we find it convenient to substitute the kinematic identity

$$\operatorname{div} \mathbf{v}^s = \frac{\dot{J}^s}{J^s} \,, \tag{2.12.14}$$

where $J^s = \det \mathbf{F}^s$ and $\mathbf{F}^s = \mathbf{I} + \operatorname{Grad} \mathbf{u}^s$ is the solid deformation gradient.

In summary, the governing equations for the FSI mixture domain are

$$\begin{aligned} &\operatorname{div} \boldsymbol{\sigma}^s = \mathbf{0} \\ &\rho^f \mathbf{a}^f = \operatorname{div} \boldsymbol{\sigma}^f + \rho^f \mathbf{b} \\ &\frac{1}{J^f} \left(\dot{J}^f + \operatorname{grad} J^f \cdot \mathbf{w} \right) = \operatorname{div} \mathbf{w} + \frac{\dot{J}^s}{J^s} \end{aligned} \tag{2.12.15}$$

where $\mathbf{a}^f$ is given in Eq.(2.12.10) above.

2.13 Hybrid Biphasic Material

In FEBio, the standard biphasic material consists of a mixture of intrinsically incompressible solid and fluid constituents, as described in Section 2.5. In this standard material, the solid and fluid dynamics are neglected, as well as the fluid viscosity. When a user wishes to consider these dynamics effects, as well as fluid viscosity, they may use a hybrid biphasic material, as described

in this section. The complete theoretical framework for such materials can be found in [89]. A hybrid biphasic domain is a mixture of an isothermal compressible viscous fluid and a hyperelastic compressible porous solid whose solid skeleton is intrinsically incompressible. Unlike the fluid-FSI material, here the solid has non-negligible mass density and elasticity, and frictional interactions may occur between the fluid and solid constituents, modeled using a hydraulic permeability (Section 5.9). In FEBio, the hybrid biphasic material is called "biphasic-FSI", since it allows dynamic fluid-structure interactions between this material and a fluid-FSI material, or a solid material. Here, we may abbreviate "biphasic-FSI" as BFSI. For BFSI domains, as with standard biphasic domains, the finite element mesh is defined on the porous solid material. The viscous fluid flows through this mesh, experiencing frictional drag caused by the porous solid. When two BFSI domains are interfaced, or when a BFSI domain is interfaced with a fluid-FSI domain, the pseudo-no slip condition [53] is enforced automatically on those interfaces. When a BFSI domain interfaces with a solid domain, the no-slip boundary condition has to be prescribed explicitly on those interfaces, where applicable.

2.13.1 BFSI Governing Equations

We model the BFSI domain as an unconstrained mixture of an isothermal, compressible, and viscous fluid and an isothermal, deformable porous solid whose skeleton material is intrinsically incompressible. As usual in mixture theory, each constituent α ($\alpha = s, f$ for solid and fluid, respectively) has its own apparent density $\rho^\alpha = dm^\alpha/dV$, which represents the ratio of the elemental mass dm^α of constituent α in the elemental mixture volume dV. This apparent density is related to the true density $\rho^\alpha_T = dm^\alpha/dV^\alpha$ (mass of α per volume of α) via $\rho^\alpha = \varphi^\alpha \rho^\alpha_T$, where $\varphi^\alpha = dV^\alpha/dV$ is the volume fraction of α in the mixture, satisfying $\varphi^s + \varphi^f = 1$. Since the solid skeleton is intrinsically incompressible, ρ^s_T is constant. The boundaries of a biphasic domain are defined on the porous solid matrix. The deformation gradient of the solid is denoted by $\mathbf{F}^s$ and its determinant, $J^s = \det \mathbf{F}^s = dV/dV_r$, represents the ratio of the mixture elemental volumes in the current (dV) and reference (dV_r) configurations. Thus, since the solid skeleton is intrinsically incompressible, J^s purely represents the compressibility of the pore volume as fluid enters or leaves the pore space, or as the compressible fluid within the pores changes in volume. The axiom of mass balance for the solid may be integrated in closed form to produce $\rho^s = \rho^s_r/J^s$, where $\rho^s_r = dm^s/dV_r$ is the solid apparent density in the mixture reference configuration. Therefore, we may define the referential solid volume fraction as $\varphi^s_r = \rho^s_r/\rho^s_T$. In the finite element analysis, $\varphi^s_r = dV^s/dV_r$ and ρ^s_T are both specified by the user, then ρ^s_r, ρ^s, φ^s and φ^f are evaluated from the above relations, given a solution for $\mathbf{F}^s$ (and thus, J^s). The solution for $\mathbf{F}^s = \mathbf{I} + \mathrm{Grad}\,\mathbf{u}$ is obtained by solving for the nodal solid displacement vector $\mathbf{u}$, where $\mathrm{Grad}\,(\cdot)$ represents the gradient operator in the material frame.

For the compressible fluid phase of a hybrid biphasic material, the true density ρ^f_T varies with the intrinsic fluid volumetric strain, or dilatation, $e^f = J^f - 1$, where J^f is the volume ratio of the fluid in its current and reference configurations, dm^f is the element mass of fluid and dV^f is the elemental volume of that fluid in the pores of the mixture, in the current configuration. It follows from this definition that

$$J^f = \frac{dV^f}{dV^f_r} = \frac{dV^f}{dm^f}\frac{dm^f}{dV^f_r} = \frac{\rho^f_{Tr}}{\rho^f_T}\,, \tag{2.13.1}$$

where dV^f_r is the elemental volume of this same fluid (having the same elemental mass dm^f) in the fluid's reference configuration. Thus, $\rho^f_{Tr} = dm^f/dV^f_r$ is a constant representing the true fluid density in its reference configuration, which is specified by the user. Accordingly, $J^f = 1$ in the limit when the fluid is idealized to be intrinsically incompressible. This definition of J^f is consistent

with that for a pure fluid, as shown in our earlier formulation of computational fluid dynamics [**?**]. As shown above, ρ^f may be evaluated as $\varphi^f \rho^f_T$, which now expands into an expression involving solid and fluid volume ratios,

$$\rho^f = \left(1 - \frac{\varphi^s_r}{J^s}\right) \frac{\rho^f_{Tr}}{J^f} \,. \tag{2.13.2}$$

The limiting case when the fluid within the solid matrix pores has been completely squeezed out corresponds to $\rho^f = 0$ (or $dm^f = 0$). Based on the above relation, this is equivalent to having the entire mixture volume dV reduce to the solid volume dV^s in the current configuration, or equivalently $J^s = \varphi^s_r$ [9]. In this limiting case, the mixture becomes an intrinsically incompressible solid and the finite element formulation presented in this study no longer applies.

We assume that $\mathbf{F}^s = \mathbf{I}$ (or equivalently, $\mathbf{u} = \mathbf{0}$) and $e^f = 0$ at the start of a finite element analysis. The fluid dilatation e^f is included as a nodal degree of freedom, implying that it is continuous across finite element boundaries. This assumption is verified below, when we review the jump conditions on axioms of mass, momentum and energy balance across interfaces.

Since the axiom of mass balance for the solid has already been solved in closed form, we only need to be concerned with the axiom of mass balance for the fluid, or alternatively, that of the mixture, which takes the form

$$\frac{D^f J^f}{Dt} = \frac{J^f}{\varphi^f} \operatorname{div}\left(\mathbf{v}^s + \mathbf{w}\right) \,, \tag{2.13.3}$$

where $\mathbf{v}^s$ is the solid velocity (the material time derivative of the solid displacement $\mathbf{u}$), and

$$\mathbf{w} = \varphi^f \left(\mathbf{v}^f - \mathbf{v}^s\right) \tag{2.13.4}$$

is the volumetric flux of the fluid relative to the solid , with $\mathbf{v}^f$ representing the fluid velocity. Here, $D^f(\cdot)/Dt$ is the material time derivative operator in the spatial frame, following the fluid motion. Since the finite element mesh is defined on the porous solid matrix of a biphasic mixture, and since the fluid flows relative to the solid, material time derivatives need to follow the solid motion in the finite element implementation. A similar scheme was used in our implementations of solute transport within deformable porous domains (Sections 2.7), to account for the motion of solutes relative to the porous solid matrix, as well as in our FSI formulation (Section 2.12) [10**? ?**]. Thus, we substitute the following identity,

$$\begin{aligned} \frac{D^f J^f}{Dt} &= \frac{\partial J^f}{\partial t} + \operatorname{grad} J^f \cdot \mathbf{v}^f \\ &= \frac{D^s J^f}{Dt} + \operatorname{grad} J^f \cdot \left(\mathbf{v}^f - \mathbf{v}^s\right) \end{aligned} \,, \tag{2.13.5}$$

into the axiom of mixture mass balance in (2.13.3) to produce the final form

$$\dot{J}^f + \frac{1}{\varphi^f} \operatorname{grad} J^f \cdot \mathbf{w} = \frac{J^f}{\varphi^f} \operatorname{div}\left(\mathbf{v}^s + \mathbf{w}\right) \,. \tag{2.13.6}$$

In this expression, the dot operator in $\dot{J}^f$ represents the material time derivative following the solid motion. In the solid material frame, this material time derivative reduces to the partial time derivative. Accordingly, we may now write $\mathbf{v}^s = \dot{\mathbf{u}}$. In the BFSI implementation, the fluid volumetric flux $\mathbf{w}$ relative to the solid is added to the list of nodal DOFs, giving us the complete set $\left(\mathbf{u}, \mathbf{w}, e^f\right)$. This choice implies that $\mathbf{w}$ is continuous across finite element boundaries, as justified further below when we review jump conditions across interfaces.

Based on the constitutive assumptions of our hybrid biphasic formulation [89], the momentum balance equations for the fluid and solid constituents reduce to

$$\rho^f \mathbf{a}^f = -\varphi^f \operatorname{grad} p + \operatorname{div} \boldsymbol{\tau}^f + \rho^f \mathbf{b}^f - \varphi^f \mathbf{k}^{-1} \cdot \mathbf{w} \,, \tag{2.13.7}$$

and

$$\rho^s \mathbf{a}^s = -\varphi^s \operatorname{grad} p + \operatorname{div} \boldsymbol{\sigma}^e + \rho^s \mathbf{b}^s + \varphi^f \mathbf{k}^{-1} \cdot \mathbf{w} \,, \tag{2.13.8}$$

where $\mathbf{a}^\alpha = D^\alpha \mathbf{v}^\alpha / Dt$ is the acceleration, $\mathbf{b}^\alpha$ is the body force per mass acting on constituent α, p is the fluid pressure, $\boldsymbol{\tau}^f$ is the apparent fluid viscous stress, and $\boldsymbol{\sigma}^e$ is the apparent solid elastic stress. These stress tensors are called apparent because their associated traction vectors represent a force acting on constituent α per elemental *mixture* area. Here, $\mathbf{k}$ is the hydraulic permeability tensor which regulates frictional drag between the fluid and solid constituents; setting $\mathbf{k}^{-1}$ to $\mathbf{0}$ implies that this frictional drag is non-existent. Since the fluid is compressible, its pressure must be given by a function of state. In the isothermal framework used here, this function only depends on e^f, and the form adopted in FEBio is

$$p = -K e^f \,, \tag{2.13.9}$$

where K is the fluid bulk modulus (a user-specified material property). In the limit when inertia and body forces are neglected ($\mathbf{a}^f = \mathbf{b}^f = \mathbf{0}$), the fluid momentum balance (2.13.7) produces the classical Darcy-Brinkman relation [**?**]. If the fluid viscous stress is also neglected ($\boldsymbol{\tau}^f = \mathbf{0}$), we recover Darcy's law, $\mathbf{w} = -\mathbf{k} \cdot \operatorname{grad} p$.

Since the finite element implementation requires all material time derivatives to follow the motion of the solid, we recognize that $\mathbf{a}^s = \ddot{\mathbf{u}}$ and we evaluate the fluid acceleration as $\mathbf{a}^f = \dot{\mathbf{v}}^f + \operatorname{grad} \mathbf{v}^f \cdot \left(\mathbf{v}^f - \mathbf{v}^s\right)$. However, since $\mathbf{v}^f$ is not a nodal degree of freedom, we use Eq.(2.13.4) to substitute

$$\mathbf{v}^f = \frac{1}{\varphi^f} \mathbf{w} + \mathbf{v}^s \tag{2.13.10}$$

into this expression. It follows that the fluid velocity gradient $\mathbf{L}^f = \operatorname{grad} \mathbf{v}^f$ may be evaluated as

$$\mathbf{L}^f = \mathbf{L}^s + \frac{1}{\varphi^f} \left(\mathbf{L}^w - \frac{1}{\varphi^f} \mathbf{w} \otimes \operatorname{grad} \varphi^f \right) \,, \tag{2.13.11}$$

where $\mathbf{L}^w = \operatorname{grad} \mathbf{w}$ and $\mathbf{L}^s = \operatorname{grad} \mathbf{v}^s$. Now, the fluid acceleration takes the form

$$\mathbf{a}^f = \frac{1}{\varphi^f} \left(\dot{\mathbf{w}} + \phi^f \ddot{\mathbf{u}} - \frac{\varphi^s}{\varphi^f} \frac{\dot{J}^s}{J^s} \mathbf{w} + \mathbf{L}^f \cdot \mathbf{w} \right) \,. \tag{2.13.12}$$

2.13.2 BFSI Continuous Variables

Jump conditions on the axioms of mass, momentum and energy balance are needed to determine which variables may be selected as nodal DOFs in the finite element implementation, and which tractions are naturally continuous across an interface. The full set of jump conditions for a hybrid biphasic material were derived in our recent study for the constitutive assumptions adopted in this formulation [89]. Here, we summarize the salient results, which apply to an interface defined on the porous solid matrix of the hybrid biphasic domain, which includes the shared faces of adjoining biphasic elements. Thus, the velocity of the interface is given by the velocity $\mathbf{v}^s$ of the solid constituent of the hybrid biphasic material. We employ the notation $[[f]] = f_+ - f_-$ to denote the jump in the function f across the interface Γ, with f_+ and f_- denoting the values of f on either

side of Γ. The unit normal on Γ is $\mathbf{n}$, which points away from the $+$ side. A variable f which is continuous across Γ satisfies $[[f]] = 0$.

Based on the jump condition on the axiom of mass balance, the normal component of the mass flux of the fluid relative to the solid is continuous across Γ, $\left[\left[\rho_T^f \mathbf{w}\right]\right] \cdot \mathbf{n} = 0$. Furthermore, a sufficient condition to satisfy the jump on the axiom of energy balance is to enforce continuity of the fluid specific free enthalpy (also known as the Gibbs function), $\left[\left[\psi^f + p/\rho_T^f\right]\right] = 0$, where ψ^f is the fluid specific free energy. This jump condition applies only when there is fluid on both sides of the interface Γ. In an isothermal framework the specific free enthalpy is a function of state that only depends on J^f, therefore this energy jump condition implies that J^f must be continuous across Γ, thus

$$\left[\left[J^f\right]\right] = 0\,, \tag{2.13.13}$$

also implying that $[[p]] = 0$. Given Eq.(2.13.1), it follows that $\left[\left[\rho_T^f\right]\right] = 0$ and the mass balance jump condition reduces to $[[\mathbf{w}]] \cdot \mathbf{n} = 0$, implying that the relative fluid flux component normal to Γ must be continuous. For the tangential component of $\mathbf{w}$ on Γ we appeal to the analysis of Hou et al. [**?**], who showed that a valid pseudo-noslip condition requires this tangential component to be continuous. Combining these two jump conditions produces

$$[[\mathbf{w}]] = 0\,. \tag{2.13.14}$$

The momentum jump condition requires that the mixture traction be continuous across Γ, thus $\left[\left[-p\mathbf{I} + \boldsymbol{\sigma}^e + \boldsymbol{\tau}^f\right]\right] \cdot \mathbf{n} = \mathbf{0}$. Since $[[p]] = 0$ based on the energy jump, this mixture momentum jump condition reduces to

$$\left[\left[\boldsymbol{\sigma}^e + \boldsymbol{\tau}^f\right]\right] \cdot \mathbf{n} = 0\,. \tag{2.13.15}$$

Finally, another relation which is sufficient to satisfy the jump condition on the energy balance is the continuity of the true fluid traction (force acting on fluid per fluid area),

$$\left[\left[\frac{\boldsymbol{\tau}^f}{\varphi^f}\right]\right] \cdot \mathbf{n} = 0\,. \tag{2.13.16}$$

This jump condition Eq.(2.13.16), which also applies only if fluid is present on both sides of Γ, is interesting because it implies that the viscous stress (and thus, the viscosity) of a fluid flowing in a porous solid matrix scales with the porosity of that medium, such that $\boldsymbol{\tau}^f = \phi^f \boldsymbol{\tau}$ where $\boldsymbol{\tau}$ would be the true fluid viscous stress. Thus, we can use FEBio's various constitutive relations for the viscous stress $\boldsymbol{\tau}$ of Newtonian or non-Newtonian fluids and adapt those models to a biphasic mixture where $\boldsymbol{\tau}^f$ is evaluated as $\varphi^f \boldsymbol{\tau}$. Accordingly, the contribution of $\boldsymbol{\tau}^f$ would properly reduce to zero in the limit as fluid content reduces to zero ($\varphi^f \to 0$), in which case the mixture momentum jump in Eq.(2.13.15) would reduce to $[[-p\mathbf{I} + \boldsymbol{\sigma}^e]] \cdot \mathbf{n} = [[\boldsymbol{\sigma}^e]] \cdot \mathbf{n} = 0$, since $[[p]] = 0$.

Letting $\mathbf{w}$ and J^f be nodal DOFs automatically enforces the jump conditions Eq.(2.13.13) and Eq.(2.13.14), acting as essential boundary conditions, along with the solid displacement $\mathbf{u}$. Finally, subtracting Eq.(2.13.16) from Eq.(2.13.15), we obtain the momentum jump condition for the solid constituent,

$$\left[\left[-\frac{\varphi^s}{\varphi^f}\boldsymbol{\tau}^f + \boldsymbol{\sigma}^e\right]\right] \cdot \mathbf{n} = 0\,. \tag{2.13.17}$$

A BFSI domain may be reduced to a FSI domain by letting $\varphi_r^s \to 0$ and $\mathbf{k}^{-1} \to \mathbf{0}$; the solid matrix would still be ascribed a material response but its stiffness would need to be negligible.

The number of nodal DOFs would remain the same. The CFD domain is a special case of the FSI domain where the mesh displacement is uniformly $\mathbf{u} = \mathbf{0}$.

However, when the biphasic domain interfaces with a non-porous solid domain across Γ^{bs}, the jump conditions Eq.(2.13.13) on J^f and Eq.(2.13.17) on $\boldsymbol{\tau}^f$ don't apply. In that case, the jump condition Eq.(2.13.14) on the relative fluid volumetric flux should reduce to $\mathbf{w} = \mathbf{0}$ for the BFSI domain on Γ^{bs}, although the user would have to enforce this no-slip condition explicitly by prescribing it as an essential boundary condition. The mixture momentum jump $\left[\left[-p\mathbf{I} + \boldsymbol{\sigma}^e + \boldsymbol{\tau}^f\right]\right] \cdot \mathbf{n} = \mathbf{0}$ implies that the mixture traction on the BFSI side of an interface with a solid is equal to the solid traction on the solid side. This jump condition would also need to be enforced explicitly.

Chapter 3

The Nonlinear FE Method

This chapter discusses the basic principles of the nonlinear finite element method. The chapter begins with a short introduction to the weak formulation and the principle of virtual work. Next, the important concept of linearization is discussed and applied to the principle of virtual work. Finally the Newton-Raphson procedure and its application to the nonlinear finite element method are described.

3.1 Weak formulation for Solid Materials

Generally, the finite element formulation is established in terms of a weak form of the differential equations under consideration. In the context of solid mechanics this implies the use of the virtual work equation:

$$\delta W = \int_v \boldsymbol{\sigma} : \delta \mathbf{d}\, dv - \int_v \mathbf{f} \cdot \delta \mathbf{v}\, dv - \int_{\partial v} \mathbf{t} \cdot \delta \mathbf{v}\, da = 0\,. \tag{3.1.1}$$

Here, $\delta \mathbf{v}$ is a virtual velocity and $\delta \mathbf{d}$ is the virtual rate of deformation tensor. This equation is known as the *spatial virtual work equation* since it is formulated using spatial quantities only. We can also define the *material virtual work equation* by expressing the principle of virtual work using only material quantities.

$$\delta W = \int_V \mathbf{S} : \delta \dot{\mathbf{E}}\, dV - \int_V \mathbf{f}_0 \cdot \delta \mathbf{v}\, dV - \int_{\partial V} \mathbf{t}_0 \cdot \delta \mathbf{v}\, dA = 0\,. \tag{3.1.2}$$

Here, $\mathbf{f}_0 = J\mathbf{f}$ is the body force per unit undeformed volume and $\mathbf{t}_0 = \mathbf{t}\,(da/dA)$ is the traction vector per unit initial area.

3.1.1 Linearization

Equation (3.1.1) is the starting point for the nonlinear finite element method. It is highly nonlinear and any method attempting to solve this equation, such as the Newton-Raphson method, necessarily has to be iterative.

To linearize the finite element equations, the directional derivative of the virtual work in Eq.(3.1.1) must be calculated. In an iterative procedure, the quantity $\boldsymbol{\phi}$ will be approximated by a trial solution $\boldsymbol{\phi}_k$. Linearization of the virtual work equation around this trial solution gives

$$\delta W\,(\boldsymbol{\phi}_k, \delta \mathbf{v}) + D\delta W\,(\boldsymbol{\phi}_k, \delta \mathbf{v})\,[\mathbf{u}] = 0\,. \tag{3.1.3}$$

The directional derivative of the virtual work will eventually lead to the definition of the stiffness matrix. In order to proceed, it is convenient to split the virtual work into an internal and external virtual work component:

$$D\delta W\left(\boldsymbol{\phi},\delta\mathbf{v}\right)\left[\mathbf{u}\right]=D\delta W_{int}\left(\boldsymbol{\phi},\delta\mathbf{v}\right)\left[\mathbf{u}\right]-D\delta W_{ext}\left(\boldsymbol{\phi},\delta\mathbf{v}\right)\left[\mathbf{u}\right], \tag{3.1.4}$$

where

$$\delta W_{int}\left(\boldsymbol{\phi},\delta\mathbf{v}\right)=\int_{v}\boldsymbol{\sigma}:\delta\mathbf{d}\,dv\,, \tag{3.1.5}$$

and

$$\delta W_{ext}\left(\boldsymbol{\phi},\delta\mathbf{v}\right)=\int_{v}\mathbf{f}\cdot\delta\mathbf{v}\,dv+\int_{\partial v}\mathbf{t}\cdot\delta\mathbf{v}\,da\,. \tag{3.1.6}$$

The result is listed here without details of the derivation – see [27] for details. The linearization of the internal virtual work is given by

$$D\delta W_{int}\left(\boldsymbol{\phi},\delta\mathbf{v}\right)\left[\mathbf{u}\right]=\int_{v}\delta\mathbf{d}:\boldsymbol{\mathcal{C}}:\boldsymbol{\varepsilon}\,dv+\int_{v}\boldsymbol{\sigma}:\left[\left(\nabla\mathbf{u}\right)^{T}\cdot\nabla\delta\mathbf{v}\right]\,dv\,. \tag{3.1.7}$$

Notice that this equation is symmetric in $\delta\mathbf{v}$ and $\mathbf{u}$. This symmetry will, upon discretization, yield a symmetric tangent matrix.

The external virtual work has contributions from both body forces and surface tractions. The precise form of the linearized external virtual work depends on the form of these forces. For surface tractions, normal pressure forces may be represented in FEBio. The linearized external work for this type of traction is given by

$$\begin{aligned}D\delta W_{ext}^{p}\left(\boldsymbol{\phi},\delta\mathbf{v}\right)\left[\mathbf{u}\right]=&\frac{1}{2}\int_{A_{\xi}}p\frac{\partial\mathbf{x}}{\partial\xi}\cdot\left[\left(\frac{\partial\mathbf{u}}{\partial\eta}\times\delta\mathbf{v}\right)+\left(\frac{\partial\delta\mathbf{v}}{\partial\eta}\times\mathbf{u}\right)\right]d\xi\,d\eta\\&-\frac{1}{2}\int_{A_{\xi}}p\frac{\partial\mathbf{x}}{\partial\eta}\cdot\left[\left(\frac{\partial\mathbf{u}}{\partial\xi}\times\delta\mathbf{v}\right)+\left(\frac{\partial\delta\mathbf{v}}{\partial\xi}\times\mathbf{u}\right)\right]d\xi\,d\eta\,.\end{aligned} \tag{3.1.8}$$

Discretization of this equation will also lead to a symmetric component of the tangent matrix.

FEBio currently supports gravity as a body force, $\mathbf{f}=\rho\mathbf{g}$. Since this force is independent of the geometry, the contribution to the linearized external work is zero. Another type of body force implemented in FEBio is the centrifugal force. For a body rotating with a constant angular speed ω, about an axis passing through the point $\mathbf{c}$ and directed along the unit vector $\mathbf{n}$, the body force is given by $\mathbf{f}=\rho\omega^{2}\mathbf{r}$, where $\mathbf{r}$ is the vector distance from a point $\mathbf{x}$ to the axis of rotation,

$$\mathbf{r}=\left(\mathbf{I}-\mathbf{n}\otimes\mathbf{n}\right)\cdot\left(\mathbf{x}-\mathbf{c}\right)\,. \tag{3.1.9}$$

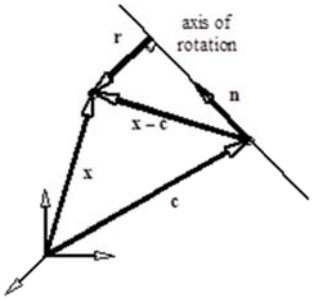

The resulting linearized external work is given by

$$D\delta W_{ext}^{f}\left(\boldsymbol{\phi},\delta\mathbf{v}\right)\left[\mathbf{u}\right]=\int_{v}\rho\omega^{2}\delta\mathbf{v}\cdot\left(\mathbf{I}-\mathbf{n}\otimes\mathbf{n}\right)\cdot\mathbf{u}\,dv, \tag{3.1.10}$$

which produces a symmetric expression that will yield a symmetric matrix.

3.1.2 Discretization

The basis of the finite element method is that the domain of the problem (that is, the volume of the object under consideration) is divided into smaller subunits, called *finite elements*. In the case of *isoparametric elements* it is further assumed that each element has a local coordinate system, named the *natural coordinates*, and the coordinates and shape of the element are discretized using the same functions. The discretization process is established by interpolating the geometry in terms of the coordinates $\mathbf{X}_a$ of the *nodes* that define the geometry of a finite element, and the *shape functions*:

$$\mathbf{X}=\sum_{a=1}^{n}N_a\left(\xi_1,\xi_2,\xi_3\right)\mathbf{X}_a\,, \tag{3.1.11}$$

where n is the number of nodes and ξ_i are the natural coordinates. Similarly, the motion is described in terms of the current position $\mathbf{x}_a\left(t\right)$ of the *same* particles:

$$\mathbf{x}\left(t\right)=\sum_{a=1}^{n}N_a\mathbf{x}_a\left(t\right)\,. \tag{3.1.12}$$

Quantities such as displacement, velocity and virtual velocity can be discretized in a similar way.

In deriving the discretized equilibrium equations, the integrations performed over the entire volume can be written as a sum of integrations constrained to the volume of an element. For this reason, the discretized equations are defined in terms of integrations over a particular element e. The discretized equilibrium equations for this particular element per node is given by

$$\delta W^{(e)}\left(\boldsymbol{\phi},N_a\delta\mathbf{v}\right)=\delta\mathbf{v}_a\cdot\left(\mathbf{T}_a^{(e)}-\mathbf{F}_a^{(e)}\right)\,, \tag{3.1.13}$$

where

$$\begin{aligned}T_a^{(e)}&=\int_{v^{(e)}}\boldsymbol{\sigma}\cdot\nabla N_a\,dv\,,\\ F_a^{(e)}&=\int_{v^{(e)}}N_a\mathbf{f}\,dv+\int_{\partial v^{(e)}}N_a\mathbf{t}\,da\,.\end{aligned} \tag{3.1.14}$$

The linearization of the internal virtual work can be split into a *material* and an *initial stress* component [27]:

$$\begin{aligned}D\delta W_{int}^{(e)}\left(\boldsymbol{\phi},\delta\mathbf{v}\right)\left[\mathbf{u}\right]&=\int_{v^{(e)}}\delta\mathbf{d}:\boldsymbol{\mathcal{C}}:\boldsymbol{\varepsilon}\,dv+\int_{v^{(e)}}\boldsymbol{\sigma}:\left[\left(\nabla\mathbf{u}\right)^{T}\cdot\nabla\delta\mathbf{v}\right]\,dv\\ &=D\delta W_{c}^{(e)}\left(\boldsymbol{\phi},\delta\mathbf{v}\right)\left[\mathbf{u}\right]+D\delta W_{\sigma}^{(e)}\left(\boldsymbol{\phi},\delta\mathbf{v}\right)\left[\mathbf{u}\right]\,.\end{aligned} \tag{3.1.15}$$

The constitutive component can be discretized as follows:

$$D\delta W_{c}^{(e)}\left(\boldsymbol{\phi},\delta\mathbf{v}\right)\left[\mathbf{u}\right]=\delta\mathbf{v}_a\cdot\left(\int_{v^{(e)}}\mathbf{B}_a^{T}\mathbf{D}\mathbf{B}_b\,dv\right)\mathbf{u}_b\,. \tag{3.1.16}$$

The term in parentheses defines the constitutive component of the tangent matrix relating node $a$to node $b$in element e:

$$\mathbf{K}_{c,ab}^{(e)} = \int_{v^{(e)}} \mathbf{B}_a^T \mathbf{D} \mathbf{B}_b \, dv \,. \tag{3.1.17}$$

Here, the linear strain-displacement matrix $\mathbf{B}$ relates the displacements to the small-strain tensor in Voigt Notation:

$$\boldsymbol{\varepsilon} = \sum_{a=1}^{n} \mathbf{B}_a \mathbf{u}_a \,. \tag{3.1.18}$$

Or, written out completely,

$$\mathbf{B}_a = \begin{bmatrix} \partial N_a/\partial x & 0 & 0 \\ 0 & \partial N_a/\partial y & 0 \\ 0 & 0 & \partial N_a/\partial z \\ \partial N_a/\partial y & \partial N_a/\partial x & 0 \\ 0 & \partial N_a/\partial z & \partial N_a/\partial y \\ \partial N_a/\partial z & 0 & \partial N_a/\partial z \end{bmatrix} . \tag{3.1.19}$$

The spatial constitutive matrix $\mathbf{D}$ is constructed from the components of the fourth-order tensor $\boldsymbol{\mathcal{C}}$ using the following table; $D_{IJ} = \mathcal{C}_{ijkl}$where

I/J	i/k	j/l
1	1	1
2	2	2
3	3	3
4	1	2
5	2	3
6	1	3

The initial stress component can be written as follows:

$$D\delta W_{\sigma}^{(e)} \left(\boldsymbol{\phi}, N_a \delta \mathbf{v}\right) \left[N_b \mathbf{u}_b\right] = \int_{v^{(e)}} \left(\nabla N_a \cdot \boldsymbol{\sigma} \cdot \nabla N_b\right) \mathbf{I} \, dv. \tag{3.1.20}$$

For the pressure component of the external virtual work, we find

$$D\delta W_{p}^{(e)} \left(\boldsymbol{\phi}, N_a \delta \mathbf{v}_a\right) \left[N_b \mathbf{u}_b\right] = \delta \mathbf{v}_a \cdot \mathbf{K}_{p,ab}^{(e)} \cdot \mathbf{u}_b \,, \tag{3.1.21}$$

where,

$$\begin{aligned} \mathbf{K}_{p,ab}^{(e)} &= \mathcal{E} \mathbf{k}_{p,ab}^{(e)}, \\ \mathbf{k}_{p,ab}^{(e)} &= \frac{1}{2} \int_{A_\xi} p \frac{\partial \mathbf{x}}{\partial \xi} \left(\frac{\partial N_a}{\partial \eta} N_b - \frac{\partial N_b}{\partial \eta} N_a \right) d\xi \, d\eta \\ &\quad + \frac{1}{2} \int_{A_\xi} p \frac{\partial \mathbf{x}}{\partial \eta} \left(\frac{\partial N_a}{\partial \xi} N_b - \frac{\partial N_b}{\partial \xi} N_a \right) d\xi \, d\eta \,. \end{aligned} \tag{3.1.22}$$

3.2 Weak formulation for biphasic materials

A weak form of the statement conservation of linear momemtum for the quasi-static case is obtained by using Eqs.(2.5.2) and (2.5.4):

$$\delta W = \int_b \left[\delta \mathbf{v}^s \cdot (\operatorname{div} \boldsymbol{\sigma} + \rho \mathbf{b}) + \delta p \, \operatorname{div} (\mathbf{v}^s + \mathbf{w})\right] dv = 0 \,, \tag{3.2.1}$$

where b is the domain of interest defined on the solid matrix, $\delta \mathbf{v}^s$ is a virtual velocity of the solid and δp is a virtual pressure of the fluid [104]. dv is an elemental volume of b. Using the divergence theorem, this expression may be rearranged as

$$\begin{aligned} \delta W = & \int_{\partial b} \delta \mathbf{v}^s \cdot \mathbf{t} \, da + \int_{\partial b} \delta p \, w_n \, da + \int_b \delta \mathbf{v}^s \cdot \rho \mathbf{b} \, dv \\ & - \int_b \boldsymbol{\sigma} : \operatorname{grad} \delta \mathbf{v}^s \, dv - \int_b \left(\mathbf{w} \cdot \operatorname{grad} \delta p - \delta p \, \operatorname{div} \mathbf{v}^s\right) \, dv \end{aligned} \,, \tag{3.2.2}$$

where $\delta \mathbf{d}^s = \left(\operatorname{grad} \delta \mathbf{v}^s + \operatorname{grad}^T \delta \mathbf{v}^s\right)/2$ is the virtual rate of deformation tensor, $\mathbf{t} = \boldsymbol{\sigma} \cdot \mathbf{n}$ is the total traction on the surface ∂b, and $w_n = \mathbf{w} \cdot \mathbf{n}$ is the component of the fluid flux normal to ∂b, with $\mathbf{n}$ representing the unit outward normal to ∂b. da represents an elemental area of ∂b. In this type of problem, essential boundary conditions are prescribed for $\mathbf{u}$ and p, and natural boundary conditions are prescribed for $\mathbf{t}$ and w_n. In the expression of Eq.(3.2.2), $\delta W\left(\boldsymbol{\chi}^s, p, \delta \mathbf{v}^s, \delta p\right)$ represents the virtual work.

3.2.1 Linearization

Since the system of equations in Eq.(3.2.2) is highly nonlinear, its solution requires an iterative scheme such as Newton's method. This requires the linearization of δW at some trial solution $(\boldsymbol{\chi}^s_k, p_k)$, along an increment $\Delta \mathbf{u}$ in $\boldsymbol{\chi}^s$ and an increment Δp in p,

$$\delta W + D\delta W\left[\Delta \mathbf{u}\right] + D\delta W\left[\Delta p\right] = 0, \tag{3.2.3}$$

where $Df\left[\Delta q\right]$ represents the directional derivative of f along Δq. For convenience, the virtual work may be separated into its internal and external parts,

$$\delta W = \delta W_{\text{ext}} - \delta W_{\text{int}}, \tag{3.2.4}$$

where

$$\delta W_{\text{int}} = \int_b \boldsymbol{\sigma} : \delta \mathbf{d}^s \, dv + \int_b \left(\mathbf{w} \cdot \operatorname{grad} \delta p - \delta p \, \frac{\dot{J}}{J}\right) \, dv, \tag{3.2.5}$$

where we have substituted $\operatorname{div} \mathbf{v}^s = \dot{J}/J$, and

$$\delta W_{\text{ext}} = \int_{\partial b} \delta \mathbf{v}^s \cdot \mathbf{t} \, da + \int_{\partial b} \delta p \, w_n \, da + \int_b \delta \mathbf{v}^s \cdot \rho \mathbf{b} \, dv \,. \tag{3.2.6}$$

The evaluation of the directional derivatives can be performed following a standard approach [27]. In particular, a backward difference scheme is used to evaluate $\dot{J} \approx \left(J - J^{-\Delta t}\right)/\Delta t$, where $J^{-\Delta t}$

is the value of J at the previous time step. For the internal part of the virtual work, the directional derivative along $\Delta\mathbf{u}$ yields

$$\begin{aligned} D\delta W_{\text{int}}\left[\Delta\mathbf{u}\right] = & \int_b \delta\mathbf{d}^s : \boldsymbol{\mathcal{C}} : \Delta\boldsymbol{\varepsilon}\, dv + \int_b \boldsymbol{\sigma} : \left(\operatorname{grad}^T \Delta\mathbf{u} \cdot \operatorname{grad} \delta\mathbf{v}^s\right)\, dv \\ & - \int_b \frac{\delta p}{\Delta t} \operatorname{div} \Delta\mathbf{u}\, dv \\ & - \int_b \operatorname{grad} \delta p \cdot \left(\boldsymbol{\mathcal{K}} : \Delta\boldsymbol{\varepsilon}\right) \cdot \left(\operatorname{grad} p - \rho_T^w \mathbf{b}^w\right)\, dv \\ & + \int_b \operatorname{grad} \delta p \cdot \mathbf{k} \cdot \rho_T^w \left(\operatorname{grad}^T \Delta\mathbf{u} \cdot \mathbf{b}^w + \operatorname{grad} \mathbf{b}^w \cdot \Delta\mathbf{u}\right) dv\,, \end{aligned} \tag{3.2.7}$$

where $\boldsymbol{\mathcal{C}}$ is the fourth-order spatial elasticity tensor for the mixture and $\Delta\boldsymbol{\varepsilon} = \left(\operatorname{grad} \Delta\mathbf{u} + \operatorname{grad}^T \Delta\mathbf{u}\right)/2$. Based on the relation of Eq.(2.5.3), the spatial elasticity tensor may also be expanded as

$$\boldsymbol{\mathcal{C}} = \boldsymbol{\mathcal{C}}^e + p\left(-\mathbf{I}\otimes\mathbf{I} + 2\mathbf{I}\,\overline{\underline{\otimes}}\,\mathbf{I}\right), \tag{3.2.8}$$

where $\boldsymbol{\mathcal{C}}^e$ is the spatial elasticity tensor for the solid matrix [34]. It is related to the material elasticity tensor $\mathbb{C}^e$ via

$$\boldsymbol{\mathcal{C}}^e = J^{-1}\left(\mathbf{F}\,\underline{\otimes}\,\mathbf{F}\right) : \mathbb{C}^e : \left(\mathbf{F}^T\,\underline{\otimes}\,\mathbf{F}^T\right), \tag{3.2.9}$$

where $\mathbf{F}$ is the deformation gradient of the solid matrix, $\mathbb{C}^e = \partial\mathbf{S}^e/\partial\mathbf{E}$ where $\mathbf{E}$ is the Lagrangian strain tensor and $\mathbf{S}^e$ is the second Piola-Kirchhoff stress tensor, related to the Cauchy stress tensor via $\boldsymbol{\sigma}^e = J^{-1}\mathbf{F}\cdot\mathbf{S}^e\cdot\mathbf{F}^T$.

Similarly, $\boldsymbol{\mathcal{K}}$ is a fourth-order tensor that represents the spatial measure of the rate of change of permeability with strain. It is related to its material frame equivalent $\mathbb{K}$ via

$$\boldsymbol{\mathcal{K}} = J^{-1}\left(\mathbf{F}\,\underline{\otimes}\,\mathbf{F}\right) : \mathbb{K} : \left(\mathbf{F}^T\,\underline{\otimes}\,\mathbf{F}^T\right), \tag{3.2.10}$$

where $\mathbb{K} = \partial\mathbf{K}/\partial\mathbf{E}$ and $\mathbf{K}$ is the permeability tensor in the material frame, such that $\mathbf{k} = J^{-1}\mathbf{F}\cdot\mathbf{K}\cdot\mathbf{F}^T$. Since $\mathbf{K}$ and $\mathbf{E}$ are symmetric tensors, it follows that $\boldsymbol{\mathcal{K}}$ and $\mathbb{K}$ exhibit two minor symmetries (e.g., $\mathcal{K}_{jikl} = \mathcal{K}_{ijkl}$ and $\mathcal{K}_{ijlk} = \mathcal{K}_{ijkl}$). However, unlike the elasticity tensor, it is not necessary that these tensors exhibit major symmetry (e.g., $\mathcal{K}_{klij} \neq \mathcal{K}_{ijkl}$ in general).

The directional derivative of δW_{int} along Δp is given by

$$D\delta W_{\text{int}}\left[\Delta p\right] = -\int_b \operatorname{grad} \delta p \cdot \mathbf{k} \cdot \operatorname{grad} \Delta p\, dv - \int_b \Delta p\, \operatorname{div} \delta\mathbf{v}^s\, dv\,. \tag{3.2.11}$$

Note that letting $p = 0$ and $\delta p = 0$ in the above equations recovers the virtual work relations for nonlinear elasticity of compressible solids. The resulting simplified equation emerging from Eq.(3.2.7) is symmetric to interchanges of $\Delta\mathbf{u}$ and $\delta\mathbf{v}^s$, producing a symmetric stiffness matrix in the finite element formulation [27]. However, the general relations of Eqs.(3.2.7) and (3.2.11) do not exhibit symmetry to interchanges of $(\Delta\mathbf{u}, \Delta p)$ and $(\delta\mathbf{v}^s, \delta p)$, implying that the finite element stiffness matrix for a solid-fluid mixture is not symmetric under general conditions.

The directional derivatives of the external virtual work δW_{ext} depend on the type of boundary conditions being considered. For a prescribed total normal traction t_n, where $\mathbf{t} = t_n\mathbf{n}$,

$$\delta W_{\text{ext}}^t = \int_{\partial b} \delta\mathbf{v}^s \cdot t_n\mathbf{n}\, da, \tag{3.2.12}$$

and

$$\begin{aligned} D\delta W^t_{\text{ext}}\left[\Delta\mathbf{u}\right] &= \int_{\partial b} \delta\mathbf{v}^s \cdot t_n \left(\mathbf{g}_1 \times \frac{\partial \Delta\mathbf{u}}{\partial \eta^2} - \mathbf{g}_2 \times \frac{\partial \Delta\mathbf{u}}{\partial \eta^1}\right) \frac{da}{|\mathbf{g}_1 \times \mathbf{g}_2|}\,, \\ D\delta W^t_{\text{ext}}\left[\Delta p\right] &= 0, \end{aligned} \tag{3.2.13}$$

where

$$\mathbf{g}_\alpha = \frac{\partial \mathbf{x}}{\partial \eta^\alpha}, \quad \alpha = 1, 2 \tag{3.2.14}$$

are covariant basis (tangent) vectors on ∂b, such that

$$\mathbf{n} = \frac{\mathbf{g}_1 \times \mathbf{g}_2}{|\mathbf{g}_1 \times \mathbf{g}_2|}\,. \tag{3.2.15}$$

For a prescribed normal effective traction t^e_n, where $\mathbf{t} = (-p + t^e_n)\,\mathbf{n}$ and p is not prescribed, then

$$\delta W^e_{\text{ext}} = \int_{\partial b} \delta\mathbf{v}^s \cdot (-p + t^e_n)\,\mathbf{n}\, da\,, \tag{3.2.16}$$

and

$$\begin{aligned} D\delta W^e_{\text{ext}}\left[\Delta\mathbf{u}\right] &= \int_{\partial b} \delta\mathbf{v}^s \cdot (-p + t^e_n) \left(\mathbf{g}_1 \times \frac{\partial \Delta\mathbf{u}}{\partial \eta^2} - \mathbf{g}_2 \times \frac{\partial \Delta\mathbf{u}}{\partial \eta^1}\right) \frac{da}{|\mathbf{g}_1 \times \mathbf{g}_2|}\,, \\ D\delta W^e_{\text{ext}}\left[\Delta p\right] &= -\int_{\partial b} \delta\mathbf{v}^s \cdot \Delta p\,\mathbf{n}\, da\,. \end{aligned} \tag{3.2.17}$$

For a prescribed normal fluid flux $w_n = \mathbf{w} \cdot \mathbf{n}$,

$$\delta W^w_{\text{ext}} = \int_{\partial b} \delta p\, w_n\, da\,, \tag{3.2.18}$$

and

$$\begin{aligned} D\delta W^w_{\text{ext}}\left[\Delta\mathbf{u}\right] &= \int_{\partial b} \delta p\, w_n\, \mathbf{n} \cdot \left(\mathbf{g}_1 \times \frac{\partial \Delta\mathbf{u}}{\partial \eta^2} - \mathbf{g}_2 \times \frac{\partial \Delta\mathbf{u}}{\partial \eta^1}\right) \frac{da}{|\mathbf{g}_1 \times \mathbf{g}_2|}\,, \\ D\delta W^w_{\text{ext}}\left[\Delta p\right] &= 0\,. \end{aligned} \tag{3.2.19}$$

Finally, for a prescribed external body force, recognizing that $\rho\mathbf{b} = \rho^s\mathbf{b}^s + \rho^w\mathbf{b}^w$ and assuming that the body forces $\mathbf{b}^s$ and $\mathbf{b}^w$ do not depend on p,

$$\begin{aligned} D\left(\delta W^b_{\text{ext}}\right)\left[\Delta\mathbf{u}\right] &= \int_b \delta\mathbf{v}^s \cdot \left[(\rho^s grad\mathbf{b}^s + \rho^w grad\mathbf{b}^w) \cdot \Delta\mathbf{u} + (\operatorname{div}\Delta\mathbf{u})\,\rho^w_T\mathbf{b}^w\right] dv\,, \\ D\left(\delta W^b_{\text{ext}}\right)\left[\Delta p\right] &= 0\,. \end{aligned} \tag{3.2.20}$$

3.2.2 Discretization

Let

$$\begin{aligned} \delta\mathbf{v}^s &= \sum_{a=1}^{m} N_a \delta\mathbf{v}_a\,, \qquad \delta p = \sum_{a=1}^{m} N_a \delta p_a\,, \\ \Delta\mathbf{u} &= \sum_{b=1}^{m} N_b \Delta\mathbf{u}_b\,, \quad \Delta p = \sum_{b=1}^{m} N_b \Delta p_b\,, \end{aligned} \tag{3.2.21}$$

where N_a represents the interpolation functions over an element, $\delta\mathbf{v}_a, \delta p_a, \Delta\mathbf{u}_b$ and Δp_b respectively represent nodal values of $\delta\mathbf{v}^s$, δp, $\Delta\mathbf{u}$ and Δp, and m is the number of nodes in an element. Then the discretized form of δW_{int} in Eq.(3.2.5) may be written as

$$\delta W_{\text{int}} = \sum_{e=1}^{n_e} \sum_{k=1}^{n_{\text{int}}^{(e)}} W_k J_\eta \sum_{a=1}^{m} \left[\begin{array}{cc} \delta\mathbf{v}_a & \delta p_a \end{array} \right] \cdot \left[\begin{array}{c} \mathbf{r}_a^u \\ r_a^p \end{array} \right] , \tag{3.2.22}$$

where n_e is the number of elements in b, $n_{\text{int}}^{(e)}$ is the number of integration points in the $e-$th element, W_k is the quadrature weight associated with the $k-$th integration point, and J_η is the Jacobian of the transformation from the spatial frame to the parametric space of the element. In the above expression,

$$\mathbf{r}_a^u = \boldsymbol{\sigma} \cdot \nabla N_a \,, \quad r_a^p = \mathbf{w} \cdot \nabla N_a - N_a \text{div}\mathbf{v}^s \,, \tag{3.2.23}$$

and it is understood that J_η, $\mathbf{r}_a^u$ and r_a^p are evaluated at the parametric coordinates of the $k-$th integration point.

Similarly, the discretized form of $D\delta W_{\text{int}}$ in Eqs.(3.2.7) and (3.2.11) may be written as

$$-D\delta W_{\text{int}} = \sum_{e=1}^{n_e} \sum_{k=1}^{n_{\text{int}}^{(e)}} W_k J_\eta \sum_{a=1}^{m} \left[\begin{array}{cc} \delta\mathbf{v}_a & \delta p_a \end{array} \right] \cdot \sum_{b=1}^{m} \left[\begin{array}{cc} \mathbf{K}_{ab}^{uu} & \mathbf{k}_{ab}^{up} \\ \mathbf{k}_{ab}^{pu} & k_{ab}^{pp} \end{array} \right] \cdot \left[\begin{array}{c} \Delta\mathbf{u}_b \\ \Delta p_b \end{array} \right] , \tag{3.2.24}$$

where

$$\begin{aligned} \mathbf{K}_{ab}^{uu} &= \nabla N_a \cdot \boldsymbol{\mathcal{C}} \cdot \nabla N_b + (\nabla N_a \cdot \boldsymbol{\sigma} \cdot \nabla N_b)\, \mathbf{I} \\ &\quad - N_a \left[N_b \left(\rho^s \nabla \mathbf{b}^s + \rho^w \nabla \mathbf{b}^w \right) + \rho_T^w \mathbf{b}^w \otimes \nabla N_b \right] , \\ \mathbf{k}_{ab}^{up} &= -N_b \nabla N_a \,, \\ \mathbf{k}_{ab}^{pu} &= -\left(\nabla N_a \cdot \boldsymbol{\mathcal{K}} \cdot \nabla N_b \right) \cdot \left(\nabla p - \rho_T^w \mathbf{b}^w \right) - \frac{1}{\Delta t} N_a \cdot \nabla N_b \\ &\quad + \rho_T^w \left(\mathbf{b}^w \otimes \nabla N_b + N_b \nabla^T \mathbf{b}^w \right) \cdot \mathbf{k} \cdot \nabla N_a \,, \\ k_{ab}^{pp} &= -\nabla N_a \cdot \mathbf{k} \cdot \nabla N_b, \end{aligned} \tag{3.2.25}$$

and Δt is a discrete increment in time. In a numerical implementation, it has been found that evaluating $\text{div}\,\mathbf{v}^s$ from $\dot{J}/J$, where $J = \det \mathbf{F}$, yields more accurate solutions than evaluating it from the trace of $\text{grad}\,\mathbf{v}^s$ [14].

For the various types of contributions to the external virtual work, a similar discretization produces

$$\delta W_{\text{ext}} = \sum_{e=1}^{n_e} \sum_{k=1}^{n_{\text{int}}^{(e)}} W_k J_\eta \sum_{a=1}^{m} \left[\begin{array}{cc} \delta\mathbf{v}_a & \delta p_a \end{array} \right] \cdot \left[\begin{array}{c} \mathbf{r}_a^u \\ r_a^p \end{array} \right] , \tag{3.2.26}$$

and

$$-D\delta W_{\text{ext}} = \sum_{e=1}^{n_e} \sum_{k=1}^{n_{\text{int}}^{(e)}} W_k J_\eta \sum_{a=1}^{m} \left[\begin{array}{cc} \delta\mathbf{v}_a & \delta p_a \end{array} \right] \cdot \sum_{b=1}^{m} \left[\begin{array}{cc} \mathbf{K}_{ab}^{uu} & \mathbf{k}_{ab}^{up} \\ \mathbf{k}_{ab}^{pu} & k_{ab}^{pp} \end{array} \right] \cdot \left[\begin{array}{c} \Delta\mathbf{u}_b \\ \Delta p_b \end{array} \right] , \tag{3.2.27}$$

where

$$J_\eta = |\mathbf{g}_1 \times \mathbf{g}_2| \,. \tag{3.2.28}$$

In this case, m represents the number of nodes on an element face. For a prescribed normal traction t_n as given in (3.2.12)-(3.2.13),

$$\begin{aligned} \mathbf{r}_a^u &= t_n N_a \mathbf{n}\,, & r_a^u &= 0\,, \\ \mathbf{K}_{ab}^{uu} &= t_n N_a \frac{1}{J_\eta} \boldsymbol{\mathcal{A}} \left\{ \frac{\partial N_b}{\partial \eta^1} \mathbf{g}_2 - \frac{\partial N_b}{\partial \eta^2} \mathbf{g}_1 \right\}\,, & \mathbf{k}_{ab}^{up} &= \mathbf{0}\,, \\ \mathbf{k}_{ab}^{pu} &= \mathbf{0}\,, & k_{ab}^{pp} &= 0\,, \end{aligned} \tag{3.2.29}$$

where $\boldsymbol{\mathcal{A}}\{\mathbf{v}\} = -\boldsymbol{\mathcal{E}} \cdot \mathbf{v}$ is the skew-symmetric tensor whose dual vector is $\mathbf{v}$ and $\boldsymbol{\mathcal{E}}$ is the third-order permutation pseudo-tensor. For a prescribed traction t_n^e as given in (3.2.16)-(3.2.17),

$$\begin{aligned} \mathbf{r}_a^u &= (-p + t_n^e)\, N_a \mathbf{n}\,, & r_a^u &= 0\,, \\ \mathbf{K}_{ab}^{uu} &= (-p + t_n^e)\, N_a \frac{1}{J_\eta} \boldsymbol{\mathcal{A}} \left\{ \frac{\partial N_b}{\partial \eta^1} \mathbf{g}_2 - \frac{\partial N_b}{\partial \eta^2} \mathbf{g}_1 \right\}\,, & \mathbf{k}_{ab}^{up} &= \mathbf{0}\,, \\ \mathbf{k}_{ab}^{pu} &= \mathbf{0}\,, & k_{ab}^{pp} &= 0\,. \end{aligned} \tag{3.2.30}$$

For a prescribed normal fluid flux w_n as given in (3.2.18)-(3.2.19),

$$\begin{aligned} \mathbf{r}_a^u &= \mathbf{0}\,, & r_a^u &= w_n N_a\,, \\ \mathbf{K}_{ab}^{uu} &= \mathbf{0}\,, & \mathbf{k}_{ab}^{up} &= \mathbf{0}\,, \\ \mathbf{k}_{ab}^{pu} &= w_n N_a \frac{1}{J_\eta} \mathbf{n} \times \left(\frac{\partial N_b}{\partial \eta^1} \mathbf{g}_2 - \frac{\partial N_b}{\partial \eta^2} \mathbf{g}_1 \right)\,, & k_{ab}^{pp} &= 0\,. \end{aligned} \tag{3.2.31}$$

3.3 Weak Formulation for Biphasic-Solute Materials

The virtual work integral for this problem is given by

$$\begin{aligned} \delta W = &\int_b \delta \mathbf{v} \cdot \operatorname{div} \boldsymbol{\sigma}\, dv + \int_b \delta \tilde{p}\, \operatorname{div} \left(\mathbf{v}^s + \mathbf{w} \right)\, dv \\ &+ \int_b \delta \tilde{c} \left[\frac{\partial \left(\varphi^w \tilde{\kappa} \tilde{c} \right)}{\partial t} + \operatorname{div} \left(\mathbf{j} + \phi^w \tilde{\kappa} \tilde{c}\, \mathbf{v}^s \right) \right]\, dv\,, \end{aligned} \tag{3.3.1}$$

where $\delta \mathbf{v}$ is the virtual velocity of the solid, $\delta \tilde{p}$ is the virtual effective fluid pressure, and $\delta \tilde{c}$ is the virtual molar energy of the solute. b represents the mixture domain in the spatial frame and dv is an elemental mixture volume in b. In the last integral of δW, note that

$$\frac{\partial \left(\varphi^w \tilde{\kappa} \tilde{c} \right)}{\partial t} + \operatorname{div} \left(\varphi^w \tilde{\kappa} \tilde{c}\, \mathbf{v}^s \right) = \frac{1}{J} \frac{D^s}{Dt} \left(J \varphi^w \tilde{\kappa} \tilde{c} \right)\,, \tag{3.3.2}$$

where $D^s f/Dt \equiv \partial f/\partial t + \mathbf{v}^s \cdot \operatorname{grad} f$ is the material time derivative of a scalar function f in the spatial frame, following the solid. Similarly, note that $\operatorname{div} \mathbf{v}^s = J^{-1} \left(D^s J/Dt \right)$. Using the divergence theorem, the virtual work integral may be separated into internal and external contributions, $\delta W = \delta W_{\text{ext}} - \delta W_{\text{int}}$, where

$$\begin{aligned} \delta W_{\text{int}} = &\int_b \boldsymbol{\sigma} : \delta \mathbf{d}^s\, dv + \int_b \left(\mathbf{w} \cdot \operatorname{grad} \delta \tilde{p} - \frac{\delta \tilde{p}}{J} \frac{D^s J}{Dt} \right)\, dv \\ &+ \int_b \left[\mathbf{j} \cdot \operatorname{grad} \delta \tilde{c} - \frac{\delta \tilde{c}}{J} \frac{D^s}{Dt} \left(J \varphi^w \tilde{\kappa} \tilde{c} \right) \right]\, dv\,, \\ \delta W_{\text{ext}} = &\int_{\partial b} \left(\delta \mathbf{v} \cdot \mathbf{t} + \delta \tilde{p}\, w_n + \delta \tilde{c}\, j_n \right)\, da\,, \end{aligned} \tag{3.3.3}$$

with δW_{ext} being evaluated on the domain's boundary surface ∂b. In the first expression $\delta\mathbf{d}^s = \left(\operatorname{grad}\delta\mathbf{v} + \operatorname{grad}^T\delta\mathbf{v}\right)/2$ represents the virtual solid rate of deformation.

To solve this nonlinear system using an iterative Newton scheme, the virtual work must be linearized at trial solutions, along increments in $\mathbf{u}$, $\tilde{p}$ and $\tilde{c}$,

$$\delta W + D\delta W\left[\Delta\mathbf{u}\right] + D\delta W\left[\Delta\tilde{p}\right] + D\delta W\left[\Delta\tilde{c}\right] \approx 0\,, \tag{3.3.4}$$

where, for any function $f\left(q\right)$, $Df\left[\Delta q\right]$ represents the directional derivative of f along Δq [27]. To operate the directional derivative on the integrand of δW_{int}, it is first necessary to convert the integrals from the spatial to the material domain [27]:

$$\delta W_{\text{int}} = \int_B \mathbf{S} : \delta\dot{\mathbf{E}}\, dV + \int_B \left(\mathbf{W}\cdot\operatorname{grad}\delta\tilde{p} - \delta\tilde{p}\frac{\partial J}{\partial t}\right) dV + \int_B \left[\mathbf{J}\cdot\operatorname{grad}\delta\tilde{c} - \delta\tilde{c}\frac{\partial}{\partial t}\left(J\varphi^w\tilde{\kappa}\tilde{c}\right)\right] dV\,, \tag{3.3.5}$$

where B represents the mixture domain in the material frame, dV is an elemental mixture volume in B, and

$$\begin{aligned} \mathbf{S} &= J\,\mathbf{F}^{-1}\cdot\boldsymbol{\sigma}\cdot\mathbf{F}^{-T}\,,\\ \delta\dot{\mathbf{E}} &= \mathbf{F}^T\cdot\delta\mathbf{d}^s\cdot\mathbf{F}\,,\\ \mathbf{W} &= J\,\mathbf{F}^{-1}\cdot\mathbf{w}\,,\\ \mathbf{J} &= J\,\mathbf{F}^{-1}\cdot\mathbf{j}\,. \end{aligned} \tag{3.3.6}$$

The second Piola-Kirchhoff stress tensor $\mathbf{S}$, and material flux vectors $\mathbf{W}$ and $\mathbf{J}$, are respectively related to $\boldsymbol{\sigma}$, $\mathbf{w}$ and $\mathbf{j}$ by the Piola transformations for tensors and vectors [27, 72]. Substituting (3.3.6) into (2.6.13) produces

$$\begin{aligned} \mathbf{W} &= -\tilde{\mathbf{K}}\cdot\left(\operatorname{grad}\tilde{p} + R\theta\frac{\tilde{\kappa}}{d_0}J^{-1}\mathbf{C}\cdot\mathbf{D}\cdot\operatorname{grad}\tilde{c}\right)\,,\\ \mathbf{J} &= \tilde{\kappa}\mathbf{D}\cdot\left(-\varphi^w\operatorname{grad}\tilde{c} + \frac{\tilde{c}}{d_0}J^{-1}\mathbf{C}\cdot\mathbf{W}\right)\,, \end{aligned} \tag{3.3.7}$$

where $\tilde{\mathbf{K}}$ and $\mathbf{D}$ are the material representations of the permeability and diffusivity tensors, related to $\tilde{\mathbf{k}}$ and $\mathbf{d}$ via the Piola transformation,

$$\begin{aligned} \tilde{\mathbf{K}} &= J\,\mathbf{F}^{-1}\cdot\tilde{\mathbf{k}}\cdot\mathbf{F}^{-T}\,,\\ \mathbf{D} &= J\,\mathbf{F}^{-1}\cdot\mathbf{d}\cdot\mathbf{F}^{-T}\,. \end{aligned} \tag{3.3.8}$$

The linearization of δW_{int} is rather involved and a summary of the resulting lengthy expressions is provided below. In consideration of the dearth of experimental data relating $\tilde{\kappa}$ and Φ to the complete state of solid matrix strain (such as $\mathbf{C}$), this implementation assumes that the dependence of these functions on the strain is restricted to a dependence on the volume ratio $J = \left(\det\mathbf{C}\right)^{1/2}$. Furthermore, it is assumed that the free solution diffusivity d_0 is independent of the strain.

The linearization of δW_{ext} is described in Section 3.3.2. Following the linearization procedure, the resulting expressions may be discretized by nodally interpolating $\mathbf{u}$, $\tilde{p}$ and $\tilde{c}$ over finite elements, producing a set of equations in matrix form, as described in Section 3.3.2.

The formulation presented in this study is implemented in FEBio by introducing an additional module dedicated to solute transport in deformable porous media. Classes are implemented to describe material functions for $\boldsymbol{\sigma}^e$, $\mathbf{k}$, $\mathbf{d}$ (and d_0), $\tilde{\kappa}$ and Φ, which allow the formulation of any desired constitutive relation for these functions of $\mathbf{C}$ and $\tilde{c}$, along with corresponding derivatives of

these functions with respect to $\mathbf{C}$ and $\tilde{c}$. The implementation accepts essential boundary conditions on $\mathbf{u}$, $\tilde{p}$ and $\tilde{c}$, or natural boundary conditions on $\mathbf{t}$, w_n and j_n; initial conditions may also be specified for $\tilde{p}$ and $\tilde{c}$. Analysis results for pressure and concentration may be displayed either as $\tilde{p}$ and $\tilde{c}$, or as p and c by inverting the relations of (2.6.11).

3.3.1 Linearization of Internal Virtual Work

The virtual work integral δW_{int} in (3.3.5) may be linearized term by term along increments in $\Delta\mathbf{u}$, $\Delta\tilde{p}$ and $\Delta\tilde{c}$ using the general form

$$D\left(\int_B F\,dV\right)[\Delta q] = \int_B DF\,[\Delta q]\;dV = \int_b f\,dv\,. \tag{3.3.9}$$

For notational simplicity, the integral sign is omitted and the linearization of each term is presented in the form $DF\,[\Delta q]\;dV = f\,dv$.

3.3.1.1 Linearization along $\Delta\mathbf{u}$

The linearization of the first term in δW_{int} along $\Delta\mathbf{u}$ yields

$$\left(\mathbf{S} : \delta\dot{\mathbf{E}}\right)[\Delta\mathbf{u}]\;dV = \left[\delta\mathbf{d}^s : \boldsymbol{\mathcal{C}} : \Delta\boldsymbol{\varepsilon} + \boldsymbol{\sigma} : \left(\operatorname{grad}^T \Delta\mathbf{u}\cdot\operatorname{grad}\delta\mathbf{v}\right)\right]\;dv\,, \tag{3.3.10}$$

where $\boldsymbol{\mathcal{C}}$ is the spatial elasticity tensor of the mixture,

$$\boldsymbol{\mathcal{C}} = \boldsymbol{\mathcal{C}}^e - (\tilde{p} + R\theta\,\Phi\tilde{\kappa}\tilde{c})\,(\mathbf{I}\otimes\mathbf{I} - 2\mathbf{I}\,\underline{\otimes}\,\mathbf{I}) - R\theta\tilde{c}\,J\frac{\partial\,(\Phi\tilde{\kappa})}{\partial J}\mathbf{I}\otimes\mathbf{I}\,, \tag{3.3.11}$$

and $\boldsymbol{\mathcal{C}}^e$ is the spatial elasticity tensor of the solid matrix,

$$\boldsymbol{\mathcal{C}}^e = J^{-1}\,(\mathbf{F}\,\underline{\otimes}\,\mathbf{F}) : 2\frac{\partial\mathbf{S}^e}{\partial\mathbf{C}} : \left(\mathbf{F}^T\,\underline{\otimes}\,\mathbf{F}^T\right)\,. \tag{3.3.12}$$

The linearization of the second term is

$$D\,(\mathbf{W}\cdot\operatorname{Grad}\delta\tilde{p})\,[\Delta\mathbf{u}]\;dV = \operatorname{grad}\delta\tilde{p}\cdot\mathbf{w}'_u\,dv\,, \tag{3.3.13}$$

where

$$\begin{aligned}\mathbf{w}'_u \equiv J^{-1}\mathbf{F}\cdot D\mathbf{W}\,[\Delta\mathbf{u}] = &-\left(\tilde{\boldsymbol{\mathcal{K}}} : \Delta\boldsymbol{\varepsilon}\right)\cdot\left(\operatorname{grad}\tilde{p} + R\theta\frac{\tilde{\kappa}}{d_0}\mathbf{d}\cdot\operatorname{grad}\tilde{c}\right)\\ &-\frac{R\theta}{d_0}\tilde{\mathbf{k}}\cdot\left(J^2\frac{\partial\left(J^{-1}\tilde{\kappa}\right)}{\partial J}\left(\operatorname{div}\Delta\mathbf{u}\right)\mathbf{I} + 2\tilde{\kappa}\,\Delta\boldsymbol{\varepsilon}\right)\cdot\mathbf{d}\cdot\operatorname{grad}\tilde{c} - \tilde{\kappa}\frac{R\theta}{d_0}\tilde{\mathbf{k}}\cdot(\boldsymbol{\mathcal{D}} : \Delta\boldsymbol{\varepsilon})\cdot\operatorname{grad}\tilde{c}\,,\end{aligned} \tag{3.3.14}$$

with

$$\begin{aligned}\tilde{\boldsymbol{\mathcal{K}}} &= J^{-1}\,(\mathbf{F}\,\underline{\otimes}\,\mathbf{F}) : 2\frac{\partial\tilde{\mathbf{K}}}{\partial\mathbf{C}} : \left(\mathbf{F}^T\,\underline{\otimes}\,\mathbf{F}^T\right)\,,\\ \boldsymbol{\mathcal{D}} &= J^{-1}\,(\mathbf{F}\,\underline{\otimes}\,\mathbf{F}) : 2\frac{\partial\mathbf{D}}{\partial\mathbf{C}} : \left(\mathbf{F}^T\,\underline{\otimes}\,\mathbf{F}^T\right)\,,\end{aligned} \tag{3.3.15}$$

representing the spatial tangents, with respect to the strain, of the effective permeability and solute diffusivity, respectively. These fourth-order tensors exhibit minor symmetries but not major

symmetry, as described recently [9]. Since $\tilde{\mathbf{K}}$ is given by substituting $(2.6.13)_3$ into $(3.3.8)_1$, the evaluation of $\tilde{\boldsymbol{\mathcal{K}}}$ is rather involved and it can be shown that

$$\tilde{\boldsymbol{\mathcal{K}}} = 2\left(\tilde{\mathbf{k}} \otimes \mathbf{I} - 2\tilde{\mathbf{k}} \underline{\otimes} \mathbf{I}\right) - \left(\tilde{\mathbf{k}} \underline{\overline{\otimes}} \tilde{\mathbf{k}}\right) : \boldsymbol{\mathcal{G}}\,, \tag{3.3.16}$$

where

$$\begin{aligned}\boldsymbol{\mathcal{G}} &= 2\left(\mathbf{k}^{-1} \otimes \mathbf{I} - 2\mathbf{k}^{-1} \underline{\overline{\otimes}} \mathbf{I}\right) - \left(\mathbf{k}^{-1} \underline{\otimes} \mathbf{k}^{-1}\right) : \boldsymbol{\mathcal{K}} \\ &+ \frac{R\theta\tilde{c}}{d_0} J \frac{\partial}{\partial J}\left(\frac{\tilde{\kappa}}{\varphi^w}\right)\left(\mathbf{I} - \frac{\mathbf{d}}{d_0}\right) \otimes \mathbf{I} \\ &+ \frac{R\theta\tilde{c}}{d_0}\frac{\tilde{\kappa}}{\varphi^w}\left(\mathbf{I} \otimes \mathbf{I} - 2\mathbf{I} \underline{\otimes} \mathbf{I} - \frac{1}{d_0}\boldsymbol{\mathcal{D}}\right)\end{aligned} \tag{3.3.17}$$

and

$$\boldsymbol{\mathcal{K}} = J^{-1}\left(\mathbf{F} \underline{\otimes} \mathbf{F}\right) : 2\frac{\partial \mathbf{K}}{\partial \mathbf{C}} : \left(\mathbf{F}^T \underline{\otimes} \mathbf{F}^T\right)\,. \tag{3.3.18}$$

The next term in δW_{int} linearizes to

$$-D\left(\delta\tilde{p}\frac{\partial J}{\partial t}\right)[\Delta\mathbf{u}]\; dV = -\delta\tilde{p}\frac{1}{\Delta t}\operatorname{div}\Delta\mathbf{u}\, dv\,, \tag{3.3.19}$$

where we used a backward difference scheme to approximate the time derivative,

$$\frac{\partial J}{\partial t} \approx \frac{1}{\Delta t}\left(J - J^{-\Delta t}\right)\,, \tag{3.3.20}$$

and Δt represents the time increment relative to the previous time point. The next term is given by

$$D\left(\mathbf{J}\cdot\operatorname{Grad}\delta\tilde{c}\right)[\Delta\mathbf{u}]\; dV = \operatorname{grad}\delta\tilde{c}\cdot\mathbf{j}'_u\, dv, \tag{3.3.21}$$

where

$$\begin{aligned}\mathbf{j}'_u \equiv J^{-1}\mathbf{F}\cdot D\mathbf{J}\left[\Delta\mathbf{u}\right] &= \left(J\frac{\partial\tilde{\kappa}}{\partial J}\left(\operatorname{div}\Delta\mathbf{u}\right)\mathbf{d} + \tilde{\kappa}\boldsymbol{\mathcal{D}} : \Delta\boldsymbol{\varepsilon}\right)\cdot\left(-\varphi^w\operatorname{grad}\tilde{c} + \frac{\tilde{c}}{d_0}\mathbf{w}\right) \\ &+ \tilde{\kappa}\mathbf{d}\cdot\left(-\varphi^s\left(\operatorname{div}\Delta\mathbf{u}\right)\operatorname{grad}\tilde{c} + \frac{\tilde{c}}{d_0}\left(2\Delta\boldsymbol{\varepsilon} - \left(\operatorname{div}\Delta\mathbf{u}\right)\mathbf{I}\right)\cdot\mathbf{w}\right) + \tilde{\kappa}\frac{\tilde{c}}{d_0}\mathbf{d}\cdot\mathbf{w}'_u\end{aligned}\,. \tag{3.3.22}$$

Using a backward difference scheme for the time derivative, the last term is

$$D\left(\delta\tilde{c}\frac{\partial\left(J\varphi^w\tilde{\kappa}\tilde{c}\right)}{\partial t}\right)[\Delta\mathbf{u}]\; dV = \frac{\delta\tilde{c}}{\Delta t}\frac{\partial\left(J\varphi^w\tilde{\kappa}\right)}{\partial J}\tilde{c}\operatorname{div}\Delta\mathbf{u}\, dv\,. \tag{3.3.23}$$

3.3.1.2 Linearization along $\Delta\tilde{p}$

The linearization of the various terms in δW_{int} along $\Delta\tilde{p}$ yields

$$D\left(\mathbf{S} : \delta\dot{\mathbf{E}}\right)[\Delta\tilde{p}]\; dV = -\Delta\tilde{p}\,\operatorname{div}\delta\mathbf{v}\, dv\,, \tag{3.3.24}$$

$$D\left(\mathbf{W}\cdot\operatorname{Grad}\delta\tilde{p} - \delta\tilde{p}\frac{\partial J}{\partial t}\right)[\Delta\tilde{p}]\; dV = -\operatorname{grad}\delta\tilde{p}\cdot\tilde{\mathbf{k}}\cdot\operatorname{grad}\Delta\tilde{p}\, dv\,, \tag{3.3.25}$$

$$D\left(\mathbf{J}\cdot\operatorname{Grad}\delta\tilde{c} - \delta\tilde{c}\frac{\partial\left(J\varphi^w\tilde{\kappa}\tilde{c}\right)}{\partial t}\right)[\Delta\tilde{p}]\; dV = -\frac{\tilde{\kappa}\tilde{c}}{d_0}\operatorname{grad}\delta\tilde{c}\cdot\mathbf{d}\cdot\tilde{\mathbf{k}}\cdot\operatorname{grad}\Delta\tilde{p}\, dv\,. \tag{3.3.26}$$

3.3.1.3 Linearization along $\Delta\tilde{c}$

The linearization of the first term in δW_{int} along $\Delta\tilde{c}$ yields

$$D\left(\mathbf{S}:\delta\dot{\mathbf{E}}\right)[\Delta\tilde{c}]\;dV=\Delta\tilde{c}\left(\boldsymbol{\sigma}'_c:\delta\mathbf{d}-R\theta\frac{\partial\left(\Phi\tilde{\kappa}\tilde{c}\right)}{\partial\tilde{c}}\operatorname{div}\delta\mathbf{v}\right)\,dv\,, \tag{3.3.27}$$

where

$$\boldsymbol{\sigma}'_c=J^{-1}\mathbf{F}\cdot\frac{\partial\mathbf{S}^e}{\partial\tilde{c}}\cdot\mathbf{F}^T \tag{3.3.28}$$

represents the spatial tangent of the stress with respect to the effective concentration. The next term is

$$D\left(\mathbf{W}\cdot\operatorname{Grad}\delta\tilde{p}\right)[\Delta\tilde{c}]\;dV=\operatorname{grad}\delta\tilde{p}\cdot\mathbf{w}'_c\,dv\,, \tag{3.3.29}$$

where

$$\begin{aligned}\mathbf{w}'_c\equiv J^{-1}\mathbf{F}\cdot D\mathbf{W}\left[\Delta\tilde{c}\right]&=-\Delta\tilde{c}\,\tilde{\mathbf{k}}'_c\cdot\left(\operatorname{grad}\tilde{p}+R\theta\frac{\tilde{\kappa}}{d_0}\mathbf{d}\cdot\operatorname{grad}\tilde{c}\right)\\&-R\theta\tilde{\mathbf{k}}\cdot\left[\Delta\tilde{c}\left(\frac{\partial}{\partial\tilde{c}}\left(\frac{\tilde{\kappa}}{d_0}\right)\mathbf{d}+\frac{\tilde{\kappa}}{d_0}\mathbf{d}'_c\right)\cdot\operatorname{grad}\tilde{c}+\frac{\tilde{\kappa}}{d_0}\mathbf{d}\cdot\operatorname{grad}\Delta\tilde{c}\right]\,,\end{aligned} \tag{3.3.30}$$

and

$$\tilde{\mathbf{k}}'_c=J^{-1}\mathbf{F}\cdot\frac{\partial\tilde{\mathbf{K}}}{\partial\tilde{c}}\cdot\mathbf{F}^T \tag{3.3.31}$$

is the spatial tangent of the effective hydraulic permeability with respect to the effective concentration.

The next term reduces to

$$-D\left(\delta\tilde{p}\frac{\partial J}{\partial t}\right)[\Delta\tilde{c}]\;dV=0\,. \tag{3.3.32}$$

The following term is

$$D\left(\mathbf{J}\cdot\operatorname{Grad}\delta\tilde{c}\right)[\Delta\tilde{c}]\;dV=\operatorname{grad}\delta\tilde{c}\cdot\mathbf{j}'_c\,dv\,, \tag{3.3.33}$$

where

$$\begin{aligned}\mathbf{j}'_c&\equiv J^{-1}\mathbf{F}\cdot D\mathbf{J}\left[\Delta\tilde{c}\right]\\&=\Delta\tilde{c}\left(\frac{\partial\tilde{\kappa}}{\partial\tilde{c}}\mathbf{d}+\tilde{\kappa}\mathbf{d}'_c\right)\cdot\left(-\varphi^w\operatorname{grad}\tilde{c}+\frac{\tilde{c}}{d_0}\mathbf{w}\right)\\&-\varphi^w\tilde{\kappa}\mathbf{d}\cdot\operatorname{grad}\Delta\tilde{c}+\tilde{\kappa}\frac{\tilde{c}}{d_0}\mathbf{d}\cdot\mathbf{w}'_c\,,\end{aligned} \tag{3.3.34}$$

and

$$\mathbf{d}'_c=J^{-1}\mathbf{F}\cdot\frac{\partial\mathbf{D}}{\partial\tilde{c}}\cdot\mathbf{F}^T \tag{3.3.35}$$

is the spatial tangent of the diffusivity with respect to the effective concentration.

The last term is

$$D\left(\frac{\partial\left(J\varphi^w\tilde{\kappa}\tilde{c}\right)}{\partial t}\delta\tilde{c}\right)[\Delta\tilde{c}]\;dV=\delta\tilde{c}\frac{\varphi^w}{\Delta t}\frac{\partial\left(\tilde{\kappa}\tilde{c}\right)}{\partial\tilde{c}}\Delta\tilde{c}\,dv\,, \tag{3.3.36}$$

where we similarly used a backward difference scheme to discretize the time derivative.

3.3.2 Linearization of External Virtual Work

The linearization of δW_{ext} in (3.3.3) depends on whether natural boundary conditions are prescribed as area densities or total net values over an area. Thus, in the case when $\mathbf{t}\,da$ (net force), $w_n da$ (net volumetric flow rate), or $j_n da$ (net molar flow rate) are prescribed over the elemental area da, there is no variation in δW_{ext} and it follows that $D\delta W_{\text{ext}} = 0$. Alternatively, in the case when $\mathbf{t}$, w_n or j_n are prescribed, the linearization may be performed by evaluating the integral in the parametric space of the boundary surface ∂b, with parametric coordinates (η^1, η^2). Accordingly, for a point $\mathbf{x}(\eta^1, \eta^2)$ on ∂b, surface tangents (covariant basis vectors) are given by

$$\mathbf{g}_\alpha = \frac{\partial \mathbf{x}}{\partial \eta^\alpha}, \quad (\alpha = 1, 2) \tag{3.3.37}$$

and the outward unit normal is

$$\mathbf{n} = \frac{\mathbf{g}_1 \times \mathbf{g}_2}{|\mathbf{g}_1 \times \mathbf{g}_2|}\,. \tag{3.3.38}$$

The elemental area on ∂b is $da = |\mathbf{g}_1 \times \mathbf{g}_2|\, d\eta^1 d\eta^2$. Consequently, the external virtual work integral may be rewritten as

$$\delta W_{\text{ext}} = \int_{\partial b} (\delta \mathbf{v} \cdot \mathbf{t} + \delta\tilde{p}\, w_n + \delta\tilde{c}\, j_n)\, |\mathbf{g}_1 \times \mathbf{g}_2|\, d\eta^1 d\eta^2\,. \tag{3.3.39}$$

The directional derivative of δW_{ext} may then be applied directly to its integrand, since the parametric space is invariant [27].

If we restrict traction boundary conditions to the special case of normal tractions, then $\mathbf{t} = t_n \mathbf{n}$ where t_n is the prescribed normal traction component. Then it can be shown that the linearization of δW_{ext} along $\Delta\mathbf{u}$ produces

$$D\left(\delta W_{\text{ext}}\right)[\Delta\mathbf{u}] = \int_{\partial b} (t_n \delta\mathbf{v} + w_n \delta\tilde{p}\,\mathbf{n} + j_n \delta\tilde{c}\,\mathbf{n}) \cdot \left(\frac{\partial \Delta\mathbf{u}}{\partial \eta^1} \times \mathbf{g}_2 + \mathbf{g}_1 \times \frac{\partial \Delta\mathbf{u}}{\partial \eta^2}\right) d\eta^1 d\eta^2\,. \tag{3.3.40}$$

The linearizations along $\Delta\tilde{p}$ and $\Delta\tilde{c}$ reduce to zero, $D\left(\delta W_{\text{ext}}\right)[\Delta\tilde{p}] = 0$ and $D\left(\delta W_{\text{ext}}\right)[\Delta\tilde{c}] = 0$.

3.3.3 Discretization

To discretize the virtual work relations, let

$$\begin{aligned}
\delta\mathbf{v} &= \sum_{a=1}^{m} N_a \delta\mathbf{v}_a\,, \quad & \Delta\mathbf{u} &= \sum_{b=1}^{m} N_b \Delta\mathbf{u}_b\,, \\
\delta\tilde{p} &= \sum_{a=1}^{m} N_a \delta\tilde{p}_a\,, \quad & \Delta\tilde{p} &= \sum_{b=1}^{m} N_b \Delta\tilde{p}_b\,, \\
\delta\tilde{c} &= \sum_{a=1}^{m} N_a \delta\tilde{c}_a\,, \quad & \Delta\tilde{c} &= \sum_{b=1}^{m} N_b \Delta\tilde{c}_b\,,
\end{aligned} \tag{3.3.41}$$

where N_a represents the interpolation functions over an element, $\delta\mathbf{v}_a$, $\delta\tilde{p}_a$, $\delta\tilde{c}_a$, $\Delta\mathbf{u}_a$, $\Delta\tilde{p}_a$ and $\Delta\tilde{c}_a$ respectively represent the nodal values of $\delta\mathbf{v}$, $\delta\tilde{p}$, $\delta\tilde{c}$, $\Delta\mathbf{u}$, $\Delta\tilde{p}$ and $\Delta\tilde{c}$; m is the number of nodes in an element.

The discretized form of δW_{int} in (3.3.3) may be written as

$$\delta W_{\text{int}} = \sum_{e=1}^{n_e} \sum_{k=1}^{n_{\text{int}}^{(e)}} W_k J_\eta \sum_{a=1}^{m} \left[\begin{array}{ccc} \delta \mathbf{v}_a & \delta \tilde{p}_a & \delta \tilde{c}_a \end{array} \right] \cdot \left[\begin{array}{c} \mathbf{r}_a^u \\ r_a^p \\ r_a^c \end{array} \right] , \tag{3.3.42}$$

where n_e is the number of elements in b, $n_{\text{int}}^{(e)}$ is the number of integration points in the $e-$th element, W_k is the quadrature weight associated with the $k-$th integration point, and J_η is the Jacobian of the transformation from the current spatial configuration to the parametric space of the element. In the above expression,

$$\begin{aligned} \mathbf{r}_a^u &= \boldsymbol{\sigma} \cdot \operatorname{grad} N_a \,, \\ r_a^p &= \mathbf{w} \cdot \operatorname{grad} N_a - N_a \frac{1}{J} \frac{\partial J}{\partial t} \,, \\ r_a^c &= \mathbf{j} \cdot \operatorname{grad} N_a - N_a \frac{1}{J} \frac{\partial}{\partial t} \left(J \varphi^w \tilde{\kappa} \tilde{c} \right) \,, \end{aligned} \tag{3.3.43}$$

and it is understood that J_η, $\mathbf{r}_a^u$, r_a^p and r_a^c are evaluated at the parametric coordinates of the $k-$th integration point. Since the parametric space is invariant, time derivatives are evaluated in a material frame. For example, the time derivative $D^s J\left(\mathbf{x}, t\right) / Dt$ appearing in (3.3.3) becomes $\partial J\left(\eta_k, t\right) / \partial t$ when evaluated at the parametric coordinates $\eta_k = \left(\eta_k^1, \eta_k^2, \eta_k^3\right)$ of the $k-$th integration point.

Similarly, the discretized form of $D\delta W_{\text{int}} = D\delta W_{\text{int}}\left[\Delta \mathbf{u}\right] + D\delta W_{\text{int}}\left[\Delta \tilde{p}\right] + D\delta W_{\text{int}}\left[\Delta \tilde{c}\right]$ may be written as

$$D\delta W_{\text{int}} = \sum_{e=1}^{n_e} \sum_{k=1}^{n_{\text{int}}^{(e)}} W_k J_\eta \sum_{a=1}^{m} \sum_{b=1}^{m} \left[\begin{array}{ccc} \delta \mathbf{v}_a & \delta \tilde{p}_a & \delta \tilde{c}_a \end{array} \right] \cdot \left[\begin{array}{ccc} \mathbf{K}_{ab}^{uu} & \mathbf{k}_{ab}^{up} & \mathbf{k}_{ab}^{uc} \\ \mathbf{k}_{ab}^{pu} & k_{ab}^{pp} & k_{ab}^{pc} \\ \mathbf{k}_{ab}^{cu} & k_{ab}^{cp} & k_{ab}^{cc} \end{array} \right] \cdot \left[\begin{array}{c} \Delta \mathbf{u}_b \\ \Delta \tilde{p}_b \\ \Delta \tilde{c}_b \end{array} \right] , \tag{3.3.44}$$

where the terms in the first column are the discretized form of the linearization along $\Delta \mathbf{u}$:

$$\mathbf{K}_{ab}^{uu} = \operatorname{grad} N_a \cdot \boldsymbol{\mathcal{C}} \cdot \operatorname{grad} N_b + \left(\operatorname{grad} N_a \cdot \boldsymbol{\sigma} \cdot \operatorname{grad} N_b \right) \mathbf{I} \,, \tag{3.3.45}$$

$$\mathbf{k}_{ab}^{pu} = \left(\mathbf{w}_b^u \right)^T \cdot \operatorname{grad} N_a + N_a \mathbf{q}_b^{pu} \,, \tag{3.3.46}$$

$$\mathbf{k}_{ab}^{cu} = \left(\mathbf{j}_b^u \right)^T \cdot \operatorname{grad} N_a + N_a \mathbf{q}_b^{cu} \,, \tag{3.3.47}$$

where

$$\begin{aligned} \mathbf{j}_b^u = {} & J \frac{\partial \tilde{\kappa}}{\partial J} \left[\mathbf{d} \cdot \left(-\varphi^w \operatorname{grad} \tilde{c} + \frac{\tilde{c}}{d_0} \mathbf{w} \right) \right] \otimes \operatorname{grad} N_b + \tilde{\kappa} \left(-\varphi^w \operatorname{grad} \tilde{c} + \frac{\tilde{c}}{d_0} \mathbf{w} \right) \cdot \mathbf{d} \cdot \operatorname{grad} N_b \\ & + \tilde{\kappa} \left(-\varphi^s \left(\mathbf{d} \cdot \operatorname{grad} \tilde{c} \right) \otimes \operatorname{grad} N_b + \frac{\tilde{c}}{d_0} \left[2 \left(\operatorname{grad} N_b \cdot \mathbf{w} \right) \mathbf{d} - \left(\mathbf{d} \cdot \mathbf{w} \right) \otimes \operatorname{grad} N_b \right] \right) + \tilde{\kappa} \frac{\tilde{c}}{d_0} \mathbf{d} \cdot \mathbf{w}_b^u \,, \end{aligned} \tag{3.3.48}$$

$$\mathbf{q}_b^{pu} = -\frac{1}{\Delta t} \operatorname{grad} N_b, \tag{3.3.49}$$

$$\mathbf{q}_b^{cu} = \tilde{c} \frac{\partial \left(J \phi^w \tilde{\kappa} \right)}{\partial J} \mathbf{q}_b^{pu}. \tag{3.3.50}$$

The terms in the second column of the stiffness matrix in (3.3.44) are the discretized form of the linearization along $\Delta \tilde{p}$:

$$\mathbf{k}_{ab}^{up} = -N_b \operatorname{grad} N_a, \tag{3.3.51}$$

$$k_{ab}^{pp} = -\operatorname{grad} N_a \cdot \tilde{\mathbf{k}} \cdot \operatorname{grad} N_b, \tag{3.3.52}$$

$$k_{ab}^{cp} = -\frac{\tilde{\kappa}\tilde{c}}{d_0} \operatorname{grad} N_a \cdot \mathbf{d} \cdot \tilde{\mathbf{k}} \cdot \operatorname{grad} N_b. \tag{3.3.53}$$

The terms in the third column of the stiffness matrix in (3.3.44) are the discretized form of the linearization along $\Delta\tilde{c}$:

$$\mathbf{k}_{ab}^{uc} = N_b \left(\boldsymbol{\sigma}_c' \cdot \operatorname{grad} N_a - R\theta \frac{\partial \left(\Phi\tilde{\kappa}\tilde{c}\right)}{\partial \tilde{c}} \operatorname{grad} N_a \right) , \tag{3.3.54}$$

$$k_{ab}^{pc} = \operatorname{grad} N_a \cdot \mathbf{w}_b^c \,, \tag{3.3.55}$$

$$k_{ab}^{cc} = \operatorname{grad} N_a \cdot \mathbf{j}_b^c + N_a q_b^c \,, \tag{3.3.56}$$

where

$$\begin{aligned} \mathbf{w}_b^c = & -N_b \tilde{\mathbf{k}}_c' \cdot \left(\operatorname{grad} \tilde{p} + R\theta \frac{\tilde{\kappa}}{d_0} \mathbf{d} \cdot \operatorname{grad} \tilde{c} \right) \\ & - R\theta \tilde{\mathbf{k}} \cdot \left[N_b \left(\frac{\partial}{\partial \tilde{c}} \left(\frac{\tilde{\kappa}}{d_0} \right) \mathbf{d} + \frac{\tilde{\kappa}}{d_0} \mathbf{d}_c' \right) \cdot \operatorname{grad} \tilde{c} + \frac{\tilde{\kappa}}{d_0} \mathbf{d} \cdot \operatorname{grad} N_b \right] , \end{aligned} \tag{3.3.57}$$

$$\mathbf{j}_b^c = N_b \left(\frac{\partial \tilde{\kappa}}{\partial \tilde{c}} \mathbf{d} + \tilde{\kappa} \mathbf{d}_c' \right) \cdot \left(-\varphi^w \operatorname{grad} \tilde{c} + \frac{\tilde{c}}{d_0} \mathbf{w} \right) + \tilde{\kappa} \mathbf{d} \cdot \left(-\varphi^w \operatorname{grad} N_b + \frac{\tilde{c}}{d_0} \mathbf{w}_b^c \right) , \tag{3.3.58}$$

$$q_b^c = -N_b \frac{\phi^w}{\Delta t} \frac{\partial \left(\tilde{\kappa}\tilde{c}\right)}{\partial \tilde{c}} \,. \tag{3.3.59}$$

The discretization of δW_{ext} in (3.3.3) has the form

$$\delta W_{\text{ext}} = \sum_{e=1}^{n_e} \sum_{k=1}^{n_{\text{int}}^{(e)}} W_k J_\eta \sum_{a=1}^{m} \left[\begin{array}{ccc} \delta \mathbf{v}_a & \delta \tilde{p}_a & \delta \tilde{c}_a \end{array} \right] \cdot \left[\begin{array}{c} N_a t_n \mathbf{n} \\ N_a w_n \\ N_a j_n \end{array} \right] , \tag{3.3.60}$$

where $J_\eta = |\mathbf{g}_1 \times \mathbf{g}_2|$. The summation is performed over all surface elements on which these boundary conditions are prescribed. The discretization of $-D\delta W_{\text{ext}}$ has the form

$$-D\delta W_{\text{ext}} = \sum_{e=1}^{n_e} \sum_{k=1}^{n_{\text{int}}^{(e)}} W_k J_\eta \sum_{a=1}^{m} \sum_{b=1}^{m} \left[\begin{array}{ccc} \delta \mathbf{v}_a & \delta \tilde{p}_a & \delta \tilde{c}_a \end{array} \right] \cdot \left[\begin{array}{ccc} \mathbf{K}_{ab}^{uu} & \mathbf{0} & \mathbf{0} \\ \mathbf{k}_{ab}^{pu} & 0 & 0 \\ \mathbf{k}_{ab}^{cu} & 0 & 0 \end{array} \right] \cdot \left[\begin{array}{c} \Delta \mathbf{u}_b \\ \Delta \tilde{p}_b \\ \Delta \tilde{c}_b \end{array} \right] , \tag{3.3.61}$$

where

$$\begin{aligned} \mathbf{K}_{ab}^{uu} &= t_n N_a \boldsymbol{\mathcal{A}} \left\{ \frac{\partial N_b}{\partial \eta^1} \mathbf{g}_2 - \frac{\partial N_b}{\partial \eta^2} \mathbf{g}_1 \right\} , \\ \mathbf{k}_{ab}^{pu} &= -w_n N_a \left(\frac{\partial N_b}{\partial \eta^1} \mathbf{g}_2 - \frac{\partial N_b}{\partial \eta^2} \mathbf{g}_1 \right) \times \mathbf{n} \,, \\ \mathbf{k}_{ab}^{cu} &= -j_n N_a \left(\frac{\partial N_b}{\partial \eta^1} \mathbf{g}_2 - \frac{\partial N_b}{\partial \eta^2} \mathbf{g}_1 \right) \times \mathbf{n} \,. \end{aligned} \tag{3.3.62}$$

In this expression, $\boldsymbol{\mathcal{A}}\{\mathbf{v}\}$ is the antisymmetric tensor whose dual vector is $\mathbf{v}$ (such that $\boldsymbol{\mathcal{A}}\{\mathbf{v}\} \cdot \mathbf{q} = \mathbf{v} \times \mathbf{q}$ for any vector $\mathbf{q}$).

3.4 Weak Formulation for Multiphasic Materials

The virtual work integral for a mixture of intrinsically incompressible constituents combines the balance of momentum for the mixture, the balance of mass for the mixture, and the balance of mass for each of the solutes. In addition, for charged mixtures, the condition of (2.7.8) may be enforced as a penalty constraint on each solute mass balance equation:

$$\begin{aligned}\delta W = &\int_b \delta\mathbf{v}\cdot\mathsf{div}\boldsymbol{\sigma}\,dv\\ &+\int_b \delta\tilde{p}\,\mathsf{div}\left(\mathbf{v}^s+\mathbf{w}\right)\,dv\\ &+\sum_{\alpha\neq s,w}\int_b \delta\tilde{c}^\alpha\left[\frac{1}{J^s}\frac{D^s}{Dt}\left(J^s\varphi^w\tilde{\kappa}^\alpha\tilde{c}^\alpha\right)+\mathsf{div}\mathbf{j}^\alpha+\sum_{\beta\neq s,w}z^\beta\mathsf{div}\mathbf{j}^\beta\right]\,dv\,,\end{aligned}\tag{3.4.1}$$

where $\delta\mathbf{v}$ is the virtual velocity of the solid, $\delta\tilde{p}$ is the virtual effective fluid pressure, and $\delta\tilde{c}^\alpha$ is the virtual molar energy of solute α. Here, b represents the mixture domain in the spatial frame and dv is an elemental volume in b. Applying the divergence theorem, δW may be split into internal and external contributions to the virtual work, $\delta W=\delta W_{\mathsf{ext}}-\delta W_{\mathsf{int}}$, where

$$\begin{aligned}\delta W_{\mathsf{int}} = &\int_b \boldsymbol{\sigma}:\delta\mathbf{D}\,dv+\int_b\left(\mathbf{w}\cdot\mathsf{grad}\delta\tilde{p}-\frac{\delta\tilde{p}}{J^s}\frac{D^sJ^s}{Dt}\right)\,dv\\ &+\sum_{\alpha\neq s,w}\int_b\left[\mathbf{j}^\alpha\cdot\mathsf{grad}\delta\tilde{c}^\alpha-\frac{\delta\tilde{c}^\alpha}{J^s}\frac{D^s}{Dt}\left(J^s\varphi^w\tilde{\kappa}^\alpha\tilde{c}^\alpha\right)\right]\,dv\\ &+\sum_{\alpha\neq s,w}\int_b\mathsf{grad}\delta\tilde{c}^\alpha\cdot\sum_{\beta\neq s,w}z^\beta\mathbf{j}^\beta\,dv\,,\end{aligned}\tag{3.4.2}$$

and

$$\delta W_{\mathsf{ext}}=\int_{\partial b}\left[\delta\mathbf{v}\cdot\mathbf{t}+\delta\tilde{p}\,w_n+\sum_{\alpha\neq s,w}\delta\tilde{c}^\alpha\left(j_n^\alpha+\sum_{\beta\neq s,w}z^\beta j_n^\beta\right)\right]\,da\,.\tag{3.4.3}$$

In these expressions, $\delta\mathbf{D}=\left(\mathsf{grad}\delta\mathbf{v}+\mathsf{grad}^T\delta\mathbf{v}\right)/2$, ∂b is the boundary of b, and da is an elemental area on ∂b. In this finite element formulation, $\mathbf{u}$, $\tilde{p}$ and $\tilde{c}^\alpha$ are used as nodal variables, and essential boundary conditions may be prescribed on these variables. Natural boundary conditions are prescribed to the mixture traction, $\mathbf{t}=\boldsymbol{\sigma}\cdot\mathbf{n}$, normal fluid flux, $w_n=\mathbf{w}\cdot\mathbf{n}$, and normal solute flux, $j_n^\alpha=\mathbf{j}^\alpha\cdot\mathbf{n}$, where $\mathbf{n}$ is the outward unit normal to ∂b. To solve the system $\delta W=0$ for nodal values of $\mathbf{u}$, $\tilde{p}$ and $\tilde{c}^\alpha$, it is necessary to linearize these equations, as shown for example in Sections 3.3.1-3.3.2 for biphasic-solute materials. If the mixture is charged, it is also necessary to solve for the electric potential ψ by solving the algebraic relation of the electroneutrality condition in (2.7.4), which may be rewritten as

$$c^F+\sum_{\beta\neq s,w}z^\beta\tilde{\kappa}^\beta\tilde{c}^\beta=0\,.\tag{3.4.4}$$

In the special case of a triphasic mixture, where solutes consist of two counter-ions ($\alpha=+,-$), this equation may be solved in closed form to produce

$$\psi=\frac{1}{z^\alpha}\frac{R\theta}{F_c}\ln\left(\frac{2z^\alpha\hat{\kappa}^\alpha\tilde{c}^\alpha}{-c^F\pm\sqrt{\left(c^F\right)^2+4\left(z^\alpha\right)^2\left(\hat{\kappa}^+\tilde{c}^+\right)\left(\hat{\kappa}^-\tilde{c}^-\right)}}\right),\quad\alpha=+,-,\tag{3.4.5}$$

Only the positive root is valid in the argument of the logarithm function.

3.4.1 Linearization along $\Delta\mathbf{u}$

The linearization of the first term in δW_{int} along $\Delta\mathbf{u}$ yields

$$\left(\mathbf{S} : \delta\dot{\mathbf{E}}\right)[\Delta\mathbf{u}]\, dV = \left[\delta\mathbf{d}^s : \boldsymbol{\mathcal{C}} : \Delta\boldsymbol{\varepsilon} + \boldsymbol{\sigma} : \left(\operatorname{grad}^T \Delta\mathbf{u} \cdot \operatorname{grad}\delta\mathbf{v}\right)\right] dv\,, \tag{3.4.6}$$

where $\boldsymbol{\mathcal{C}}$ is the spatial elasticity tensor of the mixture,

$$\boldsymbol{\mathcal{C}} = \boldsymbol{\mathcal{C}}^e - \left(\tilde{p} + R\theta\,\Phi\sum_\beta \tilde{\kappa}^\beta\tilde{c}^\beta\right)(\mathbf{I}\otimes\mathbf{I} - 2\mathbf{I}\odot\mathbf{I}) - R\theta\sum_\beta \tilde{c}^\beta\, J\frac{\partial\left(\Phi\tilde{\kappa}^\beta\right)}{\partial J}\mathbf{I}\otimes\mathbf{I}\,, \tag{3.4.7}$$

and $\boldsymbol{\mathcal{C}}^e$ is the spatial elasticity tensor of the solid matrix,

$$\boldsymbol{\mathcal{C}}^e = J^{-1}\left(\mathbf{F}\oslash\mathbf{F}\right) : 2\frac{\partial\mathbf{S}^e}{\partial\mathbf{C}} : \left(\mathbf{F}^T\oslash\mathbf{F}^T\right)\,. \tag{3.4.8}$$

The linearization of the second term is

$$D\left(\mathbf{W}\cdot\operatorname{Grad}\delta\tilde{p}\right)[\Delta\mathbf{u}]\, dV = \operatorname{grad}\delta\tilde{p}\cdot\mathbf{w}'_u\, dv\,, \tag{3.4.9}$$

where

$$\begin{aligned}\mathbf{w}'_u \equiv &-\left(\tilde{\boldsymbol{\mathcal{K}}} : \Delta\boldsymbol{\varepsilon}\right)\cdot\left(\operatorname{grad}\tilde{p} + R\theta\sum_\beta\frac{\tilde{\kappa}^\beta}{d_0^\beta}\mathbf{d}^\beta\cdot\operatorname{grad}\tilde{c}^\beta\right)\\ &-\tilde{\mathbf{k}}\cdot R\theta\sum_\beta\left(\left[J\frac{\partial}{\partial J}\left(\frac{\tilde{\kappa}^\beta}{d_0^\beta}\right) - \frac{\tilde{\kappa}^\beta}{d_0^\beta}\right](\operatorname{div}\Delta\mathbf{u})\,\mathbf{d}^\beta + \frac{\tilde{\kappa}^\beta}{d_0^\beta}\left(2\Delta\boldsymbol{\varepsilon}\cdot\mathbf{d}^\beta + \boldsymbol{\mathcal{D}}^\beta : \Delta\boldsymbol{\varepsilon}\right)\right)\cdot\operatorname{grad}\tilde{c}^\beta\end{aligned} \tag{3.4.10}$$

with

$$\begin{aligned}\tilde{\boldsymbol{\mathcal{K}}} &= J^{-1}\left(\mathbf{F}\oslash\mathbf{F}\right) : 2\frac{\partial\tilde{\mathbf{K}}}{\partial\mathbf{C}} : \left(\mathbf{F}^T\oslash\mathbf{F}^T\right)\,,\\ \boldsymbol{\mathcal{D}}^\alpha &= J^{-1}\left(\mathbf{F}\oslash\mathbf{F}\right) : 2\frac{\partial\mathbf{D}^\alpha}{\partial\mathbf{C}} : \left(\mathbf{F}^T\oslash\mathbf{F}^T\right)\,,\end{aligned} \tag{3.4.11}$$

representing the spatial tangents, with respect to the strain, of the effective permeability and solute diffusivity, respectively. These fourth-order tensors exhibit minor symmetries but not major symmetry, as described recently [9]. Since $\tilde{\mathbf{K}}$ is given by substituting $(2.6.13)_3$ into $(3.3.8)_1$, the evaluation of $\tilde{\boldsymbol{\mathcal{K}}}$ is rather involved and it can be shown that

$$\tilde{\boldsymbol{\mathcal{K}}} = \left(\tilde{\mathbf{k}}\oslash\tilde{\mathbf{k}}\right) : \left[\left(\mathbf{k}^{-1}\oslash\mathbf{k}^{-1}\right) : \boldsymbol{\mathcal{K}} + \boldsymbol{\mathcal{G}}\right]\,, \tag{3.4.12}$$

where

$$\boldsymbol{\mathcal{K}} = J^{-1}\left(\mathbf{F}\oslash\mathbf{F}\right) : 2\frac{\partial\mathbf{K}}{\partial\mathbf{C}} : \left(\mathbf{F}^T\oslash\mathbf{F}^T\right)\,, \tag{3.4.13}$$

and

$$\boldsymbol{\mathcal{G}} = \frac{R\theta}{\varphi^w}\sum_\alpha\frac{\tilde{\kappa}^\alpha\tilde{c}^\alpha}{d_0^\alpha}\begin{pmatrix}\left(\dfrac{1}{\varphi^w} - \dfrac{J}{\tilde{\kappa}^\alpha}\dfrac{\partial\tilde{\kappa}^\alpha}{\partial J}\right)\left(\mathbf{I} - \dfrac{\mathbf{d}^\alpha}{d_0^\alpha}\right)\otimes\mathbf{I}\\ +2\left(\mathbf{I}\odot\dfrac{\mathbf{d}^\alpha}{d_0^\alpha} + \dfrac{\mathbf{d}^\alpha}{d_0^\alpha}\odot\mathbf{I} - \mathbf{I}\odot\mathbf{I}\right)\\ -\dfrac{\mathbf{d}^\alpha}{d_0^\alpha}\otimes\mathbf{I} + \dfrac{\boldsymbol{\mathcal{D}}^\alpha}{d_0^\alpha}\end{pmatrix}\,. \tag{3.4.14}$$

The next term in δW_{int} linearizes to

$$- D\left(\delta\tilde{p}\frac{\partial J}{\partial t}\right)[\Delta\mathbf{u}]\; dV = -\delta\tilde{p}\frac{1}{\Delta t}\operatorname{div}\Delta\mathbf{u}\, dv\,, \tag{3.4.15}$$

where we used a backward difference scheme to approximate the time derivative,

$$\frac{\partial J}{\partial t} \approx \frac{1}{\Delta t}\left(J - J^{-\Delta t}\right)\,, \tag{3.4.16}$$

and Δt represents the time increment relative to the previous time point. The next term is given by

$$D\left(\mathbf{J}^{\alpha}\cdot\operatorname{Grad}\delta\tilde{c}^{\alpha}\right)[\Delta\mathbf{u}]\; dV = \operatorname{grad}\delta\tilde{c}^{\alpha}\cdot\mathbf{j}_{u}^{\alpha\prime}\, dv\,, \tag{3.4.17}$$

where

$$\begin{aligned}\mathbf{j}_{u}^{\alpha\prime} \equiv J^{-1}\mathbf{F}\cdot D\mathbf{J}\,[\Delta\mathbf{u}] = &\left(J\frac{\partial\tilde{\kappa}^{\alpha}}{\partial J}\left(\operatorname{div}\Delta\mathbf{u}\right)\mathbf{d}^{\alpha} + \tilde{\kappa}^{\alpha}\boldsymbol{\mathcal{D}}^{\alpha} : \Delta\boldsymbol{\varepsilon}\right)\cdot\mathbf{g}^{\alpha}\\ &+ \tilde{\kappa}^{\alpha}\mathbf{d}^{\alpha}\cdot\left(-\varphi^{s}\left(\operatorname{div}\Delta\mathbf{u}\right)\operatorname{grad}\tilde{c}^{\alpha} + \left(2\Delta\boldsymbol{\varepsilon} - \left(\operatorname{div}\Delta\mathbf{u}\right)\mathbf{I}\right)\cdot\frac{\tilde{c}^{\alpha}}{d_{0}^{\alpha}}\mathbf{w} + \frac{\tilde{c}^{\alpha}}{d_{0}^{\alpha}}\mathbf{w}_{u}^{\prime}\right)\end{aligned}\,. \tag{3.4.18}$$

where

$$\mathbf{g}^{\alpha} = -\varphi^{w}\operatorname{grad}\tilde{c}^{\alpha} + \frac{\tilde{c}^{\alpha}}{d_{0}^{\alpha}}\mathbf{w}\,. \tag{3.4.19}$$

Using a backward difference scheme for the time derivative, the last term is

$$D\left(\delta\tilde{c}^{\alpha}\frac{\partial\left(J\varphi^{w}\tilde{\kappa}^{\alpha}\tilde{c}^{\alpha}\right)}{\partial t}\right)[\Delta\mathbf{u}]\; dV = \frac{\delta\tilde{c}^{\alpha}}{\Delta t}\frac{\partial\left(J\varphi^{w}\tilde{\kappa}^{\alpha}\right)}{\partial J}\tilde{c}^{\alpha}\operatorname{div}\Delta\mathbf{u}\, dv\,. \tag{3.4.20}$$

3.4.2 Linearization along $\Delta\tilde{p}$

The linearization of the various terms in δW_{int} along $\Delta\tilde{p}$ yields

$$D\left(\mathbf{S} : \delta\dot{\mathbf{E}}\right)[\Delta\tilde{p}]\; dV = -\Delta\tilde{p}\,\operatorname{div}\delta\mathbf{v}\, dv\,, \tag{3.4.21}$$

$$D\left(\mathbf{W}\cdot\operatorname{Grad}\delta\tilde{p} - \delta\tilde{p}\frac{\partial J}{\partial t}\right)[\Delta\tilde{p}]\; dV = -\operatorname{grad}\delta\tilde{p}\cdot\tilde{\mathbf{k}}\cdot\operatorname{grad}\Delta\tilde{p}\, dv\,, \tag{3.4.22}$$

$$D\left(\mathbf{J}^{\alpha}\cdot\operatorname{Grad}\delta\tilde{c}^{\alpha} - \delta\tilde{c}^{\alpha}\frac{\partial\left(J\varphi^{w}\tilde{\kappa}^{\alpha}\tilde{c}^{\alpha}\right)}{\partial t}\right)[\Delta\tilde{p}]\; dV = -\frac{\tilde{\kappa}^{\alpha}\tilde{c}^{\alpha}}{d_{0}^{\alpha}}\operatorname{grad}\delta\tilde{c}^{\alpha}\cdot\mathbf{d}^{\alpha}\cdot\tilde{\mathbf{k}}\cdot\operatorname{grad}\Delta\tilde{p}\, dv\,. \tag{3.4.23}$$

3.4.3 Linearization along $\Delta\tilde{c}^{\gamma}$

The linearization of the first term in δW_{int} along $\Delta\tilde{c}^{\gamma}$ yields

$$D\left(\mathbf{S} : \delta\dot{\mathbf{E}}\right)[\Delta\tilde{c}^{\gamma}]\, dV = \Delta\tilde{c}^{\gamma}\left(\boldsymbol{\sigma}_{\gamma}^{\prime} : \delta\mathbf{d} - R\theta\frac{\partial\left(\Phi\tilde{\kappa}^{\alpha}\tilde{c}^{\alpha}\right)}{\partial\tilde{c}^{\gamma}}\operatorname{div}\delta\mathbf{v}\right)\, dv\,, \tag{3.4.24}$$

where

$$\boldsymbol{\sigma}_{\gamma}^{\prime} = J^{-1}\mathbf{F}\cdot\frac{\partial\mathbf{S}^{e}}{\partial\tilde{c}^{\gamma}}\cdot\mathbf{F}^{T} \tag{3.4.25}$$

represents the spatial tangent of the stress with respect to the effective concentration. The next term is

$$D\left(\mathbf{W}\cdot\operatorname{Grad}\delta\tilde{p}\right)\left[\Delta\tilde{c}^{\gamma}\right]\,dV=\operatorname{grad}\delta\tilde{p}\cdot\mathbf{w}'_{\gamma}\,dv\,, \tag{3.4.26}$$

where

$$\begin{aligned}\mathbf{w}'_{\gamma}\equiv J^{-1}\mathbf{F}\cdot D\mathbf{W}\left[\Delta\tilde{c}^{\gamma}\right]=-\tilde{\mathbf{k}}'_{\gamma}\cdot\left(\operatorname{grad}\tilde{p}+R\theta\sum_{\beta}\frac{\tilde{\kappa}^{\beta}}{d_0^{\beta}}\mathbf{d}^{\beta}\cdot\operatorname{grad}\tilde{c}^{\beta}\right)\Delta\tilde{c}^{\gamma}\\ -R\theta\tilde{\mathbf{k}}\cdot\frac{\tilde{\kappa}^{\gamma}}{d_0^{\gamma}}\mathbf{d}^{\gamma}\cdot\operatorname{grad}\Delta\tilde{c}^{\gamma}-\Delta\tilde{c}^{\gamma}R\theta\tilde{\mathbf{k}}\cdot\sum_{\beta}\left(\frac{\partial}{\partial\tilde{c}^{\gamma}}\left(\frac{\tilde{\kappa}^{\beta}}{d_0^{\beta}}\right)\mathbf{d}^{\beta}+\frac{\tilde{\kappa}^{\beta}}{d_0^{\beta}}\mathbf{d}^{\beta\prime}_{\gamma}\right)\cdot\operatorname{grad}\tilde{c}^{\beta}\end{aligned} \tag{3.4.27}$$

and

$$\tilde{\mathbf{k}}'_{\gamma}=J^{-1}\mathbf{F}\cdot\frac{\partial\tilde{\mathbf{K}}}{\partial\tilde{c}^{\gamma}}\cdot\mathbf{F}^{T},\quad\mathbf{d}^{\beta\prime}_{\gamma}=J^{-1}\mathbf{F}\cdot\frac{\partial\mathbf{d}^{\beta}}{\partial\tilde{c}^{\gamma}}\cdot\mathbf{F}^{T} \tag{3.4.28}$$

are the spatial tangents of the effective hydraulic permeability and solute diffusivity with respect to the effective concentration.

The next term reduces to

$$-D\left(\delta\tilde{p}\frac{\partial J}{\partial t}\right)\left[\Delta\tilde{c}^{\gamma}\right]\,dV=0\,. \tag{3.4.29}$$

The following term is

$$D\left(\mathbf{J}^{\alpha}\cdot\operatorname{Grad}\delta\tilde{c}^{\alpha}\right)\left[\Delta\tilde{c}^{\gamma}\right]\,dV=\operatorname{grad}\delta\tilde{c}^{\alpha}\cdot\mathbf{j}^{\alpha\prime}_{\gamma}\,dv\,, \tag{3.4.30}$$

where

$$\begin{aligned}\mathbf{j}^{\alpha\prime}_{\gamma}\equiv J^{-1}\mathbf{F}\cdot D\mathbf{J}^{\alpha}\left[\Delta\tilde{c}^{\gamma}\right]=\Delta\tilde{c}^{\gamma}\left(\frac{\partial\tilde{\kappa}^{\alpha}}{\partial\tilde{c}^{\gamma}}\mathbf{d}^{\alpha}+\tilde{\kappa}^{\alpha}\mathbf{d}^{\alpha\prime}_{\gamma}\right)\cdot\mathbf{g}^{\alpha}\\ +\tilde{\kappa}^{\alpha}\mathbf{d}^{\alpha}\cdot\left(-\varphi^{w}\delta_{\alpha\gamma}\operatorname{grad}\Delta\tilde{c}^{\gamma}+\frac{\Delta\tilde{c}^{\gamma}}{d_0^{\alpha}}\left(\delta_{\alpha\gamma}-\frac{\tilde{c}^{\alpha}}{d_0^{\alpha}}\frac{\partial d_0^{\alpha}}{\partial\tilde{c}^{\gamma}}\right)\mathbf{w}+\frac{\tilde{c}^{\alpha}}{d_0^{\alpha}}\mathbf{w}'_{\gamma}\right)\,.\end{aligned} \tag{3.4.31}$$

The last term is

$$D\left(\frac{\partial\left(J\varphi^{w}\tilde{\kappa}^{\alpha}\tilde{c}^{\alpha}\right)}{\partial t}\delta\tilde{c}^{\alpha}\right)\left[\Delta\tilde{c}^{\gamma}\right]\,dV=\delta\tilde{c}^{\alpha}\frac{\varphi^{w}}{\Delta t}\frac{\partial\left(\tilde{\kappa}^{\alpha}\tilde{c}^{\alpha}\right)}{\partial\tilde{c}^{\gamma}}\Delta\tilde{c}^{\gamma}\,dv\,, \tag{3.4.32}$$

where we similarly used a backward difference scheme to discretize the time derivative.

3.4.4 Linearization of External Virtual Work

The linearization of δW_{ext} in (3.4.3) depends on whether natural boundary conditions are prescribed as area densities or total net values over an area. Thus, in the case when $\mathbf{t}\,da$ (net force), $w_n da$ (net volumetric flow rate), or $\tilde{j}_n^{\alpha} da$ (net effective molar flow rate) are prescribed over the elemental area da, there is no variation in δW_{ext} and it follows that $D\delta W_{\text{ext}}=0$. Alternatively, in the case when $\mathbf{t}$, w_n or $\tilde{j}_n^{\alpha}$ are prescribed, the linearization may be performed by evaluating the integral in the parametric space of the boundary surface ∂b, with parametric coordinates (η^1,η^2). Accordingly, for a point $\mathbf{x}\left(\eta^1,\eta^2\right)$ on ∂b, surface tangents (covariant basis vectors) are given by

$$\mathbf{g}_{\alpha}=\frac{\partial\mathbf{x}}{\partial\eta^{\alpha}},\quad(\alpha=1,2) \tag{3.4.33}$$

and the outward unit normal is

$$\mathbf{n} = \frac{\mathbf{g}_1 \times \mathbf{g}_2}{|\mathbf{g}_1 \times \mathbf{g}_2|} \,. \tag{3.4.34}$$

The elemental area on ∂b is $da = |\mathbf{g}_1 \times \mathbf{g}_2| \, d\eta^1 d\eta^2$. Consequently, the external virtual work integral may be rewritten as

$$\delta W_{\text{ext}} = \int_{\partial b} \left(\delta \mathbf{v} \cdot \mathbf{t} + \delta \tilde{p} \, w_n + \sum_{\alpha \neq s,w} \delta \tilde{c}^{\alpha} \tilde{j}_n^{\alpha} \right) |\mathbf{g}_1 \times \mathbf{g}_2| \; d\eta^1 d\eta^2 \,, \tag{3.4.35}$$

where

$$\tilde{j}_n^{\alpha} = j_n^{\alpha} + \sum_{\beta \neq s,w} z^{\beta} j_n^{\beta} \,. \tag{3.4.36}$$

The directional derivative of δW_{ext} may then be applied directly to its integrand, since the parametric space is invariant [27].

If we restrict traction boundary conditions to the special case of normal tractions, then $\mathbf{t} = t_n \mathbf{n}$ where t_n is the prescribed normal traction component. Then it can be shown that the linearization of δW_{ext} along $\Delta \mathbf{u}$ produces

$$D\left(\delta W_{\text{ext}}\right)[\Delta \mathbf{u}] = \int_{\partial b} \left(t_n \delta \mathbf{v} + w_n \delta \tilde{p} \, \mathbf{n} + \sum_{\alpha \neq s,w} \delta \tilde{c}^{\alpha} \tilde{j}_n^{\alpha} \, \mathbf{n} \right) \cdot \left(\frac{\partial \Delta \mathbf{u}}{\partial \eta^1} \times \mathbf{g}_2 + \mathbf{g}_1 \times \frac{\partial \Delta \mathbf{u}}{\partial \eta^2} \right) d\eta^1 d\eta^2 \,. \tag{3.4.37}$$

The linearizations along $\Delta \tilde{p}$ and $\Delta \tilde{c}^{\gamma}$ reduce to zero, $D\left(\delta W_{\text{ext}}\right)[\Delta \tilde{p}] = 0$ and $D\left(\delta W_{\text{ext}}\right)[\Delta \tilde{c}^{\gamma}] = 0$.

3.4.5 Discretization

To discretize the virtual work relations, let

$$\begin{aligned}
\delta \mathbf{v} &= \sum_{a=1}^{m} N_a \delta \mathbf{v}_a \,, \quad & \Delta \mathbf{u} &= \sum_{b=1}^{m} N_b \Delta \mathbf{u}_b \,, \\
\delta \tilde{p} &= \sum_{a=1}^{m} N_a \delta \tilde{p}_a \,, \quad & \Delta \tilde{p} &= \sum_{b=1}^{m} N_b \Delta \tilde{p}_b \,, \\
\delta \tilde{c}^{\alpha} &= \sum_{a=1}^{m} N_a \delta \tilde{c}_a^{\alpha} \,, \quad & \Delta \tilde{c}^{\gamma} &= \sum_{b=1}^{m} N_b \Delta \tilde{c}_b^{\gamma} \,,
\end{aligned} \tag{3.4.38}$$

where N_a represents the interpolation functions over an element, $\delta \mathbf{v}_a$, $\delta \tilde{p}_a$, $\delta \tilde{c}_a^{\alpha}$, $\Delta \mathbf{u}_a$, $\Delta \tilde{p}_a$ and $\Delta \tilde{c}_a^{\gamma}$ respectively represent the nodal values of $\delta \mathbf{v}$, $\delta \tilde{p}$, $\delta \tilde{c}^{\alpha}$, $\Delta \mathbf{u}$, $\Delta \tilde{p}$ and $\Delta \tilde{c}^{\gamma}$; m is the number of nodes in an element.

The discretized form of δW_{int} in (3.3.3) may be written as

$$\delta W_{\text{int}} = \sum_{e=1}^{n_e} \sum_{k=1}^{n_{\text{int}}^{(e)}} W_k J_\eta \sum_{a=1}^{m} \begin{bmatrix} \delta \mathbf{v}_a & \delta \tilde{p}_a & \delta \tilde{c}_a^{\alpha} & \delta \tilde{c}_a^{\beta} \end{bmatrix} \cdot \begin{bmatrix} \mathbf{r}_a^u \\ r_a^p \\ r_a^{\alpha} \\ r_a^{\beta} \end{bmatrix} \,, \tag{3.4.39}$$

where n_e is the number of elements in b, $n_{\text{int}}^{(e)}$ is the number of integration points in the $e-$th element, W_k is the quadrature weight associated with the $k-$th integration point, and J_η is the

Jacobian of the transformation from the current spatial configuration to the parametric space of the element. In the above expression,

$$\begin{aligned} \mathbf{r}_a^u &= \boldsymbol{\sigma} \cdot \operatorname{grad} N_a \,, \\ r_a^p &= \mathbf{w} \cdot \operatorname{grad} N_a - N_a \frac{1}{J} \frac{\partial J}{\partial t} \,, \\ r_a^\alpha &= \mathbf{j}^\alpha \cdot \operatorname{grad} N_a - N_a \frac{1}{J} \frac{\partial}{\partial t} \left(J \varphi^w \tilde{\kappa}^\alpha \tilde{c}^\alpha \right) \,, \end{aligned} \tag{3.4.40}$$

and it is understood that J_η, $\mathbf{r}_a^u$, r_a^p and r_a^α are evaluated at the parametric coordinates of the $k-$th integration point. Since the parametric space is invariant, time derivatives are evaluated in a material frame. For example, the time derivative $D^s J\left(\mathbf{x}, t\right) / Dt$ appearing in (3.3.3) becomes $\partial J\left(\eta_k, t\right) / \partial t$ when evaluated at the parametric coordinates $\eta_k = \left(\eta_k^1, \eta_k^2, \eta_k^3\right)$ of the $k-$th integration point. All time derivatives are discretized using a backward difference scheme.

Similarly, the discretized form of $D\delta W_{\text{int}} = D\delta W_{\text{int}}\left[\Delta \mathbf{u}\right] + D\delta W_{\text{int}}\left[\Delta \tilde{p}\right] + \sum_\gamma D\delta W_{\text{int}}\left[\Delta \tilde{c}^\gamma\right]$ may be written as

$$D\delta W_{\text{int}} = \sum_{e=1}^{n_e} \sum_{k=1}^{n_{\text{int}}^{(e)}} W_k J_\eta \sum_{a=1}^{m} \sum_{b=1}^{m} \left[\begin{array}{cccc} \delta \mathbf{v}_a & \delta \tilde{p}_a & \delta \tilde{c}_a^\alpha & \delta \tilde{c}_a^\beta \end{array} \right] \cdot \left[\begin{array}{cccc} \mathbf{K}_{ab}^{uu} & \mathbf{k}_{ab}^{up} & \mathbf{k}_{ab}^{u\alpha} & \mathbf{k}_{ab}^{u\beta} \\ \mathbf{k}_{ab}^{pu} & k_{ab}^{pp} & k_{ab}^{p\alpha} & k_{ab}^{p\beta} \\ \mathbf{k}_{ab}^{\alpha u} & k_{ab}^{\alpha p} & k_{ab}^{\alpha\alpha} & k_{ab}^{\alpha\beta} \\ \mathbf{k}_{ab}^{\beta u} & k_{ab}^{\beta p} & k_{ab}^{\beta\alpha} & k_{ab}^{\beta\beta} \end{array} \right] \cdot \left[\begin{array}{c} \Delta \mathbf{u}_b \\ \Delta \tilde{p}_b \\ \Delta \tilde{c}_b^\alpha \\ \Delta \tilde{c}_b^\beta \end{array} \right] , \tag{3.4.41}$$

where the terms in the first column are the discretized form of the linearization along $\Delta \mathbf{u}$:

$$\mathbf{K}_{ab}^{uu} = \operatorname{grad} N_a \cdot \boldsymbol{\mathcal{C}} \cdot \operatorname{grad} N_b + \left(\operatorname{grad} N_a \cdot \boldsymbol{\sigma} \cdot \operatorname{grad} N_b \right) \mathbf{I} \,, \tag{3.4.42}$$

$$\mathbf{k}_{ab}^{pu} = \left(\mathbf{w}_b^u \right)^T \cdot \operatorname{grad} N_a + N_a \mathbf{q}_b^{pu} \,, \tag{3.4.43}$$

$$\mathbf{k}_{ab}^{\alpha u} = \left(\mathbf{j}_b^{\alpha u} + \sum\nolimits_\beta z^\beta \mathbf{j}_b^{\beta u} \right)^T \cdot \operatorname{grad} N_a + N_a \mathbf{q}_b^{\alpha u} \,, \tag{3.4.44}$$

where

$$\begin{aligned} \mathbf{w}_b^u = {} & \mathbf{g}^p \cdot \tilde{\boldsymbol{\mathcal{K}}} \cdot \operatorname{grad} N_b \\ & - R\theta \sum_\beta \frac{1}{d_0^\beta} \left(J \frac{\partial \tilde{\kappa}^\beta}{\partial J} - \tilde{\kappa}^\beta \right) \tilde{\mathbf{k}} \cdot \mathbf{d}^\beta \cdot \left(\operatorname{grad} \tilde{c}^\beta \otimes \operatorname{grad} N_b \right) \\ & - R\theta \sum_\beta \frac{\tilde{\kappa}^\beta}{d_0^\beta} \left[\tilde{\mathbf{k}} \cdot \left(\operatorname{grad} N_b \otimes \operatorname{grad} \tilde{c}^\beta \right) \cdot \mathbf{d}^\beta + \left(\operatorname{grad} N_b \cdot \mathbf{d}^\beta \cdot \operatorname{grad} \tilde{c}^\beta \right) \tilde{\mathbf{k}} \right] \\ & - R\theta \sum_\beta \frac{\tilde{\kappa}^\beta}{d_0^\beta} \tilde{\mathbf{k}} \cdot \left(\operatorname{grad} \tilde{c}^\beta \cdot \boldsymbol{\mathcal{D}}^\beta \cdot \operatorname{grad} N_b \right) \,, \end{aligned} \tag{3.4.45}$$

$$\mathbf{g}^p = - \operatorname{grad} \tilde{p} - R\theta \sum_\beta \frac{\tilde{\kappa}^\beta}{d_0^\beta} \mathbf{d}^\beta \cdot \operatorname{grad} \tilde{c}^\beta \,. \tag{3.4.46}$$

$$\begin{aligned} \mathbf{j}_b^{\alpha u} = {} & J \frac{\partial \tilde{\kappa}^\alpha}{\partial J} \mathbf{d}^\alpha \cdot \left(\mathbf{g}^\alpha \otimes \operatorname{grad} N_b \right) + \tilde{\kappa}^\alpha \mathbf{g}^\alpha \cdot \boldsymbol{\mathcal{D}}^\alpha \cdot \operatorname{grad} N_b \\ & + \tilde{\kappa}^\alpha \mathbf{d}^\alpha \cdot \left(\operatorname{grad} N_b \otimes \mathbf{w} - \mathbf{w} \otimes \operatorname{grad} N_b + \left(\operatorname{grad} N_b \cdot \mathbf{w} \right) \mathbf{I} + \mathbf{w}_b^u \right) \frac{\tilde{c}^\alpha}{d_0^\alpha} \\ & - \varphi^s \tilde{\kappa}^\alpha \mathbf{d}^\alpha \cdot \operatorname{grad} \tilde{c}^\alpha \otimes \operatorname{grad} N_b \,, \end{aligned} \tag{3.4.47}$$

$$\mathbf{g}^{\alpha} = -\varphi^{w} \operatorname{grad} \tilde{c}^{\alpha} + \frac{\tilde{c}^{\alpha}}{d_0^{\alpha}} \mathbf{w} \,, \tag{3.4.48}$$

$$\mathbf{q}_b^{pu} = -\frac{1}{\Delta t} \operatorname{grad} N_b \,, \tag{3.4.49}$$

$$\mathbf{q}_b^{\alpha u} = \tilde{c}^{\alpha} \frac{\partial \left(J \varphi^{w} \tilde{\kappa}^{\alpha} \right)}{\partial J} \mathbf{q}_b^{pu} \,. \tag{3.4.50}$$

The terms in the second column of the stiffness matrix in (3.3.44) are the discretized form of the linearization along $\Delta \tilde{p}$:

$$\mathbf{k}_{ab}^{up} = -N_b \operatorname{grad} N_a \,, \tag{3.4.51}$$

$$k_{ab}^{pp} = -\operatorname{grad} N_a \cdot \tilde{\mathbf{k}} \cdot \operatorname{grad} N_b \,, \tag{3.4.52}$$

$$k_{ab}^{\alpha p} = \operatorname{grad} N_a \cdot \left(\mathbf{j}_b^{\alpha p} + \sum_{\beta} z^{\beta} \mathbf{j}_b^{\beta p} \right) \,, \tag{3.4.53}$$

where

$$\mathbf{j}_b^{\alpha p} = -\frac{\tilde{\kappa}^{\alpha} \tilde{c}^{\alpha}}{d_0^{\alpha}} \mathbf{d}^{\alpha} \cdot \tilde{\mathbf{k}} \cdot \operatorname{grad} N_b \,. \tag{3.4.54}$$

The terms in the third column of the stiffness matrix in (3.3.44) are the discretized form of the linearization along $\Delta \tilde{c}^{\gamma}$:

$$\mathbf{k}_{ab}^{u\alpha} = N_b \left(\boldsymbol{\sigma}'_{\alpha} - R\theta \left[\Phi \tilde{\kappa}^{\alpha} + \sum_{\beta} \left(\frac{\partial \Phi}{\partial \tilde{c}^{\alpha}} \tilde{\kappa}^{\beta} + \Phi \frac{\partial \tilde{\kappa}^{\beta}}{\partial \tilde{c}^{\alpha}} \right) \tilde{c}^{\beta} \right] \mathbf{I} \right) \cdot \operatorname{grad} N_a \,, \tag{3.4.55}$$

$$k_{ab}^{p\alpha} = \operatorname{grad} N_a \cdot \mathbf{w}_b^{\alpha} \,, \tag{3.4.56}$$

$$k_{ab}^{\alpha\gamma} = \operatorname{grad} N_a \cdot \left(\mathbf{j}_b^{\alpha\gamma} + \sum_{\beta} z^{\beta} \mathbf{j}_b^{\beta\gamma} \right) + N_a q_b^{\alpha\gamma} \,, \tag{3.4.57}$$

where

$$\begin{aligned} \mathbf{w}_b^{\gamma} = {} & N_b \left(\tilde{\mathbf{k}}'_{\gamma} \cdot \mathbf{g}^{p} - R\theta \tilde{\mathbf{k}} \cdot \sum_{\beta} \left(\frac{\partial}{\partial \tilde{c}^{\gamma}} \left(\frac{\tilde{\kappa}^{\beta}}{d_0^{\beta}} \right) \mathbf{d}^{\beta} + \frac{\tilde{\kappa}^{\beta}}{d_0^{\beta}} \mathbf{d}_c^{\beta\gamma} \right) \cdot \operatorname{grad} \tilde{c}^{\beta} \right) \\ & - R\theta \tilde{\mathbf{k}} \cdot \frac{\tilde{\kappa}^{\gamma}}{d_0^{\gamma}} \mathbf{d}^{\gamma} \cdot \operatorname{grad} N_b \,, \end{aligned} \tag{3.4.58}$$

and

$$\begin{aligned} \mathbf{j}_b^{\alpha\gamma} = {} & N_b \left(\frac{\partial \tilde{\kappa}^{\alpha}}{\partial \tilde{c}^{\gamma}} \mathbf{d}^{\alpha} + \tilde{\kappa}^{\alpha} \mathbf{d}_c^{\alpha\gamma} \right) \cdot \mathbf{g}^{\alpha} \\ & + \frac{\tilde{\kappa}^{\alpha}}{d_0^{\alpha}} \mathbf{d}^{\alpha} \cdot \left[\delta_{\alpha\gamma} \left(N_b \mathbf{w} - \varphi^{w} d_0^{\alpha} \operatorname{grad} N_b \right) + \tilde{c}^{\alpha} \left(\mathbf{w}_b^{\gamma} - \frac{N_b}{d_0^{\alpha}} \frac{\partial d_0^{\alpha}}{\partial \tilde{c}^{\gamma}} \mathbf{w} \right) \right] \,, \end{aligned} \tag{3.4.59}$$

$$q_b^{\alpha\gamma} = -N_b \frac{\varphi^{w}}{\Delta t} \left(\frac{\partial \tilde{\kappa}^{\alpha}}{\partial \tilde{c}^{\gamma}} \tilde{c}^{\alpha} + \delta_{\alpha\gamma} \tilde{\kappa}^{\alpha} \right) \,. \tag{3.4.60}$$

The discretization of δW_{ext} in (3.4.35) has the form

$$\delta W_{\text{ext}} = \sum_{e=1}^{n_e} \sum_{k=1}^{n_{\text{int}}^{(e)}} W_k J_{\eta} \sum_{a=1}^{m} \begin{bmatrix} \delta \mathbf{v}_a & \delta \tilde{p}_a & \delta \tilde{c}_a^{\alpha} & \delta \tilde{c}_a^{\beta} \end{bmatrix} \cdot \begin{bmatrix} N_a t_n \mathbf{n} \\ N_a w_n \\ N_a \tilde{j}_n^{\alpha} \\ N_a \tilde{j}_n^{\beta} \end{bmatrix} \,, \tag{3.4.61}$$

where $J_\eta = |\mathbf{g}_1 \times \mathbf{g}_2|$. The summation is performed over all surface elements on which these boundary conditions are prescribed. The discretization of $-D\delta W_{\text{ext}}$ has the form

$$-D\delta W_{\text{ext}} = \sum_{e=1}^{n_e} \sum_{k=1}^{n_{\text{int}}^{(e)}} W_k J_\eta \sum_{a=1}^{m} \sum_{b=1}^{m} \left[\begin{array}{cccc} \delta\mathbf{v}_a & \delta\tilde{p}_a & \delta\tilde{c}_a^\alpha & \delta\tilde{c}_a^\beta \end{array} \right] \cdot \left[\begin{array}{cccc} \mathbf{K}_{ab}^{uu} & \mathbf{0} & \mathbf{0} & \mathbf{0} \\ \mathbf{k}_{ab}^{pu} & 0 & 0 & 0 \\ \mathbf{k}_{ab}^{\alpha u} & 0 & 0 & 0 \\ \mathbf{k}_{ab}^{\beta u} & 0 & 0 & 0 \end{array} \right] \cdot \left[\begin{array}{c} \Delta\mathbf{u}_b \\ \Delta\tilde{p}_b \\ \Delta\tilde{c}_b^\alpha \\ \Delta\tilde{c}_b^\beta \end{array} \right], \tag{3.4.62}$$

where

$$\begin{aligned} \mathbf{K}_{ab}^{uu} &= t_n N_a \boldsymbol{\mathcal{A}} \left\{ \frac{\partial N_b}{\partial \eta^1} \mathbf{g}_2 - \frac{\partial N_b}{\partial \eta^2} \mathbf{g}_1 \right\}, \\ \mathbf{k}_{ab}^{pu} &= -w_n N_a \left(\frac{\partial N_b}{\partial \eta^1} \mathbf{g}_2 - \frac{\partial N_b}{\partial \eta^2} \mathbf{g}_1 \right) \times \mathbf{n}, \\ \mathbf{k}_{ab}^{\alpha u} &= -\tilde{j}_n^\alpha N_a \left(\frac{\partial N_b}{\partial \eta^1} \mathbf{g}_2 - \frac{\partial N_b}{\partial \eta^2} \mathbf{g}_1 \right) \times \mathbf{n}. \end{aligned} \tag{3.4.63}$$

In this expression, $\boldsymbol{\mathcal{A}}\{\mathbf{v}\}$ is the antisymmetric tensor whose dual vector is $\mathbf{v}$ (such that $\boldsymbol{\mathcal{A}}\{\mathbf{v}\} \cdot \mathbf{q} = \mathbf{v} \times \mathbf{q}$ for any vector $\mathbf{q}$).

3.4.6 Electric Potential and Partition Coefficient Derivatives

When the mixture is charged it is necessary to solve for the electric potential ψ using the electroneutrality condition in (2.7.4). This equation may be rewritten as a polynomial in ζ,

$$\sum_{i=0}^{n} a_i \zeta^i, \tag{3.4.64}$$

where

$$\zeta = \exp\left(-\frac{F_c \psi}{R\theta} \right), \tag{3.4.65}$$

and

$$a_i = \begin{cases} z^\alpha \hat{\kappa}^\alpha \tilde{c}^\alpha & i = z^\alpha - z^{\min} \\ c^F & i = -z^{\min} \end{cases}. \tag{3.4.66}$$

Here, $z^{\min} = \min_\alpha z^\alpha$ and the polynomial degress is $n = z^{\max} - z^{\min}$ where $z^{\max} = \max_\alpha z^\alpha$. Since more than one solute may carry the same charge z^α, the coefficients a_i should be evaluated from the summation of $z^\alpha \hat{\kappa}^\alpha \tilde{c}^\alpha$ over all such solutes. Only real positive roots are valid, since $\psi = -R\theta (\ln \zeta)/F_c$ according to (3.4.65). Using Descartes' rule of signs, an inspection of the coefficients a_i shows tht there is only one sign change in the polynomial, regardless of the sign of c^F, implying that there will always be only one positive root ζ, which must thus be real. Therefore, there cannot be any ambiguity in the calculation of ψ, irrespective of the polynomial degree. Newton's method is used to solve for the positive real root when $n > 2$.

Using the above relations, it follows that $\tilde{\kappa}^\alpha = \hat{\kappa}^\alpha \zeta^{z^\alpha}$. An examination of the equations resulting from the linearization of the internal virtual work shows that it is necessary to evaluate derivatives of $\tilde{\kappa}^\alpha$ with respect to J and $\tilde{c}^\gamma$, which are given by

$$\begin{aligned} \frac{\partial \tilde{\kappa}^\alpha}{\partial J} &= \frac{\partial \hat{\kappa}^\alpha}{\partial J} \zeta^{z^\alpha} + z^\alpha \tilde{\kappa}^\alpha \frac{1}{\zeta} \frac{\partial \zeta}{\partial J} \\ \frac{\partial \tilde{\kappa}^\alpha}{\partial \tilde{c}^\gamma} &= \frac{\partial \hat{\kappa}^\alpha}{\partial \tilde{c}^\gamma} \zeta^{z^\alpha} + z^\alpha \tilde{\kappa}^\alpha \frac{1}{\zeta} \frac{\partial \zeta}{\partial \tilde{c}^\gamma} \end{aligned}. \tag{3.4.67}$$

In these expressions, the derivatives of $\hat{\kappa}^\alpha$ are obtained from the user-defined constitutive relations for the solubility. Derivatives of ζ may be evaluated by differentiating the electroneutrality condition to produce

$$\begin{aligned}\frac{1}{\zeta}\frac{\partial\zeta}{\partial J} &= -\frac{\frac{\partial c^F}{\partial J}+\sum_\beta z^\beta\zeta^{z^\beta}\tilde{c}^\beta\frac{\partial\hat{\kappa}^\beta}{\partial J}}{\sum_\beta\left(z^\beta\right)^2\tilde{\kappa}^\beta\tilde{c}^\beta}\\ \frac{1}{\zeta}\frac{\partial\zeta}{\partial\tilde{c}^\gamma} &= -\frac{z^\gamma\tilde{\kappa}^\gamma+\sum_\beta z^\beta\zeta^{z^\beta}\tilde{c}^\beta\frac{\partial\hat{\kappa}^\beta}{\partial\tilde{c}^\gamma}}{\sum_\beta\left(z^\beta\right)^2\tilde{\kappa}^\beta\tilde{c}^\beta}\end{aligned}\ . \tag{3.4.68}$$

The derivative $\partial c^F/\partial J$ may be evaluated from

$$c^F = \frac{1-\varphi_r^s}{J-\varphi_r^s}c_r^F\ , \tag{3.4.69}$$

where φ_r^s is the referential solid volume fraction (volume of solid in current configuration per volume of the mixture in the reference configuration) and c_r^F is the referential fixed charge density (equivalent charge in current configuration per volume of the mixture in the reference configuration).

3.4.7 Chemical Reactions

3.4.7.1 Virtual Work and Linearization

The contribution to δW due to chemical reactions is given by δG, where

$$\delta G = \int_b \delta\tilde{p}\left[\hat{\varphi}^w+\left(1-\varphi^s\right)\hat{\zeta}\overline{\mathcal{V}}\right]\,dv + \sum_\iota \nu^\iota\int_b \delta\tilde{c}^\iota\left(1-\varphi^s\right)\hat{\zeta}\,dv\,. \tag{3.4.70}$$

The linearization of δG along a solid displacement increment $\Delta\mathbf{u}$ is

$$\begin{aligned}D\delta G\left[\Delta\mathbf{u}\right] = &\int_b \delta\tilde{p}\,\left(\hat{\varphi}^w\,\operatorname{div}\Delta\mathbf{u}+\hat{\boldsymbol{\varphi}}_\varepsilon^w:\Delta\boldsymbol{\varepsilon}\right)\,dv\\ &+\overline{\mathcal{V}}\int_b \delta\tilde{p}\left[\hat{\zeta}\,\operatorname{div}\Delta\mathbf{u}+\left(J-\varphi_r^s\right)\hat{\boldsymbol{\zeta}}_\varepsilon:\Delta\boldsymbol{\varepsilon}\right]\,dv\\ &+\sum_\iota \nu^\iota\int_b \delta\tilde{c}^\iota\left[\hat{\zeta}\,\operatorname{div}\Delta\mathbf{u}+\left(J-\varphi_r^s\right)\hat{\boldsymbol{\zeta}}_\varepsilon:\Delta\boldsymbol{\varepsilon}\right]\,dv\end{aligned}\ , \tag{3.4.71}$$

where

$$\hat{\boldsymbol{\varphi}}_\varepsilon^w = \mathbf{F}\cdot\frac{\partial\hat{\varphi}^w}{\partial\mathbf{E}}\cdot\mathbf{F}^T\,,\quad \hat{\boldsymbol{\zeta}}_\varepsilon = J^{-1}\mathbf{F}\cdot\frac{\partial\hat{\zeta}}{\partial\mathbf{E}}\cdot\mathbf{F}^T\,. \tag{3.4.72}$$

Currently, $\hat{\zeta}$ is assumed to be independent of $\tilde{p}$ in FEBio; it follows that the linearization along the effective fluid pressure increment $\Delta\tilde{p}$ is

$$D\delta G\left[\Delta\tilde{p}\right] = \int_b \delta\tilde{p}\,\frac{\partial\hat{\varphi}^w}{\partial\tilde{p}}\Delta p\,dv\,. \tag{3.4.73}$$

Finally, the linearization along a concentration increment $\Delta\tilde{c}^\iota$ is

$$\begin{aligned} D\delta G\left[\Delta\tilde{c}^\iota\right] = &\int_b \delta\tilde{p}\,\frac{\partial\hat{\varphi}^w}{\partial\tilde{c}^\iota}\Delta\tilde{c}^\iota\,dv \\ &+ \overline{\mathcal{V}}\int_b \delta\tilde{p}\,(1-\varphi^s)\,\frac{\partial\hat{\zeta}}{\partial\tilde{c}^\iota}\Delta\tilde{c}^\iota\,dv \\ &+ \sum_\gamma \nu^\gamma \int_b \delta\tilde{c}^\gamma\,(1-\varphi^s)\,\frac{\partial\hat{\zeta}}{\partial\tilde{c}^\iota}\Delta\tilde{c}^\iota\,dv \end{aligned} \quad . \tag{3.4.74}$$

The discretized form of these expressions is given by

$$\delta G = \sum_a \delta\tilde{p}_a r_a^p + \sum_\gamma\sum_a \delta\tilde{c}_a^\gamma r_a^\gamma\,, \tag{3.4.75}$$

where

$$\begin{aligned} r_a^p &= \int_b N_a\,\left[\hat{\varphi}^w + (1-\varphi^s)\,\hat{\zeta}\bar{\mathcal{V}}\right]\,dv \\ r_a^\gamma &= \nu^\gamma\int_b N_a\,(1-\varphi^s)\,\hat{\zeta}\,dv \end{aligned} \quad . \tag{3.4.76}$$

Similarly,

$$\begin{aligned} D\delta G\left[\Delta\mathbf{u}\right] = &\sum_a \delta\tilde{p}_a \sum_b \mathbf{k}_{ab}^{pu}\cdot\Delta\mathbf{u}_b \\ &+ \sum_\gamma\sum_a \delta\tilde{c}_a^\gamma \sum_b \mathbf{k}_{ab}^{\gamma u}\cdot\Delta\mathbf{u}_b \end{aligned} \quad , \tag{3.4.77}$$

where

$$\begin{aligned} \mathbf{k}_{ab}^{pu} &= \int_b N_a\,(\hat{\varphi}^w\mathbf{I} + \hat{\boldsymbol{\varphi}}_\varepsilon^w)\cdot\operatorname{grad}N_b\,dv \\ &\quad + \bar{\mathcal{V}}\int_a N_a\left[\hat{\zeta}\mathbf{I} + (J-\varphi_r^s)\,\hat{\boldsymbol{\zeta}}_\varepsilon\right]\cdot\operatorname{grad}N_b\,dv \\ \mathbf{k}_{ab}^{\gamma u} &= \nu^\gamma\int_a N_a\left[\hat{\zeta}\mathbf{I} + (J-\varphi_r^s)\,\hat{\boldsymbol{\zeta}}_\varepsilon\right]\cdot\operatorname{grad}N_b\,dv \end{aligned} \quad . \tag{3.4.78}$$

Then,

$$D\delta G\left[\Delta\tilde{p}\right] = \sum_a \delta\tilde{p}_a\sum_b k_{ab}^{pp}\Delta\tilde{p}_b\,, \tag{3.4.79}$$

where

$$k_{ab}^{pp} = \int_b N_a\,\frac{\partial\hat{\varphi}^w}{\partial\tilde{p}}N_b\,dv\,. \tag{3.4.80}$$

Finally,

$$\begin{aligned} D\delta G\left[\Delta\tilde{c}^\iota\right] = &\sum_a \delta\tilde{p}_a\sum_b k_{ab}^{p\iota}\Delta\tilde{c}_b^\iota \\ &+ \sum_\gamma\sum_a \delta\tilde{c}_a^\gamma\sum_b k_{ab}^{\gamma\iota}\Delta\tilde{c}_b^\iota \end{aligned} \quad , \tag{3.4.81}$$

where

$$\begin{aligned} k_{ab}^{p\iota} &= \int_b N_a N_b\frac{\partial\hat{\varphi}^w}{\partial\tilde{c}^\iota}\,dv + \bar{\mathcal{V}}\int_b N_a N_b\,(1-\varphi^s)\,\frac{\partial\hat{\zeta}}{\partial\tilde{c}^\iota}\,dv \\ k_{ab}^{\gamma\iota} &= \nu^\gamma\int_b N_a N_b\,(1-\varphi^s)\,\frac{\partial\hat{\zeta}}{\partial\tilde{c}^\iota}\,dv \end{aligned} \quad . \tag{3.4.82}$$

3.4.7.2 Updating Solid-Bound Molecule Concentrations

The solid-bound molecule concentrations ρ_r^σ are evaluated at integration points of each element; they do not represent nodal degrees of freedom. The values of ρ_r^σ are updated at the end of each iteration in the solution of the nonlinear equations for the nodal degrees of freedom, using trapezoidal integration on $\hat{\rho}_r^\sigma$ in (2.10.6). According to (2.10.16) and (2.10.18), we have $\hat{\rho}_r^\sigma = (J - \varphi_r^s)\, M^\sigma \nu^\sigma \hat{\zeta}$, which is evaluated as the average of values at t_n and t_{n+1}, then

$$(\rho_r^\sigma)_{n+1} = (\rho_r^\sigma)_n + (\hat{\rho}_r^\sigma)_{n+\frac{1}{2}}\, \Delta t \tag{3.4.83}$$

where $\Delta t = t_{n+1} - t_n$.

3.5 Computational Fluid Dynamics

A more detailed description of the FEBio fluid solver can be found in [16].

3.5.1 Weak Formulation

The nodal unknowns in this formulation are $\mathbf{v}$ and J (or e), which may be solved using the momentum balance in eq.(2.11.1) and the kinematic constraint between J and $\mathbf{v}$ given in eq.(2.11.6). The virtual work integral for a Galerkin finite element formulation [27] is given by

$$\begin{aligned} \delta W = &\int_\Omega \delta\mathbf{v} \cdot (\operatorname{div}\boldsymbol{\sigma} + \rho\,(\mathbf{b} - \mathbf{a}))\, dv \\ &+ \int_\Omega \delta J \left(\frac{\dot{J}}{J} - \operatorname{div}\mathbf{v}\right) dv\,, \end{aligned} \tag{3.5.1}$$

where $\delta\mathbf{v}$ is a virtual velocity and δJ is a virtual energy density; Ω is the fluid finite element domain and dv is a differential volume in Ω. This virtual work statement may be directly related to the axiom of energy balance, specialized to conditions of isothermal flow of viscous compressible fluids (see Section 2.11.2). Using the divergence theorem, we may rewrite the weak form of this integral as the difference between external and internal virtual work, $\delta W = \delta W_{ext} - \delta W_{int}$, where

$$\begin{aligned} \delta W_{int} = &\int_\Omega \boldsymbol{\tau} : \operatorname{grad}\delta\mathbf{v}\, dv + \int_\Omega \delta\mathbf{v} \cdot (\operatorname{grad} p + \rho\mathbf{a})\, dv \\ &- \int_\Omega \left(\delta J \frac{\dot{J}}{J} + \operatorname{grad}\delta J \cdot \mathbf{v}\right) dv\,, \end{aligned} \tag{3.5.2}$$

and

$$\delta W_{ext} = \int_{\partial\Omega} \delta\mathbf{v} \cdot \mathbf{t}^\tau\, da + \int_\Omega \delta\mathbf{v} \cdot \rho\mathbf{b}\, dv - \int_{\partial\Omega} \delta J\, v_n\, da\,. \tag{3.5.3}$$

Here, $\partial\Omega$ is the boundary of Ω and da is a differential area on $\partial\Omega$, $\mathbf{t}^\tau = \boldsymbol{\tau}\cdot\mathbf{n}$ is the viscous component of the traction $\mathbf{t}$, and $v_n = \mathbf{v}\cdot\mathbf{n}$ is the velocity normal to the boundary $\partial\Omega$, with $\mathbf{n}$ representing the outward normal on $\partial\Omega$. From these expressions, it becomes evident that essential (Dirichlet) boundary conditions may be prescribed on $\mathbf{v}$ and J, while natural (Neumann) boundary conditions may be prescribed on $\mathbf{t}^\tau$ and v_n. The appearance of velocity in both essential and natural boundary conditions may seem surprising at first. To better understand the nature of these boundary conditions, it is convenient to separate the velocity into its normal and tangential

components, $\mathbf{v} = v_n\mathbf{n} + \mathbf{v}_t$, where $\mathbf{v}_t = (\mathbf{I} - \mathbf{n}\otimes\mathbf{n})\cdot\mathbf{v}$. In particular, for inviscid flow, the viscous stress $\boldsymbol{\tau}$ and its corresponding traction $\mathbf{t}^\tau$ are both zero, leaving v_n as the sole natural boundary condition; similarly, J becomes the only essential boundary condition in such flows, since $\mathbf{v}_t$ is unknown *a priori* on a frictionless boundary and must be obtained from the solution of the analysis.

In general, prescribing J is equivalent to prescribing the elastic fluid pressure, since p is only a function of J. On a boundary where no conditions are prescribed explicitly, we conclude that $v_n = 0$ and $\mathbf{t}^\tau = \mathbf{0}$, which represents a frictionless wall. Conversely, it is possible to prescribe v_n and $\mathbf{t}^\tau$ on a boundary to produce a desired inflow or outflow while simultaneously stabilizing the flow conditions by prescribing a suitable viscous traction. Prescribing essential boundary conditions $\mathbf{v}_t$ and J determines the tangential velocity on a boundary as well as the elastic fluid pressure p, leaving the option to also prescribe the normal component of the viscous traction, $t_n^\tau = \mathbf{t}^\tau\cdot\mathbf{n}$, to completely determine the normal traction $t_n = \mathbf{t}\cdot\mathbf{n}$ (or else t_n^τ naturally equals zero). Mixed boundary conditions represent common physical features: Prescribing v_n and $\mathbf{v}_t$ completely determines the velocity $\mathbf{v}$ on a boundary; prescribing $\mathbf{t}^\tau$ and J completely determines the traction $\mathbf{t} = \boldsymbol{\sigma}\cdot\mathbf{n}$ on a boundary. Note that v_n and J are mutually exclusive boundary conditions, and the same holds for $\mathbf{v}_t$ and the tangential component of the viscous traction, $\mathbf{t}_t^\tau = (\mathbf{I} - \mathbf{n}\otimes\mathbf{n})\cdot\mathbf{t}^\tau$.

3.5.2 Temporal Discretization and Linearization

The time derivatives, $\partial\mathbf{v}/\partial t$ which appears in the expression for $\mathbf{a}$ in eq.(2.11.2), and $\partial J/\partial t$ which similarly appears in $\dot{J}$, may be discretized upon the choice of a time integration scheme, such as the generalized-α method [57] (Section 3.9). In this scheme, δW is evaluated at an intermediate time step $t_{n+\alpha} = \alpha t_{n+1} + (1-\alpha)\,t_n$ between the current time step t_{n+1} and previous time step t_n, though different values of α are used for the primary variables and their time derivatives. The velocity and volume ratio are evaluated as $\mathbf{v}_{n+\alpha_f}$ and $J_{n+\alpha_f}$ at the intermediate time step $t_{n+\alpha_f}$, whereas their time derivatives are evaluated as $(\partial\mathbf{v}/\partial t)_{n+\alpha_m}$ and $(\partial J/\partial t)_{n+\alpha_m}$ at the intermediate time step $t_{n+\alpha_m}$. The parameters α_f and α_m are evaluated from the spectral radius for an infinite time step, ρ_∞, as described in Section 3.9. The solution of the nonlinear equation $\delta W = 0$ is obtained by linearizing this relation as

$$\delta W + D\delta W\,[\Delta\mathbf{v}] + D\delta W\,[\Delta J] \approx 0\,, \tag{3.5.4}$$

where the operator $D\delta W\,[\cdot]$ represents the directional derivative of δW at $(\mathbf{v}, J)$ along an increment $\Delta\mathbf{v}$ of $\mathbf{v}$, or ΔJ of J [27]. The aim of this analysis is to solve for the velocity $\mathbf{v}_{n+1}$ and volume ratio J_{n+1} at the current time step t_{n+1}. Using the split form of δW between external and internal work contributions, this relation may be expanded as

$$\begin{aligned} &D\delta W_{int}\,[\Delta\mathbf{v}] + D\delta W_{int}\,[\Delta J] - D\delta W_{ext}\,[\Delta\mathbf{v}] \\ &- D\delta W_{ext}\,[\Delta J] \approx \delta W_{ext} - \delta W_{int}\,. \end{aligned} \tag{3.5.5}$$

In this framework the finite element mesh is defined on the spatial domain Ω, which is fixed (time-invariant) in conventional CFD treatments. Thus, we can linearize δW_{int} along increments $\Delta\mathbf{v}$ in the velocity $\mathbf{v}_{n+1}$ and ΔJ in the volume ratio J_{n+1}, by simply bringing the directional derivative operator into the integrals of eqs.(3.5.2)-(3.5.3). The linearization of $\mathbf{v}_{n+\alpha_f}$ and $J_{n+\alpha_f}$ is given by

$$\begin{aligned} D\mathbf{v}_{n+\alpha_f}\,[\Delta\mathbf{v}] &= \alpha_f\Delta\mathbf{v} \\ DJ_{n+\alpha_f}\,[\Delta J] &= \alpha_f\Delta J \end{aligned}$$

whereas that of $(\partial \mathbf{v}/\partial t)_{n+\alpha_m}$ and $(\partial J/\partial t)_{n+\alpha_m}$ is given by

$$D\left(\frac{\partial \mathbf{v}}{dt}\right)_{n+\alpha_m}[\Delta \mathbf{v}] = \frac{\alpha_m}{\gamma}\frac{\Delta \mathbf{v}}{\Delta t}\,, \tag{3.5.6}$$

$$D\left(\frac{\partial J}{\partial t}\right)_{n+\alpha_m}[\Delta \mathbf{v}] = \frac{\alpha_m}{\gamma}\frac{\Delta J}{\Delta t}\,. \tag{3.5.7}$$

Here, Δt is the current time increment and γ is the Newmark integration parameter [57].

The linearization of δW_{int} along an increment $\Delta \mathbf{v}$ is then

$$\begin{aligned} D\left(\delta W_{int}\right)[\Delta \mathbf{v}] = {} & \alpha_f \int_\Omega \operatorname{grad}\delta\mathbf{v} : \boldsymbol{\mathcal{C}}^\tau : \operatorname{grad}\Delta\mathbf{v}\, dv \\ & + \alpha_f \int_\Omega \delta\mathbf{v}\cdot\rho\left(\left(\frac{\alpha_m}{\alpha_f\gamma}\frac{\mathbf{I}}{\Delta t}+\mathbf{L}\right)\cdot\Delta\mathbf{v}+\operatorname{grad}\Delta\mathbf{v}\cdot\mathbf{v}\right) dv \\ & - \alpha_f \int_\Omega \left(\frac{\delta J}{J}\operatorname{grad} J + \operatorname{grad}\delta J\right)\cdot\Delta\mathbf{v}\, dv \end{aligned} \tag{3.5.8}$$

where we have introduced the fourth-order tensor $\boldsymbol{\mathcal{C}}^\tau$ representing the tangent of the viscous stress with respect to the rate of deformation,

$$\boldsymbol{\mathcal{C}}^\tau = \frac{\partial \boldsymbol{\tau}}{\partial \mathbf{D}}\,. \tag{3.5.9}$$

Note that $\boldsymbol{\mathcal{C}}^\tau$ exhibits minor symmetries because of the symmetries of $\boldsymbol{\tau}$ and $\mathbf{D}$; in Cartesian components, we have $\mathcal{C}^\tau_{ijkl} = \mathcal{C}^\tau_{jikl}$ and $\mathcal{C}^\tau_{ijkl} = \mathcal{C}^\tau_{ijlk}$. In general, $\boldsymbol{\mathcal{C}}^\tau$ does not exhibit major symmetry ($\mathcal{C}^\tau_{ijkl} \neq \mathcal{C}^\tau_{klij}$), though the common constitutive relations adopted in fluid mechanics produce such symmetry as shown below.

The linearization of δW_{int} along an increment ΔJ is

$$\begin{aligned} D\left(\delta W_{int}\right)[\Delta J] = {} & \alpha_f \int_b \Delta J\, \boldsymbol{\tau}'_J : \operatorname{grad}\delta\mathbf{v}\, dv - \alpha_f \int_\Omega \delta\mathbf{v}\cdot\Delta J\frac{\rho}{J}\mathbf{a}\, dv \\ & + \alpha_f \int_\Omega \delta\mathbf{v}\cdot\left(p'\operatorname{grad}\Delta J + \Delta J\, p''\operatorname{grad} J\right) dv \\ & - \alpha_f \int_\Omega \frac{\delta J}{J}\left(\left(\frac{\alpha_m}{\alpha_f\gamma}\frac{1}{\Delta t}-\frac{\dot J}{J}\right)\Delta J + \operatorname{grad}\Delta J\cdot\mathbf{v}\right) dv \end{aligned} \tag{3.5.10}$$

where we have used $DJ[\Delta J] = \Delta J$; p' and p'' respectively represent the first and second derivatives of $p(J)$. We have also defined $\boldsymbol{\tau}'_J$ as the tangent of the viscous stress $\boldsymbol{\tau}$ with respect to J,

$$\boldsymbol{\tau}'_J = \frac{\partial \boldsymbol{\tau}}{\partial J}\,. \tag{3.5.11}$$

For the external work, when $\mathbf{t}^\tau$, $\mathbf{b}$ and v_n are prescribed, these linearizations simplify to

$$D\left(\delta W_{ext}\right)[\Delta \mathbf{v}] = 0\,, \tag{3.5.12}$$

and

$$D\left(\delta W_{ext}\right)[\Delta J] = -\alpha_f \int_b \delta\mathbf{v}\cdot\Delta J\,\frac{\rho}{J}\mathbf{b}\, dv\,. \tag{3.5.13}$$

We may define the fluid dilatation $e = J - 1$ as an alternative essential variable, since initial and boundary conditions $e = 0$ are more convenient to handle in a numerical scheme than $J = 1$. It follows that $\operatorname{grad} J = \operatorname{grad} e$ and $\partial J/\partial t = \partial e/\partial t$. Therefore the changes to the above equations are minimal, simply requiring the substitution $J = 1 + e$ and $\Delta J = \Delta e$. Steady-state analyses may be obtained by setting the terms involving Δt^{-1} to zero in eqs.(3.5.6)-(3.5.7), (3.5.8) and (3.5.10).

3.5.3 Spatial Discretization

The velocity $\mathbf{v}(\mathbf{x},t)$ and Jacobian $J(\mathbf{x},t)$ are spatially interpolated over the domain Ω using the same interpolation functions $N_a(\mathbf{x})$, with $a=1$ to n where n is the number of nodes in an element),

$$\mathbf{v}(\mathbf{x},t)=\sum_{a=1}^{n} N_a(\mathbf{x})\,\mathbf{v}_a\,,\quad J(\mathbf{x},t)=\sum_{a=1}^{n} N_a(\mathbf{x})\,J_a\,. \tag{3.5.14}$$

Here, $\mathbf{v}_a$ and J_a are nodal values of $\mathbf{v}$ and J that evolve with time. In contrast to classical mixed formulations for incompressible flow [86], which solve for the pressure p using $\operatorname{div}\mathbf{v}=0$ instead of eq.(2.11.6), equal order interpolation is acceptable in this formulation since the governing equations for $\mathbf{v}$ and J involve spatial derivatives of both variables ($\operatorname{grad}\mathbf{v}$ and $\operatorname{grad}J$). The expressions of eq.(3.5.14) may be used to evaluate $\mathbf{L}$, $\operatorname{div}\mathbf{v}$, $\mathbf{a}$, $\operatorname{grad}J$, $\dot{J}$, etc. Similar interpolations are used for virtual increments $\delta\mathbf{v}$ and δJ, as well as real increments $\Delta\mathbf{v}$ and ΔJ.

When substituted into eq.(4.2.32), we find that the discretized form of δW_{int} may be written as

$$\delta W_{int}=\sum_a \delta\mathbf{v}_a\cdot(\mathbf{f}_a^{\sigma}+\mathbf{f}_a^{\rho})+f_a^J\delta J_a\,, \tag{3.5.15}$$

where

$$\begin{aligned}
\mathbf{f}_a^{\sigma}&=\int_\Omega\left(\boldsymbol{\tau}\cdot\operatorname{grad}N_a+N_a\operatorname{grad}p\right)\,dv\,,\\
\mathbf{f}_a^{\rho}&=\int_\Omega N_a\rho\mathbf{a}\,dv\,,\\
f_a^J&=\int_\Omega-\left(N_a\frac{\dot{J}}{J}+\operatorname{grad}N_a\cdot\mathbf{v}\right)\,dv\,.
\end{aligned} \tag{3.5.16}$$

Similarly, the discretized form of $D\delta W_{int}[\Delta\mathbf{v}]$ in eq.(3.5.8) becomes

$$\begin{aligned}
D(\delta W_{int})[\Delta\mathbf{v}]=&\sum_a\delta\mathbf{v}_a\cdot\sum_b\left(\mathbf{K}_{ab}^{vv}+\mathbf{M}_{ab}^{vv}\right)\cdot\Delta\mathbf{v}_b\\
&+\sum_a\delta J_a\sum_b\mathbf{k}_{ab}^{Jv}\cdot\Delta\mathbf{v}_b\,,
\end{aligned} \tag{3.5.17}$$

where

$$\begin{aligned}
\mathbf{K}_{ab}^{vv}&=\alpha_f\int_\Omega\operatorname{grad}N_a\cdot\boldsymbol{\mathcal{C}}^v\cdot\operatorname{grad}N_b\,dv\,,\\
\mathbf{M}_{ab}^{vv}&=\alpha_f\int_\Omega N_a\rho\left(N_b\left(\frac{\alpha_m}{\alpha_f\gamma}\frac{\mathbf{I}}{\Delta t}+\operatorname{grad}\mathbf{v}\right)+(\operatorname{grad}N_b\cdot\mathbf{v})\,\mathbf{I}\right)\,dv\,,\\
\mathbf{k}_{ab}^{Jv}&=-\alpha_f\int_\Omega\left(\frac{N_a}{J}\operatorname{grad}J+\operatorname{grad}N_a\right)N_b\,dv\,,
\end{aligned} \tag{3.5.18}$$

whereas that of $D\delta W_{int}[\Delta J]$ in eq.(3.5.10) becomes

$$\begin{aligned}
D(\delta W_{int})[\Delta J]=&\sum_a\delta\mathbf{v}_a\cdot\sum_b\left(\mathbf{k}_{ab}^{vJ}+\mathbf{m}_{ab}^{vJ}\right)\,\Delta J_b\\
&+\sum_a\delta J_a\sum_b k_{ab}^{JJ}\,\Delta J_b
\end{aligned} \tag{3.5.19}$$

where

$$\begin{aligned}
\mathbf{k}_{ab}^{vJ} &= \alpha_f \int_\Omega \left[N_b \boldsymbol{\tau}'_J \cdot \operatorname{grad} N_a + N_a \left(p' \operatorname{grad} N_b + N_b p'' \operatorname{grad} J \right) \right] dv \,, \\
\mathbf{m}_{ab}^{vJ} &= -\alpha_f \int_\Omega N_a N_b \frac{\rho}{J} \mathbf{a} \, dv \,, \\
k_{ab}^{JJ} &= -\alpha_f \int_\Omega \frac{N_a}{J} \left(\left(\frac{\alpha_m}{\alpha_f \gamma} \frac{1}{\Delta t} - \frac{\dot{J}}{J} \right) N_b + \operatorname{grad} N_b \cdot \mathbf{v} \right) dv \,.
\end{aligned} \tag{3.5.20}$$

For the external work in eq.(4.2.34), its discretized form is

$$\delta W_{ext} = \sum_a \delta \mathbf{v}_a \cdot \left(\mathbf{f}_a^{\mathsf{t}} + \mathbf{f}_a^{\mathsf{b}} \right) + \delta J_a f_a^v \,, \tag{3.5.21}$$

where

$$\begin{aligned}
\mathbf{f}_a^{\mathsf{t}} &= \int_{\partial\Omega} N_a \mathbf{t}^\tau \, da \,, \\
\mathbf{f}_a^{\mathsf{b}} &= \int_\Omega N_a \rho \mathbf{b} \, dv \,, \\
f_a^v &= -\int_\Omega N_a v_n \, da \,.
\end{aligned} \tag{3.5.22}$$

The discretized form of $D\left(\delta W_{ext}\right)[\Delta J]$ in eq.(3.5.13) is

$$D\left(\delta W_{ext}\right)[\Delta J] = \sum_a \delta \mathbf{v}_a \cdot \sum_b \mathbf{k}_{ab}^{\mathsf{b}} \, \Delta J_b \,, \tag{3.5.23}$$

where

$$\mathbf{k}_{ab}^{\mathsf{b}} = -\alpha_f \int_\Omega N_a N_b \frac{\rho}{J} \mathbf{b} \, dv \,. \tag{3.5.24}$$

3.5.4 Special Boundary Conditions

3.5.4.1 Backflow Stabilization

For arterial blood flow, backflow stabilization has been proposed previously to deal with truncated domains where the entire artery is not modeled explicitly [20, 39]; for these types of problems, letting $\mathbf{t} = \mathbf{0}$ or prescribing a constant pressure at the outflow boundary may not prevent flow reversals that compromise convergence of an analysis. Instead, these authors proposed a velocity-dependent traction boundary condition, $\mathbf{t} = \beta\rho\left(\mathbf{v} \otimes \mathbf{v}\right) \cdot \mathbf{n}$ with a tensile normal component, that counters the backflow (only when $v_n < 0$). Here, β is a non-dimensional user-defined parameter; a value of $\beta = 0$ turns off this feature, while a value of $\beta = 1$ generally shows good numerical performance. We adapt this previously proposed formulation by letting the normal component of the viscous traction be given by

$$t_n^\tau = \begin{cases} \beta \rho_r v_n^2 & v_n < 0 \\ 0 & v_n \geq 0 \end{cases} . \tag{3.5.25}$$

The choice of ρ_r in lieu of ρ is for convenience, to avoid the dependence of ρ on J (which is negligible for nearly incompressible flow). Then, the contribution of this traction to the virtual external work δW_{ext} is

$$\delta G = \int_{\partial\Omega} \delta \mathbf{v} \cdot t_n^\tau \mathbf{n} \, da \,. \tag{3.5.26}$$

The linearization of δG along an increment $\Delta\mathbf{v}$ in the velocity is given by

$$D\delta G\left[\Delta\mathbf{v}\right] = \int_{\partial\Omega} \delta\mathbf{v}\cdot\mathbf{K}_n\cdot\Delta\mathbf{v}\,da\,, \tag{3.5.27}$$

where

$$\mathbf{K}_n = \begin{cases} 2\beta\rho_r v_n\left(\mathbf{n}\otimes\mathbf{n}\right) & v_n < 0 \\ \mathbf{0} & v_n \geq 0 \end{cases}. \tag{3.5.28}$$

The discretized form of δG is

$$\delta G = \sum_a \delta\mathbf{v}_a\cdot\mathbf{f}_a^n\,, \quad \mathbf{f}_a^n = \int_{\partial\Omega} N_a t_n^\tau\mathbf{n}\,da\,, \tag{3.5.29}$$

whereas the discretized form of $D\delta G\left[\Delta\mathbf{v}\right]$ is

$$D\delta G\left[\Delta\mathbf{v}\right] = \sum_a \delta\mathbf{v}_a\cdot\sum_b \mathbf{K}_{ab}^n\cdot\Delta\mathbf{v}_b\,, \quad \mathbf{K}_{ab}^n = \int_{\partial\Omega} N_a N_b\mathbf{K}_n\,da\,. \tag{3.5.30}$$

A (viscous) tangential traction is implemented as a separate flow stabilization method in the next section, applicable to inlet or outlet surfaces, without a conditional requirement based on the sign of v_n.

3.5.4.2 Tangential Flow Stabilization

For certain outlet conditions, using the natural boundary condition $\mathbf{t}_t^\tau = \mathbf{0}$ may lead to flow instabilities. It is possible to minimize these effects by prescribing a tangential viscous traction onto the boundary surface, which opposes this tangential flow. Optionally, this condition may be combined with the backflow stabilization described above.

Similar to the previous section, we introduce a non-dimensional parameter β, with the tangential traction given by

$$\mathbf{t}_t^\tau = -\beta\rho_r\left|\mathbf{v}_t\right|\mathbf{v}_t\,. \tag{3.5.31}$$

This form shows that $\mathbf{t}_t^\tau$ opposes tangential flow. The external virtual work for this traction is

$$\delta G = \int_{\partial\Omega} \delta\mathbf{v}\cdot\mathbf{t}_t^\tau\,da\,. \tag{3.5.32}$$

Its linearization along an increment $\Delta\mathbf{v}$ is

$$D\delta G\left[\Delta\mathbf{v}\right] = \int_{\partial\Omega} \delta\mathbf{v}\cdot\mathbf{K}_t\cdot\Delta\mathbf{v}\,da\,, \tag{3.5.33}$$

where it can be shown that

$$\mathbf{K}_t = -\beta\rho_r\left|\mathbf{v}_t\right|\left(\mathbf{I}-\mathbf{n}\otimes\mathbf{n}+\frac{\mathbf{v}_t}{\left|\mathbf{v}_t\right|}\otimes\frac{\mathbf{v}_t}{\left|\mathbf{v}_t\right|}\right). \tag{3.5.34}$$

The discretized form of δG is

$$\delta G = \sum_a \delta\mathbf{v}_a\cdot\mathbf{f}_a^\tau\,, \quad \mathbf{f}_a^\tau = \int_{\partial\Omega} N_a\mathbf{t}_t^\tau\,da\,. \tag{3.5.35}$$

The discretized form of $D\delta G\left[\Delta\mathbf{v}\right]$ is

$$D\delta G\left[\Delta\mathbf{v}\right] = \sum_a \delta\mathbf{v}_a\cdot\sum_b \mathbf{K}_{ab}^t\cdot\Delta\mathbf{v}_b\,, \quad \mathbf{K}_{ab}^t = \int_{\partial\Omega} N_a N_b\mathbf{K}_t\,da\,. \tag{3.5.36}$$

3.5.4.3 Flow Resistance

Flow resistance is typically implemented when modeling arterial flow, where the finite element domain only describes a portion of an arterial network [106]. A flow resistance may be imposed on downstream boundaries to simulate the resistance produced by the vascular network with its branches and bifurcations. The resistance is equivalent to a mean pressure which is proportional to the volumetric flow rate Q,

$$p = RQ\,, \quad Q = \int_{\partial\Omega} v_n \, da\,,$$

where R is the resistance. Using the pressure-dilatation relation (5.17.5), equivalent to $p = -K \cdot e$, this pressure may be prescribed as an essential boundary condition on the dilatation e.

3.6 Weak Formulation for FSI

3.6.1 General Formulation

The strong form of the virtual work statement is $\delta W = 0$ where

$$\begin{aligned} \delta W = & \int_b \delta \mathbf{v}^s \cdot \operatorname{div} \boldsymbol{\sigma}^s \, dv \\ & + \int_b \delta \mathbf{w} \cdot \left[\operatorname{div} \boldsymbol{\sigma}^f + \rho^f \left(\mathbf{b} - \mathbf{a}^f \right) \right] \, dv \\ & - \int_b \delta J^f \left[\frac{1}{J^f} \left(\dot{J}^f + \operatorname{grad} J^f \cdot \mathbf{w} \right) - \operatorname{div} \mathbf{w} - \frac{\dot{J}^s}{J^s} \right] \, dv \end{aligned} \quad . \tag{3.6.1}$$

Here, b is the mixture domain (whose boundaries are defined on the solid), $\delta \mathbf{v}^s$ is the virtual solid velocity, $\delta \mathbf{w}$ is the virtual relative fluid velocity, and δJ^f is the virtual energy density. The weak form of this statement may be written as the difference $\delta W = \delta W_{ext} - \delta W_{int}$ between external virtual work δW_{ext} and internal virtual work δW_{int}, where

$$\begin{aligned} \delta W_{int} = & \int_b \boldsymbol{\sigma}^s : \operatorname{grad} \delta \mathbf{v}^s \, dv \\ & + \int_b \boldsymbol{\tau} : \operatorname{grad} \delta \mathbf{w} \, dv + \int_b \delta \mathbf{w} \cdot \left(\operatorname{grad} p + \rho^f \mathbf{a}^f \right) \, dv \\ & + \int_b \delta J^f \left[\frac{1}{J^f} \left(\dot{J}^f + \operatorname{grad} J^f \cdot \mathbf{w} \right) - \frac{\dot{J}^s}{J^s} \right] \, dv \\ & + \int_b \mathbf{w} \cdot \operatorname{grad} \delta J^f \, dv \end{aligned} \quad , \tag{3.6.2}$$

and

$$\begin{aligned} \delta W_{ext} = & \int_{\partial b} \delta \mathbf{v}^s \cdot \mathbf{t}^s \, da \\ & + \int_{\partial b} \delta \mathbf{w} \cdot \mathbf{t}^\tau \, da + \int_b \delta \mathbf{w} \cdot \rho^f \mathbf{b} \, dv \,. \\ & + \int_{\partial b} \delta J^f w_n \, da \end{aligned} \tag{3.6.3}$$

Here, $\mathbf{t}^s = \boldsymbol{\sigma}^s \cdot \mathbf{n}$ is the solid traction, $\mathbf{t}^\tau = \boldsymbol{\tau} \cdot \mathbf{n}$ is the fluid viscous traction, and $w_n = \mathbf{w}_n \cdot \mathbf{n}$ is the normal component of the relative fluid velocity on the boundary ∂b, whose outward unit normal is

$\mathbf{n}$. In practice, both $\boldsymbol{\sigma}^s$ and $\mathbf{t}^s$ should contribute negligibly to δW, but they cannot be set exactly to zero since we need some small elasticity to regularize the deforming mixture mesh.

3.6.2 Time Integration

In the generalized $\alpha-$method we evaluate displacements and velocities at the intermediate time $t_{n+\alpha_f} = t_n + \alpha_f\,(t_{n+1} - t_n)$, such that

$$\begin{aligned}
\boldsymbol{\chi}^s_{n+\alpha_f} &= (1-\alpha_f)\,\boldsymbol{\chi}^s_n + \alpha_f \boldsymbol{\chi}^s_{n+1}\\
\mathbf{u}^s_{n+\alpha_f} &= (1-\alpha_f)\,\mathbf{u}^s_n + \alpha_f \mathbf{u}^s_{n+1}\\
\mathbf{v}^s_{n+\alpha_f} &= (1-\alpha_f)\,\mathbf{v}^s_n + \alpha_f \mathbf{v}^s_{n+1}\\
\mathbf{w}_{n+\alpha_f} &= (1-\alpha_f)\,\mathbf{w}_n + \alpha_f \mathbf{w}_{n+1}\\
J^f_{n+\alpha_f} &= (1-\alpha_f)\,J^f_n + \alpha_f J^f_{n+1}
\end{aligned}$$

In particular, it follows that

$$\mathbf{F}^s_{n+\alpha_f} = \frac{\partial \boldsymbol{\chi}^s_{n+\alpha_f}}{\partial \mathbf{X}} = (1-\alpha_f)\,\mathbf{F}^s_n + \alpha_f \mathbf{F}^s_{n+1}$$

$$J^s_{n+\alpha_f} = \det \mathbf{F}^s_{n+\alpha_f}$$

$$\dot{J}^s_{n+\alpha_f} = J^s_{n+\alpha_f} \mathbf{F}^{-T}_{n+\alpha_f} : \operatorname{Grad} \mathbf{v}^s_{n+\alpha_f}$$

$$\mathbf{L}^s_{n+\alpha_f} = \operatorname{Grad} \mathbf{v}^s_{n+\alpha_f} \cdot \mathbf{F}^{-1}_{n+\alpha_f}$$

In practice however, we get better numerical results when using

$$\dot{J}^s_{n+\alpha_f} = \frac{J^s_{n+1} - J^s_n}{\Delta t}$$

$$\mathbf{L}^s_{n+\alpha_f} = \frac{\mathbf{F}_{n+1} - \mathbf{F}_n}{\Delta t} \cdot \mathbf{F}^{-1}_{n+\alpha_f}$$

Similarly, we evaluate velocity derivatives at the intermediate time $t_{n+\alpha_m} = t_n + \alpha_m\,(t_{n+1} - t_n)$, such that

$$\begin{aligned}
\dot{\mathbf{v}}^s_{n+\alpha_m} &= (1-\alpha_m)\,\dot{\mathbf{v}}^s_n + \alpha_m \dot{\mathbf{v}}^s_{n+1}\\
\dot{\mathbf{w}}_{n+\alpha_m} &= (1-\alpha_m)\,\dot{\mathbf{w}}_n + \alpha_m \dot{\mathbf{w}}_{n+1}\\
\dot{J}^f_{n+\alpha_m} &= (1-\alpha_m)\,\dot{J}^f_n + \alpha_m \dot{J}^f_{n+1}
\end{aligned}$$

The parameters α_f and α_m are evaluated from a single parameter ρ_∞ using

$$\alpha_f = \frac{1}{1+\rho_\infty}\,, \quad \alpha_m = \frac{1}{2}\frac{3-\rho_\infty}{1+\rho_\infty}\,, \tag{3.6.4}$$

for first-order systems, or

$$\alpha_f = \frac{1}{1+\rho_\infty}\,, \quad \alpha_m = \frac{2-\rho_\infty}{1+\rho_\infty}\,, \tag{3.6.5}$$

for second-order systems, where $0 \le \rho_\infty \le 1$. This parameter is the spectral radius for an infinite time step, which controls the amount of damping of high frequencies; a value of zero produces the greatest amount of damping, anihilating the highest frequency in one step, whereas a value of one

preserves the highest frequency. Since the solid motion is governed by a second-order differential equation in time, we adopt the formulas for second-order systems.

To complete the integration scheme, we evaluate

$$\beta = \frac{1}{4}\left(1+\alpha_m-\alpha_f\right)^2$$
$$\gamma = \frac{1}{2}+\alpha_m-\alpha_f$$

then

$$\begin{aligned}
\mathbf{v}^s_{n+1} &= \mathbf{v}^s_n + \Delta t\left[(1-\gamma)\,\dot{\mathbf{v}}^s_n + \gamma\dot{\mathbf{v}}^s_{n+1}\right]\\
\mathbf{u}^s_{n+1} &= \mathbf{u}^s_n + \Delta t\mathbf{v}^s_n + \frac{\Delta t^2}{2}\left[(1-2\beta)\,\dot{\mathbf{v}}^s_n + 2\beta\dot{\mathbf{v}}^s_{n+1}\right]\\
\mathbf{w}_{n+1} &= \mathbf{w}_n + \Delta t\left[(1-\gamma)\,\dot{\mathbf{w}}_n + \gamma\dot{\mathbf{w}}_{n+1}\right]\\
J^f_{n+1} &= J^f_n + \Delta t\left[(1-\gamma)\,\dot{J}^f_n + \gamma\dot{J}^f_{n+1}\right]
\end{aligned}$$

Thus,

$$\begin{aligned}
\dot{\mathbf{v}}^s_{n+1} &= \frac{1}{\beta\Delta t}\left(\frac{\mathbf{u}^s_{n+1}-\mathbf{u}^s_n}{\Delta t}-\mathbf{v}^s_n\right)+\left(1-\frac{1}{2\beta}\right)\dot{\mathbf{v}}^s_n\\
\dot{\mathbf{w}}_{n+1} &= \frac{\mathbf{w}_{n+1}-\mathbf{w}_n}{\gamma\Delta t}+\left(1-\frac{1}{\gamma}\right)\dot{\mathbf{w}}_n = \frac{\mathbf{w}_{n+\alpha_f}-\mathbf{w}_n}{\alpha_f\gamma\Delta t}-\left(\frac{1}{\gamma}-1\right)\dot{\mathbf{w}}_n\\
\dot{J}^f_{n+1} &= \frac{J^f_{n+1}-J^f_n}{\gamma\Delta t}+\left(1-\frac{1}{\gamma}\right)\dot{J}^f_n = \frac{J^f_{n+\alpha_f}-J^f_n}{\alpha_f\gamma\Delta t}-\left(\frac{1}{\gamma}-1\right)\dot{J}^f_n
\end{aligned}$$

According to this method [57], the virtual work is evaluated using intermediate time step values, at $t_{n+\alpha_f}$ for all parameters except $\dot{\mathbf{v}}^s$, $\dot{\mathbf{w}}$, and $\dot{J}^f$, which are evaluated at $t_{n+\alpha_m}$.

3.6.3 Discretization

The discretization of the internal work produces

$$\delta W_{int} = \sum_a \delta\mathbf{v}^s_a\cdot\int_b \mathbf{f}^u_a\,dv + \delta\mathbf{w}_a\cdot\int_b \mathbf{f}^w_a\,dv + \delta J^f_a\int_b f^J_a\,dv \tag{3.6.6}$$

$$\begin{aligned}
\delta W_{int} = &\sum_a \delta\mathbf{v}^s_a\cdot\int_b \boldsymbol{\sigma}^s\cdot\operatorname{grad}N_a\,dv\\
&+\sum_a \delta\mathbf{w}_a\cdot\int_b \boldsymbol{\tau}\cdot\operatorname{grad}N_a\,dv + \sum_a \delta\mathbf{w}_a\cdot\int_b N_a\left(\operatorname{grad}p+\rho^f\mathbf{a}^f\right)\,dv\\
&+\sum_a \delta J^f_a\int_b N_a\left[\frac{1}{J^f}\left(\dot{J}^f+\operatorname{grad}J^f\cdot\mathbf{w}\right)-\frac{\dot{J}^s}{J^s}\right]\,dv\\
&+\sum_a \delta J^f_a\int_b \mathbf{w}\cdot\operatorname{grad}N_a\,dv
\end{aligned}$$

where

$$\begin{aligned}
\mathbf{f}^u_a &= \boldsymbol{\sigma}^s\cdot\operatorname{grad}N_a\\
\mathbf{f}^w_a &= \boldsymbol{\tau}\cdot\operatorname{grad}N_a + N_a\left(\operatorname{grad}p+\rho^f\mathbf{a}^f\right)\\
f^J_a &= N_a\left[\frac{1}{J^f}\left(\dot{J}^f+\operatorname{grad}J^f\cdot\mathbf{w}\right)-\frac{\dot{J}^s}{J^s}\right]+\mathbf{w}\cdot\operatorname{grad}N_a
\end{aligned} \tag{3.6.7}$$

We used the following interpolations:

$$\begin{aligned}
\delta\mathbf{v}^s &= \sum_a N_a \delta\mathbf{v}_a^s & \Delta\mathbf{u} &= \sum_b N_b \Delta\mathbf{u}_b \\
\operatorname{grad}\delta\mathbf{v}^s &= \sum_a \delta\mathbf{v}_a^s \otimes \operatorname{grad} N_a & \operatorname{grad}\Delta\mathbf{u} &= \sum_b \Delta\mathbf{u}_b \otimes \operatorname{grad} N_b \\
\operatorname{div}\delta\mathbf{v}^s &= \sum_a \delta\mathbf{v}_a^s \cdot \operatorname{grad} N_a & \operatorname{div}\Delta\mathbf{u} &= \sum_b \Delta\mathbf{u}_b \cdot \operatorname{grad} N_b \\
\delta\mathbf{w} &= \sum_a N_a \delta\mathbf{w}_a & \Delta\mathbf{w} &= \sum_b N_b \Delta\mathbf{w}_b \\
\operatorname{grad}\delta\mathbf{w} &= \sum_a \delta\mathbf{w}_a \otimes \operatorname{grad} N_a & \operatorname{grad}\Delta\mathbf{w} &= \sum_b \Delta\mathbf{w}_b \otimes \operatorname{grad} N_b \\
\delta J^f &= \sum_a N_a \delta J_a^f & \Delta J^f &= \sum_b N_b \Delta J_b^f \\
\operatorname{grad}\delta J^f &= \sum_a \delta J_a^f \operatorname{grad} N_a & \operatorname{grad}\Delta J^f &= \sum_b \Delta J_b^f \operatorname{grad} N_b
\end{aligned} \tag{3.6.8}$$

Note that the $\operatorname{grad} \equiv \frac{\partial}{\partial \mathbf{x}}$ operator should be evaluated using $\mathbf{x}_{n+\alpha_f}$.

The solution of the nonlinear equation $\delta W = 0$ is obtained by linearizing this relation as

$$\delta W + D\delta W\left[\Delta\mathbf{u}\right] + D\delta W\left[\Delta\mathbf{w}\right] + D\delta W\left[\Delta J^f\right] \approx 0\,, \tag{3.6.9}$$

where the operator $D\delta W\left[\cdot\right]$ represents the directional derivative of δW at $\left(\mathbf{u}^s, \mathbf{w}, J^f\right)$ along an increment $\Delta\mathbf{u}$ of $\mathbf{u}^s$, $\Delta\mathbf{w}$ of $\mathbf{w}$, or ΔJ^f of J^f.

To linearize the virtual work, we need to express the integrals appearing in δW_{int} and δW_{ext} over the material frame of the finite element solid domain. For notational convenience, we let $J \equiv J^s$ and $\mathbf{F} \equiv \mathbf{F}^s$. Thus,

$$\int_b \boldsymbol{\sigma}^s : \operatorname{grad}\delta\mathbf{v}^s \, dv = \int_B \mathbf{F}\cdot\mathbf{S}^s : \operatorname{Grad}\delta\mathbf{v}^s \, dV \quad , \tag{3.6.10}$$

where $\mathbf{S}^s = J\cdot\mathbf{F}^{-1}\cdot\boldsymbol{\sigma}^s\cdot\mathbf{F}^{-T}$ is the second Piola-Kirchhoff stress for the solid material. Similarly,

$$\int_b \boldsymbol{\tau} : \operatorname{grad}\delta\mathbf{w} \, dv = \int_B \boldsymbol{\tau}\cdot J\mathbf{F}^{-T} : \operatorname{Grad}\delta\mathbf{w} \, dV\,. \tag{3.6.11}$$

Next,

$$\begin{aligned}
&\int_b \delta\mathbf{w}\cdot\left(\operatorname{grad} p + \rho^f\mathbf{a}^f\right) dv \\
&= \int_B \delta\mathbf{w}\cdot\left(J\mathbf{F}^{-T}\cdot\operatorname{Grad} p + J\rho^f\left(\dot{\mathbf{w}} + \dot{\mathbf{v}}^s\right) + \rho^f\left(\operatorname{Grad}\mathbf{w} + \operatorname{Grad}\mathbf{v}^s\right)\cdot\mathbf{W}\right) dV
\end{aligned} \tag{3.6.12}$$

$$\int_b \delta J^f\left[\frac{1}{J^f}\left(\dot{J}^f + \operatorname{grad} J^f\cdot\mathbf{w}\right) - \frac{\dot{J}}{J}\right] dv = \int_B \delta J^f\left[\frac{1}{J^f}\left(J\dot{J}^f + \operatorname{Grad} J^f\cdot\mathbf{W}\right) - \dot{J}\right] dV \tag{3.6.13}$$

$$\int_b \mathbf{w}\cdot\operatorname{grad}\delta J^f \, dv = \int_B \operatorname{Grad}\delta J^f\cdot\mathbf{W} \, dV \tag{3.6.14}$$

where $\mathbf{W} = J\mathbf{F}^{-1}\cdot\mathbf{w}$.

Keep in mind that we are solving for the motions $\boldsymbol{\chi}^{\iota}_{n+1}$ at t_{n+1}. Therefore,

$$\begin{aligned}
D\mathbf{u}^s\left[\Delta\mathbf{u}\right] &= \alpha_f \Delta\mathbf{u} \\
D\mathbf{F}\left[\Delta\mathbf{u}\right] &= \alpha_f \operatorname{Grad}\Delta\mathbf{u} \\
DJ\left[\Delta\mathbf{u}\right] &= \alpha_f J\left(\operatorname{div}\Delta\mathbf{u}\right) \\
D\dot{J}\left[\Delta\mathbf{u}\right] &= D\left(J\mathbf{F}^{-T} : \operatorname{Grad}\mathbf{v}^s\right)\left[\Delta\mathbf{u}\right] \\
&= \alpha_f J\left[\left(\operatorname{div}\mathbf{v}^s + \frac{\gamma}{\beta\Delta t}\right)\left(\operatorname{div}\Delta\mathbf{u}\right) - \left(\operatorname{grad}\Delta\mathbf{u}\right)^T : \mathbf{L}^s\right] \\
D\mathbf{v}^s\left[\Delta\mathbf{u}\right] &= \frac{\alpha_f\gamma}{\beta\Delta t}\Delta\mathbf{u} \\
D\mathbf{w}\left[\Delta\mathbf{w}\right] &= \alpha_f \Delta\mathbf{w} \\
DJ^f\left[\Delta J^f\right] &= \alpha_f \Delta J^f \\
D\rho^f\left[\Delta J^f\right] &= -\alpha_f \frac{\rho^f}{J^f}\Delta J^f
\end{aligned}$$

In general, $\boldsymbol{\sigma}^s$ (and thus, $\mathbf{S}^s$) is only a function of the solid strain, such as the right Cauchy-Green tensor $\mathbf{C} = \mathbf{F}^T \cdot \mathbf{F}$ or the Green-Lagrange strain $\mathbf{E} = \left(\mathbf{C} - \mathbf{I}\right)/2$.

$$D\mathbf{E}\left[\Delta\mathbf{u}\right] = \frac{\alpha_f}{2}\left(\operatorname{Grad}^T\Delta\mathbf{u}\cdot\mathbf{F} + \mathbf{F}^T\cdot\operatorname{Grad}\Delta\mathbf{u}\right)$$

Therefore, following the standard approach in solid mechanics, the linearization of $\mathbf{S}^s$ is

$$\begin{aligned}
D\mathbf{S}^s = D\mathbf{S}^s\left[\Delta\mathbf{u}\right] &= \frac{\partial\mathbf{S}^s}{\partial\mathbf{E}} : D\mathbf{E}\left[\Delta\mathbf{u}\right] \\
&= \alpha_f\mathbb{C}^s : \frac{1}{2}\left(\operatorname{Grad}^T\Delta\mathbf{u}\cdot\mathbf{F} + \mathbf{F}^T\cdot\operatorname{Grad}\Delta\mathbf{u}\right) \\
&= \alpha_f\mathbb{C}^s : \left(\mathbf{F}^T \underline{\otimes} \mathbf{F}^T\right) : \Delta\boldsymbol{\varepsilon}
\end{aligned} \tag{3.6.15}$$

In general, $\boldsymbol{\tau}$ is a function of the fluid volume ratio J^f and the rate of deformation of the fluid, $\mathbf{D}^f = \frac{1}{2}\left(\mathbf{L}^f + \left(\mathbf{L}^f\right)^T\right)$. However, since $\mathbf{v}^f$ is not a degree of freedom, we need to let $\mathbf{D}^f = \mathbf{D}^w + \mathbf{D}^s$, where $\mathbf{D}^w = \frac{1}{2}\left(\mathbf{L}^w + \left(\mathbf{L}^w\right)^T\right)$ and $\mathbf{D}^s = \frac{1}{2}\left(\mathbf{L}^s + \left(\mathbf{L}^s\right)^T\right)$. Thus,

$$D\boldsymbol{\tau} = \boldsymbol{\mathcal{C}}^\tau : \left(D\mathbf{D}^f\left[\Delta\mathbf{w}\right] + D\mathbf{D}^f\left[\Delta\mathbf{u}\right]\right) + \frac{\partial\boldsymbol{\tau}}{\partial J^f} DJ^f\left[\Delta J^f\right] \tag{3.6.16}$$

where

$$\boldsymbol{\mathcal{C}}^\tau = \frac{\partial\boldsymbol{\tau}}{\partial\mathbf{D}^f} \tag{3.6.17}$$

3.6.4 Linearization of $\int_B \mathbf{F}\cdot\mathbf{S}^s : \operatorname{Grad}\delta\mathbf{v}^s\, dV$

$$\begin{aligned}
&D\left(\int_B \mathbf{F}\cdot\mathbf{S}^s : \operatorname{Grad}\delta\mathbf{v}^s\, dV\right)\left[\Delta\mathbf{u}\right] \\
&= \int_b \alpha_f\left(\boldsymbol{\sigma}^s : \operatorname{grad}^T\Delta\mathbf{u}\cdot\operatorname{grad}\delta\mathbf{v}^s + \operatorname{grad}\delta\mathbf{v}^s : \boldsymbol{\mathcal{C}}^s : \Delta\boldsymbol{\varepsilon}\right) dv
\end{aligned} \tag{3.6.18}$$

where

$$\boldsymbol{\mathcal{C}}^s = J^{-1}\left(\mathbf{F}\underline{\otimes}\mathbf{F}\right) : \mathbb{C}^s : \left(\mathbf{F}^T\underline{\otimes}\mathbf{F}^T\right)$$

Similarly,

$$D\left(\int_B \mathbf{F}\cdot\mathbf{S}^s : \operatorname{Grad}\delta\mathbf{v}^s\, dV\right)[\Delta\mathbf{w}] = 0 \tag{3.6.19}$$

and

$$D\left(\int_B \mathbf{F}\cdot\mathbf{S}^s : \operatorname{Grad}\delta\mathbf{v}^s\, dV\right)\left[\Delta J^f\right] = 0 \tag{3.6.20}$$

The discretized version produces

$$\begin{aligned}&\int_b \alpha_f\left(\boldsymbol{\sigma}^s : \operatorname{grad}^T\Delta\mathbf{u}\cdot\operatorname{grad}\delta\mathbf{v}^s + \operatorname{grad}\delta\mathbf{v}^s : \boldsymbol{\mathcal{C}}^s : \Delta\boldsymbol{\varepsilon}\right) dv\\ &= \sum_a \delta\mathbf{v}_a^s\cdot\sum_b\int_b \mathbf{K}_{ab}^{uu}\, dv\cdot\Delta\mathbf{u}_b\end{aligned}$$

where

$$\mathbf{K}_{ab}^{uu} = \alpha_f\left((\operatorname{grad}N_a\cdot\boldsymbol{\sigma}^s\cdot\operatorname{grad}N_b)\,\mathbf{I} + (\operatorname{grad}N_a\cdot\boldsymbol{\mathcal{C}}^s\cdot\operatorname{grad}N_b)\right) \tag{3.6.21}$$

$$\mathbf{K}_{ab}^{uw} = \mathbf{0} \tag{3.6.22}$$

$$\mathbf{k}_{ab}^{uJ} = \mathbf{0} \tag{3.6.23}$$

3.6.5 Linearization of $\int_B \boldsymbol{\tau}\cdot J\mathbf{F}^{-T} : \operatorname{Grad}\delta\mathbf{w}\, dV$

$$\begin{aligned}&D\left(\int_B \boldsymbol{\tau}\cdot J\mathbf{F}^{-T} : \operatorname{Grad}\delta\mathbf{w}\, dV\right)[\Delta\mathbf{u}]\\ &= \int_b \alpha_f\left(\boldsymbol{\tau} : \operatorname{grad}\delta\mathbf{w}\cdot\Delta\mathbf{G} + \operatorname{grad}\delta\mathbf{w} : \boldsymbol{\mathcal{C}}^\tau : \mathbf{M}\cdot\operatorname{grad}\Delta\mathbf{u}\right) dv\end{aligned} \tag{3.6.24}$$

$$\begin{aligned}D\left(\int_B \boldsymbol{\tau}\cdot J\mathbf{F}^{-T} : \operatorname{Grad}\delta\mathbf{w}\, dV\right)[\Delta\mathbf{u}] &= \int_B D\left(\boldsymbol{\tau}\cdot J\mathbf{F}^{-T}\right)[\Delta\mathbf{u}] : \operatorname{Grad}\delta\mathbf{w}\, dV\\ &= \int_B \left(D\boldsymbol{\tau}\,[\Delta\mathbf{u}]\cdot J\mathbf{F}^{-T} + \boldsymbol{\tau}\cdot D\left(J\mathbf{F}^{-T}\right)[\Delta\mathbf{u}]\right) : \operatorname{Grad}\delta\mathbf{w}\, dV\end{aligned}$$

where we used

$$\boldsymbol{\mathcal{C}}^\tau = \frac{\partial\boldsymbol{\tau}}{\partial\mathbf{D}^f}\,.$$

Similarly,

$$D\left(\int_B \boldsymbol{\tau}\cdot J\mathbf{F}^{-T} : \operatorname{Grad}\delta\mathbf{w}\, dV\right)[\Delta\mathbf{w}] = \int_b \alpha_f \operatorname{grad}\delta\mathbf{w} : \boldsymbol{\mathcal{C}}^\tau : \operatorname{grad}\Delta\mathbf{w}\, dv \tag{3.6.25}$$

$$D\left(\int_B \boldsymbol{\tau}\cdot J\mathbf{F}^{-T} : \operatorname{Grad}\delta\mathbf{w}\, dV\right)\left[\Delta J^f\right] = \int_b \alpha_f\Delta J^f\boldsymbol{\tau}'_J : \operatorname{grad}\delta\mathbf{w}\, dv \tag{3.6.26}$$

where

$$\boldsymbol{\tau}'_J = \frac{\partial\boldsymbol{\tau}}{\partial J^f}$$

The discretized version produces

$$\begin{aligned}&\int_b \alpha_f\left(\boldsymbol{\tau} : \operatorname{grad}\delta\mathbf{w}\cdot\Delta\mathbf{G} + \operatorname{grad}\delta\mathbf{w} : \boldsymbol{\mathcal{C}}^\tau : \mathbf{M}\cdot\operatorname{grad}\Delta\mathbf{u}\right) dv\\ &= \sum_a \delta\mathbf{w}_a\cdot\sum_b\int_b \mathbf{K}_{ab}^{wu}\, dv\cdot\Delta\mathbf{u}_b\end{aligned}$$

where

$$\mathbf{K}_{ab}^{wu} = \alpha_f \boldsymbol{\tau} \cdot (\operatorname{grad} N_a \otimes \operatorname{grad} N_b - \operatorname{grad} N_b \otimes \operatorname{grad} N_a) + (\operatorname{grad} N_a \cdot \boldsymbol{\mathcal{C}}^{\tau} \cdot \operatorname{grad} N_b) \cdot \mathbf{M} \tag{3.6.27}$$

$$\int_b \alpha_f \operatorname{grad} \delta\mathbf{w} : \boldsymbol{\mathcal{C}}^{\tau} : \operatorname{grad} \Delta\mathbf{w}\, dv = \sum_a \delta\mathbf{w}_a \cdot \sum_b \int_b \mathbf{K}_{ab}^{ww}\, dv \cdot \Delta\mathbf{w}_b$$

where

$$\mathbf{K}_{ab}^{ww} = \alpha_f \operatorname{grad} N_a \cdot \boldsymbol{\mathcal{C}}^{\tau} \cdot \operatorname{grad} N_b \tag{3.6.28}$$

$$\int_b \alpha_f \Delta J^f \boldsymbol{\tau}'_J : \operatorname{grad} \delta\mathbf{w}\, dv = \sum_a \delta\mathbf{w}_a \cdot \sum_b \int_b \mathbf{k}_{ab}^{wJ}\, dv\, \Delta J_b^f$$

where

$$\mathbf{k}_{ab}^{wJ} = \alpha_f N_b \boldsymbol{\tau}'_J \cdot \operatorname{grad} N_a \tag{3.6.29}$$

3.6.6 Linearization of $\int_B \delta\mathbf{w} \cdot J\mathbf{F}^{-T} \cdot \operatorname{Grad} p\, dV$

$$\boxed{\begin{aligned} &D\left(\int_B \delta\mathbf{w} \cdot J\mathbf{F}^{-T} \cdot \operatorname{Grad} p\, dV\right)[\Delta\mathbf{u}] \\ &= \int_b \alpha_f \delta\mathbf{w} \cdot \Delta\mathbf{G}^T \cdot \operatorname{grad} p\, dv \end{aligned}} \tag{3.6.30}$$

$$\boxed{D\left(\int_B \delta\mathbf{w} \cdot J\mathbf{F}^{-T} \cdot \operatorname{Grad} p\, dV\right)[\Delta\mathbf{w}] = 0} \tag{3.6.31}$$

$$\boxed{\begin{aligned} &D\left(\int_B \delta\mathbf{w} \cdot J\mathbf{F}^{-T} \cdot \operatorname{Grad} p\, dV\right)\left[\Delta J^f\right] \\ &= \int_b \alpha_f \delta\mathbf{w} \cdot \left(\Delta J^f p''\left(J^f\right) \operatorname{grad} J^f + p'\left(J^f\right) \operatorname{grad} \Delta J^f\right)\, dv \end{aligned}} \tag{3.6.32}$$

The discretization of these terms produces

$$\int_b \alpha_f \delta\mathbf{w} \cdot \Delta\mathbf{G}^T \cdot \operatorname{grad} p\, dv = \sum_a \delta\mathbf{w}_a \cdot \sum_b \int_b \mathbf{K}_{ab}^{wu}\, dv \cdot \Delta\mathbf{u}_b$$

where

$$\boxed{\mathbf{K}_{ab}^{wu} = \alpha_f N_a (\operatorname{grad} p \otimes \operatorname{grad} N_b - \operatorname{grad} N_b \otimes \operatorname{grad} p)} \tag{3.6.33}$$

$$\boxed{\mathbf{K}_{ab}^{ww} = \mathbf{0}} \tag{3.6.34}$$

$$\int_b \alpha_f \delta\mathbf{w} \cdot \left(\Delta J^f p''\left(J^f\right) \operatorname{grad} J^f + p'\left(J^f\right) \operatorname{grad} \Delta J^f\right)\, dv = \sum_a \delta\mathbf{w}_a \cdot \sum_b \int_b \mathbf{k}_{ab}^{wJ}\, dv \Delta J_b^f$$

$$\boxed{\mathbf{k}_{ab}^{wJ} = \alpha_f N_a \left(N_b p''\left(J^f\right) \operatorname{grad} J^f + p'\left(J^f\right) \operatorname{grad} N_b\right)} \tag{3.6.35}$$

3.6.7 Linearization of $\int_B \delta\mathbf{w}\cdot\rho^f\left[J\left(\dot{\mathbf{w}}+\dot{\mathbf{v}}^s\right)+\left(\operatorname{Grad}\mathbf{w}+\operatorname{Grad}\mathbf{v}^s\right)\cdot\mathbf{W}\right]\,dV$

$$\int_B \delta\mathbf{w}\cdot\rho^f\left[J\left(\dot{\mathbf{w}}+\dot{\mathbf{v}}^s\right)+\left(\operatorname{Grad}\mathbf{w}+\operatorname{Grad}\mathbf{v}^s\right)\cdot\mathbf{W}\right]\,dV$$

$$\begin{aligned}
&D\left(\int_B \delta\mathbf{w}\cdot\rho^f\left[J\left(\dot{\mathbf{w}}+\dot{\mathbf{v}}^s\right)+\left(\operatorname{Grad}\mathbf{w}+\operatorname{Grad}\mathbf{v}^s\right)\cdot\mathbf{W}\right]\,dV\right)[\Delta\mathbf{u}]\\
&=\int_b \delta\mathbf{w}\cdot\alpha_f\rho^f\left[\left(\operatorname{div}\Delta\mathbf{u}\right)\left(\dot{\mathbf{w}}+\dot{\mathbf{v}}^s\right)+\frac{\gamma}{\beta\Delta t}\operatorname{grad}\Delta\mathbf{u}\cdot\mathbf{w}+\frac{\alpha_m}{\alpha_f\beta\Delta t^2}\Delta\mathbf{u}\right]\,dv\\
&+\int_b \delta\mathbf{w}\cdot\alpha_f\rho^f\mathbf{L}^f\cdot\Delta\mathbf{G}\cdot\mathbf{w}\,dv
\end{aligned}\tag{3.6.36}$$

$$\begin{aligned}
&D\left(\int_B \delta\mathbf{w}\cdot\rho^f\left[J\left(\dot{\mathbf{w}}+\dot{\mathbf{v}}^s\right)+\left(\operatorname{Grad}\mathbf{w}+\operatorname{Grad}\mathbf{v}^s\right)\cdot\mathbf{W}\right]\,dV\right)[\Delta\mathbf{w}]\\
&=\int_b \delta\mathbf{w}\cdot\alpha_f\rho^f\left[\left(\frac{\alpha_m}{\alpha_f\gamma\Delta t}\mathbf{I}+\mathbf{L}^f\right)\cdot\Delta\mathbf{w}+\operatorname{grad}\Delta\mathbf{w}\cdot\mathbf{w}\right]\,dv
\end{aligned}\tag{3.6.37}$$

$$\begin{aligned}
&D\left(\int_B \delta\mathbf{w}\cdot\rho^f\left[J\left(\dot{\mathbf{w}}+\dot{\mathbf{v}}^s\right)+\left(\operatorname{Grad}\mathbf{w}+\operatorname{Grad}\mathbf{v}^s\right)\cdot\mathbf{W}\right]\,dV\right)\left[\Delta J^f\right]\\
&=-\int_b \delta\mathbf{w}\cdot\alpha_f\frac{\rho^f}{J^f}\Delta J^f\mathbf{a}^f\,dv
\end{aligned}\tag{3.6.38}$$

The discretized version is given by

$$\begin{aligned}
&\int_b \delta\mathbf{w}\cdot\alpha_f\rho^f\left[\left(\operatorname{div}\Delta\mathbf{u}\right)\left(\dot{\mathbf{w}}+\dot{\mathbf{v}}^s\right)+\frac{\gamma}{\beta\Delta t}\operatorname{grad}\Delta\mathbf{u}\cdot\mathbf{w}+\frac{\alpha_m}{\alpha_f\beta\Delta t^2}\Delta\mathbf{u}\right]\,dv\\
&+\int_b \delta\mathbf{w}\cdot\alpha_f\rho^f\mathbf{L}^f\cdot\Delta\mathbf{G}\cdot\mathbf{w}\,dv\\
&=\sum_a \delta\mathbf{w}_a\cdot\sum_b\int_b\mathbf{K}^{wu}_{ab}\,dv\cdot\Delta\mathbf{u}_b
\end{aligned}$$

where

$$\mathbf{K}^{wu}_{ab}=\alpha_f N_a\rho^f\left[\mathbf{a}^f\otimes\operatorname{grad}N_b-\left(\operatorname{grad}N_b\cdot\mathbf{w}\right)\mathbf{L}^f+\left(\frac{\gamma}{\beta\Delta t}\left(\operatorname{grad}N_b\cdot\mathbf{w}\right)+\frac{\alpha_m}{\alpha_f\beta\Delta t^2}N_b\right)\mathbf{I}\right]\tag{3.6.39}$$

$$\begin{aligned}
&\int_b \delta\mathbf{w}\cdot\alpha_f\rho^f\left[\left(\frac{\alpha_m}{\alpha_f\gamma\Delta t}\mathbf{I}+\mathbf{L}^f\right)\cdot\Delta\mathbf{w}+\operatorname{grad}\Delta\mathbf{w}\cdot\mathbf{w}\right]\,dv\\
&=\sum_a \delta\mathbf{w}_a\cdot\sum_b\int_b\mathbf{K}^{ww}_{ab}\,dv\cdot\Delta\mathbf{w}_b
\end{aligned}$$

where

$$\mathbf{K}^{ww}_{ab}=\alpha_f N_a\rho^f\left[N_b\left(\frac{\alpha_m}{\alpha_f\gamma\Delta t}\mathbf{I}+\mathbf{L}^f\right)+\left(\operatorname{grad}N_b\cdot\mathbf{w}\right)\mathbf{I}\right]\tag{3.6.40}$$

$$-\int_B \delta\mathbf{w}\cdot\alpha_f\frac{\rho^f}{J^f}\Delta J^f\mathbf{a}^f\,dv=\sum_a \delta\mathbf{w}_a\cdot\sum_b\int_b\mathbf{k}^{wJ}_{ab}\,dv\Delta J^f_b$$

where

$$\boxed{\mathbf{k}_{ab}^{w,J} = -\alpha_f N_a N_b \frac{\rho^f}{J^f}\mathbf{a}^f} \tag{3.6.41}$$

3.6.8 Linearization of $\int_B \delta J^f \left[\frac{1}{J^f}\left(J\dot{J}^f + \text{Grad}\, J^f \cdot \mathbf{W}\right) - \dot{J}\right] dV$

$$\int_B \delta J^f \left[\frac{1}{J^f}\left(J\dot{J}^f + \text{Grad}\, J^f \cdot \mathbf{W}\right) - \dot{J}\right] dV$$

$$D\left(\int_B \delta J^f \left[\frac{1}{J^f}\left(J\dot{J}^f + \text{Grad}\, J^f \cdot \mathbf{W}\right) - \dot{J}\right] dV\right)[\Delta\mathbf{u}]$$

$$= \int_B \delta J^f \left[\frac{1}{J^f}\left(DJ\,[\Delta\mathbf{u}]\,\dot{J}^f + \text{Grad}\, J^f \cdot D\mathbf{W}\,[\Delta\mathbf{u}]\right) - D\dot{J}\,[\Delta\mathbf{u}]\right] dV$$

$$= \int_b \delta J^f \alpha_f \left[\left(\frac{\dot{J}^f}{J^f} - \text{div}\,\mathbf{v}^s - \frac{\gamma}{\beta\Delta t}\right)(\text{div}\,\Delta\mathbf{u}) + \mathbf{w}\cdot\left[(\text{div}\,\Delta\mathbf{u})\,\mathbf{I} - \text{grad}^T\,\Delta\mathbf{u}\right]\cdot\frac{\text{grad}\, J^f}{J^f} + (\text{grad}\,\Delta\mathbf{u})^T : \mathbf{L}^s\right] dv$$

$$\boxed{\begin{aligned} &D\left(\int_B \delta J^f \left[\frac{1}{J^f}\left(J\dot{J}^f + \text{Grad}\, J^f \cdot \mathbf{W}\right) - \dot{J}\right] dV\right)[\Delta\mathbf{u}] \\ &= \int_b \delta J^f \alpha_f \left[\left(\frac{\dot{J}^f}{J^f} - \text{div}\,\mathbf{v}^s - \frac{\gamma}{\beta\Delta t}\right)(\text{div}\,\Delta\mathbf{u}) + \mathbf{w}\cdot\Delta\mathbf{G}^T\cdot\frac{\text{grad}\, J^f}{J^f} + (\text{grad}\,\Delta\mathbf{u})^T : \mathbf{L}^s\right] dv \end{aligned}} \tag{3.6.42}$$

$$\boxed{\begin{aligned} &D\left(\int_B \delta J^f \left[\frac{1}{J^f}\left(J\dot{J}^f + \text{Grad}\, J^f \cdot \mathbf{W}\right) - \dot{J}\right] dV\right)[\Delta\mathbf{w}] \\ &= \int_b \delta J^f \alpha_f \frac{1}{J^f}\Delta\mathbf{w}\cdot\text{grad}\, J^f\, dv \end{aligned}} \tag{3.6.43}$$

$$\boxed{\begin{aligned} &D\left(\int_B \delta J^f \left[\frac{1}{J^f}\left(J\dot{J}^f + \text{Grad}\, J^f \cdot \mathbf{W}\right) - \dot{J}\right] dV\right)\left[\Delta J^f\right] \\ &= \int_b \delta J^f \alpha_f \frac{1}{J^f}\left(\left[\frac{\alpha_m}{\alpha_f\gamma\Delta t} - \frac{1}{J^f}\left(\dot{J}^f + \mathbf{w}\cdot\text{grad}\, J^f\right)\right]\Delta J^f + \mathbf{w}\cdot\text{grad}\,\Delta J^f\right) dv \end{aligned}} \tag{3.6.44}$$

The discretization of these terms produces

$$\int_b \delta J^f \alpha_f \left[\left(\frac{\dot{J}^f}{J^f} - \text{div}\,\mathbf{v}^s - \frac{\gamma}{\beta\Delta t}\right)(\text{div}\,\Delta\mathbf{u}) + \mathbf{w}\cdot\Delta\mathbf{G}^T\cdot\frac{\text{grad}\, J^f}{J^f} + (\text{grad}\,\Delta\mathbf{u})^T : \mathbf{L}^s\right] dv$$

$$= \sum_a \delta J_a^f \sum_b \int_b \mathbf{k}_{ab}^{Ju}\, dv\cdot\Delta\mathbf{u}_b$$

where

$$\boxed{\mathbf{k}_{ab}^{Ju} = \alpha_f N_a\left[\left(\frac{\dot{J}^f}{J^f} - \text{div}\,\mathbf{v}^s - \frac{\gamma}{\beta\Delta t}\right)\text{grad}\, N_b + \left(\text{grad}\, N_b \otimes \frac{\text{grad}\, J^f}{J^f} - \frac{\text{grad}\, J^f}{J^f}\otimes\text{grad}\, N_b\right)\cdot\mathbf{w} + (\mathbf{L}^s)^T\cdot\text{grad}\, N_b\right]} \tag{3.6.45}$$

$$\int_b \delta J^f \alpha_f \frac{1}{J^f}\Delta\mathbf{w}\cdot\text{grad}\, J^f\, dv = \sum_a \delta J_a^f \sum_b \int_b \mathbf{k}_{ab}^{Jw}\, dv\cdot\Delta\mathbf{w}_b$$

where

$$\boxed{\mathbf{k}_{ab}^{Jw} = \alpha_f \frac{N_a N_b}{J^f} \operatorname{grad} J^f} \tag{3.6.46}$$

$$\int_b \delta J^f \alpha_f \frac{1}{J^f} \left(\left[\frac{\alpha_m}{\alpha_f \gamma \Delta t} - \frac{1}{J^f} \left(\dot{J}^f + \mathbf{w} \cdot \operatorname{grad} J^f \right) \right] \Delta J^f + \mathbf{w} \cdot \operatorname{grad} \Delta J^f \right) dv$$
$$= \sum_a \delta J_a^f \sum_b \int_b k_{ab}^{JJ} \, dv \Delta J_b^f$$

where

$$\boxed{k_{ab}^{JJ} = \alpha_f N_a \frac{1}{J^f} \left(N_b \left[\frac{\alpha_m}{\alpha_f \gamma \Delta t} - \frac{1}{J^f} \left(\dot{J}^f + \mathbf{w} \cdot \operatorname{grad} J^f \right) \right] + \mathbf{w} \cdot \operatorname{grad} N_b \right)} \tag{3.6.47}$$

3.6.9 Linearization of $-\int_B \operatorname{Grad} \delta J^f \cdot \mathbf{W} \, dV$

$$-\int_B \operatorname{Grad} \delta J^f \cdot \mathbf{W} \, dV$$

$$\boxed{D \left(\int_B \operatorname{Grad} \delta J^f \cdot \mathbf{W} \, dV \right) [\Delta \mathbf{u}] = \int_b \alpha_f \mathbf{w} \cdot \Delta \mathbf{G}^T \cdot \operatorname{grad} \delta J^f \, dv} \tag{3.6.48}$$

$$D \left(\int_B \operatorname{Grad} \delta J^f \cdot \mathbf{W} \, dV \right) [\Delta \mathbf{u}]$$
$$= \int_B \operatorname{Grad} \delta J^f \cdot D\mathbf{W} \left[\Delta \mathbf{w} \right] \, dV$$
$$= \int_B \alpha_f \Delta \mathbf{w} \cdot \operatorname{grad} \delta J^f \, dv$$

$$\boxed{D \left(\int_B \operatorname{Grad} \delta J^f \cdot \mathbf{W} \, dV \right) [\Delta \mathbf{w}] = \int_B \alpha_f \Delta \mathbf{w} \cdot \operatorname{grad} \delta J^f \, dv} \tag{3.6.49}$$

$$\boxed{D \left(\int_B \operatorname{Grad} \delta J^f \cdot \mathbf{W} \, dV \right) \left[\Delta J^f \right] = 0} \tag{3.6.50}$$

The discretization of these terms produces

$$\int_b \alpha_f \mathbf{w} \cdot \Delta \mathbf{G}^T \cdot \operatorname{grad} \delta J^f \, dv = \sum_a \delta J_a^f \sum_b \int_v \mathbf{k}_{ab}^{Ju} \, dv \cdot \Delta \mathbf{u}_b$$

where

$$\boxed{\mathbf{k}_{ab}^{Ju} = \alpha_f \left(\operatorname{grad} N_b \otimes \operatorname{grad} N_a - \operatorname{grad} N_a \otimes \operatorname{grad} N_b \right) \cdot \mathbf{w}} \tag{3.6.51}$$

$$\int_B \alpha_f \Delta \mathbf{w} \cdot \operatorname{grad} \delta J^f \, dv = \sum_a \delta J_a^f \sum_b \int_b \mathbf{k}_{ab}^{Jw} \, dv \cdot \Delta \mathbf{w}_b$$

where

$$\boxed{\mathbf{k}_{ab}^{Jw} = \alpha_f N_b \operatorname{grad} N_a} \tag{3.6.52}$$

$$\boxed{k_{ab}^{JJ} = 0} \tag{3.6.53}$$

3.6.10 Body force term $\int_b \delta\mathbf{w}\cdot\rho^f\mathbf{b}\,dv$

The body force term may be discretized as

$$\int_b \delta\mathbf{w}\cdot\rho^f\mathbf{b}\,dv = \sum_a \delta\mathbf{w}_a\cdot\int_b N_a\rho^f\mathbf{b}\,dv$$

To linearizes this expression, we first evaluate it in the material domain,

$$\int_b \delta\mathbf{w}\cdot\rho^f\mathbf{b}\,dv = \int_B \delta\mathbf{w}\cdot\rho^f J\mathbf{b}\,dV$$

Now,

$$\boxed{D\left(\int_B \delta\mathbf{w}\cdot\rho^f J\mathbf{b}\,dV\right)[\Delta\mathbf{u}] = \int_b \alpha_f\rho^f\left(\operatorname{div}\Delta\mathbf{u}\right)\delta\mathbf{w}\cdot\mathbf{b}\,dv} \tag{3.6.54}$$

$$\boxed{D\left(\int_B \delta\mathbf{w}\cdot\rho^f J\mathbf{b}\,dV\right)[\Delta\mathbf{w}] = 0} \tag{3.6.55}$$

$$\boxed{D\left(\int_B \delta\mathbf{w}\cdot\rho^f J\mathbf{b}\,dV\right)\left[\Delta J^f\right] = -\int_b \Delta J^f\frac{\alpha_f\rho^f}{J^f}\delta\mathbf{w}\cdot\mathbf{b}\,dv} \tag{3.6.56}$$

The discrete forms of these expressions are given by

$$\int_b \alpha_f\rho^f\left(\operatorname{div}\Delta\mathbf{u}\right)\delta\mathbf{w}\cdot\mathbf{b}\,dv = \sum_a \delta\mathbf{w}_a\cdot\sum_b\int_b \mathbf{K}^{wu}_{ab}\,dv\cdot\Delta\mathbf{u}_b$$

where

$$\boxed{\mathbf{K}^{wu}_{ab} = \alpha_f\rho^f N_a\mathbf{b}\otimes\operatorname{grad}N_b} \tag{3.6.57}$$

$$\boxed{\mathbf{K}^{ww}_{ab} = \mathbf{0}} \tag{3.6.58}$$

$$-\int_b \Delta J^f\frac{\alpha_f\rho^f}{J^f}\delta\mathbf{w}\cdot\mathbf{b}\,dv = \sum_a \delta\mathbf{w}_a\cdot\sum_b\int_b \mathbf{k}^{wJ}_{ab}\,dv\,\Delta J^f_b$$

where

$$\boxed{\mathbf{k}^{wJ}_{ab} = -\alpha_f N_a N_b\frac{\rho^f}{J^f}\mathbf{b}} \tag{3.6.59}$$

3.6.11 Fluid traction acting on solid interface

At a fluid-solid interface Γ, the fluid traction $\mathbf{t}^f = \boldsymbol{\sigma}^f\cdot\mathbf{n}$ acts on the solid surface, $\mathbf{t}^s = -\mathbf{t}^f$, where $\mathbf{n}$ is the outward normal to the fluid surface. The resulting virtual work on the solid domain is

$$\delta G = \int_\Gamma \delta\mathbf{v}^s\cdot\mathbf{t}^s_{n+\alpha_f}\,da = \int_\Gamma -\delta\mathbf{v}^s\cdot\boldsymbol{\sigma}^f\cdot\mathbf{n}\,da = \int_{\Gamma_\eta} -\delta\mathbf{v}^s\cdot\boldsymbol{\sigma}^f\cdot\left(\mathbf{g}_1\times\mathbf{g}_2\right)\,d\eta^1 d\eta^2$$

The linearization of this work is given by

$$D\delta G\left[\Delta\mathbf{u}\right] = \int_{\Gamma_\eta} -\delta\mathbf{v}^s\cdot\alpha_f\left[\left(\boldsymbol{\mathcal{C}}^v : \mathbf{M}\cdot\operatorname{grad}\Delta\mathbf{u}\right)\cdot\left(\mathbf{g}_1\times\mathbf{g}_2\right) + \boldsymbol{\sigma}^f\cdot\left(\frac{\partial\Delta\mathbf{u}}{\partial\eta^1}\times\mathbf{g}_2 + \mathbf{g}_1\times\frac{\partial\Delta\mathbf{u}}{\partial\eta^2}\right)\right]\,d\eta^1 d\eta^2$$

where

$$\mathbf{g}_\alpha = \frac{\partial \mathbf{x}}{\partial \eta^\alpha}$$

are covariant basis vectors on Γ. Similarly,

$$D\delta G\left[\Delta\mathbf{w}\right] = \int_{\Gamma_\eta} -\delta\mathbf{v}^s \cdot \alpha_f \left[(\boldsymbol{\mathcal{C}}^v : \operatorname{grad}\Delta\mathbf{w}) \cdot (\mathbf{g}_1 \times \mathbf{g}_2)\right] \, d\eta^1 d\eta^2$$

and

$$D\delta G\left[\Delta J^f\right] = \int_{\Gamma_\eta} -\Delta J^f \delta\mathbf{v}^s \cdot \alpha_f \left[\left(-p'\left(J^f\right) + \boldsymbol{\tau}'_J\right) \cdot (\mathbf{g}_1 \times \mathbf{g}_2)\right] \, d\eta^1 d\eta^2$$

The discretized form of these equations is

$$\delta G = \sum_a \delta\mathbf{v}_a^s \cdot \int_\Gamma \mathbf{f}_a \, d\eta^1 d\eta^2$$

where

$$\boxed{\mathbf{f}_a = -N_a \boldsymbol{\sigma}^f \cdot (\mathbf{g}_1 \times \mathbf{g}_2)} \tag{3.6.60}$$

$$D\delta G\left[\Delta\mathbf{u}\right] = \sum_a \delta\mathbf{v}_a^s \cdot \sum_b \int_{\Gamma_\eta} \mathbf{K}_{ab}^{uu} \, d\eta^1 d\eta^2 \cdot \Delta\mathbf{u}_b$$

where

$$\boxed{\mathbf{K}_{ab}^{uu} = -\alpha_f N_a \left(\left[(\mathbf{g}_1 \times \mathbf{g}_2) \cdot \boldsymbol{\mathcal{C}}^v \cdot \operatorname{grad} N_b\right] \cdot \mathbf{M} + \boldsymbol{\sigma}^f \cdot \boldsymbol{\mathcal{A}} \left\{ \frac{\partial N_b}{\partial \eta^2}\mathbf{g}_1 - \frac{\partial N_b}{\partial \eta^1}\mathbf{g}_2 \right\} \right)} \tag{3.6.61}$$

and

$$D\delta G\left[\Delta\mathbf{w}\right] = \sum_a \delta\mathbf{v}_a^s \cdot \sum_b \int_{\Gamma_\eta} \mathbf{K}_{ab}^{uw} \, d\eta^1 d\eta^2 \cdot \Delta\mathbf{w}_b$$

where

$$\boxed{\mathbf{K}_{ab}^{uw} = -\alpha_f N_a \left(\mathbf{g}_1 \times \mathbf{g}_2\right) \cdot \boldsymbol{\mathcal{C}}^v \cdot \operatorname{grad} N_b} \tag{3.6.62}$$

$$D\delta G\left[\Delta J^f\right] = \sum_a \delta\mathbf{v}_a^s \cdot \sum_b \int_{\Gamma_\eta} \mathbf{k}_{ab}^{uJ} \, d\eta^1 d\eta^2 \, \Delta J_b^f$$

where

$$\boxed{\mathbf{k}_{ab}^{uJ} = -\alpha_f N_a N_b \left(-p'\left(J^f\right) + \boldsymbol{\tau}'_J\right) \cdot (\mathbf{g}_1 \times \mathbf{g}_2)} \tag{3.6.63}$$

3.6.12 Special Boundary Conditions

3.6.12.1 Backflow Stabilization

Let the normal component of the viscous traction be given by

$$t_n^\tau = \begin{cases} \beta\rho_r w_n^2 & w_n < 0 \\ 0 & w_n \geq 0 \end{cases} . \tag{3.6.64}$$

Then, the contribution of this traction to the virtual external work δW_{ext} is

$$\delta G = \int_{\partial\Omega} \delta\mathbf{w} \cdot t_n^\tau \mathbf{n} \, da \, . \tag{3.6.65}$$

The linearization of δG along an increment $\Delta\mathbf{w}$ in the relative velocity is given by

$$D\delta G\left[\Delta\mathbf{w}\right] = \int_{\partial\Omega} \delta\mathbf{w}\cdot\alpha_f\mathbf{K}_n\cdot\Delta\mathbf{w}\,da\,, \tag{3.6.66}$$

where

$$\mathbf{K}_n = \begin{cases} 2\beta\rho_r w_n\left(\mathbf{n}\otimes\mathbf{n}\right) & v_n < 0 \\ \mathbf{0} & v_n \geq 0 \end{cases}. \tag{3.6.67}$$

Similarly,

$$D\delta G\left[\Delta\mathbf{u}\right] = \int_{\partial\Omega_\eta} \delta\mathbf{w}\cdot\alpha_f t_n^\tau\left(\mathbf{g}_1\times\frac{\partial\Delta\mathbf{u}}{\partial\eta^2} - \mathbf{g}_2\times\frac{\partial\Delta\mathbf{u}}{\partial\eta^1}\right)d\eta^1 d\eta^2$$

The discretized form of δG is

$$\delta G = \sum_a \delta\mathbf{w}_a\cdot\int_{\partial\Omega_\eta}\mathbf{f}_a^n\,d\eta^1 d\eta^2, \quad \boxed{\mathbf{f}_a^n = N_a t_n^\tau\left(\mathbf{g}_1\times\mathbf{g}_2\right)}, \tag{3.6.68}$$

whereas the discretized form of $D\delta G\left[\Delta\mathbf{v}\right]$ is

$$D\delta G\left[\Delta\mathbf{v}\right] = \sum_a \delta\mathbf{w}_a\cdot\sum_b\left(\int_{\partial\Omega_\eta}\mathbf{K}_{ab}^{wu}\,d\eta^1 d\eta^2\cdot\Delta\mathbf{u} + \int_{\partial\Omega_\eta}\mathbf{K}_{ab}^{ww}\,d\eta^1 d\eta^2\cdot\Delta\mathbf{w}_b\right), \tag{3.6.69}$$

with

$$\boxed{\mathbf{K}_{ab}^{ww} = \alpha_f N_a N_b\left|\mathbf{g}_1\times\mathbf{g}_2\right|\mathbf{K}_n}, \tag{3.6.70}$$

and

$$\boxed{\mathbf{K}_{ab}^{wu} = \alpha_f N_a t_n^\tau\boldsymbol{\mathcal{A}}\left\{\frac{\partial N_b}{\partial\eta^2}\mathbf{g}_1 - \frac{\partial N_b}{\partial\eta^1}\mathbf{g}_2\right\}} \tag{3.6.71}$$

3.6.12.2 Tangential Stabilization

The tangential traction given by

$$\mathbf{t}_t^\tau = -\beta\rho_r\left|\mathbf{w}_t\right|\mathbf{w}_t\,. \tag{3.6.72}$$

This form shows that $\mathbf{t}_t^\tau$ opposes tangential flow. The external virtual work for this traction is

$$\delta G = \int_{\partial\Omega}\delta\mathbf{w}\cdot\mathbf{t}_t^\tau\,da\,. \tag{3.6.73}$$

Its linearization along an increment $\Delta\mathbf{w}$ is

$$D\delta G\left[\Delta\mathbf{w}\right] = \int_{\partial\Omega}\delta\mathbf{w}\cdot\alpha_f\mathbf{K}_t\cdot\Delta\mathbf{w}\,da\,, \tag{3.6.74}$$

where it can be shown that

$$\mathbf{K}_t = -\beta\rho_r\left|\mathbf{w}_t\right|\left(\mathbf{I} - \mathbf{n}\otimes\mathbf{n} + \frac{\mathbf{w}_t}{\left|\mathbf{w}_t\right|}\otimes\frac{\mathbf{w}_t}{\left|\mathbf{w}_t\right|}\right). \tag{3.6.75}$$

Similarly,

$$D\delta G\left[\Delta\mathbf{u}\right] = \int_{\partial\Omega_\eta}\delta\mathbf{w}\cdot\alpha_f\left(\mathbf{t}_t^\tau\otimes\mathbf{n}\right)\cdot\left(\frac{\partial\Delta\mathbf{u}}{\partial\eta^1}\times\mathbf{g}_2 + \mathbf{g}_1\times\frac{\partial\Delta\mathbf{u}}{\partial\eta^2}\right)d\eta^1 d\eta^2\,.$$

The discretized form of δG is

$$\delta G = \sum_a \delta \mathbf{v}_a \cdot \int_{\partial\Omega} \mathbf{f}_a^\tau \, d\eta^1 d\eta^2 \,, \quad \boxed{\mathbf{f}_a^\tau = N_a \mathbf{t}_t^\tau \, |\mathbf{g}_1 \times \mathbf{g}_2|} \,. \tag{3.6.76}$$

The discretized form of $D\delta G\,[\Delta\mathbf{v}]$ is

$$D\delta G\,[\Delta\mathbf{v}] = \sum_a \delta \mathbf{w}_a \cdot \sum_b \int_{\partial\Omega_\eta} \left(\mathbf{K}_{ab}^{wu} \cdot \Delta\mathbf{u}_b + \mathbf{K}_{ab}^{ww} \cdot \Delta\mathbf{w}_b\right) \, d\eta^1 d\eta^2 \,, \tag{3.6.77}$$

where

$$\boxed{\mathbf{K}_{ab}^{ww} = \alpha_f N_a N_b \, |\mathbf{g}_1 \times \mathbf{g}_2| \, \mathbf{K}_t} \,, \tag{3.6.78}$$

and

$$\boxed{\mathbf{K}_{ab}^{wu} = \alpha_f N_a \, (\mathbf{t}_t^\tau \otimes \mathbf{n}) \cdot \boldsymbol{\mathcal{A}} \left\{ \frac{\partial N_b}{\partial \eta^2} \mathbf{g}_1 - \frac{\partial N_b}{\partial \eta^1} \mathbf{g}_2 \right\}} \,. \tag{3.6.79}$$

3.7 Weak Formulation for BFSI

3.7.1 Virtual Work and Weak Form

The virtual work statement is used to enforce the three governing equations needed to solve for the nodal DOFs $\mathbf{u}$, $\mathbf{w}$ and e^f, namely the mixture mass balance (2.13.6), the fluid momentum balance (2.13.7), and the solid momentum balance (2.13.8). We may rewrite the momentum balance equations to facilitate the enforcement of natural traction boundary conditions given in (2.13.16) and (2.13.17). Using $\boldsymbol{\tau}^f = \varphi^f \boldsymbol{\tau}$, these become

$$\begin{aligned} \varphi^s \left(-\rho_T^f \mathbf{a}^f + \rho_T^s \mathbf{a}^s\right) = & -\frac{{\varphi^s}^2}{\varphi^f} \boldsymbol{\tau} \cdot \operatorname{grad} \frac{\varphi^f}{\varphi^s} + \operatorname{div}\left(-\varphi^s \boldsymbol{\tau} + \boldsymbol{\sigma}^e\right) \\ & + \varphi^s \left(-\rho_T^f \mathbf{b}^f + \rho_T^s \mathbf{b}^s\right) + \mathbf{k}^{-1} \cdot \mathbf{w} \,, \\ \rho_T^f \mathbf{a}^f = & -\operatorname{grad} p + \frac{1}{\phi^f} \boldsymbol{\tau} \cdot \operatorname{grad} \varphi^f + \operatorname{div} \boldsymbol{\tau} \\ & + \rho_T^f \mathbf{b}^f - \mathbf{k}^{-1} \cdot \mathbf{w} \,. \end{aligned} \tag{3.7.1}$$

The virtual work statement for a Galerkin finite element formulation [27] is $\delta W = 0$, where

$$\begin{aligned} \delta W = & \int_{\Omega^b} \delta \mathbf{v}^s \cdot \left[\operatorname{div}\left(-\varphi^s \boldsymbol{\tau} + \boldsymbol{\sigma}^e\right) - \frac{{\varphi^s}^2}{\varphi^f} \boldsymbol{\tau} \cdot \operatorname{grad} \frac{\varphi^f}{\varphi^s} + \mathbf{k}^{-1} \cdot \mathbf{w}\right] dv \\ & + \int_{\Omega^b} \delta \mathbf{v}^s \cdot \varphi^s \left(-\rho_T^f \left(\mathbf{b}^f - \mathbf{a}^f\right) + \rho_T^s \left(\mathbf{b}^s - \mathbf{a}^s\right)\right) dv \\ & + \int_{\Omega^b} \delta \mathbf{w} \cdot \left[\operatorname{div} \boldsymbol{\tau} - \operatorname{grad} p + \frac{1}{\varphi^f} \boldsymbol{\tau} \cdot \operatorname{grad} \phi^f - \mathbf{k}^{-1} \cdot \mathbf{w}\right] dv \\ & + \int_{\Omega^b} \delta \mathbf{w} \cdot \rho_T^f \left(\mathbf{b}^f - \mathbf{a}^f\right) dv \\ & + \int_{\Omega^b} \delta J^f \left[\operatorname{div} \mathbf{w} + \frac{\dot{J}^s}{J^s} - \frac{1}{J^f} \left(\varphi^f \dot{J}^f + \operatorname{grad} J^f \cdot \mathbf{w}\right)\right] dv \,. \end{aligned} \tag{3.7.2}$$

These integrals are evaluated in the current configuration of Ω^b. Here, $\delta\mathbf{v}^s$ is the virtual solid velocity, $\delta\mathbf{w}$ is the virtual relative fluid volumetric flux, and δJ^f is the virtual fluid energy density. Integrating by parts and using the divergence theorem, the weak form of this statement may be written as $\delta W = \delta W_{ext} - \delta W_{int}$ where the internal virtual work is

$$\begin{aligned}
\delta W_{int} = &\int_{\Omega^b} \left[(-\varphi^s \boldsymbol{\tau} + \boldsymbol{\sigma}^e) : \operatorname{grad}\delta\mathbf{v}^s - \delta\mathbf{v}^s \cdot \mathbf{k}^{-1} \cdot \mathbf{w}\right] dv \\
&+ \int_{\Omega^b} \delta\mathbf{v}^s \cdot \varphi^s \left(\frac{\varphi^s}{\varphi^f}\boldsymbol{\tau} \cdot \operatorname{grad}\frac{\varphi^f}{\varphi^s} - \rho_T^f \mathbf{a}^f + \rho_T^s \mathbf{a}^s\right) dv \\
&+ \int_{\Omega^b} \boldsymbol{\tau} : \operatorname{grad}\delta\mathbf{w}\, dv \\
&+ \int_{\Omega^b} \delta\mathbf{w} \cdot \left(\operatorname{grad} p + \mathbf{k}^{-1} \cdot \mathbf{w}\right) dv \\
&+ \int_{\Omega^b} \delta\mathbf{w} \cdot \left(\rho_T^f \mathbf{a}^f - \frac{1}{\varphi^f}\boldsymbol{\tau} \cdot \operatorname{grad}\varphi^f\right) dv \\
&+ \int_{\Omega^b} \mathbf{w} \cdot \operatorname{grad}\delta J^f\, dv\,, \\
&+ \int_{\Omega^b} \delta J^f \left[\frac{1}{J^f}\left(\varphi^f \dot{J}^f + \operatorname{grad} J^f \cdot \mathbf{w}\right) - \frac{\dot{J}^s}{J^s}\right] dv
\end{aligned} \tag{3.7.3}$$

and the external part is

$$\begin{aligned}
\delta W_{ext} = &\int_{\partial\Omega^b} \delta\mathbf{v}^s \cdot \mathbf{t}^\sigma\, da \\
&+ \int_{\Omega^b} \delta\mathbf{v}^s \cdot \varphi^s \left(-\rho_T^f \mathbf{b}^f + \rho_T^s \mathbf{b}^s\right) dv \\
&+ \int_{\partial\Omega^b} \delta\mathbf{w} \cdot \mathbf{t}^\tau\, da + \int_{\Omega^f} \delta\mathbf{w} \cdot \rho_T^f \mathbf{b}^f\, dv \\
&+ \int_{\partial\Omega^b} \delta J^f w_n\, da\,.
\end{aligned} \tag{3.7.4}$$

where

$$\mathbf{t}^\sigma = -\varphi^s \mathbf{t}^\tau + \mathbf{t}^e\,. \tag{3.7.5}$$

Here, $\mathbf{t}^e = \boldsymbol{\sigma}^e \cdot \mathbf{n}$ is the elastic traction, $\mathbf{t}^\tau = \boldsymbol{\tau} \cdot \mathbf{n}$ is the true fluid viscous traction, and $w_n = \mathbf{w}_n \cdot \mathbf{n}$ is the normal component of the relative fluid flux on the boundary $\partial\Omega^b$, whose outward unit normal is $\mathbf{n}$. The traction $\mathbf{t}^\sigma$ emerges from the jump condition in (2.13.17). The integrands of the surface integrals represent the natural boundary conditions for this formulation. If boundary conditions are not set explicitly on $\partial\Omega^b$, the natural boundary conditions are $\mathbf{t}^\sigma = \mathbf{0}$, $\mathbf{t}^\tau = \mathbf{0}$, and $w_n = 0$. These natural boundary conditions are consistent with the jump conditions presented above. Essential boundary conditions are prescribed on the solid displacement $\mathbf{u}$, relative volumetric fluid flux $\mathbf{w}$, and fluid dilatation e^f, which are also consistent with the above jump conditions. In particular, an essential no-slip boundary condition may be prescribed on Γ^{bs} by setting $\mathbf{w} = \mathbf{0}$. A symmetry plane may be prescribed with the essential boundary condition $u_n \equiv \mathbf{u} \cdot \mathbf{n} = 0$ and the natural boundary conditions $\mathbf{t}^\tau = \mathbf{0}$ and $w_n = 0$.

In this formulation, the mixture traction is defined as $\mathbf{t} = -p\mathbf{n} + \mathbf{t}^e + \varphi^f \mathbf{t}^\tau$, which may also be written as $\mathbf{t} = -p\mathbf{n} + \mathbf{t}^\sigma + \mathbf{t}^\tau$. Because of the way we chose to split the internal and external virtual work in (3.7.3)-(3.7.4), $\mathbf{t}$ is not a natural boundary condition in this formulation. In this

expression for $\mathbf{t}$, $\mathbf{t}^\sigma$, and $\mathbf{t}^\tau$ may be prescribed as natural boundary conditions, whereas p may be prescribed as an essential boundary condition on e^f, using (2.13.9). However, there are two general scenarios where $\mathbf{t}$ needs to be prescribed on a region of the boundary $\partial\Omega^b$ with incomplete prior knowledge of p, $\mathbf{t}^\sigma$, or $\mathbf{t}^\tau$: (1) When a BFSI boundary Γ^b represents a free surface (such as the fluid surface in channel flow), the mixture traction boundary condition requires that $\mathbf{t} = \mathbf{0}$, in which case it is necessary to explicitly enforce $-p\mathbf{n} + \mathbf{t}^\sigma + \mathbf{t}^\tau = \mathbf{0}$ as a constraint equation on that boundary, to impart the free surface Γ^b its natural shape. (2) At a biphasic-solid interface Γ^{bs}, $\mathbf{t}$ must balance the traction acting on the adjoining solid domain. Since $\mathbf{u}$ is continuous across Γ^{bs} due to shared nodes, the solid natural boundary condition $\mathbf{t}^\sigma$ of $\mathbf{t}$ is already accounted for by the deformation, so that it is only necessary to prescribe the portion $-p\mathbf{n}+\mathbf{t}^\tau$ of $\mathbf{t}$ on the solid domain, thus $-p\mathbf{n} + \mathbf{t}^\tau + \mathbf{t}^s = \mathbf{0}$ where $\mathbf{t}^s$ is the (equal and opposite) traction acting on the solid domain. In both cases, the form of this traction boundary condition is the same, with $\mathbf{t}^e$ and $\mathbf{t}^s$ representing the tractions acting on Γ^b and Γ^{bs}, respectively.

For both of these cases, the resulting virtual work on the free surface Γ^b or the interface Γ^{bs} takes the form

$$\delta F = -\int_\Gamma \delta\mathbf{v}^s \cdot (-p\mathbf{n} + \mathbf{t}^\tau)\, da\,, \tag{3.7.6}$$

where the elemental area da on Γ may be evaluated from the covariant basis vectors $\mathbf{g}_\alpha$ ($\alpha = 1, 2$),

$$da = |\mathbf{g}_1 \times \mathbf{g}_2|\, d\eta^1 d\eta^2\,, \tag{3.7.7}$$

where

$$\mathbf{g}_\alpha = \frac{\partial \mathbf{x}\left(\eta^1, \eta^2\right)}{\partial \eta^\alpha}\,, \tag{3.7.8}$$

and $\mathbf{x}\left(\eta^1, \eta^2\right)$ is the parametric representation of Γ, defined on the solid constituent. The outward normal $\mathbf{n}$ to Ω^b on Γ is evaluated from

$$\mathbf{n} = \frac{\mathbf{g}_1 \times \mathbf{g}_2}{|\mathbf{g}_1 \times \mathbf{g}_2|}\,. \tag{3.7.9}$$

As a result, the virtual work can be rewritten as

$$\delta F = -\int_\Gamma \delta\mathbf{v}^s \cdot (-p\mathbf{I} + \boldsymbol{\tau}) \cdot (\mathbf{g}_1 \times \mathbf{g}_2)\, d\eta^1 d\eta^2\,. \tag{3.7.10}$$

In FEBio this boundary condition is called *BFSI traction*, which the user must explicitly prescribe on free surfaces Γ^b and deformable interfaces Γ^{bs}. The code automatically determines which of these two types of interfaces is being considered.

3.7.2 BFSI Linearization

Using the virtual work integral δW such that

$$\delta W + D\delta W\left[\Delta\mathbf{u}\right] + D\delta W\left[\Delta\mathbf{w}\right] + D\delta W\left[\Delta J^f\right] \approx 0\,, \tag{3.7.11}$$

it may be expanded as

$$\begin{aligned} &D\delta W_{int}\left[\Delta\mathbf{u}\right] + D\delta W_{int}\left[\Delta\mathbf{w}\right] + D\delta W_{int}\left[\Delta J^f\right] \\ &- D\delta W_{ext}\left[\Delta\mathbf{u}\right] - D\delta W_{ext}\left[\Delta\mathbf{w}\right] - D\delta W_{ext}\left[\Delta J^f\right] \\ &\approx \delta W_{ext} - \delta W_{int}\,. \end{aligned} \tag{3.7.12}$$

The linearizations of integrals are performed in the material frame of the solid domain of Ω^b, allowing us to linearize δW_{int} along increments $\Delta\mathbf{u}$, $\Delta\mathbf{w}$, or ΔJ^f by simply bringing the directional derivative operator inside the integrals of Eqs. (3.7.3)-(3.7.4). For notational convenience, we let $J \equiv J^s$ and $\mathbf{F} \equiv \mathbf{F}^s$. Thus, the conversion of the internal virtual work to the material frame of the solid produces

$$\begin{aligned}
\delta W_{int} = &\int_{\Omega^b} \left(-\varphi_r^s \mathbf{T}_d + \mathbf{F}\cdot\boldsymbol{\sigma}^e\cdot\mathbf{F}^T\right) : \operatorname{Grad}\delta\mathbf{v}\cdot\mathbf{F}^{-1} dV \\
&+ \int_{\Omega^b} \delta\mathbf{v}\cdot\varphi_r^s\left(\frac{\varphi^s}{\varphi^f}\boldsymbol{\tau}\cdot\mathbf{F}^{-T}\cdot\operatorname{Grad}\left(\frac{\varphi^f}{\varphi^s}\right) - \rho_T^f\mathbf{a}^f + \rho_T^s\dot{\mathbf{v}}^s\right) dV \\
&+ \int_{\Omega^b} \delta\mathbf{v}\cdot -J^2\mathbf{F}^{-T}\cdot\mathbf{K}^{-1}\cdot\mathbf{F}^{-1}\cdot\mathbf{w} dV \\
&+ \int_{\Omega^b} \delta\mathbf{w}\cdot J\left(\rho_T^f\mathbf{a}^f + \mathbf{F}^{-T}\cdot\operatorname{Grad} p\right) dV \\
&+ \int_{\Omega^b} \delta\mathbf{w}\cdot J\left(-\frac{1}{\varphi^f}\boldsymbol{\tau}\cdot\mathbf{F}^{-T}\cdot\operatorname{Grad}\varphi^f + J\mathbf{F}^{-T}\cdot\mathbf{K}^{-1}\cdot\mathbf{F}^{-1}\cdot\mathbf{w}\right) dV \\
&+ \int_{\Omega^b} J\boldsymbol{\tau} : \operatorname{Grad}\delta\mathbf{w}\cdot\mathbf{F}^{-1} dV \\
&+ \int_{\Omega^b} J\operatorname{Grad}\delta J^f\cdot\mathbf{F}^{-1}\cdot\mathbf{w} + \delta J^f\left(J\frac{\varphi^f}{J^f}\frac{D^f J^f}{Dt} - \dot{J}^s\right) dV\,,
\end{aligned} \tag{3.7.13}$$

where $\mathbf{S} = J\,\mathbf{F}^{-1}\cdot\boldsymbol{\sigma}^e\cdot\mathbf{F}^{-T}$ is the second Piola-Kirchhoff stress for the solid constituent of the mixture, $\mathbf{W} = J\mathbf{F}^{-1}\cdot\mathbf{w}$ is the Piola transformation of $\mathbf{w}$, and $dV = J^{-1}dv$ is an elemental volume of Ω^f in its material frame [27]. In addition, $\mathbf{K}^{-1} = J^{-1}\mathbf{F}^T\cdot\mathbf{k}^{-1}\cdot\mathbf{F}$ is the inverse of the permeability tensor in the material frame. Note that in the material frame, the fluid acceleration $\mathbf{a}^f$ is

$$\mathbf{a}^f = \frac{1}{\varphi^f}\left(\dot{\mathbf{w}} + \varphi^f\dot{\mathbf{v}}^s - \frac{\varphi^s}{\varphi^f}\frac{\dot{J}}{J}\mathbf{w} + \frac{1}{J}\left(\frac{1}{\varphi^f}\operatorname{Grad}\mathbf{w} + \operatorname{Grad}\mathbf{v}^s - \frac{1}{\varphi^{f2}}\mathbf{w}\otimes\operatorname{Grad}\varphi^f\right)\cdot\mathbf{W}\right)\,. \tag{3.7.14}$$

The linearization of δW_{int} is then performed along an increment $\Delta\mathbf{u}$, and the integral is reverted

back to the spatial frame, yielding for the displacement equations

$$
\begin{aligned}
D\delta W_{int}\left[\Delta\mathbf{u}\right] = & \int_{\Omega^b} \alpha_f \left(\operatorname{grad}\Delta\mathbf{u}\cdot\boldsymbol{\sigma}^e : \operatorname{grad}\delta\mathbf{v} + \operatorname{grad}\delta\mathbf{v} : \boldsymbol{\mathcal{C}} : \operatorname{grad}\Delta\mathbf{u}\right) dv \\
& + \int_{\Omega^b} \alpha_f \varphi^s \boldsymbol{\tau} : \operatorname{grad}\delta\mathbf{v} \cdot \left(\operatorname{grad}\Delta\mathbf{u} + \frac{\varphi^s}{\varphi^f}\operatorname{div}\Delta\mathbf{u}\mathbf{I}\right) dv \\
& + \int_{\Omega^b} -\alpha_f \varphi^s \operatorname{grad}\delta\mathbf{v} : \boldsymbol{\mathcal{C}}^\tau : \left(-\frac{\varphi^s}{\varphi^{f^2}}\left(\operatorname{div}\Delta\mathbf{u}\right)\mathbf{D}^w + \mathbf{M}\cdot\operatorname{grad}\Delta\mathbf{u}\right) dv \\
& + \int_{\Omega^b} -\alpha_f \varphi^s \operatorname{grad}\delta\mathbf{v} : \frac{1}{\varphi^{f^2}}\boldsymbol{\mathcal{C}}^\tau : 2\frac{\varphi^s}{\varphi^f}\left(\operatorname{div}\Delta\mathbf{u}\right)\mathbf{w}\otimes\operatorname{grad}\varphi^f dv \\
& + \int_{\Omega^b} \alpha_f \varphi^s \operatorname{grad}\delta\mathbf{v} : \frac{1}{\varphi^{f^2}}\boldsymbol{\mathcal{C}}^\tau : \mathbf{w}\otimes\left(-\operatorname{grad}^T\Delta\mathbf{u}\cdot\operatorname{grad}\varphi^f\right) dv \\
& + \int_{\Omega^b} \alpha_f \varphi^s \operatorname{grad}\delta\mathbf{v} : \frac{1}{\varphi^{f^2}}\boldsymbol{\mathcal{C}}^\tau : \mathbf{w}\otimes\left(-\left(\operatorname{div}\Delta\mathbf{u}\right)\operatorname{grad}\varphi^f + \varphi^s\operatorname{grad}\left(\operatorname{div}\Delta\mathbf{u}\right)\right) dv \\
& + \int_{\Omega^b} \delta\mathbf{v}\cdot -\alpha_f\frac{\varphi^{s^2}}{\varphi^f}\boldsymbol{\tau}\cdot\left(2\frac{\varphi^s}{\varphi^f}\operatorname{div}\Delta\mathbf{u} + \operatorname{grad}^T\Delta\mathbf{u}\right)\cdot\operatorname{grad}\frac{\varphi^f}{\varphi^s} dv \\
& + \int_{\Omega^b} \delta\mathbf{v}\cdot\alpha_f\frac{\varphi^{s^2}}{\varphi^f}\boldsymbol{\tau}\cdot\frac{1}{\varphi^s}\operatorname{grad}\left(\operatorname{div}\Delta\mathbf{u}\right) dv \\
& + \int_{\Omega^b} \delta\mathbf{v}\cdot\alpha_f\frac{\varphi^{s^2}}{\varphi^f}\boldsymbol{\mathcal{C}}^\tau : \left(-\frac{\varphi^s}{\varphi^{f^2}}\left(\operatorname{div}\Delta\mathbf{u}\right)\mathbf{D}^w + \mathbf{M}\cdot\operatorname{grad}\Delta\mathbf{u}\right)\cdot\operatorname{grad}\frac{\varphi^f}{\varphi^s} dv \\
& + \int_{\Omega^b} \delta\mathbf{v}\cdot\alpha_f\frac{\varphi^{s^2}}{\varphi^{f^3}}\boldsymbol{\mathcal{C}}^\tau : 2\frac{\varphi^s}{\varphi^f}\left(\operatorname{div}\Delta\mathbf{u}\right)\mathbf{w}\otimes\operatorname{grad}\varphi^f\cdot\operatorname{grad}\frac{\varphi^f}{\varphi^s} dv \\
& + \int_{\Omega^b} \delta\mathbf{v}\cdot -\alpha_f\frac{\varphi^{s^2}}{\varphi^{f^3}}\boldsymbol{\mathcal{C}}^\tau : \mathbf{w}\otimes\left(-\operatorname{grad}^T\Delta\mathbf{u}\cdot\operatorname{grad}\varphi^f\right)\cdot\operatorname{grad}\frac{\varphi^f}{\varphi^s} dv \\
& + \int_{\Omega^b} \delta\mathbf{v}\cdot -\alpha_f\frac{\varphi^{s^2}}{\varphi^{f^3}}\boldsymbol{\mathcal{C}}^\tau : \mathbf{w}\otimes\left(-\operatorname{div}\Delta\mathbf{u}\operatorname{grad}\varphi^f + \varphi^s\operatorname{grad}\left(\operatorname{div}\Delta\mathbf{u}\right)\right)\cdot\operatorname{grad}\frac{\varphi^f}{\varphi^s} dv \\
& + \int_{\Omega^b} \delta\mathbf{v}\cdot -\alpha_f\varphi^s\frac{\rho_T^f}{\varphi^f}\left(\varphi^s\left(\operatorname{div}\Delta\mathbf{u}\right)\dot{\mathbf{v}}^s + \varphi^f\frac{\alpha_m}{\alpha_f\beta\Delta t^2}\Delta\mathbf{u}\right) dv \\
& + \int_{\Omega^b} \delta\mathbf{v}\cdot\alpha_f\varphi^s\frac{\rho_T^f}{\varphi^f}\left(\frac{\varphi^s}{\varphi^f}\left[\left(\left(-\frac{1}{\varphi^f}\right)\frac{\dot{J}}{J} + \frac{\gamma}{\beta\Delta t}\right)\operatorname{div}\Delta\mathbf{u} - \operatorname{grad}^T\Delta\mathbf{u} : \mathbf{L}^s\right]\mathbf{w}\right) dv \\
& + \int_{\Omega^b} \delta\mathbf{v}\cdot -\alpha_f\varphi^s\frac{\rho_T^f}{\varphi^f}\left(-\frac{\varphi^s}{\varphi^{f^2}}\operatorname{div}\Delta\mathbf{u}\operatorname{grad}\mathbf{w} + \frac{\gamma}{\beta\Delta t}\operatorname{grad}\Delta\mathbf{u}\right)\cdot\mathbf{w} dv \\
& + \int_{\Omega^b} \delta\mathbf{v}\cdot -\alpha_f\varphi^s\frac{\rho_T^f}{\varphi^{f^3}}\left[\left(\left(\varphi^s+1\right)\frac{1}{\varphi^f}\operatorname{grad}\varphi^f\operatorname{div}\Delta\mathbf{u} - \varphi^s\operatorname{grad}\left(\operatorname{div}\Delta\mathbf{u}\right)\right)\cdot\mathbf{w}\right]\mathbf{w} dv \\
& + \int_{\Omega^b} \delta\mathbf{v}\cdot\alpha_f\varphi^s\frac{\rho_T^f}{\varphi^f}\left(\mathbf{L}^f\cdot\operatorname{grad}\Delta\mathbf{u}\cdot\mathbf{w} + \varphi^s\left(\operatorname{div}\Delta\mathbf{u}\right)\mathbf{a}^f\right) dv \\
& + \int_{\Omega^b} \delta\mathbf{v}\cdot\alpha_f\rho^s\frac{\alpha_m}{\alpha_f\beta\Delta t^2}\Delta\mathbf{u} dv \\
& + \int_{\Omega^b} \delta\mathbf{v}\cdot\alpha_f\left(-2\left(\operatorname{div}\Delta\mathbf{u}\right)\mathbf{k}^{-1} + \operatorname{grad}^T\Delta\mathbf{u}\cdot\mathbf{k}^{-1}\right)\cdot\mathbf{w} dv \\
& + \int_{\Omega^b} \delta\mathbf{v}\cdot\alpha_f\left(\mathbf{k}^{-1}\cdot\operatorname{grad}\Delta\mathbf{u} + \left(\mathbf{k}^{-1}\underline{\otimes}\mathbf{k}^{-1}\right) : \mathsf{k} : \operatorname{grad}\Delta\mathbf{u}\right)\cdot\mathbf{w} dv\,,
\end{aligned}
\tag{3.7.15}
$$

for the fluid flux equations

$$
\begin{aligned}
D\delta W_{int}\left[\Delta\mathbf{u}\right] = & \int_{\Omega^b} \delta\mathbf{w}\cdot\alpha_f\frac{\rho_T^f}{\varphi^f}\left(-\frac{\varphi^s}{\varphi^f}\left[\left(-\frac{1}{\varphi^f}\frac{\dot{J}}{J}+\frac{\gamma}{\beta\Delta t}\right)\operatorname{div}\Delta\mathbf{u}-\operatorname{grad}^T\Delta\mathbf{u}:\mathbf{L}^s\right]\mathbf{w}\right)dv \\
& + \int_{\Omega^b} \delta\mathbf{w}\cdot\alpha_f\frac{\rho_T^f}{\varphi^f}\left(\varphi^s\left(\operatorname{div}\Delta\mathbf{u}\right)\dot{\mathbf{v}}^s+\varphi^f\frac{\alpha_m}{\alpha_f\beta\Delta t^2}\Delta\mathbf{u}\right)dv \\
& + \int_{\Omega^b} \delta\mathbf{w}\cdot\alpha_f\frac{\rho_T^f}{\varphi^f}\left(-\frac{\varphi^s}{\varphi^{f2}}\operatorname{div}\Delta\mathbf{u}\operatorname{grad}\mathbf{w}+\frac{\gamma}{\beta\Delta t}\operatorname{grad}\Delta\mathbf{u}\right)\cdot\mathbf{w}dv \\
& + \int_{\Omega^b} \delta\mathbf{w}\cdot\alpha_f\frac{\rho_T^f}{\varphi^f}\frac{1}{\varphi^{f2}}\left[\left(\left(\varphi^s+1\right)\frac{1}{\varphi^f}\operatorname{grad}\varphi^f\left(\operatorname{div}\Delta\mathbf{u}\right)-\varphi^s\operatorname{grad}\left(\operatorname{div}\Delta\mathbf{u}\right)\right)\cdot\mathbf{w}\right]\mathbf{w}dv \\
& + \int_{\Omega^b} \delta\mathbf{w}\cdot-\alpha_f\frac{\rho_T^f}{\varphi^f}\mathbf{L}^f\cdot\operatorname{grad}\Delta\mathbf{u}\cdot\mathbf{w}dv \\
& + \int_{\Omega^b} \delta\mathbf{w}\cdot\alpha_f\left(1-\frac{\varphi^s}{\varphi^f}\right)\left(\operatorname{div}\Delta\mathbf{u}\right)\rho_T^f\mathbf{a}^f dv \\
& + \int_{\Omega^b} \delta\mathbf{w}\cdot\alpha_f\left(\left(\operatorname{div}\Delta\mathbf{u}\right)\mathbf{I}-\operatorname{grad}^T\Delta\mathbf{u}\right)\cdot\operatorname{grad}p dv \\
& + \int_{\Omega^b} \delta\mathbf{w}\cdot\alpha_f\left(2\left(\operatorname{div}\Delta\mathbf{u}\right)\mathbf{k}^{-1}-\operatorname{grad}^T\Delta\mathbf{u}\cdot\mathbf{k}^{-1}\right)\cdot\mathbf{w}dv \\
& + \int_{\Omega^b} \delta\mathbf{w}\cdot-\alpha_f\left(\mathbf{k}^{-1}\cdot\operatorname{grad}\Delta\mathbf{u}+\left(\mathbf{k}^{-1}\underline{\otimes}\mathbf{k}^{-1}\right):\mathsf{k}:\operatorname{grad}\Delta\mathbf{u}\right)\cdot\mathbf{w}dv \\
& + \int_{\Omega^b} \delta\mathbf{w}\cdot\alpha_f\frac{1}{\varphi^f}\boldsymbol{\tau}\cdot\left(2\frac{\varphi^s}{\varphi^f}\left(\operatorname{div}\Delta\mathbf{u}\right)\mathbf{I}+\operatorname{grad}^T\Delta\mathbf{u}\right)\cdot\operatorname{grad}\varphi^f dv \\
& + \int_{\Omega^b} \delta\mathbf{w}\cdot-\alpha_f\frac{\varphi^s}{\varphi^f}\boldsymbol{\tau}\cdot\operatorname{grad}\left(\operatorname{div}\Delta\mathbf{u}\right)dv \\
& + \int_{\Omega^b} \delta\mathbf{w}\cdot-\alpha_f\frac{1}{\varphi^f}\boldsymbol{\mathcal{C}}^\tau:\left(-\frac{\varphi^s}{\varphi^{f2}}\left(\operatorname{div}\Delta\mathbf{u}\right)\mathbf{D}^w+\mathbf{M}\cdot\operatorname{grad}\Delta\mathbf{u}\right)\cdot\operatorname{grad}\varphi^f dv \\
& + \int_{\Omega^b} \delta\mathbf{w}\cdot-\alpha_f\frac{1}{\varphi^{f3}}\boldsymbol{\mathcal{C}}^\tau:2\frac{\varphi^s}{\varphi^f}\left(\operatorname{div}\Delta\mathbf{u}\right)\mathbf{w}\otimes\operatorname{grad}\varphi^f\cdot\operatorname{grad}\varphi^f dv \\
& + \int_{\Omega^b} \delta\mathbf{w}\cdot\alpha_f\frac{1}{\varphi^{f3}}\boldsymbol{\mathcal{C}}^\tau:\mathbf{w}\otimes\left(-\operatorname{grad}^T\Delta\mathbf{u}\cdot\operatorname{grad}\varphi^f\right)\cdot\operatorname{grad}\varphi^f dv \\
& + \int_{\Omega^b} \delta\mathbf{w}\cdot\alpha_f\frac{1}{\varphi^{f3}}\boldsymbol{\mathcal{C}}^\tau:\mathbf{w}\otimes\left(-\left(\operatorname{div}\Delta\mathbf{u}\right)\operatorname{grad}\varphi^f+\varphi^s\operatorname{grad}\left(\operatorname{div}\Delta\mathbf{u}\right)\right)\cdot\operatorname{grad}\varphi^f dv \\
& + \int_{\Omega^b} \alpha_f\boldsymbol{\tau}:\operatorname{grad}\delta\mathbf{w}\cdot\left(\left(1-\frac{\varphi^s}{\varphi^f}\right)\left(\operatorname{div}\Delta\mathbf{u}\right)\mathbf{I}-\operatorname{grad}\Delta\mathbf{u}\right)dv
\end{aligned}
\tag{3.7.16}
$$

$$
\begin{aligned}
& + \int_{\Omega^b} \alpha_f\operatorname{grad}\delta\mathbf{w}:\boldsymbol{\mathcal{C}}^\tau:\left(-\frac{\varphi^s}{\varphi^{f2}}\left(\operatorname{div}\Delta\mathbf{u}\right)\mathbf{D}^w+\mathbf{M}\cdot\operatorname{grad}\Delta\mathbf{u}\right)dv \\
& + \int_{\Omega^b} \alpha_f\operatorname{grad}\delta\mathbf{w}:\boldsymbol{\mathcal{C}}^\tau:2\frac{\varphi^s}{\varphi^{f3}}\left(\operatorname{div}\Delta\mathbf{u}\right)\mathbf{w}\otimes\operatorname{grad}\varphi^f dv \\
& + \int_{\Omega^b} -\alpha_f\operatorname{grad}\delta\mathbf{w}:\boldsymbol{\mathcal{C}}^\tau:\frac{1}{\varphi^{f2}}\mathbf{w}\otimes\left(-\operatorname{grad}^T\Delta\mathbf{u}\cdot\operatorname{grad}\varphi^f\right)dv \\
& + \int_{\Omega^b} -\alpha_f\operatorname{grad}\delta\mathbf{w}:\boldsymbol{\mathcal{C}}^\tau:\frac{1}{\varphi^{f2}}\mathbf{w}\otimes\left(-\left(\operatorname{div}\Delta\mathbf{u}\right)\operatorname{grad}\varphi^f+\varphi^s\operatorname{grad}\left(\operatorname{div}\Delta\mathbf{u}\right)\right)dv\,,
\end{aligned}
$$

and for the fluid dilatation equations

$$
\begin{aligned}
D\delta W_{int}\left[\Delta\mathbf{u}\right] = & \int_{\Omega^b} \alpha_f \operatorname{grad}\delta J^f \cdot \left(\operatorname{div}\Delta\mathbf{u}\mathbf{I} - \operatorname{grad}\Delta\mathbf{u}\right)\cdot\mathbf{w}dv \\
& + \int_{\Omega^b} \delta J^f \alpha_f \frac{1}{J^f}\left(\dot{J}^f \operatorname{div}\Delta\mathbf{u} + \operatorname{grad} J^f \cdot \left(\left(\operatorname{div}\Delta\mathbf{u}\right)\mathbf{I} - \operatorname{grad}\Delta\mathbf{u}\right)\cdot\mathbf{w}\right)dv \\
& + \int_{\Omega^b} -\delta J^f \alpha_f \left(\operatorname{div}\mathbf{v}^s + \frac{\gamma}{\beta\Delta t}\right)\operatorname{div}\Delta\mathbf{u} + \operatorname{grad}^T\Delta\mathbf{u} : \mathbf{L}^s dv\,,
\end{aligned}
\tag{3.7.17}
$$

where $\mathbf{M} = \frac{\gamma}{\beta\Delta t}\mathbf{I} - \mathbf{L}^s$, and $\boldsymbol{\mathcal{C}}$ is the fourth-order spatial elasticity tensor associated with $\boldsymbol{\sigma}^e$ [27]. As done in the CFD formulation (Section 3.5.2) [**?**], we have introduced the fourth-order tensor $\boldsymbol{\mathcal{C}}^\tau$ representing the tangent of the viscous stress with respect to the rate of deformation,

$$
\boldsymbol{\mathcal{C}}^\tau = \frac{\partial\boldsymbol{\tau}}{\partial\mathbf{D}^f}\,,
\tag{3.7.18}
$$

where $\mathbf{D}^f$ is the fluid rate of deformation tensor (the symmetric part of $\mathbf{L}^f$). The tensors $\boldsymbol{\mathcal{C}}_d$ and $\boldsymbol{\mathcal{C}}$ depend on the choice of constitutive relations for the fluid and solid constituents of Ω^f, respectively. In addition, k is the spatial fourth order permeability tensor with respect to right Cauchy-Green tensor $\mathbf{C}$. The linearized equations include the generalized-α parameters because the virtual work is evaluated at the intermediate time step, while the increment itself ($\Delta\mathbf{u}$ in this case) is at the current time step [**?**].

Following the same procedure, the linearizations of δW_{int} along an increment $\Delta\mathbf{w}$ is given by

$$
\begin{aligned}
D\delta W_{int}\left[\Delta\mathbf{w}\right] = & \int_{\Omega^b} -\alpha_f\frac{\varphi^s}{\varphi^f}\operatorname{grad}\delta\mathbf{v} : \boldsymbol{\mathcal{C}}^\tau : \left(\operatorname{grad}\Delta\mathbf{w} - \frac{1}{\varphi^f}\Delta\mathbf{w}\otimes\operatorname{grad}\varphi^f\right)dv \\
& + \int_{\Omega^b} \delta\mathbf{v}\cdot -\alpha_f\varphi^s\frac{\rho_T^f}{\varphi^f}\left(\left(\frac{\alpha_m}{\gamma\alpha_f\Delta t} - \frac{\varphi^s}{\varphi^f}\frac{\dot{J}}{J} - \frac{1}{\varphi^{f^2}}\left(\operatorname{grad}\varphi^f\cdot\mathbf{w}\right)\right)\mathbf{I} + \mathbf{L}^f\right)\cdot\Delta\mathbf{w}dv \\
& + \int_{\Omega^b} \delta\mathbf{v}\cdot -\alpha_f\varphi^s\frac{\rho_T^f}{\varphi^{f^2}}\operatorname{grad}\Delta\mathbf{w}\cdot\mathbf{w}dv \\
& + \int_{\Omega^b} \delta\mathbf{v}\cdot\alpha_f\frac{\left(\varphi^s\right)^2}{\left(\varphi^f\right)^2}\boldsymbol{\mathcal{C}}^\tau : \left(\operatorname{grad}\Delta\mathbf{w} - \frac{1}{\varphi^f}\Delta\mathbf{w}\otimes\operatorname{grad}\varphi^f\right)\cdot\operatorname{grad}\left(\frac{\varphi^f}{\varphi^s}\right)dv \\
& + \int_{\Omega^b} \delta\mathbf{v}\cdot -\alpha_f\mathbf{k}^{-1}\cdot\Delta\mathbf{w}dv \\
& + \int_{\Omega^b} \delta\mathbf{w}\cdot\alpha_f\frac{\rho_T^f}{\varphi^f}\left(\left(\frac{\alpha_m}{\gamma\alpha_f\Delta t} - \frac{\varphi^s}{\varphi^f}\frac{\dot{J}}{J} - \frac{1}{\varphi^{f^2}}\left(\operatorname{grad}\varphi^f\cdot\mathbf{w}\right)\right)\mathbf{I} + \mathbf{L}^f\right)\cdot\Delta\mathbf{w}dv \\
& + \int_{\Omega^b} \delta\mathbf{w}\cdot\alpha_f\frac{\rho_T^f}{\varphi^{f^2}}\operatorname{grad}\Delta\mathbf{w}\cdot\mathbf{w}dv \\
& + \int_{\Omega^b} \delta\mathbf{w}\cdot\alpha_f\mathbf{k}^{-1}\cdot\Delta\mathbf{w}dv \\
& + \int_{\Omega^b} \delta\mathbf{w}\cdot\alpha_f\frac{1}{\varphi^{f^2}}\boldsymbol{\mathcal{C}}^\tau : \left(\frac{1}{\varphi^f}\Delta\mathbf{w}\otimes\operatorname{grad}\varphi^f - \operatorname{grad}\Delta\mathbf{w}\right)\cdot\operatorname{grad}\varphi^f dv \\
& + \int_{\Omega^b} \alpha_f\frac{1}{\varphi^f}\operatorname{grad}\delta\mathbf{w} : \boldsymbol{\mathcal{C}}^\tau : \left(\operatorname{grad}\Delta\mathbf{w} - \frac{1}{\varphi^f}\Delta\mathbf{w}\otimes\operatorname{grad}\varphi^f\right)dv \\
& + \int_{\Omega^b} \alpha_f\operatorname{grad}\delta J^f\cdot\Delta\mathbf{w} + \delta J^f\alpha_f\frac{1}{J^f}\operatorname{grad}J^f\cdot\Delta\mathbf{w}dv\,,
\end{aligned}
\tag{3.7.19}
$$

whereas the linearizations of δW_{int} along an increment ΔJ^f is

$$\begin{aligned} D\delta W_{int}\left[\Delta J^f\right] = &\int_{\Omega^b} -\alpha_f \varphi^s \boldsymbol{\tau}'_J : \operatorname{grad}\delta\mathbf{v}\Delta J^f dv \\ &+ \int_{\Omega^b} \delta\mathbf{v}\cdot\alpha_f\varphi^s\left(\frac{\varphi^s}{\varphi^f}\boldsymbol{\tau}'_J\cdot\operatorname{grad}\frac{\varphi^f}{\varphi^s}+\frac{\rho^f_T}{J^f}\mathbf{a}^f\right)\Delta J^f dv \\ &+ \int_{\Omega^b} \delta\mathbf{w}\cdot\alpha_f\left(p''\operatorname{grad}J^f\Delta J^f + p'\operatorname{grad}\Delta J^f\right)dv \\ &+ \int_{\Omega^b} \delta\mathbf{w}\cdot -\alpha_f\left(\frac{\rho^f_T}{J^f}\mathbf{a}^f\Delta J^f+\frac{1}{\varphi^f}\boldsymbol{\tau}'_J\Delta J^f\cdot\operatorname{grad}\varphi^f\right)dv \\ &+ \int_{\Omega^b} \alpha_f\boldsymbol{\tau}'_J : \operatorname{grad}\delta\mathbf{w}\Delta J^f dv \\ &+ \int_{\Omega^b} \delta J^f\alpha_f\frac{1}{J^f}\left(\varphi^f\frac{\alpha_m}{\gamma\alpha_f\Delta t}-\frac{1}{J^f}\left(\varphi^f\dot{J}^f+\operatorname{grad}J^f\cdot\mathbf{w}\right)\right)\Delta J^f dv \\ &+ \int_{\Omega^b} \delta J^f\alpha_f\frac{1}{J^f}\operatorname{grad}\Delta J^f\cdot\mathbf{w}dv\,. \end{aligned} \tag{3.7.20}$$

Here, p' and p'' respectively represent the first and second derivatives of $p\left(J^f\right)$. We have also defined $\boldsymbol{\tau}'_J$ as the tangent of the viscous stress $\boldsymbol{\tau}$ with respect to J^f,

$$\boldsymbol{\tau}'_J = \frac{\partial\boldsymbol{\tau}}{\partial J^f}\,. \tag{3.7.21}$$

For the external work, when $\mathbf{t}^\sigma$, $\mathbf{t}^\tau$, all $\mathbf{b}$ and w_n are prescribed, the linearizations simplify to

$$D\delta W_{ext}\left[\Delta\mathbf{u}\right] = \int_{\Omega^b}\delta\mathbf{w}\cdot\alpha_f\operatorname{div}\Delta\mathbf{u}\rho^f_T\mathbf{b}^f dv\,, \tag{3.7.22}$$

$$D\delta W_{ext}\left[\Delta\mathbf{w}\right] = 0\,, \tag{3.7.23}$$

$$\begin{aligned} D\delta W_{ext}\left[\Delta J^f\right] = &\int_{\Omega^b}\delta\mathbf{w}\cdot-\alpha_f\frac{\rho^f_T}{J^f}\mathbf{b}^f\Delta J^f dv \\ &+\int_{\Omega^b}\delta\mathbf{v}\cdot\alpha_f\varphi^s\frac{\rho^f_T}{J^f}\mathbf{b}^f\Delta J^f dv\,. \end{aligned} \tag{3.7.24}$$

As discussed in Section 2.11.1, we define the fluid dilatation $e^f = J^f - 1$ as an alternative essential variable, since initial and boundary conditions $e^f = 0$ are more convenient to handle in a numerical scheme than $J^f = 1$. It follows that $\operatorname{grad}J^f = \operatorname{grad}e^f$ and $\dot{J}^f = \dot{e}^f$. Therefore the changes to the above equations are minimal, simply requiring the substitution $J^f = 1 + e^f$ and $\Delta J^f = \Delta e^f$.

3.7.3 BFSI Spatial Discretization

The degrees of freedom $\mathbf{u}(\mathbf{x},t)$, $\mathbf{w}(\mathbf{x},t)$, $J^f(\mathbf{x},t)$ are spatially interpolated over the domain Ω^f using the same interpolation functions $N_a(\mathbf{x})$, with $a = 1$ to n, where n is the number of nodes in

an element,

$$\begin{aligned}
\mathbf{u}(\mathbf{x},t) &= \sum_{a=1}^{n} N_a(\mathbf{x})\,\mathbf{u}_a\,,\\
\mathbf{w}(\mathbf{x},t) &= \sum_{a=1}^{n} N_a(\mathbf{x})\,\mathbf{w}_a\,,\\
J^f(\mathbf{x},t) &= \sum_{a=1}^{n} N_a(\mathbf{x})\,J^f_a\,.
\end{aligned} \tag{3.7.25}$$

Here, $\mathbf{u}_a$, $\mathbf{w}_a$, and J^f_a are the nodal values of the degrees of freedom that evolve over time. These relations may be used to evaluate $\mathbf{L}^s$, $\mathbf{L}^w$, $\operatorname{div}\mathbf{w}$, $\dot{\mathbf{w}}$, $\operatorname{grad} J^f$, $\dot{J}^f$, etc. Similar interpolations are used for virtual increments $\delta\mathbf{v}$, $\delta\mathbf{w}$ and δJ^f, as well as real increments $\Delta\mathbf{u}$, $\Delta\mathbf{w}$ and ΔJ^f. In practice, interpolations N_a are performed in the parametric space of each finite element, which is a material frame.

Now, the discretized form of δW_{int}, using Eq. (3.7.3), may be written as

$$\begin{aligned}
\delta W_{int} = &\sum_a \delta\mathbf{v}_a\cdot\mathbf{f}^u_a\\
&+\sum_a \delta\mathbf{w}_a\cdot\mathbf{f}^w_a\\
&+\sum_a \delta J^f_a f^J_a\,,
\end{aligned} \tag{3.7.26}$$

where

$$\begin{aligned}
\mathbf{f}^u_a &= \int_{\Omega^b}(-\varphi^s\boldsymbol{\tau}+\boldsymbol{\sigma}^e)\cdot\operatorname{grad}N_a dv\\
&\quad+\int_{\Omega^b} N_a\left(\varphi^s\left(\frac{\varphi^s}{\varphi^f}\boldsymbol{\tau}\cdot\operatorname{grad}\frac{\varphi^f}{\varphi^s}-\rho^f_T\mathbf{a}^f+\rho^s_T\dot{\mathbf{v}}^s\right)-\mathbf{k}^{-1}\cdot\mathbf{w}\right)dv\,,\\
\mathbf{f}^w_a &= \int_{\Omega^b}\boldsymbol{\tau}\cdot\operatorname{grad}N_a+N_a\left(\rho^f_T\mathbf{a}^f+\operatorname{grad}p-\frac{1}{\varphi^f}\boldsymbol{\tau}\cdot\operatorname{grad}\varphi^f+\mathbf{k}^{-1}\cdot\mathbf{w}\right)dv\,,\\
f^J_a &= \int_{\Omega^b}\operatorname{grad}N_a\cdot\mathbf{w}+N_a\left(\frac{\varphi^f}{J^f}\frac{D^fJ^f}{Dt}-\frac{\dot{J}^s}{J^s}\right)dv\,.
\end{aligned} \tag{3.7.27}$$

The discretized form of $D\delta W_{int}[\Delta\mathbf{u}]$ becomes

$$\begin{aligned}
D\delta W_{int}[\Delta\mathbf{u}] = &\sum_a \delta\mathbf{v}_a\cdot\sum_b\mathbf{K}^{uu}_{ab}\cdot\Delta\mathbf{u}_b\\
&+\sum_a \delta\mathbf{w}_a\cdot\sum_b\mathbf{K}^{wu}_{ab}\cdot\Delta\mathbf{u}_b\\
&+\sum_a \delta J^f_a\sum_b\mathbf{k}^{Ju}_{ab}\cdot\Delta\mathbf{u}_b\,,
\end{aligned} \tag{3.7.28}$$

where

$$
\begin{aligned}
\mathbf{K}_{ab}^{uu} = & \int_{\Omega^b} \alpha_f \left((\boldsymbol{\sigma}^e : \operatorname{grad} N_b \otimes \operatorname{grad} N_a) \mathbf{I} + \operatorname{grad} N_a \cdot \boldsymbol{\mathcal{C}} \cdot \operatorname{grad} N_b \right) dv \\
& + \int_{\Omega^b} \alpha_f \varphi^s \boldsymbol{\tau} \cdot \left(\frac{\varphi^s}{\varphi^f} \operatorname{grad} N_a \otimes \operatorname{grad} N_b + \operatorname{grad} N_b \otimes \operatorname{grad} N_a \right) dv \\
& + \int_{\Omega^b} -\alpha_f \varphi^s \operatorname{grad} N_a \cdot \boldsymbol{\mathcal{C}}^\tau \cdot \operatorname{grad} N_b \cdot \left(-\frac{\varphi^s}{\varphi^{f^2}} \mathbf{D}^w + \mathbf{M} \right) dv \\
& + \int_{\Omega^b} -\alpha_f \frac{\varphi^s}{\varphi^{f^2}} \operatorname{grad} N_a \cdot \boldsymbol{\mathcal{C}}^\tau \cdot \mathbf{w} \cdot \left(2 \frac{\varphi^s}{\varphi^f} \operatorname{grad} \varphi^f \otimes \operatorname{grad} N_b \right) dv \\
& + \int_{\Omega^b} -\alpha_f \frac{\varphi^s}{\varphi^{f^2}} \operatorname{grad} N_a \cdot \boldsymbol{\mathcal{C}}^\tau \cdot \mathbf{w} \cdot \left(\operatorname{grad} N_b \otimes \operatorname{grad} \varphi^f \right) dv \\
& + \int_{\Omega^b} \alpha_f \frac{\varphi^s}{\varphi^{f^2}} \operatorname{grad} N_a \cdot \boldsymbol{\mathcal{C}}^\tau \cdot \mathbf{w} \cdot \left(- \operatorname{grad} \varphi^f \otimes \operatorname{grad} N_b + \varphi^s \operatorname{grad} \operatorname{grad} N_b \right) dv \\
& + \int_{\Omega^b} -\alpha_f N_a \frac{\varphi^{s^2}}{\varphi^f} \boldsymbol{\tau} \cdot \left(2 \frac{\varphi^s}{\varphi^f} \operatorname{grad} \frac{\varphi^f}{\varphi^s} \otimes \operatorname{grad} N_b + \operatorname{grad} N_b \otimes \operatorname{grad} \frac{\varphi^f}{\varphi^s} \right) dv \\
& + \int_{\Omega^b} \alpha_f N_a \frac{\varphi^{s^2}}{\varphi^f} \boldsymbol{\tau} \cdot \frac{1}{\varphi^s} \operatorname{grad} \operatorname{grad} N_b dv \\
& + \int_{\Omega^b} \alpha_f N_a \frac{\varphi^{s^2}}{\varphi^f} \operatorname{grad} \frac{\varphi^f}{\varphi^s} \cdot \boldsymbol{\mathcal{C}}^\tau \cdot \operatorname{grad} N_b \cdot \left(-\frac{\varphi^s}{\varphi^{f^2}} \mathbf{D}^w + \mathbf{M} \right) dv \\
& + \int_{\Omega^b} \alpha_f N_a \frac{\varphi^{s^2}}{\varphi^{f^3}} \operatorname{grad} \frac{\varphi^f}{\varphi^s} \cdot \boldsymbol{\mathcal{C}}^\tau \cdot \mathbf{w} \cdot \left(2 \frac{\varphi^s}{\varphi^f} \operatorname{grad} \varphi^f \otimes \operatorname{grad} N_b \right) dv \\
& + \int_{\Omega^b} \alpha_f N_a \frac{\varphi^{s^2}}{\varphi^{f^3}} \operatorname{grad} \frac{\varphi^f}{\varphi^s} \cdot \boldsymbol{\mathcal{C}}^\tau \cdot \mathbf{w} \cdot \left(\operatorname{grad} N_b \otimes \operatorname{grad} \varphi^f \right) dv \\
& + \int_{\Omega^b} -\alpha_f N_a \frac{\varphi^{s^2}}{\varphi^{f^3}} \operatorname{grad} \frac{\varphi^f}{\varphi^s} \cdot \boldsymbol{\mathcal{C}}^\tau \cdot \mathbf{w} \cdot \left(- \operatorname{grad} \varphi^f \otimes \operatorname{grad} N_b + \varphi^s \operatorname{grad} \operatorname{grad} N_b \right) dv \\
& + \int_{\Omega^b} -\alpha_f \frac{\varphi^s}{\varphi^f} \rho_T^f N_a \left(\varphi^s \dot{\mathbf{v}}^s \otimes \operatorname{grad} N_b + \varphi^f \frac{\alpha_m}{\alpha_f \beta \Delta t^2} N_b \mathbf{I} \right) dv \\
& + \int_{\Omega^b} \alpha_f \rho_T^f N_a \frac{\varphi^{s^2}}{\varphi^{f^2}} \left[\left(\left(-\frac{1}{\varphi^f} \right) \frac{\dot{J}}{J} + \frac{\gamma}{\beta \Delta t} \right) \mathbf{w} \otimes \operatorname{grad} N_b - \mathbf{w} \otimes \left(\mathbf{L}^{s^T} \cdot \operatorname{grad} N_b \right) \right] dv \\
& + \int_{\Omega^b} -\alpha_f N_a \varphi^s \frac{\rho_T^f}{\varphi^f} \left(-\frac{\varphi^s}{\varphi^{f^2}} \mathbf{L}^w \cdot \mathbf{w} \otimes \operatorname{grad} N_b + \frac{\gamma}{\beta \Delta t} \left(\operatorname{grad} N_b \cdot \mathbf{w} \right) \mathbf{I} \right) dv \\
& + \int_{\Omega^b} -\alpha_f N_a \rho_T^f \frac{\varphi^s}{\varphi^{f^4}} \left(\varphi^s + 1 \right) \left(\operatorname{grad} \varphi^f \cdot \mathbf{w} \right) \mathbf{w} \otimes \operatorname{grad} N_b dv
\end{aligned}
\tag{3.7.29}
$$

$$
\begin{aligned}
&+\int_{\Omega^b}\alpha_f N_a\rho_T^f\frac{\varphi^{s^2}}{\varphi^{f^3}}\mathbf{w}\otimes\operatorname{grad}\operatorname{grad}^T N_b\cdot\mathbf{w}dv\\
&+\int_{\Omega^b}\alpha_f\frac{\varphi^s}{\varphi^f}\rho_T^f N_a\left(\mathbf{L}^f\left(\operatorname{grad}N_b\cdot\mathbf{w}\right)+\varphi^s\mathbf{a}^f\otimes\operatorname{grad}N_b\right)dv\\
&+\int_{\Omega^b}\alpha_f N_a\frac{\alpha_m}{\alpha_f\beta\Delta t^2}\rho^s N_b\mathbf{I}dv\\
&+\int_{\Omega^b}\alpha_f N_a\left(-2\left(\mathbf{k}^{-1}\cdot\mathbf{w}\right)\otimes\operatorname{grad}N_b+\operatorname{grad}N_b\otimes\left(\mathbf{k}^{-1}\cdot\mathbf{w}\right)\right)dv\\
&+\int_{\Omega^b}\alpha_f N_a\left(\left(\operatorname{grad}N_b\cdot\mathbf{w}\right)\mathbf{k}^{-1}+\left(\mathbf{k}^{-1}\underline{\otimes}\mathbf{k}^{-1}\right):\mathsf{k}:\left(\operatorname{grad}N_b\cdot\mathbf{w}\right)\mathbf{I}\right)dv\,,
\end{aligned}
$$

$$
\begin{aligned}
\mathbf{K}_{ab}^{wu}=&\int_{\Omega^b}\alpha_f\frac{\rho_T^f}{\varphi^f}N_a\left(\varphi^s\dot{\mathbf{v}}^s\otimes\operatorname{grad}N_b+\varphi^f\frac{\alpha_m}{\alpha_f\beta\Delta t^2}N_b\mathbf{I}\right)dv\\
&+\int_{\Omega^b}-\alpha_f\frac{\rho_T^f}{\varphi^f}N_a\frac{\varphi^s}{\varphi^f}\left(-\frac{1}{\varphi^f}\frac{\dot{J}}{J}+\frac{\gamma}{\beta\Delta t}\right)\mathbf{w}\otimes\operatorname{grad}N_b dv\\
&+\int_{\Omega^b}\alpha_f\frac{\rho_T^f}{\varphi^f}N_a\frac{\varphi^s}{\varphi^f}\mathbf{w}\otimes\left(\mathbf{L}^{s^T}\cdot\operatorname{grad}N_b\right)dv\\
&+\int_{\Omega^b}\alpha_f N_a\frac{\rho_T^f}{\varphi^f}\left(-\frac{\varphi^s}{\varphi^{f^2}}\left(\mathbf{L}^w\cdot\mathbf{w}\right)\otimes\operatorname{grad}N_b+\frac{\gamma}{\beta\Delta t}\left(\operatorname{grad}N_b\cdot\mathbf{w}\right)\mathbf{I}\right)dv\\
&+\int_{\Omega^b}\alpha_f N_a\frac{\rho_T^f}{\varphi^{f^4}}\left(\varphi^s+1\right)\left(\operatorname{grad}\varphi^f\cdot\mathbf{w}\right)\mathbf{w}\otimes\operatorname{grad}N_b dv\\
&+\int_{\Omega^b}-\alpha_f N_a\frac{\rho_T^f}{\varphi^{f^3}}\varphi^s\mathbf{w}\otimes\left(\operatorname{grad}\operatorname{grad}^T N_b\cdot\mathbf{w}\right)dv\\
&+\int_{\Omega^b}-\alpha_f\frac{\rho_T^f}{\varphi^f}N_a\mathbf{L}^f\left(\operatorname{grad}N_b\cdot\mathbf{w}\right)dv\\
&+\int_{\Omega^b}\alpha_f N_a\left(1-\frac{\varphi^s}{\varphi^f}\right)\rho_T^f\mathbf{a}^f\otimes\operatorname{grad}N_b dv\\
&+\int_{\Omega^b}\alpha_f N_a\left(\operatorname{grad}p\otimes\operatorname{grad}N_b-\operatorname{grad}N_b\otimes\operatorname{grad}p\right)dv\\
&+\int_{\Omega^b}\alpha_f N_a\left(2\left(\mathbf{k}^{-1}\cdot\mathbf{w}\right)\otimes\operatorname{grad}N_b-\operatorname{grad}N_b\otimes\left(\mathbf{k}^{-1}\cdot\mathbf{w}\right)\right)dv\\
&+\int_{\Omega^b}-\alpha_f N_a\left(\left(\operatorname{grad}N_b\cdot\mathbf{w}\right)\mathbf{k}^{-1}+\left(\mathbf{k}^{-1}\underline{\otimes}\mathbf{k}^{-1}\right):\mathsf{k}:\left(\operatorname{grad}N_b\cdot\mathbf{w}\right)\mathbf{I}\right)dv\\
&+\int_{\Omega^b}\alpha_f N_a\frac{1}{\varphi^f}\boldsymbol{\tau}\cdot\left(2\frac{\varphi^s}{\varphi^f}\operatorname{grad}\varphi^f\otimes\operatorname{grad}N_b+\operatorname{grad}N_b\otimes\operatorname{grad}\varphi^f\right)dv\\
&+\int_{\Omega^b}-\alpha_f N_a\frac{1}{\varphi^f}\boldsymbol{\tau}\cdot\varphi^s\operatorname{grad}\operatorname{grad}N_b dv\\
&+\int_{\Omega^b}-\alpha_f N_a\frac{1}{\varphi^f}\operatorname{grad}\varphi^f\cdot\boldsymbol{\mathcal{C}}^\tau\cdot\operatorname{grad}N_b\cdot\left(-\frac{\varphi^s}{\varphi^{f^2}}\mathbf{D}^w+\mathbf{M}\right)dv\\
&+\int_{\Omega^b}-\alpha_f N_a\frac{1}{\varphi^{f^3}}\operatorname{grad}\varphi^f\cdot\boldsymbol{\mathcal{C}}^\tau\cdot\mathbf{w}\cdot\left(2\frac{\varphi^s}{\varphi^f}\operatorname{grad}\varphi^f\otimes\operatorname{grad}N_b\right)dv\\
&+\int_{\Omega^b}-\alpha_f N_a\frac{1}{\varphi^{f^3}}\operatorname{grad}\varphi^f\cdot\boldsymbol{\mathcal{C}}^\tau\cdot\mathbf{w}\cdot\left(\operatorname{grad}N_b\otimes\operatorname{grad}\varphi^f\right)dv
\end{aligned}
\tag{3.7.30}
$$

$$
\begin{aligned}
&+\int_{\Omega^b}\alpha_f N_a\frac{1}{\varphi^{f^3}}\operatorname{grad}\varphi^f\cdot\boldsymbol{\mathcal{C}}^\tau\cdot\mathbf{w}\cdot\Big(-\operatorname{grad}\varphi^f\otimes\operatorname{grad}N_b+\varphi^s\operatorname{grad}\operatorname{grad}N_b\Big)\,dv\\
&+\int_{\Omega^b}\alpha_f\boldsymbol{\tau}\cdot\left(\left(1-\frac{\varphi^s}{\varphi^f}\right)\operatorname{grad}N_a\otimes\operatorname{grad}N_b-\operatorname{grad}N_b\otimes\operatorname{grad}N_a\right)dv\\
&+\int_{\Omega^b}\alpha_f\operatorname{grad}N_a\cdot\boldsymbol{\mathcal{C}}^\tau\cdot\operatorname{grad}N_b\cdot\left(-\frac{\varphi^s}{\varphi^{f^2}}\mathbf{D}^w+\mathbf{M}\right)dv\\
&+\int_{\Omega^b}\alpha_f\frac{1}{\varphi^{f^2}}\operatorname{grad}N_a\cdot\boldsymbol{\mathcal{C}}^\tau\cdot\mathbf{w}\cdot\left(2\frac{\varphi^s}{\varphi^f}\operatorname{grad}\varphi^f\otimes\operatorname{grad}N_b\right)dv\\
&+\int_{\Omega^b}\alpha_f\frac{1}{\varphi^{f^2}}\operatorname{grad}N_a\cdot\boldsymbol{\mathcal{C}}^\tau\cdot\mathbf{w}\cdot\Big(\operatorname{grad}N_b\otimes\operatorname{grad}\varphi^f\Big)\,dv\\
&+\int_{\Omega^b}-\alpha_f\frac{1}{\varphi^{f^2}}\operatorname{grad}N_a\cdot\boldsymbol{\mathcal{C}}^\tau\cdot\mathbf{w}\cdot\Big(-\operatorname{grad}\varphi^f\otimes\operatorname{grad}N_b+\varphi^s\operatorname{grad}\operatorname{grad}N_b\Big)\,dv\,,
\end{aligned}
$$

$$
\begin{aligned}
\mathbf{k}_{ab}^{Ju}=&\int_{\Omega^b}\alpha_f\left(\operatorname{grad}N_b\otimes\mathbf{w}-\left(\operatorname{grad}N_b\cdot\mathbf{w}\right)\mathbf{I}\right)\cdot\operatorname{grad}N_a dv\\
&+\int_{\Omega^b}\alpha_f N_a\frac{1}{J^f}\left(\dot{J}^f\operatorname{grad}N_b+\left(\operatorname{grad}N_b\otimes\mathbf{w}-\operatorname{grad}N_b\cdot\mathbf{w}\mathbf{I}\right)\cdot\operatorname{grad}J^f\right)dv\\
&+\int_{\Omega^b}-\alpha_f N_a\left(\frac{\dot{J}}{J}+\frac{\gamma}{\beta\Delta t}\right)\operatorname{grad}N_b+\mathbf{L}^{s^T}\cdot\operatorname{grad}N_b dv\,,
\end{aligned}
\tag{3.7.31}
$$

whereas that of $D\delta W_{int}\left[\Delta\mathbf{w}\right]$ becomes

$$
\begin{aligned}
D\delta W_{int}\left[\Delta\mathbf{w}\right]=&\sum_a\delta\mathbf{v}_a\cdot\sum_b\mathbf{K}_{ab}^{uw}\cdot\Delta\mathbf{w}_b\\
&+\sum_a\delta\mathbf{w}_a\cdot\sum_b\mathbf{K}_{ab}^{ww}\cdot\Delta\mathbf{w}_b\\
&+\sum_a\delta J_a^f\sum_b\mathbf{k}_{ab}^{Jw}\cdot\Delta\mathbf{w}_b\,,
\end{aligned}
\tag{3.7.32}
$$

where

$$
\begin{aligned}
\mathbf{K}_{ab}^{uw} &= \int_{\Omega^b} \alpha_f \frac{\varphi^s}{\varphi^f} \operatorname{grad} N_a \cdot \boldsymbol{\mathcal{C}}^\tau \cdot \left(\frac{1}{\varphi^f} N_b \operatorname{grad} \varphi^f - \operatorname{grad} N_b \right) dv \\
&+ \int_{\Omega^b} -\alpha_f \varphi^s \frac{\rho_T^f}{\varphi^f} N_a \left(\left(\frac{\alpha_m}{\gamma \alpha_f \Delta t} - \frac{\varphi^s}{\varphi^f} \frac{\dot{J}}{J} - \frac{1}{\varphi^{f^2}} \left(\operatorname{grad} \varphi^f \cdot \mathbf{w} \right) \right) \mathbf{I} + \mathbf{L}^f \right) N_b dv \\
&+ \int_{\Omega^b} -\alpha_f \varphi^s \frac{\rho_T^f}{\varphi^{f^2}} N_a \left(\operatorname{grad} N_b \cdot \mathbf{w} \right) \mathbf{I} dv \\
&+ \int_{\Omega^b} \alpha_f N_a \frac{\left(\varphi^s\right)^2}{\left(\varphi^f\right)^2} \operatorname{grad} \frac{\varphi^f}{\varphi^s} \cdot \boldsymbol{\mathcal{C}}_d \cdot \left(-\frac{1}{\varphi^f} N_b \operatorname{grad} \varphi^f + \operatorname{grad} N_b \right) dv \\
&+ \int_{\Omega^b} -\alpha_f N_a N_b \mathbf{k}^{-1} dv \,, \\
\mathbf{K}_{ab}^{ww} &= \int_{\Omega^b} \alpha_f N_a \frac{\rho_T^f}{\varphi^f} \left(\left(\frac{\alpha_m}{\gamma \alpha_f \Delta t} - \frac{\varphi^s}{\varphi^f} \frac{\dot{J}}{J} - \frac{1}{\varphi^{f^2}} \left(\operatorname{grad} \varphi^f \cdot \mathbf{w} \right) \right) \mathbf{I} + \mathbf{L}^f \right) N_b dv \\
&+ \int_{\Omega^b} \alpha_f N_a \frac{\rho_T^f}{\varphi^{f^2}} \left(\operatorname{grad} N_b \cdot \mathbf{w} \right) \mathbf{I} dv \\
&+ \int_{\Omega^b} \alpha_f N_a \left(\frac{1}{\varphi^{f^2}} \operatorname{grad} \varphi^f \cdot \boldsymbol{\mathcal{C}}^\tau \cdot \left(\frac{1}{\varphi^f} N_b \operatorname{grad} \varphi^f - \operatorname{grad} N_b \right) + N_b \mathbf{k}^{-1} \right) dv \\
&+ \int_{\Omega^b} \alpha_f \frac{1}{\varphi^f} \operatorname{grad} N_a \cdot \boldsymbol{\mathcal{C}}^\tau \cdot \left(-\frac{1}{\varphi^f} N_b \operatorname{grad} \varphi^f + \operatorname{grad} N_b \right) dv \,, \\
\mathbf{k}_{ab}^{Jw} &= \int_{\Omega^b} \alpha_f N_b \left(\operatorname{grad} N_a + N_a \frac{1}{J^f} \operatorname{grad} J^f \right) dv \,,
\end{aligned}
\tag{3.7.33}
$$

and finally, for $D\delta W_{int}\left[\Delta J^f\right]$ the equations become

$$
\begin{aligned}
D\delta W_{int}\left[\Delta J^f\right] &= \sum_a \delta \mathbf{v}_a \cdot \sum_b \mathbf{k}_{ab}^{uJ} \Delta J_b^f \\
&+ \sum_a \delta \mathbf{w}_a \cdot \sum_b \mathbf{k}_{ab}^{wJ} \Delta J_b^f \\
&+ \sum_a \delta J_a^f \sum_b k_{ab}^{JJ} \Delta J_b^f \,,
\end{aligned}
\tag{3.7.34}
$$

where

$$
\begin{aligned}
\mathbf{k}_{ab}^{uJ} &= \int_{\Omega^b} \alpha_f \varphi^s N_a N_b \left(\frac{\varphi^s}{\varphi^f} \boldsymbol{\tau}'_J \cdot \operatorname{grad} \frac{\varphi^f}{\varphi^s} + \frac{\rho_T^f}{J^f} \mathbf{a}^f \right) dv \\
&+ \int_{\Omega^b} -\alpha_f N_b \varphi^s \boldsymbol{\tau}'_J \cdot \operatorname{grad} N_a dv \,, \\
\mathbf{k}_{ab}^{wJ} &= \int_{\Omega^b} \alpha_f N_a \left(p' \operatorname{grad} N_b + N_b \left(p'' \operatorname{grad} J^f - \frac{\rho_T^f}{J^f} \mathbf{a}^f - \frac{1}{\varphi^f} \boldsymbol{\tau}'_J \cdot \operatorname{grad} \varphi^f \right) \right) dv \Delta J_b^f \\
&+ \int_{\Omega^b} \alpha_f N_b \boldsymbol{\tau}'_J \cdot \operatorname{grad} N_a dv \,, \\
k_{ab}^{JJ} &= \int_{\Omega^b} \alpha_f N_a \frac{1}{J^f} \left(\left(\varphi^f \frac{\alpha_m}{\gamma \alpha_f \Delta t} - \frac{1}{J^f} \left(\varphi^f \dot{J}^f + \operatorname{grad} J^f \cdot \mathbf{w} \right) \right) N_b + \operatorname{grad} N_b \cdot \mathbf{w} \right) dv \,,
\end{aligned}
\tag{3.7.35}
$$

for external virtual work in Eq. (3.7.4), the discretized equations are

$$\begin{aligned}\delta W_{ext} &= \sum_a \delta \mathbf{v}_a \cdot \mathbf{f}_a^u \\ &+ \sum_a \delta \mathbf{w}_a \cdot \mathbf{f}_a^w \\ &+ \sum_a \delta J_a^f f_a^J \,,\end{aligned} \tag{3.7.36}$$

where

$$\begin{aligned}\mathbf{f}_{a,ext}^u &= \int_{\partial\Omega^b} N_a \mathbf{t}^\sigma da + \int_{\Omega^b} N_a \varphi^s \left(-\rho_T^f \mathbf{b}^f + \rho_T^s \mathbf{b}^s\right) dv \,, \\ \mathbf{f}_{a,ext}^w &= \int_{\partial\Omega^b} N_a \mathbf{t}^\tau da + \int_{\Omega^b} \rho_T^f N_a \mathbf{b}^f dv \,, \\ f_{a,ext}^J &= \int_{\partial\Omega^b} N_a w_n da \,,\end{aligned} \tag{3.7.37}$$

and the discretized forms of the linearized external virtual work are

$$\begin{aligned}D\delta W_{ext}\left[\Delta\mathbf{u}\right] &= \sum_a \delta \mathbf{w}_a \cdot \sum_b \mathbf{K}_{ab}^{wu} \cdot \Delta \mathbf{u}_b \,, \\ D\delta W_{ext}\left[\Delta J^f\right] &= \sum_a \delta \mathbf{v}_a \cdot \sum_b \mathbf{k}_{ab}^{uJ} \Delta J_b^f + \sum_a \delta \mathbf{w}_a \cdot \sum_b \mathbf{k}_{ab}^{wJ} \Delta J_b^f \,,\end{aligned} \tag{3.7.38}$$

where

$$\begin{aligned}\mathbf{K}_{ab,ext}^{wu} &= \int_{\Omega^b} \alpha_f N_a \rho_T^f \mathbf{b}^f \otimes \operatorname{grad} N_b dv \,, \\ \mathbf{k}_{ab,ext}^{uJ} &= -\int_{\Omega^b} \alpha_f \varphi^s \frac{\rho_T^f}{J^f} N_a N_b \mathbf{b}^f dv \,, \\ \mathbf{k}_{ab,ext}^{wJ} &= -\int_{\Omega^b} \alpha_f \frac{\rho_T^f}{J^f} N_a N_b \mathbf{b}^f dv \,.\end{aligned} \tag{3.7.39}$$

Combining these results, from the linearized virtual work equation of (3.5.5) we can represent the system of equations in a compact matrix form as

$$\begin{bmatrix} \mathbf{K}_{ab}^{uu} & \mathbf{K}_{ab}^{uw} & \mathbf{k}_{ab}^{uJ} - \mathbf{k}_{ab,ext}^{uJ} \\ \mathbf{K}_{ab}^{wu} - \mathbf{K}_{ab,ext}^{wu} & \mathbf{K}_{ab}^{ww} & \mathbf{k}_{ab}^{wJ} - \mathbf{k}_{ab,ext}^{wJ} \\ \mathbf{k}_{ab}^{Ju} & \mathbf{k}_{ab}^{Jw} & k_{ab}^{JJ} \end{bmatrix} \begin{bmatrix} \Delta\mathbf{u} \\ \Delta\mathbf{w} \\ \Delta J^f \end{bmatrix} = \begin{bmatrix} \mathbf{f}_{a,ext}^u - \mathbf{f}_a^u \\ \mathbf{f}_{a,ext}^w - \mathbf{f}_a^w \\ f_{a,ext}^J - f_a^J \end{bmatrix} . \tag{3.7.40}$$

3.7.4 BFSI Traction Interface

The virtual work δF on a biphasic-FSI interface was given in Eq. (3.7.10). The linearizations of δF are given by

$$
\begin{aligned}
D\delta F\left[\Delta\mathbf{u}\right] = &\int_{\partial\Omega^b} \delta\mathbf{v}\cdot\alpha_f\frac{\varphi^s}{\varphi^f}\left(\operatorname{div}\Delta\mathbf{u}\right)\mathbf{T}_d\cdot\left(\mathbf{g}_1\times\mathbf{g}_2\right)\,d\eta^1d\eta^2\\
&+\int_{\partial\Omega^b} -\delta\mathbf{v}\cdot\boldsymbol{\mathcal{C}}^\tau:\alpha_f\left(-\frac{\varphi^s}{\varphi^{f^2}}\left(\operatorname{div}\Delta\mathbf{u}\right)\mathbf{D}^w+\mathbf{M}\cdot\operatorname{grad}\Delta\mathbf{u}\right)\cdot\left(\mathbf{g}_1\times\mathbf{g}_2\right)\,d\eta^1d\eta^2\\
&+\int_{\partial\Omega^b} -\delta\mathbf{v}\cdot\boldsymbol{\mathcal{C}}^\tau:\alpha_f\left(2\frac{\varphi^s}{\varphi^{f^3}}\left(\operatorname{div}\Delta\mathbf{u}\right)\mathbf{w}\otimes\operatorname{grad}\varphi^f\right)\cdot\left(\mathbf{g}_1\times\mathbf{g}_2\right)\,d\eta^1d\eta^2\\
&+\int_{\partial\Omega^b} -\delta\mathbf{v}\cdot\boldsymbol{\mathcal{C}}^\tau:\alpha_f\left(-\frac{1}{\varphi^{f^2}}\mathbf{w}\otimes\left(-\operatorname{grad}^T\Delta\mathbf{u}\cdot\operatorname{grad}\varphi^f\right)\right)\cdot\left(\mathbf{g}_1\times\mathbf{g}_2\right)\,d\eta^1d\eta^2\\
&+\int_{\partial\Omega^b} \delta\mathbf{v}\cdot\boldsymbol{\mathcal{C}}^\tau:\alpha_f\left(\frac{\varphi^s}{\varphi^{f^2}}\mathbf{w}\otimes\left(-\frac{1}{J}\left(\operatorname{div}\Delta\mathbf{u}\right)\operatorname{grad}J+\operatorname{grad}\left(\operatorname{div}\Delta\mathbf{u}\right)\right)\right)\cdot\left(\mathbf{g}_1\times\mathbf{g}_2\right)\,d\eta^1d\eta^2\\
&+\int_{\partial\Omega^b} -\delta\mathbf{v}\cdot\alpha_f\boldsymbol{\tau}\cdot\left(\frac{\partial\Delta\mathbf{u}}{\partial\eta^1}\times\mathbf{g}_2+\mathbf{g}_1\times\frac{\partial\Delta\mathbf{u}}{\partial\eta^2}\right)\,d\eta^1d\eta^2\,,\\
D\delta F\left[\Delta\mathbf{w}\right] = &\int_{\partial\Omega^b} -\delta\mathbf{v}\cdot\alpha_f\boldsymbol{\mathcal{C}}^\tau:\left(\frac{1}{\varphi^f}\operatorname{grad}\Delta\mathbf{w}-\frac{1}{\varphi^{f^2}}\Delta\mathbf{w}\otimes\operatorname{grad}\varphi^f\right)\cdot\left(\mathbf{g}_1\times\mathbf{g}_2\right)\,d\eta^1d\eta^2\,,\\
D\delta F\left[\Delta J^f\right] = &\int_{\partial\Omega^b} -\delta\mathbf{v}\cdot\alpha_f\left(-p'\mathbf{I}+\boldsymbol{\tau}'_J\right)\cdot\left(\mathbf{g}_1\times\mathbf{g}_2\right)\Delta J^f\,d\eta^1d\eta^2\,.
\end{aligned}
\tag{3.7.41}
$$

The discretized forms of this virtual work is

$$
\delta F=\sum_a\delta\mathbf{v}_a\cdot\mathbf{f}_a\,,
\tag{3.7.42}
$$

where

$$
\mathbf{f}_a=\int_{\partial\Omega^b}-N_a\left(-p\mathbf{I}+\boldsymbol{\tau}\right)\cdot\left(\mathbf{g}_1\times\mathbf{g}_2\right)\,d\eta^1d\eta^2\,.
\tag{3.7.43}
$$

The discretized forms of the linearizations are

$$
\begin{aligned}
D\delta F\left[\Delta\mathbf{u}\right] &= \sum_a\delta\mathbf{v}_a\cdot\sum_b\mathbf{K}^{uu}_{ab}\cdot\Delta\mathbf{u}_b\,,\\
D\delta F\left[\Delta\mathbf{w}\right] &= \sum_a\delta\mathbf{v}_a\cdot\sum_b\mathbf{K}^{uw}_{ab}\cdot\Delta\mathbf{w}_b\,,\\
D\delta F\left[\Delta J^f\right] &= \sum_a\delta\mathbf{v}_a\cdot\sum_b\mathbf{k}^{uJ}_{ab}\Delta J^f_b\,,
\end{aligned}
\tag{3.7.44}
$$

where

$$\begin{aligned}
\mathbf{K}^{uu}_{ab} &= \int_{\partial\Omega^b} \alpha_f N_a \frac{\varphi^s}{\varphi^f} \left(\boldsymbol{\tau}\cdot(\mathbf{g}_1\times\mathbf{g}_2)\right)\otimes \operatorname{grad} N_b \, d\eta^1 d\eta^2 \\
&+ \int_{\partial\Omega^b} -\alpha_f N_a \left(\mathbf{g}_1\times\mathbf{g}_2\right)\cdot\boldsymbol{\mathcal{C}}_d\cdot\operatorname{grad} N_b\cdot\left(-\frac{\varphi^s}{\varphi^{f^2}}\mathbf{D}^w+\mathbf{M}\right) d\eta^1 d\eta^2 \\
&+ \int_{\partial\Omega^b} -\alpha_f N_a \left(\mathbf{g}_1\times\mathbf{g}_2\right)\cdot\boldsymbol{\mathcal{C}}^\tau\cdot\mathbf{w}\cdot\left(2\frac{\varphi^s}{\varphi^{f^3}}\operatorname{grad}\varphi^f\otimes\operatorname{grad} N_b\right) d\eta^1 d\eta^2 \\
&+ \int_{\partial\Omega^b} -\alpha_f N_a \left(\mathbf{g}_1\times\mathbf{g}_2\right)\cdot\boldsymbol{\mathcal{C}}^\tau\cdot\mathbf{w}\cdot\left(\frac{1}{\varphi^{f^2}}\operatorname{grad} N_b\otimes\operatorname{grad}\varphi^f\right) d\eta^1 d\eta^2 \\
&+ \int_{\partial\Omega^b} \alpha_f N_a \left(\mathbf{g}_1\times\mathbf{g}_2\right)\cdot\boldsymbol{\mathcal{C}}^\tau\cdot\mathbf{w}\cdot\frac{\varphi^s}{\varphi^{f^2}}\left(-\frac{1}{J}\operatorname{grad} J\otimes\operatorname{grad} N_b+\operatorname{grad}\operatorname{grad} N_b\right) d\eta^1 d\eta^2 \\
&+ \int_{\partial\Omega^b} -\alpha_f N_a \left(-p\mathbf{I}+\boldsymbol{\tau}\right)\cdot\boldsymbol{\mathcal{A}}\left\{-\mathbf{g}_2\frac{\partial N_b}{\partial\eta^1}+\mathbf{g}_1\frac{\partial N_b}{\partial\eta^2}\right\} d\eta^1 d\eta^2 \,, \\
\mathbf{K}^{uw}_{ab} &= \int_{\partial\Omega^b} -\alpha_f N_a \left(\mathbf{g}_1\times\mathbf{g}_2\right)\cdot\boldsymbol{\mathcal{C}}_d\cdot\frac{1}{\varphi^f}\left(\operatorname{grad} N_b-\frac{1}{\varphi^f}N_b\operatorname{grad}\varphi^f\right) d\eta^1 d\eta^2 \,, \\
\mathbf{k}^{uJ}_{ab} &= \int_{\partial\Omega^b} -\alpha_f N_a N_b \left(-p'\mathbf{I}+\boldsymbol{\tau}'_J\right)\cdot\left(\mathbf{g}_1\times\mathbf{g}_2\right) d\eta^1 d\eta^2 \,.
\end{aligned} \tag{3.7.45}$$

Note that $\boldsymbol{\mathcal{A}}\{\cdot\}$ represents the skew-symmetric tensor form of the bracketed vector.

3.8 Newton-Raphson Method

The Newton-Raphson method (also known as “Newton’s method”, “Full Newton method” or “the Newton method”) is the basis for solving the nonlinear finite element equations. This section will describe the *Full Newton method* and the Broyden-Fletcher-Goldfarb-Shanno (BFGS) method [73]. The latter variation is actually a *quasi-Newton method*. It is important since it provides several advantages over the full Newton method and it is this method that is implemented in FEBio [73].

3.8.1 Full Newton Method

The Newton-Raphson equation (3.1.3) can be written in terms of the discretized equilibrium equations that were derived in the previous section as follows:

$$\delta\mathbf{v}^T\cdot\mathbf{K}\cdot\mathbf{u}=-\delta\mathbf{v}^T\cdot\mathbf{R}. \tag{3.8.1}$$

Since the virtual velocities $\delta\mathbf{v}$are arbitrary, a discretized Newton-Raphson scheme can be formulated as follows:

$$\mathbf{K}\left(\mathbf{x}_k\right)\cdot\mathbf{u}=-\mathbf{R}\left(\mathbf{x}_k\right);\quad \mathbf{x}_{k+1}=\mathbf{x}_k+\mathbf{u}\ . \tag{3.8.2}$$

This is the basis of the Newton-Raphson method. For each iteration k, both the stiffness matrix and the residual vector are re-evaluated and a displacement increment $\mathbf{u}$ is calculated by pre-multiplying both sides of the above equation by $\mathbf{K}^{-1}$. This procedure is repeated until some convergence criteria are satisfied.

The formation of the stiffness matrix and, especially, calculation of its inverse, are computationally expensive. Quasi-Newton methods do not require the reevaluation of the stiffness matrix for every iteration. Instead, a quick update is calculated. One particular method that has been quite

successful in the field of computational solid mechanics is the BFGS method, which is described in the next section.

3.8.2 BFGS Method

The BFGS method updates the stiffness matrix (or rather its inverse) to provide an approximation to the exact matrix. A displacement increment is defined as

$$\mathbf{d}_k = \mathbf{x}_k - \mathbf{x}_{k-1}\,, \tag{3.8.3}$$

and an increment in the residual is defined as

$$\mathbf{G}_k = \mathbf{R}_{k-1} - \mathbf{R}_k\,. \tag{3.8.4}$$

The updated matrix $\mathbf{K}_k$ should satisfy the quasi-Newton equation:

$$\mathbf{K}_k\mathbf{d}_k = \mathbf{G}_k\,. \tag{3.8.5}$$

In order to calculate this update, as displacement increment is first calculated:

$$\mathbf{u} = \mathbf{K}_{k-1}^{-1}\mathbf{R}_{k-1}\,. \tag{3.8.6}$$

This displacement vector defines a "direction" for the actual displacement increment. A line search (see next section) can now be applied to determine the optimal displacement increment:

$$\mathbf{x}_k = \mathbf{x}_{k-1} + s\mathbf{u}\,, \tag{3.8.7}$$

where $s$is determined from the line search. With the updated position calculated, $\mathbf{R}_k$can be evaluated. Also, using equations (3.8.3) and (3.8.4), $\mathbf{d}_k$ and $\mathbf{G}_k$ can be evaluted. The stiffness update can now be expressed as

$$\mathbf{K}_k^{-1} = \mathbf{A}_k^T\mathbf{K}_{k-1}^{-1}\mathbf{A}_k\,, \tag{3.8.8}$$

where the matrix $\mathbf{A}$ is an $n \times n$ matrix of the simple form:

$$\mathbf{A}_k = \mathbf{1} + \mathbf{v}_k\mathbf{w}_k^T\,. \tag{3.8.9}$$

The vectors $\mathbf{v}$ and $\mathbf{w}$ are given by

$$\mathbf{v}_k = -\left(\frac{\mathbf{d}_k^T\mathbf{G}_k}{\mathbf{d}_k^T\mathbf{K}_{k-1}\mathbf{d}_k}\right)^{1/2}\mathbf{K}_{k-1}\mathbf{d}_k - \mathbf{G}_k\,, \tag{3.8.10}$$

$$\mathbf{w}_k = \frac{\mathbf{d}_k}{\mathbf{d}_k^T\mathbf{G}_k}\,. \tag{3.8.11}$$

The vector $\mathbf{K}_{k-1}\mathbf{d}_k$ is equal to $s\mathbf{R}_{k-1}$ and has already been calculated.

To avoid numerically dangerous updates, the condition number c of the updating matrix $\mathbf{A}$ is calculated:

$$c = \left(\frac{\mathbf{d}_k^T\mathbf{G}_k}{\mathbf{d}_k^T\mathbf{K}_{k-1}\mathbf{d}_k}\right)^{1/2}\,. \tag{3.8.12}$$

The update is not performed when this number exceeds a preset tolerance.

Considering the actual computations involved, it should be noted that using the matrix updates defined above, the calculation of the search direction in (3.8.6) can be rewritten as,

$$\mathbf{u} = \left(\mathbf{1} + \mathbf{w}_{k-1}\mathbf{v}_{k-1}^T\right)\cdots\left(\mathbf{1} + \mathbf{w}_1\mathbf{v}_1^T\right)\mathbf{K}_0^{-1}\left(\mathbf{1} + \mathbf{v}_1\mathbf{w}_1^T\right)\cdots\left(\mathbf{1} + \mathbf{v}_{k-1}\mathbf{w}_{k-1}^T\right)\mathbf{R}_{k-1}\,. \tag{3.8.13}$$

Hence, the search direction can be computed without explicitly calculating the updated matrices or performing any additional costly matrix factorizations as required in the full Newton-Raphson method.

3.8.3 Line Search Method

A powerful technique often used to improve the convergence rate of Newton based methods is the *line search method*. In this method, the direction of the displacement vector $\mathbf{u}$ is considered as optimal, but the magnitude is controlled by a parameter s:

$$\mathbf{x}_{k+1} = \mathbf{x}_k + s\mathbf{u}\,. \tag{3.8.14}$$

The value of $s$is usually chosen so that the total potential energy $W(s) = W(\mathbf{x}_k + s\mathbf{u})$at the end of the iteration is minimized in the direction of $\mathbf{u}$. This is equivalent to the requirement that the residual force $\mathbf{R}(\mathbf{x}_k + s\mathbf{u})$at the end of the iteration is orthogonal to $\mathbf{u}$:

$$R(s) = \mathbf{u}^T\mathbf{R}(\mathbf{x}_k + s\mathbf{u}) = 0\,. \tag{3.8.15}$$

However, in practice it is sufficient to obtain a value of $s$such that,

$$|R(s)| < \rho\,|R(0)|\,, \tag{3.8.16}$$

where typically a value of $\rho = 0.9$ is used. Under normal conditions the value $s = 1$ automatically satisfies equation (3.8.16) and therefore few extra operations are involved. However, when this is not the case, a more suitable value for $s$needs to be obtained. For this reason it is convenient to approximate $R(s)$as a quadratic in s:

$$R(s) \approx (1-s)\,R(0) + R(1)\,s^2 = 0\,, \tag{3.8.17}$$

which yields a value for $s$as

$$s = \frac{r}{2} \pm \sqrt{\left(\frac{r}{2}\right)^2 - r}\,, \quad r = \frac{R(0)}{R(1)}\,. \tag{3.8.18}$$

If $r < 0$, the square root is positive and a first improved value for $s$is obtained:

$$s_1 = \frac{r}{2} + \sqrt{\left(\frac{r}{2}\right)^2 - r}\,. \tag{3.8.19}$$

If $r > 0$ the $s$can be obtained by using the value that minimizes the quadratic function, that is, $s_1 = r/2$. This procedure is now repeated with $R(1)$ replaced by $R(s_1)$ until equation (3.8.16) is satisfied.

3.9 Generalized $\alpha-$Method

The generalized $\alpha-$method is used for temporal discretization of governing equations in fluid mechanics. For this method we combine the degrees of freedom into $\mathbf{Y}_n = \{\mathbf{v}, J\}_n$, where the subscript n denotes time t_n; similarly, we let $\dot{\mathbf{Y}}_n = \left\{\frac{\partial \mathbf{v}}{\partial t}, \frac{\partial J}{\partial t}\right\}_n$. According to this method [57], the virtual work is evaluated at $\delta W\left(\dot{\mathbf{Y}}_{n+\alpha_m}, \mathbf{Y}_{n+\alpha_f}\right)$, where $t_{n+\alpha} = t_n + \alpha\Delta t$ and $\Delta t = t_{n+1} - t_n$. Here,

$$\begin{aligned} \mathbf{Y}_{n+\alpha_f} &= \alpha_f\mathbf{Y}_{n+1} + (1-\alpha_f)\,\mathbf{Y}_n \\ \dot{\mathbf{Y}}_{n+\alpha_m} &= \alpha_m\dot{\mathbf{Y}}_{n+1} + (1-\alpha_m)\,\dot{\mathbf{Y}}_n \end{aligned}\,. \tag{3.9.1}$$

The parameters α_f and α_m are evaluated from a single parameter ρ_∞ using

$$\alpha_f = \frac{1}{1+\rho_\infty}\,, \quad \alpha_m = \frac{1}{2}\frac{3-\rho_\infty}{1+\rho_\infty}\,, \tag{3.9.2}$$

where $0 \le \rho_\infty \le 1$. This parameter is the spectral radius for an infinite time step, which controls the amount of damping of high frequencies; a value of zero produces the greatest amount of damping, anihilating the highest frequency in one step, whereas a value of one preserves the highest frequency.

The linearization of $\delta W\left(\dot{\mathbf{Y}}_{n+\alpha_m}, \mathbf{Y}_{n+\alpha_f}\right)$ reported in Section 3.5.2 is effectively performed along an increment $\Delta\mathbf{Y}$ of $\mathbf{Y}_{n+1}$ so that the solution to $\delta W = 0$ produces $\mathbf{Y}_{n+1}$. Based on Newmark integration, we have

$$\dot{\mathbf{Y}}_{n+1} = \frac{\mathbf{Y}_{n+1} - \mathbf{Y}_n}{\gamma\Delta t} - \left(\frac{1}{\gamma} - 1\right)\dot{\mathbf{Y}}_n\,. \tag{3.9.3}$$

where, according to the generalized $\alpha-$method,

$$\gamma = \frac{1}{2} + \alpha_m - \alpha_f\,. \tag{3.9.4}$$

Therefore, in this scheme, $\dot{\mathbf{Y}}_{n+\alpha_m}$ is evaluated from

$$\dot{\mathbf{Y}}_{n+\alpha_m} = \left(1 - \frac{\alpha_m}{\gamma}\right)\dot{\mathbf{Y}}_n + \frac{\xi}{\Delta t}\left(\mathbf{Y}_{n+\alpha_f} - \mathbf{Y}_n\right)\,, \quad \xi \equiv \frac{\alpha_m}{\alpha_f\gamma}. \tag{3.9.5}$$

Using (3.9.1) and (3.9.5), we find that

$$\begin{aligned} D\mathbf{Y}_{n+\alpha_f}\left[\Delta\mathbf{Y}\right] &= \alpha_f\Delta\mathbf{Y} \\ D\dot{\mathbf{Y}}_{n+\alpha_m}\left[\Delta\mathbf{Y}\right] &= \frac{\alpha_m}{\gamma}\frac{\Delta\mathbf{Y}}{\Delta t} \end{aligned} \tag{3.9.6}$$

Given the solution $\left(\dot{\mathbf{Y}}_{n+\alpha_m}, \mathbf{Y}_{n+\alpha_f}\right)$, the solution at t_{n+1} is evaluated from

$$\begin{aligned} \mathbf{Y}_{n+1} &= \mathbf{Y}_n + \frac{\mathbf{Y}_{n+\alpha_f} - \mathbf{Y}_n}{\alpha_f}\,, \\ \dot{\mathbf{Y}}_{n+1} &= \dot{\mathbf{Y}}_n + \frac{\dot{\mathbf{Y}}_{n+\alpha_m} - \dot{\mathbf{Y}}_n}{\alpha_m}\,. \end{aligned} \tag{3.9.7}$$

Four different options are presented in [57] for initializing $\mathbf{Y}_{n+1}$ and $\dot{\mathbf{Y}}_{n+1}$ at the beginning of time step t_{n+1}; the first three of these have been implemented in FEBio. For steady flows these authors recommend disregarding ρ_∞ and setting $\alpha_f = \alpha_m = \gamma = 1$ to recover the backward Euler scheme.

Chapter 4

Element Library

FEBio provides several element types for finite element discretization. This chapter describes these elements in more detail.

4.1 Solid Elements

The 3D solid elements available in FEBio are *isoparametric elements*. All of the solid elements are formulated in a global Cartesian coordinate system. For all these elements, a local coordinate system (so-called *isoparametric coordinates*) is defined as well. The global position vector $\mathbf{x}$ can be written as a function of the isoparametric coordinates in the following sense:

$$\mathbf{x}(r,s,t) = \sum_{i=1}^{n} N_i(r,s,t)\,\mathbf{x}_i. \tag{4.1.1}$$

Here, n is the number of nodes, r, s and t are the isoparametric coordinates, N_i are the element shape functions and $\mathbf{x}_i$ are the spatial coordinates of the element nodes. The same parametric interpolation is used for the interpolation of other scalar and vector quantities.

All elements in FEBio are integrated numerically. This implies that integrals over the volume of the element v^e are approximated by a sum:

$$\int_{v^e} f(\mathbf{x})\,dv = \int_{\square^e} f(\mathbf{r})\,J(\mathbf{r})d\square \cong \sum_{i=1}^{m} f(\mathbf{r}_i)\,J_i w_i\,. \tag{4.1.2}$$

Here, $\square$ is the biunit cube, m is the number of integration points, $\mathbf{r}_i$are the location of the integration points in isoparametric coordinates, J is the Jacobian of the transformation $\mathbf{x} = \mathbf{x}(r,s,t)$, and w_i is a weight associated with the integration point. The integration is performed over the element's volume in the natural coordinate system.

Most fully integrated solid elements are unsuitable for the analysis of (nearly-) incompressible material behavior. To deal with this type of deformation, a three-field element implementation is available in FEBio [96].

4.1.1 Hexahedral Elements

FEBio implements an 8-node trilinear hexahedral element. This element is also known as a *brick* element. The shape functions for these elements are defined in function of the isoparametric

coordinates r, s and t, and are given below.

$$\begin{aligned} N_1 &= \frac{1}{8}(1-r)(1-s)(1-t) \\ N_2 &= \frac{1}{8}(1+r)(1-s)(1-t) \\ N_3 &= \frac{1}{8}(1+r)(1+s)(1-t) \\ N_4 &= \frac{1}{8}(1-r)(1+s)(1-t) \\ N_5 &= \frac{1}{8}(1-r)(1-s)(1+t) \\ N_6 &= \frac{1}{8}(1+r)(1-s)(1+t) \\ N_7 &= \frac{1}{8}(1+r)(1+s)(1+t) \\ N_8 &= \frac{1}{8}(1-r)(1+s)(1+t) \end{aligned} \quad . \tag{4.1.3}$$

The following integration rule is implemented for this element type.

8-point Gauss rule			
r	**s**	**t**	**w**
-0.577350269	-0.577350269	-0.577350269	1
0.577350269	-0.577350269	-0.577350269	1
0.577350269	0.577350269	-0.577350269	1
-0.577350269	0.577350269	-0.577350269	1
-0.577350269	-0.577350269	0.577350269	1
0.577350269	-0.577350269	0.577350269	1
0.577350269	0.577350269	0.577350269	1
-0.577350269	0.577350269	0.577350269	1

4.1.2 Pentahedral Elements

Pentahedral elements (also knows as “wedge” elements) consist of six nodes and five faces. Their shape functions are defined in function of the isoparametric coordinates r, s and t and are given as follows.

$$\begin{aligned} N_1 &= \frac{1}{2}(1-r-s)(1-t) \\ N_2 &= \frac{1}{2}r(1-t) \\ N_3 &= \frac{1}{2}s(1-t) \\ N_4 &= \frac{1}{2}(1-r-s)(1+t) \\ N_5 &= \frac{1}{2}r(1+t) \\ N_6 &= \frac{1}{2}s(1+t) \end{aligned} \quad . \tag{4.1.4}$$

The following integration rule is implemented for this element type.

6-point Gauss rule			
r	**s**	**t**	**w**
0.166666667	0.166666667	-0.577350269	0.166666667
0.666666667	0.166666667	-0.577350269	0.166666667
0.166666667	0.666666667	-0.577350269	0.166666667
0.166666667	0.166666667	0.577350269	0.166666667
0.666666667	0.166666667	0.577350269	0.166666667
0.166666667	0.666666667	0.577350269	0.166666667

4.1.3 Tetrahedral Elements

Linear 4-node tetrahedral elements are also available in FEBio. Their shape functions are defined in function of the isoparametric coordinates r, s and t.

$$\begin{aligned} N_1 &= 1 - r - s - t \\ N_2 &= r \\ N_3 &= s \\ N_4 &= t \end{aligned} \quad . \tag{4.1.5}$$

The following integration rules are implemented for this element type.

1-point Gauss rule			
r	**s**	**t**	**w**
0.25	0.25	0.25	0.166666667

4-point Gauss rule			
r	**s**	**t**	**w**
0.13819660	0.13819660	0.13819660	0.041666667
0.58541020	0.13819660	0.13819660	0.041666667
0.13819660	0.58541020	0.13819660	0.041666667
0.13819660	0.13819660	0.58541020	0.041666667

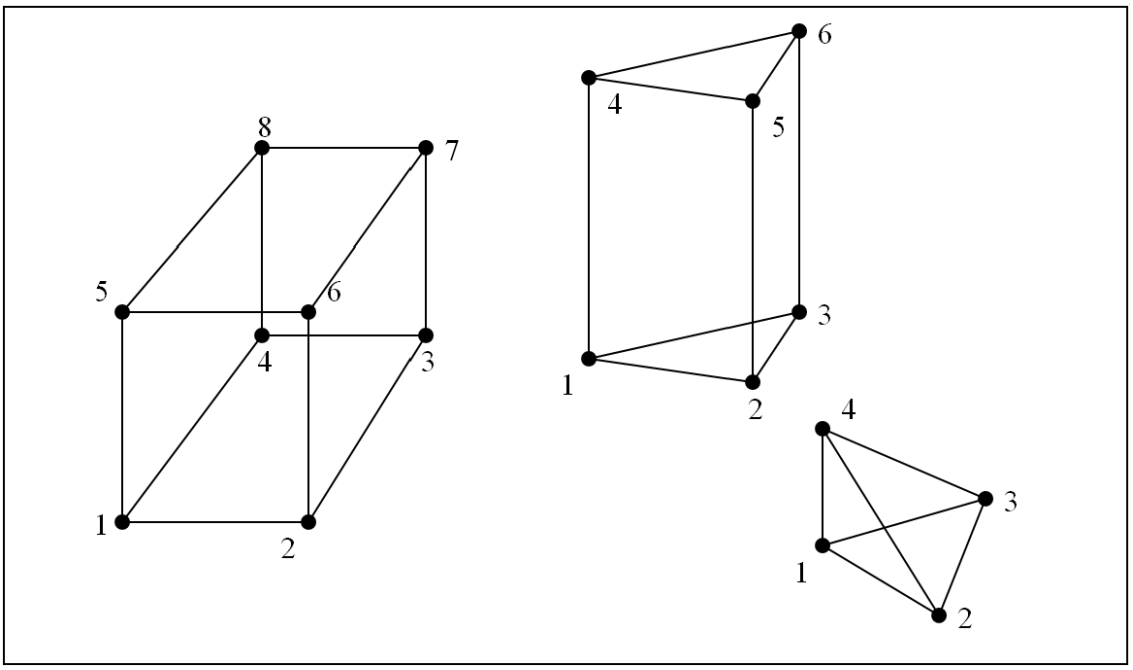

Different solid element types that are available in FEBio

4.1.4 Quadratic Tetrahedral Elements

FEBio implements a 10-node quadratic tetrahedral element. It has four corner nodes and six nodes located at the midpoint of the edges. The shape functions in terms area coordinates are given below. The area coordinates relate to the isoparametric coordinates as follows.

$$\begin{aligned} t_1 &= 1 - r - s - t \\ t_2 &= r \\ t_3 &= s \\ t_4 &= t \end{aligned} \quad . \tag{4.1.6}$$

The shape functions follow.

$$\begin{aligned} H_i &= t_i \left(2t_i - 1\right), \; i = 1 \cdots 4 \\ H_5 &= 4t_1t_2 \\ H_6 &= 4t_2t_3 \\ H_7 &= 4t_3t_1 \\ H_8 &= 4t_1t_4 \\ H_9 &= 4t_2t_4 \\ H_{10} &= 4t_3t_4 \end{aligned} \quad . \tag{4.1.7}$$

The following integration rules are implemented for this element type.

4-point Gauss rule			
r	**s**	**t**	**w**

0.58541020	0.13819660	0.13819660	0.041666667
0.13819660	0.58541020	0.13819660	0.041666667
0.13819660	0.13819660	0.58541020	0.041666667
0.13819660	0.13819660	0.13819660	0.041666667

8-point Gauss rule			
r	**s**	**t**	**w**
0.01583591	0.328054697	0.328054697	0.023087995
0.328054697	0.01583591	0.328054697	0.023087995
0.328054697	0.328054697	0.01583591	0.023087995
0.328054697	0.328054697	0.328054697	0.023087995
0.679143178	0.106952274	0.106952274	0.018578672
0.106952274	0.679143178	0.106952274	0.018578672
0.106952274	0.106952274	0.679143178	0.018578672
0.106952274	0.106952274	0.106952274	0.018578672

11-point Gauss-Lobatto rule			
r	**s**	**t**	**w**
0	0	0	0.002777778
1	0	0	0.002777778
0	1	0	0.002777778
0	0	1	0.002777778
0.5	0	0	0.011111111
0.5	0.5	0	0.011111111
0	0.5	0	0.011111111
0	0	0.5	0.011111111
0.5	0	0.5	0.011111111
0	0.5	0.5	0.011111111
0.25	0.25	0.25	0.088888889

FEBio also implements a 15-node quadratic tetrahedral element.

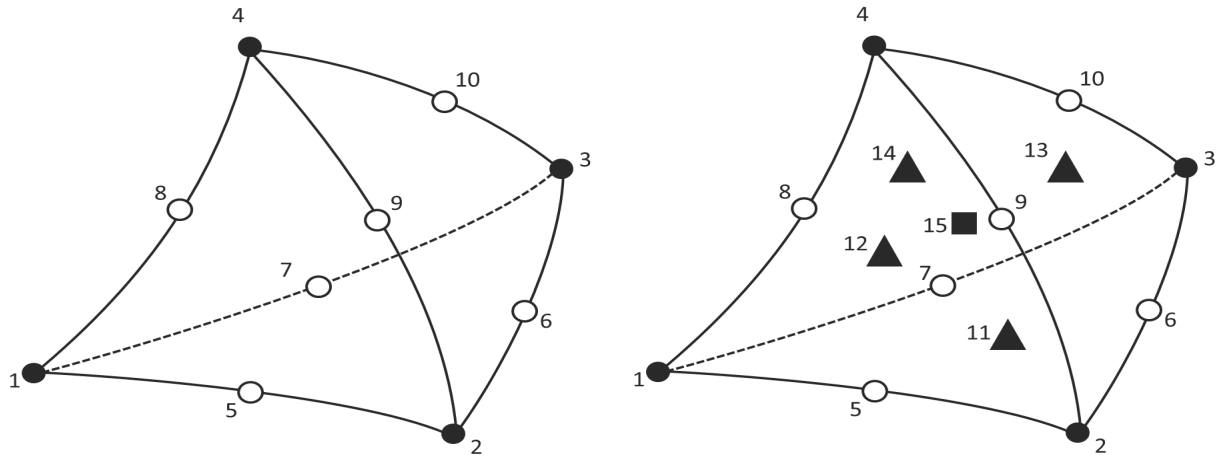

Quadratic tetrahedral elements available in FEBio. Left, a 10-node quadratic tet. Right, a 15-node quadratic tet.

The following integration rules are implemented for this element type.

8-point Gauss rule[1]			
r	**s**	**t**	**w**
0.0158359099	0.3280546970	0.3280546970	0.138527967
0.3280546970	0.0158359099	0.3280546970	0.138527967
0.3280546970	0.3280546970	0.0158359099	0.138527967
0.3280546970	0.3280546970	0.3280546970	0.138527967
0.6791431780	0.1069522740	0.1069522740	0.111472033
0.1069522740	0.6791431780	0.1069522740	0.111472033
0.1069522740	0.1069522740	0.6791431780	0.111472033
0.1069522740	0.1069522740	0.1069522740	0.111472033

11-point Gauss rule			
r	**s**	**t**	**w**
0.25	0.25	0.25	-0.01315555556
0.071428571428571	0.071428571428571	0.071428571428571	0.007622222222
0.785714285714286	0.071428571428571	0.071428571428571	0.007622222222
0.071428571428571	0.785714285714286	0.071428571428571	0.007622222222
0.071428571428571	0.071428571428571	0.785714285714286	0.007622222222
0.399403576166799	0.100596423833201	0.100596423833201	0.024888888889
0.100596423833201	0.399403576166799	0.100596423833201	0.024888888889
0.100596423833201	0.100596423833201	0.399403576166799	0.024888888889
0.399403576166799	0.399403576166799	0.100596423833201	0.024888888889
0.399403576166799	0.100596423833201	0.399403576166799	0.024888888889

[1] Note that weights sum up to one and not to the volume of the tet in the natural coordinate system (i.e. 1/6).

0.100596423833201	0.399403576166799	0.399403576166799	0.024888888889

15-point Gauss rule			
r	**s**	**t**	**w**
0.25	0.25	0.25	0.030283678097089
0.333333333333333	0.333333333333333	0.333333333333333	0.006026785714286
0.000000000000000	0.333333333333333	0.333333333333333	0.006026785714286
0.333333333333333	0.000000000000000	0.333333333333333	0.006026785714286
0.333333333333333	0.333333333333333	0.000000000000000	0.006026785714286
0.090909090909091	0.090909090909091	0.090909090909091	0.011645249086029
0.727272727272727	0.090909090909091	0.090909090909091	0.011645249086029
0.090909090909091	0.727272727272727	0.090909090909091	0.011645249086029
0.090909090909091	0.090909090909091	0.727272727272727	0.011645249086029
0.433449846426336	0.066550153573664	0.066550153573664	0.010949141561386
0.066550153573664	0.433449846426336	0.066550153573664	0.010949141561386
0.066550153573664	0.066550153573664	0.433449846426336	0.010949141561386
0.066550153573664	0.433449846426336	0.433449846426336	0.010949141561386
0.433449846426336	0.066550153573664	0.433449846426336	0.010949141561386
0.433449846426336	0.433449846426336	0.066550153573664	0.010949141561386

4.2 Shell Elements

Historically, shells have been formulated using two different approaches [54]. The difference between these approaches lies in the way the rotational degrees of freedom are defined. In the first approach, the rotational degrees of freedom are defined as angles. In addition, the plane stress condition needs to be enforced to take thickness variations into account. This approach is very useful for infinitesimal strains, but becomes very difficult to pursue in finite deformation due to the fact that finite rotations do not commute. Another disadvantage of this approach is that it requires a modification to the material formulation to enforce the plane stress condition. For complex materials this modification is very difficult or even impossible to obtain.

The alternative approach is to use an *extensible director* to describe the rotational degrees of freedom. With this approach it is not necessary to enforce the plane-stress condition and the full 3D constitutive relations can be employed. This approach is adapted in FEBio as described here.

The shell formulation implemented in FEBio is still a work in progress. The goal is to implement an extensible director formulation with strain enhancements to deal with the well-known locking effect in incompressible and bending problems [23]. With the current state of the implementation, it is advised to use quadratic elements in such problems.

Starting with FEBio 2.6, two shell formulations have become available: The original formulation, where nodes are located at the mid-surface through the thickness of the shell, and a new formulation where nodes are located on the front face of the shell. The original formulation uses

nodal displacements and directors as degrees of freedom; the new formulation uses front and back face nodal displacements. The new formulation is designed to properly accommodate shells attached to the surface of a solid element, or shells sandwiched between two solid elements, with minimal alterations to the rest of the code. The original formulation does not strictly enforce continuity of all the relevant degrees of freedom in those situations. However, this original formulation is maintained in the code for backward compatibility.

Most of the shell elements available in FEBio use a *compatible strain* formulation, where the calculation of strain components is based only on nodal displacements, similar to hexahedral or pentrahedral elements. Users should be aware that this compatible strain formulation is very susceptible to element locking when the shell thickness is much smaller than the shell size (e.g., when the aspect ratio is less than 0.01). Therefore, these shell formulations should be used with caution, keeping in mind this important constraint. Conversely, these shell elements perform very well when they are attached to solid elements (e.g., skin over muscle), or sandwiched between shell elements (e.g., cell membrane separating cytoplasm from extra-cellular matrix).

The element-locking limitation of compatible strain shell formulations has motivated the development of specialized shell formulations that attempt to overcome locking. The FE literature on this subject is rather extensive and we refer the reader to the excellent review chapter by Bischoff et al. [26] on this topic. Methods for overcoming locking include the assumed natural strain (ANS) formulation for transverse shear strains [19, 69] and transverse normal strains [24, 25]. The ANS formulation may be supplemented with the enhanced assumed strain (EAS) method [98] and extended to large deformations [60, 94, 107]. FEBio includes the ANS (*q4ans*) and EAS (*q4eas*) quadrilateral shell element formulations of Vu-Quoc and Tan [107], using a seven-parameter EAS interpolation, which is otherwise substantially similar to the five-parameter interpolation presented in an earlier study by Klinkel et al. [60]. These shell elements are not suitable for attachment to a solid element, nor sandwiching between two solid elements. Since they don't experience element locking, they should be loaded more slowly than compatible strain shell elements. The formulations presented below are for the compatible strain shell elements.

4.2.1 Shell with mid-surface nodal displacements

We create a shell formulation by reducing a solid element interpolation which is linear along the parametric coordinate ξ_3. We start with the general interpolation for a solid element,

$$\mathbf{x}\left(\xi_i\right) = \sum_{a=1}^{n} N_a\left(\xi_i\right)\mathbf{x}_a\,, \tag{4.2.1}$$

where $i = 1, 2, 3$ and n is the number of nodes, and specialize it to the case of a shell as

$$N_a\left(\xi_i\right) = \begin{cases} \frac{1-\xi_3}{2} M_a\left(\xi_\alpha\right) & 1 \leqslant a \leqslant m \\ \frac{1+\xi_3}{2} M_a\left(\xi_\alpha\right) & m+1 \leqslant a \leqslant n \end{cases}, \tag{4.2.2}$$

where $\alpha = 1, 2$, $m = n/2$ is the number of shell element nodes, and $M_a\left(\xi_\alpha\right)$ are the interpolation functions within the mid-shell surface. The description of the mid-shell surface is thus given by

$$\hat{\mathbf{x}}\left(\xi_\alpha\right) = \sum_{a=1}^{n} N_a\left(\xi_1, \xi_2, 0\right)\mathbf{x}_a \equiv \sum_{b=1}^{m} M_b\left(\xi_\alpha\right)\hat{\mathbf{x}}_b\,, \tag{4.2.3}$$

where

$$\hat{\mathbf{x}}_b = \frac{1}{2}\left(\mathbf{x}_b + \mathbf{x}_{b+m}\right) \tag{4.2.4}$$

are the nodal positions for the mid-shell surface.

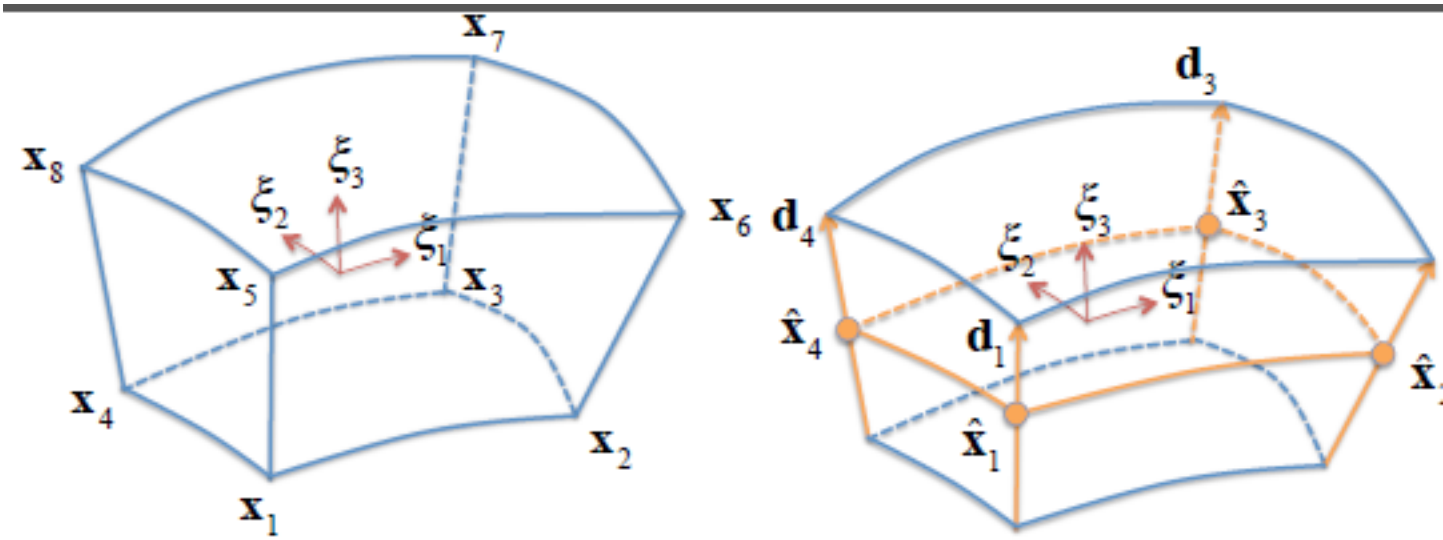

Example of shell elements with four mid-surface nodal positions $\hat{\mathbf{x}}_b$ and directors $\mathbf{d}_b$ ($b = 1 - 4$), reduced from a solid element.

We also define the director across the shell surface as

$$\mathbf{d}\left(\xi_\alpha\right) = \mathbf{x}\left(\xi_1, \xi_2, 1\right) - \mathbf{x}\left(\xi_1, \xi_2, -1\right) = \sum_{b=1}^{m} M_b\left(\xi_\alpha\right)\mathbf{d}_b\,, \tag{4.2.5}$$

where

$$\mathbf{d}_b = \mathbf{x}_{b+m} - \mathbf{x}_b, \quad b = 1 - m \tag{4.2.6}$$

are the nodal directors. Note that the magnitude of the nodal director represents the shell thickness, $h\left(\xi_\alpha\right) = \|\mathbf{d}\left(\xi_\alpha\right)\|$ and the shell thicknesses at the nodes are $h_b = \|\mathbf{d}_b\|$. With these definitions we find that the interpolation across the parametric space of the shell element is

$$\mathbf{x}\left(\xi_i\right) = \hat{\mathbf{x}}\left(\xi_\alpha\right) + \frac{1}{2}\xi_3\mathbf{d}\left(\xi_\alpha\right) = \sum_{b=1}^{m} M_b\left(\xi_\alpha\right)\left(\hat{\mathbf{x}}_b + \frac{1}{2}\xi_3\mathbf{d}_b\right)\,. \tag{4.2.7}$$

From this relation we can obtain the covariant basis vectors as

$$\begin{aligned} \mathbf{g}_\alpha\left(\xi_i\right) &= \frac{\partial \mathbf{x}}{\partial \xi_\alpha} = \sum_{b=1}^{m} \frac{\partial M_b}{\partial \xi_\alpha}\left(\hat{\mathbf{x}}_b + \frac{1}{2}\xi_3\mathbf{d}_b\right) \\ \mathbf{g}_3\left(\xi_i\right) &= \frac{\partial \mathbf{x}}{\partial \xi_3} = \frac{1}{2}\sum_{b=1}^{m} M_b\left(\xi_\alpha\right)\mathbf{d}_b \end{aligned}\,, \tag{4.2.8}$$

from which we may evaluate the contravariant basis vectors $\mathbf{g}^j$ using the identity $\mathbf{g}_i \cdot \mathbf{g}^j = \delta_i^j$. Then, the gradients of the shape functions are given by

$$\operatorname{grad} M_b = \frac{\partial M_b}{\partial \xi_\alpha}\mathbf{g}^\alpha, \quad \operatorname{grad}\left(\frac{1}{2}\xi_3 M_b\right) = \frac{1}{2}\left(\xi_3 \operatorname{grad} M_b + M_b\mathbf{g}^3\right)\,. \tag{4.2.9}$$

It follows from (4.2.7) that the virtual displacement is

$$\delta\mathbf{u}\left(\xi_i\right) = \sum_{a=1}^{m} M_a\left(\xi_\alpha\right)\left(\delta\hat{\mathbf{u}}_a + \frac{1}{2}\xi_3\delta\mathbf{d}_a\right)\,, \tag{4.2.10}$$

and the incremental displacement is

$$\Delta\mathbf{u}\left(\xi_i\right) = \sum_{b=1}^{m} M_b\left(\xi_\alpha\right)\left(\Delta\hat{\mathbf{u}}_b + \frac{1}{2}\xi_3\Delta\mathbf{d}_b\right)\,. \tag{4.2.11}$$

In FEBio, for historical reasons, the nodal director $\mathbf{d}_b$ is currently called *rotation*. This is a misnomer and users should treat this *rotation* as the vector $\mathbf{d}_a$ whose components have units of length. Thus, fixing or prescribing *rotation* components in the input file effectively places these constraints on the components of the nodal director; similarly, requesting *rotation* in the output files will produce the components of the director.

When this type of shell is connected face-to-face with a solid element, the nodes located at $\hat{\mathbf{x}}_b$ automatically share their displacement degrees of freedom $\mathbf{u}_b$ with the corresponding nodes from the face of the solid element. However, no continuity is enforced between the directors $\mathbf{d}_b$ and the solid element deformation. One consequence of this condition is that a shell sandwiched between two solid elements will not detect out-of-plane shear and normal stresses transmitted by the solid element(s). Another consequence is that bending of the solid element(s) will not produce a bending moment in the shell. Therefore, these shell elements are best used as shell-only structures.

4.2.1.1 Elastic Shell

For an elastic shell, the internal virtual work becomes

$$\delta W^e_{\text{int}} = \int\limits_{\Omega^e} \boldsymbol{\sigma} : \operatorname{grad}\delta\mathbf{u}\, dv = \sum_{a=1}^{n} \left[\begin{array}{cc} \delta\hat{\mathbf{u}}_a & \delta\mathbf{d}_a \end{array}\right] \cdot \left[\begin{array}{c} \mathbf{f}^u_a \\ \mathbf{f}^d_a \end{array}\right]\,, \tag{4.2.12}$$

where

$$\mathbf{f}^u_a = \int\limits_{\Omega^e} \boldsymbol{\sigma}\cdot\operatorname{grad} M_a\, dv, \quad \mathbf{f}^d_a = \int\limits_{\Omega^e} \boldsymbol{\sigma}\cdot\operatorname{grad}\left(\frac{1}{2}\xi_3 M_a\right)\, dv\,. \tag{4.2.13}$$

The linearization of the internal virtual work is

$$\begin{aligned} D\left(\delta W^e_{\text{int}}\right)[\Delta\mathbf{u}] = &\int\limits_{\Omega^e} \operatorname{tr}\left(\operatorname{grad}\Delta\mathbf{u}\cdot\boldsymbol{\sigma}\cdot\operatorname{grad}^T\delta\mathbf{u}\right)\, dv \\ &+ \int\limits_{\Omega^e} \operatorname{grad}\delta\mathbf{u} : \boldsymbol{\mathcal{C}} : \operatorname{grad}^T\Delta\mathbf{u}\, dv \end{aligned}\,. \tag{4.2.14}$$

The first of these integrals may be discretized as

$$\int\limits_{\Omega^e} \operatorname{tr}\left(\operatorname{grad}\Delta\mathbf{u}\cdot\boldsymbol{\sigma}\cdot\operatorname{grad}^T\delta\mathbf{u}\right)\, dv = \sum_{a=1}^{m}\sum_{b=1}^{m} \left[\begin{array}{cc} \delta\hat{\mathbf{u}}_a & \delta\mathbf{d}_a \end{array}\right] \left[\begin{array}{cc} \mathbf{K}^{uu}_{ab} & \mathbf{K}^{ud}_{ab} \\ \mathbf{K}^{du}_{ab} & \mathbf{K}^{dd}_{ab} \end{array}\right] \left[\begin{array}{c} \Delta\hat{\mathbf{u}}_b \\ \Delta\mathbf{d}_b \end{array}\right]\,, \tag{4.2.15}$$

where

$$\begin{aligned}
\mathbf{K}_{ab}^{uu} &= \int_{\Omega^e} (\operatorname{grad} M_a \cdot \boldsymbol{\sigma} \cdot \operatorname{grad} M_b)\, \mathbf{I}\, dv \\
\mathbf{K}_{ab}^{ud} &= \int_{\Omega^e} \left(\operatorname{grad} M_a \cdot \boldsymbol{\sigma} \cdot \operatorname{grad} \left(\frac{1}{2}\xi_3 M_b\right)\right) \mathbf{I}\, dv \\
\mathbf{K}_{ab}^{du} &= \int_{\Omega^e} \left(\operatorname{grad} \left(\frac{1}{2}\xi_3 M_a\right) \cdot \boldsymbol{\sigma} \cdot \operatorname{grad} M_b\right) \mathbf{I}\, dv \\
\mathbf{K}_{ab}^{dd} &= \int_{\Omega^e} \left(\operatorname{grad} \left(\frac{1}{2}\xi_3 M_a\right) \cdot \boldsymbol{\sigma} \cdot \operatorname{grad} \left(\frac{1}{2}\xi_3 M_b\right)\right) \mathbf{I}\, dv
\end{aligned} \quad . \tag{4.2.16}$$

The second integral in (4.2.14) becomes

$$\int_{\Omega^e} \operatorname{grad} \delta\mathbf{u} : \boldsymbol{\mathcal{C}} : \operatorname{grad}^T \Delta\mathbf{u}\, dv = \sum_{a=1}^{m}\sum_{b=1}^{m} \begin{bmatrix} \delta\hat{\mathbf{u}}_a & \delta\mathbf{d}_a \end{bmatrix} \begin{bmatrix} \mathbf{K}_{ab}^{uu} & \mathbf{K}_{ab}^{ud} \\ \mathbf{K}_{ab}^{du} & \mathbf{K}_{ab}^{dd} \end{bmatrix} \begin{bmatrix} \Delta\hat{\mathbf{u}}_b \\ \Delta\mathbf{d}_b \end{bmatrix}, \tag{4.2.17}$$

where

$$\begin{aligned}
\mathbf{K}_{ab}^{uu} &= \int_{\Omega^e} \operatorname{grad} M_a \cdot \boldsymbol{\mathcal{C}} \cdot \operatorname{grad} M_b\, dv \\
\mathbf{K}_{ab}^{ud} &= \int_{\Omega^e} \operatorname{grad} M_a \cdot \boldsymbol{\mathcal{C}} \cdot \operatorname{grad} \left(\frac{1}{2}\xi_3 M_b\right)\, dv \\
\mathbf{K}_{ab}^{du} &= \int_{\Omega^e} \operatorname{grad} \left(\frac{1}{2}\xi_3 M_a\right) \cdot \boldsymbol{\mathcal{C}} \cdot \operatorname{grad} M_b\, dv \\
\mathbf{K}_{ab}^{dd} &= \int_{\Omega^e} \operatorname{grad} \left(\frac{1}{2}\xi_3 M_a\right) \cdot \boldsymbol{\mathcal{C}} \cdot \operatorname{grad} \left(\frac{1}{2}\xi_3 M_b\right)\, dv
\end{aligned} \quad . \tag{4.2.18}$$

Similar expressions may be derived for the external work and inertia forces.

In FEBio a 3-point Gaussian quadrature rule is used for the through-the-thickness integration. FEBio currently supports four- and eight-node quadrilateral and three- and six-node triangular shell elements.

4.2.1.2 Quadrilateral shells

For four-node quadrilateral shells, the shape functions are given by

$$\begin{aligned}
M_1 &= \frac{1}{4}(1-r)(1-s) \\
M_2 &= \frac{1}{4}(1+r)(1-s) \\
M_3 &= \frac{1}{4}(1+r)(1+s) \\
M_4 &= \frac{1}{4}(1-r)(1+s)
\end{aligned} \quad . \tag{4.2.19}$$

For eight-node quadrilateral shells the shape functions are

$$\begin{aligned} M_1 &= \frac{1}{4}(1-r)(1-s) - \frac{1}{2}(M_8+M_5) & M_5 &= \frac{1}{2}\left(1-r^2\right)(1-s) \\ M_2 &= \frac{1}{4}(1+r)(1-s) - \frac{1}{2}(M_5+M_6) & M_6 &= \frac{1}{2}\left(1-s^2\right)(1+r) \\ M_3 &= \frac{1}{4}(1+r)(1+s) - \frac{1}{2}(M_6+M_7) & M_7 &= \frac{1}{2}\left(1-r^2\right)(1+s) \\ M_4 &= \frac{1}{4}(1-r)(1+s) - \frac{1}{2}(M_7+M_8) & M_8 &= \frac{1}{2}\left(1-s^2\right)(1-r) \end{aligned} \quad . \tag{4.2.20}$$

4.2.1.3 Triangular shells

For three-node triangular shell elements, the shape functions are given by

$$\begin{aligned} M_1 &= 1-r-s \\ M_2 &= r \\ M_3 &= s \end{aligned} \quad . \tag{4.2.21}$$

For six-node triangular shell elements they are

$$\begin{aligned} M_1 &= r_1(2r_1-1) & M_4 &= 4r_1r_2 \\ M_2 &= r_2(2r_2-1) & M_5 &= 4r_2r_3 \\ M_3 &= r_3(2r_3-1) & M_6 &= 4r_3r_1 \\ r_1 &= 1-r-s & r_2 &= r & r_3 &= s \end{aligned} \quad . \tag{4.2.22}$$

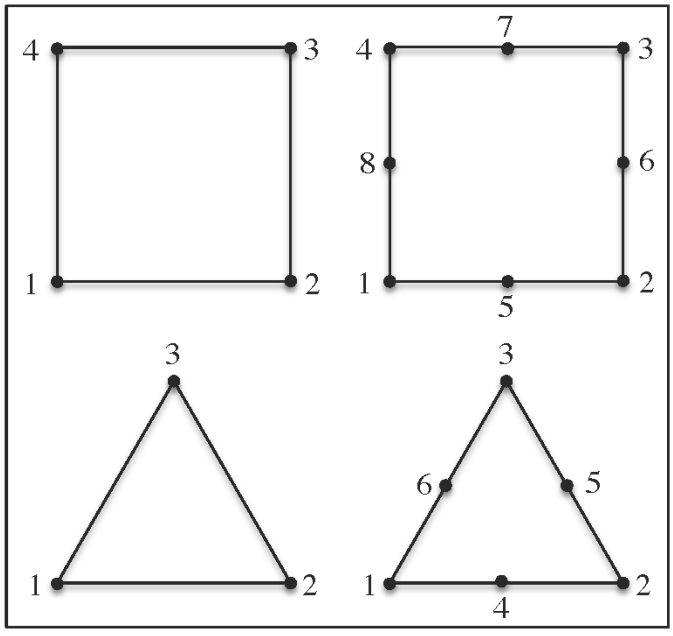

Different shell elements available in FEBio.

4.2.2 Shells with front and back face nodal displacements

We create a shell formulation by reducing a 3D element interpolation which is linear along ξ_3. The nodal positions at the back of the shell ($\xi_3 = -1$) are denoted by $\mathbf{y}_a$ and those on the front of the shell ($\xi_3 = +1$) are denoted by $\mathbf{x}_a$, thus

$$\mathbf{x}\left(\xi_i\right) = \sum_a M_a\left(\xi_1, \xi_2\right)\left(\frac{1+\xi_3}{2}\mathbf{x}_a + \frac{1-\xi_3}{2}\mathbf{y}_a\right) = \sum_a M_a\left(\xi_1, \xi_2\right)\left(\mathbf{x}_a - \frac{1-\xi_3}{2}\mathbf{d}_a\right) \tag{4.2.23}$$

The vector from $\mathbf{y}_a$ to $\mathbf{x}_a$ is the director, $\mathbf{d}_a$,

$$\mathbf{d}_a = \mathbf{x}_a - \mathbf{y}_a$$

From this relation we can get the shell covariant basis vectors,

$$\begin{aligned}
\mathbf{g}_\alpha\left(\xi_i\right) &= \frac{\partial \mathbf{x}}{\partial \xi_\alpha} = \sum_a \frac{\partial M_a}{\partial \xi_\alpha}\left(\frac{1+\xi_3}{2}\mathbf{x}_a + \frac{1-\xi_3}{2}\mathbf{y}_a\right) = \sum_a \frac{\partial M_a}{\partial \xi_\alpha}\left(\mathbf{x}_a - \frac{1-\xi_3}{2}\mathbf{d}_a\right) \\
\mathbf{g}_3\left(\xi_i\right) &= \frac{\partial \mathbf{x}}{\partial \xi_3} = \sum_a \frac{1}{2} M_a\left(\xi_1, \xi_2\right)\left(\mathbf{x}_a - \mathbf{y}_a\right) = \sum_a \frac{1}{2} M_a\left(\xi_1, \xi_2\right)\mathbf{d}_a
\end{aligned} \tag{4.2.24}$$

from which we may evaluate the contravariant basis vectors $\mathbf{g}^i$. Let the front-face and back-face displacements be denoted by $\mathbf{u}$ and $\mathbf{w}$, respectively. It follows that $\mathbf{x}_a = \mathbf{X}_a + \mathbf{u}_a$ and $\mathbf{y}_a = \mathbf{Y}_a + \mathbf{w}_a$, where $\mathbf{X}_a$ represents the shell nodal positions in the reference configuration, provided as nodal coordinates in the input file, and $\mathbf{Y}_a = \mathbf{X}_a - \mathbf{D}_a$ is evaluated from the user-defined referential shell thickness, and the surface surface normals evaluated at each node. If the shell surface is not planar in the reference configuration, users must be careful to select shell thicknesses that don't produce inverted elements (negative Jacobians) as a result of this extrapolation.

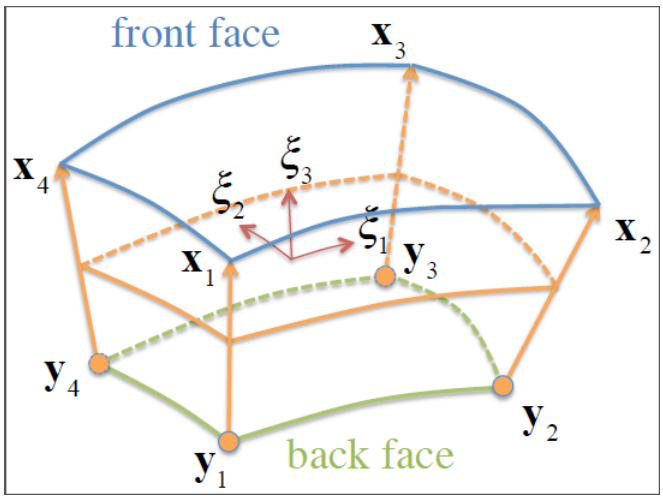

Example of shell element with front-face nodal positions $\mathbf{x}_b$ and back-face nodal positions $\mathbf{y}_b$ ($b = 1 - 4$), reduced from a solid element.

It follows that the virtual displacement is

$$\delta\mathbf{u}\left(\xi_i\right) = \sum_a M_a\left(\frac{1+\xi_3}{2}\delta\mathbf{u}_a + \frac{1-\xi_3}{2}\delta\mathbf{w}_a\right), \tag{4.2.25}$$

and the incremental displacement is

$$\Delta\mathbf{u}\left(\xi_i\right) = \sum_b M_b \left(\frac{1+\xi_3}{2}\Delta\mathbf{u}_b + \frac{1-\xi_3}{2}\Delta\mathbf{w}_b \right) , \tag{4.2.26}$$

so that

$$\operatorname{grad}\delta\mathbf{u} = \sum_a \delta\mathbf{u}_a \otimes \operatorname{grad}\left(\frac{1+\xi_3}{2}M_a\right) + \delta\mathbf{w}_a \otimes \operatorname{grad}\left(\frac{1-\xi_3}{2}M_a\right) , \tag{4.2.27}$$

and

$$\operatorname{grad}\Delta\mathbf{u} = \sum_b \Delta\mathbf{u}_b \otimes \operatorname{grad}\left(\frac{1+\xi_3}{2}M_b\right) + \Delta\mathbf{w}_b \otimes \operatorname{grad}\left(\frac{1-\xi_3}{2}M_b\right) \tag{4.2.28}$$

Note that

$$\operatorname{grad} M_b = \frac{\partial M_b}{\partial \xi_\alpha}\mathbf{g}^\alpha , \tag{4.2.29}$$

so that

$$\operatorname{grad}\left(\frac{1+\xi_3}{2}M_b\right) = \frac{1}{2}\left((1+\xi_3)\operatorname{grad} M_b + M_b\mathbf{g}^3\right) \tag{4.2.30}$$

and

$$\operatorname{grad}\left(\frac{1-\xi_3}{2}M_b\right) = \frac{1}{2}\left((1-\xi_3)\operatorname{grad} M_b - M_b\mathbf{g}^3\right) \tag{4.2.31}$$

To evaluate the deformation gradient in this shell element, we use

$$\mathbf{F} = \operatorname{Grad}\mathbf{x} = \sum_b \mathbf{u}_b \otimes \operatorname{Grad}\left(\frac{1+\xi_3}{2}M_b\right) + \mathbf{w}_b \otimes \operatorname{grad}\left(\frac{1-\xi_3}{2}M_b\right)$$

For this formulation, when a shell element is connected face-to-face with a solid element, the nodal displacements of the solid element face are set to coincide with the back-face nodal displacements $\mathbf{w}_b$ of the shell. When a user prescribes displacement components on that shared face, they apply to the front-face displacements $\mathbf{u}_b$. Similarly, prescribed pressures and contact pressures act on the shell front face.

When a shell element is sandwiched between two solid elements, the nodal displacements of the solid element facing the shell back face are set to coincide with the shell back-face nodal displacements $\mathbf{w}_b$, whereas the nodal displacements of the solid element facing the shell front face are set to coincide with the shell front-face nodal displacements $\mathbf{u}_a$. If the shell thickness exceeds the thickness of the solid element connected to its back face, results become unpredictable.

4.2.2.1 Elastic Shell

For an elastic solid, the internal virtual work is

$$\begin{aligned} \delta W_{int} &= \int_v \boldsymbol{\sigma} : \operatorname{grad}\delta\mathbf{u}\, dv \\ &= \sum_a \begin{bmatrix} \delta\mathbf{u}_a & \delta\mathbf{w}_a \end{bmatrix} \begin{bmatrix} \mathbf{f}_a^u \\ \mathbf{f}_a^w \end{bmatrix} , \end{aligned} \tag{4.2.32}$$

where

$$\begin{aligned} \mathbf{f}_a^u &= \int_v \boldsymbol{\sigma} \cdot \operatorname{grad}\left(\frac{1+\xi_3}{2} M_a\right) \, dv \\ \mathbf{f}_a^w &= \int_v \boldsymbol{\sigma} \cdot \operatorname{grad}\left(\frac{1-\xi_3}{2} M_a\right) \, dv \end{aligned} . \tag{4.2.33}$$

For the external work of body forces,

$$\begin{aligned} \delta W_{ext} &= \int_v \delta \mathbf{u} \cdot \rho \mathbf{b} \, dv \\ &= \sum_{a=1}^{m} \delta \mathbf{u}_a \cdot \mathbf{f}_a^u + \delta \mathbf{w}_a \cdot \mathbf{f}_a^w \end{aligned} , \tag{4.2.34}$$

where

$$\begin{aligned} \mathbf{f}_a^u &= \int_v \frac{1+\xi_3}{2} M_a \rho \mathbf{b} \, dv \\ \mathbf{f}_a^w &= \int_v \frac{1-\xi_3}{2} M_a \rho \mathbf{b} \, dv \end{aligned} . \tag{4.2.35}$$

The linearization of the internal virtual work is

$$\begin{aligned} D\left(\delta W_{int}\right)[\Delta \mathbf{u}] = &\int_v \operatorname{tr}\left(\operatorname{grad} \Delta \mathbf{u} \cdot \boldsymbol{\sigma} \cdot \operatorname{grad}^T \delta \mathbf{u}\right) \, dv \\ &+ \int_v \operatorname{grad} \delta \mathbf{u} : \boldsymbol{\mathcal{C}} : \operatorname{grad}^T \Delta \mathbf{u} \, dv \end{aligned} . \tag{4.2.36}$$

So

$$\int_v \operatorname{tr}\left(\operatorname{grad} \Delta \mathbf{u} \cdot \boldsymbol{\sigma} \cdot \operatorname{grad}^T \delta \mathbf{u}\right) \, dv = \sum_a \sum_b \begin{bmatrix} \delta \mathbf{u}_a & \delta \mathbf{w}_a \end{bmatrix} \begin{bmatrix} \mathbf{K}_{ab}^{uu} & \mathbf{K}_{ab}^{uw} \\ \mathbf{K}_{ab}^{wu} & \mathbf{K}_{ab}^{ww} \end{bmatrix} \begin{bmatrix} \Delta \mathbf{u}_b \\ \Delta \mathbf{w}_b \end{bmatrix} , \tag{4.2.37}$$

where

$$\begin{aligned} \mathbf{K}_{ab}^{uu} &= \int_v \left(\operatorname{grad}\left(\frac{1+\xi_3}{2} M_a\right) \cdot \boldsymbol{\sigma} \cdot \operatorname{grad}\left(\frac{1+\xi_3}{2} M_b\right)\right) \mathbf{I} \, dv \\ \mathbf{K}_{ab}^{uw} &= \int_v \left(\operatorname{grad}\left(\frac{1+\xi_3}{2} M_a\right) \cdot \boldsymbol{\sigma} \cdot \operatorname{grad}\left(\frac{1-\xi_3}{2} M_b\right)\right) \mathbf{I} \, dv \\ \mathbf{K}_{ab}^{wu} &= \int_v \left(\operatorname{grad}\left(\frac{1-\xi_3}{2} M_a\right) \cdot \boldsymbol{\sigma} \cdot \operatorname{grad}\left(\frac{1+\xi_3}{2} M_b\right)\right) \mathbf{I} \, dv \\ \mathbf{K}_{ab}^{ww} &= \int_v \left(\operatorname{grad}\left(\frac{1-\xi_3}{2} M_a\right) \cdot \boldsymbol{\sigma} \cdot \operatorname{grad}\left(\frac{1-\xi_3}{2} M_b\right)\right) \mathbf{I} \, dv \end{aligned} . \tag{4.2.38}$$

Similarly,

$$\int_v \operatorname{grad} \delta \mathbf{u} : \boldsymbol{\mathcal{C}} : \operatorname{grad}^T \Delta \mathbf{u} \, dv = \sum_a \sum_b \begin{bmatrix} \delta \mathbf{u}_a & \delta \mathbf{w}_a \end{bmatrix} \begin{bmatrix} \mathbf{K}_{ab}^{uu} & \mathbf{K}_{ab}^{uw} \\ \mathbf{K}_{ab}^{wu} & \mathbf{K}_{ab}^{ww} \end{bmatrix} \begin{bmatrix} \Delta \mathbf{u}_b \\ \Delta \mathbf{w}_b \end{bmatrix} , \tag{4.2.39}$$

where

$$\begin{aligned}
\mathbf{K}_{ab}^{uu} &= \int_v \operatorname{grad}\left(\frac{1+\xi_3}{2}M_a\right)\cdot\boldsymbol{\mathcal{C}}\cdot\operatorname{grad}\left(\frac{1+\xi_3}{2}M_b\right)\,dv \\
\mathbf{K}_{ab}^{uw} &= \int_v \operatorname{grad}\left(\frac{1+\xi_3}{2}M_a\right)\cdot\boldsymbol{\mathcal{C}}\cdot\operatorname{grad}\left(\frac{1-\xi_3}{2}M_b\right)\,dv \\
\mathbf{K}_{ab}^{wu} &= \int_v \operatorname{grad}\left(\frac{1-\xi_3}{2}M_a\right)\cdot\boldsymbol{\mathcal{C}}\cdot\operatorname{grad}\left(\frac{1+\xi_3}{2}M_b\right)\,dv \\
\mathbf{K}_{ab}^{ww} &= \int_v \operatorname{grad}\left(\frac{1-\xi_3}{2}M_a\right)\cdot\boldsymbol{\mathcal{C}}\cdot\operatorname{grad}\left(\frac{1-\xi_3}{2}M_b\right)\,dv
\end{aligned} \quad . \tag{4.2.40}$$

The linearization of the external work is

$$\begin{aligned}
D\left(\delta W_{ext}\right) &= \sum_{a=1}^{m}\sum_{b=1}^{m}\int_v \left(\frac{1+\xi_3}{2}M_a\delta\mathbf{u}_a + \frac{1-\xi_3}{2}M_a\delta\mathbf{w}_a\right)\cdot\rho\operatorname{grad}\mathbf{b}\cdot\left(\frac{1+\xi_3}{2}\Delta\mathbf{u}_b + \frac{1-\xi_3}{2}M_b\Delta\mathbf{w}_b\right)\,dv \\
&= \sum_a\sum_b \begin{bmatrix} \delta\mathbf{u}_a & \delta\mathbf{w}_a \end{bmatrix}\begin{bmatrix} \mathbf{K}_{ab}^{uu} & \mathbf{K}_{ab}^{uw} \\ \mathbf{K}_{ab}^{wu} & \mathbf{K}_{ab}^{ww} \end{bmatrix}\begin{bmatrix} \Delta\mathbf{u}_b \\ \Delta\mathbf{w}_b \end{bmatrix}
\end{aligned} \quad , \tag{4.2.41}$$

where

$$\begin{aligned}
\mathbf{K}_{ab}^{uu} &= \int_V \left(\frac{1+\xi_3}{2}\right)^2 M_aM_b\rho_0\operatorname{grad}\mathbf{b}\,dV \\
\mathbf{K}_{ab}^{uw} &= \int_V \left(\frac{1+\xi_3}{2}\right)\left(\frac{1-\xi_3}{2}\right) M_aM_b\rho_0\operatorname{grad}\mathbf{b}\,dV \\
\mathbf{K}_{ab}^{wu} &= \int_V \left(\frac{1+\xi_3}{2}\right)\left(\frac{1-\xi_3}{2}\right) M_aM_b\rho_0\operatorname{grad}\mathbf{b}\,dV \\
\mathbf{K}_{ab}^{ww} &= \int_V \left(\frac{1-\xi_3}{2}\right)^2 M_aM_b\rho_0\operatorname{grad}\mathbf{b}\,dV
\end{aligned} \quad . \tag{4.2.42}$$

4.2.2.2 External work of surface forces

We assume that surface forces are applied on the shell front face ($\xi_3 = +1$). Therefore, the external work of surface forces has the form

$$\delta W_{ext} = \int_{\partial v}\delta\mathbf{u}\left(\xi_1,\xi_2,+1\right)\cdot\mathbf{t}\,da = \sum_a \delta\mathbf{u}_a\cdot\int_{\partial v} M_a\left(\xi_1,\xi_2\right)\mathbf{t}\,da \tag{4.2.43}$$

In other words, the treatment of surface forces on a shell becomes identical to the treatment of surface forces on the face of a solid. No special treatment is needed.

4.2.2.3 Shell on top of solid element

When a shell is coincident with the face of a solid element, we assume that the face of the solid element coincides with the back face ($\xi_3 = -1$) of the shell element. This means that the solid element nodal displacements $\mathbf{u}_b$ on that face coincide with the shell nodal displacements $\mathbf{w}_b$. Therefore, when we use UnpackLM for those solid elements, we should reassign the DOF ID's of the $\mathbf{u}_b$ displacements to those of the $\mathbf{w}_b$ displacements stored in that same node.

4.2.2.4 Shell sandwiched between solid elements

When a shell is sandwiched between two solid elements, we reassign the DOF ID's of the the solid $\mathbf{u}_b$ displacements facing the back of the shell to those of the shell $\mathbf{w}_b$ displacements stored in that same node. The DOF ID's of solid $\mathbf{u}_b$ displacements facing the front of the shell remain unchanged; they will coincide with those of the corresponding solid element nodes.

4.2.2.5 Rigid-Shell Interface

When the node of a deformable shell belongs to a rigid body, we need to substitute the nodal degrees of freedom with the rigid body degrees of freedom. The positions of the shell front face and back face nodes are

$$\begin{aligned} \mathbf{x}_b &= \mathbf{r} + \mathbf{\Lambda} \cdot (\mathbf{X}_b - \mathbf{R}) \equiv \mathbf{r} + \mathbf{a}_b \\ \mathbf{y}_b &= \mathbf{r} + \mathbf{\Lambda} \cdot (\mathbf{Y}_b - \mathbf{R}) \equiv \mathbf{r} + \mathbf{b}_b \end{aligned}, \tag{4.2.44}$$

where $\mathbf{r}$ is the current position of the rigid body center of mass and $\mathbf{R}$ is its initial position; $\mathbf{\Lambda}$ is the rotation tensor for the rigid body. We assume that $\mathbf{x}_b$ and $\mathbf{y}_b$ are connected to the same rigid body. From these relations it follows that virtual displacements are

$$\begin{aligned} \delta\mathbf{u}_a &= \delta\mathbf{r} - \hat{\mathbf{a}}_a \cdot \delta\boldsymbol{\theta} \\ \delta\mathbf{w}_b &= \delta\mathbf{r} - \hat{\mathbf{b}}_a \cdot \delta\boldsymbol{\theta} \end{aligned}, \tag{4.2.45}$$

and incremental displacements are

$$\begin{aligned} \Delta\mathbf{u}_b &= \Delta\mathbf{r} - \hat{\mathbf{a}}_b \cdot \Delta\boldsymbol{\theta} \\ \Delta\mathbf{w}_b &= \Delta\mathbf{r} - \hat{\mathbf{b}}_b \cdot \Delta\boldsymbol{\theta} \end{aligned}, \tag{4.2.46}$$

where $\hat{\mathbf{a}}$ is the skew-symmetric tensor whose dual vector is $\mathbf{a}$, such that $\hat{\mathbf{a}} \cdot \mathbf{v} = \mathbf{a} \times \mathbf{v}$ for any vector $\mathbf{v}$. When nodes are flexible (when they do not belong to any rigid body), the virtual work has the general form

$$\delta W = \sum_{a=1}^{m} \delta\mathbf{u}_a \cdot \mathbf{f}_a^u + \delta\mathbf{w}_a \cdot \mathbf{f}_a^w + \delta p_a \, f_a^p = \sum_{a=1}^{m} \begin{bmatrix} \delta\mathbf{v}_a & \delta\mathbf{w}_a & \delta p_a \end{bmatrix} \begin{bmatrix} \mathbf{f}_a^u \\ \mathbf{f}_a^w \\ f_a^p \end{bmatrix}, \tag{4.2.47}$$

where p denotes any additional degree-of-freedom at that node. If node a is rigid we get

$$\begin{bmatrix} \delta\mathbf{u}_a & \delta\mathbf{w}_a & \delta p_a \end{bmatrix} = \begin{bmatrix} \delta\mathbf{r} & \delta\boldsymbol{\theta} & \delta p_a \end{bmatrix} \begin{bmatrix} \mathbf{I} & \mathbf{I} & \mathbf{0} \\ \hat{\mathbf{a}}_a & \hat{\mathbf{b}}_a & \mathbf{0} \\ \mathbf{0} & \mathbf{0} & 1 \end{bmatrix}. \tag{4.2.48}$$

If node b is rigid we get

$$\begin{bmatrix} \Delta\mathbf{u}_b \\ \Delta\mathbf{w}_b \\ \Delta p_b \end{bmatrix} = \begin{bmatrix} \mathbf{I} & -\hat{\mathbf{a}}_b & \mathbf{0} \\ \mathbf{I} & -\hat{\mathbf{b}}_b & \mathbf{0} \\ \mathbf{0} & \mathbf{0} & 1 \end{bmatrix} \begin{bmatrix} \Delta\mathbf{r} \\ \Delta\boldsymbol{\theta} \\ \Delta p_b \end{bmatrix}. \tag{4.2.49}$$

When node a belongs to a rigid body, the expression for δW must be substituted with

$$\begin{aligned} \delta W &= \sum_{a=1}^{m} \begin{bmatrix} \delta\mathbf{u}_a & \delta\mathbf{w}_a & \delta p_a \end{bmatrix} \begin{bmatrix} \mathbf{f}_a^u \\ \mathbf{f}_a^w \\ f_a^p \end{bmatrix} \\ &= \sum_{a=1}^{m} \begin{bmatrix} \delta\mathbf{r} & \delta\boldsymbol{\omega} & \delta p_a \end{bmatrix} \begin{bmatrix} \mathbf{f}_a^u + \mathbf{f}_a^w \\ \hat{\mathbf{a}}_a^{n+\alpha} \cdot \mathbf{f}_a^u + \hat{\mathbf{b}}_a^{n+\alpha} \cdot \mathbf{f}_a^w \\ f_a^p \end{bmatrix} \end{aligned}. \tag{4.2.50}$$

Similarly, the linearized virtual work has the general form

$$D\delta W = \sum_a \sum_b \left[\begin{array}{ccc} \delta\mathbf{u}_a & \delta\mathbf{w}_a & \delta p_a \end{array} \right] \left[\begin{array}{ccc} \mathbf{K}_{ab}^{uu} & \mathbf{K}_{ab}^{uw} & \mathbf{k}_{ab}^{up} \\ \mathbf{K}_{ab}^{wu} & \mathbf{K}_{ab}^{ww} & \mathbf{k}_{ab}^{wp} \\ \mathbf{k}_{ab}^{pu} & \mathbf{k}_{ab}^{pw} & k_{ab}^{pp} \end{array} \right] \left[\begin{array}{c} \Delta\mathbf{u}_b \\ \Delta\mathbf{w}_b \\ \Delta p_b \end{array} \right] . \tag{4.2.51}$$

When node a is rigid but node b is not,

$$\begin{aligned} D\delta W = & \sum_a \sum_b \left[\begin{array}{ccc} \delta\mathbf{r} & \delta\boldsymbol{\theta} & \delta p_a \end{array} \right] \times \\ & \left[\begin{array}{ccc} \mathbf{K}_{ab}^{uu} + \mathbf{K}_{ab}^{wu} & \mathbf{K}_{ab}^{uw} + \mathbf{K}_{ab}^{ww} & \mathbf{k}_{ab}^{up} + \mathbf{k}_{ab}^{wp} \\ \hat{\mathbf{a}}_a \cdot \mathbf{K}_{ab}^{uu} + \hat{\mathbf{b}}_a \cdot \mathbf{K}_{ab}^{wu} & \hat{\mathbf{a}}_a \cdot \mathbf{K}_{ab}^{uw} + \hat{\mathbf{b}}_a \cdot \mathbf{K}_{ab}^{ww} & \hat{\mathbf{a}}_a \cdot \mathbf{k}_{ab}^{up} + \hat{\mathbf{b}}_a \cdot \mathbf{k}_{ab}^{wp} \\ \mathbf{k}_{ab}^{pu} & \mathbf{k}_{ab}^{pw} & k_{ab}^{pp} \end{array} \right] . \\ & \times \left[\begin{array}{c} \Delta\mathbf{u}_b \\ \Delta\mathbf{w}_b \\ \Delta p_b \end{array} \right] \end{aligned} \tag{4.2.52}$$

If nodes a and b are both rigid,

$$\begin{aligned} D\delta W = & \sum_a \sum_b \left[\begin{array}{ccc} \delta\mathbf{r} & \delta\boldsymbol{\theta} & \delta p_a \end{array} \right] \times \\ & \left[\begin{array}{ccc} \mathbf{K}_{ab}^{uu} + \mathbf{K}_{ab}^{wu} + \mathbf{K}_{ab}^{uw} + \mathbf{K}_{ab}^{ww} & \left(\begin{array}{c} -(\mathbf{K}_{ab}^{uu} + \mathbf{K}_{ab}^{wu}) \cdot \hat{\mathbf{a}}_b \\ -(\mathbf{K}_{ab}^{uw} + \mathbf{K}_{ab}^{ww}) \cdot \hat{\mathbf{b}}_b \end{array} \right) & \mathbf{k}_{ab}^{up} + \mathbf{k}_{ab}^{wp} \\ \left(\begin{array}{c} \hat{\mathbf{a}}_a \cdot (\mathbf{K}_{ab}^{uu} + \mathbf{K}_{ab}^{uw}) \\ +\hat{\mathbf{b}}_a \cdot (\mathbf{K}_{ab}^{wu} + \mathbf{K}_{ab}^{ww}) \end{array} \right) & \left(\begin{array}{c} -\left(\hat{\mathbf{a}}_a \cdot \mathbf{K}_{ab}^{uu} + \hat{\mathbf{b}}_a \cdot \mathbf{K}_{ab}^{wu} \right) \cdot \hat{\mathbf{a}}_b \\ -\left(\hat{\mathbf{a}}_a \cdot \mathbf{K}_{ab}^{uw} + \hat{\mathbf{b}}_a \cdot \mathbf{K}_{ab}^{ww} \right) \cdot \hat{\mathbf{b}}_b \end{array} \right) & \hat{\mathbf{a}}_a \cdot \mathbf{k}_{ab}^{up} + \hat{\mathbf{b}}_a \cdot \mathbf{k}_{ab}^{wp} \\ \mathbf{k}_{ab}^{pu} + \mathbf{k}_{ab}^{pw} & \hat{\mathbf{a}}_b \cdot \mathbf{k}_{ab}^{pu} + \hat{\mathbf{b}}_b \cdot \mathbf{k}_{ab}^{pw} & k_{ab}^{pp} \end{array} \right] . \\ & \times \left[\begin{array}{c} \Delta\mathbf{r} \\ \Delta\boldsymbol{\theta} \\ \Delta p_b \end{array} \right] \end{aligned} \tag{4.2.53}$$

If node a is not rigid and node b is rigid,

$$\begin{aligned} D\delta W = & \sum_a \sum_b \left[\begin{array}{ccc} \delta\mathbf{u}_a & \delta\mathbf{w}_a & \delta p_a \end{array} \right] \times \\ & \left[\begin{array}{ccc} \mathbf{K}_{ab}^{uu} + \mathbf{K}_{ab}^{wu} & -\mathbf{K}_{ab}^{uu} \cdot \hat{\mathbf{a}}_b - \mathbf{K}_{ab}^{uw} \cdot \hat{\mathbf{b}}_b & \mathbf{k}_{ab}^{up} \\ \mathbf{K}_{ab}^{wu} + \mathbf{K}_{ab}^{ww} & -\mathbf{K}_{ab}^{wu} \cdot \hat{\mathbf{a}}_b - \mathbf{K}_{ab}^{ww} \cdot \hat{\mathbf{b}}_b & \mathbf{k}_{ab}^{wp} \\ \mathbf{k}_{ab}^{pu} + \mathbf{k}_{ab}^{pw} & \hat{\mathbf{a}}_b \cdot \mathbf{k}_{ab}^{pu} + \hat{\mathbf{b}}_b \cdot \mathbf{k}_{ab}^{pw} & k_{ab}^{pp} \end{array} \right] \left[\begin{array}{c} \Delta\mathbf{r} \\ \Delta\boldsymbol{\theta} \\ \Delta p_b \end{array} \right] . \end{aligned} \tag{4.2.54}$$

Chapter 5

Constitutive Models

This chapter describes the theoretical background behind the constitutive models that are available in FEBio. Most materials are derived from a hyperelastic strain-energy function. Please consult Section 2.4 for more background information on this class of materials.

5.1 Linear Elasticity

In the theory of linear elasticity the Cauchy stress tensor is a linear function of the small strain tensor $\boldsymbol{\varepsilon}$:

$$\boldsymbol{\sigma} = \boldsymbol{\mathcal{C}} : \boldsymbol{\varepsilon} \,. \tag{5.1.1}$$

Here, $\boldsymbol{\mathcal{C}}$ is the fourth-order elasticity tensor that contains the material properties. In the most general case this tensor has 21 independent parameters. However, in the presence of material symmetry the number of independent parameters is greatly reduced. For example, in the case of isotropic linear elasticity only two independent parameters remain. In this case, the elasticity tensor is given by $\boldsymbol{\mathcal{C}} = \lambda \mathbf{I} \otimes \mathbf{I} + 2\mu \mathbf{I} \underline{\otimes} \mathbf{I}$, or equivalently,

$$\mathcal{C}_{ijkl} = \lambda \delta_{ij} \delta_{kl} + \mu \left(\delta_{ik} \delta_{jl} + \delta_{il} \delta_{jk} \right) \,. \tag{5.1.2}$$

The material coefficients λ and μ are known as the Lamé parameters. Using this equation, the stress-strain relationship can be written as

$$\sigma_{ij} = \lambda \varepsilon_{kk} \delta_{ij} + 2\mu \varepsilon_{ij} \,. \tag{5.1.3}$$

If the stress and strain are represented inVoigt notation, the constitutive equation can be rewritten in matrix form as

$$\begin{bmatrix} \sigma_{11} \\ \sigma_{22} \\ \sigma_{33} \\ \sigma_{12} \\ \sigma_{23} \\ \sigma_{13} \end{bmatrix} = \begin{bmatrix} \lambda + 2\mu & \lambda & \lambda & 0 & 0 & 0 \\ \lambda & \lambda + 2\mu & \lambda & 0 & 0 & 0 \\ \lambda & \lambda & \lambda + 2\mu & 0 & 0 & 0 \\ 0 & 0 & 0 & \mu & 0 & 0 \\ 0 & 0 & 0 & 0 & \mu & 0 \\ 0 & 0 & 0 & 0 & 0 & \mu \end{bmatrix} \begin{bmatrix} \varepsilon_{11} \\ \varepsilon_{22} \\ \varepsilon_{33} \\ \gamma_{12} \\ \gamma_{23} \\ \gamma_{13} \end{bmatrix} . \tag{5.1.4}$$

The shear strain measures $\gamma_{ij} = 2\varepsilon_{ij}$ are called the *engineering strains*.

The following table relates the Lamé parameters to the more familiar Young's modulus E and Poisson's ratio ν or to the bulk modulus K and shear modulus G.

	E, ν	λ, μ	K, G
E, ν		$E = \frac{\mu}{\lambda+\mu}(2\mu + 3\lambda)$ $\nu = \frac{\lambda}{2(\lambda+\mu)}$	$E = \frac{9KG}{3K+G}$ $\nu = \frac{3K-2G}{6K+2G}$
λ, μ	$\lambda = \frac{\nu E}{(1+\nu)(1-2\nu)}$ $\mu = \frac{E}{2(1+\nu)}$		$\lambda = K - \frac{2}{3}G$ $\mu = G$
K, G	$K = \frac{E}{3(1-2v)}$ $G = \frac{E}{2(1+v)}$	$K = \lambda + \frac{2}{3}\mu$ $G = \mu$	

The theoretical range of the Young's modulus and Poisson's ratio for an isotropic material have the ranges

$$0 < E < \infty\,, \tag{5.1.5}$$

$$-1 \leqslant \nu < 0.5\,. \tag{5.1.6}$$

Materials with Poisson's ratio (close to) 0.5 are known as (nearly-) incompressible materials. For these materials, the bulk modulus approaches infinity. Most materials have a positive Poisson's ratio. However there do exist some materials with a negative ratio. These materials are known as *auxetic* materials and they have the remarkable property that they expand under tension.

The linear stress-strain relationship can also be derived from a strain-energy function such as in the case of hyperelastic materials. In this case the linear strain-energy is given by

$$W = \frac{1}{2}\boldsymbol{\varepsilon} : \boldsymbol{\mathcal{C}} : \varepsilon\,. \tag{5.1.7}$$

The stress is then similarly derived from $\boldsymbol{\sigma} = \frac{\partial W}{\partial \boldsymbol{\varepsilon}}$. In the case of isotropic elasticity, (5.1.7) can be simplified:

$$W = \frac{1}{2}\lambda\,(\operatorname{tr}\boldsymbol{\varepsilon})^2 + \mu\boldsymbol{\varepsilon} : \boldsymbol{\varepsilon}\,. \tag{5.1.8}$$

The Cauchy stress is now given in tensor form by

$$\boldsymbol{\sigma} = \lambda\,(\operatorname{tr}\boldsymbol{\varepsilon})\,\mathbf{I} + 2\mu\boldsymbol{\varepsilon}\,. \tag{5.1.9}$$

5.2 Compressible Materials

5.2.1 Isotropic Elasticity

The linear elastic material model as described in Section 5.1 is only valid for small strains and small rotations. A first modification to this model to the range of nonlinear deformations is given by the St. Venant-Kirchhoff model [27], which in FEBio is referred to as *isotropic elasticity*. This model is objective for large strains and rotations. For the isotropic case it can be derived from the following hyperelastic strain-energy function:

$$W = \frac{1}{2}\lambda \left(\operatorname{tr} \mathbf{E}\right)^2 + \mu \mathbf{E} : \mathbf{E} \,. \tag{5.2.1}$$

The second Piola-Kirchhoff stress can be derived from this:

$$\mathbf{S} = \frac{\partial W}{\partial \mathbf{E}} = \lambda \left(\operatorname{tr} \mathbf{E}\right) \mathbf{I} + 2\mu \mathbf{E} \,. \tag{5.2.2}$$

Note that these equations are similar to the corresponding equations in the linear elastic case, except that the small strain tensor is replaced by the Green-Lagrange elasticity tensor $\mathbf{E}$. The material elasticity tensor is then given by,

$$\mathbb{C} = \frac{\partial \mathbf{S}}{\partial \mathbf{E}} = \lambda \mathbf{I} \otimes \mathbf{I} + 2\mu \mathbf{I} \odot \mathbf{I} \,. \tag{5.2.3}$$

It is important to note that although this model is objective, it should only be used for small strains. For large strains, the response can be somewhat strange if not completely unrealistic. For example, it can be shown that under uni-axial tension the stress becomes infinite and the volume tends to zero for finite strains. Therefore, for large strains it is highly recommended to avoid this material and instead use one of the other non-linear material models described below. The Cauchy stress is

$$\boldsymbol{\sigma} = \frac{1}{J} \left(\lambda \operatorname{tr} \mathbf{E} - \mu\right) \mathbf{b} + \frac{\mu}{J} \mathbf{b}^2 \,, \tag{5.2.4}$$

where $\operatorname{tr} \mathbf{E} = \left(\operatorname{tr} \mathbf{b} - 3\right)/2$, whereas the spatial elasticity tensor is

$$\boldsymbol{\mathcal{C}} = \frac{\lambda}{J} \mathbf{b} \otimes \mathbf{b} + \frac{2}{J} \mu \mathbf{b} \odot \mathbf{b} \,. \tag{5.2.5}$$

5.2.2 Orthotropic Elasticity

An extension of the St. Venant-Kirchhoff model [27] to orthotropic symmetry is provided in FEBio, referred to as *orthotropic elasticity*. This model is objective for large strains and rotations. It can be derived from the following hyperelastic strain-energy function:

$$W = \sum_{a=1}^{3} \mu_a \mathbf{A}_a^0 : \mathbf{E}^2 + \frac{1}{2} \sum_{b=1}^{3} \lambda_{ab} \left(\mathbf{A}_a^0 : \mathbf{E}\right) \left(\mathbf{A}_b^0 : \mathbf{E}\right) \,, \tag{5.2.6}$$

where $\mathbf{A}_a^0 = \mathbf{a}_a^0 \otimes \mathbf{a}_a^0$ is the structural tensor corresponding to one of the three mutually orthogonal planes of symmetry whose unit outward normal is $\mathbf{a}_a^0$ ($\mathbf{a}_a^0 \cdot \mathbf{a}_b^0 = \delta_{ab}$). The material constants are

the three shear moduli μ_a and six moduli λ_{ab}, where $\lambda_{ba} = \lambda_{ab}$. They may be related to the Young's moduli E_a, shear moduli G_{ab} and Poisson's ratios ν_{ab} via

$$\begin{bmatrix} \lambda_{11}+2\mu_1 & \lambda_{12} & \lambda_{13} & 0 & 0 & 0 \\ \lambda_{12} & \lambda_{22}+2\mu_2 & \lambda_{23} & 0 & 0 & 0 \\ \lambda_{13} & \lambda_{23} & \lambda_{33}+2\mu_3 & 0 & 0 & 0 \\ 0 & 0 & 0 & (\mu_1+\mu_2)/2 & 0 & 0 \\ 0 & 0 & 0 & 0 & (\mu_2+\mu_3)/2 & 0 \\ 0 & 0 & 0 & 0 & 0 & (\mu_3+\mu_1)/2 \end{bmatrix}^{-1} = \begin{bmatrix} 1/E_1 & -\nu_{12}/E_1 & -\nu_{13}/E_1 & 0 & 0 & 0 \\ -\nu_{21}/E_2 & 1/E_2 & -\nu_{23}/E_2 & 0 & 0 & 0 \\ -\nu_{31}/E_3 & -\nu_{32}/E_3 & 1/E_3 & 0 & 0 & 0 \\ 0 & 0 & 0 & 1/G_{12} & 0 & 0 \\ 0 & 0 & 0 & 0 & 1/G_{23} & 0 \\ 0 & 0 & 0 & 0 & 0 & 1/G_{31} \end{bmatrix}. \tag{5.2.7}$$

The second Piola-Kirchhoff stress can be derived from this strain energy density function:

$$\begin{aligned} \mathbf{S} = \frac{\partial W}{\partial \mathbf{E}} &= \sum_{a=1}^{3} \mu_a \left(\mathbf{A}_a^0 \cdot \mathbf{E} + \mathbf{E} \cdot \mathbf{A}_a^0 \right) \\ &+ \frac{1}{2} \sum_{b=1}^{3} \lambda_{ab} \left[\left(\mathbf{A}_a^0 : \mathbf{E} \right) \mathbf{A}_b^0 + \left(\mathbf{A}_b^0 : \mathbf{E} \right) \mathbf{A}_a^0 \right] . \end{aligned} \tag{5.2.8}$$

Note that these equations are similar to the corresponding equations in the linear orthotropic elastic case, except that the small strain tensor is replaced by the Green-Lagrange elasticity tensor $\mathbf{E}$. The material elasticity tensor is then given by,

$$\mathbb{C} = \frac{\partial \mathbf{S}}{\partial \mathbf{E}} = \sum_{a=1}^{3} \mu_a \left(\mathbf{A}_a^0 \odot \mathbf{I} + \mathbf{I} \odot \mathbf{A}_a^0 \right) + \frac{1}{2} \sum_{b=1}^{3} \lambda_{ab} \left(\mathbf{A}_a^0 \otimes \mathbf{A}_b^0 + \mathbf{A}_b^0 \otimes \mathbf{A}_a^0 \right) . \tag{5.2.9}$$

It is important to note that although this model is objective, it should only be used for small strains. For large strains, the response can be somewhat strange if not completely unrealistic. For example, it can be shown that under uni-axial tension the stress becomes infinite and the volume tends to zero for finite strains. Therefore, for large strains it is highly recommended to avoid this material and instead use one of the other non-linear material models described below. The Cauchy stress is

$$\begin{aligned} \boldsymbol{\sigma} &= \sum_{a=1}^{3} \frac{\mu_a}{2J} \left(\mathbf{A}_a \cdot (\mathbf{b} - \mathbf{I}) + (\mathbf{b} - \mathbf{I}) \cdot \mathbf{A}_a \right) \\ &+ \frac{1}{2} \sum_{b=1}^{3} \frac{\lambda_{ab}}{2J} \left[\left(\mathbf{A}_a : \mathbf{I} - 1 \right) \mathbf{A}_b + \left(\mathbf{A}_b : \mathbf{I} - 1 \right) \mathbf{A}_a \right] , \end{aligned} \tag{5.2.10}$$

where $\mathbf{A}_a = \mathbf{F} \cdot \mathbf{A}_a^0 \cdot \mathbf{F}^T$ and the spatial elasticity tensor is

$$\boldsymbol{\mathcal{C}} = \sum_{a=1}^{3} \frac{\mu_a}{J} \left(\mathbf{A}_a \odot \mathbf{b} + \mathbf{b} \odot \mathbf{A}_a \right) + \frac{1}{2} \sum_{b=1}^{3} \frac{\lambda_{ab}}{J} \left(\mathbf{A}_a \otimes \mathbf{A}_b + \mathbf{A}_b \otimes \mathbf{A}_a \right) . \tag{5.2.11}$$

5.2.3 Neo-Hookean Hyperelasticity

This is a compressible neo-Hookean material. It is derived from the following hyperelastic strain energy function [27]:

$$W = \frac{\mu}{2}(I_1 - 3) - \mu \ln J + \frac{\lambda}{2}(\ln J)^2 \,. \tag{5.2.12}$$

The parameters μ and λ are the Lamé parameters from linear elasticity. This model reduces to the isotropic linear elastic model for small strains and rotations.

The Cauchy stress is given by,

$$\boldsymbol{\sigma} = \frac{\mu}{J}(\mathbf{b} - \mathbf{I}) + \frac{\lambda}{J}(\ln J)\,\mathbf{I}\,, \tag{5.2.13}$$

and the spatial elasticity tensor is given by

$$\boldsymbol{\mathcal{C}} = \frac{\lambda}{J}\mathbf{I}\otimes\mathbf{I} + \frac{2}{J}(\mu - \lambda \ln J)\,\mathbf{I}\odot\mathbf{I}\,. \tag{5.2.14}$$

The neo-Hookean material is an extension of Hooke's law for the case of large deformations. It is useable for certain plastics and rubber-like substances. A generalization of this model is the Mooney-Rivlin material, which is often used to describe the elastic response of biological tissue.

In FEBio this constitutive model uses a standard displacement-based element formulation and a "coupled" strain energy, so care must be taken when modeling materials with nearly-incompressible material behavior to avoid element locking.

5.2.4 Natural Neo-Hookean

This is a compressible isotropic neo-Hookean material that uses the natural (Hencky) strain tensor invariants to formulate its strain energy density. These invariants are reviewed in [33]. The left Hencky strain is evaluated from $\boldsymbol{\eta} = \ln \mathbf{V}$ where $\mathbf{V}$ is the left stretch tensor in the polar decomposition of the deformation gradient $\mathbf{F} = \mathbf{V}\cdot\mathbf{R}$. To evaluate $\boldsymbol{\eta}$ we first evaluate the left Cauchy-Green tensor $\mathbf{b} = \mathbf{V}^2$ from $\mathbf{F}$ as in eq.(2.3.10) and get its eigenvalues λ_i^2 and eigenvectors $\mathbf{n}_i$. Then

$$\boldsymbol{\eta} = \sum_{i=1}^{3} (\ln \lambda_i)\,\mathbf{n}_i \otimes \mathbf{n}_i \,. \tag{5.2.15}$$

The invariants K_i of the natural strain tensor are

$$\begin{aligned} K_1 &= \operatorname{tr}\boldsymbol{\eta} = \ln J && \text{amount of dilatation} \\ K_2 &= |\operatorname{dev}\boldsymbol{\eta}| = \sqrt{\operatorname{dev}\boldsymbol{\eta} : \operatorname{dev}\boldsymbol{\eta}} && \text{amount of distortion} \\ K_3 &= 3\sqrt{6}\det\boldsymbol{\Phi} && \text{mode of distortion} \end{aligned} \tag{5.2.16}$$

where $J = \det\mathbf{F}$ as usual, and

$$\boldsymbol{\Phi} = \frac{1}{K_2}\operatorname{dev}\boldsymbol{\eta}\,. \tag{5.2.17}$$

It can be shown that

$$\boldsymbol{\eta} = \frac{1}{3}K_1\mathbf{I} + K_2\boldsymbol{\Phi}\,. \tag{5.2.18}$$

Note that $K_2\boldsymbol{\Phi} \to \mathbf{0}$ as $K_2 \to 0$. It also follows that $\boldsymbol{\eta} : \boldsymbol{\eta} = \frac{1}{3}K_1^2 + K_2^2$. As explained in [33], $K_1 \in (-\infty, \infty)$ with positive K_1 implying expansion and negative K_1 implying contraction. Similarly,

$K_2 \in [0, \infty)$, with $K_2 = 0$ implying no distortion. Finally, $K_3 \in [-1, 1]$ with $K_3 = 1$ representing uniaxial extension, $K_3 = -1$ representing uniaxial contraction and $K_3 = 0$ representing pure shear.

For the natural neo-Hookean material the strain energy density is

$$W = \frac{\kappa}{2} K_1^2 + \mu K_2^2 \tag{5.2.19}$$

where κ is the material's bulk modulus and μ is its shear modulus. To evaluate the Cauchy stress $\boldsymbol{\sigma}$ and spatial elasticity tensor $\boldsymbol{\mathcal{C}}$, we use the framework of isotropic elasticity in principal directions (Section 2.4.2). This requires us to express K_1 and K_2 in terms of the eigenvalues λ_i,

$$\begin{aligned} K_1 &= \ln(\lambda_1 \lambda_2 \lambda_3) \\ K_2 &= \frac{1}{3}\sqrt{\left(\ln \frac{\lambda_1^2}{\lambda_2 \lambda_3}\right)^2 + \left(\ln \frac{\lambda_2^2}{\lambda_3 \lambda_1}\right)^2 + \left(\ln \frac{\lambda_3^2}{\lambda_1 \lambda_2}\right)^2}. \end{aligned} \tag{5.2.20}$$

Now the stress $\boldsymbol{\sigma}$ is given by eq.(2.4.18) where, based on eq.(2.4.20), the principal normal stresses are evaluated as

$$\sigma_i = \frac{1}{3J}\left[(3\kappa + 4\mu)\ln \lambda_i + (3\kappa - 2\mu)(\ln \lambda_j + \ln \lambda_k)\right], \tag{5.2.21}$$

with i, j, k forming a permutation over $1, 2, 3$. Similarly, the spatial elasticity tensor $\boldsymbol{\mathcal{C}}$ is given by eq.(2.4.21) where we substitute

$$J^{-1}\lambda_i^2 \frac{\partial^2 W}{\partial \lambda_i^2} - \sigma_i = \frac{1}{3J}\left[(3\kappa + 4\mu)(1 - 2\ln \lambda_i) - 2(3\kappa - 2\mu)(\ln \lambda_j + \ln \lambda_k)\right] \tag{5.2.22}$$

and

$$J^{-1}\lambda_j \lambda_k \frac{\partial^2 W}{\partial \lambda_j \partial \lambda_k} = \frac{3\kappa - 2\mu}{3J}. \tag{5.2.23}$$

Finally, in the limiting case when pairs of eigenvalues are repeated, we substitute

$$\lim_{\lambda_k^2 \to \lambda_j^2} 2\frac{\lambda_k^2 \sigma_j - \lambda_j^2 \sigma_k}{\lambda_j^2 - \lambda_k^2} = \frac{2\mu}{J} - \frac{4(3\kappa + \mu)\ln \lambda_j + 2(3\kappa - 2\mu)\ln \lambda_i}{3J}. \tag{5.2.24}$$

5.2.5 Ogden Unconstrained

The Ogden unconstrained material is defined using the following hyperelastic strain energy function:

$$W(\lambda_1, \lambda_2, \lambda_3) = \frac{1}{2} c_p (J - 1)^2 + \sum_{k=1}^{N} \frac{c_k}{m_k^2}\left(\lambda_1^{m_k} + \lambda_2^{m_k} + \lambda_3^{m_k} - 3 - m_k \ln J\right). \tag{5.2.25}$$

Here, λ_i are the principal stretches and c_p, c_k and m_k are material parameters.

The Cauchy stress tensor for this material may be obtained using the general formula for isotropic elasticity in principal directions given in (2.4.18), with

$$\sigma_i = c_p (J - 1) + \sum_{k=1}^{N} \frac{1}{J}\frac{c_k}{m_k}\left(\lambda_i^{m_k} - 1\right). \tag{5.2.26}$$

Similarly, the spatial elasticity tensor is given by

$$\begin{aligned}\boldsymbol{\mathcal{C}} = &\sum_{i=1}^{3}\left(c_p + \sum_{k=1}^{N}\frac{1}{J}\frac{c_k}{m_k}\left[\left(m_k-2\right)\lambda_i^{m_k}+2\right]\right)\mathbf{a}_i\otimes\mathbf{a}_i \\ &+\sum_{i=1}^{3}\sum_{j=i+1}^{3} c_p\left(2J-1\right)\left(\mathbf{a}_i\otimes\mathbf{a}_j+\mathbf{a}_j\otimes\mathbf{a}_i\right) \\ &+\sum_{i=1}^{3}\sum_{j=i+1}^{3} 2\frac{\lambda_j^2\sigma_i-\lambda_i^2\sigma_j}{\lambda_i^2-\lambda_j^2}\left(\mathbf{a}_i\odot\mathbf{a}_j+\mathbf{a}_j\odot\mathbf{a}_i\right)\,,\end{aligned} \tag{5.2.27}$$

where $\mathbf{a}_i = \mathbf{n}_i\otimes\mathbf{n}_i$ and $\mathbf{n}_i$ are the eigenvectors of $\mathbf{b}$. In the limit when eigenvalues coincide,

$$\lim_{\lambda_j\to\lambda_i} 2\frac{\sigma_i\lambda_j^2-\sigma_j\lambda_i^2}{\lambda_i^2-\lambda_j^2} = 2c_p\left(1-J\right)+\sum_{k=1}^{N}\frac{1}{J}\frac{c_k}{m_k}\left[2+\left(m_k-2\right)\lambda_i^{m_k}\right]\,. \tag{5.2.28}$$

In the reference configuration the elasticity tensor reduces to

$$\boldsymbol{\mathcal{C}}|_{\mathbf{b}=\mathbf{I}} = c_p\mathbf{I}\otimes\mathbf{I}+\left(\sum_{k=1}^{N}c_k\right)\mathbf{I}\odot\mathbf{I}\,, \tag{5.2.29}$$

which has the form of Hooke's law for infinitesimal isotropic elasticity (see Section 5.1), with equivalent Lamé coefficients $c_p \equiv \lambda$ and $2\mu \equiv \sum_{k=1}^{N} c_k$.

5.2.6 Holmes-Mow

The coupled hyperelastic strain-energy function for this material is given by [50],

$$\Psi\left(I_1,I_2,J\right) = \frac{1}{2}c\left(e^{Q}-1\right)\,, \tag{5.2.30}$$

where $I_1$and $I_2$are the first and second invariants of the right Cauchy-Green tensor and $J$the jacobian of the deformation. Furthermore,

$$\begin{aligned}Q &= \frac{\beta}{\lambda+2\mu}\left[\left(2\mu-\lambda\right)\left(I_1-3\right)+\lambda\left(I_2-3\right)-\left(\lambda+2\mu\right)\ln J^2\right]\,, \\ c &= \frac{\lambda+2\mu}{2\beta}\,,\end{aligned} \tag{5.2.31}$$

and λ and μ are the Lamé parameters. The corresponding Cauchy stress tensor is

$$\boldsymbol{\sigma} = \frac{1}{2J}e^{Q}\left(\left[2\mu+\lambda\left(I_1-1\right)\right]\mathbf{b}-\lambda\mathbf{b}^2-\left(\lambda+2\mu\right)\mathbf{I}\right)\,, \tag{5.2.32}$$

and the spatial elasticity tensor is

$$\boldsymbol{\mathcal{C}} = \frac{4\beta}{\lambda+2\mu}Je^{-Q}\boldsymbol{\sigma}\otimes\boldsymbol{\sigma}+J^{-1}e^{Q}\left[\lambda\left(\mathbf{b}\otimes\mathbf{b}-\mathbf{b}\odot\mathbf{b}\right)+\left(\lambda+2\mu\right)\mathbf{I}\odot\mathbf{I}\right]\,. \tag{5.2.33}$$

5.2.7 Conewise Linear Elasticity

Curnier et al. [34] formulated a model for describing bimodular elastic solids exhibiting orthotropic material symmetry. This can be derived from the following hyperelastic strain-energy function:

$$W = \sum_{a=1}^{3} \mu_a \mathbf{A}_a^0 : \mathbf{E}^2 + \frac{1}{2}\lambda_{aa}\left[\mathbf{A}_a^0 : \mathbf{E}\right]\left(\mathbf{A}_a^0 : \mathbf{E}\right) + \sum_{b=1,\, b\neq a}^{3} \frac{1}{2}\lambda_{ab}\left(\mathbf{A}_a^0 : \mathbf{E}\right)\left(\mathbf{A}_b^0 : \mathbf{E}\right), \tag{5.2.34}$$

where $\mathbf{A}_a^0 = \mathbf{a}_a^0 \otimes \mathbf{a}_a^0$ is the structural tensor corresponding to one of the three mutually orthogonal planes of symmetry whose unit outward normal is $\mathbf{a}_a^0$ ($\mathbf{a}_a^0 \cdot \mathbf{a}_b^0 = \delta_{ab}$). The bimodular response is described by

$$\lambda_{aa}\left[\mathbf{A}_a^0 : \mathbf{E}\right] = \begin{cases} \lambda_{+aa} & \mathbf{A}_a^0 : \mathbf{E} \geqslant 0 \\ \lambda_{-aa} & \mathbf{A}_a^0 : \mathbf{E} < 0 \end{cases}. \tag{5.2.35}$$

The material constants are the three shear moduli μ_a, three tensile moduli λ_{+aa}, three compressive moduli λ_{-aa}, and three moduli λ_{ab} ($b \neq a$), where $\lambda_{ba} = \lambda_{ab}$. The second Piola-Kirchhoff stress can be derived from this strain energy density function:

$$\begin{aligned} \mathbf{S} = \frac{\partial W}{\partial \mathbf{E}} &= \sum_{a=1}^{3} \mu_a \left(\mathbf{A}_a^0 \cdot \mathbf{E} + \mathbf{E} \cdot \mathbf{A}_a^0\right) \\ &+ \lambda_{aa}\left[\mathbf{A}_a^0 : \mathbf{E}\right]\left(\mathbf{A}_a^0 : \mathbf{E}\right)\mathbf{A}_a^0 + \sum_{b=1,\, b\neq a}^{3} \lambda_{ab}\left(\mathbf{A}_a^0 : \mathbf{E}\right)\mathbf{A}_b^0 . \end{aligned} \tag{5.2.36}$$

The material elasticity tensor is then given by,

$$\begin{aligned} \mathbb{C} = \frac{\partial \mathbf{S}}{\partial \mathbf{E}} &= \sum_{a=1}^{3} \mu_a \left(\mathbf{A}_a^0 \odot \mathbf{I} + \mathbf{I} \odot \mathbf{A}_a^0\right) \\ &+ \lambda_{aa}\left[\mathbf{A}_a^0 : \mathbf{E}\right]\mathbf{A}_a^0 \otimes \mathbf{A}_a^0 + \sum_{b=1,\, b\neq a}^{3} \lambda_{ab}\mathbf{A}_a^0 \otimes \mathbf{A}_b^0 \end{aligned} . \tag{5.2.37}$$

It is important to note that although this model is objective, it should only be used for small strains. For large strains, the response may be unrealistic. The Cauchy stress is

$$\begin{aligned} \boldsymbol{\sigma} = J^{-1} \Bigg(&\sum_{a=1}^{3} \frac{\mu_a}{2}\left(\mathbf{A}_a \cdot (\mathbf{b} - \mathbf{I}) + (\mathbf{b} - \mathbf{I}) \cdot \mathbf{A}_a\right) \\ &+ \lambda_{aa}\left[K_a\right] K_a \mathbf{A}_a + \sum_{b=1,\, b\neq a}^{3} \lambda_{ab} K_a \mathbf{A}_b \Bigg) , \end{aligned} \tag{5.2.38}$$

where $\mathbf{A}_a = \mathbf{F} \cdot \mathbf{A}_a^0 \cdot \mathbf{F}^T$ and $K_a = \frac{1}{2}\left(\mathbf{A}_a : \mathbf{I} - 1\right)$. The spatial elasticity tensor is

$$\boldsymbol{\mathcal{C}} = J^{-1}\left(\sum_{a=1}^{3} \mu_a \left(\mathbf{A}_a \odot \mathbf{b} + \mathbf{b} \odot \mathbf{A}_a\right) + \lambda_{aa}\left[K_a\right]\mathbf{A}_a \otimes \mathbf{A}_a + \sum_{b=1,\, b\neq a}^{3} \lambda_{ab}\mathbf{A}_a \otimes \mathbf{A}_b\right) . \tag{5.2.39}$$

In the special case of cubic symmetry the number of material constants reduces to four,

$$\begin{aligned} \lambda_{+11} = \lambda_{+22} = \lambda_{+33} &\equiv \lambda_{+1} \\ \lambda_{-11} = \lambda_{-22} = \lambda_{-33} &\equiv \lambda_{-1} \\ \lambda_{12} = \lambda_{23} = \lambda_{31} &\equiv \lambda_2 \\ \mu_1 = \mu_2 = \mu_3 &\equiv \mu \end{aligned} . \tag{5.2.40}$$

5.2.8 Donnan Equilibrium Swelling

The swelling pressure is described by the equations for ideal Donnan equilibrium, assuming that the material is porous, with a charged solid matrix, and the external bathing environment consists of a salt solution of monovalent counter-ions. Since osmotic swelling must be resisted by a solid material, this material is not stable on its own. It must be combined with an elastic material that resists the swelling.

The Cauchy stress for this material is the stress from the Donnan equilibrium response [7]:

$$\boldsymbol{\sigma} = -\pi \mathbf{I}\,, \tag{5.2.41}$$

where π is the osmotic pressure, given by

$$\pi = R\theta \left(\sqrt{\left(c^F\right)^2 + \left(\bar{c}^*\right)^2} - \bar{c}^* \right), \tag{5.2.42}$$

$\bar{c}^*$ is the bath osmolarity (twice the concentration) and c^F is the fixed charge density in the current configuration, related to the reference configuration via,

$$c^F = \frac{\varphi_0^w}{J - 1 + \varphi_0^w} c_0^F\,, \tag{5.2.43}$$

where $J = \det \mathbf{F}$ is the relative volume, R is the universal gas constant and θ is the absolute temperature.

Note that c_0^F may be negative or positive. The gel porosity φ_0^w is unitless and must be in the range $0 < \varphi_0^w < 1$. The corresponding spatial elasticity tensor is [17]

$$\begin{aligned} \boldsymbol{\mathcal{C}} = & \frac{R\theta J \left(c^F\right)^2}{\left(J - 1 + \varphi_0^w\right) \sqrt{\left(c^F\right)^2 + \left(\bar{c}^*\right)^2}} \mathbf{I} \otimes \mathbf{I} \\ & + R\theta \left[\sqrt{\left(c^F\right)^2 + \left(\bar{c}^*\right)^2} - \bar{c}^* \right] \left(2\mathbf{I} \odot \mathbf{I} - \mathbf{I} \otimes \mathbf{I} \right)\,. \end{aligned} \tag{5.2.44}$$

5.2.9 Perfect Osmometer Equilibrium Osmotic Pressure

The swelling pressure is described by the equations for a perfect osmometer, assuming that the material is porous, containing an interstitial solution whose solutes cannot be exchanged with the external bathing environment. Similarly, solutes in the external bathing solution cannot be exchanged with the interstitial fluid of the porous material. Therefore, osmotic pressurization occurs when there is an imbalance between the interstitial and bathing solution osmolarities. Since osmotic swelling must be resisted by a solid matrix, this material is not stable on its own. It must be combined with an elastic material that resists the swelling.

The Cauchy stress for this material is the stress from the perfect osmometer equilibrium response [6]:

$$\boldsymbol{\sigma} = -\pi \mathbf{I}\,, \tag{5.2.45}$$

where π is the osmotic pressure, given by

$$\pi = R\theta \left(\bar{c} - \bar{c}^* \right)\,. \tag{5.2.46}$$

Here, R is the universal gas constant and θ is the absolute temperature, $\bar{c}^*$ is the external bath osmolarity and $\bar{c}$ is the interstitial fluid osmolarity in the current configuration, related to the reference configuration osmolarity $\bar{c}_0$ via,

$$\bar{c} = \frac{\varphi_0^w}{J - 1 + \varphi_0^w} \bar{c}_0 \,. \tag{5.2.47}$$

Though this material is porous, this is not a full-fledged poroelastic material. The behavior described by this material is strictly valid only after the transient response of interstitial fluid and solute fluxes has subsided. The corresponding spatial elasticity tensor is

$$\boldsymbol{\mathcal{C}} = R\theta \left[\frac{J\,\bar{c}}{J - 1 + \varphi_0^w} \mathbf{I} \otimes \mathbf{I} + (\bar{c} - \bar{c}^*) \left(2\mathbf{I} \odot \mathbf{I} - \mathbf{I} \otimes \mathbf{I} \right) \right] . \tag{5.2.48}$$

5.2.10 Large Poisson's Ratio Ligament

This material captures the transversely isotropic behavior of tendon and ligaments while enforcing a large Poisson's ratio. The material utilizes a three part strain energy equation:

$$W = W_{\text{fiber}} + W_{\text{matrix}} + W_{\text{vol}} \,,$$

where:

$$\begin{aligned} W_{\text{fiber}} &= \frac{1}{2} \frac{c_1}{c_2} \left(e^{c_2 (\lambda - 1)^2 - 1} \right) \,, \\ W_{\text{matrix}} &= \frac{\mu}{2} \left(I_1 - 3 \right) - \mu \ln \left(\sqrt{I_3} \right) \,, \\ W_{\text{vol}} &= \frac{\kappa}{2} \left(\ln \left(\frac{I_5 - I_1 I_4 + I_2}{I_4^{2(m - v_0)} e^{-4m(\lambda - 1)}} \right) \right)^2 \,. \end{aligned}$$

The transversely isotropic strain energy W_{fiber} takes into account the behavior of the collagen fibers. The isotropic strain energy W_{matrix} takes into account the mechanical contribution of the extrafibrillar matrix and provides the majority of support when loaded transverse to the fiber direction. The variables c_1, c_2 and μ are material parameters controlling the stress-strain response of the material.

The volumetric strain energy W_{vol} acts as a penalty term which enforces a Poisson's ratio based on user selection of the parameters m and v_0. The variable κ acts as a penalty parameter. Raising κ will cause the prescribed Poisson's ratio to be enforced. The Poisson's ratio in question is given by the following function:

$$v_{\text{apparent}} = -\frac{\lambda^{m - v_0} e^{-m(\lambda - 1)} - 1}{\lambda - 1} \,.$$

5.2.11 Porous Neo-Hookean Material

Consider a porous neo-Hookean material with referential porosity φ_r^w. The pores are compressible but the skeleton is intrinsically incompressible. Thus, upon pore closure, the material behavior needs to switch from compressible to incompressible.

In the current configuration, the porosity is given by

$$\varphi^w = \frac{J - 1 + \varphi_r^w}{J} \,.$$

We may define a new variable,

$$\bar{J} \equiv \frac{J - 1 + \varphi_r^w}{\varphi_r^w} = \frac{J - \varphi_r^s}{1 - \varphi_r^s}\,,$$

which represents the pore volume ratio. It is equal to 1 when $J = 1$ and is equal to J when $\varphi_r^w = 1$ (or $\varphi_r^s = 1 - \varphi_r^w = 0$). Now,

$$\varphi^w = \varphi_r^w \frac{\bar{J}}{J}\,,$$

and

$$\frac{\partial \bar{J}}{\partial J} = \frac{1}{\varphi_r^w}\,.$$

Pore closure occurs when $\varphi^w = 0$, which corresponds to $J = \varphi_r^s$ and $\bar{J} = 0$.

Let us also define a modified deformation gradient,

$$\bar{\mathbf{F}} = \left(\frac{\bar{J}}{J}\right)^{1/3} \mathbf{F}\,,$$

such that $\det \bar{\mathbf{F}} = \bar{J}$. Let the corresponding modified right Cauchy-Green tensor be given by

$$\bar{\mathbf{C}} = \bar{\mathbf{F}}^T \cdot \bar{\mathbf{F}} = \left(\frac{\bar{J}}{J}\right)^{2/3} \mathbf{C}\,,$$

so that

$$\frac{\partial \bar{\mathbf{C}}}{\partial \mathbf{C}} = \left(\frac{\bar{J}}{J}\right)^{2/3} \left(\frac{\varphi_r^s}{3\left(J - \varphi_r^s\right)} \mathbf{C} \otimes \mathbf{C}^{-1} + \mathbf{I} \odot \mathbf{I}\right)\,.$$

The constitutive relation for the strain energy density of the compressible porous neo-Hookean material may be given by

$$\Psi_r = \frac{\mu}{2}\left(\bar{I}_1 - 3\right) - \mu \ln \bar{J}\,,$$

where $\bar{I}_1 = \mathrm{tr}\bar{\mathbf{C}}$. This relation shows that the material develops an infinite strain energy density as $\bar{J}$ approaches zero. From this expression, the 2nd Piola-Kirchhoff stress is given by

$$\mathbf{S} = 2\frac{\partial \Psi_r}{\partial \mathbf{C}} = \mu\left[\left(\frac{\bar{J}}{J}\right)^{2/3} \mathbf{I} + \frac{1}{J - \varphi_r^s}\left(\varphi_r^s \left(\frac{\bar{J}}{J}\right)^{2/3} \frac{I_1}{3} - J\right)\mathbf{C}^{-1}\right]\,.$$

When $\mathbf{C} = \mathbf{I}$ we can verify that $\mathbf{S} = \mathbf{0}$. The corresponding Cauchy stress is

$$\boldsymbol{\sigma} = \frac{\mu}{J}\left[\left(\frac{\bar{J}}{J}\right)^{2/3} \mathbf{b} + \frac{1}{J - \varphi_r^s}\left(\varphi_r^s \left(\frac{\bar{J}}{J}\right)^{2/3} \frac{I_1}{3} - J\right)\mathbf{I}\right]\,,$$

where $\mathbf{b}$ is the left Cauchy-Green tensor.

The material elasticity tensor is given by

$$\begin{aligned}
\mathbb{C} &= 2\frac{\partial \mathbf{S}}{\partial \mathbf{C}} \\
&= \frac{2}{3} g\left(J\right)\left(\mathbf{I} \otimes \mathbf{C}^{-1} + \mathbf{C}^{-1} \otimes \mathbf{I}\right) + \left(J\frac{dg}{dJ}\frac{I_1}{3} + J\frac{dh}{dJ}\right)\mathbf{C}^{-1} \otimes \mathbf{C}^{-1}\,, \\
&- 2\left[g\left(J\right)\frac{I_1}{3} + h\left(J\right)\right]\mathbf{C}^{-1} \odot \mathbf{C}^{-1}
\end{aligned}$$

where

$$f(J) = \mu \left(\frac{\bar{J}}{J}\right)^{2/3}$$
$$g(J) = \frac{\varphi_r^s}{J - \varphi_r^s} f(J),$$
$$h(J) = -\mu \frac{J}{J - \varphi_r^s}$$

and

$$J\frac{dg}{dJ} = \mu \frac{(2\varphi_r^s - 3J)\,\varphi_r^s}{3\left(J - \varphi_r^s\right)^2} \left(\frac{\bar{J}}{J}\right)^{2/3}$$
$$J\frac{dh}{dJ} = \mu \frac{J\varphi_r^s}{\left(J - \varphi_r^s\right)^2}$$

.

Then, the spatial elasticity tensor may be evaluated as

$$\boldsymbol{\mathcal{C}} = J^{-1}\left[\frac{2}{3} g(J)\left(\mathbf{b}\otimes\mathbf{I} + \mathbf{I}\otimes\mathbf{b}\right) + \left(J\frac{dg}{dJ}\frac{I_1}{3} + J\frac{dh}{dJ}\right)\mathbf{I}\otimes\mathbf{I} - 2\left[g(J)\frac{I_1}{3} + h(J)\right]\mathbf{I}\odot\mathbf{I}\right].$$

In the limit of infinitesimal strains and rotations, when $\mathbf{b} = \mathbf{I}$ and $J = 1$, we find that

$$f(1) = \mu \qquad J\frac{dg}{dJ} = \mu\frac{(2\varphi_r^s - 3)\,\varphi_r^s}{3\left(1 - \varphi_r^s\right)^2}$$
$$g(J) = \mu\frac{\varphi_r^s}{1 - \varphi_r^s} \qquad J\frac{dh}{dJ} = \mu\frac{\varphi_r^s}{\left(1 - \varphi_r^s\right)^2}$$
$$h(J) = -\mu\frac{1}{1 - \varphi_r^s}\mu$$

and

$$\boldsymbol{\mathcal{C}} = \frac{2\mu}{3}\left(\frac{1}{\left(\varphi_r^w\right)^2} - 1\right)\mathbf{I}\otimes\mathbf{I} + 2\mu\mathbf{I}\odot\mathbf{I}.$$

Thus, by comparison to a standard neo-Hookean material, this porous neo-Hookean material has an effective Young's modulus equal to

$$E = \frac{3\mu}{1 + \frac{1}{2}\left(\varphi_r^w\right)^2},$$

and an effective Poisson's ratio equal to

$$\nu = \frac{1 - \left(\varphi_r^w\right)^2}{2 + \left(\varphi_r^w\right)^2}.$$

The two material properties that need to be provided are E and the referential porosity φ_r^w (or referential solid volume fraction $\varphi_r^s = 1 - \varphi_r^w$). Poisson's ratio in the limit of infinitesimal strains is dictated by the porosity according to the above formula. In particular, a highly porous material ($\varphi_r^w \to 1$) has an effective (infinitesimal strain) Poisson ratio that approaches zero ($\nu \to 0$) and $E \to 2\mu$. A low porosity material ($\varphi_r^w \to 0$) has $\nu \to \frac{1}{2}$ and $E \to 3\mu$, which is the expected behavior of an incompressible neo-Hookean solid. Note that setting $\varphi_r^w = 0$ would not produce good numerical behavior, since the Cauchy stress in an incompressible material would need to be supplemented by a pressure term (a Lagrange multiplier that enforces the incompressibility constraint). Nevertheless, this compressible porous neo-Hookean material behaves well even for values of φ^w as low as ~ 0.015.

5.2.12 Cell Growth

The cell growth material implements a swelling pressure π such that the Cauchy stress is given by

$$\boldsymbol{\sigma} = -\pi \mathbf{I}\,,$$

where

$$\pi = RT\left(\frac{c_r}{J-\varphi_r^s} - c_e\right)\,.$$

Here, c_r represents the referential molar concentration of intracellular solutes (moles of solutes per mixture volume in the reference configuration), φ_r^s is the referential intracellular solid volume fraction, and $J = \det \mathbf{F}$ is the determinant of the deformation gradient, representing the volume ratio in the current configuration. The extracellular osmolarity is c_e. This model assumes that neither intracellular solutes nor extracellular solutes may transport across the cell membrane passively. When a cell divides, it must use active transport mechanisms to bring in membrane-impermeant extracellular solutes inside, some of which are converted into intracellular solid matrix (e.g., cytoskeletal structures). As the intracellular osmolarity increases, water is transported into the cell, thus causing it to swell. The process of cell division is not modeled explicitly in this continuum representation, though the net effect is that cell proliferation leads to an increase in intracellular osmotic pressure, which generally translates into an increase in volume (unless the cell growth is constrained significantly). In a cell growth model, the initial condition (when $J = 1$) should be selected for c_r and φ_r^s such that $\pi = 0$, thus

$$\frac{c_r}{1-\varphi_r^s} = c_e \quad \text{initial condition}\,.$$

The spatial elasticity tensor associated with this osmotic pressure is

$$\boldsymbol{\Pi} = -\left(\pi + J\frac{\partial \pi}{\partial J}\right)\mathbf{I}\otimes\mathbf{I} + 2\pi\mathbf{I}\odot\mathbf{I}\,,$$

where

$$J\frac{\partial \pi}{\partial J} = -RT\frac{J}{(J-\varphi_r^s)^2}c_r\,.$$

This elasticity tensor has the same form as that of an isotropic elastic material whose effective Young's modulus E_Y and Poisson's ratio ν are given by

$$\begin{aligned} E_Y &= \pi\frac{\left(\pi + 3J\frac{\partial \pi}{\partial J}\right)}{J\frac{\partial \pi}{\partial J}} \\ \nu &= \frac{\pi + J\frac{\partial \pi}{\partial J}}{2J\frac{\partial \pi}{\partial J}} \end{aligned}\,.$$

In the reference configuration, when $\pi = 0$, it follows that $E_Y = 0$ and $\nu = \frac{1}{2}$.

$$\tilde{\boldsymbol{\sigma}} = \tilde{\boldsymbol{\sigma}}_m + \tilde{\boldsymbol{\sigma}}_f\,. \tag{5.2.49}$$

5.2.13 Fiber with Exponential Power Law

This material model describes a constitutive model for fibers, where a single fiber family follows an exponential power law strain energy function. The Cauchy stress is given by:

$$\boldsymbol{\sigma} = 2J^{-1}H\left(I_n - I_0\right) I_n \frac{\partial \Psi_r}{\partial I_n} \mathbf{n} \otimes \mathbf{n}\,, \tag{5.2.50}$$

and the corresponding spatial elasticity tensor is

$$\boldsymbol{\mathcal{C}} = 4J^{-1}H\left(I_n - I_0\right) I_n^2 \frac{\partial^2 \Psi_r}{\partial I_n^2} \mathbf{n} \otimes \mathbf{n} \otimes \mathbf{n} \otimes \mathbf{n}\,, \tag{5.2.51}$$

where $I_n = \lambda_n^2 = \mathbf{n}_r \cdot \mathbf{C} \cdot \mathbf{n}_r$ is the square of the fiber stretch, $\mathbf{n}_r$ is the fiber orientation in the reference configuration,

$$\mathbf{n}_r = \sin\varphi\cos\theta\,\mathbf{e}_1 + \sin\varphi\sin\theta\,\mathbf{e}_2 + \cos\varphi\,\mathbf{e}_3\,, \tag{5.2.52}$$

and $\mathbf{n} = \mathbf{F} \cdot \mathbf{n}_r/\lambda_n$. The function $H\left(\cdot\right)$ is the unit step function that enforces the tension-only contribution. Thus, the stress and elasticity tensors are non-zero only when $I_n > I_0$, where $I_0 = \lambda_0^2$ is the square of the stretch at which the fiber's tensile response engages. By default we may take $I_0 = 1$, though the actual value of I_0 may be set by the user. The fiber strain energy density is given by

$$\Psi_r = \frac{\xi}{\alpha\beta}\left(\exp\left[\alpha\left(I_n - I_0\right)^\beta\right] - 1\right)\,, \tag{5.2.53}$$

where $\xi > 0$, $\alpha \geqslant 0$and $\beta \geqslant 2$. From this expression we get

$$\begin{aligned} \frac{\partial \Psi_r}{\partial I_n} &= \xi\left(I_n - I_0\right)^{\beta-1}\exp\left[\alpha\left(I_n - I_0\right)^\beta\right] \\ \frac{\partial^2 \Psi_r}{\partial I_n^2} &= \xi\left(\beta\left(1 + \alpha\left(I_n - I_0\right)^\beta\right) - 1\right)\left(I_n - I_0\right)^{\beta-2}\exp\left[\alpha\left(I_n - I_0\right)^\beta\right] \end{aligned}\,. \tag{5.2.54}$$

Note: In the limit when $\alpha \to 0$, this expression produces a power law,

$$\lim_{\alpha\to 0}\Psi_r = \frac{\xi}{\beta}\left(I_n - I_0\right)^\beta\,. \tag{5.2.55}$$

Note: According to (5.2.51) and (5.2.54), when $\beta > 2$ the fiber modulus is zero at the strain origin ($I_n = I_0$). Therefore, use $\beta > 2$ when a smooth transition in the stress is desired from compression to tension.

There is an option to also add a shear modulus μ to account for the interaction of a fiber with the ground matrix. This additional contribution does not depend on whether the fiber is in tension. It has a strain energy density

$$W = \frac{\mu}{4}\left(K_n - 1 - 2\left(I_n - 1\right)\right)\,, \quad K_n = \mathbf{n}_r \cdot \mathbf{C}^2 \cdot \mathbf{n}_r \tag{5.2.56}$$

The corresponding stress is

$$\begin{aligned} \boldsymbol{\sigma} &= 2\frac{I_n}{J}\left(\frac{\partial W}{\partial I_n}\mathbf{n} \otimes \mathbf{n} + \frac{\partial W}{\partial K_n}\left(\mathbf{n} \otimes \mathbf{n} \cdot \mathbf{b} + \mathbf{b} \cdot \mathbf{n} \otimes \mathbf{n}\right)\right) \\ &= \frac{\mu}{2}\frac{I_n}{J}\left(\mathbf{n} \otimes \mathbf{n} \cdot \left(\mathbf{b} - \mathbf{I}\right) + \left(\mathbf{b} - \mathbf{I}\right) \cdot \mathbf{n} \otimes \mathbf{n}\right) \end{aligned} \tag{5.2.57}$$

where $\mathbf{b} = \mathbf{F} \cdot \mathbf{F}^T$ is the left Cauchy-Green tensor. The elasticity tensor is

$$\begin{aligned}\boldsymbol{\mathcal{C}} &= 4\frac{I_n^2}{J}\left(\frac{\partial^2 W}{\partial I_n^2}\mathbf{N}\otimes\mathbf{N} + \frac{\partial^2 W}{\partial K_n^2}\left(\mathbf{N}\cdot\mathbf{b}+\mathbf{b}\cdot\mathbf{N}\right)\otimes\left(\mathbf{N}\cdot\mathbf{b}+\mathbf{b}\cdot\mathbf{N}\right)\right)\\ &+ 4\frac{I_n^2}{J}\frac{\partial^2 W}{\partial I_n \partial K_n}\left(\mathbf{N}\otimes\left(\mathbf{N}\cdot\mathbf{b}+\mathbf{b}\cdot\mathbf{N}\right) + \left(\mathbf{N}\cdot\mathbf{b}+\mathbf{b}\cdot\mathbf{N}\right)\otimes\mathbf{N}\right)\\ &+ \frac{4I_n}{J}\frac{\partial W}{\partial K_n}\left(\mathbf{N}\odot\mathbf{b}+\mathbf{b}\odot\mathbf{N}\right)\\ &= \mu\frac{I_n}{J}\left(\mathbf{N}\odot\mathbf{b}+\mathbf{b}\odot\mathbf{N}\right)\end{aligned}, \tag{5.2.58}$$

where $\mathbf{N} = \mathbf{n}\otimes\mathbf{n}$.

5.2.14 Fiber with Natural Neo-Hookean Response

This model is an adaptation of the natural neo-Hookean material presented in Section (5.2.4). Consider that the state of strain in a fiber is given by the unidirectional natural (left Hencky) strain along the fiber,

$$\boldsymbol{\eta} = \ln\lambda_n\,\mathbf{n}\otimes\mathbf{n} \tag{5.2.59}$$

where λ_n is the stretch ratio along the current fiber unit vector $\mathbf{n}$. For this special state of strain the invariants K_i of the natural strain tensor reduce to $K_1 = \ln\lambda_n$, $K_2 = \sqrt{3/2}\ln\lambda_n$, and $K_3 = 1$. In this case, a natural neo-Hookean fiber response is given by

$$\Psi_r = \frac{\xi}{2}H\left(\ln\lambda_n\right)\left(\ln\lambda_n\right)^2 . \tag{5.2.60}$$

The corresponding Cauchy stress is

$$\boldsymbol{\sigma} = \xi J^{-1}H\left(\ln\lambda_n\right)\ln\lambda_n\mathbf{n}\otimes\mathbf{n} \tag{5.2.61}$$

and the elasticity tensor is

$$\boldsymbol{\mathcal{C}} = \xi J^{-1}H\left(\ln\lambda_n\right)\left(1-2\ln\lambda_n\right)\mathbf{N}\otimes\mathbf{N} \tag{5.2.62}$$

where ξ is the fiber modulus. This expression shows that the components of the elasticity tensor become negative when $1-2\ln\lambda_n < 0$, or equivalently when $\lambda_n > e^{\frac{1}{2}}$. However, the stress always remains positive.

If we want the tensile response to engage only beyond a threshold stretch ratio λ_0, we may rewrite the strain energy density as

$$\Psi_r = \frac{\xi}{2}H\left(\ln\lambda_n-\ln\lambda_0\right)\left(\ln\lambda_n-\ln\lambda_0\right)^2 = \frac{\xi}{2}H\left(\ln\frac{\lambda_n}{\lambda_0}\right)\left(\ln\frac{\lambda_n}{\lambda_0}\right)^2 . \tag{5.2.63}$$

Then

$$\boldsymbol{\sigma} = \xi J^{-1}H\left(\ln\frac{\lambda_n}{\lambda_0}\right)\ln\frac{\lambda_n}{\lambda_0}\mathbf{n}\otimes\mathbf{n}\,, \tag{5.2.64}$$

and

$$\boldsymbol{\mathcal{C}} = \xi J^{-1}H\left(\ln\frac{\lambda_n}{\lambda_0}\right)\left(1-2\ln\frac{\lambda_n}{\lambda_0}\right)\mathbf{N}\otimes\mathbf{N}\,. \tag{5.2.65}$$

5.3 Nearly-Incompressible Materials

5.3.1 Mooney-Rivlin Hyperelasticity

This material model is a hyperelastic Mooney-Rivlin type with uncoupled deviatoric and volumetric behavior. The uncoupled strain energy W is given by:

$$W = c_1\left(\tilde{I}_1 - 3\right) + c_2\left(\tilde{I}_2 - 3\right) + \frac{1}{2}K\left(\ln J\right)^2 . \tag{5.3.1}$$

Here, c_1 and c_2 are the Mooney-Rivlin material coefficients, $\tilde{I}_1$ and $\tilde{I}_2$ are the invariants of the deviatoric part of the right Cauchy-Green deformation tensor, $\tilde{\mathbf{C}} = \tilde{\mathbf{F}}^T \cdot \tilde{\mathbf{F}}$, where $\tilde{\mathbf{F}} = J^{-1/3}\mathbf{F}$, $\mathbf{F}$ is the deformation gradient and $J = \det \mathbf{F}$ is the Jacobian of the deformation. When $c_2 = 0$, this model reduces to an uncoupled version of the incompressible neo-Hookean constitutive model.

The Cauchy stress is given by

$$\boldsymbol{\sigma} = p\mathbf{I} + \frac{2}{J}\left[\left(c_1 + c_2\tilde{I}_1\right)\tilde{\mathbf{b}} - c_2\tilde{\mathbf{b}}^2 - \frac{1}{3}\left(c_1\tilde{I}_1 + 2c_2\tilde{I}_2\right)\mathbf{I}\right] . \tag{5.3.2}$$

The spatial elasticity tensor is given by

$$\boldsymbol{\mathcal{C}} = p\left(\mathbf{I}\otimes\mathbf{I} - 2\mathbf{I}\odot\mathbf{I}\right) - \frac{2}{3}\left(\operatorname{dev}\boldsymbol{\sigma}\otimes\mathbf{I} + \mathbf{I}\otimes\operatorname{dev}\boldsymbol{\sigma}\right) + \boldsymbol{\mathcal{C}}_w , \tag{5.3.3}$$

where,

$$\begin{aligned}\boldsymbol{\mathcal{C}}_w = {} & \frac{4}{3J}\left(c_1\tilde{I}_1 + 2c_2\tilde{I}_2\right)\left(\mathbf{I}\odot\mathbf{I} - \frac{1}{3}\mathbf{I}\otimes\mathbf{I}\right) + \frac{4c_2}{J}\left(\tilde{\mathbf{b}}\otimes\tilde{\mathbf{b}} - \tilde{\mathbf{b}}\odot\tilde{\mathbf{b}}\right) \\ & - \frac{4c_2}{3J}\left[\left(\tilde{I}_1\tilde{\mathbf{b}} - \tilde{\mathbf{b}}^2\right)\otimes\mathbf{I} + \mathbf{I}\otimes\left(\tilde{I}_1\tilde{\mathbf{b}} - \tilde{\mathbf{b}}^2\right)\right] + \frac{8c_2\tilde{I}_2}{9J}\mathbf{I}\otimes\mathbf{I} .\end{aligned} \tag{5.3.4}$$

This material model uses a three-field element formulation, interpolating displacements as linear field variables and pressure and volume ratio as piecewise constant in each element [96].

5.3.2 Ogden Hyperelastic

The Ogden material is defined using the following hyperelastic strain energy function:

$$W\left(\lambda_1, \lambda_2, \lambda_3, J\right) = \sum_{i=1}^{N}\frac{c_i}{m_i^2}\left(\tilde{\lambda}_1^{m_i} + \tilde{\lambda}_2^{m_i} + \tilde{\lambda}_3^{m_i} - 3\right) + U\left(J\right) . \tag{5.3.5}$$

Here, $\tilde{\lambda}_i$ are the deviatoric principal stretches and c_i and m_i are material parameters. The term $U\left(J\right)$ is the volumetric component and J is the determinant of the deformation gradient.

Note that the neo-Hookean and Mooney-Rivlin models can also be obtained from the general Ogden strain energy function using special choices for c_i and m_i.

5.3.3 Veronda-Westmann Hyperelasticity

This model is similar to the Mooney-Rivlin model in that it also uses an uncoupled strain energy. However, in this case the strain energy is given by an exponential form:

$$W = C_1\left[e^{\left(C_2\left(\tilde{I}_1 - 3\right)\right)} - 1\right] - \frac{C_1C_2}{2}\left(\tilde{I}_2 - 3\right) + U\left(J\right) . \tag{5.3.6}$$

The dilatational term U is identical to the Mooney-Rivlin model.

The Cauchy stress $\boldsymbol{\sigma}$ is found from

$$\boldsymbol{\sigma} = p\mathbf{I} + \operatorname{dev} \tilde{\boldsymbol{\sigma}} \,, \tag{5.3.7}$$

where

$$\tilde{\boldsymbol{\sigma}} = \frac{2}{J}\left[(W_1 + I_1 W_2)\,\tilde{\mathbf{b}} - W_2 \tilde{\mathbf{b}}^2\right] \,. \tag{5.3.8}$$

The strain energy derivatives are given by

$$W_1 = C_1 C_2 e^{C_2(I_1-3)} \,, \tag{5.3.9}$$

$$W_2 = -\frac{C_1 C_2}{2} \,. \tag{5.3.10}$$

This material model was the result from the research of the elastic response of skin tissue [105].

5.3.4 Arruda-Boyce Hyperelasticity

Arruda and Boyce proposed a model for the deformation of rubber materials [3]. Their main motivation was to develop a model that accurately captures the behavior of rubbers in different loading scenarios and that can be described with a limited number of physically motivated parameters. Their model is based on the Langevin chain statistics, which models a rubber chain segment between chemical crosslinks as a number N of rigid links of equal length l. The parameter N is related to the locking stretch λ_L, the stretch at which the chains reach their full extended state, $\lambda_L = \sqrt{N}$.

Their proposed strain-energy is a truncated Taylor series of the inverse Langevin function. A formulation that retains the first five terms of this function takes on the following form:

$$\tilde{W} = \mu \sum_{i=1}^{5} \frac{\alpha_i}{N^{i-1}} \left(\tilde{I}_1^i - 3^i\right) + U\left(J\right) \,, \tag{5.3.11}$$

where μ is a shear-modulus like parameter and the coefficients α_i are

$$\alpha_1 = \frac{1}{2} \,, \quad \alpha_2 = \frac{1}{20} \,, \quad \alpha_3 = \frac{11}{1050} \,, \quad \alpha_4 = \frac{19}{7000} \,, \quad \alpha_5 = \frac{519}{673750} \,. \tag{5.3.12}$$

The Cauchy stress is given by

$$\boldsymbol{\sigma} = p\mathbf{I} + \frac{2}{J} \operatorname{dev}\left(W_1 \tilde{\mathbf{b}}\right) = p\mathbf{I} + \frac{2W_1}{J}\left(\tilde{\mathbf{b}} - \frac{1}{3}\tilde{I}_1 \mathbf{I}\right) \,, \tag{5.3.13}$$

where,

$$W_1 = \frac{\partial \tilde{W}}{\partial \tilde{I}_1} = \mu \sum_{i=1}^{5} \alpha_i i \left(\frac{\tilde{I}_1}{N}\right)^{i-1} \,. \tag{5.3.14}$$

5.3.5 Transversely Isotropic Hyperelastic

This constitutive model can be used to represent a material that has a single preferred fiber direction and was developed for application to biological soft tissues [81, 83, 108]. It can be used to model tissues such as tendons, ligaments and muscle. The elastic response of the tissue is assumed to arise from the resistance of the fiber family and an isotropic matrix. It is assumed that the strain energy function can be written as follows:

$$W = F_1\left(\tilde{I}_1, \tilde{I}_2\right) + F_2\left(\tilde{\lambda}\right) + \frac{K}{2}\left[\ln\left(J\right)\right]^2 . \tag{5.3.15}$$

Here, $\tilde{I}_1$ and $\tilde{I}_2$ are the first and second invariants of the deviatoric version of the right Cauchy Green deformation tensor $\tilde{\mathbf{C}}$ and $\tilde{\lambda}$ is the deviatoric part of the stretch along the fiber direction ($\tilde{\lambda}^2 = \mathbf{A}\cdot\tilde{\mathbf{C}}\cdot\mathbf{A}$, where $\mathbf{A}$ is the initial fiber direction). The function F_1 represents the material response of the isotropic ground substance matrix, while F_2represents the contribution from the fiber family. The strain energy of the fiber family is as follows:

$$\tilde{\lambda}\frac{\partial F_2}{\partial \tilde{\lambda}} = \begin{cases} 0 & \tilde{\lambda} \leqslant 1 \\ C_3\left(e^{C_4(\tilde{\lambda}-1)} - 1\right) & 1 < \tilde{\lambda} < \lambda_m \\ C_5 + C_6\tilde{\lambda} & \tilde{\lambda} \geqslant \lambda_m \end{cases} . \tag{5.3.16}$$

Here, λ_m is the stretch at which the fibers are straightened, C_3 scales the exponential stresses, C_4 is the rate of uncrimping of the fibers, and C_5 is the modulus of the straightened fibers. C_6 is determined from the requirement that the stress is continuous at λ_m,

$$C_6 = \frac{1}{\lambda_m}\left[C_3\left(e^{C_4(\lambda_m-1)} - 1\right) - C_5\right] . \tag{5.3.17}$$

It also follows that

$$F_2\left(\tilde{\lambda}\right) = \begin{cases} 0 & \tilde{\lambda} \leqslant 1 \\ C_3\left(e^{-C_4}\left[\mathrm{Ei}\left(C_4\tilde{\lambda}\right) - \mathrm{Ei}\left(C_4\right)\right] - \ln\tilde{\lambda}\right) & 1 < \tilde{\lambda} < \lambda_m \\ \left(C_5 + \frac{C_6}{2}\tilde{\lambda}\right)\tilde{\lambda} + C_7 & \tilde{\lambda} \geqslant \lambda_m \end{cases} , \tag{5.3.18}$$

where

$$C_7 = C_3\left(e^{-C_4}\left[\mathrm{Ei}\left(C_4\lambda_m\right) - \mathrm{Ei}\left(C_4\right)\right] - \ln\lambda_m\right) - \left(C_5 + \frac{C_6}{2}\lambda_m\right)\lambda_m . \tag{5.3.19}$$

This material model uses a three-field element formulation, interpolating displacements as linear field variables and pressure and volume ratio as piecewise constant on each element [96].

5.3.6 Ellipsoidal Fiber Distribution

This constitutive model describes a material that is composed of an ellipsoidal continuous fiber distribution in an uncoupled formulation. The deviatoric part of the stress is given by [4, 7, 62],

$$\tilde{\boldsymbol{\sigma}} = \int_0^{2\pi}\int_0^{\pi} H\left(\tilde{I}_n - 1\right)\tilde{\boldsymbol{\sigma}}_n\left(\mathbf{n}\right)\sin\varphi\, d\varphi\, d\theta , \tag{5.3.20}$$

and the corresponding elasticity tensor is

$$\tilde{\boldsymbol{\mathcal{C}}} = \int_0^{2\pi}\int_0^{\pi} H\left(\tilde{I}_n - 1\right)\tilde{\boldsymbol{\mathcal{C}}}_n\left(\mathbf{n}\right)\sin\phi\, d\phi\, d\theta . \tag{5.3.21}$$

$\tilde{I}_n = \tilde{\lambda}_n^2 = \mathbf{N} \cdot \tilde{\mathbf{C}} \cdot \mathbf{N}$ is the square of the fiber stretch $\mathbf{F}$, $\mathbf{N}$ is the unit vector along the fiber direction (in the reference configuration), which in spherical angles is directed along (θ, φ), $\mathbf{n} = \tilde{\mathbf{F}} \cdot \mathbf{N}/\tilde{\lambda}_n$ and $H(\cdot)$ is the unit step function that enforces the tension-only contribution. The fiber stress is determined from a fiber strain energy function in the usual manner:

$$\tilde{\boldsymbol{\sigma}}_n(\mathbf{n}) = 2J^{-1}\tilde{I}_n \frac{\partial \tilde{\Psi}}{\partial \tilde{I}_n} \mathbf{n} \otimes \mathbf{n}\,, \tag{5.3.22}$$

whereas the fiber elasticity tensor is

$$\tilde{\boldsymbol{\mathcal{C}}}_n(\mathbf{n}) = 4J^{-1}\tilde{I}_n^2 \frac{\partial^2 \tilde{\Psi}}{\partial \tilde{I}_n^2} \mathbf{n} \otimes \mathbf{n} \otimes \mathbf{n} \otimes \mathbf{n}\,, \tag{5.3.23}$$

where in this material

$$\tilde{\Psi}\left(\mathbf{n}, \tilde{I}_n\right) = \xi(\mathbf{n}) \left(\tilde{I}_n - 1\right)^{\beta(\mathbf{n})}\,. \tag{5.3.24}$$

The materials parameters β and ξ are determined from:

$$\begin{aligned} \xi(\mathbf{n}) &= \left(\frac{\cos^2\theta \sin^2\varphi}{\xi_1^2} + \frac{\sin^2\theta \sin^2\varphi}{\xi_2^2} + \frac{\cos^2\varphi}{\xi_3^2}\right)^{-1/2}, \\ \beta(\mathbf{n}) &= \left(\frac{\cos^2\theta \sin^2\varphi}{\beta_1^2} + \frac{\sin^2\theta \sin^2\varphi}{\beta_2^2} + \frac{\cos^2\varphi}{\beta_3^2}\right)^{-1/2}. \end{aligned} \tag{5.3.25}$$

Since fibers can only sustain tension, this material is not stable on its own. It must be combined with a material that acts as the ground matrix. The total stress is then given by the sum of the fiber stress and the ground matrix stress:

$$\tilde{\boldsymbol{\sigma}} = \tilde{\boldsymbol{\sigma}}_m + \tilde{\boldsymbol{\sigma}}_f\,. \tag{5.3.26}$$

5.3.7 Fiber with Exponential Power Law Uncoupled

This material model describes a constitutive model for fibers, where a single fiber family follows an exponential power law strain energy function. The deviatoric part of the Cauchy stress is given by:

$$\tilde{\boldsymbol{\sigma}} = 2J^{-1} H\left(\tilde{I}_n - 1\right) \tilde{I}_n \frac{\partial \tilde{\Psi}}{\partial \tilde{I}_n} \mathbf{n} \otimes \mathbf{n}\,, \tag{5.3.27}$$

and the corresponding spatial elasticity tensor is

$$\tilde{\boldsymbol{\mathcal{C}}} = 4J^{-1} H\left(\tilde{I}_n - 1\right) \tilde{I}_n^2 \frac{\partial^2 \tilde{\Psi}}{\partial \tilde{I}_n^2} \mathbf{n} \otimes \mathbf{n} \otimes \mathbf{n} \otimes \mathbf{n}\,, \tag{5.3.28}$$

where $\tilde{I}_n = \tilde{\lambda}_n^2 = \mathbf{N} \cdot \tilde{\mathbf{C}} \cdot \mathbf{N}$ is the square of the fiber stretch, $\mathbf{N}$ is the fiber orientation in the reference configuration,

$$\mathbf{N} = \sin\varphi \cos\theta\, \mathbf{e}_1 + \sin\varphi \sin\theta\, \mathbf{e}_2 + \cos\varphi\, \mathbf{e}_3\,, \tag{5.3.29}$$

and $\mathbf{n} = \tilde{\mathbf{F}} \cdot \mathbf{N}/\tilde{\lambda}_n$ and $H(\cdot)$ is the unit step function that enforces the tension-only contribution. The fiber strain energy density is given by

$$\tilde{\Psi} = \frac{\xi}{\alpha\beta}\left(\exp\left[\alpha\left(\tilde{I}_n - 1\right)^{\beta}\right] - 1\right)\,, \tag{5.3.30}$$

where $\xi > 0$, $\alpha \geqslant 0$and $\beta \geqslant 2$.

Note: In the limit when $\alpha \to 0$, this expression produces a power law,

$$\lim_{\alpha \to 0} \tilde{\Psi} = \frac{\xi}{\beta} \left(\tilde{I}_n - 1 \right)^{\beta} . \tag{5.3.31}$$

Note: When $\beta > 2$, the fiber modulus is zero at the strain origin ($\tilde{I}_n = 1$). Therefore, use $\beta > 2$when a smooth transition in the stress is desired from compression to tension.

5.3.8 Fung Orthotropic

The hyperelastic strain energy function for a Fung Orthotropic material is given by [42, 43]

$$\tilde{\Psi} = \frac{1}{2} c \left(e^{\tilde{Q}} - 1 \right) + U(J) , \tag{5.3.32}$$

where

$$\tilde{Q} = c^{-1} \sum_{a=1}^{3} \left[2\mu_a \mathbf{M}_a : \tilde{\mathbf{E}}^2 + \sum_{b=1}^{3} \lambda_{ab} \left(\mathbf{M}_a : \tilde{\mathbf{E}} \right) \left(\mathbf{M}_b : \tilde{\mathbf{E}} \right) \right] . \tag{5.3.33}$$

Here, $\tilde{\mathbf{E}} = \frac{1}{2} \left(\tilde{\mathbf{C}} - \mathbf{I} \right)$ and $\mathbf{M}_a = \mathbf{A}_a \otimes \mathbf{A}_a$, where $\mathbf{A}_a$ are orthonormal vectors that define the initial direction of material axes. The orthotropic Lamé coefficients should be chosen such that the stiffness matrix,

$$\begin{bmatrix} \lambda_{11} + 2\mu_1 & \lambda_{12} & \lambda_{13} & 0 & 0 & 0 \\ \lambda_{12} & \lambda_{22} + 2\mu_2 & \lambda_{23} & 0 & 0 & 0 \\ \lambda_{13} & \lambda_{23} & \lambda_{33} + 2\mu_3 & 0 & 0 & 0 \\ 0 & 0 & 0 & \frac{1}{2}(\mu_1 + \mu_2) & 0 & 0 \\ 0 & 0 & 0 & 0 & \frac{1}{2}(\mu_2 + \mu_3) & 0 \\ 0 & 0 & 0 & 0 & 0 & \frac{1}{2}(\mu_1 + \mu_3) \end{bmatrix} \tag{5.3.34}$$

is positive definite.

5.3.9 Tension-Compression Nonlinear Orthotropic

This material model is based on the following uncoupled hyperelastic strain energy function [14]:

$$\Psi(\mathbf{C}, \lambda_1, \lambda_2, \lambda_3) = \tilde{\Psi}_{\text{iso}} \left(\tilde{\mathbf{C}} \right) + \sum_{i=1}^{3} \tilde{\Psi}_i^{TC} \left(\tilde{\lambda}_i \right) + U(J) . \tag{5.3.35}$$

The isotropic strain energy $\tilde{\Psi}_{\text{iso}}$ and the dilatational energy U are the same as for the Mooney-Rivlin material (Section 5.3.1). The tension-compression term is defined as follows:

$$\tilde{\Psi}_i^{TC} \left(\tilde{\lambda}_i \right) = \begin{cases} \xi_i \left(\tilde{\lambda}_i - 1 \right)^{\beta_i} & \tilde{\lambda}_i > 1 \\ 0 & \tilde{\lambda}_i \leqslant 1 \end{cases} , \xi_i \geqslant 0 \quad \text{(no sum over } i\text{)}. \tag{5.3.36}$$

The $\tilde{\lambda}_i$ parameters are the deviatoric fiber stretches of the local material fibers,

$$\tilde{\lambda}_i = \left(\mathbf{A}_i \cdot \tilde{\mathbf{C}} \cdot \mathbf{A}_i \right)^{1/2} . \tag{5.3.37}$$

The local material fibers are defined (in the reference frame) as an orthonormal set of vectors $\mathbf{A}_i$. The corresponding deviatoric part of the Cauchy stress is

$$\tilde{\boldsymbol{\sigma}} = J^{-1} \sum_{i=1}^{3} \frac{1}{\tilde{\lambda}_i} \frac{\partial \tilde{\Psi}}{\partial \tilde{\lambda}_i} \mathbf{a}_i \otimes \mathbf{a}_i \,, \tag{5.3.38}$$

and the spatial elasticity tensor is

$$\tilde{\boldsymbol{\mathcal{C}}} = J^{-1} \sum_{i=1}^{3} \frac{1}{\tilde{\lambda}_i} \frac{\partial}{\partial \tilde{\lambda}_i} \left(\frac{1}{\tilde{\lambda}_i} \frac{\partial \tilde{\Psi}}{\partial \tilde{\lambda}_i} \right) \mathbf{a}_i \otimes \mathbf{a}_i \otimes \mathbf{a}_i \otimes \mathbf{a}_i \,, \tag{5.3.39}$$

where $\mathbf{a}_i = \tilde{\mathbf{F}} \cdot \mathbf{A}_i$.

5.3.10 Holmes-Mow Uncoupled

The uncoupled hyperelastic strain-energy function for this material is given by [50],

$$\Psi\left(\mathbf{C}\right) = \tilde{\Psi}\left(\tilde{\mathbf{C}}\right) + U\left(J\right) \,, \tag{5.3.40}$$

where

$$\tilde{\Psi}\left(\tilde{\mathbf{C}}\right) = \frac{1}{2}\frac{\mu}{\beta}\left(e^{\tilde{Q}} - 1\right) \,, \tag{5.3.41}$$

and

$$\tilde{Q} = \beta\left(\tilde{I}_1 - 3\right) \,. \tag{5.3.42}$$

Here, μ is the shear modulus and β is the exponential nonlinearity coefficient. The corresponding spatial stress and elasticity tensors are

$$\tilde{\boldsymbol{\sigma}} = \frac{\mu}{J} e^{\tilde{Q}} \tilde{\mathbf{b}} \,, \tag{5.3.43}$$

and

$$\tilde{\boldsymbol{\mathcal{C}}} = 2\beta \frac{\mu}{J} e^{\tilde{Q}} \tilde{\mathbf{b}} \otimes \tilde{\mathbf{b}} \tag{5.3.44}$$

respectively. Note that $\tilde{\boldsymbol{\sigma}}$ does not reduce to zero when $\tilde{\mathbf{b}} = \mathbf{I}$, but $\operatorname{dev} \tilde{\boldsymbol{\sigma}}$ does. These expressions can be substituted into (2.4.31) and (2.4.37) to evaluate the final expressions for the Cauchy stress and spatial elasticity tensors, respectively.

5.4 Viscoelasticity

For a viscoelastic material the second Piola Kirchhoff stress can be written as follows [81]:

$$\mathbf{S}\left(t\right) = \int_{-\infty}^{t} G\left(t-s\right) \frac{d\mathbf{S}^e}{ds} \, ds \,, \tag{5.4.1}$$

where $\mathbf{S}^e$ is the elastic stress and $G(t)$ is the relaxation function. Here we consider the special case where the relaxation function is given by

$$G\left(t\right) = \gamma_0 + \sum_{i=1}^{N} \gamma_i \exp\left(-t/\tau_i\right) \,. \tag{5.4.2}$$

With this function chosen for the relaxation function, we can write the total stress as

$$\mathbf{S}(t) = \int_{-\infty}^{t} \left(\gamma_0 + \sum_{i=1}^{N} \gamma_i \exp\left((-t+s)/\tau_i \right) \frac{d\mathbf{S}^e}{ds} \right) ds\,. \tag{5.4.3}$$

Introducing the internal variables,

$$\mathbf{H}^{(i)}(t) = \int_{-\infty}^{t} \exp\left[-(t-s)/\tau_i \right] \frac{d\mathbf{S}^e}{ds}\, ds\,, \tag{5.4.4}$$

we can rewrite (5.4.3) as follows,

$$\mathbf{S}(t) = \gamma_0 \mathbf{S}^e(t) + \sum_{i=1}^{N} \gamma_i \mathbf{H}^{(i)}(t)\ . \tag{5.4.5}$$

In FEBio, $\gamma_0 = 1$, so $\mathbf{S}^e$ is the long-term elastic response of the material.

The question now remains how to evaluate the internal variables. From equation (5.4.4) it appears that we have to integrate over the entire time domain. However, we can find a recurrence relationship that will allow us to evaluate the internal variables at a time $t + \Delta t$ given the values at time t.

$$\begin{aligned}
\mathbf{H}^{(i)}(t+\Delta t) &= \int_{-\infty}^{t+\Delta t} \exp\left[-(t+\Delta t-s)/\tau_i \right] \frac{d\mathbf{S}^e}{ds}\, ds \\
&= \exp\left(-\Delta t/\tau_i\right) \int_{-\infty}^{t} \exp\left[-(t-s)/\tau_i \right] \frac{d\mathbf{S}^e}{ds}\, ds + \int_{t}^{t+\Delta t} \exp\left[-(t+\Delta t-s)/\tau_i \right] \frac{d\mathbf{S}^e}{ds}\, ds \\
&= \exp\left(-\Delta t/\tau_i\right) \mathbf{H}^{(i)}(t) + \int_{t}^{t+\Delta t} \exp\left[-(t+\Delta t-s)/\tau_i \right] \frac{d\mathbf{S}^e}{ds}\, ds\,.
\end{aligned} \tag{5.4.6}$$

The last term can now be simplified using the midpoint rule to approximate the derivate. In that case we find the recurrence relation:

$$\mathbf{H}^{(i)}(t+\Delta t) = \exp\left(-\Delta t/\tau_i\right) \mathbf{H}^{(i)}(t) + \frac{1-\exp\left(-\Delta t/\tau_i\right)}{\Delta t/\tau_i} \left(\mathbf{S}^e(t+\Delta t) - \mathbf{S}^e(t) \right)\ . \tag{5.4.7}$$

The following procedure can now be applied to calculate the new stress. Given $\mathbf{S}^e_n$ and $\mathbf{H}^{(i)}_n$ corresponding to time t, find $\mathbf{S}^e_{n+1}$ and $\mathbf{H}^{(i)}_{n+1}$ corresponding to time $t + \Delta t$:

1. calculate elastic stress:
$$\mathbf{S}^e_{n+1} = \frac{\partial W^e}{\partial \mathbf{C}_{n+1}}\,,$$
2. evaluate internal variables:
$$\mathbf{H}^i_{n+1} = \exp\left(-\Delta t/\tau_i\right) \mathbf{H}^i_n + \frac{1-\exp\left(-\Delta t/\tau_i\right)}{\Delta t/\tau_i} \left(\mathbf{S}^e_{n+1} - \mathbf{S}^e_n \right)\ ,$$
3. find the total stress:
$$\mathbf{S}_{n+1} = \gamma_0 \mathbf{S}^e_{n+1} + \sum_{i=1}^{N} \gamma_i \mathbf{H}^i_{n+1}\,.$$

5.5 Reactive Viscoelasticity

Reactive viscoelasticity models a material as a mixture of strong bonds, which are permanent, and weak bonds, which break and reform in response to loading [13]. This framework is based on constrained reactive mixtures of solids (Section 2.8). Strong bonds produce the equilibrium elastic response, whereas weak bonds produce the transient viscous response. Strong bonds are in a stress-free state when in their reference configuration $\mathbf{X}$. Their deformation gradient is defined as usual, $\mathbf{F}(\mathbf{X},t)=\partial\boldsymbol{\chi}(\mathbf{X},t)/\partial\mathbf{X}$. When weak bonds break in response to loading at some time u, they reform instantaneously in a stress-free configuration $\mathbf{X}^u$ that coincides with the current configuration at time u, thus, $\mathbf{X}^u=\boldsymbol{\chi}(\mathbf{X},u)$. Therefore, a reaction transforms intact loaded bonds into reformed unloaded bonds. Weak bonds that reform at time u may be called $u-$generation bonds. The deformation gradient of $u-$generation weak bonds relative to their reference configuration $\mathbf{X}^u$ is denoted by $\mathbf{F}^u(\mathbf{X},t)$, which may be evaluated from the chain rule,

$$\mathbf{F}(\mathbf{X},t)=\mathbf{F}^u(\mathbf{X},t)\cdot\mathbf{U}(\mathbf{X},u)\ , \tag{5.5.1}$$

where $\mathbf{U}$ is the right-stretch tensor of $\mathbf{F}$. The strain energy density Ψ_r in a reactive viscoelastic material is given by

$$\Psi_r(\mathbf{F})=\Psi_r^e(\mathbf{F})+\sum_u w^u\Psi_0^b(\mathbf{F}^u)\ , \tag{5.5.2}$$

where Ψ_r^e is the strain energy density of strong bonds and Ψ_0^b is the strain energy density of weak bonds, when they all belong to the same generation. In this expression, $w^u(\mathbf{X},t)$ is the mass fraction of $u-$generation weak bonds, which evolves over time as described below. The summation is taken over all generations u that were created prior to the current time t. Based on Eq.(2.8.15), the mixture Cauchy stress σ in a reactive viscoelastic material is similarly given by

$$\boldsymbol{\sigma}(\mathbf{F}^s)=\boldsymbol{\sigma}^e(\mathbf{F}^s)+\sum_u w^u J^{-1}(u)\,\boldsymbol{\sigma}_0^b(\mathbf{F}^u)\ , \tag{5.5.3}$$

where $\boldsymbol{\sigma}^e$ is the stress in the strong bonds and $\boldsymbol{\sigma}_0^b$ is the stress in the weak bonds. These stresses are related to the respective strain energy densities of strong and weak bonds according to

$$\boldsymbol{\sigma}^e(\mathbf{F}^s)=\frac{1}{J^s}\frac{\partial\Psi_r^e(\mathbf{F}^s)}{\partial\mathbf{F}^s}\cdot(\mathbf{F}^s)^T\ ,\quad \boldsymbol{\sigma}_0^b(\mathbf{F}^u)=\frac{1}{J^u}\frac{\partial\Psi_0^b(\mathbf{F}^u)}{\partial\mathbf{F}^u}\cdot(\mathbf{F}^u)^T\ . \tag{5.5.4}$$

The mass fractions $w^u(\mathbf{X},t)$ are obtained by solving the equation of mass balance for reactive constrained mixtures,

$$\dot{w}^u=\hat{w}^u(\mathbf{F},w^\gamma)\ , \tag{5.5.5}$$

where the mass fraction supply $\hat{w}^u$ must be specified as a constitutive function of the deformation gradient $\mathbf{F}$ and the mass fractions w^γ from all generations. Since mass must be conserved over all generations, it follows that

$$\sum_u\hat{w}^u=0,\quad \sum_u w^u=1\,. \tag{5.5.6}$$

Any number of valid solutions may exist for w^u, based on constitutive assumptions for $\hat{w}^u$. For example, for $u-$generation bonds reforming in an unloaded state during the time interval $u\leqslant t<v$, and subsequently breaking in response to loading at $t=v$, Type I bond kinetics provides a solution of the form

$$w^u(\mathbf{X},t)=\begin{cases}0 & t<u\\ f^u(\mathbf{X},t) & u\leqslant t<v\\ f^u(\mathbf{X},v)\,g(\mathbf{F}(v);\mathbf{X},t-v) & v\leqslant t\end{cases}\ , \tag{5.5.7}$$

where

$$f^u(\mathbf{X},t) = 1 - \sum_{\gamma<u} w^\gamma(\mathbf{X},t)\ , \tag{5.5.8}$$

and $g(\mathbf{F}(v);\mathbf{X},t-v)$ is a reduced relaxation function which may assume any number of valid forms. (A reduced relaxation function $g(t)$ satisfies $g(0)=1$ and $g(t\to\infty)=0$, and decreases monotonically with t.) In particular, g may depend on the state of strain at time v when the $u-$generation starts breaking and reforming. In the recursive expression of Eq.(5.5.7), the earliest generation $u=-\infty$, which is initially at rest, produces $w^u(t)=1$ for $t<v$ and $w^u(t)=g(\mathbf{F}(v);\mathbf{X},t-v)$ for $t\geqslant v$; this latter expression seeds the recursion for subsequent generations. Therefore, providing a functional form for g suffices to produce the solution for all bond generations u.

For Type II bond kinetics, the solution for the mass fractions is given by

$$w^u(t) = \begin{cases} 0 & t<u \\ 1-g(t-u) & u\leqslant t<v \\ g(t-v)-g(t-u) & v\leqslant t \end{cases}\ . \tag{5.5.9}$$

For this type of bond kinetics, the reduced relaxation function g cannot depend on the magnitude of the strain, because strain-dependence might violate the constraint $0\leqslant w^u\leqslant 1$. Thus, type II bond kinetics is only valid for quasilinear viscoelasticity, whereas type I bond kinetics also encompasses nonlinear viscoelasticity.

For all bond kinetics, it is also possible to constrain the occurrence of the breaking-and-reforming reaction to specific forms of the strain. For example, the reaction may be allowed to proceed only in the case of dilatational strain, or only in the case of distortional strain.

The finite element implementation of reactive viscoelasticity stores the value of time v, mass fraction of reformed bonds $f^u(\mathbf{X},v)$, and the right stretch tensor $\mathbf{U}(\mathbf{X},v)$ needed to evaluate w^u in Eq.(5.5.7) and $\mathbf{F}^v(\mathbf{X},t)$ in Eq.(5.5.1).

5.5.1 Reduced Relaxation Functions

Reduced relaxation functions are monotonically decreasing functions of time $g(t)$ that satisfy $g(0)=1$ and $\lim_{t\to\infty} g(t)=0$. Many different forms of reduced relaxation functions are available in FEBio, given in the *FEBio User's Manual*. The simplest and most commonly used relaxation function is the exponential function $g(t)=e^{-t/\tau}$, where τ is the relaxation constant. In viscoelasticity theory it is common to use a combination of relaxation functions with distinct relaxation constants τ_i, described as a Prony series of the form

$$g(t) = \frac{\sum_i \gamma_i e^{-t/\tau_i}}{\sum_i \gamma_i}\ . \tag{5.5.10}$$

The coefficients γ_i are normalized by $\sum_i \gamma_i$ to enforce $g(0)=1$. Alternatively, we could have written

$$g(t) = \sum_i \hat{\gamma}_i e^{-t/\tau_i}\ ,\quad \sum_i \hat{\gamma}_i = 1\ . \tag{5.5.11}$$

This type of relaxation function $g(t)$ is said to have a discrete spectrum of coefficients $\hat{\gamma}_i$ corresponding to each τ_i.

It is also possible to define a continuous relaxation spectrum $\hat{\gamma}(\tau)$ such that the reduced relaxation function is given by

$$g(t) = \int_0^\infty \hat{\gamma}(\tau)\, e^{-t/\tau}\, d\tau\,. \tag{5.5.12}$$

To satisfy $g(0) = 1$ the continous relaxation spectrum $\hat{\gamma}(\tau)$ must satisfy

$$\int_0^\infty \hat{\gamma}(\tau)\; d\tau = 1\,. \tag{5.5.13}$$

For example, Fung [44] proposed a relaxation spectrum of the form

$$\hat{\gamma}(\tau) = \begin{cases} \frac{1}{\ln\frac{\tau_2}{\tau_1}}\frac{1}{\tau} & \tau_1 \le \tau \le \tau_2 \\ 0 & \text{otherwise} \end{cases}. \tag{5.5.14}$$

When substituted into Eq.(5.5.12) it produces

$$g(t) = \frac{\Gamma\left(0, \frac{t}{\tau_2}\right) - \Gamma\left(0, \frac{t}{\tau_1}\right)}{\ln\frac{\tau_2}{\tau_1}} = \frac{-\operatorname{Ei}\left(-\frac{t}{\tau_2}\right) + \operatorname{Ei}\left(-\frac{t}{\tau_1}\right)}{\ln\frac{\tau_2}{\tau_1}}\,, \tag{5.5.15}$$

where $\Gamma(a, z)$ is the incomplete gamma function and $\operatorname{Ei}(z)$ is the exponential integral function, which satisfy $\Gamma(0, z) = -\operatorname{Ei}(-z)$. An alternative model proposed later by Fung [41] is

$$\hat{\gamma}(\tau) = \begin{cases} \frac{1}{\tau_2 - \tau_1} & \tau_1 \le \tau \le \tau_2 \\ 0 & \text{otherwise} \end{cases}, \tag{5.5.16}$$

which produces

$$g(t) = \frac{\tau_2 e^{-t/\tau_2} - \tau_1 e^{-t/\tau_1} + t\left[\operatorname{Ei}\left(-\frac{t}{\tau_2}\right) - \operatorname{Ei}\left(-\frac{t}{\tau_1}\right)\right]}{\tau_2 - \tau_1}\,. \tag{5.5.17}$$

A generalization of Fung's earlier continuous relaxation spectrum may be derived from the work of Malkin [71] who proposed to use a function proportional to $\tau^{-\beta}$. If we constrain this spectrum to the range $\tau_1 \le \tau \le \tau_2$ it takes the form

$$\hat{\gamma}(\tau) = \begin{cases} \frac{\beta - 1}{\tau_1^{1-\beta} - \tau_2^{1-\beta}}\frac{1}{\tau^\beta} & \tau_1 \le \tau \le \tau_2 \\ 0 & \text{otherwise} \end{cases}. \tag{5.5.18}$$

When substituted into (5.5.12) this continuous relaxation spectrum produces the reduced relaxation function

$$g(t) = \frac{(\beta - 1)\, t^{1-\beta}}{\tau_1^{1-\beta} - \tau_2^{1-\beta}}\left[\Gamma\left(\beta - 1, \frac{t}{\tau_2}\right) - \Gamma\left(\beta - 1, \frac{t}{\tau_1}\right)\right]\,. \tag{5.5.19}$$

In the limit as $\beta \to 1$, the expression of Eq.(5.5.19) reduces to Eq.(5.5.15).

Another example for a continuous relaxation spectrum is the exponential spectrum

$$\hat{\gamma}(\tau) = \frac{1}{\tau_0} e^{-\tau/\tau_0}\,, \quad 0 \le \tau < \infty\,, \tag{5.5.20}$$

which produces

$$g(t) = 2\sqrt{\frac{t}{\tau_0}} K_1\left(2\sqrt{\frac{t}{\tau_0}}\right)\,, \tag{5.5.21}$$

where $K_1(z)$ is the modified Bessel function of the second kind, of order 1.

5.6 Reactive Damage Mechanics

5.6.1 Bond-Breaking Reaction

The reactive damage mechanics framework was first described in [77]. It is based on constrained reactive mixtures of solids (Section 2.8) and used to model damage in an elastic solid as a reaction that transforms intact (elastic) bonds into broken bonds,

$$\mathcal{E}^i \to \mathcal{E}^b \,. \tag{5.6.1}$$

Here, $\mathcal{E}^\alpha$ is the material associated with bonds α ($\alpha = i$ for intact bonds and $\alpha = b$ for broken bonds). The material is modeled as a constrained mixture of these two constituents α. Whereas intact bonds may store free energy, broken bond sustain none. This framework assumes that isothermal conditions prevail. Thus, any heat generated by the dissipative damage reaction must be radiated from the continuum to preserve a constant temperature. In an isothermal framework, the free energy density is also equal to the strain energy density.

The referential mass density of the solid mixture is ρ_r (mass of solid per volume in its referential, stress-free configuration), which remains constant throughout an analysis. The material associated with intact bonds has an apparent mass density ρ_r^i while that associated with broken bonds is ρ_r^b,such that the mixture mass balance is satisfied by

$$\rho_r = \rho_r^i + \rho_r^b \,. \tag{5.6.2}$$

5.6.2 Strain Energy Density and Stress

Let the specific free energy stored in intact bonds be represented by $\psi\left(\mathbf{F}\right)$; that of broken bonds is zero. Therefore, the free energy density of the mixture is

$$\Psi_r\left(\mathbf{F}\right) = \rho_r^i \psi\left(\mathbf{F}\right) \,. \tag{5.6.3}$$

We may define the mass fraction w^α of bond species α as

$$w^\alpha = \frac{\rho_r^\alpha}{\rho_r} \,. \tag{5.6.4}$$

Now, the mixture mass balance in Eq.(5.6.2) may be rewritten as $\sum_\alpha w^\alpha = 1$, or more specifically,

$$w^i + w^b = 1 \,. \tag{5.6.5}$$

We may also rewrite the mixture free energy density in Eq.(5.6.3) as

$$\Psi_r\left(\mathbf{F}\right) = w^i \rho_r \psi\left(\mathbf{F}\right) = \left(1 - w^b\right) \rho_r \psi\left(\mathbf{F}\right) \,, \tag{5.6.6}$$

where we have made use of Eq.(5.6.5). The corresponding Cauchy stress may be evaluated using the standard hyperelasticity formula,

$$\boldsymbol{\sigma} = J^{-1} \frac{\partial \Psi_r}{\partial \mathbf{F}} \cdot \mathbf{F}^T = \left(1 - w^b\right) \frac{\rho_r}{J} \frac{\partial \psi}{\partial \mathbf{F}} \cdot \mathbf{F}^T . \tag{5.6.7}$$

These relation show that the free energy density and stress of a damaged material are scaled by the mass fraction $w^i = 1 - w^b$ of remaining intact bonds. Comparing these formulas to those of classical damage mechanics [31, 58, 66, 67, 84, 97], it becomes immediately apparent that the

classical damage variable D appearing in those theories is equivalent to the mass fraction w^b of broken bonds,

$$D \equiv w^b. \tag{5.6.8}$$

To further clarify this equivalence, we may let $\Psi_0 \equiv \rho_r \psi$ represent the free energy density of an intact elastic solid, such that Eq.(5.6.6) may be rewritten as $\Psi_r = (1-D)\,\Psi_0$. Similarly, Eq.(5.6.7) may be rewritten as $\boldsymbol{\sigma} = (1-D)\,\boldsymbol{\sigma}_0$, where $\boldsymbol{\sigma}_0$ is the stress in the intact elastic solid, derived from the hyperelasticity relation $\boldsymbol{\sigma}_0 = J^{-1}\left(\partial\Psi_0/\partial\mathbf{F}\right)\cdot\mathbf{F}^T$.

For nearly-incompressible hyperelastic materials (Section 2.4.3), the strain energy density of the intact material has the form of Eq.(2.4.23), thus $\Psi_0(\mathbf{C}) = \tilde{\Psi}_0\left(\tilde{\mathbf{C}}\right) + U(J)$. In this case, we assume that the damage only affects the distortional part of the strain energy density $\tilde{\Psi}_0\left(\tilde{\mathbf{C}}\right)$, consistent with the general framework advocated in [51]. Thus, for *uncoupled damage*, we assume that $\Psi_r(\mathbf{C}) = (1-D)\,\tilde{\Psi}_0\left(\tilde{\mathbf{C}}\right) + U(J)$. The resulting damage stress similarly takes the form $\boldsymbol{\sigma} = (1-D)\,\mathrm{dev}\,\tilde{\boldsymbol{\sigma}}_0 + p\mathbf{I}$, consistent with Eq.(2.4.31), where $\tilde{\boldsymbol{\sigma}}_0$ is evaluated from $\tilde{\Psi}_0\left(\tilde{\mathbf{C}}\right)$ as given in Eq.(2.4.32) and p is evaluated from $U(J)$ as given in Eq.(2.4.25).

When investigating the damage mechanics of tension-bearing fibrous materials, described in Section 2.4.5, it is important to use the unconstrained version of the fiber and damage mechanics models, even when the fibers are embedded in a ground matrix with a nearly-incompressible response (uncoupled formulation). This is a necessary requirement since uncoupled fiber formulations are now understood to be non-physical. Nevertheless, for historical reasons, FEBio allows users to use uncoupled fiber formulations in an uncoupled damage material.

5.6.3 Damage Criterion

At each material point $\mathbf{X}$ in the continuum, damage occurs when a scalar damage (or failure) measure $\Xi(\mathbf{F})$ achieves a critical value Ξ_m over the loading history,

$$\Xi_m(\mathbf{X}) = \max_{-\infty<s\le t} \Xi\left(\mathbf{F}(\mathbf{X},s)\right)\,. \tag{5.6.9}$$

The scalar damage measure $\Xi(\mathbf{F})$ must be invariant to orthogonal transformations $\mathbf{Q}$ that preserve material symmetry, or else the damage formulation would not be observer-independent. For example, for isotropic materials, $\Xi(\mathbf{F})$ must be an isotropic function of the deformation, in which case it should be expressed as $\Xi(\mathbf{U})$ or $\Xi(\mathbf{E})$, where $\mathbf{U}$ is the right stretch tensor in the polar decomposition $\mathbf{F} = \mathbf{R}\cdot\mathbf{U}$ of the deformation gradient, and

$$\mathbf{E} = \frac{1}{2}\left(\mathbf{F}^T\cdot\mathbf{F} - \mathbf{I}\right) = \frac{1}{2}\left(\mathbf{U}^2 - \mathbf{I}\right) \tag{5.6.10}$$

is the Green-Lagrange strain tensor. It follows that

$$\left(\frac{\partial\mathbf{E}}{\partial\mathbf{U}}\right)_{ijmn} = \frac{1}{2}\left(\frac{1}{2}\left(\delta_{im}U_{nj} + \delta_{in}U_{mj}\right) + \frac{1}{2}\left(U_{im}\delta_{jn} + U_{in}\delta_{jm}\right)\right)\,.$$

For anisotropic materials where $\mathbf{a}$ is the unit normal to a symmetry plane and $\mathbf{A} = \mathbf{a}\otimes\mathbf{a}$, the damage measure Ξ must satisfy

$$\Xi(\mathbf{U},\mathbf{A}) = \Xi\left(\mathbf{Q}\cdot\mathbf{U}\cdot\mathbf{Q}^T, \mathbf{Q}\cdot\mathbf{A}\cdot\mathbf{Q}^T\right)\,, \tag{5.6.11}$$

for transformations $\mathbf{Q}$ that satisfy $\mathbf{Q}\cdot\mathbf{A}\cdot\mathbf{Q}^T=\mathbf{A}$ (or $\mathbf{Q}\cdot\mathbf{a}=\mathbf{a}$). We may replace $\mathbf{U}$ with $\mathbf{E}$ in the above expression.

We assume that the amount of damage (the fraction D of broken bonds) is given by the function of state

$$D=F\left(\Xi_m\right)\,, \tag{5.6.12}$$

where $0\leq F\left(\Xi_m\right)\leq 1$. As shown in [77], the Clausius-Duhem inequality imposes the constraint that $F\left(\Xi_m\right)$ must be a monotonically increasing function of its argument. Therefore, we may understand F to represent a cumulative density function (CDF), whose derivative $f\left(\Xi_m\right)=F'\left(\Xi_m\right)$ is a probability distribution function (PDF) that describes the probability of bonds breaking at the specific threshold Ξ_m.

5.6.4 Reaction Kinetics and Thermodynamics

The axiom of mass balance in a reactive constrained mixture reduces to

$$\dot{\rho}_r^\alpha=\hat{\rho}_r^\alpha\,, \tag{5.6.13}$$

where $\dot{\rho}_r^\alpha$ is the material time derivative of ρ_r^α and $\hat{\rho}_r^\alpha$ is a function of state representing the referential mass supply density to constituent α due to reactions with all other constituents. In the damage framework, the above relations show that

$$\begin{aligned}\rho_r^i&=\rho_r\left(1-F\left(\Xi_m\right)\right)\\ \rho_r^b&=\rho_r F\left(\Xi_m\right)\end{aligned}\,. \tag{5.6.14}$$

Substituting these expressions into Eq.(5.6.13) shows that the referential mass density supplies are given by

$$\begin{aligned}\hat{\rho}_r^i&=-\rho_r\dot{F}\left(\Xi_m\right)\\ \hat{\rho}_r^b&=\rho_r\dot{F}\left(\Xi_m\right)\end{aligned}\,, \tag{5.6.15}$$

where

$$\dot{F}\left(\Xi_m\right)=\begin{cases}f\left(\Xi\right)\dot{\Xi}\Big|_{\Xi_m} & \text{advancing damage}\\ 0 & \text{otherwise}\end{cases}\,. \tag{5.6.16}$$

In these expressions, the damage is advancing when Ξ_m increases over two consecutive time points. In this expression for $\dot{F}$ we need to evaluate

$$\dot{\Xi}\left(\mathbf{U}\right)=\frac{\partial\Xi}{\partial\mathbf{U}}:\dot{\mathbf{U}}=\mathbf{N}:\dot{\mathbf{U}}\,, \tag{5.6.17}$$

where we defined

$$\mathbf{N}\equiv\frac{\partial\Xi}{\partial\mathbf{U}} \tag{5.6.18}$$

to represent the tensorial normal to the damage hypersurface, which needs to be evaluated at Ξ_m.

In this isothermal damage framework it can be shown from the energy balance that a heat supply density $\rho_r r$ must radiate the bond-breaking energy out of the continuum to maintain isothermal conditions, where

$$\rho_r r=\hat{\rho}_r^i\psi\left(\mathbf{F}\right)=-\rho_r\dot{F}\left(\Xi_m\right)\psi\left(\mathbf{F}\right)\,. \tag{5.6.19}$$

Since F is a monotonically increasing function of Ξ_m, its material time derivative $\dot{F}$ is always positive when the damage is increasing, and zero otherwise as per Eq.(5.6.17). Since the specific strain energy $\psi\left(\mathbf{F}\right)$ is always positive, it follows that the specific heat supply $r=-\dot{F}\left(\Xi_m\right)\psi\left(\mathbf{F}\right)$ in Eq.(5.6.19) is negative or zero, consistent with the expectation that heat needs to leave the continuum to maintain isothermal conditions.

5.6.5 Constitutive Models for Damage and Yield Criteria

Constitutive models for the damage or yield measure $\Xi(\mathbf{U})$ may be derived from energy- or stress-based potentials or (less commonly) strain measures. A summary of constitutive models for damage or yield criteria currently implemented in FEBio is presented below.

5.6.5.1 Strain Energy Density

It may be assumed that damage occurs when the strain energy density Ψ_r achieves a certain threshold Ψ_m. In that case, the constitutive model for the damage measure is

$$\Xi(\mathbf{U}) = \Psi_r(\mathbf{U}) \ . \tag{5.6.20}$$

This damage measure is valid for isotropic or anisotropic materials, since the strain energy density Ψ_r must satisfy the frame-invariance of Eq.165 by construction. The resulting damage surface normal is

$$\mathbf{N} = \frac{\partial \Psi_r}{\partial \mathbf{U}} = \frac{1}{2}(\mathbf{S}\cdot\mathbf{U} + \mathbf{U}\cdot\mathbf{S}) \ , \tag{5.6.21}$$

where $\mathbf{S} = \partial\Psi_r/\partial\mathbf{E} = J\mathbf{F}^{-1}\cdot\boldsymbol{\sigma}\cdot\mathbf{F}^{-T}$ is the second Piola-Kirchhoff stress associated with the material.

5.6.5.2 Simo Damage Criterion

Simo [92, 97] proposed a damage criterion related to the strain energy density,

$$\Xi(\mathbf{U}) = \sqrt{2\Psi_r(\mathbf{U})} \, . \tag{5.6.22}$$

This damage measure is valid for isotropic or anisotropic materials, since the strain energy density Ψ_r must satisfy the frame-invariance of Eq.165 by construction. Its resulting damage surface normal is

$$\mathbf{N} = \frac{1}{\sqrt{2\Psi_r}}\frac{1}{2}(\mathbf{S}\cdot\mathbf{U} + \mathbf{U}\cdot\mathbf{S}) \ , \tag{5.6.23}$$

where we have used the result of Eq.(5.6.21). The normal reduces to the null tensor in the limit when Ψ_r and $\boldsymbol{\sigma}$ tend to zero.

5.6.5.3 Specific Strain Energy

It may be assumed that damage occurs when the specific strain energy Ψ_r/ρ_r achieves a certain threshold ψ_m. In that case, the constitutive model for the damage measure is

$$\Xi(\mathbf{U}) = \frac{1}{\rho_r}\Psi_r(\mathbf{U}) \ . \tag{5.6.24}$$

This damage measure is valid for isotropic or anisotropic materials, since the strain energy density Ψ_r must satisfy the frame-invariance of Eq.165 by construction. The resulting damage surface normal is

$$\mathbf{N} = \frac{1}{\rho_r}\frac{\partial \Psi_r}{\partial \mathbf{U}} = \frac{1}{2\rho_r}(\mathbf{S}\cdot\mathbf{U} + \mathbf{U}\cdot\mathbf{S}) \ , \tag{5.6.25}$$

where we have used the result of Eq.(5.6.21).

5.6.5.4 Von Mises Stress

For this criterion it is assumed that damage or yield is initiated by increases in the von Mises (or effective) stress, σ_Y. Thus,

$$\Xi\left(\mathbf{U}\right) = \sigma_Y\left(\mathbf{U}\right) = \sqrt{\frac{3}{2}\,\mathrm{dev}\,\boldsymbol{\sigma} : \mathrm{dev}\,\boldsymbol{\sigma}}\,, \tag{5.6.26}$$

where $\mathrm{dev}\,\boldsymbol{\sigma}$ is the deviatoric part of $\boldsymbol{\sigma}$. To evaluate the damage surface normal in this case, we must use the chain rule,

$$\mathbf{N} = \frac{\partial \Xi}{\partial \boldsymbol{\sigma}} : \frac{\partial \boldsymbol{\sigma}}{\partial \mathbf{F}} : \frac{\partial \mathbf{F}}{\partial \mathbf{U}}\,. \tag{5.6.27}$$

From the hyperelasticity relation in Eq.(5.6.7) it can be shown that

$$\frac{\partial \boldsymbol{\sigma}}{\partial \mathbf{F}} = \left(\boldsymbol{\mathcal{C}} + \mathbf{I} \oslash \boldsymbol{\sigma} + \boldsymbol{\sigma} \oslash \mathbf{I} - \boldsymbol{\sigma} \otimes \mathbf{I}\right) \cdot \mathbf{F}^{-T}\,, \tag{5.6.28}$$

where $\boldsymbol{\mathcal{C}}$ is the fourth-order spatial elasticity tensor associated with the strain energy density Ψ_r. Then, it can be shown that

$$\mathbf{N} = \frac{1}{2}\mathbf{R}^T \cdot \mathbf{M} \cdot \mathbf{R} \cdot \mathbf{U}^{-1} + \frac{1}{2}\mathbf{U}^{-1} \cdot \mathbf{R}^T \cdot \mathbf{M}^T \cdot \mathbf{R}\,, \tag{5.6.29}$$

where

$$\mathbf{M} = \frac{\partial \Xi}{\partial \boldsymbol{\sigma}} : \boldsymbol{\mathcal{C}} + 2\frac{\partial \Xi}{\partial \boldsymbol{\sigma}} \cdot \boldsymbol{\sigma} - \left(\frac{\partial \Xi}{\partial \boldsymbol{\sigma}} : \boldsymbol{\sigma}\right)\mathbf{I}\,. \tag{5.6.30}$$

From the von Mises criterion in Eq.(5.6.26), it can be shown that

$$\frac{\partial \Xi}{\partial \boldsymbol{\sigma}} = \frac{3}{2\sigma_Y}\,\mathrm{dev}\,\boldsymbol{\sigma}\,. \tag{5.6.31}$$

Substituting Eqs.(5.6.30)-(5.6.31) into Eq.(5.6.29) provides the surface normal $\mathbf{N}$.

5.6.5.5 Maximum Normal Stress

For this criterion, the damage measure takes the form

$$\Xi\left(\mathbf{U}\right) = \sigma_1\,, \tag{5.6.32}$$

where σ_1 is the maximum principal stress (under the assumption that the three principal stresses of $\boldsymbol{\sigma}$ are ordered such that $\sigma_1 \geq \sigma_2 \geq \sigma_3$). To evaluate the damage surface normal, we may use Eqs.(5.6.29)-(5.6.30) where

$$\frac{\partial \Xi}{\partial \boldsymbol{\sigma}} = \frac{\partial \sigma_1}{\partial \boldsymbol{\sigma}} = \mathbf{n}_1 \otimes \mathbf{n}_1\,. \tag{5.6.33}$$

Here, $\mathbf{n}_1$ is a unit vector along the principal direction of maximum normal stress (the eigenvector of $\boldsymbol{\sigma}$ corresponding to the eigenvalue σ_1).

5.6.5.6 Maximum Shear Stress

For this criterion, the damage measure takes the form

$$\Xi(\mathbf{U}) = \frac{\sigma_1 - \sigma_3}{2}, \tag{5.6.34}$$

where σ_1 and σ_3 are the maximum and minimum principal normal stresses (under the assumption that the three principal stresses of $\boldsymbol{\sigma}$ are ordered such that $\sigma_1 \geq \sigma_2 \geq \sigma_3$). To evaluate the damage surface normal, we may use Eqs.(5.6.29)-(5.6.30) where

$$\frac{\partial \Xi}{\partial \boldsymbol{\sigma}} = \frac{1}{2}\left(\mathbf{n}_1 \otimes \mathbf{n}_1 - \mathbf{n}_3 \otimes \mathbf{n}_3\right). \tag{5.6.35}$$

Here, $\mathbf{n}_1$ and $\mathbf{n}_3$ are unit vectors along the principal directions of maximum and minimum normal stress, respectively.

5.6.5.7 Drucker Shear Stress

This criterion is based on the yield criterion for plasticity introduced in [37]. Its damage (or yield) measure takes the form

$$\Xi(\mathbf{U}) = k = \left(J_2^3 - cJ_3^2\right)^{1/6}, \tag{5.6.36}$$

where $J_2 = \frac{1}{2}\operatorname{dev}\boldsymbol{\sigma} : \operatorname{dev}\boldsymbol{\sigma}$, $J_3 = \det(\operatorname{dev}\boldsymbol{\sigma})$, k is the yield limit in simple shear and c is a user-specified non-dimensional material constant which must lie in the range $-\frac{27}{8} \leq c \leq \frac{9}{4}$. To better understand the meaning of k, consider uniaxial loading of a bar which yields at the normal stress value of σ_y. In this case,

$$k = \frac{\sigma_y}{\sqrt{3}}\left(1 - \frac{4}{27}c\right)^{1/6} \quad \frac{\sigma_y}{\sqrt{3}}\left(\frac{2}{3}\right)^{1/6} \leq k \leq \frac{\sigma_y}{\sqrt{3}}\left(\frac{3}{2}\right)^{1/6}. \tag{5.6.37}$$

In the special case when $c = 0$ the Drucker criterion reduces to the von Mises criterion, with $k = \sigma_y/\sqrt{3}$. To evaluate the damage or yield surface normal, we may use Eqs.(5.6.29)-(5.6.30) where

$$\frac{\partial \Xi}{\partial \boldsymbol{\sigma}} = \frac{1}{k^5}\left(\frac{J_2^2}{2}\operatorname{dev}\boldsymbol{\sigma} - \frac{cJ_3^2}{3}\operatorname{dev}(\operatorname{dev}\boldsymbol{\sigma})^{-1}\right). \tag{5.6.38}$$

5.6.5.8 Maximum Normal Lagrange Strain

The Lagrange strain tensor $\mathbf{E}$ is related to $\mathbf{F}$ via Eq.(5.6.10). Its maximum principal value is denoted by E_1. For this criterion, we let

$$\Xi(\mathbf{U}) = E_1. \tag{5.6.39}$$

Then, the damage surface normal is given by

$$\mathbf{N} = \frac{\partial E_1}{\partial \mathbf{U}} = \sqrt{1 + 2E_1}\,\mathbf{n}_1 \otimes \mathbf{n}_1, \tag{5.6.40}$$

where $\mathbf{n}_1$ is a unit vector along the principal direction of normal strain.

5.6.5.9 Octahedral Lagrange Strain

The octahedral Lagrange strain is given by

$$e\left(\mathbf{U}\right)=\sqrt{\frac{2}{3}\operatorname{dev}\mathbf{E}:\operatorname{dev}\mathbf{E}}\,, \tag{5.6.41}$$

where $\operatorname{dev}\mathbf{E}$ is the deviatoric part of the Lagrange strain tensor,

$$\operatorname{dev}\mathbf{E}=\mathbf{E}-\frac{1}{3}\operatorname{tr}\left(\mathbf{E}\right)\mathbf{I}\,, \tag{5.6.42}$$

and $\mathbf{E}$ is given in Eq.(5.6.10). For this damage measure we let

$$\Xi\left(\mathbf{U}\right)=e\left(\mathbf{U}\right)\,. \tag{5.6.43}$$

The damage surface normal can be evaluated from

$$\mathbf{N}=\frac{\partial e}{\partial\mathbf{E}}:\frac{\partial\mathbf{E}}{\partial\mathbf{U}}=\frac{1}{3e}\left(\operatorname{dev}\mathbf{E}\cdot\mathbf{U}+\mathbf{U}\cdot\operatorname{dev}\mathbf{E}\right)\,, \tag{5.6.44}$$

where we used

$$\frac{\partial e}{\partial\mathbf{E}}=\frac{2}{3e}\operatorname{dev}\mathbf{E} \tag{5.6.45}$$

and

$$\frac{\partial\mathbf{E}}{\partial\mathbf{U}}=\frac{1}{2}\frac{\partial\mathbf{U}^{2}}{\partial\mathbf{U}}=\frac{1}{2}\left(\mathbf{I}\odot\mathbf{U}+\mathbf{U}\odot\mathbf{I}\right)\,. \tag{5.6.46}$$

5.7 Reactive Plasticity

Reactive plasticity models a material as a mixture of bonds that break in response to loading and reform in a stressed state [115]. This framework is based on constrained reactive mixtures of solids (Section 2.8).

5.7.1 Elastic-Perfectly Plastic Response

This section describes a reactive framework in which all loaded bonds in an elemental region break and reform simultaneously into a stressed state with a new reference configuration, resulting in elastic-perfectly plastic behavior. The theory outlined here is similar to reactive viscoelasticity (Section 5.5) [13, 76], although bonds now reform in a stressed rather than a stress-free state.

The elastic response of this material is achieved when bonds have not yet failed in response to loading. In this case it is assumed that the bonds belong to generation s (the master constituent) whose reference configuration is represented by material points located at $\mathbf{X}^s$. When bonds break and reform at time t^σ, a new $\sigma-$generation is formed. Consider that bonds of the $\sigma-$generation yield based on a scalar *yield measure* $\Phi\left(\mathbf{U}^\sigma\right)$ (e.g., the von Mises stress), where $\mathbf{U}^\sigma$ is the right stretch tensor from the polar decomposition $\mathbf{F}^\sigma = \mathbf{R}\cdot\mathbf{U}^\sigma$, and $\mathbf{R}$ is the rotation tensor, assumed to also be the rotation tensor of $\mathbf{F}^s$. Thus, according to Eq.(2.8.2), $\mathbf{U}^s = \mathbf{U}^\sigma\cdot\mathbf{F}^{\sigma s}$.

Let the *yield threshold* for the $\sigma-$generation be given by Φ_m, which represents the threshold value at which yielding begins. For $\sigma-$generation bonds the *yield criterion* may thus be defined as

$$\varphi\left(\mathbf{U}^\sigma\right) = \Phi\left(\mathbf{U}^\sigma\right) - \Phi_m \leq 0\,, \tag{5.7.1}$$

where $\varphi\left(\mathbf{U}^\sigma\right)$ represents the *yield surface* of $\sigma-$generation bonds whose *tensorial normal* is

$$\mathbf{N}^\sigma = \frac{\partial\varphi}{\partial\mathbf{U}^\sigma} = \frac{\partial\Phi\left(\mathbf{U}^\sigma\right)}{\partial\mathbf{U}^\sigma}\,. \tag{5.7.2}$$

When yield thresholds are formulated in stress space, the dependence on the deformation takes the form $\Phi = \Phi\left(\boldsymbol{\sigma}^\sigma\left(\mathbf{U}^\sigma\right)\right)$.

Consider two consecutive generations σ, denoted by u and v, such that the bond-breaking-and-reforming reaction is $\mathcal{E}^u \to \mathcal{E}^v$. Upon breaking of the $u-$generation to form the $v-$generation the plastic consistency condition is given by $d\varphi = 0$, which reduces to

$$\mathbf{N}^u\left(u\right) : \left(\mathbf{U}^v\left(v\right) - \mathbf{U}^u\left(u\right)\right) = 0\,. \tag{5.7.3}$$

The constitutive model for $\mathbf{F}^{\sigma s}$ is given by

$$\left(\mathbf{F}^{vs}\right)^{-1} = \left(\mathbf{F}^{us}\right)^{-1}\cdot\left(\mathbf{I} - \lambda\hat{\mathbf{N}}^v\right) \tag{5.7.4}$$

where

$$\hat{\mathbf{N}}^v = \frac{\mathbf{N}^v}{\sqrt{\mathbf{N}^v : \mathbf{N}^v}} \tag{5.7.5}$$

is the unit tensor along $\mathbf{N}^v$ and λ is a non-dimensional scalar which may be determined analytically by enforcing the plastic consistency condition in Eq.(5.7.3). When the plastic deformation is assumed to be isochoric the solution for λ is obtained while enforcing $\det\mathbf{F}^{\sigma s} = 1$. For the earliest yielded generation u, the preceding $s-$generation is in the elastic regime; therefore, $\mathbf{F}^{us} = \mathbf{I}$ at the start of the recursive relation in Eq.(5.7.4).

The stress response of this solid mixture is given generically by Eq.(2.8.13), specialized to the case where each generation σ is assumed to have the same constitutive model Ψ_0 for its strain energy density, $\Psi_r^\sigma = J^{\sigma s}\Psi_0$. For example, in the case of the three consecutive σ generations s, u and v, the strain energy density is $\Psi_r\left(\mathbf{F}^s\right) = \sum_\sigma w^\sigma J^{\sigma s}\Psi_0\left(\mathbf{U}^\sigma\right)$ and the stress is

$$\boldsymbol{\sigma} = w^s\boldsymbol{\sigma}_0\left(\mathbf{U}^s\right) + w^u\boldsymbol{\sigma}_0\left(\mathbf{U}^u\right) + w^v\boldsymbol{\sigma}_0\left(\mathbf{U}^v\right) , \tag{5.7.6}$$

where $\mathbf{U}^u$ and $\mathbf{U}^v$ are evaluated from $\mathbf{U}^s \cdot \left(\mathbf{F}^{\sigma s}\right)^{-1} = \mathbf{U}^\sigma$ ($\sigma = u, v$) and Eq.(5.7.4), and $\boldsymbol{\sigma}_0$ is given in Eq.(2.8.16). For an elastic-perfectly plastic response the bond mass fractions are constitutively assumed to satisfy

$$w^s = 1 - H\left(t - t^u\right) \quad , \quad w^u = H\left(t - t^u\right) - H\left(t - t^v\right) , \quad w^v = H\left(t - t^v\right) , \tag{5.7.7}$$

where $H\left(\cdot\right)$ is the Heaviside unit step function. The corresponding constitutive models for $\hat{\rho}_r^\sigma$ may be obtained by substituting these expressions into (2.8.5). The onset of yielding of generations u and v is the time t when $\varphi\left(\mathbf{U}^s\right) = 0$ ($\mathcal{E}^s \rightarrow \mathcal{E}^u$, $t = t^u$) and $\varphi\left(\mathbf{U}^u\right) = 0$ ($\mathcal{E}^u \rightarrow \mathcal{E}^v$, $t = t^v$), respectively. In summary $w^\sigma = 1$ during the lifetime of generation σ ($t^\sigma \leq t < t^{\sigma+1}$) and 0 at other times t.

5.7.2 Kinematic "Hardening" Response

The framework presented in Section 5.7.1 has considered an elastic-perfectly plastic response, i.e., all the bonds yield when a single yield threshold Φ_m is met. However, a wealth of experimental results show a more progressive yielding, rather than a sudden onset, and an increase in the stress with increasing plastic deformation, a phenomenon alternately termed strain hardening or work hardening. Real materials typically exhibit the Bauschinger effect, where loading to yield in one direction changes the yield threshold in the reverse direction. The hardening behavior that accounts for this effect is known as kinematic hardening; for a load reversal, it predicts yielding occurs when the change in load achieves twice the monotonic yield strength. The reactive plasticity framework can be extended to allow for kinematic hardening by introducing multiple families of bonds. In the current FEBio implementation each bond family β shares the same yield criterion Φ but distinct associated yield thresholds $\Phi_{m\beta}$, and it follows the elastic-perfectly plastic behavior for multiple generations outlined in Section 5.7.1. The superposition of multiple bond families β in parallel naturally develops behavior consistent with kinematic hardening, as different bond families yield at different thresholds.

We consider n_f *bond families* $\beta = 0, \ldots, n_f - 1$, which may yield under different thresholds, where each bond family may evolve over multiple generations σ. This framework requires us to update our notation to include a subscript β for suitable variables introduced in the presentation above. In particular, the reference configuration of generation σ in bond family β is now denoted by $\mathbf{X}_\beta^\sigma$ and the corresponding deformation gradient is $\mathbf{F}_\beta^\sigma$. We assume that the free energy density of each bond family β is $\Psi_{\beta r} = J_\beta^{\sigma s}\Psi_0\left(\mathbf{F}_\beta^\sigma\right)$, when the mixture consists entirely of bonds of family β in generation σ. The master reference configuration of all bond families remains $\mathbf{X}^s$ and the associated (total) deformation gradient is still $\mathbf{F}^s$. Therefore, each bond family β requires a constitutive relation for the function of state $\mathbf{F}_\beta^{\sigma s}$ in the updated form of Eq.(2.8.2), such as that given in Eq.(5.7.4), where each term should now include a subscript β.

The referential mass density of bond family β is $\rho_{r\beta}$, such that the mixture referential mass density is given by $\rho_r = \sum_\beta \rho_{r\beta}$. The referential mass density of generation σ in bond family β is

$\rho^\sigma_{r\beta}$, which satisfies $\sum_\sigma \rho^\sigma_{r\beta} = \rho_{r\beta}$, as per Eq.(2.8.6). For convenience, we define

$$w_\beta \equiv \frac{\rho_{r\beta}}{\rho_r}\,, \quad \sum_\beta w_\beta = 1\,, \tag{5.7.8}$$

which represents the mass fraction of each bond family β within the constrained solid mixture, and

$$w^\sigma_\beta = \frac{\rho^\sigma_{r\beta}}{\rho_{r\beta}}\,, \quad \sum_\sigma w^\sigma_\beta = 1\,, \tag{5.7.9}$$

which represents the mass fraction of each generation σ within the bond family β. From these definitions, it follows that bond family mass fractions w_β are time-invariant (thus user-selected for a particular material response), whereas generation mass fractions w^σ_β evolve with bond-breaking-and-reforming reactions.

The mixture strain energy density Ψ_r is now given by

$$\Psi_r = \sum_\beta w_\beta \sum_\sigma w^\sigma_\beta J^{\sigma s}_\beta \Psi_0\left(\mathbf{F}^\sigma_\beta\right)\,, \tag{5.7.10}$$

whereas the mixture stress is

$$\boldsymbol{\sigma} = \sum_\beta w_\beta \underbrace{\sum_\sigma w^\sigma_\beta \boldsymbol{\sigma}_0\left(\mathbf{F}^\sigma_\beta\right)}_{\boldsymbol{\sigma}_\beta}\,, \quad \boldsymbol{\sigma}_0\left(\mathbf{F}^\sigma_\beta\right) = \frac{1}{J^\sigma_\beta}\frac{\partial \Psi_0}{\partial \mathbf{F}^\sigma_\beta}\cdot\left(\mathbf{F}^\sigma_\beta\right)^T\,. \tag{5.7.11}$$

To simplify the remainder of this presentation, we introduce the concept of *yielded bonds*, denoted by y, to represent bonds of the current extant generation in a plasticity formulation. The yielded bond fraction for each family β is given by

$$w^y_\beta = \sum_{\sigma\neq s} w^\sigma_\beta = 1 - w^s_\beta \tag{5.7.12}$$

where the summation runs over all possible yielded generations $\sigma \neq s$. In particular, at time $t = u$, Eq.(5.7.12) reduces to the statement $w^y_\beta = w^u_\beta$. We then define the relative deformation gradient of yielded bonds as $\mathbf{F}^y_\beta$, which equals $\mathbf{F}^\sigma_\beta$ for the extant generation σ in family β. With these notational changes, we may write the yielding reactions in the form

$$\mathcal{E}^s \to \underbrace{\mathcal{E}^u \to \mathcal{E}^v \to \ldots}_{\mathcal{E}^y}\,. \tag{5.7.13}$$

Then the mixture stress in Eq.(5.7.11) may be rewritten as $\boldsymbol{\sigma} = \sum_\beta w_\beta \boldsymbol{\sigma}_\beta$ where $\boldsymbol{\sigma}_\beta = w^s_\beta \boldsymbol{\sigma}_0\left(\mathbf{F}^s\right) + \left(1 - w^s_\beta\right)\boldsymbol{\sigma}_0\left(\mathbf{F}^y_\beta\right)$. We may also define the total fraction w^s of intact bonds in the mixture as $w^s = \sum_\beta w_\beta w^s_\beta$, and the total fraction of yielded bonds as $w^y = \sum_\beta w_\beta w^y_\beta = 1 - w^s$, such that $w^s + w^y = 1$. Then $\boldsymbol{\sigma} = w^s \boldsymbol{\sigma}_0\left(\mathbf{F}^s\right) + \sum_\beta w_\beta \left(1 - w^s_\beta\right)\boldsymbol{\sigma}_0\left(\mathbf{F}^y_\beta\right)$. The summation in this last expression does not simplify further since $\mathbf{F}^y_\beta$ is different for each bond family β.

Let each bond family β exhibit an elastic-perfectly plastic response, following the model of Section 5.7.1. Once the yield threshold $\Phi_{m\beta}$ is reached, all the intact bonds of that family yield at once, such that $w^s_\beta = 0$ and $w^y_\beta = 1$ as shown for the mixture stress response in Figure 5.7.1a-c. Now consider that there are three bond families, $\beta = 0, 1, 2$ which are weighted evenly, $w_\beta =$

$1/3 \, \forall \beta$. The stress response for this illustrative example is shown in Figure 5.7.1d-f. Though each bond family is elastic-perfectly plastic, their superposition develops "hardening"-like behavior. At the onset of yielding, when family $\beta = 0$ yields, its bond mass fractions are $w_0^s = 0$ and $w_0^y = 1$, implying that this entire family has yielded. However, since the family has a mass fraction $w_0 = 1/3$ in the solid mixture, two-thirds of the bonds in the mixture remain intact at this juncture, $1 - w_0^s = 2/3$. As subsequent families β yield, their bonds transition from intact to yielded generations in the same manner. Though the resulting stress response in Figure 5.7.1d is classically described as a "hardening" behavior, the reactive plasticity mixture framework proposes a different interpretation, namely that there are multiple elastic-perfectly plastic bond families in the material, each with a different threshold of yielding.

For each bond family β, the family mass fraction w_β and the associated yield threshold $\Phi_{m\beta}$ must be provided by constitutive assumption, along with a single constitutive model for Ψ_0 which applies to all generations of all bond families. The total number n_f of bond families must also be provided. Parameters n_f and $\{w_\beta, \Phi_{m\beta}\}$, $\beta \in [0, n_f - 1]$ suffice to define an elastoplastic material which exhibits classical kinematic hardening behavior, for a given elastic response Ψ_0 and yield criterion Φ.

5.7.3 Constitutive Modeling of Yield Response

Here, we provide basic constitutive relations for the parameters $\{w_\beta, \Phi_{m\beta}\}$, $\beta \in [0, n_f - 1]$ which define an elastoplastic material. We also demonstrate how these various parameters affect the uniaxial stress-strain response of a material. The example in Figure 5.7.1d shows how superposition of multiple elastic-perfectly plastic bond families may create a hardening-like curve. In particular, we present a constitutive modeling framework that requires at most six scalar parameters, regardless of the value of n_f.

Since each family behaves elastically until it yields, a family's yield threshold $\Phi_{m\beta}$ is generally not the value recorded on a stress-strain curve when the slope changes (Figure 5.7.2). That value may be called the *apparent yield threshold* Υ_β, which can be related to the true yield threshold $\Phi_{m\beta}$ by assuming a linear elastic stress-strain relationship prior to yielding. For simplicity, we assume that Υ_β values are evenly distributed between an *initial yield threshold* Υ_0 and a *final yield threshold* Υ_{max}, parameters which may be identified from a stress strain curve (Figure 5.7.3a-b). Beyond Υ_{max}, the material either behaves as if it is perfectly plastic (a scenario which may be valid around the ultimate strength, for example), or it transitions to a linear hardening regime. The constitutive model thus specifies

$$\begin{aligned} \Upsilon_\beta &= \Upsilon_0 + \beta \frac{\Upsilon_{\text{max}} - \Upsilon_0}{n_f - 1}, \qquad \beta = 0, \ldots, n_f - 1 \\ \Phi_{m\beta} &= \Phi_{m,\beta-1} + \frac{\Upsilon_\beta - \Upsilon_{\beta-1}}{1 - \sum_{b=0}^{\beta-1} w_b}, \quad \Phi_{m0} = \Upsilon_0 \end{aligned} \tag{5.7.14}$$

The relationships between Υ_β and $\Phi_{m\beta}$ embodied in Eq.(5.7.14) are illustrated graphically in Figure 5.7.2. Through this relationship, only the values of Υ_0 and Υ_{max} must be specified, along with n_f.

The family mass fractions w_β govern the influence of each family on the overall material response. The simplest model for w_β involves specifying the mass fraction of the first yielding family w_0, which controls the slope of the initial post-yield response (Figure 5.7.3a), and then evenly weighting the rest of the bond families, $w_\beta = (1 - w_0) / (n_f - 1)$. However, in cases where the material transitions to a linear hardening regime, we can recover this behavior by adding one more

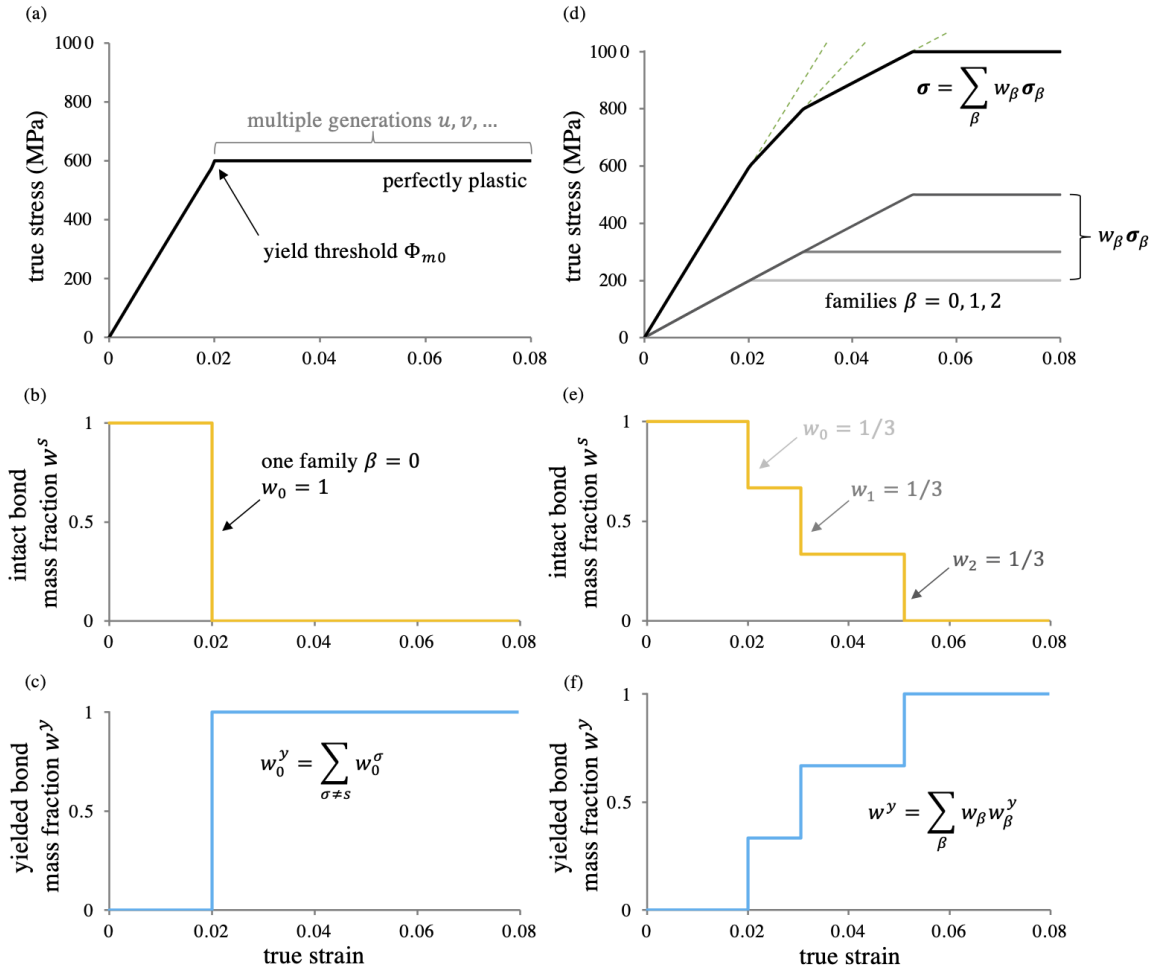

Figure 5.7.1: The phenomenon described as "kinematic hardening" in classical plasticity may be represented by the superposition of multiple elastic-perfectly plastic bond families with different yield thresholds. The elastic-perfectly plastic stress response of a single bond family $\beta = 0$ in the reactive framework is presented in (a), with the initial linear response contributed by the intact bonds s; upon yielding at the threshold Φ_{m0}, the perfectly plastic response consists of multiple generations of breaking and reforming bonds $\sigma = u, v, \ldots$. The evolution of mass fractions w_0^s of intact and w_0^y of yielded bonds is presented in (b) and (c), respectively. The stress response obtained from the superposition of three bond families $\beta = 0, 1, 2$ is shown in (d), where each family occupies the same mass fraction w_β in the mixture, $w_0 = w_1 = w_2 = \frac{1}{3}$, reproducing the classical kinematic hardening behavior. Green dashed lines help indicate changes in slope due to yielding of each bond family. The corresponding mixture mass fractions of (e) intact bonds w^s, and (f) yielded bonds $w^y = 1 - w^s$ further illustrates the occurence of each yielding reaction.

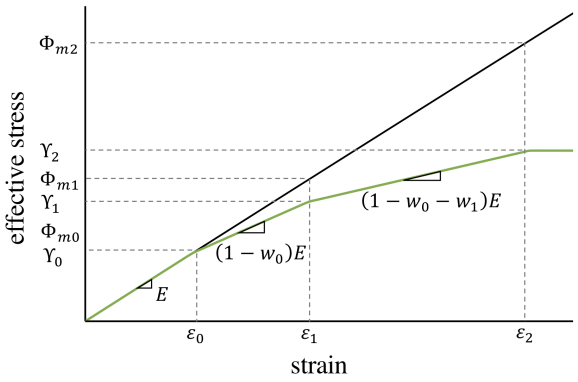

Figure 5.7.2: Schematic stress-strain curve illustrating derivation of constitutive models for $\Phi_{m\beta}$. E is Young's modulus of the elastic solid (whose value does not matter here), Υ_β are the effective yield thresholds for the global material (given), ε_β are the yield strains and $\Phi_{m\beta}$ are the true yield thresholds for each bond family, which need to be determined, and w_β are the family mass fractions (given).

bond family, $\beta = n_f$, that never yields, thus remaining elastic. The associated mass fraction w_β for $\beta = n_f$ is called the *elastic mass fraction* and denoted w_e; a non-zero value for this parameter may be specified whenever we wish to include linear hardening behavior (Figure 5.7.3b). Given initial and elastic mass fractions w_0 and w_e, the simplest constitutive assumption for the remaining w_β's assumes the remaining mass is evenly divided, such that

$$w_\beta = \frac{1 - w_e - w_0}{n_f - 1},\ \beta \in [1, n_f - 1]\ . \tag{5.7.15}$$

The effect of the mass fraction parameters w_0 and w_e is explored parametrically in Figure 5.7.3c and Figure 5.7.3d, respectively. In general, most ductile materials have w_0 very close to unity, which provides hardening behavior over a finite strain range. As $w_0 \to 1$ the stress-strain behavior approaches perfect plasticity. In contrast, when $w_e = 0$, the material response becomes perfectly plastic once the final yield threshold Υ_{max} has been exceeded. As w_e increases, a region of linear hardening is seen on a plot of the true stress against strain. For most ductile materials, w_e is usually 0 or on the order of 0.001.

It is also possible to refine the constitutive relations of Eqs. (5.7.14)-(5.7.15) by introducing a *bias factor* r, which allows a geometric progression rather than uniform spacing of the apparent yield thresholds and family mass fractions. The bias factor r has the effect of modifying the shape of the hardening region between Υ_0 and Υ_{max} (Figure 5.7.3b). The modified constitutive relations for w_β and $\Phi_{m\beta}$ take the form

$$\begin{aligned}
c &= \frac{1-r}{1-r^{n_f-1}} & \Phi_{m0} &= \Upsilon_0 \\
\Upsilon_1 &= \Upsilon_0 + c\,(\Upsilon_{\mathsf{max}} - \Upsilon_0)\,, & \Phi_{m1} &= \Upsilon_0 + \frac{\Upsilon_1 - \Upsilon_0}{1 - w_0} \\
\Upsilon_\beta &= \Upsilon_{\beta-1} + r\,(\Upsilon_{\beta-1} - \Upsilon_{\beta-2})\,, & \Phi_{m\beta} &= \Phi_{m,\beta-1} + \frac{\Upsilon_\beta - \Upsilon_{\beta-1}}{1 - \sum_{b=0}^{\beta-1} w_b}
\end{aligned} \tag{5.7.16}$$

The mass fractions w_β are similarly biased, where w_0 and w_e are specified and

$$\begin{aligned}
w_1 &= c\,(1 - w_e - w_0) \\
w_\beta &= w_{\beta-1} r
\end{aligned} \tag{5.7.17}$$

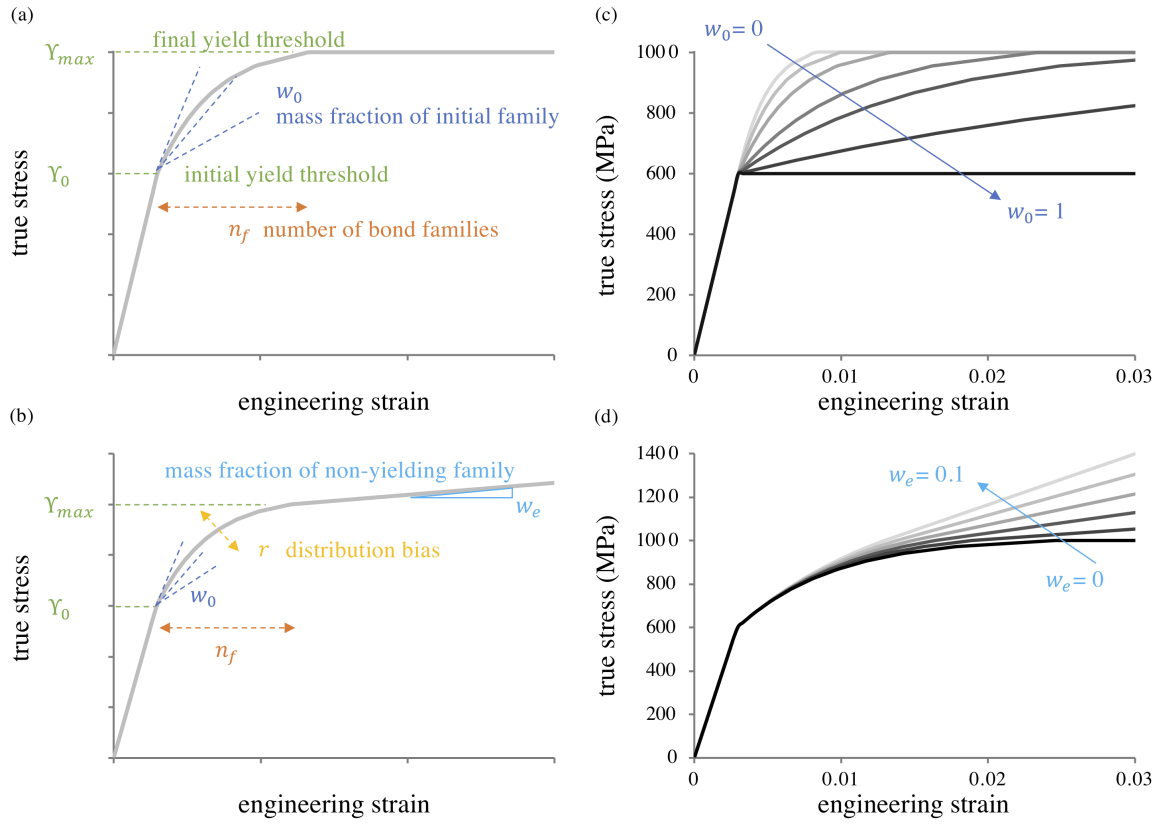

Figure 5.7.3: Modeling uniaxial stress-strain curves using the constitutive model for scalar bond family parameters given in Section 5.7.3. Identification of parameters on idealized stress-strain curves showing (a) a plateau in the stress, or (b) exhibiting a region of linear hardening. The yielding behavior is fully described by the set of parameters $\{n_f, \Upsilon_0, \Upsilon_{\text{max}}, w_0, w_e, r\}$. Parametric variations of (c) w_0 and (d) w_e illustrate their influence on the stress-strain response; other parameters are held fixed. In (c-d) $n_f = 10$, $\Upsilon_0 = 600$ MPa, $\Upsilon_{\text{max}} = 1000$ MPa, and $r = 1$. In (c), $w_e = 0$ and in (d) $w_0 = 0.75$. For all cases, $E = 200$ GPa and $\nu = 0.3$.

The full set of parameters is then given by $\{n_f, \Upsilon_0, \Upsilon_{\max}, w_0, w_e, r\}$. Setting $r = 1$ recovers the uniform distribution presented in Eqs.(5.7.14)-(5.7.15). Figure 5.7.3a-b graphically describes the influence of each parameter on simplified stress-strain curves, showing how these parameters may be extracted from experimental data.

5.8 Reactive Elastoplastic Damage Mechanics

Plastic deformation (Section 5.7) is often coupled with damage, as the finite deformation and plastic flow of a loaded material typically induces some amount of failure. Within the constrained reactive mixture framework adopted in FEBio (Section 2.8), damage is produced by bonds breaking permanently (Section 5.6), which reduces the generation mass fractions w_β^σ [115]. In our treatment of elastoplastic damage we assume that both intact and yielded bonds may become damaged. Damage to intact bonds may represent some initial damage value for a material with defects, or damage due to intermolecular failure of bonds that never yielded; we refer to this as *elastic damage*. Damage to yielded bonds represents *plastic damage*. The mechanism of damage and the failure measure may be different for these two types of bonds, particularly since a stress- or energy-based failure measure may not be appropriate for plastic damage. Intact bonds belong to the $s-$generation which is present at $t = -\infty$. Once yielding occurs, all successive generations of that family are labeled as yielded bonds y. This distinction is necessary so we can then distinguish between damage to intact bonds (elastic damage) and damage to yielded bonds (plastic damage), since intact bonds which get damaged never have the ability to yield. It is important to note that the nature of the plastic deformation described in Section 5.7 remains unchanged. Damage modifies the material behavior by reducing the fraction of bonds in various generations, which scales the response accordingly.

In a reactive constrained mixture framework the insertion of damage into the reactive plasticity formulation is straightforward. Since bonds break permanently in a damage reaction, there is no need to define a function of state $\mathbf{F}_\beta^{\sigma s}$ to describe a (non-existing) reformed configuration. Furthermore, the specific free energy of broken bonds is zero. The scalar *elastic damage criterion* $\Xi^e\left(\mathbf{F}^s\right)$, which is taken to have the same functional form for all bond families β, is the analog to the yield criterion Φ for plasticity. As shown in Section 5.6, the main contrast with reactive plasticity is that not all bonds in the family β break simultaneously at a single *elastic damage threshold* $\Xi_{m\beta}^e$. Instead, the fraction of broken bonds varies as a function of $\Xi^e\left(\mathbf{F}^s\right)$, denoted by $F^e\left(\Xi_\beta^e\right)$, such that $0 \leq F^e\left(\Xi_\beta^e\right) \leq 1$. Here, $F^e\left(\Xi_\beta^e\right)$ is a function of state; it must be a monotonically increasing function of its argument to satisfy the Clausius-Duhem inequality [77]. We may view F^e as a cumulative distribution function (CDF), whose corresponding probability distribution function (PDF) represents the probability of damage at a particular value of Ξ_β^e.

5.8.1 Theoretical Formulation

We first briefly sketch the structure of the elastoplastic damage theory in FEBio for a single bond family β. Since each bond family in reactive plasticity yields all at once, we can easily split an elastoplastic damage theory into two parts to represent elastic and plastic damage regimes. Assume that the first yielding reaction for bond family β occurs at time $t = u_\beta$. Prior to this initial yielding, the damage behavior described in Section 5.6 applies, and the material composition is generally a mixture of intact ($\sigma = s$) and broken ($\sigma = b$) bonds satisfying the reaction $\mathcal{E}_\beta^s \rightarrow \mathcal{E}_\beta^b$. The corresponding bond mass fractions satisfy $1 = w_\beta^s + w_\beta^b$ and $w_\beta^y = 0$, where $w_\beta^b = F^e\left(\Xi_\beta^e\right)$ is the elastic damage in bond family β. At $t = u_\beta$, the remaining intact bonds $w_\beta^s = 1 - w_\beta^b$ all yield, following the reaction in Eq.(5.7.13). The family mass balance is then given as $1 = w_\beta^y + w_\beta^b$, since $w_\beta^s = 0$ after yielding. The mass fraction of broken bonds $w^b = \sum_\beta w_\beta w_\beta^b$ is equal to the elastic damage variable D as defined in classical damage mechanics.

For time $t > u_\beta$, yielded bonds may continue to yield, but they may also sustain damage

according to the reaction $\mathcal{E}^y_\beta \rightarrow \mathcal{E}^b_\beta$, which reduces their mass fraction w^y_β. Damage to yielded bonds may occur based on a function of state (often described as a plastic strain, though it is not an observable kinematic variable), which is distinct from the measure of elastic damage. Therefore, we denote the *plastic damage measure* as $\Xi^p\left(\mathbf{F}^{ys}_\beta\right)$ and its cumulative distribution function by $F^p\left(\Xi^p_\beta\right)$, under the assumption that all bond families β share the same functional forms for Ξ^p and F^p. For each bond family β, only the remaining undamaged fraction $1 - F^p\left(\Xi^p_\beta\right)$ of yielded bonds may break and reform as the next yielded generation.

The modern understanding is that plastic strain is ill-defined and not a suitable state variable. It must be recognized that, just as $\mathbf{F}^{ys}_\beta$ is a constitutively-prescribed function of state and does not carry the meaning of a plastic deformation gradient, the plastic damage measure $\Xi^p\left(\mathbf{F}^{ys}_\beta\right)$ is also a function of state. This quantity is called a plastic strain for convenience only.

When plastic deformation occurs simultaneously with damage, the mass fraction of each successive yielded generation will have decreased. The following treatment now considers the superposition of multiple plastic bond families, as described in Section 5.7.2.

5.8.1.1 Damage to Intact Bonds

At any given time t, there is a maximum value of Ξ^e that has been achieved over the past deformation history. This maximum value may be distinct for each bond family β, since intact bond families may yield at different values of $\mathbf{F}^s$; it is thus denoted by $\Xi^e_{m\beta}$,

$$\Xi^e_{m\beta} = \max_{-\infty < \tau \leq t < u_\beta} \Xi^e\left(\mathbf{F}^s\left(\tau\right)\right) . \tag{5.8.1}$$

Any damage sustained by intact bonds reduces their mass fraction, such that

$$\begin{cases} w^s_\beta = 1 - F^e\left(\Xi^e_{m\beta}\right) \\ w^y_\beta = 0 \\ w^b_\beta = F^e\left(\Xi^e_{m\beta}\right) \end{cases} , \quad t < u_\beta \, , \tag{5.8.2}$$

and hence the mass balance of Eq.(5.7.9) is satisfied. Since all remaining intact bonds yield at $t = u_\beta$ and thus no intact bonds are left to sustain damage, $F^e\left(\Xi^e_{m\beta}\right)$ remains constant constant for bond family β when $t \geq u_\beta$.

5.8.1.2 Damage to Yielded Bonds

At time $t = u_\beta$, the yield threshold $\Phi_{m\beta}$ for family β is reached and all remaining intact bonds in family β yield such that

$$\begin{cases} w^s_\beta = 0 \\ w^y_\beta = 1 - F^e\left(\Xi^e_{m\beta}\right) \\ w^b_\beta = F^e\left(\Xi^e_{m\beta}\right) \end{cases} , \quad t = u_\beta \, . \tag{5.8.3}$$

Once they have formed, yielded bonds may sustain plastic damage. The maximum value of the plastic damage measure Ξ^p experienced by family β up until the current time t is denoted by $\Xi^p_{m\beta}$,

$$\Xi^p_{m\beta} = \max_{u_\beta \leq \tau < t} \Xi^p\left(\mathbf{F}^y_\beta\left(\tau\right)\right) . \tag{5.8.4}$$

For $t > u_\beta$, yielded bonds may continue to yield, breaking and reforming into successive generations. However, in contrast to Section 5.7, the mass fraction w_β^y of yielded bonds in family β no longer remains constant over successive yield generations, due to the plastic damage reaction. Each time a yielded bond breaks and reforms into a new generation, w_β^y is given by the undamaged fraction of yielded bonds,

$$\begin{cases} w_\beta^s = 0 \\ w_\beta^y = \left(1 - F^p\left(\Xi_{m\beta}^p\right)\right)\left(1 - F^e\left(\Xi_{m\beta}^e\right)\right) \\ w_\beta^b = F^e\left(\Xi_{m\beta}^e\right) + F^p\left(\Xi_{m\beta}^p\right)\left(1 - F^e\left(\Xi_{m\beta}^e\right)\right) \end{cases} , \quad t > u_\beta \,. \tag{5.8.5}$$

Equations (5.8.2),(5.8.3), and (5.8.5) govern the temporal behavior of the bond species mass fractions.

5.8.1.3 Strain Energy Density, Stress, and Damage

Recognizing that damaged (broken) bonds do not store free energy, the referential mixture free energy density in Eq.(5.7.10) may be rewritten as

$$\Psi_r = \sum_\beta w_\beta \left(w_\beta^s \Psi_0\left(\mathbf{F}^s\right) + w_\beta^y J^{ys} \Psi_0\left(\mathbf{F}_\beta^y\right)\right) , \tag{5.8.6}$$

where the bond mass fractions w_β^s and w_β^y are given in Eqs.(5.8.2)-(5.8.5) prior to, during, and after yielding of each bond family β. Similarly, the mixture stress may be evaluated from Eq.(5.7.11) as

$$\boldsymbol{\sigma} = \sum_\beta w_\beta \left(w_\beta^s \boldsymbol{\sigma}_0\left(\mathbf{F}^s\right) + w_\beta^y \boldsymbol{\sigma}_0\left(\mathbf{F}_\beta^y\right)\right) , \tag{5.8.7}$$

where the stresses $\boldsymbol{\sigma}_0$ are given by the standard hyperelasticity relation in Eq.(5.7.11). These expressions may be simplified further when assuming that the functional form of ψ_β remains the same for all bond families β. Finally, the reactive mixture equivalent of the damage variable D may be evaluated for elastoplastic damage as the fraction of all bonds that are broken,

$$D = w^b = \sum_\beta w_\beta w_\beta^b \,. \tag{5.8.8}$$

5.8.1.4 Damage Measures

For elastic damage, we may use the same functional measure as proposed for plastic yielding (e.g., the von Mises stress); this implies that the functions Ξ^e and Φ have the same form. For plastic damage, experimental results show that during plastic flow damage is coupled with measures of plastic strain [68], necessitating a (pseudo-)strain-based plastic damage measure Ξ^p. For yielded bonds in a bond family β, we can use the constitutively-determined mapping $\mathbf{F}_\beta^{ys}$ to define plastic right Cauchy-Green and Lagrange strain tensors through

$$\begin{aligned} \mathbf{C}_\beta^{ys} &= \left(\mathbf{F}_\beta^{ys}\right)^T \cdot \mathbf{F}_\beta^{ys} \\ \mathbf{E}_\beta^{ys} &= \frac{1}{2}\left(\mathbf{C}_\beta^{ys} - \mathbf{I}\right) \end{aligned} . \tag{5.8.9}$$

One possible constitutive relation for Ξ^p, which remains valid for general deformations, is to set it equal to the *effective plastic strain* e^p_β for the various bond families β,

$$e^p_\beta = \sqrt{\frac{2}{3}\,\mathrm{dev}\,\mathbf{E}^{ys}_\beta : \mathrm{dev}\,\mathbf{E}^{ys}_\beta}\,. \tag{5.8.10}$$

In a numerical implementation, the effective plastic strain e^p_0 of the first bond family to yield may be reported as the effective plastic strain in the entire material, for consistency with plastic strain measures in classical models of plasticity.

Quantities in this section do not represent plastic strains or plastic strain tensors, though we adopt the terminology due to similarities. Recall that the non-observable function of state $\mathbf{F}^{ys}_\beta = \mathbf{F}^{ys}_\beta\left(\mathbf{F}^s, \rho^\alpha_{r\beta}\right)$ is a time-invariant mapping providing the reference configuration of a yielded bond y with respect to the reference configuration of the master constituent s, for family β. The quantities $\mathbf{C}^{ys}_\beta$ and $\mathbf{E}^{ys}_\beta$ then also represent non-observable functions of state calculated as strain tensors. Consequently, e^p_β is a measure of the relative motion of the reference configuration of bond family β , expressed as a scalar "strain". Physically, this amounts to the modeling assumption that once the breaking-and-reforming process takes a bond family out of a local neighborhood centered about its original position, the bond begins to degrade with further breaking-and-reforming processes. That each of these quantities exists for every bond family β emphasizes the lack of any true or unique plastic strain measure in this framework.

5.8.1.5 Cumulative Damage Distribution Functions

The final set of constitutive relations required to fully define an elastoplastic damage material are the two CDFs, $F^e\left(\Xi^e_{m\beta}\right)$ and $F^p\left(\Xi^p_{m\beta}\right)$. As shown by **(author?)** [77], the only requirement imposed by the Clausius-Duhem inequality is that these be monotonically increasing functions. Whereas these CDFs may be characterized directly from experimental data, here we illustrate the FEBio elastoplastic damage framework using a Weibull distribution of the form

$$F\left(\Xi\right) = 1 - \exp\left(-\left(\frac{\Xi}{\kappa}\right)^\gamma\right)\,, \tag{5.8.11}$$

where κ (same units as Ξ) is the value of Ξ at which the fraction $1 - e^{-1}$ of bonds have failed and the exponent γ (unitless) controls the slope of the response, such that $F\left(\Xi\right)$ approaches a step function with a jump at $\Xi = \kappa$ as $\gamma \to \infty$. Therefore, each damage function has two free parameters κ and γ. Based on experimental evidence, we may let Ξ^e be given by the von Mises (effective) stress, while Ξ^p is taken to be the effective plastic strain (Section 5.8.1.4). Figure 5.8.1 shows the effect of the Weibull parameter γ^p on the stress-strain and damage-strain responses, with κ^p fixed. The damage response as a function of plastic strain is identically the prescribed CDF (Figure 5.8.1b). The shape of the CDF changes from logarithmic-like to exponential as γ^p increases, demonstrating the ability of this formulation to recover a broad variety of experimentally measured damage-strain behaviors [28].]

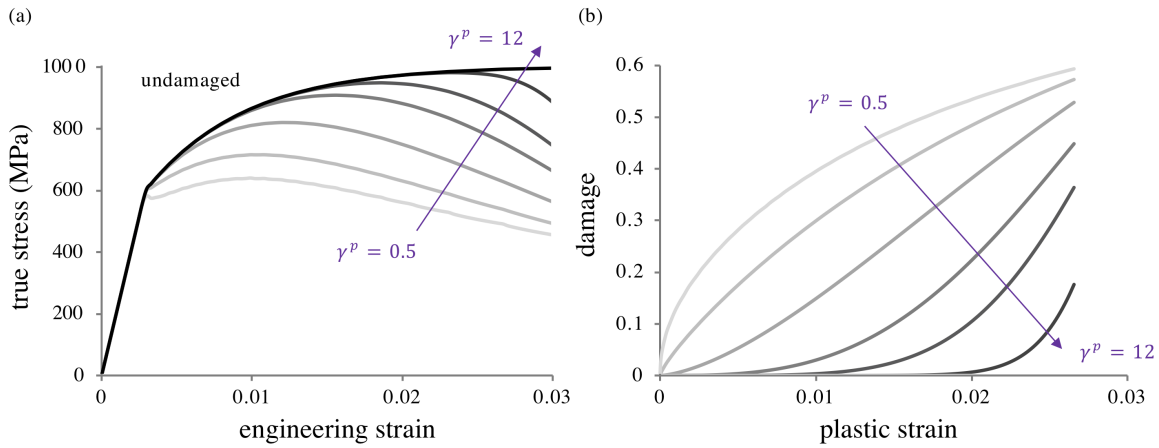

Figure 5.8.1: Parametric study of the effect of the damage parameter γ^p for a Weibull distribution, with no intact damage taking place. (a) As γ^p increases, the onset of noticeable damage shifts to higher strains and becomes more rapid. (b) Plot of the damage variable $D = \sum_\beta w_\beta F^p\left(\Xi^p_{m\beta}\right)$. The response becomes more nonlinear as γ^p deviates from unity. Other plasticity and damage parameters are $n_f = 20$, $\Upsilon_0 = 600$ MPa, $\Upsilon_{\max} = 1000$ MPa, $w_0 = 0.75$, $w_e = 0$, $r = 1$, and $\kappa^p = 0.03$.

5.9 Hydraulic Permeability

Hydraulic permeability is a material function needed for biphasic and multiphasic materials.

5.9.1 Constant Isotropic Permeability

When the permeability is isotropic,

$$\mathbf{k} = k\,\mathbf{I}\,. \tag{5.9.1}$$

For this material model, k is constant. Generally, this assumption is only reasonable when strains are small.

5.9.2 Exponential Isotropic Permeability

This isotropic material has a permeability that varies as a function of the determinant J of the deformation gradient. Its general form is

$$\mathbf{k} = k\,(J)\,\mathbf{I}\,, \tag{5.9.2}$$

where,

$$k\,(J) = k_0 \exp\left(M\frac{J-1}{J-\varphi_0}\right)\,. \tag{5.9.3}$$

Pore closure occurs as J approaches φ_0 from above, in which case the permeability reduces to zero,

$$\lim_{J\to\varphi_0} k\,(J) = 0\,. \tag{5.9.4}$$

In the special case when $M = 0$, the permeability becomes constant. In the limit of infinitesimal strains, the permeability has the form

$$k(J) = k_0 \left(1 + \frac{M}{1-\varphi_0}(J-1) + \mathcal{O}\left((J-1)^2\right)\right). \tag{5.9.5}$$

For the type of isotropic permeability given in (5.9.2), the spatial permeability tangent $\boldsymbol{\mathcal{K}}$ with respect to the solid matrix strain has the general form

$$\boldsymbol{\mathcal{K}} = \left(k + Jk'\right)\mathbf{I}\otimes\mathbf{I} - 2k\mathbf{I}\odot\mathbf{I}, \tag{5.9.6}$$

where

$$k'(J) = M\frac{1-\varphi_0}{(J-\varphi_0)^2}k(J) \tag{5.9.7}$$

in this case.

5.9.3 Holmes-Mow

This isotropic material uses a strain-dependent permeability tensor as formulated by [50]:

$$\mathbf{k} = k(J)\,\mathbf{I}, \tag{5.9.8}$$

where,

$$k(J) = k_0\left(\frac{J-\varphi_0}{1-\varphi_0}\right)^{\alpha} e^{\frac{1}{2}M\left(J^2-1\right)}. \tag{5.9.9}$$

When $\alpha > 0$, pore closure occurs as $J \to \varphi_0$ from above, in which case k reduces to 0. Setting $\alpha = 0$ and $M = 0$ produces a constant permeability. In the limit of infinitesimal strains,

$$k(J) = k_0\left(1 + \left(M + \frac{\alpha}{1-\varphi_0}\right)(J-1) + \mathcal{O}\left((J-1)^2\right)\right). \tag{5.9.10}$$

The spatial tangent of the permeability tensor with respect to strain may be evaluated from (5.9.6) using

$$k'(J) = \left(J\,M + \frac{\alpha}{J-\varphi_0}\right)k(J). \tag{5.9.11}$$

5.9.4 Referentially Isotropic Permeability

This material uses a strain-dependent permeability tensor that accommodates strain-induced anisotropy [9]:

$$\mathbf{k} = \left(k_{0r}\mathbf{I} + \frac{k_{1r}}{J^2}\mathbf{b} + \frac{k_{2r}}{J^4}\mathbf{b}^2\right)\left(\frac{J-\varphi_r^s}{1-\varphi_r^s}\right)e^{M\left(J^2-1\right)/2}, \tag{5.9.12}$$

Note that the permeability in the reference state ($\mathbf{F} = \mathbf{I}$) is isotropic and given by $\mathbf{k} = (k_{0r} + k_{1r} + k_{2r})\,\mathbf{I}$.

5.9.5 Referentially Orthotropic Permeability

This material uses a strain-dependent permeability tensor that is orthotropic in the reference configuration, and accommodates strain-induced anisotropy [9]:

$$\mathbf{k} = k_0\mathbf{I} + \sum_{a=1}^{3} k_1^a \mathbf{m}_a + k_2^a \left(\mathbf{m}_a \cdot \mathbf{b} + \mathbf{b} \cdot \mathbf{m}_a\right) , \tag{5.9.13}$$

where,

$$\begin{aligned} k_0 &= k_{0r} \left(\frac{J-\varphi_r^s}{1-\varphi_r^s}\right)^{\alpha_0} e^{M_0\left(J^2-1\right)/2} , \\ k_1^a &= \frac{k_{1r}^a}{J^2} \left(\frac{J-\varphi_r^s}{1-\varphi_r^s}\right)^{\alpha_a} e^{M_a\left(J^2-1\right)/2} , \quad a = 1,2,3 \\ k_2^a &= \frac{k_{2r}^a}{2J^4} \left(\frac{J-\varphi_r^s}{1-\varphi_r^s}\right)^{\alpha_a} e^{M_a\left(J^2-1\right)/2} . \end{aligned} \tag{5.9.14}$$

Here, $\mathbf{m}_a$ are second order tensors representing the spatial structural tensors describing the orthogonal planes of symmetry, given by

$$\mathbf{m}_a = \mathbf{F} \cdot \left(\mathbf{V}_a \otimes \mathbf{V}_a\right) \cdot \mathbf{F}^T , \quad a = 1-3, \tag{5.9.15}$$

where $\mathbf{V}_a$ are orthonormal vectors normal to the planes of symmetry. Note that the permeability in the reference state ($\mathbf{F} = \mathbf{I}$) is given by $\mathbf{k} = k_{0r}\mathbf{I} + \sum\limits_{a=1}^{3} \left(k_{1r}^a + k_{2r}^a\right) \mathbf{V}_a \otimes \mathbf{V}_a$.

5.9.6 Referentially Transversely Isotropic Permeability

This material uses a strain-dependent permeability tensor that is transversely isotropic in the reference configuration, and accommodates strain-induced anisotropy [9]:

$$\begin{aligned} \mathbf{k} = {} & k_{0r} \left(\frac{J-\varphi_r^s}{1-\varphi_r^s}\right)^{\alpha_0} e^{M_0\left(J^2-1\right)/2}\mathbf{I} \\ & + \left(\frac{k_{1r}^T}{J^2}\left(\mathbf{b}-\mathbf{m}\right) + \frac{k_{2r}^T}{2J^4}\left[2\mathbf{b}^2 - \left(\mathbf{m}\cdot\mathbf{b} + \mathbf{b}\cdot\mathbf{m}\right)\right]\right) \left(\frac{J-\varphi_r^s}{1-\varphi_r^s}\right)^{\alpha_T} e^{M_T\left(J^2-1\right)/2} \\ & + \left(\frac{1}{J^2}k_{1r}^A\mathbf{m} + \frac{1}{2J^4}k_{2r}^A\left(\mathbf{m}\cdot\mathbf{b} + \mathbf{b}\cdot\mathbf{m}\right)\right) \left(\frac{J-\varphi_r^s}{1-\varphi_r^s}\right)^{\alpha_A} e^{M_A\left(J^2-1\right)/2} , \end{aligned} \tag{5.9.16}$$

where $\mathbf{m}$ is a second order tensor representing the spatial structural tensor describing the axial direction, given by

$$\mathbf{m} = \mathbf{F} \cdot \left(\mathbf{V} \otimes \mathbf{V}\right) \cdot \mathbf{F}^T , \tag{5.9.17}$$

and $\mathbf{V}$ is a unit vector along the axial direction. Note that the permeability in the reference state ($\mathbf{F} = \mathbf{I}$) is given by $\mathbf{k} = \left(k_{0r} + k_{1r}^T + k_{2r}^T\right)\mathbf{I} + \left(k_{1r}^A - k_{1r}^T + k_{2r}^A - k_{2r}^T\right)\left(\mathbf{V} \otimes \mathbf{V}\right)$.

5.10 Solute Diffusivity

Diffusivity materials provide a constitutive relation for the solute diffusivity in a biphasic-solute material. In general, the diffusivity tensor $\mathbf{d}$ may be a function of strain and solute concentration.

5.10.1 Constant Isotropic Diffusivity

When the permeability is isotropic,

$$\mathbf{d} = d\,\mathbf{I}\,. \tag{5.10.1}$$

For this material model, d is constant. This assumption is only true when strains are small. Note that the user must specify $d \leqslant d_0$, where d_0 is the solute diffusivity in free solution, since a solute cannot diffuse through the biphasic-solute mixture faster than in free solution.

5.10.2 Constant Orthotropic Diffusivity

When the permeability is orthotropic,

$$\mathbf{d} = \sum_{a=1}^{3} d^a \mathbf{V}_a \otimes \mathbf{V}_a\,, \tag{5.10.2}$$

where $\mathbf{V}_a$ are orthonormal vectors normal to the planes of symmetry. For this material model, the d^a are constant. Therefore this model should be used only when strains are small. Note that the user must specify $d^a \leqslant d_0$, where d_0 is the solute diffusivity in free solution, since a solute cannot diffuse through the biphasic-solute mixture faster than in free solution.

5.10.3 Referentially Isotropic Diffusivity

This material uses a strain-dependent diffusivity tensor that is isotropic in the reference configuration and accommodates strain-induced anisotropy:

$$\mathbf{d} = \left(d_{0r}\mathbf{I} + \frac{d_{1r}}{J^2}\mathbf{b} + \frac{d_{2r}}{J^4}\mathbf{b}^2\right)\left(\frac{J-\varphi_r^s}{1-\varphi_r^s}\right)e^{M(J^2-1)/2}, \tag{5.10.3}$$

where J is the jacobian of the deformation, i.e. $J = \det\mathbf{F}$ where $\mathbf{F}$ is the deformation gradient, and $\mathbf{b} = \mathbf{F}\cdot\mathbf{F}^T$ is the left Cauchy-Green tensor. Note that the diffusivity in the reference state ($\mathbf{F} = \mathbf{I}$) is isotropic and given by $\mathbf{d} = (d_{0r} + d_{1r} + d_{2r})\,\mathbf{I}$.

5.10.4 Referentially Orthotropic Diffusivity

This material uses a strain-dependent diffusivity tensor that is orthotropic in the reference configuration and accommodates strain-induced anisotropy:

$$\mathbf{d} = d_0\mathbf{I} + \sum_{a=1}^{3} d_1^a\mathbf{m}_a + d_2^a\left(\mathbf{m}_a\cdot\mathbf{b} + \mathbf{b}\cdot\mathbf{m}_a\right)\,, \tag{5.10.4}$$

where

$$
\begin{aligned}
d_0 &= d_{0r}\left(\frac{J-\varphi_r^s}{1-\varphi_r^s}\right)^{\alpha_0} e^{M_0\left(J^2-1\right)/2}\,,\\
d_1^a &= \frac{d_{1r}^a}{J^2}\left(\frac{J-\varphi_r^s}{1-\varphi_r^s}\right)^{\alpha_a} e^{M_a\left(J^2-1\right)/2}\,, \quad a=1,2,3\\
d_2^a &= \frac{d_{2r}^a}{2J^4}\left(\frac{J-\varphi_r^s}{1-\varphi_r^s}\right)^{\alpha_a} e^{M_a\left(J^2-1\right)/2}\,.
\end{aligned}
\tag{5.10.5}
$$

Here, J is the Jacobian of the deformation, i.e. $J=\det\mathbf{F}$ where $\mathbf{F}$ is the deformation gradient. $\mathbf{m}_a$ are second order tensor representing the spatial structural tensors describing the orthogonal planes of symmetry, given by

$$
\mathbf{m}_a = \mathbf{F}\cdot\left(\mathbf{V}_a\otimes\mathbf{V}_a\right)\cdot\mathbf{F}^T, \quad a=1-3\,,
\tag{5.10.6}
$$

where $\mathbf{V}_a$ are orthonormal vectors normal to the planes of symmetry. Note that the permeability in the reference state ($\mathbf{F}=\mathbf{I}$) is given by $\mathbf{k}=k_{0r}\mathbf{I}+\sum_{a=1}^{3}\left(k_{1r}^a+k_{2r}^a\right)\mathbf{V}_a\otimes\mathbf{V}_a$.

5.11 Solute Solubility

Solubility constitutive equations provide a relation for $\tilde{\kappa}$ as a function of solid matrix strain and effective solute concentrations.

5.11.1 Constant Solubility

For this material model, $\tilde{\kappa}$ is constant.

5.12 Osmotic Coefficient

Osmotic coefficient constitutive equations provide a relation for Φ as a function of solid matrix strain and effective solute concentrations.

5.12.1 Constant Osmotic Coefficient

For this material model, Φ is constant.

5.13 Active Contraction Model

A time varying "elastance" active contraction model [47] was added to the transversely isotropic materials. When active contraction is activated, the total Cauchy stress $\sigma$is defined as the sum of the active stress tensor $\boldsymbol{\sigma}^a = T^a \mathbf{a} \otimes \mathbf{a}$ and the passive stress tensor $\boldsymbol{\sigma}^p$:

$$\boldsymbol{\sigma} = \boldsymbol{\sigma}^p + \boldsymbol{\sigma}^a, \tag{5.13.1}$$

where ***a*** is the deformed fiber vector (unit length), defined as $\lambda \mathbf{a} = \mathbf{F} \cdot \mathbf{a}$. The time varying elastance model is a modification of the standard Hill equation that scales the standard equation by an activation curve $C\left(t\right)$. The active fiber stress T^a is defined as:

$$T^a = T_{\max} \frac{Ca_0^2}{Ca_0^2 + ECa_{50}^2} C\left(t\right), \tag{5.13.2}$$

where $T_{max} = 135.7$ kPa is the isometric tension under maximal activation at the peak intracellular calcium concentration of $Ca_0 = 4.35\,\mu M$. The length dependent calcium sensitivity is governed by the following equation:

$$ECa_{50} = \frac{\left(\mathrm{Ca}_0\right)_{\max}}{\sqrt{\exp\left[B(l - l_0)\right] - 1}}, \tag{5.13.3}$$

where $\left(\mathrm{Ca}_0\right)_{\max} = 4.35\,\mu$M is the maximum peak intracellular calcium concentration, $B = 4.75\,\mu\mathrm{m}^{-1}$ governs the shape of the peak isometric tension-sarcomere length relation, $l_0 = 1.58\,\mu$m is the sarcomere length at which no active tension develops, and l is the sarcomere length which is the product of the fiber stretch λ and the sarcomere unloaded length $l_r = 2.04\,\mu$m.

5.14 Prescribed Active Contraction

Prescribed active contraction models allow the user to directly specify the time history of the active contractile stress.

5.14.1 Uniaxial Active Contraction

For this model, the active stress is acting along a prescribed direction given by the unit vector $\mathbf{a}_r$ in the reference configuration. The 2^{nd} Piola-Kirchhoff stress is

$$\mathbf{S}^a = T^a \mathbf{a}_r \otimes \mathbf{a}_r \,, \tag{5.14.1}$$

and the Cauchy stress is

$$\boldsymbol{\sigma}^a = J^{-1} T^a \mathbf{a} \otimes \mathbf{a} \,, \tag{5.14.2}$$

where T^a is the prescribed contractile stress and $\mathbf{a} = \mathbf{F} \cdot \mathbf{a}_r$. Since $\mathbf{S}^a$ is not a function of deformation, the material and spatial tangents are both zero.

5.14.2 Transversely Isotropic Active Contraction

In this case, the active stress is isotropic in a plane transverse to the direction $\mathbf{a}_r$,

$$\mathbf{S}^a = T^a \left(\mathbf{I} - \mathbf{a}_r \otimes \mathbf{a}_r \right) \,, \tag{5.14.3}$$

and the corresponding Cauchy stress is

$$\boldsymbol{\sigma}^a = J^{-1} T^a \left(\mathbf{B} - \mathbf{a} \otimes \mathbf{a} \right) \,, \tag{5.14.4}$$

where $\mathbf{B} = \mathbf{F} \cdot \mathbf{F}^T$ is the left Cauchy-Green tensor. The material and spatial tangents are zero.

5.14.3 Isotropic Active Contraction

An isotropic active contractile stress is given by

$$\mathbf{S}^a = T^a \mathbf{I} \tag{5.14.5}$$

and the corresponding Cauchy stress is

$$\boldsymbol{\sigma}^a = J^{-1} T^a \mathbf{B} \,. \tag{5.14.6}$$

The material and spatial tangents are zero.

5.15 Chemical Reaction Production Rate

Production rate constitutive equations provide a relation for $\hat{\zeta}$ as a function of solid matrix strain, solute concentrations, and the concentrations of solid-bound molecular species.

5.15.1 Mass Action Forward

According to the law of mass action for forward reactions,

$$\hat{\zeta} = k\left(\theta, \mathbf{F}, \rho_r^\sigma\right) \prod_\alpha \left(c^\alpha\right)^{\nu_R^\alpha} . \tag{5.15.1}$$

A constitutive relation for the specific reaction rate $k\left(\theta, \mathbf{F}, \rho_r^\sigma\right)$ must also be provided.

5.15.2 Mass Action Reversible

According to the law of mass action for reversible reactions,

$$\begin{aligned} \hat{\zeta}_F &= k_F\left(\theta, \mathbf{F}, \rho_r^\sigma\right) \prod_\alpha \left(c^\alpha\right)^{\nu_R^\alpha} \\ \hat{\zeta}_R &= k_R\left(\theta, \mathbf{F}, \rho_r^\sigma\right) \prod_\alpha \left(c^\alpha\right)^{\nu_P^\alpha} \\ \hat{\zeta} &= \hat{\zeta}_F - \hat{\zeta}_R = \hat{\zeta}_F \left[1 - K_c\left(\theta, \mathbf{F}, \rho_r^\sigma\right) \prod_\alpha \left(c^\alpha\right)^{\nu^\alpha}\right] , \end{aligned} \tag{5.15.2}$$

where $K_c = k_R/k_F$ is a function that reduces to the equilibrium constant of the reversible reaction at chemical equilibrium (when $\hat{\zeta} = 0$). Constitutive relations for the specific forward and reverse reaction rates, $k_F\left(\theta, \mathbf{F}, \rho_r^\sigma\right)$ and $k_R\left(\theta, \mathbf{F}, \rho_r^\sigma\right)$ respectively, must also be provided.

5.15.3 Michaelis-Menten

Michaelis-Menten is a model for enzyme kinetics as represented by the reactions

$$\mathcal{E}^e + \mathcal{E}^s \rightleftharpoons \mathcal{E}^{es} \rightarrow \mathcal{E}^e + \mathcal{E}^p , \tag{5.15.3}$$

where $\mathcal{E}^e$ is the enzyme, $\mathcal{E}^s$ is the substrate, $\mathcal{E}^{es}$ is the enzyme-substrate complex, and $\mathcal{E}^p$ is the product. The molar mass supply $\hat{c}^p$ producing $\mathcal{E}^p$ is related to the concentration of the substrate $\mathcal{E}^s$ via

$$\hat{c}^p = \frac{V_{max} c^s}{K_m + c^s} , \tag{5.15.4}$$

where V_{max} is the maximum rate achieved by the system, at maximum (saturating) substrate concentrations. K_m is the substrate concentration at which the reaction rate is half of V_{max}.

This relation may be derived by applying the law of mass action to the two reactions in (5.15.3). under the simplifying assumption that the reversible reaction between the enzyme and substrate reaches steady state much faster than the subsequent forward reaction forming the product. If the first and second reactions are denoted by subscripts 1 and 2, respectively, the law of mass action for the first (reversible) and second (forwar) reaction produces

$$\begin{aligned} &\hat{\zeta}_1 = k_{F1} c^e c^s - k_{R1} c^{es}, \quad \hat{\zeta}_2 = k_{F2} c^{es} , \\ &\hat{c}^s = -\hat{\zeta}_1, \quad \hat{c}^p = \hat{\zeta}_2, \quad \hat{c}^{es} = \hat{\zeta}_1 - \hat{\zeta}_2 . \end{aligned} \tag{5.15.5}$$

The total enzyme concentration remains constant at $c_0^e = c^e + c^{es}$, so that $\hat{\zeta}_1 = k_{F1} c_0^e c^s - (k_{F1} c^s + k_{R1})\, c^{es}$. Assuming that the first reaction equilibrates much faster than the second is equivalent to letting $\hat{\zeta}_1 \approx 0$, in which case

$$c^{es} \approx \frac{c_0^e c^s}{c^s + K_m}\,, \tag{5.15.6}$$

where $K_m = k_{R1}/k_{F1}$. Then,

$$\hat{\zeta}_2 = \frac{V_{\max} c^s}{c^s + K_m}\,,$$

where $V_{\max} = k_{F2} c_0^e$ represents the maximum value of $\hat{\zeta}_2$, when $K_m \ll c^s$. In practice, choosing $k_{F1} \gg k_{F2}$ can produce the desired effect.

5.16 Specific Reaction Rate

Specific reaction rate constitutive equations provide a relation for k as a function of solid matrix strain and the concentrations of solid-bound molecular species.

5.16.1 Constant Specific Reaction Rate

For this material model, k is constant.

5.16.2 Huiskes Remodeling

For this material, the specific reaction rate depends on the deviation of the specific strain energy from a threshold value,

$$k\left(\mathbf{F}, \rho_r^s\right) = \frac{B}{\left(J - \varphi_r^s\right) M^s} \left(\frac{\Psi_r}{\rho_r^s} - \psi_0 \right) ,, \tag{5.16.1}$$

where B is a constant, Ψ_r is the strain energy density of the solid, ρ_r^s is the referential mass density of the solid, ψ_0 is the threshold value for the specific strain energy. In this relation, $J = \det \mathbf{F}$ is evaluated from the solid deformation and φ_r^s is evaluated from (2.10.7).

5.17 Viscous Fluids

The most common family of constitutive relations employed for viscous fluids, including Newtonian fluids, is given by

$$\boldsymbol{\tau}\left(J, \mathbf{D}\right) = \left(\kappa - \frac{2}{3}\mu \right) \left(\operatorname{tr} \mathbf{D}\right)\, \mathbf{I} + 2\mu\, \mathbf{D}\,, \tag{5.17.1}$$

where μ and κ are, respectively, the dynamic shear and bulk viscosity coefficients (both positive), which may generally depend on J and, for non-Newtonian fluids, on invariants of $\mathbf{D}$. In practice, most constitutive models for non-Newtonian viscous fluids only use a dependence on $\dot{\gamma} = \sqrt{2\mathbf{D} : \mathbf{D}}$, since it is the only non-zero invariant in viscometric flows [85]. In this case, substituting eq.(5.17.1) into eq.(3.5.9) produces

$$\begin{aligned} \boldsymbol{\mathcal{C}}^{\tau} = &\left(\kappa - \frac{2}{3}\mu \right) \mathbf{I} \otimes \mathbf{I} + \frac{2}{\dot{\gamma}} \left(\frac{\partial \kappa}{\partial \dot{\gamma}} - \frac{2}{3} \frac{\partial \mu}{\partial \dot{\gamma}} \right) \left(\operatorname{tr} \mathbf{D}\right) \mathbf{I} \otimes \mathbf{D} \\ &+ 2 \left(\frac{2}{\dot{\gamma}} \frac{\partial \mu}{\partial \dot{\gamma}} \mathbf{D} \otimes \mathbf{D} + \mu\, \mathbf{I} \odot \mathbf{I} \right) . \end{aligned} \tag{5.17.2}$$

The term containing $\mathbf{I} \otimes \mathbf{D}$ is the only one that does not exhibit major symmetry. In Newtonian fluids, μ and κ are independent of $\mathbf{D}$; in incompressible fluids they are independent of J (since $J = 1$ remains constant and $\operatorname{tr} \mathbf{D} = 0$). Thus, for both of these cases the term containing $\mathbf{I} \otimes \mathbf{D}$ drops out and $\mathcal{C}^\tau$ exhibits major symmetry.

Similarly, using eq.(5.17.1), the tangent $\boldsymbol{\tau}'_J$ in eq.(3.5.11) reduces to

$$\boldsymbol{\tau}'_J = \left(\frac{\partial \kappa}{\partial J} - \frac{2}{3} \frac{\partial \mu}{\partial J} \right) (\operatorname{tr} \mathbf{D})\, \mathbf{I} + 2 \frac{\partial \mu}{\partial J} \mathbf{D} \,. \tag{5.17.3}$$

Explicit forms for the dependence of μ or κ on J are not illustrated here, since viscosity generally shows negligible dependence on pressure (thus J) over typical ranges of pressures in fluids, hence $\boldsymbol{\tau}'_J \approx \mathbf{0}$ in most analyses.

Many fluid mechanics textbooks employ Stoke's condition ($\kappa = 0$) for the purpose of equating the elastic pressure p with the mean normal stress $-\frac{1}{3} \operatorname{tr} \boldsymbol{\sigma}$ [79]; in FEBio, κ is kept as a user-defined material property, which may be set to zero if desired. A common example of a non-Newtonian fluid is the Carreau model, where $\boldsymbol{\tau} = 2\mu(\dot{\gamma})\, \mathbf{D}$, which is a special case of eq.(5.17.1), with $\kappa = 2\mu/3$ and

$$\mu = \mu_\infty + (\mu_0 - \mu_\infty) \left(1 + (\lambda \dot{\gamma})^2 \right)^{(n-1)/2} , \tag{5.17.4}$$

where λ is a time constant, n is a parameter governing the power-law response, μ_0 is the viscosity when $\dot{\gamma} = 0$ and μ_∞ is the viscosity as $\dot{\gamma} \to \infty$. Other common models of non-Newtonian viscous fluids are summarized in [32], though it should be noted that some of these models produce infinite values when evaluating $\dot{\gamma}^{-1} \partial \mu / \partial \dot{\gamma}$ as $\dot{\gamma} \to 0$, which is problematic in the evaluation of $\mathcal{C}^\tau$ in eq.(5.17.2).

For nearly incompressible fluids, a simple constitutive relation may be adopted for the pressure,

$$p(J) = K(1 - J) \,, \tag{5.17.5}$$

where K is the bulk modulus of the fluid in the limit when $J = 1$. It follows that $p'(J) = -K$ and $p''(J) = 0$ in eq.(3.5.10). This constitutive relation is adopted for nearly-incompressible CFD analyses in FEBio, though alternative formulations may be easily implemented.

Chapter 6

Dynamics

FEBio can perform a nonlinear dynamic analysis by iteratively solving the following nonlinear semi-discrete finite element equations [18].

$$\begin{aligned} \mathbf{M}\ddot{\mathbf{d}}_{n+1}^{k} + \mathbf{K}\Delta\mathbf{d}^{k} &= \mathbf{T}_{n+1}^{k} - \mathbf{F}_{n+1} \\ \mathbf{d}_{n+1}^{k} &= \mathbf{d}_{n+1}^{k-1} + \Delta\mathbf{d}^{k} \end{aligned} . \tag{6.0.1}$$

Here, $\mathbf{M}$ is the mass matrix, $\mathbf{K}$ the stiffness matrix, $\mathbf{T}$ the internal force (stress) vector and $\mathbf{F}$ the externally applied loads. The upperscript index k refers to the iteration number, the subscript $n$refers to the time increment. The trapezoidal (or midpoint) rule is used to perform the time integration. This results in the following approximations for the displacement and velocity updates.

$$\begin{aligned} \mathbf{d}_{n+1} &= \mathbf{d}_{n} + \frac{h}{2}\left(\dot{\mathbf{d}}_{n} + \dot{\mathbf{d}}_{n+1}\right) \\ \dot{\mathbf{d}}_{n+1} &= \dot{\mathbf{d}}_{n} + \frac{h}{2}\left(\ddot{\mathbf{d}}_{n} + \ddot{\mathbf{d}}_{n+1}\right) \end{aligned} . \tag{6.0.2}$$

Using (6.0.2) we can solve for $\ddot{\mathbf{d}}_{n+1}$,

$$\ddot{\mathbf{d}}_{n+1}^{k} = \frac{4}{h^2}\left(\mathbf{d}_{n+1}^{k-1} - \mathbf{d}_{n} + \Delta\mathbf{d}^{k}\right) - \frac{4}{h}\dot{\mathbf{d}}_{n} - \ddot{\mathbf{d}}_{n} . \tag{6.0.3}$$

Substituting this into equation (6.0.1) results in the following linear system of equations.

$$\left(\frac{4}{h^2}\mathbf{M} + \mathbf{K}\right)\Delta\mathbf{d}^{k} = \mathbf{T}_{n+1}^{k} - \mathbf{F}_{n+1} - \mathbf{M}\left(\frac{4}{h^2}\left(\mathbf{d}_{n+1}^{k-1} - \mathbf{d}_{n}\right) - \frac{4}{h}\dot{\mathbf{d}}_{n} - \ddot{\mathbf{d}}_{n}\right) . \tag{6.0.4}$$

Solving this equation for $\Delta\mathbf{d}^{k}$ and using (6.0.1) gives the new displacement vector $\mathbf{d}_{n+1}^{k}$. The acceleration vector $\ddot{\mathbf{d}}_{n+1}^{k}$ can then be found from (6.0.3) and the velocity vector $\dot{\mathbf{d}}_{n+1}^{k}$ from(6.0.3). This algorithm is repeated until convergence is reached.

6.1 Newmark Integration

To solve a differential equation which is second-order in time, we need to perform a numerical integration in the time domain. Let $\theta(t)$ denote the function of interest and let t_n and t_{n+1} represent consecutive time steps such that $\Delta t = t_{n+1} - t_n$. The function $\theta(t)$ may be represented at each time point as $\theta_n = \theta(t_n)$ and $\theta_{n+1} = \theta(t_{n+1})$. The Newmark integration formulas are used to

evaluate θ_{n+1} and $\dot{\theta}_{n+1}$ at time θ_{n+1}, assuming that they can be integrated from a judiciously selected $\ddot{\theta}\left(t_{n+\gamma}\right)$ in the time interval $[t_n, t_{n+1}]$. Using the mean value theorem for definite integrals, we know that an exact solution may be found for the integral according to

$$\int_{t_n}^{t_{n+1}} \ddot{\theta}\left(t\right)\, dt = \dot{\theta}_{n+1} - \dot{\theta}_n \equiv \ddot{\theta}\left(t_{n+\gamma}\right) \Delta t\,, \tag{6.1.1}$$

where γ is generally unknown *a priori*. In the Newmark integration scheme we let

$$\ddot{\theta}\left(t_{n+\gamma}\right) = \gamma \ddot{\theta}_{n+1} + \left(1-\gamma\right) \ddot{\theta}_n\,, \tag{6.1.2}$$

where γ is a user-selected parameter in the range 0 to 1. It follows that

$$\dot{\theta}_{n+1} = \dot{\theta}_n + \Delta t \left[\gamma \ddot{\theta}_{n+1} + \left(1-\gamma\right) \ddot{\theta}_n\right]\,. \tag{6.1.3}$$

We can similarly integrate this function twice to obtain θ_{n+1},

$$\int_{t_n}^{t_{n+1}} \int_{t_n}^{t} \ddot{\theta}\left(\tau\right)\, d\tau\, dt = \int_{t_n}^{t_{n+1}} \left(\dot{\theta}\left(t\right) - \dot{\theta}_n\right)\, dt = \theta_{n+1} - \theta_n - \dot{\theta}_n \Delta t \equiv \ddot{\theta}\left(t_{n+2\beta}\right) \frac{\Delta t^2}{2}$$

where we let

$$\ddot{\theta}\left(t_{n+2\beta}\right) = 2\beta \ddot{\theta}_{n+1} + \left(1-2\beta\right) \ddot{\theta}_n\,.$$

Here, β represents a parameter that varies from 0 to $\frac{1}{2}$. It follows that

$$\theta_{n+1} = \theta_n + \dot{\theta}_n \Delta t + \frac{\Delta t^2}{2} \left[2\beta \ddot{\theta}_{n+1} + \left(1-2\beta\right) \ddot{\theta}_n\right]\,, \tag{6.1.4}$$

or alternatively,

$$\ddot{\theta}_{n+1} = \frac{1}{\beta \Delta t^2} \left(\theta_{n+1} - \theta_n - \dot{\theta}_n \Delta t\right) - \left(\frac{1}{2\beta} - 1\right) \ddot{\theta}_n\,, \tag{6.1.5}$$

from which we may re-evaluate (6.1.3) as

$$\dot{\theta}_{n+1} = \dot{\theta}_n + \Delta t \left[\frac{\gamma}{\beta \Delta t^2} \left(\theta_{n+1} - \theta_n - \dot{\theta}_n \Delta t\right) + \left(1 - \frac{\gamma}{2\beta}\right) \ddot{\theta}_n\right]\,. \tag{6.1.6}$$

Stability of this integration scheme is guaranteed when

$$\gamma \geq \frac{1}{2}\,, \quad \beta \geq \frac{\left(\gamma + \frac{1}{2}\right)^2}{4}\,. \tag{6.1.7}$$

6.2 Elastodynamics

6.2.1 Governing Equations

The linear momentum balance for elastodynamics is

$$\rho \mathbf{a} = \operatorname{div} \boldsymbol{\sigma} + \rho \mathbf{b}\,, \tag{6.2.1}$$

where ρ is the density, $\mathbf{a}$ is the acceleration, $\boldsymbol{\sigma}$ is the Cauchy stress, and $\mathbf{b}$ is the body force per mass. The angular momentum balance is satisfied by letting $\boldsymbol{\sigma}^T = \boldsymbol{\sigma}$. The integrated form of the mass balance equations yields

$$\rho = \frac{\rho_r}{J}\,, \tag{6.2.2}$$

where ρ_r is the density in the reference configuration and $J = \det \mathbf{F}$, where $\mathbf{F}$ is the deformation gradient. The acceleration is given by the material time derivative of the velocity $\mathbf{v}$, evaluated either in a spatial or a material frame,

$$\mathbf{a} = \dot{\mathbf{v}} \tag{6.2.3}$$

6.2.2 Virtual Work

The virtual work for the domain b is given by

$$\delta W = \int_b \delta\mathbf{v} \cdot (\operatorname{div}\boldsymbol{\sigma} + \rho\,(\mathbf{b} - \mathbf{a}))\; dv\,, \tag{6.2.4}$$

where $\delta\mathbf{v}$ is the virtual velocity. Using the divergence theorem, this virtual work may be expressed as the difference $\delta W = \delta W_{ext} - \delta W_{int}$ between external virtual work δW_{ext} and internal virtual work δW_{int}, where

$$\begin{aligned} \delta W_{int} &= \int_b \boldsymbol{\sigma} : \operatorname{grad}\delta\mathbf{v}\, dv + \int_b \delta\mathbf{v}\cdot\rho\mathbf{a}\, dv\,, \\ \delta W_{ext} &= \int_{\partial b} \delta\mathbf{v}\cdot\mathbf{t}\, da + \int_b \delta\mathbf{v}\cdot\rho\mathbf{b}\, dv\,, \end{aligned} \tag{6.2.5}$$

where $\mathbf{t} = \boldsymbol{\sigma}\cdot\mathbf{n}$ is the traction on the boundary ∂b.

6.2.3 Generalized $\alpha-$Method for Elastodynamics

In the generalized $\alpha-$method, we evaluate displacements and velocities at the intermediate time $t_{n+\alpha_f} = t_n + \alpha_f\,(t_{n+1} - t_n)$, where α_f is a user-defined parameter ($0 < \alpha_f \leq 1$), such that

$$\begin{aligned} \boldsymbol{\chi}_{n+\alpha_f} &= (1-\alpha_f)\,\boldsymbol{\chi}_n + \alpha_f\boldsymbol{\chi}_{n+1}\,, \\ \mathbf{u}_{n+\alpha_f} &= (1-\alpha_f)\,\mathbf{u}_n + \alpha_f\mathbf{u}_{n+1}\,, \\ \mathbf{v}_{n+\alpha_f} &= (1-\alpha_f)\,\mathbf{v}_n + \alpha_f\mathbf{v}_{n+1}\,, \end{aligned} \tag{6.2.6}$$

where $\boldsymbol{\chi}$ is the motion and $\mathbf{u}$ is the displacement. In particular, it follows that the deformation gradient and its determinant are given at the intermediate time by

$$\mathbf{F}_{n+\alpha_f} = \frac{\partial\boldsymbol{\chi}_{n+\alpha_f}}{\partial\mathbf{X}} = (1-\alpha_f)\,\mathbf{F}_n + \alpha_f\mathbf{F}_{n+1}\,, \tag{6.2.7}$$

and

$$J_{n+\alpha_f} = \det\mathbf{F}_{n+\alpha_f}\,. \tag{6.2.8}$$

The material time derivative of $J_{n+\alpha_f}$, and the velocity gradient $\mathbf{L}_{n+\alpha_f}$ are normally evaluated as

$$\dot{J}_{n+\alpha_f} = J_{n+\alpha_f}\mathbf{F}^{-T}_{n+\alpha_f} : \operatorname{Grad}\mathbf{v}_{n+\alpha_f}\,, \tag{6.2.9}$$

and

$$\mathbf{L}_{n+\alpha_f} = \operatorname{Grad}\mathbf{v}_{n+\alpha_f}\cdot\mathbf{F}^{-1}_{n+\alpha_f}\,. \tag{6.2.10}$$

In practice however, we get better numerical results when using

$$\dot{J}_{n+\alpha_f} = \frac{J_{n+1} - J_n}{\Delta t}\,, \tag{6.2.11}$$

and

$$\mathbf{L}_{n+\alpha_f} = \frac{\mathbf{F}_{n+1} - \mathbf{F}_n}{\Delta t}\cdot\mathbf{F}^{-1}_{n+\alpha_f}\,. \tag{6.2.12}$$

According to the generalized$-\alpha$ method, we evaluate the velocity derivative at a different intermediate time $t_{n+\alpha_m} = t_n + \alpha_m\,(t_{n+1} - t_n)$, such that

$$\dot{\mathbf{v}}_{n+\alpha_m} = (1-\alpha_m)\,\dot{\mathbf{v}}_n + \alpha_m\dot{\mathbf{v}}_{n+1}\,. \tag{6.2.13}$$

Since elastodynamics represent a second-order system of equations in time, the parameters α_f and α_m are evaluated from a single parameter ρ_∞ using [21]

$$\alpha_f = \frac{1}{1+\rho_\infty}\,, \quad \alpha_m = \frac{2-\rho_\infty}{1+\rho_\infty}\,, \tag{6.2.14}$$

where $0 \leq \rho_\infty \leq 1$. This parameter is the spectral radius for an infinite time step, which controls the amount of damping of high frequencies; a value of zero produces the greatest amount of damping, anihilating the highest frequency in one step, whereas a value of one preserves the highest frequency.

To complete the integration scheme [57], we evaluate

$$\begin{aligned} \beta &= \frac{1}{4}\left(1+\alpha_m-\alpha_f\right)^2 \\ \gamma &= \frac{1}{2}+\alpha_m-\alpha_f \end{aligned}\,, \tag{6.2.15}$$

then we use the Newmark integration formulas (Section 6.1),

$$\begin{aligned} \mathbf{v}_{n+1} &= \mathbf{v}_n + \Delta t\left[(1-\gamma)\,\dot{\mathbf{v}}_n + \gamma\dot{\mathbf{v}}_{n+1}\right] \\ \mathbf{u}_{n+1} &= \mathbf{u}_n + \Delta t\mathbf{v}_n + \frac{\Delta t^2}{2}\left[(1-2\beta)\,\dot{\mathbf{v}}_n + 2\beta\dot{\mathbf{v}}_{n+1}\right] \\ \dot{\mathbf{v}}_{n+1} &= \frac{1}{\beta\Delta t}\left(\frac{\mathbf{u}_{n+1}-\mathbf{u}_n}{\Delta t}-\mathbf{v}_n\right)+\left(1-\frac{1}{2\beta}\right)\dot{\mathbf{v}}_n \end{aligned}\,. \tag{6.2.16}$$

At the start of each time step, we initialize the variables as follows:

$$\begin{aligned} \mathbf{u}_{n+1} &= \mathbf{u}_n \\ \dot{\mathbf{v}}_{n+1} &= \left(1-\frac{1}{2\beta}\right)\dot{\mathbf{v}}_n - \frac{1}{\beta\Delta t}\mathbf{v}_n \\ \mathbf{v}_{n+1} &= \left(1-\frac{\gamma}{\beta}\right)\mathbf{v}_n + \Delta t\left(1-\frac{\gamma}{2\beta}\right)\dot{\mathbf{v}}_n \end{aligned}\,. \tag{6.2.17}$$

6.2.4 Linearization

The solution of the nonlinear equation $\delta W = 0$ is obtained by linearizing this relation as

$$\delta W + D\delta W\left[\Delta\mathbf{u}\right] \approx 0\,, \tag{6.2.18}$$

where the operator $D\delta W\left[\cdot\right]$ represents the directional derivative of δW at $\mathbf{u}$ along an increment $\Delta\mathbf{u}$ of $\mathbf{u}_{n+1}$ [27]. According to the generalized$-\alpha$ method [57], the virtual work is evaluated using intermediate time step values, at $t_{n+\alpha_f}$ for all parameters except $\dot{\mathbf{v}}$, which is evaluated at $t_{n+\alpha_m}$. It follows from these definitions that the linearizations of critical variables are given by

$$\begin{aligned} D\mathbf{u}\left[\Delta\mathbf{u}\right] &= \alpha_f\Delta\mathbf{u} \\ D\mathbf{F}\left[\Delta\mathbf{u}\right] &= \alpha_f\,\mathrm{Grad}\,\Delta\mathbf{u} \\ DJ\left[\Delta\mathbf{u}\right] &= \alpha_f J\left(\mathrm{div}\,\Delta\mathbf{u}\right) \\ D\dot{J}\left[\Delta\mathbf{u}\right] &= D\left(J\mathbf{F}^{-T} : \mathrm{Grad}\,\mathbf{v}\right)\left[\Delta\mathbf{u}\right] \\ &= \alpha_f J\left[\left(\mathrm{div}\,\mathbf{v}+\frac{\gamma}{\beta\Delta t}\right)\left(\mathrm{div}\,\Delta\mathbf{u}\right)-\left(\mathrm{grad}\,\Delta\mathbf{u}\right)^T : \mathbf{L}\right] \\ D\mathbf{v}\left[\Delta\mathbf{u}\right] &= \frac{\alpha_f\gamma}{\beta\Delta t}\Delta\mathbf{u} \\ D\dot{\mathbf{v}}\left[\Delta\mathbf{u}\right] &= \frac{\alpha_m}{\beta\Delta t^2}\Delta\mathbf{u} \end{aligned}\,. \tag{6.2.19}$$

To linearize the virtual work, we need to express the integrals appearing in δW_{int} and δW_{ext} over the material frame of the finite element solid domain.

6.2.4.1 Internal Work

The first term in the internal work becomes

$$\int_b \boldsymbol{\sigma} : \operatorname{grad} \delta\mathbf{v}\, dv = \int_B \mathbf{F}\cdot\mathbf{S} : \operatorname{Grad} \delta\mathbf{v}\, dV \quad , \tag{6.2.20}$$

where $\mathbf{S} = J\cdot\mathbf{F}^{-1}\cdot\boldsymbol{\sigma}\cdot\mathbf{F}^{-T}$ is the second Piola-Kirchhoff stress for the solid material. In general, $\boldsymbol{\sigma}$ (and thus, $\mathbf{S}$) is only a function of the solid strain, such as the right Cauchy-Green tensor $\mathbf{C} = \mathbf{F}^T\cdot\mathbf{F}$ or the Green-Lagrange strain $\mathbf{E} = (\mathbf{C}-\mathbf{I})/2$.

$$D\mathbf{E}[\Delta\mathbf{u}] = \frac{\alpha_f}{2}\left(\operatorname{Grad}^T \Delta\mathbf{u}\cdot\mathbf{F} + \mathbf{F}^T\cdot\operatorname{Grad}\Delta\mathbf{u}\right) . \tag{6.2.21}$$

Therefore, following the standard approach in solid mechanics, the linearization of $\mathbf{S}$ is

$$\begin{aligned} D\mathbf{S}[\Delta\mathbf{u}] &= \frac{\partial\mathbf{S}}{\partial\mathbf{E}} : D\mathbf{E}[\Delta\mathbf{u}] \\ &= \alpha_f\mathbb{C} : \frac{1}{2}\left(\operatorname{Grad}^T\Delta\mathbf{u}\cdot\mathbf{F} + \mathbf{F}^T\cdot\operatorname{Grad}\Delta\mathbf{u}\right), \\ &= \alpha_f\mathbb{C} : \left(\mathbf{F}^T \oslash \mathbf{F}^T\right) : \Delta\boldsymbol{\varepsilon} \end{aligned} \tag{6.2.22}$$

where $\mathbb{C}$ is the material elasticity tensor. Now, the linearization of the first term in δW_{int} is

$$\boxed{\begin{aligned} &D\left(\int_B \mathbf{F}\cdot\mathbf{S} : \operatorname{Grad}\delta\mathbf{v}\, dV\right)[\Delta\mathbf{u}] \\ &= \int_v \alpha_f\left(\operatorname{grad}\delta\mathbf{v} : \operatorname{grad}\Delta\mathbf{u}\cdot\boldsymbol{\sigma} + \operatorname{grad}\delta\mathbf{v} : \boldsymbol{\mathcal{C}} : \operatorname{grad}\Delta\mathbf{u}\right) dv \end{aligned}} . \tag{6.2.23}$$

where $\boldsymbol{\mathcal{C}}$ is the spatial elasticity tensor. Similarly, the second term in δW_{int} produces

$$\boxed{D\left(\int_B \delta\mathbf{v}\cdot\rho_r\mathbf{a}\, dV\right)[\Delta\mathbf{u}] = \int_b \delta\mathbf{v}\cdot\frac{\alpha_m}{\beta\Delta t^2}\rho\Delta\mathbf{u}\, dv} . \tag{6.2.24}$$

6.2.4.2 External Work

The linearization of the body force term is

$$D\left(\int_B \delta\mathbf{v}\cdot\rho_r\mathbf{b}\, dV\right)[\Delta\mathbf{u}] = \int_b \delta\mathbf{v}\cdot\alpha_f\rho\operatorname{grad}\mathbf{b}\cdot\Delta\mathbf{u}\, dv . \tag{6.2.25}$$

The linearization of the traction force term is

$$\begin{aligned} &D\left(\int_{\Gamma_\eta} \delta\mathbf{v}\cdot\mathbf{t}\,|\mathbf{g}_1\times\mathbf{g}_2|\; d\eta^1 d\eta^2\right)[\Delta\mathbf{u}] \\ &= \int_{\Gamma_\eta} \alpha_f\delta\mathbf{v}\cdot(\mathbf{t}\otimes\mathbf{n})\cdot\left(\mathbf{g}_1\times\frac{\partial\Delta\mathbf{u}}{\partial\eta^2} - \mathbf{g}_2\times\frac{\partial\Delta\mathbf{u}}{\partial\eta^1}\right) d\eta^1 d\eta^2 . \\ &+ \int_{\Gamma_\eta} \delta\mathbf{v}\cdot D\mathbf{t}[\Delta\mathbf{u}]\,|\mathbf{g}_1\times\mathbf{g}_2|\; d\eta^1 d\eta^2 \end{aligned} \tag{6.2.26}$$

Note that $D\mathbf{t}\left[\Delta\mathbf{u}\right]$ depends on the nature of the surface traction. For a prescribed traction we have $D\mathbf{t}\left[\Delta\mathbf{u}\right] = \mathbf{0}$. A contact analysis needs more elaborate derivations (not yet implemented as of FEBio 2.7). In the above expression we used

$$\begin{aligned} D\left|\mathbf{g}_1 \times \mathbf{g}_2\right|\left[\Delta\mathbf{u}\right] &= \mathbf{n} \cdot D\left(\mathbf{g}_1 \times \mathbf{g}_2\right)\left[\Delta\mathbf{u}\right] \\ &= \alpha_f \mathbf{n} \cdot \left(\mathbf{g}_1 \times \frac{\partial \Delta\mathbf{u}}{\partial \eta^2} - \mathbf{g}_2 \times \frac{\partial \Delta\mathbf{u}}{\partial \eta^1}\right) \end{aligned} \tag{6.2.27}$$

where the unit outward normal is evaluated as

$$\mathbf{n} = \frac{\mathbf{g}_1 \times \mathbf{g}_2}{\left|\mathbf{g}_1 \times \mathbf{g}_2\right|}\,. \tag{6.2.28}$$

6.2.5 Discretization

We use the following interpolations:

$$\begin{aligned} \delta\mathbf{v} &= \sum_a N_a \delta\mathbf{v}_a & \Delta\mathbf{u} &= \sum_b N_b \Delta\mathbf{u}_b \\ \operatorname{grad}\delta\mathbf{v} &= \sum_a \delta\mathbf{v}_a \otimes \operatorname{grad} N_a & \operatorname{grad}\Delta\mathbf{u} &= \sum_b \Delta\mathbf{u}_b \otimes \operatorname{grad} N_b \\ \operatorname{div}\delta\mathbf{v} &= \sum_a \delta\mathbf{v}_a \cdot \operatorname{grad} N_a & \operatorname{div}\Delta\mathbf{u} &= \sum_b \Delta\mathbf{u}_b \cdot \operatorname{grad} N_b \end{aligned}\,, \tag{6.2.29}$$

where $N_a\left(\eta^1, \eta^2, \eta^3\right)$ are shape functions of the element parametric coordinates $\left(\eta^1, \eta^2, \eta^3\right)$. Note that the $\operatorname{grad} \equiv \frac{\partial}{\partial \mathbf{x}}$ operator should be evaluated at $t_{n+\alpha_f}$, using $\mathbf{x}_{n+\alpha_f}$. For example, in the case of a scalar function f,

$$\begin{aligned} \operatorname{grad} f &= \frac{\partial f}{\partial \mathbf{x}_{n+\alpha_f}} = \frac{\partial f}{\partial \eta^i}\mathbf{g}^i_{n+\alpha_f} \\ \mathbf{g}^i_{n+\alpha_f} &= \frac{\partial \eta^i}{\partial \mathbf{x}_{n+\alpha_f}} \end{aligned}\,,$$

where the contravariant basis vectors $\mathbf{g}^i_{n+\alpha_f}$ may be evaluated from the covariant basis vectors

$$\mathbf{g}_i^{n+\alpha_f} = \frac{\partial \mathbf{x}_{n+\alpha_f}}{\partial \eta^i} = \left(1-\alpha_f\right)\frac{\partial \mathbf{x}_n}{\partial \eta^i} + \alpha_f \frac{\partial \mathbf{x}_{n+1}}{\partial \eta^i}$$

using $\mathbf{g}_i^{n+\alpha_f} \cdot \mathbf{g}^j_{n+\alpha_f} = \delta^j_i$.

The discretization of the internal work produces

$$\delta W_{int} = \sum_a \delta\mathbf{v}_a \cdot \int_b \left(\mathbf{f}^u_a + \mathbf{f}^\rho_a\right)\, dv\,, \tag{6.2.30}$$

where

$$\boxed{\begin{aligned} \mathbf{f}^u_a &= \boldsymbol{\sigma} \cdot \operatorname{grad} N_a \\ \mathbf{f}^\rho_a &= N_a \rho \mathbf{a} \end{aligned}}\,. \tag{6.2.31}$$

The discretization of the stress and elasticity terms in the internal work is

$$\begin{aligned} &\int_v \alpha_f \left(\operatorname{grad}\delta\mathbf{v} : \operatorname{grad}\Delta\mathbf{u} \cdot \boldsymbol{\sigma} + \operatorname{grad}\delta\mathbf{v} : \boldsymbol{\mathcal{C}} : \operatorname{grad}\Delta\mathbf{u}\right)\, dv \\ &= \sum_a \delta\mathbf{v}_a \cdot \sum_b \int_v \mathbf{K}_{ab}\, dv \cdot \Delta\mathbf{u}_b \end{aligned}\,,$$

where

$$\boxed{\mathbf{K}_{ab} = \alpha_f \left((\operatorname{grad} N_a \cdot \boldsymbol{\sigma} \cdot \operatorname{grad} N_b)\, \mathbf{I} + \operatorname{grad} N_a \cdot \boldsymbol{\mathcal{C}} \cdot \operatorname{grad} N_b \right)}. \tag{6.2.32}$$

The discretization of the mass term in the internal work is

$$\int_b \delta\mathbf{v} \cdot \frac{\alpha_m}{\beta \Delta t^2} \rho \Delta\mathbf{u}\, dv = \sum_a \delta\mathbf{v}_a \cdot \sum_b \int_b \mathbf{M}_{ab}\, dv \cdot \Delta\mathbf{u}_b\,,$$

where

$$\boxed{\mathbf{M}_{ab} = \frac{\alpha_m}{\beta \Delta t^2} \rho N_a N_b \mathbf{I}}. \tag{6.2.33}$$

For the external work of body forces,

$$\int_b \delta\mathbf{v} \cdot \rho\mathbf{b}\, dv = \sum_a \delta\mathbf{v}_a \cdot \int_b \mathbf{f}_a^{\mathbf{b}}\, dv$$

where

$$\boxed{\mathbf{f}_a^{\mathbf{b}} = N_a \rho^s \mathbf{b}}, \tag{6.2.34}$$

and

$$\int_b \delta\mathbf{v}^s \cdot \alpha_f \rho^s \operatorname{grad} \mathbf{b} \cdot \Delta\mathbf{u}\, dv = \sum_a \delta\mathbf{v}_a^s \cdot \sum_b \int_b \mathbf{K}_{ab}^{\mathbf{b}}\, dv \cdot \Delta\mathbf{u}_b$$

where

$$\boxed{\mathbf{K}_{ab}^{\mathbf{b}} = \alpha_f N_a N_b \rho^s \operatorname{grad} \mathbf{b}}. \tag{6.2.35}$$

For prescribed tractions,

$$\int_{\partial b} \delta\mathbf{v}^s \cdot \mathbf{t}^s\, da = \sum_a \delta\mathbf{v}_a^s \cdot \int_{\Gamma_\eta} \mathbf{f}_a^t\, d\eta^1 d\eta^2$$

where

$$\boxed{\mathbf{f}_a^t = N_a \mathbf{t}^s\, |\mathbf{g}_1 \times \mathbf{g}_2|}, \tag{6.2.36}$$

and

$$\begin{aligned} &\int_{\Gamma_\eta} \alpha_f \delta\mathbf{v}^s \cdot (\mathbf{t}^s \otimes \mathbf{n}) \cdot \left(\mathbf{g}_1 \times \frac{\partial \Delta\mathbf{u}}{\partial \eta^2} - \mathbf{g}_2 \times \frac{\partial \Delta\mathbf{u}}{\partial \eta^1} \right) d\eta^1 d\eta^2 \\ &= \sum_a \delta\mathbf{v}_a^s \cdot \sum_b \int_{\Gamma_\eta} \mathbf{K}_{ab}^t\, d\eta^1 d\eta^2 \cdot \Delta\mathbf{u}_b \end{aligned}$$

where

$$\boxed{\mathbf{K}_{ab}^t = \alpha_f N_a \left(\mathbf{t}^s \otimes \mathbf{n}\right) \cdot \left(\frac{\partial N_b}{\partial \eta^2} \hat{\mathbf{g}}_1 - \frac{\partial N_b}{\partial \eta^1} \hat{\mathbf{g}}_2 \right)}, \tag{6.2.37}$$

where $\hat{\mathbf{g}}$ is the skew-symmetric tensor whose dual vector is $\mathbf{g}$.

6.2.6 Energy-Momentum Conservation Scheme

The time discretization scheme may be selected in a manner that enforces linear and angular momentum, and energy conservation over consecutive time steps t_n and t_{n+1}, when boundary conditions and external loads are time-independent. Based on the prior literature [46, 82, 95], this momentum and energy conservation may be achieved by using the midpoint rule ($\rho_\infty = 1$, leading to $\alpha_f = \alpha_m = \frac{1}{2}$), and evaluating the virtual work at $t_{n+\frac{1}{2}}$. However, since the virtual work strictly enforces momentum balance only, there is no guarantee that energy conservation will be satisfied as a result of time discretization. Therefore, we need to enforce a specific scheme to satisfy energy balance.

6.2.6.1 Energy Balance

For an elastic solid, in the absence of heat exchanges (i.e., in elastodynamics), the equation of energy balance reduces

$$\rho\dot{\varepsilon} = \boldsymbol{\sigma} : \mathbf{D}\,, \tag{6.2.38}$$

where ε is the specific internal energy and $\mathbf{D}$ is the rate of deformation tensor. Recall that $\varepsilon = \psi + \theta\eta$, where ψ is the specific free energy, θ is the absolute temperature and η is the specific entropy. Since $\eta = 0$ in elasticity (due to the temperature remaining constant), the above energy balance may be combined with the mass balance (6.2.2) as

$$\rho\dot{\psi} = \frac{\rho_r}{J}\dot{\psi} = \boldsymbol{\sigma} : \mathbf{D}\,, \tag{6.2.39}$$

or

$$\dot{\Psi}_r = J\boldsymbol{\sigma} : \mathbf{D}\,, \tag{6.2.40}$$

where $\Psi_r = \rho_r\psi$ is the free energy density (per volume of the material in the reference configuration).

In our time integration scheme, to satisfy energy balance, this equation needs to be evaluated at $t_{n+\alpha_f}$, thus

$$\left(\dot{\Psi}_r\right)_{n+\alpha_f} = J_{n+\alpha_f}\boldsymbol{\sigma}_{n+\alpha_f} : \mathbf{D}_{n+\alpha_f}\,. \tag{6.2.41}$$

However, the solution for $\boldsymbol{\sigma}_{n+\alpha_f} \equiv \boldsymbol{\sigma}\left(\mathbf{F}_{n+\alpha_f}\right)$ obtained from the momentum balance may not necessarity satisfy this equation. Thus, to satisfy energy balance over consecutive time steps, we want to evaluate an effective stress $\tilde{\boldsymbol{\sigma}}_{n+\alpha_f}$ such that

$$J_{n+\alpha_f}\tilde{\boldsymbol{\sigma}}_{n+\alpha_f} : \mathbf{D}_{n+\alpha_f} = \frac{(\Psi_r)_{n+1} - (\Psi_r)_n}{\Delta t}\,. \tag{6.2.42}$$

To find a solution for $\tilde{\boldsymbol{\sigma}}_{n+\alpha_f}$, we follow the procedure of Gonzalez [46] and let

$$\tilde{\boldsymbol{\sigma}}_{n+\alpha_f} = \boldsymbol{\sigma}_{n+\alpha_f} + f\mathbf{D}_{n+\alpha_f}\,, \tag{6.2.43}$$

where f is some scalar function to be determined. Substituting this relation, (6.2.43), into the previous equation, (6.2.42), produces

$$f = \left(\frac{(\Psi_r)_{n+1} - (\Psi_r)_n}{J^s_{n+\alpha_f}\Delta t} - \boldsymbol{\sigma}_{n+\alpha_f} : \mathbf{D}_{n+\alpha_f}\right)\frac{1}{\mathbf{D}_{n+\alpha_f} : \mathbf{D}_{n+\alpha_f}}\,. \tag{6.2.44}$$

Hence, the equation for an effective stress needed to satisfy energy balance between consecutive time steps is

$$\boxed{\tilde{\boldsymbol{\sigma}}_{n+\alpha_f} = \boldsymbol{\sigma}_{n+\alpha_f} + \left(\frac{(\Psi_r)_{n+1} - (\Psi_r)_n}{J_{n+\alpha_f}\Delta t} - \boldsymbol{\sigma}_{n+\alpha_f} : \mathbf{D}_{n+\alpha_f}\right)\frac{\mathbf{D}_{n+\alpha_f}}{\mathbf{D}_{n+\alpha_f} : \mathbf{D}_{n+\alpha_f}}}\,. \tag{6.2.45}$$

In the limit when $\mathbf{D}_{n+\alpha_f} : \mathbf{D}_{n+\alpha_f} = 0$, we use $\tilde{\boldsymbol{\sigma}}_{n+\alpha_f} = \boldsymbol{\sigma}_{n+\alpha_f}$. Recall that this scheme produces conservation of linear and angular momentum and total energy only with $\rho_\infty = 1$, or equivalently, $\alpha_f = \alpha_m = \frac{1}{2}$, $\beta = \frac{1}{2}$ and $\gamma = 1$. Therefore, this effective stress calculation is only applied when the user employs $\rho_\infty = 1$.

6.3 Rigid Body Dynamics

6.3.1 Rigid Body Rotation

6.3.1.1 Exponential Map

Conventionally, the rigid body rotation tensor $\mathbf{\Lambda}$ corresponding to a rotation of angle χ about the unit vector $\mathbf{n}$ may be expressed in terms of the vector $\boldsymbol{\chi} = \chi\mathbf{n}$ as

$$\mathbf{\Lambda}(\boldsymbol{\chi}) = \cos\chi\,\mathbf{I} - \sin\chi\,\boldsymbol{\mathcal{E}}\cdot\mathbf{n} + (1-\cos\chi)\,\mathbf{n}\otimes\mathbf{n} \tag{6.3.1}$$

where $\boldsymbol{\mathcal{E}}$ is the third-order permutation pseudo-tensor with Cartesian components ε_{ijk}. Making use of the trigonometric identity,

$$\cos\chi = 1 - 2\sin^2\frac{1}{2}\chi\,, \tag{6.3.2}$$

this expression may be rearranged as

$$\mathbf{\Lambda}(\boldsymbol{\chi}) = \mathbf{I} - \frac{\sin\chi}{\chi}\,\boldsymbol{\mathcal{E}}\cdot\boldsymbol{\chi} + \frac{2}{\chi^2}\sin^2\frac{1}{2}\chi\,(\boldsymbol{\mathcal{E}}\cdot\boldsymbol{\chi})^2\,, \tag{6.3.3}$$

where we have made use of the identity

$$(\boldsymbol{\mathcal{E}}\cdot\boldsymbol{\chi})^2 = \boldsymbol{\chi}\otimes\boldsymbol{\chi} - \chi^2\mathbf{I}\,. \tag{6.3.4}$$

Letting

$$\hat{\boldsymbol{\chi}} = -\boldsymbol{\mathcal{E}}\cdot\boldsymbol{\chi} \tag{6.3.5}$$

represent the antisymmetric tensor with axial vector $\boldsymbol{\chi}$, $\mathbf{\Lambda}(\boldsymbol{\chi})$ may now be represented as

$$\mathbf{\Lambda}(\boldsymbol{\chi}) \equiv \exp[\hat{\boldsymbol{\chi}}] = \mathbf{I} + \frac{\sin\chi}{\chi}\hat{\boldsymbol{\chi}} + \frac{2}{\chi^2}\sin^2\left(\frac{1}{2}\chi\right)\hat{\boldsymbol{\chi}}^2\,, \tag{6.3.6}$$

where $\exp[\hat{\boldsymbol{\chi}}]$ is known as the *exponential map*. Thus, the exponential map provides the rotation tensor for a rotation χ about the unit vector $\mathbf{n}$. Note that $\mathbf{\Lambda}\cdot\boldsymbol{\chi} = \boldsymbol{\chi}$, since $\hat{\boldsymbol{\chi}}\cdot\boldsymbol{\chi} = \boldsymbol{\chi}\times\boldsymbol{\chi} = \mathbf{0}$.

Let $\mathbf{Q}$ be any orthogonal transformation, then

$$\begin{aligned}\mathbf{Q}\cdot\exp[\hat{\boldsymbol{\chi}}]\cdot\mathbf{Q}^T &= \mathbf{I} + \frac{\sin\chi}{\chi}\mathbf{Q}\cdot\hat{\boldsymbol{\chi}}\cdot\mathbf{Q}^T + \frac{2}{\chi^2}\sin^2\frac{1}{2}\chi\left(\mathbf{Q}\cdot\hat{\boldsymbol{\chi}}\cdot\mathbf{Q}^T\right)^2 \\ &= \exp\left[\mathbf{Q}\cdot\hat{\boldsymbol{\chi}}\cdot\mathbf{Q}^T\right] \equiv \exp\left[\hat{\boldsymbol{\theta}}\right]\end{aligned} \tag{6.3.7}$$

where $\hat{\boldsymbol{\theta}} = \mathbf{Q}\cdot\hat{\boldsymbol{\chi}}\cdot\mathbf{Q}^T$ and its corresponding axial vector is $\boldsymbol{\theta} = \mathbf{Q}\cdot\boldsymbol{\chi}$, implying that $\theta = \chi$. This property of the exponential map is used in the next derivation.

Consider a vector $\mathbf{Z}$ in the reference configuration of a rigid body. Upon rigid body rotation, this vector is currently at

$$\mathbf{z}(t) = \mathbf{\Lambda}(t)\cdot\mathbf{Z}\,. \tag{6.3.8}$$

The corresponding axial vector of $\mathbf{\Lambda}(t)$ is $\boldsymbol{\chi}(t)$. At a subsequent time t', we would similarly have

$$\mathbf{z}(t') = \mathbf{\Lambda}(t')\cdot\mathbf{Z} = \exp\left[\hat{\boldsymbol{\theta}}\right]\cdot\mathbf{\Lambda}(t)\cdot\mathbf{Z}\,, \tag{6.3.9}$$

where here, $\boldsymbol{\theta}$ is the incremental (finite) rotation from t to t'. Alternatively, we may choose to write

$$\mathbf{z}(t') = \mathbf{\Lambda}(t')\cdot\mathbf{Z} = \mathbf{\Lambda}(t)\cdot\exp\left[\hat{\boldsymbol{\Theta}}\right]\cdot\mathbf{Z}\,, \tag{6.3.10}$$

such that

$$\begin{aligned} \boldsymbol{\Lambda}\left(t'\right) &= \exp\left[\hat{\boldsymbol{\theta}}\right] \cdot \boldsymbol{\Lambda}\left(t\right) \\ &= \boldsymbol{\Lambda}\left(t\right) \cdot \exp\left[\hat{\boldsymbol{\Theta}}\right] \end{aligned}, \tag{6.3.11}$$

implying that

$$\begin{aligned} \exp\left[\hat{\boldsymbol{\theta}}\right] &= \exp\left[\boldsymbol{\Lambda}\left(t\right) \cdot \hat{\boldsymbol{\Theta}} \cdot \boldsymbol{\Lambda}^T\left(t\right)\right] \\ \boldsymbol{\theta} &= \boldsymbol{\Lambda}\left(t\right) \cdot \boldsymbol{\Theta} \end{aligned}. \tag{6.3.12}$$

Note from these relations that $\theta = \Theta$. Thus, $\boldsymbol{\Theta}$ is the material representation of the incremental rotation from t to t', while $\boldsymbol{\theta}$ is the corresponding spatial representation.

6.3.1.2 Cayley Transform

An alternative to the exponential map is the Cayley transform,

$$\boldsymbol{\Lambda}\left(\boldsymbol{\chi}\right) = \mathrm{cay}\left[\hat{\boldsymbol{\chi}}\right] = \mathbf{I} + \frac{2}{1 + \left(\frac{1}{2}\chi\right)^2}\left(\frac{1}{2}\hat{\boldsymbol{\chi}} + \frac{1}{4}\hat{\boldsymbol{\chi}}^2\right) \tag{6.3.13}$$

which is a second order approximation to the exponential map. This formula is a correction to that appearing in [82] (which has $\frac{1}{2}\chi^2$ in the denominator). According to Puso [82], the Cayley transform must be used to enforce conservation of momentum and energy in a midpoint rule discretization scheme, whenever the rigid body is connected to a deformable body, or whenever two rigid bodies are connected by a joint. Comparing the above expression to the exponential map $\exp\left[\hat{\boldsymbol{\theta}}\right]$ using (6.3.6), we find that $\boldsymbol{\chi}$ and $\boldsymbol{\theta}$ are related via

$$\boldsymbol{\chi} = 2\tan\frac{\theta}{2}\mathbf{n}\,. \tag{6.3.14}$$

6.3.1.3 Linearization Along Rotational Increment

Let $\boldsymbol{\theta}$ represent a spatial rotational increment, such that a rotation tensor compounded by an infinitesimal incremental rotation is given by

$$\boldsymbol{\Lambda}_\varepsilon = \mathrm{cay}\left[\varepsilon\hat{\boldsymbol{\theta}}\right] \cdot \boldsymbol{\Lambda}\,. \tag{6.3.15}$$

Using the Cayley transform for illustration, the linearization of $\boldsymbol{\Lambda}$ along the increment $\boldsymbol{\theta}$ is obtained from

$$\begin{aligned} D\boldsymbol{\Lambda}\left[\boldsymbol{\theta}\right] &= \left.\frac{d}{d\varepsilon}\right|_{\varepsilon=0} \mathrm{cay}\left[\varepsilon\hat{\boldsymbol{\theta}}\right] \cdot \boldsymbol{\Lambda} \\ &= \left.\frac{d}{d\varepsilon}\right|_{\varepsilon=0} \left(\mathbf{I} + \frac{2}{1 + \frac{1}{4}\varepsilon^2\theta^2}\left(\frac{1}{2}\varepsilon\hat{\boldsymbol{\theta}} + \frac{1}{4}\varepsilon^2\hat{\boldsymbol{\theta}}^2\right)\right) \cdot \boldsymbol{\Lambda}\,. \\ &= \hat{\boldsymbol{\theta}} \cdot \boldsymbol{\Lambda} \end{aligned} \tag{6.3.16}$$

The same result may be obtained with the exponential map. Similarly, using an infinitesimal material rotational increment such that $\boldsymbol{\Lambda}_\varepsilon = \boldsymbol{\Lambda} \cdot \mathrm{cay}\left[\varepsilon\hat{\boldsymbol{\Theta}}\right]$, we may find

$$D\boldsymbol{\Lambda}\left[\boldsymbol{\Theta}\right] = \boldsymbol{\Lambda} \cdot \hat{\boldsymbol{\Theta}}\,. \tag{6.3.17}$$

6.3.2 General Rigid Body Motion

If the point $\mathbf{x}$ is connected to a rigid body, its motion is given by

$$\mathbf{x} = \mathbf{r}(t) + \mathbf{\Lambda}(t) \cdot \mathbf{Z} = \mathbf{r}(t) + \mathbf{z}(t) \tag{6.3.18}$$

where $\mathbf{r}(t)$ is the position of the rigid body center of mass and $\mathbf{\Lambda}(t)$ is the body's rotation tensor, which satisfies $\mathbf{\Lambda}(t_0) = \mathbf{I}$ at the initial time t_0; here, $\mathbf{z}(t) = \mathbf{\Lambda}(t) \cdot \mathbf{Z}$ is the distance of the point from the body's center of mass, and $\mathbf{X} = \mathbf{r}(t_0) + \mathbf{Z}$ is the initial position. The velocity of that point is

$$\dot{\mathbf{x}} = \dot{\mathbf{r}}(t) + \dot{\mathbf{\Lambda}}(t) \cdot \mathbf{Z} \quad , \tag{6.3.19}$$

where

$$\dot{\mathbf{\Lambda}}(t) = \hat{\boldsymbol{\omega}}(t) \cdot \mathbf{\Lambda}(t) = \mathbf{\Lambda}(t) \cdot \hat{\mathbf{W}}(t) \ . \tag{6.3.20}$$

Here, $\hat{\boldsymbol{\omega}}$ is an antisymmetric tensor with axial vector $\boldsymbol{\omega}$ which represents the spatial angular velocity vector; similarly, $\hat{\mathbf{W}}$ is an antisymmetric tensor with axial vector $\mathbf{W}$ (the material angular velocity), such that $\boldsymbol{\omega} = \mathbf{\Lambda} \cdot \mathbf{W}$ and

$$\hat{\boldsymbol{\omega}} = \mathbf{\Lambda} \cdot \hat{\mathbf{W}} \cdot \mathbf{\Lambda}^T . \tag{6.3.21}$$

We may now rewrite

$$\begin{aligned} \dot{\mathbf{x}} &= \dot{\mathbf{r}}(t) + \hat{\boldsymbol{\omega}}(t) \cdot \mathbf{z}(t) \\ &= \dot{\mathbf{r}}(t) + \mathbf{\Lambda}(t) \cdot \hat{\mathbf{W}}(t) \cdot \mathbf{Z} \end{aligned}^{\prime} \tag{6.3.22}$$

so that the acceleration of the point is

$$\begin{aligned} \ddot{\mathbf{x}} &= \ddot{\mathbf{r}}(t) + \left(\hat{\boldsymbol{\alpha}}(t) + \hat{\boldsymbol{\omega}}^2(t)\right) \cdot \mathbf{z} \\ &= \ddot{\mathbf{r}}(t) + \mathbf{\Lambda}(t) \cdot \left(\hat{\mathbf{A}}(t) + \hat{\mathbf{W}}^2(t)\right) \cdot \mathbf{Z} \end{aligned}^{\prime} \tag{6.3.23}$$

where $\boldsymbol{\alpha} = \dot{\boldsymbol{\omega}} = \mathbf{\Lambda} \cdot \mathbf{A}$ is the spatial angular acceleration vector, $\mathbf{A} = \dot{\mathbf{W}}$ is the material angular acceleration vector. As shown below, the time discretization is performed in the material frame.

6.3.3 Rigid Body Momentum Balance

For a rigid body, the conservation of linear momentum is given by

$$\frac{d}{dt}(m\dot{\mathbf{r}}) = \dot{\mathbf{p}} = \mathbf{f}^{ext}(t) \tag{6.3.24}$$

where m is the mass of the rigid body, $\dot{\mathbf{r}}$ is the velocity of the center of mass, $\mathbf{p} = m\dot{\mathbf{r}}$ is the linear momentum, and $\mathbf{f}^{ext}(t)$ represents the sum of external forces acting on the body. Here, m is constant for a rigid body. There are typically four contributions to $\mathbf{f}^{ext}(t)$: Body forces $\mathbf{f}_b^{ext}(t) = m\mathbf{b}(t)$ (where $\mathbf{b}$ represents the body force per mass, such as gravitational acceleration), other user-prescribed forces $\mathbf{f}_p^{ext}(t)$ (which act at the center of mass), forces $\mathbf{f}_c^{ext}(t)$ produced by rigid body connectors (such as revolute and prismatic joints, or contact forces), and forces $\mathbf{f}_f^{ext}(t)$ produced by rigid-flexible connections (where deformable materials interface with the rigid body), in which case $\mathbf{f}_f^{ext}$ is evaluated from the traction $\mathbf{t} = \boldsymbol{\sigma} \cdot \mathbf{n}$ over that interface, with $\boldsymbol{\sigma}$ representing the stress in the deformable material.

The conservation of angular momentum is similarly given by

$$\frac{d}{dt}(\mathbf{J} \cdot \boldsymbol{\omega}) = \dot{\mathbf{h}} = \boldsymbol{\omega} \times \mathbf{h} + \mathbf{J} \cdot \boldsymbol{\alpha} = \mathbf{m}^{ext}(t) \tag{6.3.25}$$

where $\mathbf{J}$ is the rigid body mass moment of inertia about its center of mass, $\boldsymbol{\omega}$ is its angular velocity, $\mathbf{h} = \mathbf{J} \cdot \boldsymbol{\omega}$ is its angular momentum, $\boldsymbol{\alpha} = \dot{\boldsymbol{\omega}}$ is the rigid body angular acceleration, and $\mathbf{m}^{ext}(t)$ is the sum of moments acting on the rigid body. External moments include contributions from user-prescribed moments/torques $\mathbf{m}_p^{ext}(t)$, from rigid body connectors, $\mathbf{m}_c^{ext}(t) = \mathbf{z}_c(t) \times \mathbf{f}_c^{ext}(t)$ where $\mathbf{z}_c(t)$ is the connector insertion relative to the rigid body center of mass, and rigid-flexible interfaces, $\mathbf{m}_f^{ext}(t) = \mathbf{z}_f(t) \times \mathbf{f}_f^{ext}(t)$ where $\mathbf{z}_f(t)$ is the position of the interface point relative to the rigid body center of mass. Since body forces $\mathbf{f}_b^{ext}$ and user-prescribed forces $\mathbf{f}_p^{ext}$ act at the center of mass, they do not contribute to $\mathbf{m}^{ext}(t)$. Note that

$$\mathbf{J}(t) = \boldsymbol{\Lambda}(t) \cdot \mathbf{J}_r \cdot \boldsymbol{\Lambda}^T(t) \ , \tag{6.3.26}$$

where $\mathbf{J}_r$ is the mass moment of inertia about the center of mass in the reference configuration and $\boldsymbol{\Lambda}(t)$ is the rotation tensor representing the orientation of the rigid body at time t, with $\boldsymbol{\Lambda} = \mathbf{I}$ in the reference configuration.

The virtual work statement is given by

$$\delta W = \delta\mathbf{r} \cdot \left(\mathbf{f}^{ext}(t) - \dot{\mathbf{p}}\right) + \delta\boldsymbol{\theta} \cdot \left(\mathbf{m}^{ext}(t) - \dot{\mathbf{h}}\right) \ , \tag{6.3.27}$$

where $\delta\mathbf{r}$ is the virtual velocity of the center of mass and $\delta\boldsymbol{\theta}$ is the virtual angular velocity of the rigid body.

6.3.4 Time Discretization

6.3.4.1 Newmark Integration for Rigid Body Dynamics

Let t_n and t_{n+1} represent consecutive time points. According to the Newmark integration scheme, the rigid body center of mass velocity and acceleration at t_{n+1} may be expressed in terms of their values at t_n as

$$\begin{aligned} \dot{\mathbf{r}}_{n+1} &= \dot{\mathbf{r}}_n + \Delta t \left[(1-\gamma)\,\ddot{\mathbf{r}}_n + \gamma\ddot{\mathbf{r}}_{n+1}\right] \\ \ddot{\mathbf{r}}_{n+1} &= \frac{1}{\beta\Delta t}\left[\frac{1}{\Delta t}\left(\mathbf{r}_{n+1} - \mathbf{r}_n\right) - \dot{\mathbf{r}}_n\right] + \left(1 - \frac{1}{2\beta}\right)\ddot{\mathbf{r}}_n \end{aligned} \ , \tag{6.3.28}$$

where β and γ are Newmark parameters that satisfy $0 \le 2\beta \le 1$ and $0 \le \gamma \le 1$.

Let the rigid body rotation tensor $\boldsymbol{\Lambda}(t)$ be expressed as $\boldsymbol{\Lambda}(t) = \exp[\boldsymbol{\xi}(t)]$, and $\boldsymbol{\xi}(t)$ is the material rotation of the rigid body from its reference configuration. Thus, $\boldsymbol{\Lambda}_n = \exp[\boldsymbol{\xi}_n]$ and $\boldsymbol{\Lambda}_{n+1} = \exp\left[\boldsymbol{\xi}_{n+1}\right]$ respectively represent the rigid body rotation tensors at t_n and t_{n+1}. (In practice, $\boldsymbol{\xi}$ is stored as a quaternion to facilitate the multiplication of rotation tensors.) These tensors are related by the incremental spatial rotation $\boldsymbol{\theta}$ or material rotation $\boldsymbol{\Theta}$ from t_n to t_{n+1} according to

$$\boldsymbol{\Lambda}_{n+1} = \mathrm{cay}[\boldsymbol{\theta}] \cdot \boldsymbol{\Lambda}_n = \boldsymbol{\Lambda}_n \cdot \mathrm{cay}[\boldsymbol{\Theta}] \ . \tag{6.3.29}$$

Here, it should be understood that the material frame for this incremental rotation is the configuration at time t_n, while the spatial frame is the configuration at t_{n+1}. For rotational motion, the Newmark scheme is applied in the material frame as

$$\begin{aligned} \mathbf{W}_{n+1} &= \frac{\gamma}{\beta\Delta t}\boldsymbol{\Theta} - \mathbf{W}_n + \left(2 - \frac{\gamma}{\beta}\right)\left(\mathbf{W}_n + \frac{\Delta t}{2}\mathbf{A}_n\right) \\ \mathbf{A}_{n+1} &= \frac{1}{\gamma\Delta t}\left(\mathbf{W}_{n+1} - \mathbf{W}_n\right) + \left(1 - \frac{1}{\gamma}\right)\mathbf{A}_n \\ &= \frac{1}{\beta\Delta t}\left(\frac{1}{\Delta t}\boldsymbol{\Theta} - \mathbf{W}_n\right) + \left(1 - \frac{1}{2\beta}\right)\mathbf{A}_n \end{aligned} \ . \tag{6.3.30}$$

Then, using the relations $\boldsymbol{\omega} = \boldsymbol{\Lambda} \cdot \mathbf{W}$ and $\boldsymbol{\alpha} = \boldsymbol{\Lambda} \cdot \mathbf{A}$ at t_n and t_{n+1}, along with (6.3.29), we may express these relations in the spatial frame as

$$\begin{aligned} \boldsymbol{\omega}_{n+1} &= \operatorname{cay}[\boldsymbol{\theta}] \cdot \left(\frac{\gamma}{\beta \Delta t} \boldsymbol{\theta} - \boldsymbol{\omega}_n + \left(2 - \frac{\gamma}{\beta} \right) \left(\boldsymbol{\omega}_n + \frac{\Delta t}{2} \boldsymbol{\alpha}_n \right) \right) \\ \boldsymbol{\alpha}_{n+1} &= \operatorname{cay}[\boldsymbol{\theta}] \cdot \left(\frac{1}{\beta \Delta t} \left(\frac{1}{\Delta t} \boldsymbol{\theta} - \boldsymbol{\omega}_n \right) + \left(1 - \frac{1}{2\beta} \right) \boldsymbol{\alpha}_n \right) \end{aligned} . \tag{6.3.31}$$

In a nonlinear solution scheme we solve for $\boldsymbol{\Theta}$ incrementally. According to (6.3.17), the linearization of $\operatorname{cay}[\boldsymbol{\Theta}]$ along an increment $\Delta\boldsymbol{\Theta}$ is given by

$$D(\operatorname{cay}[\boldsymbol{\Theta}])[\Delta\boldsymbol{\Theta}] = \operatorname{cay}[\boldsymbol{\Theta}] \cdot \widehat{\Delta\boldsymbol{\Theta}}, \tag{6.3.32}$$

so that

$$D\boldsymbol{\Lambda}_{n+1}[\Delta\boldsymbol{\Theta}] = \boldsymbol{\Lambda}_{n+1} \cdot \widehat{\Delta\boldsymbol{\Theta}}. \tag{6.3.33}$$

The linearizations of $\mathbf{W}_{n+1}$ and $\mathbf{A}_{n+1}$, as given in (6.3.30), along an increment $\Delta\boldsymbol{\Theta}$ requires us to first evaluate $D\boldsymbol{\Theta}[\Delta\boldsymbol{\Theta}]$. According to Puso [82],

$$D\boldsymbol{\Theta}[\Delta\boldsymbol{\Theta}] = \mathbf{T}(\boldsymbol{\Theta}) \cdot \Delta\boldsymbol{\Theta}, \tag{6.3.34}$$

where

$$\mathbf{T}(\boldsymbol{\Theta}) = \mathbf{I} + \frac{1}{2}\hat{\boldsymbol{\Theta}} + \frac{1}{4}\boldsymbol{\Theta} \otimes \boldsymbol{\Theta}. \tag{6.3.35}$$

Thus,

$$\begin{aligned} D\mathbf{W}_{n+1}[\Delta\boldsymbol{\Theta}] &= \frac{\gamma}{\beta \Delta t} \mathbf{T}(\boldsymbol{\Theta}) \cdot \Delta\boldsymbol{\Theta} \\ D\mathbf{A}_{n+1}[\Delta\boldsymbol{\Theta}] &= \frac{1}{\beta \Delta t^2} \mathbf{T}(\boldsymbol{\Theta}) \cdot \Delta\boldsymbol{\Theta} \end{aligned} . \tag{6.3.36}$$

6.3.5 Generalized-α Method for Rigid Body Dynamics

In the generalized-α method, we evaluate forces and moments at time $t_{n+\alpha_f} = (1-\alpha_f)\, t_n + \alpha_f t_{n+1}$ and the time rate of change of linear and angular momenta at time $t_{n+\alpha_m} = (1-\alpha_m)\, t_n + \alpha_m t_{n+1}$, where α_f and α_m may be evaluated from the spectral radius for an infinite time step, ρ_∞ (Section 3.9). For second-order systems these parameters may be evaluated from [**?**]

$$\alpha_f = \frac{1}{1+\rho_\infty}, \quad \alpha_m = \frac{2-\rho_\infty}{1+\rho_\infty}, \tag{6.3.37}$$

Then, the Newmark parameters are given by

$$\begin{aligned} \beta &= \frac{1}{4}(1 + \alpha_m - \alpha_f)^2, \\ \gamma &= \frac{1}{2} + \alpha_m - \alpha_f. \end{aligned} \tag{6.3.38}$$

Accordingly, to solve numerically for $\delta W = 0$ over the time domain, we express (6.3.27) in the discretized time domain as

$$\delta\mathbf{r} \cdot \left(\mathbf{f}^{ext}_{n+\alpha_f} - \dot{\mathbf{p}}_{n+\alpha_m} \right) + \delta\boldsymbol{\theta} \cdot \left(\mathbf{m}^{ext}_{n+\alpha_f} - \dot{\mathbf{h}}_{n+\alpha_m} \right) = 0, \tag{6.3.39}$$

or equivalently,

$$\left[\begin{array}{cc} \delta\mathbf{r} & \delta\boldsymbol{\theta} \end{array}\right] \cdot \left[\begin{array}{c} \mathbf{f}^{ext}_{n+\alpha_f} - \dot{\mathbf{p}}_{n+\alpha_m} \\ \mathbf{m}^{ext}_{n+\alpha_f} - \dot{\mathbf{h}}_{n+\alpha_m} \end{array}\right] = 0\,, \tag{6.3.40}$$

Thus, the residual vector is given by

$$[\mathbf{R}] = \left[\begin{array}{c} \mathbf{f}^{ext}_{n+\alpha_f} \\ \mathbf{m}^{ext}_{n+\alpha_f} \end{array}\right] - \left[\begin{array}{c} \dot{\mathbf{p}}_{n+\alpha_m} \\ \dot{\mathbf{h}}_{n+\alpha_m} \end{array}\right] \tag{6.3.41}$$

where

$$\begin{aligned} \dot{\mathbf{p}}_{n+\alpha_m} &= (1-\alpha_m)\,\dot{\mathbf{p}}_n + \alpha_m \dot{\mathbf{p}}_{n+1} \\ \dot{\mathbf{h}}_{n+\alpha_m} &= (1-\alpha_m)\,\dot{\mathbf{h}}_n + \alpha_m \dot{\mathbf{h}}_{n+1} \end{aligned}\,. \tag{6.3.42}$$

According to the Newmark integration scheme,

$$\begin{aligned} \dot{\mathbf{p}}_{n+1} &= \frac{\mathbf{p}_{n+1} - \mathbf{p}_n}{\gamma \Delta t} + \left(1 - \frac{1}{\gamma}\right) \dot{\mathbf{p}}_n \\ \dot{\mathbf{h}}_{n+1} &= \frac{\mathbf{h}_{n+1} - \mathbf{h}_n}{\gamma \Delta t} + \left(1 - \frac{1}{\gamma}\right) \dot{\mathbf{h}}_n \end{aligned}\,, \tag{6.3.43}$$

where $\mathbf{p}_{n+1} = m\dot{\mathbf{r}}_{n+1}$ and $\mathbf{h}_{n+1} = \mathbf{J}_{n+1} \cdot \boldsymbol{\omega}_{n+1}$.

The nonlinear system $\mathbf{R} = \mathbf{0}$ is solved using a Newton scheme that requires linearizing $\mathbf{R}$ along increments $\Delta\mathbf{r}$ and $\Delta\boldsymbol{\theta}$. Thus,

$$\mathbf{R} + D\mathbf{R}\,[\Delta\mathbf{r}] + D\mathbf{R}\,[\Delta\boldsymbol{\theta}] \approx \mathbf{0}\,. \tag{6.3.44}$$

The increments $\Delta\mathbf{r}$ and $\Delta\boldsymbol{\theta}$ are evaluated at t_{n+1} and the iterative Newton scheme requires updates of the form

$$\begin{aligned} \mathbf{r}^{j+1}_{n+1} &= \mathbf{r}^{j}_{n+1} + \Delta\mathbf{r} \\ \mathrm{cay}\left[\boldsymbol{\theta}^{j+1}\right] &= \mathrm{cay}\left[\Delta\boldsymbol{\theta}\right] \cdot \mathrm{cay}\left[\boldsymbol{\theta}^{j}\right] \end{aligned}\,, \tag{6.3.45}$$

where j represents the Newton iteration. At each Newton iteration, the current value of $\mathrm{cay}\left[\boldsymbol{\theta}^{j+1}\right]$ is used to perform the update

$$\boldsymbol{\Lambda}^{j+1}_{n+1} = \mathrm{cay}\left[\boldsymbol{\theta}^{j+1}\right] \cdot \boldsymbol{\Lambda}_n\,, \tag{6.3.46}$$

until convergence is achieved.

In practice, it is convenient to store $\boldsymbol{\theta}$ and $\Delta\boldsymbol{\theta}$ in quaternions, recognizing that

$$\mathrm{cay}\,[\theta\mathbf{n}] = \exp\left[\left(2\tan^{-1}\frac{\theta}{2}\right)\mathbf{n}\right]\,,$$

where $\mathbf{n}$ is the unit vector along $\boldsymbol{\theta}$ and $\theta = \|\boldsymbol{\theta}\|$. Thus, it is $\left(2\tan^{-1}\frac{\theta}{2}\right)\mathbf{n}$ which is stored in the quaternion, instead of $\theta\mathbf{n}$.

In the linearization of $\mathbf{R}$, the contributions from the rate of change of linear momentum $\dot{\mathbf{p}}_{n+\alpha_m}$ reduce to

$$\begin{aligned} D\dot{\mathbf{p}}_{n+\alpha_m}\,[\Delta\mathbf{r}] &= \frac{\alpha_m}{\beta\Delta t^2} m\Delta\mathbf{r} \\ D\dot{\mathbf{p}}_{n+\alpha_m}\,[\Delta\boldsymbol{\theta}] &= \mathbf{0} \end{aligned}\,.$$

To evaluate the contributions from the rate of change of angular momentum $\dot{\mathbf{h}}_{n+\alpha_m}$, we start from $D\dot{\mathbf{h}}_{n+\alpha_m} = \alpha_m D\dot{\mathbf{h}}_{n+1}$. Then, it becomes necessary to transform the variables to the material frame,

$$\begin{aligned} \dot{\mathbf{h}}_{n+1} &= \boldsymbol{\omega}_{n+1} \times \mathbf{h}_{n+1} + \mathbf{J}_{n+1} \cdot \boldsymbol{\alpha}_{n+1} \\ &= \boldsymbol{\Lambda}_{n+1} \cdot \left(\hat{\mathbf{W}}_{n+1} \cdot \mathbf{J}_r \cdot \mathbf{W}_{n+1} + \mathbf{J}_r \cdot \mathbf{A}_{n+1}\right)\,. \end{aligned}$$

It follows that

$$D\dot{\mathbf{h}}_{n+\alpha_m}\left[\Delta\mathbf{r}\right]=\mathbf{0}\,.$$

Then, using the relations in Section 6.3.4.1, it can be shown that

$$D\dot{\mathbf{h}}_{n+\alpha_m}\left[\Delta\boldsymbol{\Theta}\right]=\alpha_m\left[\frac{1}{\beta\Delta t}\left(\left(\gamma\hat{\boldsymbol{\omega}}_{n+1}+\frac{1}{\Delta t}\mathbf{I}\right)\cdot\mathbf{J}_{n+1}-\gamma\hat{\mathbf{h}}_{n+1}\right)\cdot\mathbf{T}\left(\boldsymbol{\theta}\right)-\hat{\dot{\mathbf{h}}}_{n+1}\right]\cdot\Delta\boldsymbol{\theta}\equiv\alpha_m\mathbf{K}\cdot\Delta\boldsymbol{\theta}\,.$$

Alternatively, we may use the discretization in (6.3.43) to produce

$$D\dot{\mathbf{h}}_{n+\alpha_m}\left[\Delta\boldsymbol{\Theta}\right]=\frac{\alpha_m}{\gamma\Delta t}D\mathbf{h}_{n+1}\left[\Delta\boldsymbol{\Theta}\right]$$

where

$$D\mathbf{h}_{n+1}\left[\Delta\boldsymbol{\Theta}\right]=\left(\frac{\gamma}{\beta\Delta t}\mathbf{J}_{n+1}\cdot\mathbf{T}\left(\boldsymbol{\theta}\right)-\hat{\mathbf{h}}_{n+1}\right)\cdot\Delta\boldsymbol{\theta}$$

so that

$$D\dot{\mathbf{h}}_{n+\alpha_m}\left[\Delta\boldsymbol{\Theta}\right]=\frac{\alpha_m}{\Delta t}\left(\frac{1}{\beta\Delta t}\mathbf{J}_{n+1}\cdot\mathbf{T}\left(\boldsymbol{\theta}\right)-\frac{1}{\gamma}\hat{\mathbf{h}}_{n+1}\right)\cdot\Delta\boldsymbol{\theta}\equiv\alpha_m\mathbf{K}\cdot\Delta\boldsymbol{\theta}$$

Therefore, the contribution to $D\mathbf{R}$ from the linear and angular momenta produces a stiffness matrix called the mass matrix,

$$D\left[\begin{array}{c}\dot{\mathbf{p}}_{n+\alpha_m}\\ \dot{\mathbf{h}}_{n+\alpha_m}\end{array}\right]=\alpha_m\left[\begin{array}{cc}\frac{m}{\beta\Delta t^2}\mathbf{I} & \mathbf{0}\\ \mathbf{0} & \mathbf{K}\end{array}\right]\left[\begin{array}{c}\Delta\mathbf{r}\\ \Delta\boldsymbol{\theta}\end{array}\right].$$

Consider that the moments $\mathbf{m}^{ext}_{n+\alpha_f}$ about the rigid body center of mass are produced by the forces $\mathbf{f}^{ext}_{n+\alpha_f}$ according to

$$\mathbf{m}^{ext}_{n+\alpha_f}=\mathbf{z}_{n+\alpha_f}\times\mathbf{f}^{ext}_{n+\alpha_f}=\hat{\mathbf{z}}_{n+\alpha_f}\cdot\mathbf{f}^{ext}_{n+\alpha_f}\,,$$

where $\mathbf{z}_{n+\alpha_f}$ is the moment arm at $t_{n+\alpha_f}$,

$$\begin{aligned}\mathbf{z}_{n+\alpha_f}&=\left(1-\alpha_f\right)\mathbf{z}_n+\alpha_f\mathbf{z}_{n+1}\\&=\left[\left(1-\alpha_f\right)\boldsymbol{\Lambda}_n+\alpha_f\boldsymbol{\Lambda}_{n+1}\right]\cdot\mathbf{Z}\\&\equiv\boldsymbol{\Lambda}_{n+\alpha_f}\cdot\mathbf{Z}\end{aligned}$$

where $\mathbf{Z}$ is the moment arm in the reference configuration. Note that

$$\begin{aligned}D\mathbf{z}_{n+\alpha_f}\left[\Delta\mathbf{r}\right]&=\mathbf{0}\\D\mathbf{z}_{n+\alpha_f}\left[\Delta\boldsymbol{\theta}\right]&=\alpha_f D\boldsymbol{\Lambda}_{n+1}\left[\Delta\boldsymbol{\theta}\right]\cdot\mathbf{Z}=-\alpha_f\hat{\mathbf{z}}_{n+1}\cdot\Delta\boldsymbol{\theta}\end{aligned}$$

Thus,

$$\left[\begin{array}{c}D\mathbf{f}^{ext}_{n+\alpha_f}\left[\Delta\mathbf{r}\right]\\ D\mathbf{m}^{ext}_{n+\alpha_f}\left[\Delta\mathbf{r}\right]\end{array}\right]=\left[\begin{array}{c}D\mathbf{f}^{ext}_{n+\alpha_f}\left[\Delta\mathbf{r}\right]\\ \mathbf{z}_{n+\alpha_f}\times D\mathbf{f}^{ext}_{n+\alpha_f}\left[\Delta\mathbf{r}\right]\end{array}\right]$$

and

$$\left[\begin{array}{c}D\mathbf{f}^{ext}_{n+\alpha_f}\left[\Delta\boldsymbol{\theta}\right]\\ D\mathbf{m}^{ext}_{n+\alpha_f}\left[\Delta\boldsymbol{\theta}\right]\end{array}\right]=\left[\begin{array}{c}D\mathbf{f}^{ext}_{n+\alpha_f}\left[\Delta\boldsymbol{\theta}\right]\\ \mathbf{z}_{n+\alpha_f}\times D\mathbf{f}^{ext}_{n+\alpha_f}\left[\Delta\boldsymbol{\theta}\right]-\left(\alpha_f\hat{\mathbf{z}}_{n+1}\cdot\Delta\boldsymbol{\theta}\right)\times\mathbf{f}^{ext}_{n+\alpha_f}\end{array}\right].$$

Chapter 7

Contact and Coupling

FEBio allows the user to connect the different parts of the model in various ways. Deformable parts can be connected to rigid bodies. Deformable objects can be brought in contact with each other. Rigid bodies can be connected with rigid joints. This chapter describes the different ways to couple parts together.

7.1 Sliding Interfaces

This section summarizes the theoretical developments of the two body contact problem. After introducing some notation and terminology, the contact integral is presented, which contains the contribution to the virtual work equation from the contact tractions. Since the nonlinear contact problem is solved using a Newton based iterative method, the contact integral is linearized. Next, anticipating a finite element implementation, the contact integral and its linearization are discretized using a standard finite element approach. Finally the augmented Lagrangian method for enforcing the contact constraints is described.

7.1.1 Contact Kinematics

For the most part the notation of this section follows [65], with a few simplifications here and there since the implementation in FEBio is currently for quasi-static, frictionless, two body contact problem.

The volume occupied by body i in the reference configuration is denoted by $\Omega^{(i)} \subset \mathbb{R}^3$where $i = 1, 2$. The boundary of body i is denoted by $\Gamma^{(i)}$ and is divided into three regions $\Gamma^{(i)} = \Gamma_\sigma^{(i)} \cup \Gamma_u^{(i)} \cup \Gamma_c^{(i)}$, where $\Gamma_\sigma^{(i)}$ is the boundary where tractions are applied, $\Gamma_u^{(i)}$ the boundary where the solution is prescribed and $\Gamma_c^{(i)}$ the part of the boundary that will be in contact with the other body. It is assumed that $\Gamma_\sigma^{(i)} \cap \Gamma_u^{(i)} \cap \Gamma_c^{(i)} = \emptyset$.

The deformation of body i is defined by $\boldsymbol{\varphi}^{(i)}$. The boundary of the deformed body i, that is the boundary of $\boldsymbol{\varphi}^{(i)}\left(\Omega^{(i)}\right)$ is denoted by $\gamma^{(i)} = \gamma_\sigma^{(i)} \cup \gamma_u^{(i)} \cup \gamma_c^{(i)}$ where $\gamma_\sigma^{(i)} = \boldsymbol{\varphi}^{(i)}\left(\Gamma_\sigma^{(i)}\right)$ is the boundary in the current configuration where the tractions are applied and similar definitions for $\gamma_u^{(i)}$ and $\gamma_c^{(i)}$. See the figure below for a graphical illustration of the defined regions.

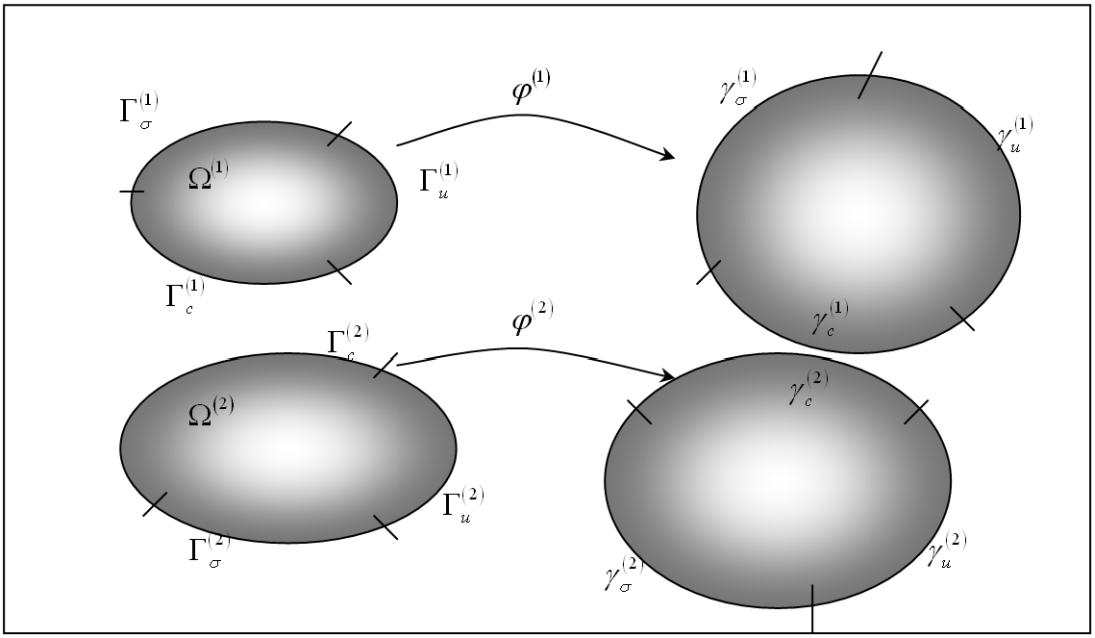

The two-body contact problem.

Points in body 1 are denoted by $\mathbf{X}$ in the reference configuration and $\mathbf{x}$ in the current configuration. For body 2 these points are denoted by $\mathbf{Y}$ and $\mathbf{y}$. To define contact, the location where the two bodies are in contact with each other must be established. If body 1 is the *slave body* and body 2 is the *master body*, then for a given point $\mathbf{X}$ on the slave reference contact surface there is a point $\bar{\mathbf{Y}}(\mathbf{X})$ on the master contact surface that is in some sense closest to point $\mathbf{X}$. This closest point is defined in a closest point projection sense:

$$\bar{\mathbf{Y}}(\mathbf{X}) = \arg \min_{\mathbf{Y} \in \Gamma_c^{(2)}} \left\| \boldsymbol{\varphi}^{(1)}(\mathbf{X}) - \boldsymbol{\varphi}^{(2)}(\mathbf{Y}) \right\| . \tag{7.1.1}$$

With the definition of $\bar{\mathbf{Y}}(\mathbf{X})$ established the *gap function* can be defined, which is a measure for the distance between $\mathbf{X}$ and $\bar{\mathbf{Y}}(\mathbf{X})$,

$$g(\mathbf{X}) = -\boldsymbol{\nu} \cdot \left(\boldsymbol{\varphi}^{(1)}(\mathbf{X}) - \boldsymbol{\varphi}^{(2)}\left(\bar{\mathbf{Y}}(\mathbf{X})\right) \right) , \tag{7.1.2}$$

where $\boldsymbol{\nu}$ is the local surface normal of surface $\gamma_c^{(2)}$ evaluated at $\bar{\mathbf{y}} = \boldsymbol{\varphi}^{(2)}\left(\bar{\mathbf{Y}}(\mathbf{X})\right)$. Note that $g > 0$ when $\mathbf{X}$ has penetrated body 2, so that the constraint condition to be satisfied at all time is $g \leqslant 0$.

7.1.2 Weak Form of Two Body Contact

The balance of linear momentum can be written for each of the two bodies in the reference configuration,

$$G^{(i)}\left(\boldsymbol{\varphi}^{(i)}, \mathbf{w}^{(i)}\right) = \int_{\Omega^{(i)}} \operatorname{Grad} \mathbf{w}^{(i)} : \mathbf{P}^{(i)} \, d\Omega - \int_{\Omega^{(i)}} \mathbf{w}^{(i)} \cdot \mathbf{F}^{(i)} \, d\Omega - \int_{\Gamma_s^{(i)}} \mathbf{w}^{(i)} \cdot \mathbf{T}^{(i)} \, d\Gamma - \int_{\Gamma_c^{(i)}} \mathbf{w}^{(i)} \cdot \mathbf{T}^{(i)} \, d\Gamma = 0 , \tag{7.1.3}$$

where $\mathbf{w}^{(i)}$ is a weighting function and $\mathbf{P}$ is the 1^{st} Piola-Kirchhoff stress tensor. The last term corresponds to the virtual work of the contact tractions on body i. For notational convenience, the

notations $\varphi$and w are introduced to denote the collection of the respective mappings $\boldsymbol{\varphi}^{(i)}$ and $\mathbf{w}^{(i)}$ (for i =1,2). In other words,

$$\begin{aligned} \varphi &: \bar{\Omega}^{(1)} \cup \bar{\Omega}^{(2)} \to \mathbb{R}^3 \,, \\ w &: \bar{\Omega}^{(1)} \cup \bar{\Omega}^{(2)} \to \mathbb{R}^3 \,. \end{aligned} \tag{7.1.4}$$

The variational principle for the two body system is the sum of (7.1.3) for body 1 and 2 and can be expressed as,

$$\begin{aligned} G\left(\boldsymbol{\varphi}, \mathbf{w}\right) &:= \sum_{i=1}^{2} G^{(i)}\left(\boldsymbol{\varphi}^{(i)}, \mathbf{w}^{(i)}\right) \\ &= \underbrace{\sum_{i=1}^{2} \left\{ \int_{\Omega^{(i)}} \operatorname{Grad} \mathbf{w}^{(i)} : \mathbf{P}^{(i)} \, d\Omega - \int_{\Omega^{(i)}} \mathbf{w}^{(i)} \cdot \mathbf{F}^{(i)} \, d\Omega - \int_{\Gamma_s^{(i)}} \mathbf{w}^{(i)} \cdot \mathbf{T}^{(i)} \, d\Gamma \right\}}_{G^{\text{int,ext}}(\boldsymbol{\varphi}, \mathbf{w})} \\ &\underbrace{- \sum_{i=1}^{2} \int_{\Gamma_c^{(i)}} \mathbf{w}^{(i)} \cdot \mathbf{T}^{(i)} \, d\Gamma}_{G^{c}(\boldsymbol{\varphi}, \mathbf{w})} \,. \end{aligned} \tag{7.1.5}$$

Or in short,

$$G\left(\boldsymbol{\varphi}, \mathbf{w}\right) = G^{\text{int,ext}}\left(\boldsymbol{\varphi}, \mathbf{w}\right) + G^{c}\left(\boldsymbol{\varphi}, \mathbf{w}\right) \,. \tag{7.1.6}$$

Note that the minus sign is included in the definition of the contact integral G^c. The contact integral can be written as an integration over the contact surface of body 1 by balancing linear momentum across the contact surface:

$$\mathbf{t}^{(2)}\left(\bar{\mathbf{y}}\left(\mathbf{x}\right)\right) d\Gamma^{(2)} = -\mathbf{t}^{(1)}\left(\mathbf{x}\right) \, d\Gamma^{(1)} \,. \tag{7.1.7}$$

The contact integral can now be rewritten over the contact surface of body 1:

$$G^{c} = - \int_{\Gamma_c^{(1)}} \mathbf{t}^{(1)}\left(\mathbf{x}\right) \cdot \left[\mathbf{w}^{(1)}\left(\mathbf{x}\right) - \mathbf{w}^{(2)}\left(\bar{\mathbf{y}}\left(\mathbf{x}\right)\right) \right] \, d\Gamma \,. \tag{7.1.8}$$

In the case of frictionless contact, the contact traction is taken as perpendicular to surface 2 and therefore can be written as, $\mathbf{t}^{(1)} = t_N \boldsymbol{\nu}$ where $\boldsymbol{\nu}$ is the (outward) surface normal and t_N is to be determined from the solution strategy. For example in a Lagrange multiplier method the t_N's would be the Lagrange multipliers.

By noting that the variation of the gap function is given by

$$\delta g = -\boldsymbol{\nu} \cdot \left(\mathbf{w}^{(1)}\left(\mathbf{x}\right) - \mathbf{w}^{(2)}\left(\bar{\mathbf{y}}\left(\mathbf{x}\right)\right) \right) \,, \tag{7.1.9}$$

equation (7.1.8) can be simplified as,

$$G^{c} = \int_{\Gamma_c^{(1)}} t_N \delta g \, d\Gamma \,. \tag{7.1.10}$$

7.1.3 Linearization of the Contact Integral

In a Newton-Raphson implementation the contact integral must be linearized with respect to the current configuration:

$$\Delta G^c(\boldsymbol{\varphi}, \mathbf{w}) = \int_{\Gamma_c^{(1)}} \Delta(t_N \delta g)\, d\Gamma\,. \tag{7.1.11}$$

Examining the normal contact term first, the directional derivative of t_N is given (for the case of the penalty regularization) by:

$$\begin{aligned} \Delta t_N &= \Delta\{\varepsilon_N \langle g \rangle\} \\ &= H(g)\, \varepsilon_N \Delta g\,, \end{aligned} \tag{7.1.12}$$

where ε_N is the penalty factor and $H(g)$ is the Heaviside function. The quantity $\Delta(\delta g)$ is given by

$$\begin{aligned} \Delta(\delta g) = {} & g\left[\boldsymbol{\nu}\cdot\delta\boldsymbol{\varphi}^{(2)}_{,\gamma}\left(\bar{\mathbf{Y}}(\mathbf{X})\right) + \kappa_{\alpha\gamma}\left(\bar{\mathbf{Y}}(\mathbf{X})\right)\delta\bar{\xi}_\alpha\right] m^{\gamma\beta} \\ & \left[\boldsymbol{\nu}\cdot\Delta\boldsymbol{\varphi}^{(2)}_{,\beta}\left(\bar{\mathbf{Y}}(\mathbf{X})\right) + \kappa_{\alpha\beta}\left(\bar{\mathbf{Y}}(\mathbf{X})\right)\Delta\bar{\xi}^\alpha\right] \\ & + \delta\bar{\xi}^\beta\boldsymbol{\nu}\cdot\left[\Delta\boldsymbol{\varphi}^{(2)}_{,\beta}\left(\bar{\mathbf{Y}}(\mathbf{X})\right)\right] + \Delta\bar{\xi}^\beta\boldsymbol{\nu}\cdot\left[\delta\boldsymbol{\varphi}^{(2)}_{,\beta}\left(\bar{\mathbf{Y}}(\mathbf{X})\right)\right] \\ & + \kappa_{\alpha\beta}\left(\bar{\mathbf{Y}}(\mathbf{X})\right)\delta\bar{\xi}^\beta\Delta\bar{\xi}^\alpha\,. \end{aligned} \tag{7.1.13}$$

7.1.4 Discretization of the Contact Integral

The contact integral, which is repeated here,

$$G^c(\boldsymbol{\varphi}, \mathbf{w}) = \int_{\Gamma^{(1)}} t_N \delta g\, d\Gamma\,, \tag{7.1.14}$$

will now be discretized using a standard finite element procedure. First it is noted that the integration can be written as a sum over the surface element areas:

$$G^c(\boldsymbol{\varphi}, \mathbf{w}) = \sum_{e=1}^{N_{sel}} \int_{\Gamma^{(1)e}} t_N \delta g\, d\Gamma\,, \tag{7.1.15}$$

where N_{sel} is the number of surface elements. The integration can be approximated using a quadrature rule,

$$G^c(\boldsymbol{\varphi}, \mathbf{w}) \cong \sum_{e=1}^{N_{sel}} \left\{ \sum_{i=1}^{N^e_{int}} w^i j(\boldsymbol{\xi}_i)\, t_N(\boldsymbol{\xi}_i)\, \delta g(\boldsymbol{\xi}_i) \right\}, \tag{7.1.16}$$

where N^e_{int} are the number of integration points for element e. It is now assumed that the integration points coincide with the element's nodes (e.g. for a quadrilateral surface element we have $\boldsymbol{\xi}_1 = (-1,-1)$, $\boldsymbol{\xi}_2 = (1,-1)$, $\boldsymbol{\xi}_3 = (1,1)$ and $\boldsymbol{\xi}_4 = (-1,1)$). With this quadrature rule, we have

$$\begin{aligned} w^{(1)}(\boldsymbol{\xi}_i) &= \mathbf{c}^{(1)}_i \\ w^{(2)}(\bar{\boldsymbol{\xi}}_i) &= \sum_{j=1}^{n} N_j(\bar{\boldsymbol{\xi}}_i)\, \mathbf{c}^{(2)}_j\,, \end{aligned} \tag{7.1.17}$$

so that,

$$\delta g\left(\boldsymbol{\xi}_i\right) = -\boldsymbol{\nu} \cdot \left(\mathbf{c}_i^{(1)} - \sum_{j=1}^{n} N_j^{(2)}\left(\bar{\boldsymbol{\xi}}_i\right) \mathbf{c}_j^{(2)} \right) . \tag{7.1.18}$$

If the following vectors are defined,

$$\begin{aligned} \delta\boldsymbol{\Phi}^T &= \left[\begin{array}{cccc} \mathbf{c}_i^{(1)} & \mathbf{c}_1^{(2)} & \cdots & \mathbf{c}_n^{(2)} \end{array} \right] \\ \mathbf{N}^T &= \left[\begin{array}{cccc} \boldsymbol{\nu} & -\boldsymbol{\nu} N_1^{(2)} & \cdots & -\boldsymbol{\nu} N_n^{(2)} \end{array} \right] \end{aligned} , \tag{7.1.19}$$

equation (7.1.16) can then be rewritten as follows,

$$G^c\left(\boldsymbol{\varphi}, \mathbf{w}\right) \cong \sum_{e=1}^{N_{sel}} \left\{ \sum_{i=1}^{N_{int}^e} w^i j\left(\boldsymbol{\xi}_i\right) t_N\left(\boldsymbol{\xi}_i\right) \delta\boldsymbol{\Phi}^T \mathbf{N}^T \right\} . \tag{7.1.20}$$

The specific form for $t_N$will depend on the method employed for enforcing the contact constraint.

7.1.5 Discretization of the Contact Stiffness

A similar procedure can now be used to calculate the discretized contact stiffness matrix. The linearization of the contact integral is repeated here:

$$\begin{aligned} \Delta G^c\left(\boldsymbol{\varphi}, \mathbf{w}\right) &= \sum_{e=1}^{N_{sel}} \int_{\Gamma^{(1)e}} \Delta\left(t_N \delta g\right) \, d\Gamma \\ &= \sum_{e=1}^{N_{sel}} \sum_{i=1}^{N_{int}^e} w_i j\left(\boldsymbol{\xi}_i\right) \Delta\left(t_N \delta g\right)\left(\boldsymbol{\xi}_i\right) \end{aligned} . \tag{7.1.21}$$

Using matrix notation we can rewrite equation (7.1.21) as,

$$\Delta W^c\left(\boldsymbol{\varphi}, \mathbf{w}\right) = \sum_{e=1}^{N_{sel}} \sum_{i}^{N_{int}^e} w_i j\left(\xi_i\right) \delta\boldsymbol{\Phi} \cdot \mathbf{k}^c \Delta\boldsymbol{\Phi} , \tag{7.1.22}$$

where $\delta\boldsymbol{\Phi}$ is as above and $\Delta\boldsymbol{\Phi}$ similar to $\delta\boldsymbol{\Phi}$ with δ replaced with Δ, and $\mathbf{k}^c$ is

$$\begin{aligned} \mathbf{k}^c = \varepsilon_N H\left(\lambda_N^k + \varepsilon_N g\right) \mathbf{N}\mathbf{N}^T + t_N \{ & g\left[m^{11} \bar{\mathbf{N}}_1 \bar{\mathbf{N}}_1^T \right. \\ & + m^{12}\left(\bar{\mathbf{N}}_1 \bar{\mathbf{N}}_2^T + \bar{\mathbf{N}}_2 \bar{\mathbf{N}}_1^T\right) + \left. m^{22} \bar{\mathbf{N}}_2 \bar{\mathbf{N}}_2^T \right] - \mathbf{D}_1 \mathbf{N}_1^T \\ & - \mathbf{D}_2 \mathbf{N}_2^T - \mathbf{N}_1 \mathbf{D}_1^T - \mathbf{N}_2 \mathbf{D}_2^T + \kappa_{12}\left(\mathbf{D}_1 \mathbf{D}_2^T + \mathbf{D}_2 \mathbf{D}_1^T\right) \} \end{aligned} , \tag{7.1.23}$$

where,

$$\mathbf{N} = \left[\begin{array}{c} \boldsymbol{\nu} \\ -N_1\left(\bar{\boldsymbol{\xi}}\right) \boldsymbol{\nu} \\ \vdots \\ -N_4\left(\bar{\boldsymbol{\xi}}\right) \boldsymbol{\nu} \end{array} \right] , \quad \mathbf{T}_\alpha = \left[\begin{array}{c} \boldsymbol{\tau}_\alpha \\ -N_1\left(\bar{\boldsymbol{\xi}}\right) \boldsymbol{\tau}_\alpha \\ \vdots \\ -N_4\left(\bar{\boldsymbol{\xi}}\right) \boldsymbol{\tau}_\alpha \end{array} \right] , \quad \mathbf{N}_\alpha = \left[\begin{array}{c} \mathbf{0} \\ -N_{1,\alpha}\left(\bar{\boldsymbol{\xi}}\right) \boldsymbol{\nu} \\ \vdots \\ -N_{4,\alpha}\left(\bar{\boldsymbol{\xi}}\right) \boldsymbol{\nu} \end{array} \right] . \tag{7.1.24}$$

The following vectors are also defined which depend on the vectors of (7.1.24):

$$\begin{aligned}\mathbf{D}_1 &= \frac{1}{\det \mathbf{A}} \left[A_{22} \left(\mathbf{T}_1 + g\mathbf{N}_1 \right) - A_{12} \left(\mathbf{T}_2 + g\mathbf{N}_2 \right) \right] \\ \mathbf{D}_2 &= \frac{1}{\det \mathbf{A}} \left[A_{11} \left(\mathbf{T}_2 + g\mathbf{N}_2 \right) - A_{12} \left(\mathbf{T}_1 + g\mathbf{N}_1 \right) \right], \\ \bar{\mathbf{N}}_1 &= \mathbf{N}_1 - \kappa_{12}\mathbf{D}_2 \\ \bar{\mathbf{N}}_2 &= \mathbf{N}_2 - \kappa_{12}\mathbf{D}_1\end{aligned} \tag{7.1.25}$$

where the matrix $\mathbf{A}$ is defined as,

$$A_{ij} = m_{ij} + g\kappa_{ij} \,. \tag{7.1.26}$$

Here, $m_{ij} = \boldsymbol{\tau}_i \cdot \boldsymbol{\tau}_j$ is the surface metric tensor and $\kappa_{ij} = \boldsymbol{\nu} \cdot \boldsymbol{\varphi}^{(2)}_{t,ij} \left(\bar{\mathbf{Y}} \right)$ denotes the components of the surface curvature at $\bar{\boldsymbol{\xi}}$.

7.1.6 Augmented Lagrangian Method

The augmented Lagrangian method is used in FEBio to enforce the contact constraints to a user-specified tolerance. This implies that the normal contact tractions are given by,

$$t_N = \langle \lambda_N + \varepsilon_N g \rangle \,. \tag{7.1.27}$$

Note that this assumption is consistent with the approach that was used in establishing the discretization of the linearization of the contact integral (7.1.23). In (7.1.27) ε_N is a penalty factor that is chosen arbitrarily.

The Newton-Raphson iterative method is now used to solve the nonlinear contact problem where Uzawa's method (REF) is employed to calculate the Lagrange multipliers λ_N. This implies that the Lagrange multipliers are kept fixed during the Newton-Raphson iterations. After convergence the multipliers are updated and a new NR procedure is started. This procedure can be summarized by the following four steps.

1. **Initialize** the augmented Lagrangian iteration counter k, and the initial guesses for the multipliers:

$$\begin{aligned}\lambda^{(0)}_{N_{n+1}} &= \lambda_{N_n} \,, \\ k &= 0 \,.\end{aligned} \tag{7.1.28}$$

2. **Solve** for $\mathbf{d}^{(k)}_{n+1}$, the solution vector corresponding to the fixed kth iterate for the multipliers,

$$\mathbf{F}^{int} \left(\mathbf{d}^{(k)}_{n+1} \right) + \mathbf{F}^{c} \left(\mathbf{d}^{(k)}_{n+1} \right) = \mathbf{F}^{ext}_{n+1} \,, \tag{7.1.29}$$

   where the contact tractions used to compute $\mathbf{F}^c$, the contact force, are governed by

$$t^{(k)}_{N_{n+1}} = \left\langle \lambda^{(k)}_{N_{n+1}} + \varepsilon_N g^{k}_{n+1} \right\rangle \,. \tag{7.1.30}$$

3. **Update** the Lagrange multipliers and iteration counters:

$$\begin{aligned}\lambda^{(k+1)}_{N_{n+1}} &= \left\langle \lambda^{(k)}_{N_{n+1}} + \varepsilon_N g^{(k)}_{n+1} \right\rangle \,, \\ k &= k + 1 \,.\end{aligned} \tag{7.1.31}$$

4. **Return** to the solution phase.

Steps 2-4 of the above algorithm are generally repeated until all contact constraints are satisfied to a user-specified tolerance or little change in the solution vector from augmentation to augmentation is noted.

7.1.7 Automatic Penalty Calculation

The determination of the penalty factor ε_N can be a difficult task, since a good value may depend on both material parameters and geometrical factors. In FEBio the value of this penalty factor can be determined automatically. In this case FEBio will calculate a penalty factor for each facet using the following formula.

$$\varepsilon_i = \frac{f_{SI} E_i A_i}{V_i} \,. \tag{7.1.32}$$

Here, E_i is the effective Young's modulus along the facet normal, A_i the surface area of the facet, V_i the volume of the element to which this facet belongs and f_{SI} a user defined scale factor. The parameter E_i is evaluated from the elasticity tensor $\boldsymbol{\mathcal{C}}$ and the facet unit normal $\mathbf{n}$ according to

$$\frac{1}{E_i} = (\mathbf{n} \otimes \mathbf{n}) : \boldsymbol{\mathcal{C}}^{-1} : (\mathbf{n} \otimes \mathbf{n}) \;, \tag{7.1.33}$$

where $\boldsymbol{\mathcal{C}}^{-1}$ is the compliance tensor.

7.1.8 Facet-To-Facet Sliding

As of FEBio version 1.2, two alternative formulations for sliding contact are available. The first method, which is referred to as the *facet-to-facet sliding*, is very similar to the formulation described above. It only differs in that it uses a Gaussian quadrature rule instead of nodal integration. Because of the more accurate integration rule, it was noted that this method in many situations was more stable and resulted in better convergence.

7.1.9 Sliding-Elastic

This algorithm was presented in [114] and differs considerably from the previous two. Consider a domain b consisting of two bodies $b^{(1)}$ and $b^{(2)}$ with respective boundaries $\partial b^{(1)}$ and $\partial b^{(2)}$. The two bodies are in contact over portions of $\partial b^{(1)}$ and $\partial b^{(2)}$, respectively denoted $\gamma^{(1)}$ and $\gamma^{(2)}$. The contribution of contact to the external virtual work may be written as

$$\delta G_c = \sum_{i=1}^{2} \int_{\gamma^{(i)}} \delta \mathbf{v}^{(i)} \cdot \mathbf{t}^{(i)} \, da^{(i)} \tag{7.1.34}$$

where $\delta \mathbf{v}^{(i)}$ is a virtual velocity, $\mathbf{t}^{(i)}$ represents the traction on $\gamma^{(i)}$, and $da^{(i)}$ is an elemental area of $\gamma^{(i)}$. In contact analyses, the tractions on $\gamma^{(i)}$ are equal and opposite, $\mathbf{t}^{(1)} = -\mathbf{t}^{(2)}$, and the contact surfaces are shared, hence we may select one surface to perform the integration over. The virtual work arising from contact may be written as an integral over the primary surface $\gamma^{(1)}$ only, yielding

$$\delta G_c = \int_{\gamma^{(1)}} \left(\delta \mathbf{v}^{(1)} - \delta \mathbf{v}^{(2)} \right) \cdot \mathbf{t}^{(1)} \, da^{(1)} \tag{7.1.35}$$

Eq.(7.1.35) is commonly referred to as the contact integral.

To evaluate the directional derivatives of δG_c along increments in the displacements $\Delta \mathbf{u}^{(i)}$ of $\gamma^{(i)}$, as required for an iterative technique such as Newton's method, it is necessary to formulate the integration over an invariant domain so that the directional derivative may be brought inside

the integral without concern for variations in the domain of integration. In our approach the integral is formulated over the invariant parametric space of $\gamma^{(1)}$ [11, 27].

Each surface $\gamma^{(i)}$ is expressed in parametric form using coordinates $\eta^{\alpha}_{(i)}$, and material points $X^{(i)}$ are identified through their parametric coordinates. On each surface $\gamma^{(i)}$, covariant basis vectors are given by

$$\mathbf{g}^{(i)}_{\alpha} = \frac{\partial \mathbf{x}^{(i)}}{\partial \eta^{\alpha}_{(i)}} \,. \tag{7.1.36}$$

Here, $\mathbf{x}^{(i)}\left(\eta^{\alpha}_{(i)}, t\right)$ is the spatial representation of surface $\gamma^{(i)}$ as it deforms over time t, in terms of contravariant surface parametric coordinates $\eta^{\alpha}_{(i)}$. These covariant basis vectors are tangent to $\gamma^{(i)}$, and it follows that the unit outward normal to $\gamma^{(i)}$ is

$$\mathbf{n}^{(i)} = \frac{\mathbf{g}^{(i)}_1 \times \mathbf{g}^{(i)}_2}{\left|\mathbf{g}^{(i)}_1 \times \mathbf{g}^{(i)}_2\right|} \,. \tag{7.1.37}$$

Furthermore, the elemental area on $\gamma^{(i)}$ is evaluated as

$$da^{(i)} = J^{(i)}_{\eta}\, d\eta^1_{(i)} d\eta^2_{(i)} \,, \quad J^{(i)}_{\eta} = \left|\mathbf{g}^{(i)}_1 \times \mathbf{g}^{(i)}_2\right| \,. \tag{7.1.38}$$

Therefore the contact integral of Eq.(7.1.35) may be placed into matrix form and rewritten as

$$\delta G_c = \int_{\Gamma^{(1)}_{\eta}} \begin{bmatrix} \delta \mathbf{v}^{(1)} & \delta \mathbf{v}^{(2)} \end{bmatrix} \cdot \begin{bmatrix} \mathbf{t}^{(1)} \\ -\mathbf{t}^{(1)} \end{bmatrix} J^{(1)}_{\eta}\, d\eta^1_{(1)} d\eta^2_{(1)} \,, \tag{7.1.39}$$

where $\Gamma^{(1)}_{\eta}$ represents the invariant parametric space of surface $\gamma^{(1)}$ and integration is performed over points $X^{(1)}$ with prescribed parametric coordinates $\eta^{\alpha}_{(1)}$. Since $\Gamma^{(1)}_{\eta}$ represents a material frame, it is possible to linearize δG_c by applying the directional derivative operator directly to the integrand,

$$D\delta G_c = \int_{\Gamma^{(1)}_{\eta}} D\left(\begin{bmatrix} \delta \mathbf{v}^{(1)} & \delta \mathbf{v}^{(2)} \end{bmatrix} \cdot \begin{bmatrix} \mathbf{t}^{(1)} \\ -\mathbf{t}^{(1)} \end{bmatrix} J^{(1)}_{\eta} \right) d\eta^1_{(1)} d\eta^2_{(1)} \,, \tag{7.1.40}$$

where it is understood that for any function f,

$$Df \equiv \sum_{i=1}^{2} Df\left[\Delta \mathbf{u}^{(i)}\right] \,. \tag{7.1.41}$$

To proceed with this linearization, it is necessary to formulate the kinematics of points on $\gamma^{(i)}$ and provide expressions for the contact traction $\mathbf{t}^{(1)}$ that can differentiate between frictional stick and slip.

7.1.9.1 Slip Kinematics

During contact slip, $\gamma^{(1)}$ and $\gamma^{(2)}$ move relative to one another as their configurations evolve. Performing a contact analysis requires mapping points between these surfaces. For the spatial position $\mathbf{x}^{(1)}\left(\eta^{\alpha}_{(1)}, t\right)$ of each material point on the primary surface, we define the intersection point

$\mathbf{x}^{(2)}\left(\eta^{\alpha}_{(2)}, t\right)$ on the secondary surface as the point intersected by a ray directed along the unit outward normal to the primary surface $\mathbf{n}^{(1)}\left(\eta^{\alpha}_{(1)}, t\right)$,

$$\mathbf{x}^{(2)} = \mathbf{x}^{(1)} + g\mathbf{n}^{(1)}, \tag{7.1.42}$$

where the gap function g is defined to be positive when the surfaces $\gamma^{(1)}$ and $\gamma^{(2)}$ are separated, and negative when they penetrate,

$$g = \left(\mathbf{x}^{(2)} - \mathbf{x}^{(1)}\right) \cdot \mathbf{n}^{(1)}. \tag{7.1.43}$$

The ray intersects $\gamma^{(2)}$ at a spatial position $\mathbf{x}^{(2)}$ through which different material points $X^{(2)}$ identified by parametric coordinates $\eta^{\alpha}_{(2)}$ may convect. Computationally, this ray intersection and contact detection is performed with an Octree method [40].

The projection approach of Eq.(7.1.42), described in our previous study [11] and commonly termed *ray-tracing* [80], can be characterized as an inverse projection relative to the classical contact mechanics approach used for NTS contact [65, 109]. Although the definition of this projection and its associated gap function is not new, it has typically been employed mostly for mortar contact (e.g. as in Tur et al. [103]). The benefits associated with a projection method such as Eq.(7.1.42) for non-mortar contact have been developed in detail [80]. Here it suffices to note that avoiding a reliance on secondary surface normal vectors eliminates many contact-searching difficulties that plague NTS algorithms [112], and also serves to greatly reduce the complexity of the linearizations and the resulting stiffness matrices.

7.1.9.2 Stick Kinematics

Equations (7.1.42) and (7.1.43) describe searching for evolving contact and are only valid during slip. In stick no relative motion occurs between contacting points, thus the intersection point $X^{(2)}$ on $\gamma^{(2)}$ does not evolve during the iterative solution process, allowing the development of kinematics of sticking contact. Implicit in this condition is the assumption that the contact projection was previously resolved, and thus contact searching is not performed again; rather, the contact point on $\gamma^{(2)}$ is given by the parametric coordinates of intersection $\eta^{\alpha}_{(2)}$ found from the previous time point, which will be denoted as $\eta^{\alpha}_{(2)p}$, with the subscripted p referring to the previous time. Thus, we write the spatial position of $X^{(2)}$ in stick as

$$\mathbf{x}^{(2)}_s = \mathbf{x}^{(2)}\left(\eta^{\alpha}_{(2)p}, t\right) = \mathbf{x}^{(1)}\left(\eta^{\alpha}_{(1)}, t\right) + \mathbf{g}_s\,, \tag{7.1.44}$$

where $\mathbf{g}_s$ is a vectorial gap function,

$$\mathbf{g}_s = \mathbf{x}^{(2)}_s - \mathbf{x}^{(1)}\,. \tag{7.1.45}$$

Here, $\mathbf{g}_s$ is the vectorial distance, at the current time t, between material points which were in contact at the previous time step; for perfect stick we must have $\mathbf{g}_s = \mathbf{0}$. In a finite element implementation however, it is important to note that the intersection point $\mathbf{x}^{(2)}_s$ is not in general the point that would be found from a ray directed from $\eta^{\alpha}_{(1)}$ along the unit outward normal $\mathbf{n}^{(1)}$. This is because stick will not be enforced exactly, so the points $\mathbf{x}^{(1)}$ and $\mathbf{x}^{(2)}_s$ will separate slightly when using a penalty method for enforcing this constraint. How to minimize this separation and enforce perfect stick behavior is the subject of the forthcoming sections.

7.1.9.3 Velocities

The kinematics developed above can be used to formulate velocities. The formulation for stick developed in Section 7.1.9.4 does not rely on velocity constraints, therefore we are only concerned with velocities of opposing contact points in slip. The development of velocities presented below anticipates the need for a relative velocity as required by Coulomb's law of kinetic friction, which aligns the friction force with this slip direction.

Since the parametric coordinates $\eta^\alpha_{(1)}$ of integration points represent material points on $\gamma^{(1)}$, the velocity $\mathbf{v}^{(1)}$ of these points on the primary surface is evaluated from the material time derivative in the material frame,

$$\mathbf{v}^{(1)}\left(\eta^\alpha_{(1)},t\right)=\frac{\partial\mathbf{x}^{(1)}\left(\eta^\alpha_{(1)},t\right)}{\partial t}\,. \tag{7.1.46}$$

In contrast, since material may convect through the intersection point of the ray with $\gamma^{(2)}$, the total velocity $\mathbf{v}^{(2)}$ at the intersection point on $\gamma^{(2)}$ needs to be evaluated using the material time derivative in the spatial frame,

$$\mathbf{v}^{(2)}\left(\eta^\alpha_{(2)},t\right)=\frac{\partial\mathbf{x}^{(2)}\left(\eta^\alpha_{(2)},t\right)}{\partial t}+\dot\eta^\alpha_{(2)}\mathbf{g}^{(2)}_\alpha\,. \tag{7.1.47}$$

Here, $\partial\mathbf{x}^{(2)}/\partial t$ represents the velocity of the intersection point on $\gamma^{(2)}$, whereas $\dot\eta^\alpha_{(2)}$ are the contravariant components of the convective velocity of material passing through this intersection point. In effect, $\dot\eta^\alpha_{(2)}\mathbf{g}^{(2)}_\alpha$ represents the relative (slip) velocity between the material on $\gamma^{(2)}$ and that on $\gamma^{(1)}$. Importantly, as noted below when performing time discretization and linearization, by definition $\partial\mathbf{x}^{(2)}/\partial t$ is evaluated while keeping $\eta^\alpha_{(2)}$ constant.

We now use these relations to produce a more practical formulation of the slip velocity for our frictional contact implementation. Taking the material time derivative of Eq.(7.1.42) and using the contact persistency condition $\dot g=0$ [64] produces $\mathbf{v}^{(2)}=\mathbf{v}^{(1)}+g\dot{\mathbf{n}}^{(1)}$. Substituting Eqs.(7.1.46)-(7.1.47) into this expression yields a frame-invariant measure of relative velocity between $\gamma^{(1)}$ and $\gamma^{(2)}$ [35, 80],

$$\mathbf{v}^r\equiv\dot\eta^\alpha_{(2)}\mathbf{g}^{(2)}_\alpha=g\dot{\mathbf{n}}^{(1)}+\frac{\partial\mathbf{x}^{(1)}\left(\eta^\alpha_{(1)},t\right)}{\partial t}-\frac{\partial\mathbf{x}^{(2)}\left(\eta^\alpha_{(2)},t\right)}{\partial t}, \tag{7.1.48}$$

where $\dot{\mathbf{n}}^{(1)}$ is the material time derivative of $\mathbf{n}^{(1)}$ in the parametric material frame of $\gamma^{(1)}$, evaluated from Eq.(7.1.37) as

$$\dot{\mathbf{n}}^{(1)}=\mathbf{P}_N\cdot\frac{\dot{\mathbf{g}}^{(1)}_1\times\mathbf{g}^{(1)}_2+\mathbf{g}^{(1)}_1\times\dot{\mathbf{g}}^{(1)}_2}{J^{(1)}_\eta}\,. \tag{7.1.49}$$

Here, $\dot{\mathbf{g}}^{(1)}_\alpha$ denotes the material time derivative of $\mathbf{g}^{(1)}_\alpha$ in the material frame,

$$\dot{\mathbf{g}}^{(1)}_\alpha\left(\eta^\beta_{(1)},t\right)=\frac{\partial\mathbf{g}^{(1)}_\alpha\left(\eta^\beta_{(1)},t\right)}{\partial t}\,, \tag{7.1.50}$$

and we define the tangential plane projection tensor $\mathbf{P}_N$ as

$$\mathbf{P}_N=\mathbf{I}-\mathbf{n}^{(1)}\otimes\mathbf{n}^{(1)}\,. \tag{7.1.51}$$

Previous authors have utilized $\mathbf{v}^r=\dot\eta^\alpha_{(2)}\mathbf{g}^{(2)}_\alpha$ directly instead of the right-hand-side of Eq.(7.1.48); this expression requires the evaluation of time derivatives of parametric coordinates [64, 88, 111],

which necessitates special integration algorithms to handle crossing element boundaries [36]. The relative velocity measure on the right-hand-side of Eq.(7.1.48) obviates the need for any such special treatment. In particular, the choice of $\partial \mathbf{x}^{(2)}/\partial t$ ensures that element boundaries will never be crossed when calculating this velocity, since it is evaluated while keeping $\eta^{\alpha}_{(2)}$ constant.

The tangential frictional traction in slip depends only on the tangential component of the relative velocity, therefore we may define the slip direction $\mathbf{s}^{(1)}$ as the unit vector of the projection $\mathbf{P}_N \cdot \mathbf{v}^r$ of $\mathbf{v}^r$ onto the tangent plane of $\gamma^{(1)}$,

$$\mathbf{s}^{(1)} = \frac{\mathbf{P}_N \cdot \mathbf{v}^r}{|\mathbf{P}_N \cdot \mathbf{v}^r|} \,, \tag{7.1.52}$$

These definitions of contact kinematics may now be used to formulate frictional contact.

7.1.9.4 Coulomb Frictional Contact

This work considers Coulomb frictional contact, with no distinction made between static and kinetic coefficients of friction. Although classical Coulomb friction is the most frequently adopted behavior, it should be noted that other constitutive equations, including micromechanically-inspired formulations which consider local phenomena, have been proposed as well [109, 111]. During frictional contact, the contact traction $\mathbf{t}^{(i)}$ on the opposing surfaces is determined by the sticking or slipping behavior. For Coulomb friction, the relationship between sticking and slipping is described by a slip criterion Φ, where on the primary surface

$$\Phi = \left|\mathbf{t}^{(1)}_T\right| - \mu \left|t_n\right| \,. \tag{7.1.53}$$

Here, $t_n = \mathbf{t}^{(1)} \cdot \mathbf{n}^{(1)}$ is the normal component of the contact traction (negative in compression), $\mathbf{t}^{(1)}_T = \mathbf{t}^{(1)} - t_n \mathbf{n}^{(1)}$ is the tangential component of the contact traction, and μ is the friction coefficient. The value of the slip criterion determines the stick-slip status,

$$\Phi \begin{cases} < 0 & \text{sticking} \\ = 0 & \text{slipping} \end{cases} \tag{7.1.54}$$

Algorithmically, stick and slip are typically based on a predictor-corrector approach derived from an analogy with elastoplasticity [45], leading to constitutive relations for the rate of the traction and thus requiring numerical integration [36]. Variations of this approach have been utilized in differing forms [64, 88, 111].

In contrast, this presentation proposes to treat stick and slip separately, controlled by an exact return mapping based on the slip criterion. The return mapping defines a rule for correcting a calculated traction which exceeds the slip limit and is thus not permissible. Stick will be treated as a special case of a tied interface, whereas in slip the traction will be directly prescribed. The formulation of Coulomb frictional contact is presented for both penalty and augmented Lagrangian regularization schemes.

7.1.9.5 Penalty Scheme

During stick, no relative motion may occur between surfaces; thus, points on $\gamma^{(1)}$ and $\gamma^{(2)}$ that were in contact at the previous time must remain in contact. The stick traction may be obtained by penalizing any relative motion between such points,

$$\mathbf{t}^{(1)} = \varepsilon \mathbf{g}_s \,, \tag{7.1.55}$$

where ε is the penalty parameter and we have employed Eq.(7.1.45).

During slip, we first calculate the normal component of the contact traction by penalizing the normal gap of Eq.(7.1.43),

$$t_n = \varepsilon g \,. \tag{7.1.56}$$

The total traction vector is then directly obtained as

$$\mathbf{t}^{(1)} = t_n \left(\mathbf{n}^{(1)} + \mu \mathbf{s}^{(1)} \right) \,. \tag{7.1.57}$$

Here we have achieved an exact expression for the tangential traction in slip and remark that since t_n is strictly negative in contact, the frictional contact traction $\mu t_n \mathbf{s}^{(1)}$ acting on $\gamma^{(1)}$ is in the direction opposing the motion of $\gamma^{(1)}$ relative to $\gamma^{(2)}$. A trial state and return map, presented in Section 7.1.9.7, is employed to differentiate between stick and slip.

7.1.9.6 Augmented Lagrangian Scheme

The augmented Lagrangian scheme employed in this study is first order and utilizes Uzawa's algorithm [22], where multipliers are updated outside of the Newton step, producing a double loop algorithm (see the texts by Laursen [65] and Wriggers [109] for a discussion of Uzawa's algorithm applied to frictional contact problems). Such an approach preserves the quadratic convergence of Newton's method near solution points. The presented scheme is a modification of the approach suggested by Simo and Laursen [91].

During stick, the traction is calculated by augmenting the vector gap $\mathbf{g}_s$,

$$\mathbf{t}^{(1)} = \boldsymbol{\lambda}_s + \varepsilon \mathbf{g}_s \,, \tag{7.1.58}$$

where $\boldsymbol{\lambda}_s$ is the vectorial Lagrange multiplier in stick. In slip, we first calculate the normal component of the contact traction by augmenting the normal gap g,

$$t_n = \lambda_n + \varepsilon g \,, \tag{7.1.59}$$

where λ_n is the normal Lagrange multiplier. The total traction vector in slip is then defined to be

$$\mathbf{t}^{(1)} = t_n \left(\mathbf{n}^{(1)} + \mu \mathbf{s}^{(1)} \right) \,, \tag{7.1.60}$$

where t_n is given by Eq.(7.1.59). In this approach the Lagrange multiplier $\boldsymbol{\lambda}_s$ augments the traction $\mathbf{t}^{(1)}$ in stick, but in slip only the normal component of traction t_n is augmented by λ_n and the tangential traction is directly prescribed from the augmented normal component. This approach has the advantage of preserving an exact mapping to the proper tangential traction in slip, which is consistent with the augmented normal traction. As in the penalty case, a trial state and return map controlled by the slip criterion is employed to differentiate between stick and slip, presented in Section 7.1.9.7.

The Lagrange multipliers λ_n and $\boldsymbol{\lambda}_s$ are held constant during each Newton step. Outside of the Newton loop, in this study we propose a novel update scheme where one of these multipliers is considered active and is updated from the kinematic data ($\mathbf{g}_s$ or g), and the other is considered passive and is derived from the active multiplier. The contact status is determined via Eq.(7.1.54). If the current status is stick ($\Phi < 0$), we update $\boldsymbol{\lambda}_s$ (active) and derive λ_n (passive),

$$\begin{aligned} \boldsymbol{\lambda}_s &\leftarrow \boldsymbol{\lambda}_s + \varepsilon \mathbf{g}_s \\ \lambda_n &= \boldsymbol{\lambda}_s \cdot \mathbf{n}^{(1)} \end{aligned} \tag{7.1.61}$$

Alternatively, if the current contact status is slip ($\Phi = 0$), we update λ_n (active) and derive $\boldsymbol{\lambda}_s$ (passive),

$$\begin{aligned} \lambda_n &\leftarrow \lambda_n + \varepsilon g \\ \boldsymbol{\lambda}_s &= \lambda_n \left(\mathbf{n}^{(1)} + \mu \mathbf{s}^{(1)} \right) \end{aligned} \tag{7.1.62}$$

An active-passive strategy for the multipliers ensures consistency when the contact status switches between stick and slip and is made possible due to this formulation's use of a single penalty parameter ε, in conjunction with an exact return mapping for slip.

Augmentations proceed until a tolerance related to a convergence criterion is met. In this formulation, two separate convergence criteria and their associated tolerances are defined. The first criterion considers the relative change of the norms of the active Lagrange multipliers between successive iterations, where the associated unitless tolerance P_{tol} specifies the largest allowable change. Convergence is achieved when

$$\left| \frac{L^r - L^{r-1}}{L^r} \right| < P_{tol} \,, \tag{7.1.63}$$

where L^r represents the total norm of the active multipliers across the contact surface at augmentation step r, calculated by summing all the individual norms,

$$L^r = \sum_{e=1}^{n_e^{(1)}} \sum_{k=1}^{n_{int}^{(e)}} l_{k,e}^r \tag{7.1.64}$$

In this expression, $n_e^{(1)}$ is the number of element faces on $\gamma^{(1)}$, $n_{int}^{(e)}$ is the number of integration points on the eth element face, and $l_{k,e}^r$ is the norm of the active Lagrange multiplier at the kth integration point on the eth element of $\gamma^{(1)}$ at augmentation step r, defined by

$$l_{k,e}^r = \begin{cases} \boldsymbol{\lambda}_s^r \cdot \boldsymbol{\lambda}_s^r & \Phi < 0, \quad \text{sticking} \\ (\lambda_n^r)^2 & \Phi = 0, \quad \text{slipping} \end{cases} \tag{7.1.65}$$

The second criterion is a gap tolerance, where augmentations will continue until the magnitude of the gap is lower than the specified tolerance G_{tol} at every location. Convergence of the augmentations requires

$$\text{max } (|\mathbf{g}_s| \,, |g|) < G_{tol} \tag{7.1.66}$$

where $|\mathbf{g}_s|$ is associated with points currently sticking and $|g|$ with those in slip. The tolerance G_{tol} has units of length, allowing enforcement of the non-penetration and stick constraints to arbitrarily small precision.

7.1.9.7 Stick-Slip Algorithm

Determination of whether stick or slip is active is accomplished by a trial state and return map, and follows the same procedure for both penalty and augmented Lagrangian regularizations. We begin by calculating a trial traction $\tilde{\mathbf{t}}^{(1)}$ assuming stick, utilizing either Eq.(7.1.55) or Eq.(7.1.58). The trial normal and tangential components $\tilde{t}_n$ and $\tilde{\mathbf{t}}_T^{(1)}$ are evaluated from $\tilde{\mathbf{t}}^{(1)}$ and inserted into the slip criterion Φ,

$$\Phi = \left| \tilde{\mathbf{t}}_T^{(1)} \right| - \mu \left| \tilde{t}_n \right| . \tag{7.1.67}$$

Based on the slip criterion and trial traction vector, we perform a return mapping and obtain the traction vector as

$$\mathbf{t}^{(1)} = \begin{cases} \tilde{\mathbf{t}}^{(1)} & \Phi < 0\,, \quad \text{sticking} \\ t_n(\mathbf{n}^{(1)} + \mu \mathbf{s}^{(1)}) & \Phi = 0\,, \quad \text{slipping} \end{cases} \tag{7.1.68}$$

where t_n is given by either Eq.(7.1.56) or Eq.(7.1.59). In the case of first contact, a trial stick traction cannot be calculated, as stick requires a previous intersection point. Consequently, first contact is treated as a case of slip in this framework. The alternative of treating first contact as frictionless is unsatisfying, as the lack of friction at the first iteration can lead to premature failure and thus precludes the modeling of certain problems that rely on frictional forces for stability (such as load-control analyses). After one iteration, the traction can be evaluated via the return map described above.

Computationally, care must be taken to ensure that augmentation does not unnecessarily change the stick-slip status. For normal contact, the update $\lambda_n \leftarrow \lambda_n + \varepsilon g$ will augment the normal traction until the non-penetration contact constraint is adequately satisfied, with no adverse consequence if λ_n slightly overshoots the final target value during an intermediate augmentation. For tangential contact however, augmentation of the tangential traction that overshoots the final target value may cross the boundary between stick and slip, thus changing the nature of the solution. For example, at the first augmentation step, the stick traction is $\mathbf{t}^{(1)} = \varepsilon \mathbf{g}_s$ and the multiplier $\boldsymbol{\lambda}_s$ is augmented from its initial zero value to $\boldsymbol{\lambda}_s = \varepsilon \mathbf{g}_s$ according to Eq.(7.1.61). Thus, at the start of the next iteration, when $\mathbf{g}_s$ has not yet changed, the traction is calculated as $\mathbf{t}^{(1)} = \boldsymbol{\lambda}_s + \varepsilon \mathbf{g}_s = 2\varepsilon \mathbf{g}_s$ according to Eq.(7.1.58), which essentially counts the gap function twice and can in some cases shift the contact from stick to slip. To circumvent potential error introduced by this step, our implementation freezes the stick-slip status until the completion of the first iteration following an augmentation step. After the first iteration, the gap function has been reduced by the augmentation and the traction is split appropriately between the remaining gap and the multiplier. In this way, the double-counting of the gap function does not unnecessarily shift the contact status, but augmentation is able to modify the stick-slip status if accurate enforcement of the contact constraints requires it.

7.1.9.8 Linearization

To evaluate the linearization in Eq.(7.1.40) requires directional derivatives of kinematic quantities, some of which are dependent on the stick-slip status. In an attempt to simplify the presentation, the continuum linearization of only a few kinematic quantities is described below, and the majority of the linearization will be deferred until after the discretization presented in Section 7.1.9.9. We note that, as a consequence of the double-loop Uzawa algorithm discussed in Section 7.1.9.6, the Lagrange multipliers are updated outside of each Newton step and thus $D\lambda_n = 0$ and $D\boldsymbol{\lambda}_s = \mathbf{0}$ in the following linearizations. Furthermore, in forthcoming sections, $\Delta\mathbf{u}^{(i)}$ refers to an increment in displacement in the trial solution $\boldsymbol{\chi}$. All other expressions which employ Δ are slight abuses of notation, used to compactly denote changes in a quantity from the previous time step.

Stick Parametric coordinates on the primary surface are always invariant since they represent material points $X^{(1)}$ where the contact integral is to be evaluated (integration points), and in stick the parametric coordinates of contact on the secondary surface are similarly fixed by definition. Accordingly, directional derivatives of $\delta\mathbf{v}^{(i)}$ and $\mathbf{x}^{(i)}$ are given by

$$\begin{aligned} D\mathbf{x}^{(1)} &= \Delta\mathbf{u}^{(1)}\,, \qquad D\mathbf{x}^{(2)} = \Delta\mathbf{u}^{(2)} \\ D\delta\mathbf{v}^{(1)} &= \mathbf{0}\,, \qquad\quad D\delta\mathbf{v}^{(2)} = \mathbf{0} \end{aligned} \tag{7.1.69}$$

From the above expressions and Eqs.(7.1.36) and (7.1.38), we find directional derivatives of $\mathbf{g}_\alpha^{(1)}$ and $J_\eta^{(1)}$ to be

$$\begin{aligned} D\mathbf{g}_\alpha^{(1)} &= \frac{\partial \Delta\mathbf{u}^{(1)}}{\partial \eta_{(1)}^\alpha} \\ DJ_\eta^{(1)} &= \mathbf{n}^{(1)} \cdot \left(\hat{\mathbf{g}}_1^{(1)} \cdot \frac{\partial \Delta\mathbf{u}^{(1)}}{\partial \eta_{(1)}^2} - \hat{\mathbf{g}}_2^{(1)} \cdot \frac{\partial \Delta\mathbf{u}^{(1)}}{\partial \eta_{(1)}^1} \right) \end{aligned} \tag{7.1.70}$$

where $\hat{\mathbf{g}}_\alpha^{(1)}$ is a skew-symmetric tensor whose dual vector is $\mathbf{g}_\alpha^{(1)}$; thus $\hat{\mathbf{g}}_\alpha^{(1)} \cdot \mathbf{z} = \mathbf{g}_\alpha^{(1)} \times \mathbf{z}$ for any vector $\mathbf{z}$. Given the definitions of Eqs.(7.1.45) and (7.1.55), along with the relations of Eq.(7.1.69), it follows that

$$D\mathbf{t}^{(1)} = \varepsilon \left(\Delta\mathbf{u}^{(2)} - \Delta\mathbf{u}^{(1)} \right) . \tag{7.1.71}$$

The linearization operator may be brought inside the contact integral of Eq.(7.1.39) to find

$$\begin{aligned} D\delta G_c = \int_{\Gamma_\eta^{(1)}} \begin{bmatrix} \delta\mathbf{v}^{(1)} & \delta\mathbf{v}^{(2)} \end{bmatrix} \cdot \Bigg(& \begin{bmatrix} 1 \\ -1 \end{bmatrix} D\mathbf{t}^{(1)} J_\eta^{(1)} \\ & + \begin{bmatrix} \mathbf{t}^{(1)} \\ -\mathbf{t}^{(1)} \end{bmatrix} DJ_\eta^{(1)} \Bigg) \, d\eta_{(1)}^1 d\eta_{(1)}^2 \end{aligned} \tag{7.1.72}$$

where we recall that $D\delta\mathbf{v}^{(1)} = D\delta\mathbf{v}^{(2)} = \mathbf{0}$ from Eq.(7.1.69).

Slip As in stick, the contact integral over $\gamma^{(1)}$ is performed over integration points of prescribed parametric coordinates $\eta_{(1)}^\alpha$. However, the point on $\gamma^{(2)}$ in contact with $\gamma^{(1)}$ has parametric coordinates $\eta_{(2)}^\alpha$ that change with variations in $\mathbf{x}^{(1)}$ and $\mathbf{n}^{(1)}$, in accordance with Eq.(7.1.42). Thus, directional derivatives of $\delta\mathbf{v}^{(i)}$ and $\mathbf{x}^{(i)}$ are given by

$$\begin{aligned} D\mathbf{x}^{(1)} &= \Delta\mathbf{u}^{(1)} , \qquad D\mathbf{x}^{(2)} = \Delta\mathbf{u}^{(2)} + \mathbf{g}_\alpha^{(2)} D\eta_{(2)}^\alpha \\ D\delta\mathbf{v}^{(1)} &= \mathbf{0} , \qquad\quad D\delta\mathbf{v}^{(2)} = \frac{\partial \delta\mathbf{v}^{(2)}}{\partial \eta_{(2)}^\alpha} D\eta_{(2)}^\alpha \end{aligned} \tag{7.1.73}$$

where we recall that $\mathbf{x}^{(2)}$ is the spatial location of the intersection point $\eta_{(2)}^\alpha$ at the current time t.

We evaluate $D\eta_{(2)}^\alpha$ in terms of increments in solid displacements by means of our modification [9] of a method proposed by Laursen and Simo [64]. Briefly, recognizing that $\left(\mathbf{x}^{(2)} - \mathbf{x}^{(1)}\right) \cdot \mathbf{g}_\alpha^{(1)} = 0$, the directional derivative of this expression is evaluated and the resulting linear system is inverted to yield

$$D\eta_{(2)}^\alpha = \left(\Delta\mathbf{u}^{(1)} - \Delta\mathbf{u}^{(2)} \right) \cdot \bar{\mathbf{g}}_{(2)}^\alpha - a^{\alpha\beta} g \mathbf{n}^{(1)} \cdot \frac{\partial \Delta\mathbf{u}^{(1)}}{\partial \eta_{(1)}^\beta} \tag{7.1.74}$$

where $a^{\alpha\beta} = (A_{\alpha\beta})^{-1}$, $A_{\alpha\beta} = \mathbf{g}_\alpha^{(1)} \cdot \mathbf{g}_\beta^{(2)}$, and

$$\bar{\mathbf{g}}_{(1)}^\beta = a^{\alpha\beta} \mathbf{g}_\alpha^{(2)}, \quad \bar{\mathbf{g}}_{(2)}^\alpha = a^{\alpha\beta} \mathbf{g}_\beta^{(1)}. \tag{7.1.75}$$

In this expression, $\bar{\mathbf{g}}_{(i)}^\alpha$ are approximate contravariant basis vectors on $\gamma^{(i)}$. In the limit of perfect contact ($g \to 0$), $\gamma^{(1)}$ and $\gamma^{(2)}$ become true mating surfaces and a number of relations emerge,

including $\bar{\mathbf{g}}^{\alpha}_{(i)} \rightarrow \mathbf{g}^{\alpha}_{(i)}$ since $a^{\alpha\beta} \rightarrow \mathbf{g}^{\alpha}_{(2)} \cdot \mathbf{g}^{\beta}_{(1)}$ (see the discussion following Eq.(40) in [9]). In the present formulation, this simplification to perfect contact is not adopted, as it was determined that retaining all terms provides better convergence and stability.

From Eq.(7.1.57) it follows that

$$D\mathbf{t}^{(1)} = Dt_n \left(\mathbf{n} + \mu \mathbf{s}^{(1)}\right) + t_n \left(D\mathbf{n}^{(1)} + \mu D\mathbf{s}^{(1)}\right) . \tag{7.1.76}$$

By Eq.(7.1.56), $Dt_n = \varepsilon Dg$, and

$$Dg = \left(\Delta\mathbf{u}^{(2)} - \Delta\mathbf{u}^{(1)} + \mathbf{g}^{(2)}_{\alpha} D\eta^{\alpha}_{(2)}\right) \cdot \mathbf{n}^{(1)} \quad . \tag{7.1.77}$$

Applying the linearization operator to Eq.(7.1.52) yields

$$D\mathbf{s}^{(1)} = \frac{1}{|\mathbf{P}_N \cdot \mathbf{v}^r|} (\mathbf{I} - \mathbf{s}^{(1)} \otimes \mathbf{s}^{(1)}) \cdot \left(D\mathbf{P}_N \cdot \mathbf{v}^r + \mathbf{P}_N \cdot D\mathbf{v}^r\right) \tag{7.1.78}$$

where $D\mathbf{v}^r = Dg\, \dot{\mathbf{n}}^{(1)} + g\, D\dot{\mathbf{n}}^{(1)} + D\left(\partial \mathbf{x}^{(1)}/\partial t\right) - D\left(\partial \mathbf{x}^{(2)}/\partial t\right)$ according to Eq.(7.1.48).

To linearize partial time derivatives of positions $\mathbf{x}^{(i)}$, we adopt Euler integration and find

$$\frac{\partial \mathbf{x}^{(i)}\left(\eta^{\alpha}_{(i)}, t\right)}{\partial t} \approx \frac{\mathbf{x}^{(i)}\left(\eta^{\alpha}_{(i)}, t\right) - \mathbf{x}^{(i)}\left(\eta^{\alpha}_{(i)}, t - \Delta t\right)}{\Delta t} = \frac{\Delta \mathbf{x}^{(i)}}{\Delta t} \tag{7.1.79}$$

where Δt represents the time increment and $\Delta\mathbf{x}^{(i)}$ denotes the change in $\mathbf{x}^{(i)}$ from the previous time step. Since $\eta^{\alpha}_{(i)}$ is kept constant when evaluating the partial time derivative, the linearization of this expression reduces to

$$D\left(\frac{\partial \mathbf{x}^{(i)}\left(\eta^{\alpha}_{(i)}, t\right)}{\partial t}\right) \approx \frac{\Delta \mathbf{u}^{(i)}}{\Delta t} . \tag{7.1.80}$$

Finally, linearizing Eqs.(7.1.37) and (7.1.51) produces

$$D\mathbf{n}^{(1)} = \frac{1}{J^{(1)}_{\eta}} \mathbf{P}_N \cdot \left(\hat{\mathbf{g}}^{(1)}_1 \cdot \frac{\partial \Delta\mathbf{u}^{(1)}}{\partial \eta^2_{(1)}} - \hat{\mathbf{g}}^{(1)}_2 \cdot \frac{\partial \Delta\mathbf{u}^{(1)}}{\partial \eta^1_{(1)}}\right) \tag{7.1.81}$$

and

$$D\mathbf{P}_N = -\left(D\mathbf{n}^{(1)} \otimes \mathbf{n}^{(1)} + \mathbf{n}^{(1)} \otimes D\mathbf{n}^{(1)}\right) . \tag{7.1.82}$$

7.1.9.9 Discretization

Let the continuous variables on the primary and secondary surfaces be interpolated over each element face according to

$$\begin{aligned} \delta\mathbf{v}^{(1)} &= \sum_{a=1}^{m^{(1)}} N^{(1)}_a \delta\mathbf{v}^{(1)}_a , \qquad \delta\mathbf{v}^{(2)} = \sum_{b=1}^{m^{(2)}_k} N^{(2)}_b \delta\mathbf{v}^{(2)}_b \\ \Delta\mathbf{u}^{(1)} &= \sum_{c=1}^{m^{(1)}} N^{(1)}_c \Delta\mathbf{u}^{(1)}_c , \quad \Delta\mathbf{u}^{(2)} = \sum_{d=1}^{m^{(2)}_k} N^{(2)}_d \Delta\mathbf{u}^{(2)}_d \end{aligned} \tag{7.1.83}$$

where $N_a^{(i)}$ represent interpolation functions on the element faces of $\gamma^{(i)}$, $m^{(1)}$ is the number of nodes and interpolation functions on each primary element face, $m_k^{(2)}$ is the number of nodes and interpolation functions on the secondary element face which is intersected by the ray issued from the kth integration point on the primary element face, and $\delta\mathbf{v}_a^{(i)}$ and $\Delta\mathbf{u}_a^{(i)}$ represent respective nodal values of $\delta\mathbf{v}^{(i)}$ and $\Delta\mathbf{u}^{(i)}$. From this point forward, the summation signs will be written simply as $\sum_a$, where it is assumed they have the same meaning described above.

Stick Applying the discretization to Eq.(7.1.39), the contact integral becomes

$$\delta G_c = \begin{bmatrix} \sum_a \delta\mathbf{v}_a^{(1)} & \sum_b \delta\mathbf{v}_b^{(2)} \end{bmatrix} \cdot \int_{\Gamma_\eta^{(1)}} \begin{bmatrix} \mathbf{f}_a^{(1)} \\ \mathbf{f}_b^{(2)} \end{bmatrix} J_\eta^{(1)} d\eta_{(1)}^1 d\eta_{(1)}^2 \tag{7.1.84}$$

where

$$\mathbf{f}_a^{(1)} = N_a^{(1)}\mathbf{t}^{(1)}, \quad \mathbf{f}_b^{(2)} = -N_b^{(2)}\mathbf{t}^{(1)} \tag{7.1.85}$$

and $\mathbf{t}^{(1)}$ is defined by Eq.(7.1.55) in the penalty case and Eq.(7.1.58) when augmented Lagrangian regularization is used. Individual terms may now be discretized and placed into matrix notation, facilitating their substitution into Eq.(7.1.72). A straightforward application of Eq.(7.1.83) to Eq.(7.1.70)$_2$ yields

$$DJ_\eta^{(1)} = \begin{bmatrix} \sum_c J_\eta^{(1)} \mathbf{A}_c^{(1)} \cdot \mathbf{n}^{(1)} & \sum_d \mathbf{0} \end{bmatrix} \cdot \begin{bmatrix} \Delta\mathbf{u}_c^{(1)} \\ \Delta\mathbf{u}_d^{(2)} \end{bmatrix} \tag{7.1.86}$$

where

$$\mathbf{A}_c^{(1)} = \frac{1}{J_\eta^{(1)}} \left(\frac{\partial N_c^{(1)}}{\partial \eta_{(1)}^1} \hat{\mathbf{g}}_2^{(1)} - \frac{\partial N_c^{(1)}}{\partial \eta_{(1)}^2} \hat{\mathbf{g}}_1^{(1)} \right) \tag{7.1.87}$$

and $\begin{bmatrix} \Delta\mathbf{u}_c^{(1)} & \Delta\mathbf{u}_d^{(2)} \end{bmatrix}^T$ is the vector of incremental changes in the degrees of freedom to the cth node associated with the element face on $\gamma^{(1)}$, and to the dth node of the element face on $\gamma^{(2)}$ associated with the current integration point on $\gamma^{(1)}$. Furthermore, discretizing Eq.(7.1.71) produces

$$D\mathbf{t}^{(1)} = \begin{bmatrix} \sum_c -\varepsilon N_c^{(1)} \mathbf{I} & \sum_d \varepsilon N_d^{(2)} \mathbf{I} \end{bmatrix} \cdot \begin{bmatrix} \Delta\mathbf{u}_c^{(1)} \\ \Delta\mathbf{u}_d^{(2)} \end{bmatrix} . \tag{7.1.88}$$

Substituting Eq.(7.1.86) and Eq.(7.1.88) into Eq.(7.1.72) and applying the discretization of Eq.(7.1.83) yields the directional derivative of the virtual work in stick as

$$\begin{aligned} D\delta G_c = & \begin{bmatrix} \sum_a \delta\mathbf{v}_a^{(1)} & \sum_b \delta\mathbf{v}_b^{(2)} \end{bmatrix} \\ & \cdot \int_{\Gamma_\eta^{(1)}} \left(\begin{bmatrix} \sum_c -N_a^{(1)} N_c^{(1)} & \sum_d N_a^{(1)} N_d^{(2)} \\ \sum_c N_b^{(2)} N_c^{(1)} & \sum_d -N_b^{(2)} N_d^{(2)} \end{bmatrix} \varepsilon\mathbf{I} \right. \\ & \left. + \begin{bmatrix} \sum_c -N_a^{(1)} & \sum_d 0 \\ \sum_c N_b^{(2)} & \sum_d 0 \end{bmatrix} \left(-\mathbf{t}^{(1)} \otimes \mathbf{A}_c^{(1)} \cdot \mathbf{n}^{(1)} \right) \right) \\ & \times J_\eta^{(1)} d\eta_{(1)}^1 d\eta_{(1)}^2 \cdot \begin{bmatrix} \Delta\mathbf{u}_c^{(1)} \\ \Delta\mathbf{u}_d^{(2)} \end{bmatrix} \end{aligned} \tag{7.1.89}$$

An examination of Eq.(7.1.89) shows that the stiffness matrix associated with this contact formulation is not symmetric in stick.

Although the stiffness matrix of Eq.(7.1.89) can be cast in a more traditional form,

$$\begin{aligned} D\delta G_c = &\begin{bmatrix} \sum_a \delta \mathbf{v}_a^{(1)} & \sum_b \delta \mathbf{v}_b^{(2)} \end{bmatrix} \\ &\cdot \int_{\Gamma_\eta^{(1)}} \begin{bmatrix} \sum_c \mathbf{K}_{ac}^{(1,1)} & \sum_d \mathbf{K}_{ad}^{(1,2)} \\ \sum_c \mathbf{K}_{bc}^{(2,1)} & \sum_d \mathbf{K}_{bd}^{(2,2)} \end{bmatrix} J_\eta^{(1)} d\eta_{(1)}^1 d\eta_{(1)}^2 \cdot \begin{bmatrix} \Delta \mathbf{u}_c^{(1)} \\ \Delta \mathbf{u}_d^{(2)} \end{bmatrix} \end{aligned} \tag{7.1.90}$$

as was done in [11], splitting up like terms is a more natural way to implement the final equations, and provides some insight into the resulting matrix structure. A discussion of how to numerically evaluate the integrals in the above equations is deferred until Section 7.1.9.12.

Slip In the case of slip, the contact integral of Eq.(7.1.39) can be split into normal and tangential parts, $\delta G_c = \delta G_c^n + \delta G_c^t$, such that

$$\begin{aligned} \delta G_c = &\int_{\Gamma_\eta^{(1)}} \begin{bmatrix} \delta \mathbf{v}^{(1)} & \delta \mathbf{v}^{(2)} \end{bmatrix} \cdot \begin{bmatrix} t_n \mathbf{n}^{(1)} \\ -t_n \mathbf{n}^{(1)} \end{bmatrix} J_\eta^{(1)} d\eta_{(1)}^1 d\eta_{(1)}^2 \\ &+ \int_{\Gamma_\eta^{(1)}} \begin{bmatrix} \delta \mathbf{v}^{(1)} & \delta \mathbf{v}^{(2)} \end{bmatrix} \cdot \begin{bmatrix} \mu t_n \mathbf{s}^{(1)} \\ -\mu t_n \mathbf{s}^{(1)} \end{bmatrix} J_\eta^{(1)} d\eta_{(1)}^1 d\eta_{(1)}^2 \end{aligned} \tag{7.1.91}$$

Discretizing this expression yields

$$\delta G_c = \begin{bmatrix} \sum_a \delta \mathbf{v}_a^{(1)} & \sum_b \delta \mathbf{v}_b^{(2)} \end{bmatrix} \cdot \int_{\Gamma_\eta^{(1)}} \begin{bmatrix} \mathbf{f}_a^{(1)} \\ \mathbf{f}_b^{(2)} \end{bmatrix} J_\eta^{(1)} d\eta_{(1)}^1 d\eta_{(1)}^2 \tag{7.1.92}$$

where

$$\mathbf{f}_a^{(1)} = t_n N_a^{(1)} \left(\mathbf{n}^{(1)} + \mu \mathbf{s}^{(1)} \right), \quad \mathbf{f}_b^{(2)} = -t_n N_b^{(2)} \left(\mathbf{n}^{(1)} + \mu \mathbf{s}^{(1)} \right) \tag{7.1.93}$$

and t_n is given by Eq.(7.1.56) in the penalty formulation and Eq.(7.1.59) with augmented Lagrangian regularization.

For the following linearization and discretization the normal and tangential components, representing frictionless and frictional contributions to the contact integral, will be treated separately and may then be added together as in Eq.(7.1.91).

7.1.9.10 Frictionless Terms

The linearization of the frictionless contribution δG_c^n makes use of Eq.(7.1.73) to find

$$\begin{aligned} D\delta G_c^n = &\int_{\Gamma_\eta^{(1)}} \begin{bmatrix} \mathbf{0} & \frac{\partial \delta \mathbf{v}^{(2)}}{\partial \eta_{(2)}^\alpha} \end{bmatrix} \cdot \begin{bmatrix} t_n \mathbf{n}^{(1)} \\ -t_n \mathbf{n}^{(1)} \end{bmatrix} D\eta_{(2)}^\alpha J_\eta^{(1)} d\eta_{(1)}^1 d\eta_{(1)}^2 \\ &+ \int_{\Gamma_\eta^{(1)}} \begin{bmatrix} \delta \mathbf{v}^{(1)} & \delta \mathbf{v}^{(2)} \end{bmatrix} \cdot \left(\begin{bmatrix} t_n \mathbf{n}^{(1)} \\ -t_n \mathbf{n}^{(1)} \end{bmatrix} DJ_\eta^{(1)} \right. \\ &\left. + \begin{bmatrix} \mathbf{n}^{(1)} \\ -\mathbf{n}^{(1)} \end{bmatrix} Dt_n J_\eta^{(1)} + \begin{bmatrix} t_n \\ -t_n \end{bmatrix} D\mathbf{n}^{(1)} J_\eta^{(1)} \right) d\eta_{(1)}^1 d\eta_{(1)}^2 \end{aligned} \tag{7.1.94}$$

Evaluating Eq.(7.1.94) requires $D\mathbf{n}^{(1)}$, Dt_n, and $D\eta^{\alpha}_{(2)}$. Directly inserting Eqs.(7.1.73) and (7.1.83) into Eqs.(7.1.74), (7.1.77), and (7.1.81) yields

$$\begin{aligned} D\eta^{\alpha}_{(2)} &= \left[\sum_c N^{(1)}_c \bar{\mathbf{g}}^{\alpha}_{(2)} - ga^{\alpha\beta}\frac{\partial N^{(1)}_c}{\partial \eta^{\beta}_{(1)}}\mathbf{n}^{(1)} \quad \sum_d -N^{(2)}_d \bar{\mathbf{g}}^{\alpha}_{(2)}\right] \cdot \begin{bmatrix}\Delta\mathbf{u}^{(1)}_c \\ \Delta\mathbf{u}^{(2)}_d\end{bmatrix} \\ Dt_n &= \left[\sum_c -\varepsilon N^{(1)}_c \bar{\mathbf{N}}^{(1)}\cdot\mathbf{n}^{(1)} - t_n\mathbf{N}^{(1)}\cdot\bar{\mathbf{m}}^{(1)}_c \quad \sum_d \varepsilon N^{(2)}_d \bar{\mathbf{N}}^{(1)}\cdot\mathbf{n}^{(1)}\right] \cdot \begin{bmatrix}\Delta\mathbf{u}^{(1)}_c \\ \Delta\mathbf{u}^{(2)}_d\end{bmatrix} \\ D\mathbf{n}^{(1)} &= \left[\sum_c -\mathbf{P}_N\cdot\mathbf{A}^{(1)}_c \quad \sum_d \mathbf{0}\right] \cdot \begin{bmatrix}\Delta\mathbf{u}^{(1)}_c \\ \Delta\mathbf{u}^{(2)}_d\end{bmatrix} \end{aligned} \tag{7.1.95}$$

with the definitions

$$\begin{aligned} &\mathbf{N}^{(1)} = \mathbf{n}^{(1)}\otimes\mathbf{n}^{(1)}, \quad \bar{\mathbf{N}}^{(1)} = \mathbf{I} - \mathbf{g}^{(1)}_{\beta}\otimes\bar{\mathbf{g}}^{\beta}_{(1)} \\ &\bar{\mathbf{m}}^{(1)}_c = \frac{\partial N^{(1)}_c}{\partial\eta^{\beta}_{(1)}}\bar{\mathbf{g}}^{\beta}_{(1)}, \quad \bar{\mathbf{m}}^{(2)}_b = \frac{\partial N^{(2)}_b}{\partial\eta^{\alpha}_{(2)}}\bar{\mathbf{g}}^{\alpha}_{(2)} \end{aligned} \tag{7.1.96}$$

Applying the discretization in Eq.(7.1.83) to Eq.(7.1.94) and employing the linearizations of Eqs.(7.1.86) and (7.1.95) to evaluate the resulting matrix products yields the directional derivative of δG^n_c as

$$\begin{aligned} D\delta G^n_c = &\left[\sum_a \delta\mathbf{v}^{(1)}_a \quad \sum_b \delta\mathbf{v}^{(2)}_b\right] \\ &\cdot\int_{\Gamma^{(1)}_{\eta}}\left(\begin{bmatrix}\sum_c -N^{(1)}_a N^{(1)}_c & \sum_d N^{(1)}_a N^{(2)}_d \\ \sum_c N^{(2)}_b N^{(1)}_c & \sum_d -N^{(2)}_b N^{(2)}_d\end{bmatrix}\varepsilon\tilde{\mathbf{N}}^{(1)}\right. \\ &+\begin{bmatrix}\sum_c -N^{(1)}_a & \sum_d 0 \\ \sum_c N^{(2)}_b & \sum_d 0\end{bmatrix} t_n\left(\mathbf{A}^{(1)}_c + \bar{\mathbf{M}}^{(1)}_c\cdot\mathbf{N}^{(1)}\right) \\ &+\begin{bmatrix}\sum_c 0 & \sum_d 0 \\ \sum_c N^{(1)}_c & \sum_d -N^{(2)}_d\end{bmatrix} t_n\bar{\mathbf{M}}^{(2)}_b \\ &\left.+\begin{bmatrix}\sum_c 0 & \sum_d 0 \\ \sum_c G_{bc} & \sum_d 0\end{bmatrix} t_n\mathbf{N}^{(1)}\right) J^{(1)}_{\eta}\, d\eta^1_{(1)} d\eta^2_{(1)} \cdot \begin{bmatrix}\Delta\mathbf{u}^{(1)}_c \\ \Delta\mathbf{u}^{(2)}_d\end{bmatrix} \end{aligned} \tag{7.1.97}$$

where

$$\begin{aligned} \tilde{\mathbf{N}}^{(1)} &= \mathbf{n}^{(1)}\otimes\bar{\mathbf{N}}^{(1)}\cdot\mathbf{n}^{(1)} \\ \bar{\mathbf{M}}^{(1)}_c &= \mathbf{n}^{(1)}\otimes\bar{\mathbf{m}}^{(1)}_c \\ \bar{\mathbf{M}}^{(2)}_b &= -\mathbf{n}^{(1)}\otimes\bar{\mathbf{m}}^{(2)}_b \\ G_{bc} &= ga^{\alpha\beta}\frac{\partial N_b}{\partial\eta^{\alpha}_{(2)}}\frac{\partial N_c}{\partial\eta^{\beta}_{(1)}} \end{aligned} \tag{7.1.98}$$

and it is apparent that the resulting frictionless stiffness matrix is also nonsymmetric. Eq.(7.1.97) is very similar to that which may be found by reducing our previous frictionless biphasic contact algorithm to the case of contact between two nonporous solids (eliminating all fluid degrees of freedom) [11], although the present framework is more general, since that previous study evaluated expressions in the limit as $g \to 0$.

7.1.9.11 Frictional Terms

The linearization of the frictional contribution follows from the second term of Eq.(7.1.91) as

$$\begin{aligned} D\delta G_c^t = &\int_{\Gamma_\eta^{(1)}} \begin{bmatrix} \mathbf{0} & \frac{\partial \delta \mathbf{v}^{(2)}}{\partial \eta_{(2)}^\alpha} \end{bmatrix} \cdot \begin{bmatrix} \mu t_n \mathbf{s}^{(1)} \\ -\mu t_n \mathbf{s}^{(1)} \end{bmatrix} D\eta_{(2)}^\alpha J_\eta^{(1)} \, d\eta_{(1)}^1 d\eta_{(1)}^2 \\ &+ \int_{\Gamma_\eta^{(1)}} \begin{bmatrix} \delta \mathbf{v}^{(1)} & \delta \mathbf{v}^{(2)} \end{bmatrix} \cdot \left(\begin{bmatrix} \mu t_n \mathbf{s}^{(1)} \\ -\mu t_n \mathbf{s}^{(1)} \end{bmatrix} DJ_\eta^{(1)} \right. \\ &\left. + \begin{bmatrix} \mu \mathbf{s}^{(1)} \\ -\mu \mathbf{s}^{(1)} \end{bmatrix} Dt_n J_\eta^{(1)} + \begin{bmatrix} \mu t_n \\ -\mu t_n \end{bmatrix} D\mathbf{s}^{(1)} J_\eta^{(1)} \right) d\eta_{(1)}^1 d\eta_{(1)}^2 \end{aligned} \tag{7.1.99}$$

The remaining quantity to be determined in this expression is the linearization $D\mathbf{s}^{(1)}$; according to Eq.(7.1.78), $D\dot{\mathbf{n}}^{(1)}$ must also be evaluated. As $\dot{\mathbf{n}}^{(1)}$ depends on $\dot{\mathbf{g}}_\alpha^{(1)}$ via Eq.(7.1.49), we must first propose a temporal discretization scheme for these rate quantities.

In a similar fashion to Eq.(7.1.79), let the material time derivative in the material frame of the covariant basis vectors of $\gamma^{(1)}$ be discretized as

$$\dot{\mathbf{g}}_\alpha^{(1)} \approx \frac{\mathbf{g}_\alpha^{(1)}\left(\eta_{(i)}^\beta, t\right) - \mathbf{g}_\alpha^{(1)}\left(\eta_{(i)}^\beta, t - \Delta t\right)}{\Delta t} = \frac{\Delta \mathbf{g}_\alpha^{(1)}}{\Delta t} \tag{7.1.100}$$

where $\Delta \mathbf{g}_\alpha^{(1)}$ denotes the change in $\mathbf{g}_\alpha^{(1)}$ from the previous time step. A temporally discretized form of Eq.(7.1.49) may now be written as

$$\dot{\mathbf{n}}^{(1)} \approx \frac{1}{\Delta t} \mathbf{c}^{(1)} \tag{7.1.101}$$

where

$$\begin{aligned} \mathbf{c}^{(1)} &= \frac{1}{J_\eta^{(1)}} \mathbf{P}_N \cdot \mathbf{m}^{(1)} \\ \mathbf{m}^{(1)} &= \Delta \mathbf{g}_1^{(1)} \times \mathbf{g}_2^{(1)} + \mathbf{g}_1^{(1)} \times \Delta \mathbf{g}_2^{(1)} \end{aligned} \tag{7.1.102}$$

The directional derivative of $\dot{\mathbf{n}}^{(1)}$ may now be evaluated as

$$\begin{aligned} D\dot{\mathbf{n}}^{(1)} = &\frac{1}{\Delta t} \begin{bmatrix} \sum_c \mathbf{Q}^{(1)} \cdot \mathbf{P}_N \cdot \mathbf{A}_c^{(1)} - \mathbf{P}_N \cdot \left(\mathbf{A}_c^{(1)} + \bar{\mathbf{A}}_c^{(1)} \right) - \mathbf{c}^{(1)} \otimes \mathbf{A}_c^{(1)} \cdot \mathbf{n}^{(1)} \\ \sum_d \mathbf{0} \end{bmatrix}^T \\ &\cdot \begin{bmatrix} \Delta \mathbf{u}_c^{(1)} \\ \Delta \mathbf{u}_d^{(2)} \end{bmatrix} \end{aligned} \tag{7.1.103}$$

where

$$\mathbf{Q}^{(1)} = \frac{1}{J_\eta^{(1)}} \left(\left(\mathbf{n}^{(1)} \cdot \mathbf{m}^{(1)} \right) \mathbf{I} + \mathbf{n}^{(1)} \otimes \mathbf{m}^{(1)} \right) \tag{7.1.104}$$

and $\bar{\mathbf{A}}_c^{(1)}$ is defined by analogy with Eq.(7.1.87) to be

$$\bar{\mathbf{A}}_c^{(1)} = \frac{1}{J_\eta^{(1)}} \left(\frac{\partial N_c^{(1)}}{\partial \eta_{(1)}^1} \Delta \hat{\mathbf{g}}_2^{(1)} - \frac{\partial N_c^{(1)}}{\partial \eta_{(1)}^2} \Delta \hat{\mathbf{g}}_1^{(1)} \right) , \tag{7.1.105}$$

where $\Delta \hat{\mathbf{g}}_\alpha^{(1)}$ is a skew-symmetric tensor whose dual vector is $\Delta \mathbf{g}_\alpha^{(1)}$.

Utilizing the discrete-time equations Eqs.(7.1.79) and (7.1.101) in Eq.(7.1.48), we find

$$\mathbf{v}^r \approx \frac{\mathbf{r}^{(1)}}{\Delta t} = \frac{g\mathbf{c}^{(1)} + \Delta\mathbf{x}^{(1)} - \Delta\mathbf{x}^{(2)}}{\Delta t} \tag{7.1.106}$$

and thus Eq.(7.1.78) may be discretized in time,

$$D\mathbf{s}^{(1)} = \mathbf{P}_S \cdot \left(D\mathbf{P}_N \cdot \mathbf{r}^{(1)} + \mathbf{P}_N \cdot D\mathbf{r}^{(1)} \right) \tag{7.1.107}$$

where $D\mathbf{r}^{(1)} = Dg\,\mathbf{c}^{(1)} + g\,D\mathbf{c}^{(1)} + \Delta\mathbf{u}^{(1)} - \Delta\mathbf{u}^{(2)}$ and

$$\begin{aligned} |\mathbf{P}_N \cdot \mathbf{v}^r| &= \frac{\Delta h}{\Delta t} \\ \mathbf{P}_S &= \frac{1}{\Delta h}\left(\mathbf{I} - \mathbf{s}^{(1)} \otimes \mathbf{s}^{(1)} \right) \end{aligned} \tag{7.1.108}$$

In Eq.(7.1.108), Δh is a spatial increment defined to simplify notation and $\mathbf{P}_S$ is a projection tensor.

Defining the tensors

$$\begin{aligned} \mathbf{R}^{(1)} &= \frac{1}{g}\left(\left(\mathbf{n}^{(1)} \cdot \mathbf{r}^{(1)} \right) \mathbf{I} + \mathbf{n}^{(1)} \otimes \mathbf{r}^{(1)} \right) \\ \mathbf{B}^{(1)} &= \mathbf{P}_S \cdot \mathbf{c}^{(1)} \otimes \bar{\mathbf{N}}^{(1)} \cdot \mathbf{n}^{(1)} - \mathbf{P}_S \cdot \mathbf{P}_N \\ \mathbf{L}^{(1)} &= g\mathbf{P}_S \cdot \left(\mathbf{P}_N \cdot \mathbf{Q}^{(1)} + \mathbf{R}^{(1)} - \mathbf{I} \right) \cdot \mathbf{P}_N \\ \mathbf{J}_c^{(1)} &= \mathbf{L}^{(1)} \cdot \mathbf{A}_c^{(1)} - g\mathbf{P}_S \cdot \mathbf{P}_N \cdot \bar{\mathbf{A}}_c^{(1)} \end{aligned} \tag{7.1.109}$$

and vectors

$$\begin{aligned} \mathbf{h}_{c+}^{(1)} &= \mathbf{N}^{(1)} \cdot \bar{\mathbf{m}}_c^{(1)} + \mathbf{A}_c^{(1)} \cdot \mathbf{n}^{(1)} \\ \mathbf{h}_{c-}^{(1)} &= \mathbf{N}^{(1)} \cdot \bar{\mathbf{m}}_c^{(1)} - \mathbf{A}_c^{(1)} \cdot \mathbf{n}^{(1)} \end{aligned}, \tag{7.1.110}$$

the directional derivative $D\mathbf{s}^{(1)}$ may be written fairly compactly as

$$\begin{aligned} D\mathbf{s}^{(1)} = &\begin{bmatrix} \sum_c -N_c^{(1)}\mathbf{B}^{(1)} - g\mathbf{P}_S \cdot \mathbf{c}^{(1)} \otimes \mathbf{h}_{c+}^{(1)} + \mathbf{J}_c^{(1)} & \sum_d N_d^{(2)}\mathbf{B}^{(1)} \end{bmatrix} \\ &\cdot \begin{bmatrix} \Delta\mathbf{u}_c^{(1)} \\ \Delta\mathbf{u}_d^{(2)} \end{bmatrix} \end{aligned} \tag{7.1.111}$$

Finally, the tangential stiffness matrix is found to be

$$\begin{aligned} D\delta G_c^t = &\begin{bmatrix} \sum_a \delta\mathbf{v}_a^{(1)} & \sum_b \delta\mathbf{v}_b^{(2)} \end{bmatrix} \\ &\cdot \int_{\Gamma_\eta^{(1)}} \left(\begin{bmatrix} \sum_c -N_a^{(1)}N_c^{(1)} & \sum_d N_a^{(1)}N_d^{(2)} \\ \sum_c N_b^{(2)}N_c^{(1)} & \sum_d -N_b^{(2)}N_d^{(2)} \end{bmatrix} \mu\left(\varepsilon\tilde{\mathbf{S}}^{(1)} + t_n\mathbf{B}^{(1)} \right) \right. \\ &+ \begin{bmatrix} \sum_c -N_a^{(1)} & \sum_d 0 \\ \sum_c N_b^{(2)} & \sum_d 0 \end{bmatrix} \mu t_n \left(\mathbf{s}^{(1)} \otimes \mathbf{h}_{c-}^{(1)} + g\mathbf{P}_S \cdot \mathbf{c}^{(1)} \otimes \mathbf{h}_{c+}^{(1)} - \mathbf{J}_c^{(1)} \right) \\ &+ \begin{bmatrix} \sum_c 0 & \sum_d 0 \\ \sum_c N_c^{(1)} & \sum_d -N_d^{(2)} \end{bmatrix} \mu t_n \left(-\mathbf{s}^{(1)} \otimes \bar{\mathbf{m}}_b^{(2)} \right) \\ &\left. + \begin{bmatrix} \sum_c 0 & \sum_d 0 \\ \sum_c G_{bc} & \sum_d 0 \end{bmatrix} \mu t_n \mathbf{S}^{(1)} \right) J_\eta^{(1)} d\eta_{(1)}^1 d\eta_{(1)}^2 \cdot \begin{bmatrix} \Delta\mathbf{u}_c^{(1)} \\ \Delta\mathbf{u}_d^{(2)} \end{bmatrix} \end{aligned} \tag{7.1.112}$$

where

$$\begin{aligned}\mathbf{S}^{(1)} &= \mathbf{s}^{(1)} \otimes \mathbf{n}^{(1)} \\ \tilde{\mathbf{S}}^{(1)} &= \mathbf{s}^{(1)} \otimes \bar{\mathbf{N}}^{(1)} \cdot \mathbf{n}^{(1)}\end{aligned} \tag{7.1.113}$$

The stiffness matrix of the frictional contribution to the virtual work, Eq.(7.1.112), is nonsymmetric. Summing Eq.(7.1.97) and Eq.(7.1.112) produces the total stiffness matrix for the case of frictional slip, which is also nonsymmetric.

7.1.9.12 Integration Scheme

In this formulation, a Gaussian quadrature integration scheme is adopted. The general form of the contact integral (e.g. Eq.(7.1.84) or Eq.(7.1.92)) may be integrated numerically as

$$\delta G_c = \sum_{e=1}^{n_e^{(1)}} \sum_{k=1}^{n_{int}^{(e)}} W_k J_\eta^{(1)} \begin{bmatrix} \sum_a \delta \mathbf{v}_a^{(1)} & \sum_b \delta \mathbf{v}_{b,k}^{(2)} \end{bmatrix} \cdot \begin{bmatrix} \mathbf{f}_a^{(1)} \\ \mathbf{f}_{b,k}^{(2)} \end{bmatrix} \tag{7.1.114}$$

where $n_e^{(1)}$ is the number of element faces on $\gamma^{(1)}$, $n_{int}^{(e)}$ is the number of integration points on the eth element face of $\gamma^{(1)}$, W_k is the weight associated with the kth integration point, and where it should be understood that terms associated with $\gamma^{(1)}$ (such as $J_\eta^{(1)}$, $\delta \mathbf{v}_a^{(1)}$, etc.) are evaluated at the parametric coordinates $\eta_{(1)}^\alpha$, associated with the kth integration point, and terms associated with $\gamma^{(2)}$ (such as $\mathbf{f}_{b,k}^{(2)}$) are evaluated at the parametric coordinates of contact $\eta_{(2)p}^\alpha$ or $\eta_{(2)}^\alpha$, defined by Eqs.(7.1.44) and (7.1.42) for cases of stick and slip, respectively. The subscript k appearing in the terms associated with $\gamma^{(2)}$ has been added to emphasize that there may be up to $n_{int}^{(e)}$ distinct element faces on $\gamma^{(2)}$ associated with all the integration points on the eth element face of $\gamma^{(1)}$, based on the location of the contact point on $\gamma^{(2)}$ as defined by either Eq.(7.1.44) or (7.1.42).

In a similar fashion, the contact stiffness may be integrated numerically as

$$\begin{aligned} D\delta G_c = \sum_{e=1}^{n_e^{(1)}} \sum_{k=1}^{n_{int}^{(e)}} & W_k J_\eta^{(1)} \begin{bmatrix} \sum_a \delta \mathbf{v}_a^{(1)} & \sum_b \delta \mathbf{v}_{b,k}^{(2)} \end{bmatrix} \\ & \cdot \begin{bmatrix} \sum_c \mathbf{K}_{ac}^{(1,1)} & \sum_d \mathbf{K}_{ad,k}^{(1,2)} \\ \sum_c \mathbf{K}_{bc,k}^{(2,1)} & \sum_d \mathbf{K}_{bd,k}^{(2,2)} \end{bmatrix} \cdot \begin{bmatrix} \Delta \mathbf{u}_c^{(1)} \\ \Delta \mathbf{u}_{d,k}^{(2)} \end{bmatrix} \end{aligned} \tag{7.1.115}$$

where the matrix of tensors $\mathbf{K}_{ab}^{(i,j)}$ is a general representation of the stiffness terms given explicitly in either Eq.(7.1.89) or Eqs.(7.1.97) and (7.1.112). In this expression, $\begin{bmatrix} \Delta \mathbf{u}_c^{(1)} & \Delta \mathbf{u}_{d,k}^{(2)} \end{bmatrix}^T$ is the vector of incremental changes in the degrees of freedom of the cth node of the eth element face on $\gamma^{(1)}$, and the dth node of the element face on $\gamma^{(2)}$ which contains the contact point $\eta_{(2)}^\alpha$ associated with the kth integration point on the eth element face of $\gamma^{(1)}$; the specific form of $\eta_{(2)}^\alpha$ will be dictated by the stick/slip status. A more detailed treatment of Gaussian quadrature, and a discussion of the benefits of this scheme versus nodal integration, may be found in our previous work [9].

7.2 Biphasic Contact

7.2.1 Contact Integral

See Section 2.5 for a review of biphasic materials, reference [11] for additional details on biphasic frictionless contact, and reference [113] for biphasic frictional contact. The presentation here follows that of [113]. The contact interface is defined between surfaces $\gamma^{(1)}$ and $\gamma^{(2)}$. Due to continuity requirements on the traction and fluxes, the external virtual work resulting from contact tractions $\mathbf{t}^{(i)}$ and solvent fluxes $w_n^{(i)}$ $(i = 1, 2)$, may be combined into the contact integral

$$\delta G_c = \int_{\gamma^{(1)}} \left(\left(\delta \mathbf{v}^{(1)} - \delta \mathbf{v}^{(2)} \right) \cdot \mathbf{t}^{(1)} + \left(\delta p^{(1)} - \delta p^{(2)} \right) w_n \right) da^{(1)} \tag{7.2.1}$$

where $\mathbf{t}^{(1)}$ is the contact traction on the primary surface, which is equal and opposite to that on the secondary surface, $\mathbf{t}^{(1)} = -\mathbf{t}^{(2)}$; $w_n \equiv w_n^{(1)}$ is the outward normal component of the fluid flux $\mathbf{w}^{(1)}$ from the primary surface, $\delta \mathbf{v}^{(i)}$ are virtual velocities, $\delta p^{(i)}$ are virtual fluid pressures, and $da^{(1)}$ is an elemental area on the primary surface $\gamma^{(1)}$. The contact integral is then written over the invariant parametric space of $\gamma^{(1)}$, which is denoted by $\Gamma_\eta^{(1)}$ [27], facilitating its linearization as required for use with an iterative solution method such as Newton's method. The elemental area is given by

$$da^{(1)} = J_\eta^{(1)} d\eta_{(1)}^1 d\eta_{(1)}^2, \quad J_\eta^{(1)} = \left| \mathbf{g}_1^{(1)} \times \mathbf{g}_2^{(1)} \right| \tag{7.2.2}$$

using the covariant basis vectors

$$\mathbf{g}_\alpha^{(i)} = \frac{\partial \mathbf{x}^{(i)}}{\partial \eta_{(i)}^\alpha} \tag{7.2.3}$$

where $\mathbf{x}^{(i)} \left(\eta_{(i)}^\alpha, t \right)$ is the spatial representation of surface $\gamma^{(i)}$ as it deforms in time t, in terms of contravariant surface parametric coordinates $\eta_{(i)}^\alpha$. Casting Eq.(7.2.1) into convenient matrix notation and switching the domain of integration to the parametric frame yields the invariant biphasic contact integral

$$\delta G_c = \int_{\Gamma_\eta^{(1)}} \left(\begin{bmatrix} \delta \mathbf{v}^{(1)} & \delta p^{(1)} \end{bmatrix} \cdot \begin{bmatrix} \mathbf{t}^{(1)} \\ w_n \end{bmatrix} + \begin{bmatrix} \delta \mathbf{v}^{(2)} & \delta p^{(2)} \end{bmatrix} \cdot \begin{bmatrix} -\mathbf{t}^{(1)} \\ -w_n \end{bmatrix} \right) J_\eta^{(1)} d\eta_{(1)}^1 d\eta_{(1)}^2 \tag{7.2.4}$$

Since $\Gamma_\eta^{(1)}$ represents an invariant material frame, the linearization of δG_c can be accomplished by applying the directional derivative operator directly to the integrand,

$$D\delta G_c = \int_{\Gamma_\eta^{(1)}} D \left(\begin{bmatrix} \delta \mathbf{v}^{(1)} & \delta p^{(1)} \end{bmatrix} \cdot \begin{bmatrix} \mathbf{t}^{(1)} \\ w_n \end{bmatrix} J_\eta^{(1)} + \begin{bmatrix} \delta \mathbf{v}^{(2)} & \delta p^{(2)} \end{bmatrix} \cdot \begin{bmatrix} -\mathbf{t}^{(1)} \\ -w_n \end{bmatrix} J_\eta^{(1)} \right) d\eta_{(1)}^1 d\eta_{(1)}^2 \tag{7.2.5}$$

where it is understood that for any function f in this biphasic analysis,

$$Df \equiv \sum_{i=1}^{2} Df \left[\Delta \mathbf{u}^{(i)} \right] + Df \left[\Delta p^{(i)} \right] \tag{7.2.6}$$

7.2.2 Biphasic Friction Formulation

An examination of Eq.(7.2.4) reveals that a contact framework must provide expressions for both the normal fluid flux w_n and the contact traction $\mathbf{t}^{(1)}$. For the contact traction, this work implements

a Coulomb-like framework for frictional contact [114]. In this framework the relationship between sticking and slipping, and thus the contact traction $\mathbf{t}^{(i)}$ on the opposing surfaces, is described by a slip criterion Ψ, where on the primary surface

$$\Psi = \left|\mathbf{t}_T^{(1)}\right| - \mu_{\text{eff}}\left|t_n\right| \tag{7.2.7}$$

where

$$\mu_{\text{eff}} = \mu_{\text{eq}}\left[1 + (1-\varphi)\,\frac{p}{t_n}\right] \tag{7.2.8}$$

Here, $t_n = \mathbf{t}^{(1)} \cdot \mathbf{n}^{(1)}$ is the normal component of the contact traction (negative in compression), $\mathbf{t}_T^{(1)} = \mathbf{t}^{(1)} - t_n\mathbf{n}^{(1)}$ is the tangential component of the contact traction, and the effective friction coefficient μ_{eff} is given by Eq.(7.2.8) with no distinction made between static and kinetic coefficients of friction. The user-defined parameter μ_{eq} represents the friction coefficient when the fluid pressure has subsided ($p = 0$), whereas the user-defined parameter φ represents the fraction of the apparent contact area where solid-on-solid contact takes place [12]. The ratio $-p/t_n$ represents the local fluid load support at each point on the contact surface. Since the friction coefficient μ_{eff} cannot be negative, the theoretical upper bound on the local fluid load support is $-p/t_n|_{\max} = (1-\varphi)^{-1}$. This upper bound is enforced whenever numerical errors produce a greater value of the local fluid load support.

The value of the slip criterion determines the stick-slip status via

$$\Psi \begin{cases} < 0 & \text{sticking} \\ = 0 & \text{slipping} \end{cases} \tag{7.2.9}$$

Following our prior study [114], this work treats stick and slip separately, controlled by an exact return mapping predicated on the value of the slip criterion. The return mapping defines a rule for correcting a calculated stick traction which exceeds the slip limit and is thus not permissible. Stick is treated as a special case of a tied biphasic interface (Section 7.6), whereas in slip the traction is directly prescribed as a natural boundary condition. The formulation of biphasic frictional contact is presented for both penalty and augmented Lagrangian regularization schemes.

7.2.3 Contact Kinematics

7.2.3.1 Slip Kinematics

The kinematics of slip are developed by mapping points between the surfaces $\gamma^{(i)}$ as they move relative to one another. The relationship between spatial points $\mathbf{x}^{(i)}\left(\eta_{(i)}^{\alpha}, t\right)$ on each surface is given by

$$\mathbf{x}^{(2)} = \mathbf{x}^{(1)} + g\mathbf{n}^{(1)} \tag{7.2.10}$$

where $\mathbf{n}^{(1)}$ is the unit outward normal to $\gamma^{(1)}$ given by

$$\mathbf{n}^{(1)} = \frac{\mathbf{g}_1^{(1)} \times \mathbf{g}_2^{(1)}}{\left|\mathbf{g}_1^{(1)} \times \mathbf{g}_2^{(1)}\right|} \tag{7.2.11}$$

and the gap function g is defined as

$$g = \left(\mathbf{x}^{(2)} - \mathbf{x}^{(1)}\right) \cdot \mathbf{n}^{(1)} \tag{7.2.12}$$

Here we note that $\mathbf{x}^{(1)}\left(\eta^{\alpha}_{(1)}, t\right)$ is the spatial position of a material point $X^{(1)}$ on the primary surface, and $\mathbf{x}^{(2)}\left(\eta^{\alpha}_{(2)}, t\right)$ is the corresponding spatial intersection point on the secondary surface, through which different material points $X^{(2)}$ identified by parametric coordinates $\eta^{\alpha}_{(2)}$ may convect. At any given instant, $\eta^{\alpha}_{(2)}$ are termed the parametric coordinates of intersection.

7.2.3.2 Stick Kinematics

Implicit in the concept of stick is the assumption that the contact projection was previously resolved; thus points are not mapped between surfaces during stick. Rather, the current contact point on $\gamma^{(2)}$ is given by the parametric coordinates of intersection $\eta^{\alpha}_{(2)}$ from the previous time point, now denoted as $\eta^{\alpha}_{(2)p}$ with the subscripted p referring to the previous time. The spatial position of the material point $X^{(2)}$ identified by $\eta^{\alpha}_{(2)p}$ is then given by

$$\mathbf{x}^{(2)}_s = \mathbf{x}^{(2)}\left(\eta^{\alpha}_{(2)p}, t\right) = \mathbf{x}^{(1)}\left(\eta^{\alpha}_{(1)}, t\right) + \mathbf{g}_s \tag{7.2.13}$$

where the vector gap $\mathbf{g}_s$ in stick is defined to be

$$\mathbf{g}_s = \mathbf{x}^{(2)}_s - \mathbf{x}^{(1)} \tag{7.2.14}$$

Here $\mathbf{g}_s$ is the vectorial distance, at the current time t, between material points which were in contact at the previous time step; for perfect stick we must have $\mathbf{g}_s = \mathbf{0}$.

7.2.3.3 Velocities

Coulomb's law of kinetic friction requires that the friction force be aligned with the relative slip velocity between the two surfaces. Despite the name, Coulomb's law is a constitutive relation, and hence must obey the Principle of Material-Frame Indifference; this requires a frame-invariant relative velocity. As points in stick do not experience relative motion, the development of velocities below is only concerned with opposing contact points in slip.

As parametric coordinates $\eta^{\alpha}_{(1)}$ of integration points on the primary surface $\gamma^{(1)}$ represent material points, the velocity $\mathbf{v}^{(1)}$ of these points is evaluated from the material time derivative in the material frame,

$$\mathbf{v}^{(1)}\left(\eta^{\alpha}_{(1)}, t\right) = \frac{\partial \mathbf{x}^{(1)}\left(\eta^{\alpha}_{(1)}, t\right)}{\partial t} \tag{7.2.15}$$

In contrast, different material points $X^{(2)}$ may convect through the intersection point $\mathbf{x}^{(2)}$, and so the velocity $\mathbf{v}^{(2)}$ at the intersection point on $\gamma^{(2)}$ is evaluated from the material time derivative in the spatial frame,

$$\mathbf{v}^{(2)}\left(\eta^{\alpha}_{(2)}, t\right) = \frac{\partial \mathbf{x}^{(2)}\left(\eta^{\alpha}_{(2)}, t\right)}{\partial t} + \dot{\eta}^{\alpha}_{(2)}\mathbf{g}^{(2)}_{\alpha} \tag{7.2.16}$$

where $\partial \mathbf{x}^{(2)}/\partial t$ represents the velocity of the intersection point on $\gamma^{(2)}$, while $\dot{\eta}^{\alpha}_{(2)}$ are the contravariant components of the convective velocity of material passing through the intersection point $\mathbf{x}^{(2)}$. The quantity $\dot{\eta}^{\alpha}_{(2)}\mathbf{g}^{(2)}_{\alpha}$ represents the relative slip velocity between the material on $\gamma^{(2)}$ and that on $\gamma^{(1)}$. Importantly, by definition $\partial \mathbf{x}^{(2)}/\partial t$ is evaluated while holding $\eta^{\alpha}_{(2)}$ constant. From these relations, a more practical formulation of the slip velocity can be achieved [114]. Taking

the material time derivative of Eq.(7.2.10) and recalling the contact persistency condition $\dot{g} = 0$ [110] produces $\mathbf{v}^{(2)} = \mathbf{v}^{(1)} + g\dot{\mathbf{n}}^{(1)}$. Substituting Eqs.(7.2.15)-(7.2.16) into this expression yields the desired frame-invariant measure of relative velocity between $\gamma^{(1)}$ and $\gamma^{(2)}$ [35],

$$\mathbf{v}^r \equiv \dot{\eta}^\alpha_{(2)}\mathbf{g}^{(2)}_\alpha = g\dot{\mathbf{n}}^{(1)} + \frac{\partial \mathbf{x}^{(1)}\left(\eta^\alpha_{(1)}, t\right)}{\partial t} - \frac{\partial \mathbf{x}^{(2)}\left(\eta^\alpha_{(2)}, t\right)}{\partial t}, \tag{7.2.17}$$

where $\dot{\mathbf{n}}^{(1)}$ is evaluated from Eq.(7.2.11) as

$$\dot{\mathbf{n}}^{(1)} = \mathbf{P}_N \cdot \frac{\dot{\mathbf{g}}^{(1)}_1 \times \mathbf{g}^{(1)}_2 + \mathbf{g}^{(1)}_1 \times \dot{\mathbf{g}}^{(1)}_2}{J^{(1)}_\eta}\,. \tag{7.2.18}$$

Here, $\dot{\mathbf{g}}^{(1)}_\alpha$ is the material time derivative of $\mathbf{g}^{(1)}_\alpha$ in the material frame, evaluated from Eq.(7.2.3) as

$$\dot{\mathbf{g}}^{(1)}_\alpha\left(\eta^\beta_{(1)}, t\right) = \frac{\partial \mathbf{g}^{(1)}_\alpha\left(\eta^\beta_{(1)}, t\right)}{\partial t}\,, \tag{7.2.19}$$

and $\mathbf{P}_N$ is the tangential plane projection tensor,

$$\mathbf{P}_N = \mathbf{I} - \mathbf{n}^{(1)} \otimes \mathbf{n}^{(1)}\,. \tag{7.2.20}$$

A unit vector in the slip direction can then be found by projecting the relative velocity $\mathbf{v}^r$ onto the tangent plane of $\gamma^{(1)}$, yielding

$$\mathbf{s}^{(1)} = \frac{\mathbf{P}^{(1)}_N \cdot \mathbf{v}^r}{\left|\mathbf{P}^{(1)}_N \cdot \mathbf{v}^r\right|}\,. \tag{7.2.21}$$

7.2.4 Penalty Scheme

The defining characteristic of frictional stick is a lack of relative motion between points which were previously in contact. Consequently, the stick traction is obtained by penalizing relative motion between such points,

$$\mathbf{t}^{(1)} = \varepsilon \mathbf{g}_s\,, \tag{7.2.22}$$

where ε is the contact penalty parameter and we have utilized Eq.(7.2.14) to define the gap vector $\mathbf{g}_s$ during stick.

During slip, the normal component of the contact traction is first calculated by penalizing the normal component g of the gap, given by Eq.(7.2.12),

$$t_n = \varepsilon g\,. \tag{7.2.23}$$

The total traction vector in slip is then directly prescribed as

$$\mathbf{t}^{(1)} = t_n\left(\mathbf{n}^{(1)} + \mu_{\text{eff}}\mathbf{s}^{(1)}\right)\,, \tag{7.2.24}$$

where $\mathbf{s}^{(1)}$ is the unit vector in the slip direction, given by Eq.(7.2.21). We note that Eq.(7.2.24) has the same form as the classical Coulomb friction considered in Section 7.1.9 and [114], with the standard Coulomb friction coefficient replaced by μ_{eff}, as evaluated from (7.2.8). A trial state and return map, adapted from Section 7.1.9.7 [114] and presented in Section 7.2.6, is employed to differentiate between stick and slip.

The jump conditions for a biphasic mixture require continuity of the fluid pressure across an interface and therefore an expression for the normal fluid flux w_n can be obtained by penalizing the fluid pressure gap π between contacting points [9],

$$\begin{aligned} w_n &= \varepsilon_p \pi \,, \quad t_n < 0 \\ p^{(i)} &= 0 \,, \qquad t_n = 0 \end{aligned} \tag{7.2.25}$$

where $p^{(i)} = 0$ prescribes zero fluid pressure (free-draining conditions) on the portions of the boundary where no contact takes place. We define the fluid pressure gap as

$$\pi = p^{(1)} - p^{(2)} \tag{7.2.26}$$

and ε_p is the pressure penalty parameter which has units of hydraulic permeability per unit length (e.g. m^3/N·s, similar to the hydraulic permeability of a membrane). Equation (7.2.25) is valid for both stick and slip. Note that $p^{(1)} = p^{(1)}\left(\eta^{\alpha}_{(1)}\right)$ is evaluated at a point with parametric coordinates $\eta^{\alpha}_{(1)}$ on the primary surface, whereas the pressure on the secondary surface, $p^{(2)} = p^{(2)}\left(\eta^{\alpha}_{(2)}, t\right)$, is evaluated at the parametric coordinates of the intersection of a ray issued from that primary surface point and normal to $\gamma^{(1)}$. As detailed previously [114] and summarized in Section7.2.3, the parametric coordinates of intersection are dependent on the stick-slip status, so care must be taken to evaluate w_n from Eq.(7.2.25) using the contact kinematics determined by Eq.(7.2.9). In practice this is accomplished by calculating w_n once the stick-slip status has been resolved for each iteration.

7.2.5 Augmented Lagrangian Scheme

The augmented Lagrangian scheme presented herein was developed in Section 7.1.9.6 [114] as a modification of the approach proposed by Simo and Laursen [93]. Briefly, this is a first-order augmentation scheme that utilizes Uzawa's algorithm [22], where the multipliers are updated outside of the Newton step, producing a double loop algorithm [110] and preserving quadratic convergence of Newton's method near solution points.

During stick, the traction is calculated by augmenting the vector gap $\mathbf{g}_s$,

$$\mathbf{t}^{(1)} = \boldsymbol{\lambda}_s + \varepsilon \mathbf{g}_s \,, \tag{7.2.27}$$

where $\boldsymbol{\lambda}_s$ is the vectorial Lagrange multiplier in stick. In slip, the normal component of the contact traction is first calculated by augmenting the normal gap g,

$$t_n = \lambda_n + \varepsilon g \,, \tag{7.2.28}$$

where λ_n is the normal Lagrange multiplier. The total traction vector in slip is then directly prescribed as

$$\mathbf{t}^{(1)} = t_n \left(\mathbf{n}^{(1)} + \mu_{\text{eff}} \mathbf{s}^{(1)} \right) \tag{7.2.29}$$

where Eq.(7.2.28) has been used. The update formulas for the Lagrange multipliers can be found in Section 7.1.9.6 [114]. Here it suffices to note that by augmenting only the normal gap and employing Eq.(7.2.29), we have ensured an exact mapping to the proper tangential traction in slip, which is consistent with the augmented normal traction. As in the penalty case, a trial state and return map, presented in Section 7.2.6 and controlled by the slip criterion, is used to differentiate between stick and slip.

In this augmentation scheme, the normal fluid flux is given by

$$\begin{aligned} w_n &= \lambda_p + \varepsilon_p \pi\,, \quad t_n < 0 \\ p^{(i)} &= 0\,, \qquad\qquad t_n = 0 \end{aligned} \tag{7.2.30}$$

where λ_p is the fluid pressure Lagrange multiplier, and the update formula for λ_p has been detailed in our prior work on frictionless biphasic contact [9] and is given by

$$\lambda_p \leftarrow \lambda_p + \varepsilon_p \pi \tag{7.2.31}$$

Unlike $\boldsymbol{\lambda}_s$ and λ_n [114], λ_p is not dependent on the stick-slip status. However, as noted before, Eq.(7.2.30) must be evaluated after the stick-slip status has been resolved.

7.2.6 Stick-Slip Algorithm

Determining whether stick or slip is occurring at a given instant is accomplished by a trial state and return map, and has the same form for both penalty and augmented Lagrangian regularization schemes [114]. We initially assume stick and calculate a trial traction $\tilde{\mathbf{t}}^{(1)}$, utilizing either Eq.(7.2.22) or Eq.(7.2.27). The trial normal and tangential components $\tilde{t}_n$ and $\tilde{\mathbf{t}}_T^{(1)}$ are evaluated from $\tilde{\mathbf{t}}^{(1)}$ and inserted into the slip criterion Ψ,

$$\Psi = \left|\tilde{\mathbf{t}}_T^{(1)}\right| - \mu_{\text{eff}} \left|\tilde{t}_n\right|. \tag{7.2.32}$$

Based on the slip criterion and trial traction vector, the traction vector is calculated from the return mapping as

$$\mathbf{t}^{(1)} = \begin{cases} \tilde{\mathbf{t}}^{(1)} & \Psi < 0\,, \quad \text{sticking} \\ t_n(\mathbf{n}^{(1)} + \mu_{\text{eff}}\mathbf{s}^{(1)}) & \Psi = 0\,, \quad \text{slipping} \end{cases} \tag{7.2.33}$$

where t_n is given by either Eq.(7.2.23) or Eq.(7.2.28).

7.2.7 Linearization and Discretization Outline

The following sections provide the linearization and discretization of stick and slip for biphasic frictional contact, culminating in the final forms of the residual vectors and stiffness matrices which have been implemented into FEBio. Section 7.2.8 begins with an important discussion of kinematic definitions and notation which is assumed to hold without repetition. Sections 7.2.9 and 7.2.10 linearize and discretize biphasic stick and slip, respectively. Importantly, Section 7.2.9 sets up and uses more formal notation and definitions, before we dispense of this cumbersome notation for the remainder of the treatment.

7.2.8 Definitions and Notation

Evaluating the linearizations of Eq.(7.2.4) requires directional derivatives of kinematic quantities, some of which depend on the stick-slip status. To simplify the presentation, the continuum linearization is presented only for a few select quantities. The remainder of the linearization is deferred until after discretization, as many expressions are much easier to manipulate in discretized form. To keep the equations more manageable, the discretization of slip is split into frictionless and frictional terms, and the final form of the stiffness matrices follows this split. The full model is easily obtained by summing the frictionless and frictional contributions. Here we emphasize that,

as a consequence of the double-loop Uzawa algorithm discussed in Section 7.2.5 (reprised from [114]), all Lagrange multipliers are updated outside of each Newton step, thus $D\lambda = 0$, where λ is any Lagrange multiplier, i.e. $\lambda = \lambda_n, \boldsymbol{\lambda}_s, \lambda_p$, etc. As a consequence, Lagrange multipliers do not appear in any of the linearized or discretized equations. In what follows, Greek indices are associated with covariant basis vectors on the contacting surfaces, and thus vary from 1 to 2. Repeated Greek indices indicate implicit summation over their range.

Many kinematic quantities remain unchanged from Section 7.1.9 on elastic frictional contact [114]. We thus accept without repetition the definitions of $\mathbf{N}^{(1)}$, $\bar{\mathbf{N}}^{(1)}$, $\bar{\mathbf{m}}_c^{(1)}$, $\bar{\mathbf{m}}_b^{(2)}$, $\tilde{\mathbf{N}}^{(1)}$, $\bar{\mathbf{M}}_c^{(1)}$, $\bar{\mathbf{M}}_b^{(2)}$, $\mathbf{c}^{(1)}$, $\mathbf{m}^{(1)}$, $\mathbf{Q}^{(1)}$, $\bar{\mathbf{A}}_c^{(1)}$, $\mathbf{A}_c^{(1)}$, $\mathbf{P}_N$, $\mathbf{P}_S$, $\mathbf{R}^{(1)}$, $\mathbf{B}^{(1)}$, $\mathbf{L}^{(1)}$, $\mathbf{J}_c^{(1)}$, $\mathbf{S}^{(1)}$, and $\tilde{\mathbf{S}}^{(1)}$. These terms are all defined in Sections 7.1.9.10-7.1.9.11 [114]. Directional derivatives which will not be duplicated here include $D\mathbf{n}^{(1)}$, $D\dot{\mathbf{n}}^{(1)}$, $D\mathbf{s}^{(1)}$, $Dt_n = \varepsilon Dg$, Dg, $DJ_\eta^{(1)}$, $D\eta^\alpha_{(2)}$, and $D\mathbf{P}_N$ (see Sections 7.1.9.8, 7.1.9.10 and 7.1.9.11).

The final residual vectors and stiffness matrices presented below are written in integral form. In the FEBio implementation, a Gaussian quadrature scheme is adopted to perform numerical integration. A detailed treatment of Gaussian quadrature, and equations for numerically integrating the contact integrals and stiffnesses, may be found in Section 7.1.9.12.

As a final implementation detail, we note that multiplying all biphasic entries in the residual vector and stiffness matrices by the time step leads to better convergence. In this context, biphasic refers to all terms which are not purely related to solid-solid contact. In the residual, this is all terms which are not $\mathbf{f}_m^{(i)}$ (see below). Similarly, this includes all stiffness entries except the solid-solid $\mathbf{K}_{mn}^{(i,j)}$ terms (see below).

7.2.9 Biphasic Stick

7.2.9.1 Linearization

In stick parametric coordinates are fixed on both surfaces, hence directional derivatives of $\mathbf{x}^{(i)}$, $p^{(i)}$, $\delta\mathbf{v}^{(i)}$, and $\delta p^{(i)}$ are given by

$$\begin{aligned} D\mathbf{x}^{(1)} &= \Delta\mathbf{u}^{(1)} & D\mathbf{x}^{(2)} &= \Delta\mathbf{u}^{(2)} \\ Dp^{(1)} &= \Delta p^{(1)} & Dp^{(2)} &= \Delta p^{(2)} \\ D\delta\mathbf{v}^{(1)} &= \mathbf{0} & D\delta\mathbf{v}^{(2)} &= \mathbf{0} \\ D\delta p^{(1)} &= 0 & D\delta p^{(2)} &= 0 \end{aligned} \tag{7.2.34}$$

From the definitions of Eq.(7.2.14) and Eq.(7.2.22), and utilizing Eq.(7.2.34), it follows that

$$D\mathbf{t}^{(1)} = \varepsilon\left(\Delta\mathbf{u}^{(2)} - \Delta\mathbf{u}^{(1)}\right). \tag{7.2.35}$$

Similarly, application of Eq.(7.2.34) to Eqs.(7.2.25)-(7.2.26) yields

$$Dw_n = \varepsilon_p\left(\Delta p^{(1)} - \Delta p^{(2)}\right) \tag{7.2.36}$$

The biphasic contact integral of Eq.(7.2.1), written over an invariant domain, can then be linearized directly to find

$$\begin{aligned} D\delta G_c = \int_{\Gamma_\eta^{(1)}} \Bigg(&\begin{bmatrix}\delta\mathbf{v}^{(1)} & \delta\mathbf{v}^{(2)}\end{bmatrix} \cdot \left(\begin{bmatrix}1\\-1\end{bmatrix} D\mathbf{t}^{(1)} J_\eta^{(1)} + \begin{bmatrix}\mathbf{t}^{(1)}\\-\mathbf{t}^{(1)}\end{bmatrix} DJ_\eta^{(1)} \right) \\ &+ \begin{bmatrix}\delta p^{(1)} & \delta p^{(2)}\end{bmatrix} \cdot \left(\begin{bmatrix}1\\-1\end{bmatrix} Dw_n J_\eta^{(1)} + \begin{bmatrix}w_n\\-w_n\end{bmatrix} DJ_\eta^{(1)} \right) \Bigg) d\eta^1_{(1)} d\eta^2_{(1)} \end{aligned} \tag{7.2.37}$$

Note that for convenience, terms in Eq.(7.2.37) have been grouped differently than in Eq.(7.2.5).

7.2.9.2 Discretization

Let the continuous variables on the primary and secondary surfaces be interpolated over element faces according to [9, 114]

$$\begin{aligned}
\delta\mathbf{v}^{(1)} &= \sum_{a=1}^{m^{(1)}} N_a^{(1)}\delta\mathbf{v}_a^{(1)} \qquad \delta\mathbf{v}^{(2)} = \sum_{b=1}^{m_k^{(2)}} N_b^{(2)}\delta\mathbf{v}_b^{(2)} \\
\Delta\mathbf{u}^{(1)} &= \sum_{c=1}^{m^{(1)}} N_c^{(1)}\Delta\mathbf{u}_c^{(1)} \quad \Delta\mathbf{u}^{(2)} = \sum_{d=1}^{m_k^{(2)}} N_d^{(2)}\Delta\mathbf{u}_d^{(2)} \\
\delta p^{(1)} &= \sum_{a=1}^{m^{(1)}} N_a^{(1)}\delta p_a^{(1)} \qquad \delta p^{(2)} = \sum_{b=1}^{m_k^{(2)}} N_b^{(2)}\delta p_b^{(2)} \\
\Delta p^{(1)} &= \sum_{c=1}^{m^{(1)}} N_c^{(1)}\Delta p_c^{(1)} \quad \Delta p^{(2)} = \sum_{d=1}^{m_k^{(2)}} N_d^{(2)}\Delta p_d^{(2)}
\end{aligned} \tag{7.2.38}$$

where $N_a^{(i)}$ represent interpolation functions on the element faces of $\gamma^{(i)}$, $m^{(1)}$ is the number of nodes and interpolation functions on each primary element face, $m_k^{(2)}$ is the number of nodes and interpolation functions on the secondary element face which is intersected by the ray issued from the kth integration point on the primary element face, and $\delta\mathbf{v}_a^{(i)}$, $\Delta\mathbf{u}_a^{(i)}$,$\delta p_a^{(i)}$, and $\Delta p_a^{(i)}$ represent respective nodal values of $\delta\mathbf{v}^{(i)}$, $\Delta\mathbf{u}^{(i)}$, $\delta p^{(i)}$, and $\Delta p^{(i)}$. From this point forward the summation signs will be written simply as $\sum_a$, where it is assumed they have the same meaning described above.

Inserting the discretization of Eq.(7.2.38) into Eq.(7.2.4) yields

$$\begin{aligned}
\delta G_c = &\sum_a \begin{bmatrix}\delta\mathbf{v}_a^{(1)} & \delta p_a^{(1)}\end{bmatrix} \cdot \int_{\Gamma_\eta^{(1)}} \begin{bmatrix}\mathbf{f}_a^{(1)} \\ w_a^{(1)}\end{bmatrix} J_\eta^{(1)} d\eta_{(1)}^1 d\eta_{(1)}^2 \\
&+ \sum_b \begin{bmatrix}\delta\mathbf{v}_b^{(2)} & \delta p_b^{(2)}\end{bmatrix} \cdot \int_{\Gamma_\eta^{(1)}} \begin{bmatrix}\mathbf{f}_b^{(2)} \\ w_b^{(2)}\end{bmatrix} J_\eta^{(1)} d\eta_{(1)}^1 d\eta_{(1)}^2
\end{aligned} \tag{7.2.39}$$

where the residuals are

$$\begin{aligned}
\mathbf{f}_a^{(1)} &= N_a^{(1)}\mathbf{t}^{(1)}\,, \quad \mathbf{f}_b^{(2)} = -\,N_b^{(2)}\mathbf{t}^{(1)} \\
w_a^{(1)} &= N_a^{(1)} w_n\,, \quad w_b^{(2)} = -\,N_b^{(2)} w_n
\end{aligned} \tag{7.2.40}$$

and $\mathbf{t}^{(1)}$ is obtained from Eq.(7.2.22) in the penalty case and from Eq.(7.2.27) if augmented Lagrangian regularization is employed. Similarly, w_n is calculated from either Eq.(7.2.25) or Eq.(7.2.30) for penalty and augmented Lagrange methods, respectively.

We may now discretize individual terms and place them into matrix notation, anticipating their substitution into Eq.(7.2.37). By placing Eq.(7.2.39) into Eqs.(7.2.35)-(7.2.36) and inserting the

resulting linearizations into Eq.(7.2.37), we obtain the stiffness matrix for biphasic stick as

$$\begin{aligned} D\delta G_c = &\sum_a \begin{bmatrix} \delta \mathbf{v}_a^{(1)} & \delta p_a^{(1)} \end{bmatrix} \cdot \int_{\Gamma_\eta^{(1)}} \left(\sum_c \begin{bmatrix} \mathbf{K}_{ac}^{(1,1)} & \mathbf{0} \\ \mathbf{g}_{ac}^{(1,1)} & g_{ac}^{(1,1)} \end{bmatrix} \cdot \begin{bmatrix} \Delta \mathbf{u}_c^{(1)} \\ \Delta p_c^{(1)} \end{bmatrix} \right. \\ &\left. + \sum_d \begin{bmatrix} \mathbf{K}_{ad}^{(1,2)} & \mathbf{0} \\ \mathbf{g}_{ad}^{(1,2)} & g_{ad}^{(1,2)} \end{bmatrix} \cdot \begin{bmatrix} \Delta \mathbf{u}_d^{(2)} \\ \Delta p_d^{(2)} \end{bmatrix} \right) J_\eta^{(1)} d\eta_{(1)}^1 d\eta_{(1)}^2 \\ + &\sum_b \begin{bmatrix} \delta \mathbf{v}_b^{(2)} & \delta p_b^{(2)} \end{bmatrix} \cdot \int_{\Gamma_\eta^{(1)}} \left(\sum_c \begin{bmatrix} \mathbf{K}_{bc}^{(2,1)} & \mathbf{0} \\ \mathbf{g}_{bc}^{(2,1)} & g_{bc}^{(2,1)} \end{bmatrix} \cdot \begin{bmatrix} \Delta \mathbf{u}_c^{(1)} \\ \Delta p_c^{(1)} \end{bmatrix} \right. \\ &\left. + \sum_d \begin{bmatrix} \mathbf{K}_{bd}^{(2,2)} & \mathbf{0} \\ \mathbf{g}_{bd}^{(2,2)} & g_{bd}^{(2,2)} \end{bmatrix} \cdot \begin{bmatrix} \Delta \mathbf{u}_d^{(2)} \\ \Delta p_d^{(2)} \end{bmatrix} \right) J_\eta^{(1)} d\eta_{(1)}^1 d\eta_{(1)}^2 \end{aligned} \tag{7.2.41}$$

where

$$\begin{aligned} \mathbf{K}_{ac}^{(1,1)} &= -\varepsilon_n N_a^{(1)} N_c^{(1)} \mathbf{I} + N_a^{(1)} \mathbf{t}^{(1)} \otimes \mathbf{A}_c^{(1)} \cdot \mathbf{n}^{(1)} \\ \mathbf{K}_{ad}^{(1,2)} &= \varepsilon_n N_a^{(1)} N_d^{(2)} \mathbf{I} \\ \mathbf{K}_{bc}^{(2,1)} &= \varepsilon_n N_b^{(2)} N_c^{(1)} \mathbf{I} - N_b^{(2)} \mathbf{t}^{(1)} \otimes \mathbf{A}_c^{(1)} \cdot \mathbf{n}^{(1)} \\ \mathbf{K}_{bd}^{(2,2)} &= -\varepsilon_n N_b^{(2)} N_d^{(2)} \mathbf{I} \end{aligned} \tag{7.2.42}$$

and

$$\begin{aligned} \mathbf{g}_{ac}^{(1,1)} &= N_a^{(1)} w_n \mathbf{A}_c^{(1)} \cdot \mathbf{n}^{(1)} & g_{ac}^{(1,1)} &= \varepsilon_p N_a^{(1)} N_c^{(1)} \\ \mathbf{g}_{ad}^{(1,2)} &= \mathbf{0} & g_{ad}^{(1,2)} &= -\varepsilon_p N_a^{(1)} N_d^{(2)} \\ \mathbf{g}_{bc}^{(2,1)} &= -N_b^{(2)} w_n \mathbf{A}_c^{(1)} \cdot \mathbf{n}^{(1)} & g_{bc}^{(2,1)} &= -\varepsilon_p N_b^{(2)} N_c^{(1)} \\ \mathbf{g}_{bd}^{(2,2)} &= \mathbf{0} & g_{bd}^{(2,2)} &= \varepsilon_p N_b^{(2)} N_d^{(2)} \end{aligned} \tag{7.2.43}$$

In Eq.(7.2.41), $\begin{bmatrix} \Delta \mathbf{u}_c^{(1)} & \Delta p_c^{(1)} \end{bmatrix}^T$ is the vector of incremental changes in the degrees of freedom of the cth node of the current element face on $\gamma^{(1)}$. Similarly, $\begin{bmatrix} \Delta \mathbf{u}_d^{(2)} & \Delta p_d^{(2)} \end{bmatrix}^T$ represents the incremental changes in the degrees of freedom of the dth node of the element face on $\gamma^{(2)}$ which contains the intersection point $X^{(2)}$ associated with the kth integration point on the current element face on $\gamma^{(1)}$ [11, 114]. See Section 7.1.9.12 for a description of the Gaussian quadrature integration scheme used to evaluate residuals and stiffness matrices (e.g. Eqs.(7.2.39) and (7.2.41)). Briefly, it should be noted that for all terms associated with $\gamma^{(2)}$ (e.g. $\mathbf{K}_{ad}^{(1,2)}$, $\Delta \mathbf{u}_d^{(2)}$, $\delta p_b^{(2)}$) there may be $k \in \begin{bmatrix} 1, & n_{int}^{(e)} \end{bmatrix}$ distinct element faces on $\gamma^{(2)}$ associated with all the integration points $X^{(1)}$ on the eth element face of $\gamma^{(1)}$, based on the location of $X^{(2)}$ obtained from Eq.(7.2.13).

In Section 7.1.9 on sliding-elastic frictional contact, we split the contact stiffness matrices in a different way, which allowed us to clearly separate like terms. Here, due to the complexity of the biphasic contact formulation, it was determined that the form of Eq.(7.2.41) provides more clarity.

7.2.10 Biphasic Slip

7.2.10.1 Linearization

During slip, the contact integral over $\gamma^{(1)}$ is performed over integration points $X^{(1)}$ with prescribed parametric coordinates $\eta_{(1)}^\alpha$. However, the point on $\gamma^{(2)}$ in contact with $\gamma^{(1)}$ has parametric coordi-

nates $\eta^{\alpha}_{(2)}$ which change with variations in $\mathbf{x}^{(1)}$ and $\mathbf{n}^{(1)}$, in accordance with Eq.(7.2.12). Consequently, directional derivatives of $\mathbf{x}^{(i)}$, $p^{(i)}$, $\delta\mathbf{v}^{(i)}$, and $\delta p^{(i)}$ are given by

$$\begin{aligned} D\mathbf{x}^{(1)} &= \Delta\mathbf{u}^{(1)} \qquad D\mathbf{x}^{(2)} = \Delta\mathbf{u}^{(2)} + \mathbf{g}^{(2)}_{\alpha} D\eta^{\alpha}_{(2)} \\ Dp^{(1)} &= \Delta p^{(1)} \qquad Dp^{(2)} = \Delta p^{(2)} + \frac{\partial p^{(2)}}{\partial \eta^{\alpha}_{(2)}} D\eta^{\alpha}_{(2)} \\ D\delta\mathbf{v}^{(1)} &= \mathbf{0} \qquad D\delta\mathbf{v}^{(2)} = \frac{\partial \delta\mathbf{v}^{(2)}}{\partial \eta^{\alpha}_{(2)}} D\eta^{\alpha}_{(2)} \\ D\delta p^{(1)} &= 0 \qquad D\delta p^{(2)} = \frac{\partial \delta p^{(2)}}{\partial \eta^{\alpha}_{(2)}} D\eta^{\alpha}_{(2)} \end{aligned} \tag{7.2.44}$$

where $D\eta^{\alpha}_{(2)}$ is evaluated by our modification [11] of a method proposed by Laursen and Simo [64], and may be found in Section 7.1.9.10. The linearization of the slip traction proceeds as before [114], with the addition of a term involving the linearization of μ_{eff}. From Eq.(7.2.8) it follows that

$$D\mu_{\text{eff}} = \mu_{\text{eq}} \left(1 - \varphi\right) \frac{\Delta p^{(1)}}{t_n} - \mu_{\text{eq}} \left(1 - \varphi\right) \frac{p^{(1)}}{t_n^2} Dt_n \tag{7.2.45}$$

where $Dt_n = \varepsilon Dg$ according to Eq.(7.2.23); this term has been provided previously in Eq.(7.1.77) [114]. Equation (7.2.45) was derived by recalling that μ_{eq} and φ are constants. We then obtain

$$D\mathbf{t}^{(1)} = Dt_n \left(\mathbf{n}^{(1)} + \mu_{\text{eff}}\mathbf{s}^{(1)}\right) + t_n \left(D\mathbf{n}^{(1)} + \left(D\mu_{\text{eff}}\right)\mathbf{s}^{(1)} + \mu_{\text{eff}} D\mathbf{s}^{(1)}\right) \tag{7.2.46}$$

Finally, from Eq.(7.2.25) (evaluated at $\mathbf{x}^{(2)}$ determined by Eq.(7.2.10)) and Eq.(7.2.44) it follows that

$$Dw_n = \varepsilon_p \left(\Delta p^{(1)} - \Delta p^{(2)} - \frac{\partial p^{(2)}}{\partial \eta^{\alpha}_{(2)}} D\eta^{\alpha}_{(2)}\right) \tag{7.2.47}$$

Note that the form of Dw_n given in Eq.(7.2.47) contains additional terms not present in Eq.(7.2.36). This is because the parametric coordinates of intersection may vary in slip, but are invariant in stick; as a consequence, whether or not the linearization of $p^{(2)}$ depends on $\eta^{\alpha}_{(2)}$ is determined by the stick-slip status. Per the discussion following Eq.(7.2.26) in the main text, the fluid flux must be calculated after the stick-slip status has been resolved.

7.2.10.2 Discretization

Let the continuous variables on the primary and secondary surfaces be interpolated over each element face according to

$$\begin{aligned} \delta\mathbf{v}^{(1)} &= \sum_a N^{(1)}_a \delta\mathbf{v}^{(1)}_a \qquad \delta\mathbf{v}^{(2)} = \sum_b N^{(2)}_b \delta\mathbf{v}^{(2)}_b \\ \Delta\mathbf{u}^{(1)} &= \sum_c N^{(1)}_c \Delta\mathbf{u}^{(1)}_c \quad \Delta\mathbf{u}^{(2)} = \sum_d N^{(2)}_d \Delta\mathbf{u}^{(2)}_d \\ \delta p^{(1)} &= \sum_a N^{(1)}_a \delta p^{(1)}_a \qquad \delta p^{(2)} = \sum_b N^{(2)}_b \delta p^{(2)}_b \\ \Delta p^{(1)} &= \sum_c N^{(1)}_c \Delta p^{(1)}_c \quad \Delta p^{(2)} = \sum_d N^{(2)}_d \Delta p^{(2)}_d \end{aligned} \tag{7.2.48}$$

In the case of slip, the contact integral of Eq.(7.2.4) can be split into normal and tangential parts, $\delta G_c = \delta G_c^n + \delta G_c^t$, such that

$$\begin{aligned}\delta G_c = &\int_{\Gamma_\eta^{(1)}} \left(\begin{bmatrix} \delta\mathbf{v}^{(1)} & \delta\mathbf{v}^{(2)} \end{bmatrix} \cdot \begin{bmatrix} t_n\mathbf{n}^{(1)} \\ -t_n\mathbf{n}^{(1)} \end{bmatrix} + \begin{bmatrix} \delta p^{(1)} & \delta p^{(2)} \end{bmatrix} \cdot \begin{bmatrix} w_n \\ -w_n \end{bmatrix} \right) J_\eta^{(1)} d\eta_{(1)}^1 d\eta_{(1)}^2 \\ &+ \int_{\Gamma_\eta^{(1)}} \begin{bmatrix} \delta\mathbf{v}^{(1)} & \delta\mathbf{v}^{(2)} \end{bmatrix} \cdot \begin{bmatrix} \mu_{\text{eff}} t_n \mathbf{s}^{(1)} \\ -\mu_{\text{eff}} t_n \mathbf{s}^{(1)} \end{bmatrix} J_\eta^{(1)} d\eta_{(1)}^1 d\eta_{(1)}^2\end{aligned} \tag{7.2.49}$$

This split will be useful for the full linearization. Discretizing this expression yields

$$\begin{aligned}\delta G_c = &\sum_a \begin{bmatrix} \delta\mathbf{v}_a^{(1)} & \delta p_a^{(1)} \end{bmatrix} \cdot \int_{\Gamma_\eta^{(1)}} \begin{bmatrix} \mathbf{f}_a^{(1)} \\ w_a^{(1)} \end{bmatrix} J_\eta^{(1)} d\eta_{(1)}^1 d\eta_{(1)}^2 \\ &+ \sum_b \begin{bmatrix} \delta\mathbf{v}_b^{(2)} & \delta p_b^{(2)} \end{bmatrix} \cdot \int_{\Gamma_\eta^{(1)}} \begin{bmatrix} \mathbf{f}_b^{(2)} \\ w_b^{(2)} \end{bmatrix} J_\eta^{(1)} d\eta_{(1)}^1 d\eta_{(1)}^2\end{aligned} \tag{7.2.50}$$

where

$$\begin{aligned}\mathbf{f}_a^{(1)} =& N_a^{(1)} \mathbf{t}^{(1)}, \quad \mathbf{f}_b^{(2)} = -N_b^{(2)} \mathbf{t}^{(1)} \\ w_a^{(1)} =& N_a^{(1)} w_n, \quad w_b^{(2)} = -N_b^{(2)} w_n\end{aligned} \tag{7.2.51}$$

and $\mathbf{t}^{(1)}$ is given by Eqs.(7.2.23)-(7.2.24) for the penalty method and Eqs.(7.2.28)-(7.2.29) for augmented Lagrangian regularization; similarly, w_n is given by Eq.(7.2.25) or Eq.(7.2.30) for penalty and augmented Lagrangian schemes, respectively. For the following linearization and discretization the normal and tangential components, representing frictionless and frictional contributions to the contact integral, will be treated separately and may then be added together as in Eq.(7.2.49).

Frictionless Terms The linearization of the frictional part of Eq.(7.2.49) makes use of Eq.(7.2.44) to find

$$\begin{aligned}D\delta G_c = &\int_{\Gamma_\eta^{(1)}} \begin{bmatrix} \delta\mathbf{v}^{(1)} & \delta p^{(1)} \end{bmatrix} \cdot \left(\begin{bmatrix} t_n\mathbf{n}^{(1)} \\ w_n \end{bmatrix} \frac{1}{J_\eta^{(1)}} DJ_\eta^{(1)} + \begin{bmatrix} t_n \\ 0 \end{bmatrix} D\mathbf{n}^{(1)} + \begin{bmatrix} \mathbf{n}^{(1)} \\ 0 \end{bmatrix} Dt_n \right. \\ &\left. + \begin{bmatrix} 0 \\ 1 \end{bmatrix} Dw_n \right) J_\eta^{(1)} d\eta_{(1)}^1 d\eta_{(1)}^2 \\ &+ \int_{\Gamma_\eta^{(1)}} \begin{bmatrix} \frac{\partial\delta\mathbf{v}^{(2)}}{\partial\eta_{(2)}^\alpha} & \frac{\partial\delta p^{(2)}}{\partial\eta_{(2)}^\alpha} \end{bmatrix} \cdot \begin{bmatrix} -t_n\mathbf{n}^{(1)} \\ -w_n \end{bmatrix} D\eta_{(2)}^\alpha J_\eta^{(1)} d\eta_{(1)}^1 d\eta_{(1)}^2 \\ &+ \int_{\Gamma_\eta^{(1)}} \begin{bmatrix} \delta\mathbf{v}^{(2)} & \delta p^{(2)} \end{bmatrix} \cdot \left(\begin{bmatrix} -t_n\mathbf{n}^{(1)} \\ -w_n \end{bmatrix} \frac{1}{J_\eta^{(1)}} DJ_\eta^{(1)} + \begin{bmatrix} -t_n \\ 0 \end{bmatrix} D\mathbf{n}^{(1)} + \begin{bmatrix} -\mathbf{n}^{(1)} \\ 0 \end{bmatrix} Dt_n \right. \\ &\left. \begin{bmatrix} 0 \\ -1 \end{bmatrix} Dw_n \right) J_\eta^{(1)} d\eta_{(1)}^1 d\eta_{(1)}^2\end{aligned} \tag{7.2.52}$$

where we note that the virtual variables on the secondary surface now enter the linearization, as parametric coordinates on the secondary surface vary during slip according to Eq.(7.2.12). The only linearization which has not been previously discretized is Dw_n, and it follows from placing Eq.(7.2.48) into Eq.(7.2.47) that

$$Dw_n = \sum_c \begin{bmatrix} -\varepsilon_p N_c^{(1)} \mathbf{p}^{(2)} + \varepsilon_p P_c \mathbf{n}^{(1)} & \varepsilon_p N_c^{(1)} \end{bmatrix} \cdot \begin{bmatrix} \Delta\mathbf{u}_c^{(1)} \\ \Delta p_c^{(1)} \end{bmatrix} + \sum_d \begin{bmatrix} \varepsilon_p N_d^{(2)} \mathbf{p}^{(2)} & -\varepsilon_p N_d^{(2)} \end{bmatrix} \cdot \begin{bmatrix} \Delta\mathbf{u}_d^{(2)} \\ \Delta p_d^{(2)} \end{bmatrix} \tag{7.2.53}$$

where we define

$$\begin{aligned}\mathbf{p}^{(2)} &= \frac{\partial p^{(2)}}{\partial \eta^{\alpha}_{(2)}} \bar{\mathbf{g}}^{\alpha}_{(2)} \\ P_c &= g a^{\alpha\beta} \frac{\partial p^{(2)}}{\partial \eta^{\alpha}_{(2)}} \frac{\partial N^{(1)}_c}{\partial \eta^{\beta}_{(1)}}\end{aligned} \tag{7.2.54}$$

and for convenience we note that

$$\frac{\partial p^{(2)}}{\partial \eta^{\alpha}_{(2)}} D\eta^{\alpha}_{(2)} = \sum_c \begin{bmatrix} N^{(1)}_c \mathbf{p}^{(2)} - P_c \mathbf{n}^{(1)} & 0 \end{bmatrix} \cdot \begin{bmatrix} \Delta \mathbf{u}^{(1)}_c \\ \Delta p^{(1)}_c \end{bmatrix} + \sum_d \begin{bmatrix} -N^{(2)}_d \mathbf{p}^{(2)} & 0 \end{bmatrix} \cdot \begin{bmatrix} \Delta \mathbf{u}^{(2)}_d \\ \Delta p^{(2)}_d \end{bmatrix} \tag{7.2.55}$$

Directional derivatives of virtual variables on the secondary surface will lead to expressions of the form $\left(\partial N^{(2)}_b / \partial \eta^{\lambda}_{(2)}\right) D\eta^{\lambda}_{(2)}$, where

$$\frac{\partial N^{(2)}_b}{\partial \eta^{\lambda}_{(2)}} D\eta^{\lambda}_{(2)} = \begin{bmatrix} \sum_c N^{(1)}_c \bar{\mathbf{m}}^{(2)}_b - G_{bc} \mathbf{n}^{(1)} & \sum_d -N^{(2)}_d \bar{\mathbf{m}}^{(2)}_b \end{bmatrix} \cdot \begin{bmatrix} \Delta \mathbf{u}^{(1)}_c \\ \Delta \mathbf{u}^{(2)}_d \end{bmatrix} \tag{7.2.56}$$

In Eq.(7.2.56), the pressure degrees of freedom do not enter into the linearization. In an effort to keep the expression more compact, we have not included these variables. However, this expression could easily be cast into the form of e.g. Eq.(7.2.55) by adding zeros where necessary. Discretizing Eq.(7.2.52) and making use of linearizations found previously [114], along with Eqs.(7.2.53) and (7.2.55), allows the resulting stiffness matrix to be expressed as

$$\begin{aligned} D\delta G_c = \sum_a \begin{bmatrix} \delta \mathbf{v}^{(1)}_a & \delta p^{(1)}_a \end{bmatrix} \cdot \int_{\Gamma^{(1)}_\eta} \Bigg(\sum_c \begin{bmatrix} \mathbf{K}^{(1,1)}_{ac} & \mathbf{0} \\ \mathbf{g}^{(1,1)}_{ac} & g^{(1,1)}_{ac} \end{bmatrix} \cdot \begin{bmatrix} \Delta \mathbf{u}^{(1)}_c \\ \Delta p^{(1)}_c \end{bmatrix} \\ + \sum_d \begin{bmatrix} \mathbf{K}^{(1,2)}_{ad} & \mathbf{0} \\ \mathbf{g}^{(1,2)}_{ad} & g^{(1,2)}_{ad} \end{bmatrix} \cdot \begin{bmatrix} \Delta \mathbf{u}^{(2)}_d \\ \Delta p^{(2)}_d \end{bmatrix} \Bigg) J^{(1)}_\eta d\eta^1_{(1)} d\eta^2_{(1)} \\ + \sum_b \begin{bmatrix} \delta \mathbf{v}^{(2)}_b & \delta p^{(2)}_b \end{bmatrix} \cdot \int_{\Gamma^{(1)}_\eta} \Bigg(\sum_c \begin{bmatrix} \mathbf{K}^{(2,1)}_{bc} & \mathbf{0} \\ \mathbf{g}^{(2,1)}_{bc} & g^{(2,1)}_{bc} \end{bmatrix} \cdot \begin{bmatrix} \Delta \mathbf{u}^{(1)}_c \\ \Delta p^{(1)}_c \end{bmatrix} \\ + \sum_d \begin{bmatrix} \mathbf{K}^{(2,2)}_{bd} & \mathbf{0} \\ \mathbf{g}^{(2,2)}_{bd} & g^{(2,2)}_{bd} \end{bmatrix} \cdot \begin{bmatrix} \Delta \mathbf{u}^{(2)}_d \\ \Delta p^{(2)}_d \end{bmatrix} \Bigg) J^{(1)}_\eta d\eta^1_{(1)} d\eta^2_{(1)} \end{aligned} \tag{7.2.57}$$

where

$$\begin{aligned} \mathbf{K}^{(1,1)}_{ac} &= -N^{(1)}_a N^{(1)}_c \left(\varepsilon \tilde{\mathbf{N}}^{(1)} \right) - N^{(1)}_a \left(t_n \mathbf{A}^{(1)}_c + t_n \bar{\mathbf{M}}^{(1)}_c \cdot \mathbf{N}^{(1)} \right) \\ \mathbf{K}^{(1,2)}_{ad} &= N^{(1)}_a N^{(2)}_d \left(\varepsilon \tilde{\mathbf{N}}^{(1)} \right) \\ \mathbf{K}^{(2,1)}_{bc} &= N^{(2)}_b N^{(1)}_c \left(\varepsilon \tilde{\mathbf{N}}^{(1)} \right) + N^{(2)}_b \left(t_n \mathbf{A}^{(1)}_c + t_n \bar{\mathbf{M}}^{(1)}_c \cdot \mathbf{N}^{(1)} \right) \\ &\quad + N^{(1)}_c \left(t_n \bar{\mathbf{M}}^{(2)}_b \right) + G_{bc} \left(t_n \mathbf{N}^{(1)} \right) \\ \mathbf{K}^{(2,2)}_{bd} &= -N^{(2)}_b N^{(2)}_d \left(\varepsilon \tilde{\mathbf{N}}^{(1)} \right) - N^{(2)}_d \left(t_n \bar{\mathbf{M}}^{(2)}_b \right) \end{aligned} \tag{7.2.58}$$

and

$$\begin{aligned}
\mathbf{g}_{ac}^{(1,1)} &= -N_a^{(1)} N_c^{(1)} \left(\varepsilon_p \mathbf{p}^{(2)}\right) + N_a^{(1)} \left(w_n \mathbf{A}_c^{(1)} \cdot \mathbf{n}^{(1)} + \varepsilon_p P_c \mathbf{n}^{(1)}\right) \\
\mathbf{g}_{ad}^{(1,2)} &= N_a^{(1)} N_d^{(2)} \left(\varepsilon_p \mathbf{p}^{(2)}\right) \\
\mathbf{g}_{bc}^{(2,1)} &= N_b^{(2)} N_c^{(1)} \left(\varepsilon_p \mathbf{p}^{(2)}\right) - N_b^{(2)} \left(w_n \mathbf{A}_c^{(1)} \cdot \mathbf{n}^{(1)} + \varepsilon_p P_c \mathbf{n}^{(1)}\right) - N_c^{(1)} \left(w_n \bar{\mathbf{m}}_b^{(2)}\right) + G_{bc} \left(w_n \mathbf{n}^{(1)}\right) \\
\mathbf{g}_{bd}^{(2,2)} &= -N_b^{(2)} N_d^{(2)} \left(\varepsilon_p \mathbf{p}^{(2)}\right) + N_d^{(2)} \left(w_n \bar{\mathbf{m}}_b^{(2)}\right)
\end{aligned} \tag{7.2.59}$$

and

$$\begin{aligned}
g_{ac}^{(1,1)} &= -N_a^{(1)} N_c^{(1)} \left(-\varepsilon_p\right) \\
g_{ad}^{(1,2)} &= N_a^{(1)} N_d^{(2)} \left(-\varepsilon_p\right) \\
g_{bc}^{(2,1)} &= N_b^{(2)} N_c^{(1)} \left(-\varepsilon_p\right) \\
g_{bd}^{(2,2)} &= -N_b^{(2)} N_d^{(2)} \left(-\varepsilon_p\right)
\end{aligned} \tag{7.2.60}$$

The expressions above are very similar to those which can be found in our frictionless biphasic contact paper [9], although the present framework is more general, as that previous study evaluated expressions in the limit as $g \to 0$ (see Zimmerman and Ateshian [114] for a detailed discussion of this assumption and the benefits of relaxing it).

Frictional Terms Linearizing the frictional contribution follows from the second term of Eq.(7.2.49) as

$$\begin{aligned}
D\delta G_c = &\int_{\Gamma_\eta^{(1)}} \begin{bmatrix} \delta \mathbf{v}^{(1)} & \delta p^{(1)} \end{bmatrix} \cdot \left(\begin{bmatrix} t_n \mathbf{s}^{(1)} \\ 0 \end{bmatrix} D\mu_{\text{eff}} + \begin{bmatrix} \mu_{\text{eff}} \mathbf{s}^{(1)} \\ 0 \end{bmatrix} Dt_n \right. \\
&\left. + \begin{bmatrix} \mu_{\text{eff}} t_n \\ 0 \end{bmatrix} D\mathbf{s}^{(1)} + \begin{bmatrix} \mu_{\text{eff}} t_n \mathbf{s}^{(1)} \\ 0 \end{bmatrix} \frac{1}{J_\eta^{(1)}} DJ_\eta^{(1)} \right) J_\eta^{(1)} d\eta_{(1)}^1 d\eta_{(1)}^2 \\
&+ \int_{\Gamma_\eta^{(1)}} \begin{bmatrix} \delta \mathbf{v}^{(2)} & \delta p^{(2)} \end{bmatrix} \cdot \left(\begin{bmatrix} -t_n \mathbf{s}^{(1)} \\ 0 \end{bmatrix} D\mu_{\text{eff}} + \begin{bmatrix} -\mu_{\text{eff}} \mathbf{s}^{(1)} \\ 0 \end{bmatrix} Dt_n \right. \\
&\left. + \begin{bmatrix} -\mu_{\text{eff}} t_n \\ 0 \end{bmatrix} D\mathbf{s}^{(1)} + \begin{bmatrix} -\mu_{\text{eff}} t_n \mathbf{s}^{(1)} \\ 0 \end{bmatrix} \frac{1}{J_\eta^{(1)}} DJ_\eta^{(1)} \right) J_\eta^{(1)} d\eta_{(1)}^1 d\eta_{(1)}^2 \\
&+ \int_{\Gamma_\eta^{(1)}} \begin{bmatrix} \frac{\partial \delta \mathbf{v}^{(2)}}{\partial \eta_{(2)}^\alpha} & \frac{\partial \delta p^{(2)}}{\partial \eta_{(2)}^\alpha} \end{bmatrix} \cdot \begin{bmatrix} -\mu_{\text{eff}} t_n \mathbf{s}^{(1)} \\ 0 \end{bmatrix} D\eta_{(2)}^\alpha J_\eta^{(1)} d\eta_{(1)}^1 d\eta_{(1)}^2
\end{aligned} \tag{7.2.61}$$

The remaining quantity in this expression to be determined is the discretization of $D\mu_{\text{eff}}$; from Eq.(7.2.45) and Eq.(7.2.48) it follows that

$$\begin{aligned}
D\mu_{\text{eff}} = &\sum_c \left[\varepsilon N_c^{(1)} \mu_{\text{eq}} \Gamma_p \tfrac{1}{t_n^2} \bar{\mathbf{N}}^{(1)} \cdot \mathbf{n}^{(1)} + \mu_{\text{eq}} \Gamma_p \tfrac{1}{t_n} \mathbf{N}^{(1)} \cdot \bar{\mathbf{m}}_c^{(1)} \quad N_c^{(1)} \mu_{\text{eq}} \left(1 - \varphi\right) \tfrac{1}{t_n} \right] \cdot \begin{bmatrix} \Delta \mathbf{u}_c^{(1)} \\ \Delta p_c^{(1)} \end{bmatrix} \\
&+ \sum_d \left[-\varepsilon_n N_d^{(2)} \mu_{\text{eq}} \Gamma_p \tfrac{1}{t_n^2} \bar{\mathbf{N}}^{(1)} \cdot \mathbf{n}^{(1)} \quad 0 \right] \cdot \begin{bmatrix} \Delta \mathbf{u}_d^{(2)} \\ \Delta p_d^{(2)} \end{bmatrix}
\end{aligned} \tag{7.2.62}$$

where we made the definition

$$\Gamma_p = \left(1 - \varphi\right) p^{(1)} \tag{7.2.63}$$

just to be used in Eq.(7.2.62) for space considerations. Finally, inserting Eqs.(7.2.48) and (7.2.62) into Eq.(7.2.61) yields the stiffness matrix for the frictional terms

$$\begin{aligned} D\delta G_c = \sum_a \begin{bmatrix} \delta\mathbf{v}_a^{(1)} & \delta p_a^{(1)} \end{bmatrix} \cdot \int_{\Gamma_\eta^{(1)}} \left(\sum_c \begin{bmatrix} \mathbf{K}_{ac}^{(1,1)} & \mathbf{k}_{ac}^{(1,1)} \\ \mathbf{0} & 0 \end{bmatrix} \cdot \begin{bmatrix} \Delta\mathbf{u}_c^{(1)} \\ \Delta p_c^{(1)} \end{bmatrix} \right. \\ \left. + \sum_d \begin{bmatrix} \mathbf{K}_{ad}^{(1,2)} & \mathbf{k}_{ad}^{(1,2)} \\ \mathbf{0} & 0 \end{bmatrix} \cdot \begin{bmatrix} \Delta\mathbf{u}_d^{(2)} \\ \Delta p_d^{(2)} \end{bmatrix} \right) J_\eta^{(1)} d\eta_{(1)}^1 d\eta_{(1)}^2 \\ + \sum_b \begin{bmatrix} \delta\mathbf{v}_b^{(2)} & \delta p_b^{(2)} \end{bmatrix} \cdot \int_{\Gamma_\eta^{(1)}} \left(\sum_c \begin{bmatrix} \mathbf{K}_{bc}^{(2,1)} & \mathbf{k}_{bc}^{(2,1)} \\ \mathbf{0} & 0 \end{bmatrix} \cdot \begin{bmatrix} \Delta\mathbf{u}_c^{(1)} \\ \Delta p_c^{(1)} \end{bmatrix} \right. \\ \left. + \sum_d \begin{bmatrix} \mathbf{K}_{bd}^{(2,2)} & \mathbf{k}_{bd}^{(2,2)} \\ \mathbf{0} & 0 \end{bmatrix} \cdot \begin{bmatrix} \Delta\mathbf{u}_d^{(2)} \\ \Delta p_d^{(2)} \end{bmatrix} \right) J_\eta^{(1)} d\eta_{(1)}^1 d\eta_{(1)}^2 \end{aligned} \tag{7.2.64}$$

where

$$\begin{aligned} \mathbf{K}_{ac}^{(1,1)} &= -N_a^{(1)} N_c^{(1)} \left(\varepsilon\mu_{\text{eq}} \tilde{\mathbf{S}}^{(1)} + \mu_{\text{eff}} t_n \mathbf{B}^{(1)} \right) - N_a^{(1)} \left(t_n \mathbf{s}^{(1)} \otimes \bar{\mathbf{h}}_{c-}^{(1)} \right. \\ &\quad \left. + \mu_{\text{eff}} t_n g \mathbf{P}_S \cdot \mathbf{c}^{(1)} \otimes \mathbf{h}_{c+}^{(1)} - \mu_{\text{eff}} t_n \mathbf{J}_c^{(1)} \right) \\ \mathbf{K}_{ad}^{(1,2)} &= N_a^{(1)} N_d^{(2)} \left(\varepsilon\mu_{\text{eq}} \tilde{\mathbf{S}}^{(1)} + \mu_{\text{eff}} t_n \mathbf{B}^{(1)} \right) \\ \mathbf{K}_{bc}^{(2,1)} &= N_b^{(2)} N_c^{(1)} \left(\varepsilon\mu_{\text{eq}} \tilde{\mathbf{S}}^{(1)} + \mu_{\text{eff}} t_n \mathbf{B}^{(1)} \right) + N_b^{(2)} \left(t_n \mathbf{s}^{(1)} \otimes \bar{\mathbf{h}}_{c-}^{(1)} \right. \\ &\quad \left. + \mu_{\text{eff}} t_n g \mathbf{P}_S \cdot \mathbf{c}^{(1)} \otimes \mathbf{h}_{c+}^{(1)} - \mu_{\text{eff}} t_n \mathbf{J}_c^{(1)} \right) \\ &\quad + N_c^{(1)} \left(-\mu_{\text{eff}} t_n \mathbf{s}^{(1)} \otimes \bar{\mathbf{m}}_b^{(2)} \right) + G_{bc} \left(\mu_{\text{eff}} t_n \mathbf{S}^{(1)} \right) \\ \mathbf{K}_{bd}^{(2,2)} &= -N_b^{(2)} N_d^{(2)} \left(\varepsilon\mu_{\text{eq}} \tilde{\mathbf{S}}^{(1)} + \mu_{\text{eff}} t_n \mathbf{B}^{(1)} \right) - N_d^{(2)} \left(-\mu_{\text{eff}} t_n \mathbf{s}^{(1)} \otimes \bar{\mathbf{m}}_b^{(2)} \right) \end{aligned} \tag{7.2.65}$$

and

$$\begin{aligned} \mathbf{k}_{ac}^{(1,1)} &= -N_a^{(1)} N_c^{(1)} \left(-\mu_{\text{eq}} (1-\varphi) \mathbf{s}^{(1)} \right) \\ \mathbf{k}_{ad}^{(1,2)} &= \mathbf{0} \\ \mathbf{k}_{bc}^{(2,1)} &= N_b^{(2)} N_c^{(1)} \left(-\mu_{\text{eq}} (1-\varphi) \mathbf{s}^{(1)} \right) \\ \mathbf{k}_{bd}^{(2,2)} &= \mathbf{0} \end{aligned} \tag{7.2.66}$$

In Eq.(7.2.65), we have defined

$$\bar{\mathbf{h}}_{c-}^{(1)} = \mu_{\text{eq}} \mathbf{N}^{(1)} \cdot \bar{\mathbf{m}}_c^{(1)} - \mu_{\text{eff}} \mathbf{A}_c^{(1)} \cdot \mathbf{n}^{(1)} \tag{7.2.67}$$

by analogy with our definitions for $\mathbf{h}_{c+}^{(1)}$ and $\mathbf{h}_{c-}^{(1)}$ in Section 7.1.9.11. The stiffness matrix of the frictional contribution to the virtual work, given by Eq.(7.2.64), is nonsymmetric. Summing Eqs.(7.2.57) and (7.2.64) produces the total stiffness matrix for the case of frictional biphasic slip; this total stiffness matrix is also nonsymmetric. However, as noted before [9], the stiffness matrix for biphasic materials is nonsymmetric by construction, so there is no expectation that the contact stiffness matrices be symmetric.

Equation (7.2.65) contains the solid-solid stiffness terms. Comparing Eq.(7.2.65) with Eq.(7.1.112) shows that the same form of the equations is recovered. Interestingly, however, some of the terms in sliding-elastic (Section 7.1.9) which were multiplied by the friction coefficient μ are now multiplied by μ_{eff}, which indicates certain terms which are important in biphasic contact. Of course, in the absence of pressurized fluid, $\mu_{\text{eff}} \to \mu$ and we recover the sliding-elastic formulation.

7.3 Biphasic-Solute Contact

7.3.1 Contact Integral

See Section 2.6 for a review of biphasic-solute materials. The contact interface is defined between surfaces $\gamma^{(1)}$ and $\gamma^{(2)}$. Due to continuity requirements on the traction and fluxes, the external virtual work resulting from contact tractions $\mathbf{t}^{(i)}$, solvent fluxes $w_n^{(i)}$ and solute fluxes $j_n^{(i)}$ $(i = 1, 2)$, may be combined into the contact integral

$$\begin{aligned}\delta G_c = &\int_{\gamma^{(1)}} \left(\delta\mathbf{v}^{(1)} - \delta\mathbf{v}^{(2)}\right) \cdot \mathbf{t}^{(1)}\, da^{(1)} \\ &+ \int_{\gamma^{(1)}} \left(\delta\tilde{p}^{(1)} - \delta\tilde{p}^{(2)}\right) w_n^{(1)}\, da^{(1)} \\ &+ \int_{\gamma^{(1)}} \left(\delta\tilde{c}^{(1)} - \delta\tilde{c}^{(2)}\right) j_n^{(1)}\, da^{(1)}\,.\end{aligned} \tag{7.3.1}$$

In the current implementation, only frictionless contact is taken into consideration, so that the contact traction has only a normal component, $\mathbf{t}^{(i)} = t_n\mathbf{n}^{(i)}$. To evaluate and linearize δG_c, define the covariant basis vectors on each surface as

$$\mathbf{g}_\alpha^{(i)} = \frac{\partial\mathbf{x}^{(i)}}{\partial\eta^\alpha_{(i)}}, \quad \alpha = 1, 2, \tag{7.3.2}$$

where $\mathbf{x}^{(i)}$ represents the spatial position of points on $\gamma^{(i)}$, and $\eta^\alpha_{(i)}$ represent the parametric coordinates of that point. The unit outward normal on each surface is then given by

$$\mathbf{n}^{(i)} = \frac{\mathbf{g}_1^{(i)} \times \mathbf{g}_2^{(i)}}{\left|\mathbf{g}_1^{(i)} \times \mathbf{g}_2^{(i)}\right|}. \tag{7.3.3}$$

Now the contact integral may be rewritten as

$$\begin{aligned}\delta G_c = &\int_{\gamma^{(1)}} \left(\delta\mathbf{v}^{(1)} - \delta\mathbf{v}^{(2)}\right) t_n\mathbf{g}_1^{(1)} \times \mathbf{g}_2^{(1)}\, d\eta^1_{(1)} d\eta^2_{(1)} \\ &+ \int_{\gamma^{(1)}} \left(\delta\tilde{p}^{(1)} - \delta\tilde{p}^{(2)}\right) w_n^{(1)} \left|\mathbf{g}_1^{(1)} \times \mathbf{g}_2^{(1)}\right| d\eta^1_{(1)} d\eta^2_{(1)} \\ &+ \int_{\gamma^{(1)}} \left(\delta\tilde{c}^{(1)} - \delta\tilde{c}^{(2)}\right) j_n^{(1)} \left|\mathbf{g}_1^{(1)} \times \mathbf{g}_2^{(1)}\right| d\eta^1_{(1)} d\eta^2_{(1)}\,,\end{aligned} \tag{7.3.4}$$

and the linearization $D\delta G_c$ of δG_c has the form

$$D\delta G_c = \sum_{i=1}^{2} D\delta G_c\left[\Delta\mathbf{u}^{(i)}\right] + D\delta G_c\left[\Delta\tilde{p}^{(i)}\right] + D\delta G_c\left[\Delta\tilde{c}^{(i)}\right]\,. \tag{7.3.5}$$

7.3.2 Gap Function

The gap function g, representing the distance between the contact surfaces, is defined by

$$\mathbf{x}^{(2)} = \mathbf{x}^{(1)} + g\mathbf{n}^{(1)}, \quad g = \left(\mathbf{x}^{(2)} - \mathbf{x}^{(1)}\right) \cdot \mathbf{n}^{(1)}\,. \tag{7.3.6}$$

The linearization of variables associated with motion, pressure, and concentration, is given by

$$\begin{aligned}
D\mathbf{x}^{(1)} &= \Delta\mathbf{u}^{(1)} \qquad D\mathbf{x}^{(2)} = \Delta\mathbf{u}^{(2)} + \mathbf{g}_\alpha^{(2)}\Delta\eta_{(2)}^\alpha \\
D\tilde{p}^{(1)} &= \Delta\tilde{p}^{(1)} \qquad D\tilde{p}^{(2)} = \Delta\tilde{p}^{(2)} + \frac{\partial\tilde{p}^{(2)}}{\partial\eta_{(2)}^\alpha}\Delta\eta_{(2)}^\alpha \\
D\tilde{c}^{(1)} &= \Delta\tilde{c}^{(1)} \qquad D\tilde{c}^{(2)} = \Delta\tilde{c}^{(2)} + \frac{\partial\tilde{c}^{(2)}}{\partial\eta_{(2)}^\alpha}\Delta\eta_{(2)}^\alpha \\
D\delta\mathbf{v}^{(1)} &= \mathbf{0} \qquad\quad D\mathbf{v}^{(2)} = \frac{\partial\delta\mathbf{v}^{(2)}}{\partial\eta_{(2)}^\alpha}\Delta\eta_{(2)}^\alpha \\
D\delta\tilde{p}^{(1)} &= 0 \qquad\quad D\delta\tilde{p}^{(2)} = \frac{\partial\delta\tilde{p}^{(2)}}{\partial\eta_{(2)}^\alpha}\Delta\eta_{(2)}^\alpha \\
D\delta\tilde{c}^{(1)} &= 0 \qquad\quad D\delta\tilde{c}^{(2)} = \frac{\partial\delta\tilde{c}^{(2)}}{\partial\eta_{(2)}^\alpha}\Delta\eta_{(2)}^\alpha
\end{aligned} \,, \tag{7.3.7}$$

where

$$\Delta\eta_{(2)}^\alpha = \left(\Delta\mathbf{u}^{(1)} - \Delta\mathbf{u}^{(2)}\right)\cdot a^{\alpha\beta}\mathbf{g}_\beta^{(1)} - a^{\alpha\beta}g\mathbf{n}^{(1)}\cdot\frac{\partial\Delta\mathbf{u}^{(1)}}{\partial\eta_{(1)}^\beta}\,, \tag{7.3.8}$$

with $a^{\alpha\beta} = (A_{\alpha\beta})^{-1}$ and $A_{\alpha\beta} = \mathbf{g}_\alpha^{(1)}\cdot\mathbf{g}_\beta^{(2)}$.

7.3.3 Penalty Method

Let the normal component of the contact traction be described by the penalty function,

$$t_n = \begin{cases} \varepsilon_n g & g < 0 \\ 0 & g \geqslant 0 \end{cases}, \tag{7.3.9}$$

where ε_n is a penalty factor associated with t_n. Similarly, let

$$\begin{cases} w_n = \varepsilon_p\pi = \varepsilon_p\left(\tilde{p}^{(1)} - \tilde{p}^{(2)}\right) & t_n < 0 \\ \tilde{p}^{(i)} = \tilde{p}^* & t_n = 0 \end{cases}, \tag{7.3.10}$$

and

$$\begin{cases} j_n = \varepsilon_c\chi = \varepsilon_c\left(\tilde{c}^{(1)} - \tilde{c}^{(2)}\right) & t_n < 0 \\ \tilde{c}^{(i)} = \tilde{c}^* & t_n = 0 \end{cases}, \tag{7.3.11}$$

where ε_p and ε_c are penalty factors associated with w_n and j_n, respectively. It follows that

$$\begin{aligned}
Dt_n &= \varepsilon_n\left(\Delta\mathbf{u}^{(2)} - \Delta\mathbf{u}^{(1)} + \mathbf{g}_\alpha^{(2)}\Delta\eta_{(2)}^\alpha\right)\cdot\mathbf{n}^{(1)} \\
Dw_n &= \varepsilon_p\left(\Delta\tilde{p}^{(1)} - \Delta\tilde{p}^{(2)} - \frac{\partial\tilde{p}^{(2)}}{\partial\eta_{(2)}^\alpha}\Delta\eta_{(2)}^\alpha\right) \\
Dj_n &= \varepsilon_c\left(\Delta\tilde{c}^{(1)} - \Delta\tilde{c}^{(2)} - \frac{\partial\tilde{c}^{(2)}}{\partial\eta_{(2)}^\alpha}\Delta\eta_{(2)}^\alpha\right)
\end{aligned} \,. \tag{7.3.12}$$

Given these relations, it can be shown that the directional derivatives of the various terms appearing in the integrand of δG_c are

$$\begin{aligned}
&D\left(t_n\left(\delta\mathbf{v}^{(1)}-\delta\mathbf{v}^{(2)}\right)\cdot\mathbf{g}_1^{(1)}\times\mathbf{g}_2^{(1)}\right)=\\
&-J_\eta^{(1)}\varepsilon_n\left(\delta\mathbf{v}^{(1)}-\delta\mathbf{v}^{(2)}\right)\cdot\left(\mathbf{n}^{(1)}\otimes\mathbf{n}^{(1)}\right)\cdot\left(\Delta\mathbf{u}^{(1)}-\Delta\mathbf{u}^{(2)}\right)\\
&+J_\eta^{(1)}t_n\frac{\partial\delta\mathbf{v}^{(2)}}{\partial\eta_{(2)}^\alpha}\cdot\left(\mathbf{n}^{(2)}\otimes\mathbf{g}_{(2)}^\alpha\right)\cdot\left(\Delta\mathbf{u}^{(1)}-\Delta\mathbf{u}^{(2)}\right) \qquad ,\\
&+t_n\left(\delta\mathbf{v}^{(1)}-\delta\mathbf{v}^{(2)}\right)\cdot\left(\frac{\partial\Delta\mathbf{u}^{(1)}}{\partial\eta_{(1)}^1}\times\mathbf{g}_2^{(1)}+\mathbf{g}_1^{(1)}\times\frac{\partial\Delta\mathbf{u}^{(1)}}{\partial\eta_{(1)}^2}\right)
\end{aligned} \tag{7.3.13}$$

$$\begin{aligned}
&D\left(w_n\left(\delta\tilde{p}^{(1)}-\delta\tilde{p}^{(2)}\right)\left|\mathbf{g}_1^{(1)}\times\mathbf{g}_2^{(1)}\right|\right)=\\
&J_\eta^{(1)}\varepsilon_p\left(\delta\tilde{p}^{(1)}-\delta\tilde{p}^{(2)}\right)\left(\Delta\tilde{p}^{(1)}-\Delta\tilde{p}^{(2)}\right)\\
&-J_\eta^{(1)}\left[\varepsilon_p\left(\delta\tilde{p}^{(1)}-\delta\tilde{p}^{(2)}\right)\frac{\partial\tilde{p}^{(1)}}{\partial\eta_{(1)}^\alpha}\mathbf{g}_{(1)}^\alpha+w_n\frac{\partial\delta\tilde{p}^{(2)}}{\partial\eta_{(2)}^\alpha}\mathbf{g}_{(2)}^\alpha\right]\cdot\left(\Delta\mathbf{u}^{(1)}-\Delta\mathbf{u}^{(2)}\right),\\
&+w_n\left(\delta\tilde{p}^{(1)}-\delta\tilde{p}^{(2)}\right)\mathbf{n}^{(1)}\cdot\left(\frac{\partial\Delta\mathbf{u}^{(1)}}{\partial\eta_{(1)}^1}\times\mathbf{g}_2^{(1)}+\mathbf{g}_1^{(1)}\times\frac{\partial\Delta\mathbf{u}^{(1)}}{\partial\eta_{(1)}^2}\right)
\end{aligned} \tag{7.3.14}$$

$$\begin{aligned}
&D\left(j_n\left(\delta\tilde{c}^{(1)}-\delta\tilde{c}^{(2)}\right)\left|\mathbf{g}_1^{(1)}\times\mathbf{g}_2^{(1)}\right|\right)=\\
&J_\eta^{(1)}\varepsilon_c\left(\delta\tilde{c}^{(1)}-\delta\tilde{c}^{(2)}\right)\left(\Delta\tilde{c}^{(1)}-\Delta\tilde{c}^{(2)}\right)\\
&-J_\eta^{(1)}\left[\varepsilon_c\left(\delta\tilde{c}^{(1)}-\delta\tilde{c}^{(2)}\right)\frac{\partial\tilde{c}^{(1)}}{\partial\eta_{(1)}^\alpha}\mathbf{g}_{(1)}^\alpha+j_n\frac{\partial\delta\tilde{c}^{(2)}}{\partial\eta_{(2)}^\alpha}\mathbf{g}_{(2)}^\alpha\right]\cdot\left(\Delta\mathbf{u}^{(1)}-\Delta\mathbf{u}^{(2)}\right),\\
&+j_n\left(\delta\tilde{c}^{(1)}-\delta\tilde{c}^{(2)}\right)\mathbf{n}^{(1)}\cdot\left(\frac{\partial\Delta\mathbf{u}^{(1)}}{\partial\eta_{(1)}^1}\times\mathbf{g}_2^{(1)}+\mathbf{g}_1^{(1)}\times\frac{\partial\Delta\mathbf{u}^{(1)}}{\partial\eta_{(1)}^2}\right)
\end{aligned} \tag{7.3.15}$$

where $J_\eta^{(1)}=\left|\mathbf{g}_1^{(1)}\times\mathbf{g}_2^{(1)}\right|$.

7.3.4 Discretization

The contact integral may be discretized as

$$\delta G_c=\sum_{e=1}^{n_e^{(1)}}\sum_{k=1}^{n_{\text{int}}^{(e)}}W_kJ_\eta^{(1)}\left[t_n\left(\delta\mathbf{v}^{(1)}-\delta\mathbf{v}^{(2)}\right)\cdot\mathbf{n}^{(1)}+w_n\left(\delta\tilde{p}^{(1)}-\delta\tilde{p}^{(2)}\right)+j_n\left(\delta\tilde{c}^{(1)}-\delta\tilde{c}^{(2)}\right)\right]. \tag{7.3.16}$$

The variables may be interpolated over each element face according to

$$\begin{aligned}
\delta\mathbf{v}^{(1)} &= \sum_{a=1}^{m^{(1)}} N_a^{(1)}\delta\mathbf{v}_a^{(1)} \qquad \delta\mathbf{v}^{(2)} = \sum_{b=1}^{m^{(2)}} N_b^{(2)}\delta\mathbf{v}_b^{(2)} \\
\Delta\mathbf{u}^{(1)} &= \sum_{c=1}^{m^{(1)}} N_c^{(1)}\Delta\mathbf{u}_c^{(1)} \quad \Delta\mathbf{u}^{(2)} = \sum_{d=1}^{m^{(2)}} N_d^{(2)}\Delta\mathbf{u}_d^{(2)} \\
\delta\tilde{p}^{(1)} &= \sum_{a=1}^{m^{(1)}} N_a^{(1)}\delta\tilde{p}_a^{(1)} \qquad \delta\tilde{p}^{(2)} = \sum_{b=1}^{m^{(2)}} N_b^{(2)}\delta\tilde{p}_b^{(2)} \\
\Delta\tilde{p}^{(1)} &= \sum_{c=1}^{m^{(1)}} N_c^{(1)}\Delta\tilde{p}_c^{(1)} \quad \Delta\tilde{p}^{(2)} = \sum_{d=1}^{m^{(2)}} N_d^{(2)}\Delta\tilde{p}_d^{(2)} \\
\delta\tilde{c}^{(1)} &= \sum_{a=1}^{m^{(1)}} N_a^{(1)}\delta\tilde{c}_a^{(1)} \qquad \delta\tilde{c}^{(2)} = \sum_{b=1}^{m^{(2)}} N_b^{(2)}\delta\tilde{c}_b^{(2)} \\
\Delta\tilde{c}^{(1)} &= \sum_{c=1}^{m^{(1)}} N_c^{(1)}\Delta\tilde{c}_c^{(1)} \quad \Delta\tilde{c}^{(2)} = \sum_{d=1}^{m^{(2)}} N_d^{(2)}\Delta\tilde{c}_d^{(2)}
\end{aligned} \quad . \tag{7.3.17}$$

Then,

$$\begin{aligned}
\delta G_c = \sum_{e=1}^{n_e^{(1)}} \sum_{k=1}^{n_{\text{int}}^{(e)}} W_k J_\eta^{(1)} \Bigg(& \sum_{a=1}^{m^{(1)}} \begin{bmatrix} \delta\mathbf{v}_a^{(1)} & \delta\tilde{p}_a^{(1)} & \delta\tilde{c}_a^{(1)} \end{bmatrix} \cdot \begin{bmatrix} \mathbf{f}_a^{(1)} \\ w_a^{(1)} \\ j_a^{(1)} \end{bmatrix} \\
& + \sum_{b=1}^{m_k^{(2)}} \begin{bmatrix} \delta\mathbf{v}_{b,k}^{(1)} & \delta\tilde{p}_{b,k}^{(1)} & \delta\tilde{c}_{b,k}^{(1)} \end{bmatrix} \cdot \begin{bmatrix} \mathbf{f}_{b,k}^{(1)} \\ w_{b,k}^{(1)} \\ j_{b,k}^{(1)} \end{bmatrix} \Bigg) ,
\end{aligned} \tag{7.3.18}$$

where

$$\begin{aligned}
\mathbf{f}_a^{(1)} &= N_a^{(1)} t_n \mathbf{n}^{(1)} \quad \mathbf{f}_{b,k}^{(2)} = -N_b^{(2)} t_n \mathbf{n}^{(1)} \\
w_a^{(1)} &= N_a^{(1)} w_n \qquad w_{b,k}^{(2)} = -N_b^{(2)} w_n \quad . \\
j_a^{(1)} &= N_a^{(1)} j_n \qquad j_{b,k}^{(2)} = -N_b^{(2)} j_n
\end{aligned} \tag{7.3.19}$$

Similarly,

$$
\begin{aligned}
-D\delta G_c = \sum_{e=1}^{n_e^{(1)}} \sum_{k=1}^{n_{\text{int}}^{(e)}} W_k J_\eta^{(1)} \\
\times \Bigg(\sum_{a=1}^{m^{(1)}} \begin{bmatrix} \delta\mathbf{v}_a^{(1)} & \delta\tilde{p}_a^{(1)} & \delta\tilde{c}_a^{(1)} \end{bmatrix} \cdot \Bigg(\sum_{c=1}^{m^{(1)}} \begin{bmatrix} \mathbf{K}_{ac}^{(1,1)} & \mathbf{0} & \mathbf{0} \\ \mathbf{g}_{ac}^{(1,1)} & g_{ac}^{(1,1)} & 0 \\ \mathbf{h}_{ac}^{(1,1)} & 0 & h_{ac}^{(1,1)} \end{bmatrix} \cdot \begin{bmatrix} \Delta\mathbf{u}_c^{(1)} \\ \Delta\tilde{p}_c^{(1)} \\ \Delta\tilde{c}_c^{(1)} \end{bmatrix} \\
+ \sum_{d=1}^{m_k^{(2)}} \begin{bmatrix} \mathbf{K}_{ad,k}^{(1,2)} & \mathbf{0} & \mathbf{0} \\ \mathbf{g}_{ad,k}^{(1,2)} & g_{ad,k}^{(1,2)} & 0 \\ \mathbf{h}_{ad,k}^{(1,2)} & 0 & h_{ad,k}^{(1,2)} \end{bmatrix} \cdot \begin{bmatrix} \Delta\mathbf{u}_d^{(2)} \\ \Delta\tilde{p}_d^{(2)} \\ \Delta\tilde{c}_d^{(2)} \end{bmatrix} \Bigg) \\
+ \sum_{b=1}^{m_k^{(2)}} \begin{bmatrix} \delta\mathbf{v}_{b,k}^{(2)} & \delta\tilde{p}_{b,k}^{(2)} & \delta\tilde{c}_{b,k}^{(2)} \end{bmatrix} \cdot \Bigg(\sum_{c=1}^{m^{(1)}} \begin{bmatrix} \mathbf{K}_{bc,k}^{(2,1)} & \mathbf{0} & \mathbf{0} \\ \mathbf{g}_{bc,k}^{(2,1)} & g_{bc,k}^{(2,1)} & 0 \\ \mathbf{h}_{bc,k}^{(2,1)} & 0 & h_{bc,k}^{(2,1)} \end{bmatrix} \cdot \begin{bmatrix} \Delta\mathbf{u}_c^{(1)} \\ \Delta\tilde{p}_c^{(1)} \\ \Delta\tilde{c}_c^{(1)} \end{bmatrix} \\
+ \sum_{d=1}^{m_k^{(2)}} \begin{bmatrix} \mathbf{K}_{bd,k}^{(2,2)} & \mathbf{0} & \mathbf{0} \\ \mathbf{g}_{bd,k}^{(2,2)} & g_{bd,k}^{(2,2)} & 0 \\ \mathbf{h}_{bd,k}^{(2,2)} & 0 & h_{bd,k}^{(2,2)} \end{bmatrix} \cdot \begin{bmatrix} \Delta\mathbf{u}_d^{(2)} \\ \Delta\tilde{p}_d^{(2)} \\ \Delta\tilde{c}_d^{(2)} \end{bmatrix} \Bigg) \Bigg) \,,
\end{aligned}
\tag{7.3.20}
$$

where

$$
\begin{aligned}
\mathbf{K}_{ac}^{(1,1)} &= N_a^{(1)} \left(\varepsilon_n N_c^{(1)} \mathbf{N}^{(1)} + t_n \mathbf{A}_c^{(1)} \right) \\
\mathbf{K}_{ad,k}^{(1,2)} &= -\varepsilon_n N_a^{(1)} N_d^{(2)} \mathbf{N}^{(1)} \\
\mathbf{K}_{bc,k}^{(2,1)} &= -N_c^{(1)} \left(\varepsilon_n N_b^{(2)} \mathbf{N}^{(1)} + t_n \mathbf{M}_b^{(2)} \right) - t_n N_b^{(2)} \mathbf{A}_c^{(1)} \,, \\
\mathbf{K}_{bd,k}^{(2,2)} &= N_d^{(2)} \left(\varepsilon_n N_b^{(2)} \mathbf{N}^{(1)} + t_n \mathbf{M}_b^{(2)} \right)
\end{aligned}
\tag{7.3.21}
$$

$$
\begin{aligned}
\mathbf{g}_{ac}^{(1,1)} &= N_a^{(1)} \left(\varepsilon_p N_c^{(1)} \mathbf{p}^{(1)} - w_n \mathbf{A}_c^{(1)} \cdot \mathbf{n}^{(1)} \right) \\
\mathbf{g}_{ad,k}^{(1,2)} &= -\varepsilon_p N_a^{(1)} N_d^{(2)} \mathbf{p}^{(1)} \\
\mathbf{g}_{bc,k}^{(2,1)} &= N_c^{(1)} \left(-\varepsilon_p N_b^{(2)} \mathbf{p}^{(1)} + w_n \mathbf{m}_b^{(2)} \right) + w_n N_b^{(2)} \mathbf{A}_c^{(1)} \cdot \mathbf{n}^{(1)} \,, \\
\mathbf{g}_{bd,k}^{(2,2)} &= N_d^{(2)} \left(\varepsilon_p N_b^{(2)} \mathbf{p}^{(1)} - w_n \mathbf{m}_b^{(2)} \right)
\end{aligned}
\tag{7.3.22}
$$

$$
\begin{aligned}
g_{ac}^{(1,1)} &= -\varepsilon_p N_a^{(1)} N_c^{(1)} \\
g_{ad,k}^{(1,2)} &= \varepsilon_p N_a^{(1)} N_d^{(2)} \\
g_{bc,k}^{(2,1)} &= \varepsilon_p N_b^{(2)} N_c^{(1)} \quad , \\
g_{bd,k}^{(2,2)} &= -\varepsilon_p N_b^{(2)} N_d^{(2)}
\end{aligned}
\tag{7.3.23}
$$

$$
\begin{aligned}
\mathbf{h}_{ac}^{(1,1)} &= N_a^{(1)} \left(\varepsilon_c N_c^{(1)} \mathbf{q}^{(1)} - j_n \mathbf{A}_c^{(1)} \cdot \mathbf{n}^{(1)} \right) \\
\mathbf{h}_{ad,k}^{(1,2)} &= -\varepsilon_c N_a^{(1)} N_d^{(2)} \mathbf{q}^{(1)} \\
\mathbf{h}_{bc,k}^{(2,1)} &= N_c^{(1)} \left(-\varepsilon_c N_b^{(2)} \mathbf{q}^{(1)} + j_n \mathbf{m}_b^{(2)} \right) + j_n N_b^{(2)} \mathbf{A}_c^{(1)} \cdot \mathbf{n}^{(1)} \,, \\
\mathbf{h}_{bd,k}^{(2,2)} &= N_d^{(2)} \left(\varepsilon_c N_b^{(2)} \mathbf{q}^{(1)} - j_n \mathbf{m}_b^{(2)} \right)
\end{aligned}
\tag{7.3.24}
$$

$$\begin{aligned} h_{ac}^{(1,1)} &= -\varepsilon_c N_a^{(1)} N_c^{(1)} \\ h_{ad,k}^{(1,2)} &= \varepsilon_c N_a^{(1)} N_d^{(2)} \\ h_{bc,k}^{(2,1)} &= \varepsilon_c N_b^{(2)} N_c^{(1)} \\ h_{bd,k}^{(2,2)} &= -\varepsilon_c N_b^{(2)} N_d^{(2)} \end{aligned} \quad , \tag{7.3.25}$$

and

$$\begin{aligned} \mathbf{N}^{(1)} &= \mathbf{n}^{(1)} \otimes \mathbf{n}^{(1)} \\ \mathbf{A}_c^{(1)} &= \frac{1}{J_\eta^{(1)}} \boldsymbol{\mathcal{A}} \left\{ \frac{\partial N_c^{(1)}}{\partial \eta^1_{(1)}} \mathbf{g}_2^{(1)} - \frac{\partial N_c^{(1)}}{\partial \eta^2_{(1)}} \mathbf{g}_1^{(1)} \right\} \\ \mathbf{M}_b^{(2)} &= \mathbf{n}^{(2)} \otimes \mathbf{m}_b^{(2)} \\ \mathbf{m}_b^{(2)} &= \frac{\partial N_b^{(2)}}{\partial \eta^\alpha_{(2)}} \mathbf{g}^\alpha_{(2)} \\ \mathbf{p}^{(1)} &= \frac{\partial \tilde{p}^{(1)}}{\partial \eta^\alpha_{(1)}} \mathbf{g}^\alpha_{(1)} \\ \mathbf{q}^{(1)} &= \frac{\partial \tilde{c}^{(1)}}{\partial \eta^\alpha_{(1)}} \mathbf{g}^\alpha_{(1)} \end{aligned} \quad . \tag{7.3.26}$$

7.4 Multiphasic Contact

7.4.1 Contact Integral

See Section 2.7 for a review of multiphasic materials. The contact interface is defined between surfaces $\gamma^{(1)}$ and $\gamma^{(2)}$. Due to continuity requirements on the traction and fluxes, the external virtual work resulting from contact tractions $\mathbf{t}^{(i)}$, solvent fluxes $w_n^{(i)}$ and solute fluxes $j_n^{\alpha(i)}$ for solute α $(i = 1, 2)$, may be combined into the contact integral

$$\begin{aligned} \delta G_c = &\int_{\gamma^{(1)}} \left(\delta \mathbf{v}^{(1)} - \delta \mathbf{v}^{(2)} \right) \cdot \mathbf{t}^{(1)} \, da^{(1)} \\ &+ \int_{\gamma^{(1)}} \left(\delta \tilde{p}^{(1)} - \delta \tilde{p}^{(2)} \right) w_n^{(1)} \, da^{(1)} \\ &+ \sum_\alpha \int_{\gamma^{(1)}} \left(\delta \tilde{c}^{\alpha(1)} - \delta \tilde{c}^{\alpha(2)} \right) j_n^{\alpha(1)} \, da^{(1)} \end{aligned} \quad . \tag{7.4.1}$$

In the current implementation, only frictionless contact is taken into consideration, so that the contact traction has only a normal component, $\mathbf{t}^{(i)} = t_n \mathbf{n}^{(i)}$. To evaluate and linearize δG_c, define the covariant basis vectors on each surface as

$$\mathbf{g}_\alpha^{(i)} = \frac{\partial \mathbf{x}^{(i)}}{\partial \eta^\alpha_{(i)}}, \quad \alpha = 1, 2, \tag{7.4.2}$$

where $\mathbf{x}^{(i)}$ represents the spatial position of points on $\gamma^{(i)}$, and $\eta^\alpha_{(i)}$ represent the parametric coordinates of that point. The unit outward normal on each surface is then given by

$$\mathbf{n}^{(i)} = \frac{\mathbf{g}_1^{(i)} \times \mathbf{g}_2^{(i)}}{\left| \mathbf{g}_1^{(i)} \times \mathbf{g}_2^{(i)} \right|}. \tag{7.4.3}$$

Now the contact integral may be rewritten as

$$\begin{aligned}\delta G_c = &\int_{\gamma^{(1)}} \left(\delta\mathbf{v}^{(1)} - \delta\mathbf{v}^{(2)}\right) t_n \mathbf{g}_1^{(1)} \times \mathbf{g}_2^{(1)}\, d\eta^1_{(1)} d\eta^2_{(1)} \\ &+ \int_{\gamma^{(1)}} \left(\delta\tilde{p}^{(1)} - \delta\tilde{p}^{(2)}\right) w_n^{(1)} \left|\mathbf{g}_1^{(1)} \times \mathbf{g}_2^{(1)}\right| d\eta^1_{(1)} d\eta^2_{(1)} \\ &+ \sum_\alpha \int_{\gamma^{(1)}} \left(\delta\tilde{c}^{\alpha(1)} - \delta\tilde{c}^{\alpha(2)}\right) j_n^{\alpha(1)} \left|\mathbf{g}_1^{(1)} \times \mathbf{g}_2^{(1)}\right| d\eta^1_{(1)} d\eta^2_{(1)}\end{aligned} \quad , \tag{7.4.4}$$

and the linearization $D\delta G_c$ of δG_c has the form

$$D\delta G_c = \sum_{i=1}^{2} D\delta G_c\left[\Delta\mathbf{u}^{(i)}\right] + D\delta G_c\left[\Delta\tilde{p}^{(i)}\right] + \sum_\alpha D\delta G_c\left[\Delta\tilde{c}^{\alpha(i)}\right] . \tag{7.4.5}$$

7.4.2 Gap Function

The gap function g, representing the distance between the contact surfaces, is defined by

$$\mathbf{x}^{(2)} = \mathbf{x}^{(1)} + g\mathbf{n}^{(1)}, \quad g = \left(\mathbf{x}^{(2)} - \mathbf{x}^{(1)}\right) \cdot \mathbf{n}^{(1)} . \tag{7.4.6}$$

The linearization of variables associated with motion, pressure, and concentration, is given by

$$\begin{aligned}
D\mathbf{x}^{(1)} =& \Delta\mathbf{u}^{(1)} & D\mathbf{x}^{(2)} &= \Delta\mathbf{u}^{(2)} + \mathbf{g}_\alpha^{(2)} \Delta\eta^\alpha_{(2)} \\
D\tilde{p}^{(1)} =& \Delta\tilde{p}^{(1)} & D\tilde{p}^{(2)} &= \Delta\tilde{p}^{(2)} + \frac{\partial\tilde{p}^{(2)}}{\partial\eta^\alpha_{(2)}} \Delta\eta^\alpha_{(2)} \\
D\tilde{c}^{\gamma(1)} =& \Delta\tilde{c}^{\gamma(1)} & D\tilde{c}^{\gamma(2)} &= \Delta\tilde{c}^{\gamma(2)} + \frac{\partial\tilde{c}^{\gamma(2)}}{\partial\eta^\alpha_{(2)}} \Delta\eta^\alpha_{(2)} \\
D\delta\mathbf{v}^{(1)} =& \mathbf{0} & D\mathbf{v}^{(2)} &= \frac{\partial\delta\mathbf{v}^{(2)}}{\partial\eta^\alpha_{(2)}} \Delta\eta^\alpha_{(2)} \\
D\delta\tilde{p}^{(1)} =& 0 & D\delta\tilde{p}^{(2)} &= \frac{\partial\delta\tilde{p}^{(2)}}{\partial\eta^\alpha_{(2)}} \Delta\eta^\alpha_{(2)} \\
D\delta\tilde{c}^{\gamma(1)} =& 0 & D\delta\tilde{c}^{\gamma(2)} &= \frac{\partial\delta\tilde{c}^{\gamma(2)}}{\partial\eta^\alpha_{(2)}} \Delta\eta^\alpha_{(2)}
\end{aligned} \quad , \tag{7.4.7}$$

where

$$\Delta\eta^\alpha_{(2)} = \left(\Delta\mathbf{u}^{(1)} - \Delta\mathbf{u}^{(2)}\right) \cdot a^{\alpha\beta}\mathbf{g}_\beta^{(1)} - a^{\alpha\beta} g\mathbf{n}^{(1)} \cdot \frac{\partial\Delta\mathbf{u}^{(1)}}{\partial\eta^\beta_{(1)}} , \tag{7.4.8}$$

with $a^{\alpha\beta} = (A_{\alpha\beta})^{-1}$ and $A_{\alpha\beta} = \mathbf{g}_\alpha^{(1)} \cdot \mathbf{g}_\beta^{(2)}$.

7.4.3 Penalty Method

Let the normal component of the contact traction be described by the penalty function,

$$t_n = \begin{cases} \varepsilon_n g & g < 0 \\ 0 & g \geqslant 0 \end{cases} , \tag{7.4.9}$$

where ε_n is a penalty factor associated with t_n. Similarly, let

$$\begin{cases} w_n = \varepsilon_p \pi = \varepsilon_p \left(\tilde{p}^{(1)} - \tilde{p}^{(2)} \right) & t_n < 0 \\ \tilde{p}^{(i)} = \tilde{p}^* & t_n = 0 \end{cases}, \tag{7.4.10}$$

and

$$\begin{cases} j_n^\alpha = \varepsilon_c \chi^\alpha = \varepsilon_c \left(\tilde{c}^{\alpha(1)} - \tilde{c}^{\alpha(2)} \right) & t_n < 0 \\ \tilde{c}^{\alpha(i)} = \tilde{c}^{\alpha *} & t_n = 0 \end{cases}, \tag{7.4.11}$$

where ε_p and ε_c are penalty factors associated with $w_n \equiv w_n^{(1)}$ and $j_n^\alpha \equiv j_n^{\alpha(1)}$, respectively. It follows that

$$\begin{aligned} Dt_n &= \varepsilon_n \left(\Delta \mathbf{u}^{(2)} - \Delta \mathbf{u}^{(1)} + \mathbf{g}_\alpha^{(2)} \Delta \eta_{(2)}^\alpha \right) \cdot \mathbf{n}^{(1)} \\ Dw_n &= \varepsilon_p \left(\Delta \tilde{p}^{(1)} - \Delta \tilde{p}^{(2)} - \frac{\partial \tilde{p}^{(2)}}{\partial \eta_{(2)}^\alpha} \Delta \eta_{(2)}^\alpha \right) \\ Dj_n^\gamma &= \varepsilon_c \left(\Delta \tilde{c}^{\gamma(1)} - \Delta \tilde{c}^{\gamma(2)} - \frac{\partial \tilde{c}^{\gamma(2)}}{\partial \eta_{(2)}^\alpha} \Delta \eta_{(2)}^\alpha \right) \end{aligned} . \tag{7.4.12}$$

Given these relations, it can be shown that the directional derivatives of the various terms appearing in the integrand of δG_c are

$$\begin{aligned} &- D \left(t_n \left(\delta \mathbf{v}^{(1)} - \delta \mathbf{v}^{(2)} \right) \cdot \mathbf{g}_1^{(1)} \times \mathbf{g}_2^{(1)} \right) = \\ &J_\eta^{(1)} \varepsilon_n \left(\delta \mathbf{v}^{(1)} - \delta \mathbf{v}^{(2)} \right) \cdot \left(\mathbf{n}^{(1)} \otimes \mathbf{n}^{(1)} \right) \cdot \left(\Delta \mathbf{u}^{(1)} - \Delta \mathbf{u}^{(2)} \right) \\ &- J_\eta^{(1)} t_n \frac{\partial \delta \mathbf{v}^{(2)}}{\partial \eta_{(2)}^\alpha} \cdot \left(\mathbf{n}^{(2)} \otimes \mathbf{g}_{(2)}^\alpha \right) \cdot \left(\Delta \mathbf{u}^{(1)} - \Delta \mathbf{u}^{(2)} \right) \\ &+ t_n \left(\delta \mathbf{v}^{(1)} - \delta \mathbf{v}^{(2)} \right) \cdot \left(\mathbf{g}_2^{(1)} \times \frac{\partial \Delta \mathbf{u}^{(1)}}{\partial \eta_{(1)}^1} - \mathbf{g}_1^{(1)} \times \frac{\partial \Delta \mathbf{u}^{(1)}}{\partial \eta_{(1)}^2} \right) \end{aligned} , \tag{7.4.13}$$

$$\begin{aligned} &- D \left(w_n \left(\delta \tilde{p}^{(1)} - \delta \tilde{p}^{(2)} \right) \left| \mathbf{g}_1^{(1)} \times \mathbf{g}_2^{(1)} \right| \right) = \\ &- J_\eta^{(1)} \varepsilon_p \left(\delta \tilde{p}^{(1)} - \delta \tilde{p}^{(2)} \right) \left(\Delta \tilde{p}^{(1)} - \Delta \tilde{p}^{(2)} \right) \\ &+ J_\eta^{(1)} \left[\varepsilon_p \left(\delta \tilde{p}^{(1)} - \delta \tilde{p}^{(2)} \right) \frac{\partial \tilde{p}^{(1)}}{\partial \eta_{(1)}^\alpha} \mathbf{g}_{(1)}^\alpha + w_n \frac{\partial \delta \tilde{p}^{(2)}}{\partial \eta_{(2)}^\alpha} \mathbf{g}_{(2)}^\alpha \right] \cdot \left(\Delta \mathbf{u}^{(1)} - \Delta \mathbf{u}^{(2)} \right) , \\ &+ w_n \left(\delta \tilde{p}^{(1)} - \delta \tilde{p}^{(2)} \right) \mathbf{n}^{(1)} \cdot \left(\mathbf{g}_2^{(1)} \times \frac{\partial \Delta \mathbf{u}^{(1)}}{\partial \eta_{(1)}^1} - \mathbf{g}_1^{(1)} \times \frac{\partial \Delta \mathbf{u}^{(1)}}{\partial \eta_{(1)}^2} \right) \end{aligned} \tag{7.4.14}$$

$$\begin{aligned} &- D \left(j_n^\gamma \left(\delta \tilde{c}^{\gamma(1)} - \delta \tilde{c}^{\gamma(2)} \right) \left| \mathbf{g}_1^{(1)} \times \mathbf{g}_2^{(1)} \right| \right) = \\ &- J_\eta^{(1)} \varepsilon_c \left(\delta \tilde{c}^{\gamma(1)} - \delta \tilde{c}^{\gamma(2)} \right) \left(\Delta \tilde{c}^{\gamma(1)} - \Delta \tilde{c}^{\gamma(2)} \right) \\ &+ J_\eta^{(1)} \varepsilon_c \left(\delta \tilde{c}^{\gamma(1)} - \delta \tilde{c}^{\gamma(2)} \right) \frac{\partial \tilde{c}^{\gamma(1)}}{\partial \eta_{(1)}^\alpha} \mathbf{g}_\alpha^{(1)} \cdot \left(\Delta \mathbf{u}^{(1)} - \Delta \mathbf{u}^{(2)} \right) \\ &+ J_\eta^{(1)} j_n^\gamma \frac{\partial \delta \tilde{c}^{\gamma(1)}}{\partial \eta_{(1)}^\alpha} \mathbf{g}_\alpha^{(1)} \cdot \left(\Delta \mathbf{u}^{(1)} - \Delta \mathbf{u}^{(2)} \right) \\ &+ j_n^\gamma \left(\delta \tilde{c}^{\gamma(1)} - \delta \tilde{c}^{\gamma(2)} \right) \mathbf{n}^{(1)} \cdot \left(\mathbf{g}_2^{(1)} \times \frac{\partial \Delta \mathbf{u}^{(1)}}{\partial \eta_{(1)}^1} - \mathbf{g}_1^{(1)} \times \frac{\partial \Delta \mathbf{u}^{(1)}}{\partial \eta_{(1)}^2} \right) \end{aligned} \tag{7.4.15}$$

where $J_\eta^{(1)} = \left|\mathbf{g}_1^{(1)} \times \mathbf{g}_2^{(1)}\right|$.

7.4.4 Discretization

The contact integral may be discretized as

$$\delta G_c = \sum_{e=1}^{n_e^{(1)}} \sum_{k=1}^{n_{\text{int}}^{(e)}} W_k J_\eta^{(1)} \left[t_n \left(\delta \mathbf{v}^{(1)} - \delta \mathbf{v}^{(2)} \right) \cdot \mathbf{n}^{(1)} + w_n \left(\delta \tilde{p}^{(1)} - \delta \tilde{p}^{(2)} \right) + \sum_\gamma j_n^\gamma \left(\delta \tilde{c}^{\gamma(1)} - \delta \tilde{c}^{\gamma(2)} \right) \right] . \tag{7.4.16}$$

The variables may be interpolated over each element face according to

$$\begin{aligned}
\delta \mathbf{v}^{(1)} &= \sum_{a=1}^{m^{(1)}} N_a^{(1)} \delta \mathbf{v}_a^{(1)} & \delta \mathbf{v}^{(2)} &= \sum_{b=1}^{m^{(2)}} N_b^{(2)} \delta \mathbf{v}_b^{(2)} \\
\Delta \mathbf{u}^{(1)} &= \sum_{c=1}^{m^{(1)}} N_c^{(1)} \Delta \mathbf{u}_c^{(1)} & \Delta \mathbf{u}^{(2)} &= \sum_{d=1}^{m^{(2)}} N_d^{(2)} \Delta \mathbf{u}_d^{(2)} \\
\delta \tilde{p}^{(1)} &= \sum_{a=1}^{m^{(1)}} N_a^{(1)} \delta \tilde{p}_a^{(1)} & \delta \tilde{p}^{(2)} &= \sum_{b=1}^{m^{(2)}} N_b^{(2)} \delta \tilde{p}_b^{(2)} \\
\Delta \tilde{p}^{(1)} &= \sum_{c=1}^{m^{(1)}} N_c^{(1)} \Delta \tilde{p}_c^{(1)} & \Delta \tilde{p}^{(2)} &= \sum_{d=1}^{m^{(2)}} N_d^{(2)} \Delta \tilde{p}_d^{(2)} \\
\delta \tilde{c}^{\gamma(1)} &= \sum_{a=1}^{m^{(1)}} N_a^{(1)} \delta \tilde{c}_a^{\gamma(1)} & \delta \tilde{c}^{\gamma(2)} &= \sum_{b=1}^{m^{(2)}} N_b^{(2)} \delta \tilde{c}_b^{\gamma(2)} \\
\Delta \tilde{c}^{\gamma(1)} &= \sum_{c=1}^{m^{(1)}} N_c^{(1)} \Delta \tilde{c}_c^{\gamma(1)} & \Delta \tilde{c}^{\gamma(2)} &= \sum_{d=1}^{m^{(2)}} N_d^{(2)} \Delta \tilde{c}_d^{\gamma(2)}
\end{aligned} \quad . \tag{7.4.17}$$

Then,

$$\begin{aligned}
\delta G_c = \sum_{e=1}^{n_e^{(1)}} \sum_{k=1}^{n_{\text{int}}^{(e)}} W_k J_\eta^{(1)} \Bigg(& \sum_{a=1}^{m^{(1)}} \left[\begin{array}{cccc} \delta \mathbf{v}_a^{(1)} & \delta \tilde{p}_a^{(1)} & \delta \tilde{c}_a^{\alpha(1)} & \delta \tilde{c}_a^{\beta(1)} \end{array} \right] \cdot \left[\begin{array}{c} \mathbf{f}_a^{(1)} \\ w_a^{(1)} \\ j_a^{\alpha(1)} \\ j_a^{\beta(1)} \end{array} \right] \\
& + \sum_{b=1}^{m^{(2)}} \left[\begin{array}{cccc} \delta \mathbf{v}_b^{(2)} & \delta \tilde{p}_b^{(2)} & \delta \tilde{c}_b^{\alpha(2)} & \delta \tilde{c}_b^{\beta(2)} \end{array} \right] \cdot \left[\begin{array}{c} \mathbf{f}_{b,k}^{(2)} \\ w_{b,k}^{(2)} \\ j_{b,k}^{\alpha(2)} \\ j_{b,k}^{\beta(2)} \end{array} \right] \Bigg) ,
\end{aligned} \tag{7.4.18}$$

where

$$\begin{aligned}
\mathbf{f}_a^{(1)} &= t_n N_a^{(1)} \mathbf{n}^{(1)} & \mathbf{f}_{b,k}^{(2)} &= -t_n N_b^{(2)} \mathbf{n}^{(1)} \\
w_a^{(1)} &= w_n N_a^{(1)} & w_{b,k}^{(2)} &= -w_n N_b^{(2)} \\
j_a^{\gamma(1)} &= j_n^\gamma N_a^{(1)} & j_{b,k}^{\gamma(2)} &= -j_n^\gamma N_b^{(2)}
\end{aligned} \quad . \tag{7.4.19}$$

Similarly,

$$
\begin{aligned}
-D\delta G_c = \sum_{e=1}^{n_e^{(1)}} \sum_{k=1}^{n_{\text{int}}^{(e)}} W_k J_\eta^{(1)} \times \Bigg(& \sum_{a=1}^{m^{(1)}} \left[\begin{array}{cccc} \delta \mathbf{v}_a^{(1)} & \delta \tilde{p}_a^{(1)} & \delta \tilde{c}_a^{\alpha(1)} & \delta \tilde{c}_a^{\beta(1)} \end{array} \right] \cdot \\
& \Bigg(\sum_{c=1}^{m^{(1)}} \left[\begin{array}{cccc} \mathbf{K}_{ac}^{(1,1)} & 0 & 0 & 0 \\ \mathbf{g}_{ac}^{(1,1)} & g_{ac}^{(1,1)} & 0 & 0 \\ \mathbf{h}_{ac}^{\alpha(1,1)} & 0 & h_{ac}^{\alpha\alpha(1,1)} & 0 \\ \mathbf{h}_{ac}^{\beta(1,1)} & 0 & 0 & h_{ac}^{\beta\beta(1,1)} \end{array} \right] \cdot \left[\begin{array}{c} \Delta \mathbf{u}_c^{(1)} \\ \Delta \tilde{p}_c^{(1)} \\ \Delta \tilde{c}_c^{\alpha(1)} \\ \Delta \tilde{c}_c^{\beta(1)} \end{array} \right] \\
& + \sum_{d=1}^{m_k^{(2)}} \left[\begin{array}{cccc} \mathbf{K}_{ad,k}^{(1,2)} & 0 & 0 & 0 \\ \mathbf{g}_{ad,k}^{(1,2)} & g_{ad,k}^{(1,2)} & 0 & 0 \\ \mathbf{h}_{ad,k}^{\alpha(1,2)} & 0 & h_{ad,k}^{\alpha\alpha(1,2)} & 0 \\ \mathbf{h}_{ad,k}^{\beta(1,2)} & 0 & 0 & h_{ad,k}^{\beta\beta(1,2)} \end{array} \right] \cdot \left[\begin{array}{c} \Delta \mathbf{u}_d^{(2)} \\ \Delta \tilde{p}_d^{(2)} \\ \Delta \tilde{c}_d^{\alpha(2)} \\ \Delta \tilde{c}_d^{\beta(2)} \end{array} \right] \Bigg) \\
& + \sum_{b=1}^{m_k^{(2)}} \left[\begin{array}{cccc} \delta \mathbf{v}_{b,k}^{(2)} & \delta \tilde{p}_{b,k}^{(2)} & \delta \tilde{c}_{b,k}^{\alpha(2)} & \delta \tilde{c}_{b,k}^{\beta(2)} \end{array} \right] \cdot \\
& \Bigg(\sum_{c=1}^{m^{(1)}} \left[\begin{array}{cccc} \mathbf{K}_{bc,k}^{(2,1)} & 0 & 0 & 0 \\ \mathbf{g}_{bc,k}^{(2,1)} & g_{bc,k}^{(2,1)} & 0 & 0 \\ \mathbf{h}_{bc,k}^{\alpha(2,1)} & 0 & h_{bc,k}^{\alpha\alpha(2,1)} & 0 \\ \mathbf{h}_{bc,k}^{\beta(2,1)} & 0 & 0 & h_{bc,k}^{\beta\beta(2,1)} \end{array} \right] \cdot \left[\begin{array}{c} \Delta \mathbf{u}_c^{(1)} \\ \Delta \tilde{p}_c^{(1)} \\ \Delta \tilde{c}_c^{\alpha(1)} \\ \Delta \tilde{c}_c^{\beta(1)} \end{array} \right] \\
& + \sum_{d=1}^{m_k^{(2)}} \left[\begin{array}{cccc} \mathbf{K}_{bd,k}^{(2,2)} & 0 & 0 & 0 \\ \mathbf{g}_{bd,k}^{(2,2)} & g_{bd,k}^{(2,2)} & 0 & 0 \\ \mathbf{h}_{bd,k}^{\alpha(2,2)} & 0 & h_{bd,k}^{\alpha\alpha(2,2)} & 0 \\ \mathbf{h}_{bd,k}^{\beta(2,2)} & 0 & 0 & h_{bd,k}^{\beta\beta(2,2)} \end{array} \right] \cdot \left[\begin{array}{c} \Delta \mathbf{u}_d^{(2)} \\ \Delta \tilde{p}_d^{(2)} \\ \Delta \tilde{c}_d^{\alpha(2)} \\ \Delta \tilde{c}_d^{\beta(2)} \end{array} \right] \Bigg) \Bigg) \Bigg) ,
\end{aligned}
\tag{7.4.20}
$$

where

$$
\begin{aligned}
\mathbf{K}_{ac}^{(1,1)} &= N_a^{(1)} \left(\varepsilon_n N_c^{(1)} \mathbf{N}^{(1)} + t_n \mathbf{A}_c^{(1)} \right) \\
\mathbf{K}_{ad,k}^{(1,2)} &= -\varepsilon_n N_a^{(1)} N_d^{(2)} \mathbf{N}^{(1)} \\
\mathbf{K}_{bc,k}^{(2,1)} &= -N_c^{(1)} \left(\varepsilon_n N_b^{(2)} \mathbf{N}^{(1)} + t_n \mathbf{M}_b^{(2)} \right) - t_n N_b^{(2)} \mathbf{A}_c^{(1)} , \\
\mathbf{K}_{bd,k}^{(2,2)} &= N_d^{(2)} \left(\varepsilon_n N_b^{(2)} \mathbf{N}^{(1)} + t_n \mathbf{M}_b^{(2)} \right)
\end{aligned}
\tag{7.4.21}
$$

$$
\begin{aligned}
\mathbf{g}_{ac}^{(1,1)} &= N_a^{(1)} \left(\varepsilon_p N_c^{(1)} \mathbf{p}^{(1)} - w_n \mathbf{A}_c^{(1)} \cdot \mathbf{n}^{(1)} \right) \\
\mathbf{g}_{ad,k}^{(1,2)} &= -\varepsilon_p N_a^{(1)} N_d^{(2)} \mathbf{p}^{(1)} \\
\mathbf{g}_{bc,k}^{(2,1)} &= N_c^{(1)} \left(-\varepsilon_p N_b^{(2)} \mathbf{p}^{(1)} + w_n \mathbf{m}_b^{(2)} \right) + w_n N_b^{(2)} \mathbf{A}_c^{(1)} \cdot \mathbf{n}^{(1)} , \\
\mathbf{g}_{bd,k}^{(2,2)} &= N_d^{(2)} \left(\varepsilon_p N_b^{(2)} \mathbf{p}^{(1)} - w_n \mathbf{m}_b^{(2)} \right)
\end{aligned}
\tag{7.4.22}
$$

$$
\begin{aligned}
g_{ac}^{(1,1)} &= -\varepsilon_p N_a^{(1)} N_c^{(1)} \quad g_{ad,k}^{(1,2)} = \varepsilon_p N_a^{(1)} N_d^{(2)} \\
g_{bc,k}^{(2,1)} &= \varepsilon_p N_b^{(2)} N_c^{(1)} \quad\quad g_{bd,k}^{(2,2)} = -\varepsilon_p N_b^{(2)} N_d^{(2)} ,
\end{aligned}
\tag{7.4.23}
$$

$$\begin{aligned}
\mathbf{h}_{ac}^{\gamma(1,1)} &= N_a^{(1)}\left(N_c^{(1)}\varepsilon_c\mathbf{q}^{\gamma(1)} - \mathbf{A}_c^{(1)}\cdot j_n^{\gamma}\mathbf{n}^{(1)}\right)\\
\mathbf{h}_{ad,k}^{\gamma(1,2)} &= -N_a^{(1)}N_d^{(2)}\varepsilon_c\mathbf{q}^{\gamma(1)}\\
\mathbf{h}_{bc,k}^{\gamma(2,1)} &= N_b^{(2)}\left(-N_c^{(1)}\varepsilon_c\mathbf{q}^{\gamma(1)} + \mathbf{A}_c^{(1)}\cdot j_n^{\gamma}\mathbf{n}^{(1)}\right) + N_c^{(1)}j_n^{\gamma}\mathbf{m}_b^{(2)}\\
\mathbf{h}_{bd,k}^{\gamma(2,2)} &= N_b^{(2)}N_d^{(2)}\varepsilon_c\mathbf{q}^{\gamma(1)} - N_d^{(2)}j_n^{\gamma}\mathbf{m}_b^{(2)}
\end{aligned}, \tag{7.4.24}$$

$$\begin{aligned}
h_{ac}^{\gamma\gamma(1,1)} &= -\varepsilon_c N_a^{(1)}N_c^{(1)}\\
h_{ad,k}^{\gamma\gamma(1,2)} &= \varepsilon_c N_a^{(1)}N_d^{(2)}\\
h_{bc,k}^{\gamma\gamma(2,1)} &= \varepsilon_c N_b^{(2)}N_c^{(1)}\\
h_{bd,k}^{\gamma\gamma(2,2)} &= -\varepsilon_c N_b^{(2)}N_d^{(2)}
\end{aligned}, \tag{7.4.25}$$

and

$$\begin{aligned}
\mathbf{N}^{(1)} &= \mathbf{n}^{(1)}\otimes\mathbf{n}^{(1)} \qquad \mathbf{A}_c^{(1)} = \frac{1}{J_\eta^{(1)}}\boldsymbol{\mathcal{A}}\left\{\frac{\partial N_c^{(1)}}{\partial\eta_{(1)}^1}\mathbf{g}_2^{(1)} - \frac{\partial N_c^{(1)}}{\partial\eta_{(1)}^2}\mathbf{g}_1^{(1)}\right\}\\
\mathbf{M}_b^{(2)} &= \mathbf{n}^{(2)}\otimes\mathbf{m}_b^{(2)} \quad \mathbf{m}_b^{(2)} = \frac{\partial N_b^{(2)}}{\partial\eta_{(2)}^{\alpha}}\mathbf{g}_{(2)}^{\alpha}\\
\mathbf{p}^{(1)} &= \frac{\partial\tilde{p}^{(1)}}{\partial\eta_{(1)}^{\alpha}}\mathbf{g}_{(1)}^{\alpha} \qquad \mathbf{q}^{\gamma(1)} = \frac{\partial\tilde{c}^{\gamma(1)}}{\partial\eta_{(1)}^{\alpha}}\mathbf{g}_{(1)}^{\alpha}
\end{aligned}. \tag{7.4.26}$$

7.5 Tied Contact

In some situations it is useful to connect two non-conforming meshes together. This can be done by defining a tied contact interface. In FEBio, the tied contact works very similar to the sliding contact interface. We need to define a slave surface and a master surface, where it is assumed that the slave surface nodes will be tied to the master surface faces.

7.5.1 Gap Function

Just as in sliding contact, we need to define a gap function that measures the distance between the slave and master surface. In order to do that, we first define the projection of a slave node to the master surface.

$$\bar{\mathbf{Y}}\left(\mathbf{X}\right) = \arg\min_{\mathbf{Y}\in\Gamma^{(2)}}\left\|\mathbf{X}-\mathbf{Y}\right\|. \tag{7.5.1}$$

This definition is similar to that of the sliding interface, except that now the projection is done in the material reference frame. This implies that the projection only needs to be calculated once, at the beginning of the analysis. We can now proceed to the definition of the gap function.

$$\mathbf{g}\left(\mathbf{X}\right) = \boldsymbol{\varphi}^{(1)}\left(\mathbf{X}\right) - \boldsymbol{\varphi}^{(2)}\left(\bar{\mathbf{Y}}\left(\mathbf{X}\right)\right). \tag{7.5.2}$$

An important observation is that the gap function is now a vector quantity since the gap needs to be closed in all direction, not just the normal direction as is the case in sliding contact.

7.5.2 Tied Contact Integral

With the definition of the gap function at hand (equation (7.5.2)), we can define the contribution to the virtual work equation from the tied contact reaction forces.

$$W_t = \int_{\Gamma_c} \mathbf{T} \cdot \delta\mathbf{g}\, d\Gamma\,. \tag{7.5.3}$$

Here, $\mathbf{T}$ is the reaction force that enforces the constraint $\mathbf{g}(\mathbf{X}) = 0$. Since we anticipate the use of an augmented Lagrangian formalism, we can write this reaction force as follows,

$$\mathbf{T} = \boldsymbol{\lambda} + \varepsilon\mathbf{g}\,. \tag{7.5.4}$$

The vector quantity $\boldsymbol{\lambda}$ is the Lagrangian multiplier and ε is a penalty factor.

7.5.3 Linearization of the Contact Integral

Since equation (7.5.3) is nonlinear we need to calculate the linearization. For tied contact, this is simply given by the following equation.

$$\Delta W_t = \int_{\Gamma_c} \varepsilon\Delta\mathbf{g} \cdot \delta\mathbf{g}\, d\Gamma\,. \tag{7.5.5}$$

Where

$$\delta\mathbf{g} = \mathbf{w}^{(1)} - \mathbf{w}^{(2)} \tag{7.5.6}$$

and

$$\Delta\mathbf{g} = \Delta\boldsymbol{\varphi}^{(1)}(\mathbf{X}) - \Delta\boldsymbol{\varphi}^{(2)}\left(\bar{\mathbf{Y}}(\mathbf{X})\right)\,. \tag{7.5.7}$$

We also introduced the notation $\mathbf{w}^{(i)} = \delta\boldsymbol{\varphi}^{(i)}$.

The discretization of (7.5.5) will lead to a contribution to the stiffness matrix. Notice that due to symmetry between $\delta\mathbf{g}$ and$\Delta\mathbf{g}$ this matrix will be symmetric.

7.5.4 Discretization

The contact integral (7.5.3) can be discretized as follows. First, we split the integration over all the slave surface elements.

$$W_t = \sum_{e=1}^{nel} \int_{\Gamma_c^{(e)}} \mathbf{T} \cdot \delta\mathbf{g}\, d\Gamma^{(e)}\,. \tag{7.5.8}$$

The integration can be approximated by a quadrature rule,

$$W_t = \sum_{e=1}^{nel} \sum_{i=1}^{N_{int}^{(e)}} w^i j(\xi_i)\, \mathbf{T}(\xi_i) \cdot \delta\mathbf{g}(\xi_i)\,. \tag{7.5.9}$$

If we use a nodally integrated elements, we have

$$\begin{aligned} \mathbf{w}^{(1)}(\xi_i) &= \mathbf{c}_i^{(1)}\,, \\ \mathbf{w}^{(2)}(\xi_i) &= \sum_j N_j\left(\bar{\xi}_i\right)\mathbf{c}_j^{(2)}\,, \end{aligned} \tag{7.5.10}$$

so that,

$$\delta \mathbf{g}\left(\xi_i\right) = \mathbf{c}_i^{(1)} - \sum_j N_j\left(\bar{\xi}_i\right)\mathbf{c}_j^{(2)}\,. \tag{7.5.11}$$

We can now write the contact integral (7.5.8) in its final form,

$$W_t = \sum_{e=1}^{nel}\sum_{i=1}^{N_{int}^{(e)}} w^i j\left(\xi_i\right)\left(\mathbf{N}\left(\xi_i\right)\mathbf{T}\left(\xi_i\right)\right)\cdot\delta\mathbf{\Phi}\,, \tag{7.5.12}$$

where

$$\delta\mathbf{\Phi}^T\left(\xi_i\right) = \left[\begin{array}{cccc}\mathbf{c}_i^{(1)} & \mathbf{c}_1^{(2)} & \mathbf{c}_2^{(2)} & \cdots & \mathbf{c}_n^{(2)}\end{array}\right], \tag{7.5.13}$$

$$\mathbf{N}\left(\xi_i\right) = \left[\begin{array}{cccc}\mathbf{I} & -\mathbf{N}_1 & \cdots & -\mathbf{N}_n\end{array}\right], \tag{7.5.14}$$

and

$$\mathbf{N}_i = \left[\begin{array}{ccc}N_i & 0 & 0\\ 0 & N_i & 0\\ 0 & 0 & N_i\end{array}\right]. \tag{7.5.15}$$

For the linearized tied contact integral (7.5.5), a similar discretization procedure leads to,

$$\Delta W_t = \sum_{e=1}^{nel}\sum_{i=1}^{N_{int}^{(e)}} w^i j\left(\xi_i\right)\Delta\mathbf{\Phi}\cdot\mathbf{K}_c\delta\mathbf{\Phi}\,, \tag{7.5.16}$$

where

$$\mathbf{K}_c = \varepsilon\mathbf{N}^T\mathbf{N}\,. \tag{7.5.17}$$

7.6 Tied Biphasic Contact

7.6.1 Contact Integral

See Section 2.5 for a review of biphasic materials, and [11] for additional details on biphasic contact. The contact interface is defined between surfaces $\gamma^{(1)}$ and $\gamma^{(2)}$. Due to continuity requirements on the traction and fluxes, the external virtual work resulting from contact tractions $\mathbf{t}^{(i)}$ and solvent fluxes $w_n^{(i)}$ $(i = 1, 2)$ may be combined into the contact integral

$$\begin{aligned}\delta G_c = &\int_{\gamma^{(1)}}\left(\delta\mathbf{v}^{(1)} - \delta\mathbf{v}^{(2)}\right)\cdot\mathbf{t}^{(1)}da^{(1)}\\ &+\int_{\gamma^{(1)}}\left(\delta p^{(1)} - \delta p^{(2)}\right)w_n^{(1)}da^{(1)}\,.\end{aligned} \tag{7.6.1}$$

To evaluate and linearize δG_c, define the covariant basis vectors on each surface as

$$\mathbf{g}_\alpha^{(i)} = \frac{\partial\mathbf{x}^{(i)}}{\partial\eta_{(i)}^\alpha}, \quad \alpha = 1, 2, \tag{7.6.2}$$

where $\mathbf{x}^{(i)}$ represents the spatial position of points on $\gamma^{(i)}$, and $\eta_{(i)}^\alpha$ represent the parametric coordinates of that point. The unit outward normal on each surface is then given by

$$\mathbf{n}^{(i)} = \frac{\mathbf{g}_1^{(i)}\times\mathbf{g}_2^{(i)}}{\left|\mathbf{g}_1^{(i)}\times\mathbf{g}_2^{(i)}\right|}\,. \tag{7.6.3}$$

Now the contact integral may be rewritten as

$$\begin{aligned}\delta G_c = &\int_{\gamma^{(1)}} \left(\delta\mathbf{v}^{(1)} - \delta\mathbf{v}^{(2)}\right)\cdot\mathbf{t}\left|\mathbf{g}_1^{(1)}\times\mathbf{g}_2^{(1)}\right| d\eta^1_{(1)}d\eta^2_{(1)} \\ &+ \int_{\gamma^{(1)}} \left(\delta p^{(1)} - \delta p^{(2)}\right) w_n \left|\mathbf{g}_1^{(1)}\times\mathbf{g}_2^{(1)}\right| d\eta^1_{(1)}d\eta^2_{(1)}\end{aligned}\,, \tag{7.6.4}$$

where $\mathbf{t}\equiv\mathbf{t}^{(1)}$ and $w_n\equiv w_n^{(1)}$. The linearization $D\delta G_c$ of δG_c has the form

$$D\delta G_c = \sum_{i=1}^{2} D\delta G_c\left[\Delta\mathbf{u}^{(i)}\right] + D\delta G_c\left[\Delta p^{(i)}\right]\,. \tag{7.6.5}$$

7.6.2 Gap Function

The vector gap function $\mathbf{g}$, representing the distance between the contact surfaces, is defined by

$$\mathbf{g} = \mathbf{x}^{(2)} - \mathbf{x}^{(1)}\,. \tag{7.6.6}$$

The premise of a tied interface is that the parametric coordinates of $\mathbf{x}^{(1)}$ and $\mathbf{x}^{(2)}$ are both invariants (i.e., they are determined in the reference configuration and remain unchanged over time). The parametric coordinates of $\mathbf{x}^{(1)}$ correspond to the integration points on $\gamma^{(1)}$, and those of $\mathbf{x}^{(2)}$ are evaluated once, in the reference configuration, by shooting a ray from the integration point on $\gamma^{(1)}$ to intersect $\gamma^{(2)}$. It follows from this premise that

$$\begin{aligned} D\mathbf{x}^{(1)} &= \Delta\mathbf{u}^{(1)} & D\mathbf{x}^{(2)} &= \Delta\mathbf{u}^{(2)} \\ Dp^{(1)} &= \Delta p^{(1)} & Dp^{(2)} &= \Delta p^{(2)} \\ D\delta\mathbf{v}^{(1)} &= \mathbf{0} & D\delta\mathbf{v}^{(2)} &= \mathbf{0} \\ D\delta p^{(1)} &= 0 & D\delta p^{(2)} &= 0 \end{aligned}\,. \tag{7.6.7}$$

If $\gamma^{(1)}$ and $\gamma^{(2)}$ are not initially conforming, continuity of fluid pressure and normal flux will only be enforced within the contact interface; unlike the sliding biphasic contact interface (Section 7.2), free-draining conditions are not set automatically on regions of $\gamma^{(1)}$ and $\gamma^{(2)}$ where a solution for $\mathbf{g}$ was not found. Therefore, these regions naturally enforce zero fluid flux (impermeable boundary), unless an explicit boundary condition on the pressure p is prescribed over those regions.

7.6.3 Penalty Method

Let the tied contact traction be described by the penalty function,

$$\mathbf{t} = \varepsilon_n\mathbf{g}\,, \tag{7.6.8}$$

where ε_n is a penalty factor associated with $\mathbf{t}$. Similarly, let

$$w_n = \varepsilon_p\pi = \varepsilon_p\left(p^{(1)} - p^{(2)}\right)\,, \tag{7.6.9}$$

where ε_p is a penalty factor associated with w_n. It follows that

$$\begin{aligned} D\mathbf{t} &= \varepsilon_n\left(\Delta\mathbf{u}^{(2)} - \Delta\mathbf{u}^{(1)}\right)\,, \\ Dw_n &= \varepsilon_p\left(\Delta p^{(1)} - \Delta p^{(2)}\right)\,. \end{aligned} \tag{7.6.10}$$

Given these relations, it can be shown that the directional derivatives of the various terms appearing in the integrand of δG_c are

$$\begin{aligned}
&-D\left(J_\eta^{(1)}\left(\delta\mathbf{v}^{(1)}-\delta\mathbf{v}^{(2)}\right)\cdot\mathbf{t}\right)= \\
&\left(\delta\mathbf{v}^{(1)}-\delta\mathbf{v}^{(2)}\right)\cdot\varepsilon_n J_\eta^{(1)}\mathbf{I}\cdot\left(\Delta\mathbf{u}^{(1)}-\Delta\mathbf{u}^{(2)}\right) \\
&+\left(\delta\mathbf{v}^{(1)}-\delta\mathbf{v}^{(2)}\right)\cdot\mathbf{t}\otimes\left[\left(\mathbf{g}_1^{(1)}\times\mathbf{n}^{(1)}\right)\cdot\frac{\partial\Delta\mathbf{u}^{(1)}}{\partial\eta^2_{(1)}}-\left(\mathbf{g}_2^{(1)}\times\mathbf{n}^{(1)}\right)\cdot\frac{\partial\Delta\mathbf{u}^{(1)}}{\partial\eta^1_{(1)}}\right]
\end{aligned}, \tag{7.6.11}$$

$$\begin{aligned}
&-D\left(w_n\left(\delta p^{(1)}-\delta p^{(2)}\right)J_\eta^{(1)}\right)= \\
&-J_\eta^{(1)}\varepsilon_p\left(\delta p^{(1)}-\delta p^{(2)}\right)\left(\Delta p^{(1)}-\Delta p^{(2)}\right) \\
&+w_n\left(\delta p^{(1)}-\delta p^{(2)}\right)\mathbf{n}^{(1)}\cdot\left(\mathbf{g}_2^{(1)}\times\frac{\partial\Delta\mathbf{u}^{(1)}}{\partial\eta^1_{(1)}}-\mathbf{g}_1^{(1)}\times\frac{\partial\Delta\mathbf{u}^{(1)}}{\partial\eta^2_{(1)}}\right)
\end{aligned}, \tag{7.6.12}$$

where $J_\eta^{(1)}=\left|\mathbf{g}_1^{(1)}\times\mathbf{g}_2^{(1)}\right|$.

7.6.4 Discretization

The contact integral may be discretized as

$$\delta G_c=\sum_{e=1}^{n_e^{(1)}}\sum_{k=1}^{n_{\text{int}}^{(e)}}W_k J_\eta^{(1)}\left[\left(\delta\mathbf{v}^{(1)}-\delta\mathbf{v}^{(2)}\right)\cdot\mathbf{t}+w_n\left(\delta p^{(1)}-\delta p^{(2)}\right)\right]. \tag{7.6.13}$$

The variables may be interpolated over each element face according to

$$\begin{aligned}
\delta\mathbf{v}^{(1)}&=\sum_{a=1}^{m^{(1)}}N_a^{(1)}\delta\mathbf{v}_a^{(1)} & \delta\mathbf{v}^{(2)}&=\sum_{b=1}^{m^{(2)}}N_b^{(2)}\delta\mathbf{v}_b^{(2)} \\
\Delta\mathbf{u}^{(1)}&=\sum_{c=1}^{m^{(1)}}N_c^{(1)}\Delta\mathbf{u}_c^{(1)} & \Delta\mathbf{u}^{(2)}&=\sum_{d=1}^{m^{(2)}}N_d^{(2)}\Delta\mathbf{u}_d^{(2)} \\
\delta p^{(1)}&=\sum_{a=1}^{m^{(1)}}N_a^{(1)}\delta p_a^{(1)} & \delta p^{(2)}&=\sum_{b=1}^{m^{(2)}}N_b^{(2)}\delta p_b^{(2)} \\
\Delta p^{(1)}&=\sum_{c=1}^{m^{(1)}}N_c^{(1)}\Delta p_c^{(1)} & \Delta p^{(2)}&=\sum_{d=1}^{m^{(2)}}N_d^{(2)}\Delta p_d^{(2)}
\end{aligned}. \tag{7.6.14}$$

Then,

$$\begin{aligned}
\delta G_c=\sum_{e=1}^{n_e^{(1)}}\sum_{k=1}^{n_{\text{int}}^{(e)}}W_k J_\eta^{(1)}\Bigg(&\sum_{a=1}^{m^{(1)}}\begin{bmatrix}\delta\mathbf{v}_a^{(1)} & \delta p_a^{(1)}\end{bmatrix}\cdot\begin{bmatrix}\mathbf{f}_a^{(1)}\\ w_a^{(1)}\end{bmatrix} \\
&+\sum_{b=1}^{m_k^{(2)}}\begin{bmatrix}\delta\mathbf{v}_{b,k}^{(1)} & \delta p_{b,k}^{(1)}\end{bmatrix}\cdot\begin{bmatrix}\mathbf{f}_{b,k}^{(1)}\\ w_{b,k}^{(1)}\end{bmatrix}\Bigg)
\end{aligned}, \tag{7.6.15}$$

where

$$\begin{aligned} \mathbf{f}_a^{(1)} &= N_a^{(1)}\mathbf{t} \qquad \mathbf{f}_{b,k}^{(2)} = -N_b^{(2)}\mathbf{t} \\ w_a^{(1)} &= N_a^{(1)} w_n \quad w_{b,k}^{(2)} = -N_b^{(2)} w_n \end{aligned} \; . \tag{7.6.16}$$

Similarly,

$$\begin{aligned} -D\delta G_c = & \sum_{e=1}^{n_e^{(1)}} \sum_{k=1}^{n_{\text{int}}^{(e)}} W_k J_\eta^{(1)} \\ & \times \left(\sum_{a=1}^{m^{(1)}} \left[\begin{array}{cc} \delta\mathbf{v}_a^{(1)} & \delta p_a^{(1)} \end{array} \right] \cdot \left(\sum_{c=1}^{m^{(1)}} \left[\begin{array}{cc} \mathbf{K}_{ac}^{(1,1)} & \mathbf{0} \\ \mathbf{k}_{ac}^{(1,1)} & k_{ac}^{(1,1)} \end{array} \right] \cdot \left[\begin{array}{c} \Delta\mathbf{u}_c^{(1)} \\ \Delta p_c^{(1)} \end{array} \right] \right. \right. \\ & \left. \left. + \sum_{d=1}^{m_k^{(2)}} \left[\begin{array}{cc} \mathbf{K}_{ad,k}^{(1,2)} & \mathbf{0} \\ \mathbf{0} & k_{ad,k}^{(1,2)} \end{array} \right] \cdot \left[\begin{array}{c} \Delta\mathbf{u}_d^{(2)} \\ \Delta p_d^{(2)} \end{array} \right] \right) \\ & + \sum_{b=1}^{m_k^{(2)}} \left[\begin{array}{cc} \delta\mathbf{v}_{b,k}^{(2)} & \delta p_{b,k}^{(2)} \end{array} \right] \cdot \left(\sum_{c=1}^{m^{(1)}} \left[\begin{array}{cc} \mathbf{K}_{bc,k}^{(2,1)} & \mathbf{0} \\ \mathbf{k}_{bc,k}^{(2,1)} & k_{bc,k}^{(2,1)} \end{array} \right] \cdot \left[\begin{array}{c} \Delta\mathbf{u}_c^{(1)} \\ \Delta p_c^{(1)} \end{array} \right] \right. \\ & \left. \left. + \sum_{d=1}^{m_k^{(2)}} \left[\begin{array}{cc} \mathbf{K}_{bd,k}^{(2,2)} & \mathbf{0} \\ \mathbf{0} & k_{bd,k}^{(2,2)} \end{array} \right] \cdot \left[\begin{array}{c} \Delta\mathbf{u}_d^{(2)} \\ \Delta p_d^{(2)} \end{array} \right] \right) \right) \; , \end{aligned} \tag{7.6.17}$$

where

$$\begin{aligned} \mathbf{K}_{ac}^{(1,1)} &= N_a^{(1)} \left(\varepsilon_n N_c^{(1)} \mathbf{I} + \mathbf{t} \otimes \mathbf{a}_c^{(1)} \right) \\ \mathbf{K}_{ad,k}^{(1,2)} &= -\varepsilon_n N_a^{(1)} N_d^{(2)} \mathbf{I} \\ \mathbf{K}_{bc,k}^{(2,1)} &= -N_b^{(2)} \left(\varepsilon_n N_c^{(1)} \mathbf{I} + \mathbf{t} \otimes \mathbf{a}_c^{(1)} \right) \\ \mathbf{K}_{bd,k}^{(2,2)} &= \varepsilon_n N_b^{(2)} N_d^{(2)} \mathbf{I} \end{aligned} \; , \tag{7.6.18}$$

$$\begin{aligned} \mathbf{k}_{ac}^{(1,1)} &= N_a^{(1)} w_n \mathbf{a}_c^{(1)} \\ \mathbf{k}_{bc,k}^{(2,1)} &= -N_b^{(2)} w_n \mathbf{a}_c^{(1)} \end{aligned} \; , \tag{7.6.19}$$

$$\begin{aligned} k_{ac}^{(1,1)} &= -\varepsilon_p N_a^{(1)} N_c^{(1)} \\ k_{ad,k}^{(1,2)} &= \varepsilon_p N_a^{(1)} N_d^{(2)} \\ k_{bc,k}^{(2,1)} &= \varepsilon_p N_b^{(2)} N_c^{(1)} \\ k_{bd,k}^{(2,2)} &= -\varepsilon_p N_b^{(2)} N_d^{(2)} \end{aligned} \; , \tag{7.6.20}$$

and

$$\mathbf{a}_c^{(1)} = \frac{1}{J_\eta^{(1)}} \mathbf{n}^{(1)} \times \left(\mathbf{g}_2^{(1)} \frac{\partial N_c^{(1)}}{\partial \eta_{(1)}^1} - \mathbf{g}_1^{(1)} \frac{\partial N_c^{(1)}}{\partial \eta_{(1)}^2} \right) \; . \tag{7.6.21}$$

7.7 Tied Multiphasic Contact

See Section 2.7 for a review of multiphasic materials, and [15] for additional details on contact interfaces involving solutes. The contact interface is defined between surfaces $\gamma^{(1)}$ and $\gamma^{(2)}$. Due to

continuity requirements on the traction and fluxes, the external virtual work resulting from contact tractions $\mathbf{t}^{(i)}$, solvent fluxes $w_n^{(i)}$ and solute fluxes $j_n^{\alpha(i)}$ $(i = 1, 2)$ may be combined into the contact integral

$$\begin{aligned}\delta G_c = &\int_{\gamma^{(1)}} \left(\delta \mathbf{v}^{(1)} - \delta \mathbf{v}^{(2)}\right) \cdot \mathbf{t}^{(1)}\, da^{(1)} \\ &+ \int_{\gamma^{(1)}} \left(\delta \tilde{p}^{(1)} - \delta \tilde{p}^{(2)}\right) w_n^{(1)}\, da^{(1)} \\ &+ \sum_{\alpha} \int_{\gamma^{(1)}} \left(\delta \tilde{c}^{\alpha(1)} - \delta \tilde{c}^{\alpha(2)}\right) j_n^{\alpha(1)}\, da^{(1)}\,.\end{aligned} \tag{7.7.1}$$

Note that the summation in (7.7.1) is performed only over solutes that are present on both sides of the contact interface. No special treatment is needed for solutes that only belong to one side, since the natural boundary condition for these solutes enforces zero normal flux across the contact interface.

To evaluate and linearize δG_c, define the covariant basis vectors on each surface as

$$\mathbf{g}_\alpha^{(i)} = \frac{\partial \mathbf{x}^{(i)}}{\partial \eta^\alpha_{(i)}}, \quad \alpha = 1, 2, \tag{7.7.2}$$

where $\mathbf{x}^{(i)}$ represents the spatial position of points on $\gamma^{(i)}$, and $\eta^\alpha_{(i)}$ represent the parametric coordinates of that point. The unit outward normal on each surface is then given by

$$\mathbf{n}^{(i)} = \frac{\mathbf{g}_1^{(i)} \times \mathbf{g}_2^{(i)}}{\left|\mathbf{g}_1^{(i)} \times \mathbf{g}_2^{(i)}\right|}\,. \tag{7.7.3}$$

Now the contact integral may be rewritten as

$$\begin{aligned}\delta G_c = &\int_{\gamma^{(1)}} \left(\delta \mathbf{v}^{(1)} - \delta \mathbf{v}^{(2)}\right) \cdot \mathbf{t} \left|\mathbf{g}_1^{(1)} \times \mathbf{g}_2^{(1)}\right| d\eta^1_{(1)} d\eta^2_{(1)} \\ &+ \int_{\gamma^{(1)}} \left(\delta \tilde{p}^{(1)} - \delta \tilde{p}^{(2)}\right) w_n \left|\mathbf{g}_1^{(1)} \times \mathbf{g}_2^{(1)}\right| d\eta^1_{(1)} d\eta^2_{(1)} \\ &+ \sum_{\alpha} \int_{\gamma^{(1)}} \left(\delta \tilde{c}^{\alpha(1)} - \delta \tilde{c}^{\alpha(2)}\right) j_n^{\alpha} \left|\mathbf{g}_1^{(1)} \times \mathbf{g}_2^{(1)}\right| d\eta^1_{(1)} d\eta^2_{(1)}\end{aligned}, \tag{7.7.4}$$

where $\mathbf{t} \equiv \mathbf{t}^{(1)}$, $w_n \equiv w_n^{(1)}$ and $j_n^\alpha \equiv j_n^{\alpha(1)}$. The linearization $D\delta G_c$ of δG_c has the form

$$D\delta G_c = \sum_{i=1}^{2} D\delta G_c \left[\Delta \mathbf{u}^{(i)}\right] + D\delta G_c \left[\Delta \tilde{p}^{(i)}\right] + \sum_{\alpha} D\delta G_c \left[\Delta \tilde{c}^{\alpha(i)}\right]\,. \tag{7.7.5}$$

7.7.1 Gap Function

The vector gap function $\mathbf{g}$, representing the distance between the contact surfaces, is defined by

$$\mathbf{g} = \mathbf{x}^{(2)} - \mathbf{x}^{(1)}\,. \tag{7.7.6}$$

The premise of a tied interface is that the parametric coordinates of $\mathbf{x}^{(1)}$ and $\mathbf{x}^{(2)}$ are both invariants (i.e., they are determined in the reference configuration and remain unchanged over time). The parametric coordinates of $\mathbf{x}^{(1)}$ correspond to the integration points on $\gamma^{(1)}$, and those of $\mathbf{x}^{(2)}$ are

evaluated once, in the reference configuration, by shooting a ray from the integration point on $\gamma^{(1)}$ to intersect $\gamma^{(2)}$. It follows from this premise that

$$\begin{aligned} D\mathbf{x}^{(i)} &= \Delta\mathbf{u}^{(i)} \quad & D\delta\mathbf{v}^{(i)} &= \mathbf{0} \\ D\tilde{p}^{(i)} &= \Delta\tilde{p}^{(i)} \quad & D\delta\tilde{p}^{(i)} &= 0 \quad i = 1, 2\,. \\ D\tilde{c}^{\alpha(i)} &= \Delta\tilde{c}^{\alpha(i)} \quad & D\delta\tilde{c}^{\alpha(i)} &= 0 \end{aligned} \tag{7.7.7}$$

If $\gamma^{(1)}$ and $\gamma^{(2)}$ are not initially conforming, continuity of effective fluid pressure and solute concentration, as well as normal fluid and solute fluxes, will only be enforced within the contact interface; unlike the sliding multiphasic contact interface (Section 7.4), ambient conditions are not set automatically on regions of $\gamma^{(1)}$ and $\gamma^{(2)}$ where a solution for $\mathbf{g}$ was not found. Therefore, these regions naturally enforce zero fluid and solute flux (impermeable boundary), unless an explicit boundary condition on the effective pressure $\tilde{p}$ or solute concentrations $\tilde{c}^{\alpha}$ are prescribed over those regions.

7.7.2 Penalty Method

Let the tied contact traction be described by the penalty function,

$$\mathbf{t} = \varepsilon_n \mathbf{g}\,, \tag{7.7.8}$$

where ε_n is a penalty factor associated with $\mathbf{t}$. Similarly, let

$$w_n = \varepsilon_p \pi = \varepsilon_p \left(\tilde{p}^{(1)} - \tilde{p}^{(2)} \right)\,, \tag{7.7.9}$$

where ε_p is a penalty factor associated with w_n, and

$$j_n^{\alpha} = \varepsilon_c \chi^{\alpha} = \varepsilon_c^{\alpha} \left(\tilde{c}^{\alpha(1)} - \tilde{c}^{\alpha(2)} \right)\,, \tag{7.7.10}$$

where ε_c^{α} is a penalty factor associated with j_n^{α}. It follows that

$$\begin{aligned} D\mathbf{t} &= \varepsilon_n \left(\Delta\mathbf{u}^{(2)} - \Delta\mathbf{u}^{(1)} \right)\,, \\ Dw_n &= \varepsilon_p \left(\Delta\tilde{p}^{(1)} - \Delta\tilde{p}^{(2)} \right)\,, \\ Dj_n^{\alpha} &= \varepsilon_c^{\alpha} \left(\Delta\tilde{c}^{\alpha(1)} - \Delta\tilde{c}^{\alpha(2)} \right)\,. \end{aligned} \tag{7.7.11}$$

Given these relations, it can be shown that the directional derivatives of the various terms appearing in the integrand of δG_c are

$$\begin{aligned} &- D\left(J_{\eta}^{(1)} \left(\delta\mathbf{v}^{(1)} - \delta\mathbf{v}^{(2)} \right) \cdot \mathbf{t} \right) = \\ &\left(\delta\mathbf{v}^{(1)} - \delta\mathbf{v}^{(2)} \right) \cdot \varepsilon_n J_{\eta}^{(1)} \mathbf{I} \cdot \left(\Delta\mathbf{u}^{(1)} - \Delta\mathbf{u}^{(2)} \right) \\ &+ \left(\delta\mathbf{v}^{(1)} - \delta\mathbf{v}^{(2)} \right) \cdot \mathbf{t} \otimes \left[\left(\mathbf{g}_1^{(1)} \times \mathbf{n}^{(1)} \right) \cdot \frac{\partial \Delta\mathbf{u}^{(1)}}{\partial \eta^2_{(1)}} - \left(\mathbf{g}_2^{(1)} \times \mathbf{n}^{(1)} \right) \cdot \frac{\partial \Delta\mathbf{u}^{(1)}}{\partial \eta^1_{(1)}} \right] \end{aligned}\,, \tag{7.7.12}$$

$$\begin{aligned} &- D\left(w_n \left(\delta p^{(1)} - \delta p^{(2)} \right) J_{\eta}^{(1)} \right) = \\ &- J_{\eta}^{(1)} \varepsilon_p \left(\delta p^{(1)} - \delta p^{(2)} \right) \left(\Delta\tilde{p}^{(1)} - \Delta\tilde{p}^{(2)} \right) \\ &+ w_n \left(\delta p^{(1)} - \delta p^{(2)} \right) \mathbf{n}^{(1)} \cdot \left(\mathbf{g}_2^{(1)} \times \frac{\partial \Delta\mathbf{u}^{(1)}}{\partial \eta^1_{(1)}} - \mathbf{g}_1^{(1)} \times \frac{\partial \Delta\mathbf{u}^{(1)}}{\partial \eta^2_{(1)}} \right) \end{aligned}\,, \tag{7.7.13}$$

$$
\begin{aligned}
&- D\left(j_n^\alpha\left(\delta\tilde{c}^{\alpha(1)}-\delta\tilde{c}^{\alpha(2)}\right)J_\eta^{(1)}\right)= \\
&- J_\eta^{(1)}\left(\delta\tilde{c}^{\alpha(1)}-\delta\tilde{c}^{\alpha(2)}\right)\varepsilon_c^\alpha\left(\Delta\tilde{c}^{\alpha(1)}-\Delta\tilde{c}^{\alpha(2)}\right) \\
&+ j_n^\alpha\left(\delta\tilde{c}^{\alpha(1)}-\delta\tilde{c}^{\alpha(2)}\right)\mathbf{n}^{(1)}\cdot\left(\mathbf{g}_2^{(1)}\times\frac{\partial\Delta\mathbf{u}^{(1)}}{\partial\eta^1_{(1)}}-\mathbf{g}_1^{(1)}\times\frac{\partial\Delta\mathbf{u}^{(1)}}{\partial\eta^2_{(1)}}\right)
\end{aligned}
, \tag{7.7.14}
$$

where $J_\eta^{(1)}=\left|\mathbf{g}_1^{(1)}\times\mathbf{g}_2^{(1)}\right|$.

7.7.3 Discretization

The contact integral may be discretized as

$$
\delta G_c=\sum_{e=1}^{n_e^{(1)}}\sum_{k=1}^{n_{\text{int}}^{(e)}}W_kJ_\eta^{(1)}\left[\left(\delta\mathbf{v}^{(1)}-\delta\mathbf{v}^{(2)}\right)\cdot\mathbf{t}+w_n\left(\delta p^{(1)}-\delta p^{(2)}\right)+\sum_\alpha j_n^\alpha\left(\delta\tilde{c}^{\alpha(1)}-\delta\tilde{c}^{\alpha(2)}\right)\right]. \tag{7.7.15}
$$

The variables may be interpolated over each element face according to

$$
\begin{aligned}
\delta\mathbf{v}^{(1)}&=\sum_{a=1}^{m^{(1)}}N_a^{(1)}\delta\mathbf{v}_a^{(1)} & \delta\mathbf{v}^{(2)}&=\sum_{b=1}^{m^{(2)}}N_b^{(2)}\delta\mathbf{v}_b^{(2)} \\
\Delta\mathbf{u}^{(1)}&=\sum_{c=1}^{m^{(1)}}N_c^{(1)}\Delta\mathbf{u}_c^{(1)} & \Delta\mathbf{u}^{(2)}&=\sum_{d=1}^{m^{(2)}}N_d^{(2)}\Delta\mathbf{u}_d^{(2)} \\
\delta\tilde{p}^{(1)}&=\sum_{a=1}^{m^{(1)}}N_a^{(1)}\delta\tilde{p}_a^{(1)} & \delta p^{(2)}&=\sum_{b=1}^{m^{(2)}}N_b^{(2)}\delta\tilde{p}_b^{(2)} \\
\Delta\tilde{p}^{(1)}&=\sum_{c=1}^{m^{(1)}}N_c^{(1)}\Delta\tilde{p}_c^{(1)} & \Delta\tilde{p}^{(2)}&=\sum_{d=1}^{m^{(2)}}N_d^{(2)}\Delta\tilde{p}_d^{(2)} \\
\delta\tilde{c}^{\alpha(1)}&=\sum_{a=1}^{m^{(1)}}N_a^{(1)}\delta\tilde{c}_a^{\alpha(1)} & \delta c^{\alpha(2)}&=\sum_{b=1}^{m^{(2)}}N_b^{(2)}\delta\tilde{c}_b^{\alpha(2)} \\
\Delta\tilde{c}^{\alpha(1)}&=\sum_{c=1}^{m^{(1)}}N_c^{(1)}\Delta\tilde{c}_c^{\alpha(1)} & \Delta\tilde{c}^{\alpha(2)}&=\sum_{d=1}^{m^{(2)}}N_d^{(2)}\Delta\tilde{c}_d^{\alpha(2)}
\end{aligned}
. \tag{7.7.16}
$$

Then,

$$
\begin{aligned}
\delta G_c=\sum_{e=1}^{n_e^{(1)}}\sum_{k=1}^{n_{\text{int}}^{(e)}}W_kJ_\eta^{(1)}\Bigg(&\sum_{a=1}^{m^{(1)}}\left[\begin{array}{cccc}\delta\mathbf{v}_a^{(1)} & \delta\tilde{p}_a^{(1)} & \delta\tilde{c}^{\alpha(1)} & \delta\tilde{c}^{\beta(1)}\end{array}\right]\cdot\left[\begin{array}{c}\mathbf{f}_a^{(1)}\\ w_a^{(1)}\\ j_n^{\alpha(1)}\\ j_n^{\beta(1)}\end{array}\right] \\
&+\sum_{b=1}^{m_k^{(2)}}\left[\begin{array}{cccc}\delta\mathbf{v}_{b,k}^{(1)} & \delta\tilde{p}_{b,k}^{(1)} & \delta\tilde{c}_{b,k}^{\alpha(1)} & \delta\tilde{c}_{b,k}^{\beta(1)}\end{array}\right]\cdot\left[\begin{array}{c}\mathbf{f}_{b,k}^{(1)}\\ w_{b,k}^{(1)}\\ j_{b,k}^{\alpha(1)}\\ j_{b,k}^{\beta(1)}\end{array}\right]\Bigg)
\end{aligned}
, \tag{7.7.17}
$$

where

$$\begin{aligned} \mathbf{f}_a^{(1)} &= N_a^{(1)}\mathbf{t} \qquad \mathbf{f}_{b,k}^{(2)} = -N_b^{(2)}\mathbf{t} \\ w_a^{(1)} &= N_a^{(1)} w_n \quad w_{b,k}^{(2)} = -N_b^{(2)} w_n \,. \\ j_a^{\gamma(1)} &= N_a^{(1)} j_n^{\gamma} \quad j_{b,k}^{\gamma(2)} = -N_b^{(2)} j_n^{\gamma} \end{aligned} \tag{7.7.18}$$

Similarly,

$$\begin{aligned} -D\delta G_c = & \sum_{e=1}^{n_e^{(1)}} \sum_{k=1}^{n_{\text{int}}^{(e)}} W_k J_\eta^{(1)} \\ & \times \left(\sum_{a=1}^{m^{(1)}} \left[\begin{array}{cccc} \delta\mathbf{v}_a^{(1)} & \delta\tilde{p}_a^{(1)} & \delta\tilde{c}_a^{\alpha(1)} & \delta\tilde{c}_a^{\beta(1)} \end{array} \right] \cdot \left(\sum_{c=1}^{m^{(1)}} \left[\begin{array}{cccc} \mathbf{K}_{ac}^{(1,1)} & \mathbf{0} & \mathbf{0} & \mathbf{0} \\ \mathbf{k}_{ac}^{(1,1)} & k_{ac}^{(1,1)} & 0 & 0 \\ \mathbf{k}_{ac}^{\alpha(1,1)} & 0 & k_{ac}^{\alpha\alpha(1,1)} & 0 \\ \mathbf{k}_{ac}^{\beta(1,1)} & 0 & 0 & k_{ac}^{\beta\beta(1,1)} \end{array} \right] \cdot \left[\begin{array}{c} \Delta\mathbf{u}_c^{(1)} \\ \Delta\tilde{p}_c^{(1)} \\ \Delta\tilde{c}_c^{\alpha(1)} \\ \Delta\tilde{c}_c^{\beta(1)} \end{array} \right] \right. \right. \\ & \left. \left. + \sum_{d=1}^{m_k^{(2)}} \left[\begin{array}{cccc} \mathbf{K}_{ad,k}^{(1,2)} & \mathbf{0} & \mathbf{0} & \mathbf{0} \\ \mathbf{0} & k_{ad,k}^{(1,2)} & 0 & 0 \\ \mathbf{0} & 0 & k_{ad,k}^{\alpha\alpha(1,2)} & 0 \\ \mathbf{0} & 0 & 0 & k_{ad,k}^{\beta\beta(1,2)} \end{array} \right] \cdot \left[\begin{array}{c} \Delta\mathbf{u}_d^{(2)} \\ \Delta\tilde{p}_d^{(2)} \\ \Delta\tilde{c}_d^{\alpha(2)} \\ \Delta\tilde{c}_d^{\beta(2)} \end{array} \right] \right) \\ & + \sum_{b=1}^{m_k^{(2)}} \left[\begin{array}{cccc} \delta\mathbf{v}_{b,k}^{(2)} & \delta\tilde{p}_{b,k}^{(2)} & \delta\tilde{c}_{b,k}^{\alpha(2)} & \delta\tilde{c}_{b,k}^{\beta(2)} \end{array} \right] \cdot \left(\sum_{c=1}^{m^{(1)}} \left[\begin{array}{cccc} \mathbf{K}_{bc,k}^{(2,1)} & \mathbf{0} & \mathbf{0} & \mathbf{0} \\ \mathbf{k}_{bc,k}^{(2,1)} & k_{bc,k}^{(2,1)} & 0 & 0 \\ \mathbf{k}_{bc,k}^{\alpha(2,1)} & 0 & k_{bc,k}^{\alpha\alpha(2,1)} & 0 \\ \mathbf{k}_{bc,k}^{\beta(2,1)} & 0 & 0 & k_{bc,k}^{\beta\beta(2,1)} \end{array} \right] \cdot \left[\begin{array}{c} \Delta\mathbf{u}_c^{(1)} \\ \Delta\tilde{p}_c^{(1)} \\ \Delta\tilde{c}_c^{\alpha(1)} \end{array} \right] \right. \\ & \left. \left. + \sum_{d=1}^{m_k^{(2)}} \left[\begin{array}{cccc} \mathbf{K}_{bd,k}^{(2,2)} & \mathbf{0} & \mathbf{0} & \mathbf{0} \\ \mathbf{0} & k_{bd,k}^{(2,2)} & 0 & 0 \\ \mathbf{0} & 0 & k_{bd,k}^{\alpha\alpha(2,2)} & 0 \\ \mathbf{0} & 0 & 0 & k_{bd,k}^{\beta\beta(2,2)} \end{array} \right] \cdot \left[\begin{array}{c} \Delta\mathbf{u}_d^{(2)} \\ \Delta\tilde{p}_d^{(2)} \\ \Delta\tilde{c}_d^{\alpha(2)} \\ \Delta\tilde{c}_d^{\beta(2)} \end{array} \right] \right) \right) , \end{aligned} \tag{7.7.19}$$

where

$$\begin{aligned} \mathbf{K}_{ac}^{(1,1)} &= N_a^{(1)} \left(\varepsilon_n N_c^{(1)} \mathbf{I} + \mathbf{t} \otimes \mathbf{a}_c^{(1)} \right) \\ \mathbf{K}_{ad,k}^{(1,2)} &= -\varepsilon_n N_a^{(1)} N_d^{(2)} \mathbf{I} \\ \mathbf{K}_{bc,k}^{(2,1)} &= -N_b^{(2)} \left(\varepsilon_n N_c^{(1)} \mathbf{I} + \mathbf{t} \otimes \mathbf{a}_c^{(1)} \right) \\ \mathbf{K}_{bd,k}^{(2,2)} &= \varepsilon_n N_b^{(2)} N_d^{(2)} \mathbf{I} \end{aligned} \,, \tag{7.7.20}$$

$$\begin{aligned} \mathbf{k}_{ac}^{(1,1)} &= N_a^{(1)} w_n \mathbf{a}_c^{(1)} \\ \mathbf{k}_{bc,k}^{(2,1)} &= -N_b^{(2)} w_n \mathbf{a}_c^{(1)} \\ \mathbf{k}_{ac}^{\alpha(1,1)} &= N_a^{(1)} j_n^{\alpha} \mathbf{a}_c^{(1)} \\ \mathbf{k}_{bc,k}^{\alpha(2,1)} &= -N_b^{(2)} j_n^{\alpha} \mathbf{a}_c^{(1)} \end{aligned} \,, \tag{7.7.21}$$

$$\begin{aligned} k_{ac}^{(1,1)} &= -\varepsilon_p N_a^{(1)} N_c^{(1)} \\ k_{ad,k}^{(1,2)} &= \varepsilon_p N_a^{(1)} N_d^{(2)} \\ k_{bc,k}^{(2,1)} &= \varepsilon_p N_b^{(2)} N_c^{(1)} \\ k_{bd,k}^{(2,2)} &= -\varepsilon_p N_b^{(2)} N_d^{(2)} \end{aligned} \quad , \tag{7.7.22}$$

$$\begin{aligned} k_{ac}^{\gamma\gamma(1,1)} &= -\varepsilon_c^{\gamma} N_a^{(1)} N_c^{(1)} \\ k_{ad,k}^{\gamma\gamma(1,2)} &= \varepsilon_c^{\gamma} N_a^{(1)} N_d^{(2)} \\ k_{bc,k}^{\gamma\gamma(2,1)} &= \varepsilon_c^{\gamma} N_b^{(2)} N_c^{(1)} \\ k_{bd,k}^{\gamma\gamma(2,2)} &= -\varepsilon_c^{\gamma} N_b^{(2)} N_d^{(2)} \end{aligned} \tag{7.7.23}$$

and

$$\mathbf{a}_c^{(1)} = \frac{1}{J_\eta^{(1)}} \mathbf{n}^{(1)} \times \left(\mathbf{g}_2^{(1)} \frac{\partial N_c^{(1)}}{\partial \eta_{(1)}^1} - \mathbf{g}_1^{(1)} \frac{\partial N_c^{(1)}}{\partial \eta_{(1)}^2} \right) . \tag{7.7.24}$$

7.8 Tied Fluid Interface

A tied fluid interface may be used to enforces continuity of viscous shear traction and normal fluid velocity at the interface between dissimilar meshes.

7.8.1 Contact Integral

See Section 2.11 for a review of fluid materials, and [16] for additional details on the FEBio fluid solver. The tied fluid interface is defined between surfaces $\gamma^{(1)}$ and $\gamma^{(2)}$. Due to continuity requirements on the viscous traction and normal fluid velocity, the external virtual work resulting from tractions $\mathbf{t}^{\tau(i)}$ and normal velocities $v_n^{(i)}$ $(i = 1, 2)$ may be combined into the tied interface integral

$$\begin{aligned} \delta G_c = &\int_{\gamma^{(1)}} \left(\delta \mathbf{v}^{(1)} - \delta \mathbf{v}^{(2)} \right) \cdot \mathbf{t}^{\tau(1)} da^{(1)} \\ &- \int_{\gamma^{(1)}} \left(\delta J^{(1)} - \delta J^{(2)} \right) v_n^{(1)} da^{(1)} . \end{aligned} \tag{7.8.1}$$

To evaluate and linearize δG_c, define the covariant basis vectors on each surface as

$$\mathbf{g}_\alpha^{(i)} = \frac{\partial \mathbf{x}^{(i)}}{\partial \eta_{(i)}^\alpha}, \quad \alpha = 1, 2, \tag{7.8.2}$$

where $\mathbf{x}^{(i)}$ represents the spatial position of points on $\gamma^{(i)}$, and $\eta_{(i)}^\alpha$ represent the parametric coordinates of that point. The unit outward normal on each surface is then given by

$$\mathbf{n}^{(i)} = \frac{\mathbf{g}_1^{(i)} \times \mathbf{g}_2^{(i)}}{\left| \mathbf{g}_1^{(i)} \times \mathbf{g}_2^{(i)} \right|} . \tag{7.8.3}$$

Now the contact integral may be rewritten as

$$\begin{aligned} \delta G_c = &\int_{\gamma^{(1)}} \left(\delta \mathbf{v}^{(1)} - \delta \mathbf{v}^{(2)} \right) \cdot \mathbf{t}^{\tau} \left| \mathbf{g}_1^{(1)} \times \mathbf{g}_2^{(1)} \right| d\eta_{(1)}^1 d\eta_{(1)}^2 \\ &- \int_{\gamma^{(1)}} \left(\delta J^{(1)} - \delta J^{(2)} \right) v_n \left| \mathbf{g}_1^{(1)} \times \mathbf{g}_2^{(1)} \right| d\eta_{(1)}^1 d\eta_{(1)}^2 \end{aligned} , \tag{7.8.4}$$

where $\mathbf{t}^\tau \equiv \mathbf{t}^{\tau(1)}$ and $v_n \equiv v_n^{(1)}$. The linearization $D\delta G_c$ of δG_c has the form

$$D\delta G_c = \sum_{i=1}^{2} D\delta G_c \left[\Delta \mathbf{v}^{(i)}\right] + D\delta G_c \left[\Delta J^{(i)}\right] . \tag{7.8.5}$$

7.8.2 Gap Functions

The premise of a tied interface is that the parametric coordinates of coincident points $\mathbf{x}^{(1)}$ and $\mathbf{x}^{(2)}$ on $\gamma^{(1)}$ and $\gamma^{(2)}$ are both invariants (i.e., they are determined in the reference configuration and remain unchanged over time). The parametric coordinates of $\mathbf{x}^{(1)}$ correspond to the integration points on $\gamma^{(1)}$, and those of $\mathbf{x}^{(2)}$ are evaluated once by shooting a ray from the integration point on $\gamma^{(1)}$ to intersect $\gamma^{(2)}$.

The vector gap function $\mathbf{g}$, representing the difference between tangential velocities across the interface, is defined by

$$\mathbf{g} = \mathbf{v}_t^{(2)} - \mathbf{v}_t^{(1)} , \tag{7.8.6}$$

where the tangential velocity is evaluate from

$$\mathbf{v}_t^{(i)} = \left(\mathbf{I} - \mathbf{n}^{(i)} \otimes \mathbf{n}^{(i)}\right) \cdot \mathbf{v}^{(i)} . \tag{7.8.7}$$

We may similarly define the scalar gap function π, representing the difference between fluid pressures across the interface,

$$\pi = K\left(J^{(2)} - J^{(1)}\right) = K\left(e^{(2)} - e^{(1)}\right) , \tag{7.8.8}$$

where K is the fluid bulk modulus.

7.8.3 Penalty Method

Let the tied interface viscous traction be described by the penalty function,

$$\mathbf{t}^\tau = \varepsilon_t \mathbf{g} , \tag{7.8.9}$$

where ε_t is a penalty factor associated with $\mathbf{t}^\tau$. The penalty factor ε_t is expressed in units of viscosity per length. Therefore, in an auto-penalty scheme, it may be scaled to the ratio of fluid viscosity to element thickness. Similarly, let

$$v_n = \varepsilon_n \pi = K\varepsilon_n \left(J^{(2)} - J^{(1)}\right) , \tag{7.8.10}$$

where ε_n is a penalty factor associated with v_n. Note that ε_n has units of length per viscosity. It follows that

$$\begin{aligned} D\mathbf{t}^\tau &= \varepsilon_t \left(\left(\mathbf{I} - \mathbf{n}^{(2)} \otimes \mathbf{n}^{(2)}\right) \cdot \Delta\mathbf{v}^{(2)} - \left(\mathbf{I} - \mathbf{n}^{(1)} \otimes \mathbf{n}^{(1)}\right) \cdot \Delta\mathbf{v}^{(1)}\right) , \\ Dv_n &= K\varepsilon_n \left(\Delta J^{(2)} - \Delta J^{(1)}\right) . \end{aligned} \tag{7.8.11}$$

Given these relations, it can be shown that the directional derivatives of the various terms appearing in the integrand of δG_c are

$$\begin{aligned} &- D\left(J_\eta^{(1)} \left(\delta\mathbf{v}^{(1)} - \delta\mathbf{v}^{(2)}\right) \cdot \mathbf{t}^\tau\right) = \\ &\varepsilon_t J_\eta^{(1)} \left(\delta\mathbf{v}^{(1)} - \delta\mathbf{v}^{(2)}\right) \cdot \left(\left(\mathbf{I} - \mathbf{n}^{(1)} \otimes \mathbf{n}^{(1)}\right) \cdot \Delta\mathbf{v}^{(1)} - \left(\mathbf{I} - \mathbf{n}^{(2)} \otimes \mathbf{n}^{(2)}\right) \cdot \Delta\mathbf{v}^{(2)}\right) , \end{aligned} \tag{7.8.12}$$

$$D\left(v_n\left(\delta J^{(1)}-\delta J^{(2)}\right)J_\eta^{(1)}\right)=-\varepsilon_n K J_\eta^{(1)}\left(\delta J^{(1)}-\delta J^{(2)}\right)\left(\Delta J^{(1)}-\Delta J^{(2)}\right), \tag{7.8.13}$$

where $J_\eta^{(1)}=\left|\mathbf{g}_1^{(1)}\times\mathbf{g}_2^{(1)}\right|$.

7.8.4 Discretization

The contact integral may be discretized as

$$\delta G_c=\sum_{e=1}^{n_e^{(1)}}\sum_{k=1}^{n_{\text{int}}^{(e)}}W_k J_\eta^{(1)}\left[\left(\delta\mathbf{v}^{(1)}-\delta\mathbf{v}^{(2)}\right)\cdot\mathbf{t}^\tau-\left(\delta J^{(1)}-\delta J^{(2)}\right)v_n\right]. \tag{7.8.14}$$

The variables may be interpolated over each element face according to

$$\begin{aligned}
\delta\mathbf{v}^{(1)}&=\sum_{a=1}^{m^{(1)}}N_a^{(1)}\delta\mathbf{v}_a^{(1)} & \delta\mathbf{v}^{(2)}&=\sum_{b=1}^{m^{(2)}}N_b^{(2)}\delta\mathbf{v}_b^{(2)}\\
\Delta\mathbf{v}^{(1)}&=\sum_{c=1}^{m^{(1)}}N_c^{(1)}\Delta\mathbf{v}_c^{(1)} & \Delta\mathbf{v}^{(2)}&=\sum_{d=1}^{m^{(2)}}N_d^{(2)}\Delta\mathbf{v}_d^{(2)}\\
\delta J^{(1)}&=\sum_{a=1}^{m^{(1)}}N_a^{(1)}\delta J_a^{(1)} & \delta J^{(2)}&=\sum_{b=1}^{m^{(2)}}N_b^{(2)}\delta J_b^{(2)}\\
\Delta J^{(1)}&=\sum_{c=1}^{m^{(1)}}N_c^{(1)}\Delta J_c^{(1)} & \Delta J^{(2)}&=\sum_{d=1}^{m^{(2)}}N_d^{(2)}\Delta J_d^{(2)}
\end{aligned}. \tag{7.8.15}$$

Then,

$$\begin{aligned}
\delta G_c=\sum_{e=1}^{n_e^{(1)}}\sum_{k=1}^{n_{\text{int}}^{(e)}}W_k J_\eta^{(1)}\Bigg(&\sum_{a=1}^{m^{(1)}}\begin{bmatrix}\delta\mathbf{v}_a^{(1)} & \delta J_a^{(1)}\end{bmatrix}\cdot\begin{bmatrix}\mathbf{f}_a^{(1)}\\ v_a^{(1)}\end{bmatrix}\\
&+\sum_{b=1}^{m_k^{(2)}}\begin{bmatrix}\delta\mathbf{v}_{b,k}^{(1)} & \delta J_{b,k}^{(1)}\end{bmatrix}\cdot\begin{bmatrix}\mathbf{f}_{b,k}^{(1)}\\ v_{b,k}^{(1)}\end{bmatrix}\Bigg)
\end{aligned}, \tag{7.8.16}$$

where

$$\begin{aligned}
\mathbf{f}_a^{(1)}&=N_a^{(1)}\mathbf{t}^\tau & \mathbf{f}_{b,k}^{(2)}&=-N_b^{(2)}\mathbf{t}^\tau\\
w_a^{(1)}&=-N_a^{(1)}v_n & w_{b,k}^{(2)}&=N_b^{(2)}v_n
\end{aligned}. \tag{7.8.17}$$

Similarly,

$$
\begin{aligned}
-D\delta G_c = & \sum_{e=1}^{n_e^{(1)}} \sum_{k=1}^{n_{\text{int}}^{(e)}} W_k J_\eta^{(1)} \\
& \times \left(\sum_{a=1}^{m^{(1)}} \left[\begin{array}{cc} \delta \mathbf{v}_a^{(1)} & \delta J_a^{(1)} \end{array} \right] \cdot \left(\sum_{c=1}^{m^{(1)}} \left[\begin{array}{cc} \mathbf{K}_{ac}^{(1,1)} & \mathbf{0} \\ \mathbf{0} & k_{ac}^{(1,1)} \end{array} \right] \cdot \left[\begin{array}{c} \Delta \mathbf{v}_c^{(1)} \\ \Delta J_c^{(1)} \end{array} \right] \right. \right. \\
& \left. + \sum_{d=1}^{m_k^{(2)}} \left[\begin{array}{cc} \mathbf{K}_{ad,k}^{(1,2)} & \mathbf{0} \\ \mathbf{0} & k_{ad,k}^{(1,2)} \end{array} \right] \cdot \left[\begin{array}{c} \Delta \mathbf{v}_d^{(2)} \\ \Delta J_d^{(2)} \end{array} \right] \right) \\
& + \sum_{b=1}^{m_k^{(2)}} \left[\begin{array}{cc} \delta \mathbf{v}_{b,k}^{(2)} & \delta J_{b,k}^{(2)} \end{array} \right] \cdot \left(\sum_{c=1}^{m^{(1)}} \left[\begin{array}{cc} \mathbf{K}_{bc,k}^{(2,1)} & \mathbf{0} \\ \mathbf{0} & k_{bc,k}^{(2,1)} \end{array} \right] \cdot \left[\begin{array}{c} \Delta \mathbf{v}_c^{(1)} \\ \Delta J_c^{(1)} \end{array} \right] \right. \\
& \left. \left. + \sum_{d=1}^{m_k^{(2)}} \left[\begin{array}{cc} \mathbf{K}_{bd,k}^{(2,2)} & \mathbf{0} \\ \mathbf{0} & k_{bd,k}^{(2,2)} \end{array} \right] \cdot \left[\begin{array}{c} \Delta \mathbf{v}_d^{(2)} \\ \Delta J_d^{(2)} \end{array} \right] \right) \right) ,
\end{aligned}
\tag{7.8.18}
$$

where

$$
\begin{aligned}
\mathbf{K}_{ac}^{(1,1)} &= \varepsilon_t N_a^{(1)} N_c^{(1)} \left(\mathbf{I} - \mathbf{n}^{(1)} \otimes \mathbf{n}^{(1)} \right) \\
\mathbf{K}_{ad,k}^{(1,2)} &= -\varepsilon_t N_a^{(1)} N_d^{(2)} \left(\mathbf{I} - \mathbf{n}^{(2)} \otimes \mathbf{n}^{(2)} \right) \\
\mathbf{K}_{bc,k}^{(2,1)} &= -\varepsilon_t N_b^{(2)} N_c^{(1)} \left(\mathbf{I} - \mathbf{n}^{(1)} \otimes \mathbf{n}^{(1)} \right) \\
\mathbf{K}_{bd,k}^{(2,2)} &= \varepsilon_t N_b^{(2)} N_d^{(2)} \left(\mathbf{I} - \mathbf{n}^{(2)} \otimes \mathbf{n}^{(2)} \right)
\end{aligned} ,
\tag{7.8.19}
$$

$$
\begin{aligned}
k_{ac}^{(1,1)} &= -K\varepsilon_n N_a^{(1)} N_c^{(1)} \\
k_{ad,k}^{(1,2)} &= K\varepsilon_n N_a^{(1)} N_d^{(2)} \\
k_{bc,k}^{(2,1)} &= K\varepsilon_n N_b^{(2)} N_c^{(1)} \\
k_{bd,k}^{(2,2)} &= -K\varepsilon_n N_b^{(2)} N_d^{(2)}
\end{aligned} .
\tag{7.8.20}
$$

7.9 Rigid Connectors

A *rigid connector* connects two rigid bodies denoted by (1) and (2). The connector origin (e.g., its insertion point) on rigid body (i) is located at

$$
\mathbf{x}^{(i)} = \mathbf{r}^{(i)} + \mathbf{\Lambda}^{(i)} \cdot \mathbf{Z}^{(i)} = \mathbf{r}^{(i)} + \mathbf{z}^{(i)} ,
\tag{7.9.1}
$$

where $\mathbf{z}^{(i)}$ is the connector origin position relative to the center of mass at the current time, whereas $\mathbf{Z}^{(i)}$ is its relative position in the reference configuration, when the rotation tensor $\mathbf{\Lambda}^{(i)}$ is equal to the identity tensor. The connector is exerting a reaction force $\mathbf{f}^{(i)}$ at $\mathbf{x}^{(i)}$ and a reaction moment $\mathbf{m}^{(i)}$ on rigid body (i), such that $\mathbf{f}^{(1)} + \mathbf{f}^{(2)} = \mathbf{0}$ and $\mathbf{m}^{(1)} + \mathbf{m}^{(2)} = \mathbf{0}$.

Rigid body joints, such as spherical, revolute, prismatic, cylindrical and planar joints, are a special category of rigid connectors that have a large stiffness spring connecting the joint origins on

each rigid body, in a manner that only allows relative motion along the joint translational degree(s) of freedom. Similarly, a large stiffness torsional spring connects the rigid bodies in a manner that only allows relative rotation along the joint rotational degree(s) of freedom.

Other connectors include springs, dampers, and contractile forces that may connect rigid bodies. Optionally, a joint may include a linear damper connecting its origins, and an angular damper restricting its relative rotation.

7.9.1 Virtual Work

The virtual work of a connector represents the work of external forces on the rigid body; it is given by

$$\delta G = \sum_{i=1}^{2} \delta \mathbf{v}^{(i)} \cdot \mathbf{f}^{(i)} + \delta \boldsymbol{\theta}^{(i)} \cdot \mathbf{m}^{(i)} \,, \tag{7.9.2}$$

where $\delta \mathbf{v}^{(i)}$ is the virtual velocity of the joint origin and $\delta \boldsymbol{\theta}^{(i)}$ is the virtual angular velocity of rigid body (i). Using the above relations for $\mathbf{f}^{(i)}$ and $\mathbf{m}^{(i)}$, it reduces to

$$\delta G = \left(\delta \mathbf{v}^{(1)} - \delta \mathbf{v}^{(2)} \right) \cdot \mathbf{f}^{(1)} + \left(\delta \boldsymbol{\theta}^{(1)} - \delta \boldsymbol{\theta}^{(2)} \right) \cdot \mathbf{m}^{(1)} \,. \tag{7.9.3}$$

The analysis thus returns the values of the reaction force and moment acting on rigid body (1). The virtual velocities at the joint may be evaluated from (7.9.1) as

$$\delta \mathbf{v}^{(i)} = \delta \mathbf{r}^{(i)} - \hat{\mathbf{z}}^{(i)} \cdot \delta \boldsymbol{\theta}^{(i)} \,, \tag{7.9.4}$$

where $\hat{\mathbf{z}}$ is the skew-symmetric tensor whose dual vector is $\mathbf{z}$, such that $\hat{\mathbf{z}} \cdot \mathbf{v} = \mathbf{z} \times \mathbf{v}$ for any vector $\mathbf{v}$. Substituting this expression into (7.9.3) allows us to express the virtual work in terms of the virtual velocities of the centers of mass and the virtual angular velocities of the rigid bodies,

$$\delta G = \begin{bmatrix} \delta \mathbf{r}^{(1)} & \delta \boldsymbol{\theta}^{(1)} & \delta \mathbf{r}^{(2)} & \delta \boldsymbol{\theta}^{(2)} \end{bmatrix} \begin{bmatrix} \mathbf{f}^{(1)} \\ \hat{\mathbf{z}}^{(1)} \cdot \mathbf{f}^{(1)} + \mathbf{m}^{(1)} \\ -\mathbf{f}^{(1)} \\ -\hat{\mathbf{z}}^{(2)} \cdot \mathbf{f}^{(1)} - \mathbf{m}^{(1)} \end{bmatrix} . \tag{7.9.5}$$

When using time discretization in the interval $[t_n, t_{n+1}]$, the external forces and moments may be evaluated at the intermediate time point $t_{n+\alpha}$ using

$$\begin{aligned} \mathbf{f}^{(1)}_{n+\alpha} &= \alpha \mathbf{f}^{(1)}_{n+1} + (1-\alpha)\, \mathbf{f}^{(1)}_{n} \\ \left(\hat{\mathbf{z}}^{(1)} \cdot \mathbf{f}^{(1)} \right)_{n+\alpha} &= \alpha \hat{\mathbf{z}}^{(1)}_{n+1} \cdot \mathbf{f}^{(1)}_{n+1} + (1-\alpha)\, \hat{\mathbf{z}}^{(1)}_{n} \cdot \mathbf{f}^{(1)}_{n} \\ \mathbf{m}^{(1)}_{n+\alpha} &= \alpha \mathbf{m}^{(1)}_{n+1} + (1-\alpha)\, \mathbf{m}^{(1)}_{n} \end{aligned}$$

We solve for $\delta G = 0$ using Newton's method in the usual manner, by evaluating the linearization of δG along increments in the rigid body degrees of freedom at t_{n+1},

$$\delta G + \sum_{i=1}^{2} D\delta G \left[\Delta \mathbf{r}^{(i)} \right] + D\delta G \left[\Delta \boldsymbol{\theta}^{(i)} \right] \approx 0 \,. \tag{7.9.6}$$

Assuming that

$$D\mathbf{f}^{(1)}_{n+1} = \begin{bmatrix} \mathbf{K}^{(1)}_{fr} & \mathbf{K}^{(1)}_{f\theta} & \mathbf{K}^{(2)}_{fr} & \mathbf{K}^{(2)}_{f\theta} \end{bmatrix} \begin{bmatrix} \Delta \mathbf{r}^{(1)} \\ \Delta \boldsymbol{\theta}^{(1)} \\ \Delta \mathbf{r}^{(2)} \\ \Delta \boldsymbol{\theta}^{(2)} \end{bmatrix} , \tag{7.9.7}$$

and

$$D\mathbf{m}_{n+1}^{(1)} = \left[\begin{array}{cccc} \mathbf{K}_{mr}^{(1)} & \mathbf{K}_{m\theta}^{(1)} & \mathbf{K}_{mr}^{(2)} & \mathbf{K}_{m\theta}^{(2)} \end{array} \right] \left[\begin{array}{c} \Delta\mathbf{r}^{(1)} \\ \Delta\boldsymbol{\theta}^{(1)} \\ \Delta\mathbf{r}^{(2)} \\ \Delta\boldsymbol{\theta}^{(2)} \end{array} \right], \tag{7.9.8}$$

it follows that

$$\begin{aligned} D\delta G = & \left[\begin{array}{cccc} \delta\mathbf{r}^{(1)} & \delta\boldsymbol{\theta}^{(1)} & \delta\mathbf{r}^{(2)} & \delta\boldsymbol{\theta}^{(2)} \end{array} \right] \times \\ & \alpha \left[\begin{array}{cccc} \mathbf{K}_{fr}^{(1)} & \mathbf{K}_{f\theta}^{(1)} & \mathbf{K}_{fr}^{(2)} & \mathbf{K}_{f\theta}^{(2)} \\ \hat{\mathbf{z}}_{n+1}^{(1)} \cdot \mathbf{K}_{fr}^{(1)} + \mathbf{K}_{mr}^{(1)} & \hat{\mathbf{z}}_{n+1}^{(1)} \cdot \mathbf{K}_{f\theta}^{(1)} + \mathbf{K}_{m\theta}^{(1)} & \hat{\mathbf{z}}_{n+1}^{(1)} \cdot \mathbf{K}_{fr}^{(2)} + \mathbf{K}_{mr}^{(2)} & \hat{\mathbf{z}}_{n+1}^{(1)} \cdot \mathbf{K}_{f\theta}^{(2)} + \mathbf{K}_{m\theta}^{(2)} \\ -\mathbf{K}_{fr}^{(1)} & -\mathbf{K}_{f\theta}^{(1)} & -\mathbf{K}_{fr}^{(2)} & -\mathbf{K}_{f\theta}^{(2)} \\ -\hat{\mathbf{z}}_{n+1}^{(2)} \cdot \mathbf{K}_{fr}^{(1)} - \mathbf{K}_{mr}^{(1)} & -\hat{\mathbf{z}}_{n+1}^{(2)} \cdot \mathbf{K}_{f\theta}^{(1)} - \mathbf{K}_{m\theta}^{(1)} & -\hat{\mathbf{z}}_{n+1}^{(2)} \cdot \mathbf{K}_{fr}^{(2)} - \mathbf{K}_{mr}^{(2)} & -\hat{\mathbf{z}}_{n+1}^{(2)} \cdot \mathbf{K}_{f\theta}^{(2)} - \mathbf{K}_{m\theta}^{(2)} \end{array} \right] \\ & \times \left[\begin{array}{c} \Delta\mathbf{r}^{(1)} \\ \Delta\boldsymbol{\theta}^{(1)} \\ \Delta\mathbf{r}^{(2)} \\ \Delta\boldsymbol{\theta}^{(2)} \end{array} \right] \end{aligned} \tag{7.9.9}$$

It becomes immediately apparent that the stiffness matrix for a rigid connector is not symmetric. Therefore, rigid body dynamics should be analyzed using non-symmetric solvers.

7.9.2 Joint Axes

Joint axes are used to define the directions of degrees of freedom in rigid joints, which represent one of the major categories of rigid connectors. The axes are defined with respect to a body-based coordinate system centered at the origin of a joint, given by the orthonormal triad $\left\{\mathbf{e}_1^{(i)}, \mathbf{e}_2^{(i)}, \mathbf{e}_3^{(i)}\right\}$ for rigid body i ($i = 1, 2$). In the reference configuration, the bases coincide on both rigid bodies, $\mathbf{e}_j^{(1)} = \mathbf{e}_j^{(2)} \equiv \mathbf{E}_j$ ($j = 1, 2, 3$), where $\mathbf{E}_j$ is the $j-$th basis vector in the reference configuration. Thus, at any time t, we may evaluate the basis vectors as

$$\mathbf{e}_j^{(i)} = \boldsymbol{\Lambda}^{(i)} \cdot \mathbf{E}_j \tag{7.9.10}$$

Using this relation, the linearization of a basis vector along increments in the rigid body motion is given by

$$D\mathbf{e}_j^{(i)} = -\hat{\mathbf{e}}_j^{(i)} \cdot \Delta\boldsymbol{\theta}^{(i)}, \tag{7.9.11}$$

which shows a dependence only on $\Delta\boldsymbol{\theta}^{(i)}$.

7.9.3 Relative Joint Motion

The position of a joint in each rigid body i is given in (7.9.1). The relative motion across a joint is given by the relative translation

$$\mathbf{x} = \mathbf{x}^{(2)} - \mathbf{x}^{(1)}, \tag{7.9.12}$$

and the relative rotation

$$\mathbf{Q} = \boldsymbol{\Lambda}^{(2)} \cdot \left(\boldsymbol{\Lambda}^{(1)}\right)^T \equiv \exp\left[\hat{\boldsymbol{\theta}}\right], \tag{7.9.13}$$

where $\hat{\boldsymbol{\theta}} = -\boldsymbol{\mathcal{E}} \cdot \boldsymbol{\theta}$ is the skew-symmetric tensor with dual vector $\boldsymbol{\theta}$. As usual, $\boldsymbol{\theta}$ is a vector whose direction represents the axis of rotation and whose magnitude is the angle of (counter-clockwise) rotation about that axis. To report the relative motion of a joint, we may project $\mathbf{x}$ and $\boldsymbol{\theta}$ along the basis vectors $\mathbf{e}_j^{(1)} = \boldsymbol{\Lambda}^{(1)} \cdot \mathbf{E}_j$ of the first rigid body. Thus,

$$\begin{aligned} x_j &= \mathbf{x} \cdot \mathbf{e}_j^{(1)} \\ \theta_j &= \boldsymbol{\theta} \cdot \mathbf{e}_j^{(1)} \end{aligned} . \tag{7.9.14}$$

7.9.4 Joint Reaction Forces and Moments

Reaction forces are used to constrain the degrees of freedom of a joint that connects two rigid bodies. Typically, these forces are generated by very stiff springs and dampers that only allow unrestricted motion along the joint degrees of freedom.

7.9.4.1 Reaction Forces from Springs

The reaction force $\mathbf{f}^{(1)}$ generated by a spring acting on rigid body (1) is given by

$$\boxed{\mathbf{f}^{(1)} = \boldsymbol{\lambda} + \varepsilon_c \mathbf{P} \cdot \mathbf{g}}, \tag{7.9.15}$$

where

$$\boxed{\mathbf{g} = \mathbf{x}^{(2)} - \mathbf{x}^{(1)}} \tag{7.9.16}$$

is a gap function that represents the vector distance between the joint origins, $\boldsymbol{\lambda}$ is the (optional) Lagrange multiplier used when invoking the augmented Lagrangian method, and ε_c is a penalty parameter that represents the spring stiffness. The tensor $\mathbf{P}$ is a projection that limits the reaction force to the directions that are not free to move. In general, there are three possible options for $\mathbf{P}$:

$$\mathbf{P} = \begin{cases} \mathbf{P}_1 = \mathbf{I} & \text{constrain relative translation along all directions} \\ \mathbf{P}_2 = \mathbf{I} - \mathbf{n}^{(1)} \otimes \mathbf{n}^{(1)} & \text{constrain relative translation within plane normal to } \mathbf{n}^{(1)} \\ \mathbf{P}_3 = \mathbf{n}^{(1)} \otimes \mathbf{n}^{(1)} & \text{constrain relative translation along } \mathbf{n}^{(1)} \end{cases} . \tag{7.9.17}$$

For example, $\mathbf{P}_1 = \mathbf{I}$ in a spherical or revolute joint, whereas $\mathbf{P}_2 = \mathbf{I} - \mathbf{n}^{(1)} \otimes \mathbf{n}^{(1)}$ in an unconstrained prismatic joint, with $\mathbf{n}^{(1)}$ representing the axis of motion; and $\mathbf{P}_3 = \mathbf{n}^{(1)} \otimes \mathbf{n}^{(1)}$ in an unconstrained planar joint, with $\mathbf{n}^{(1)}$ representing the normal to the plane. Note that in all cases we choose to define the axis in the basis of rigid body (1). If the constraint is enforced properly, then $\mathbf{n}^{(1)}$ should be the same as $\mathbf{n}^{(2)}$, within a user-defined numerical tolerance. In practice, we let $\mathbf{n}^{(1)} \equiv \mathbf{e}_1^{(1)}$.

The linearization of $\mathbf{f}^{(1)}$ in (7.9.15) is given by

$$D\mathbf{f}^{(1)} = \varepsilon_c \left(\mathbf{P} \cdot D\mathbf{g} + D\mathbf{P} \cdot \mathbf{g} \right) . \tag{7.9.18}$$

The linearization of the gap function produces

$$\mathbf{P} \cdot D\mathbf{g} = \begin{bmatrix} -\mathbf{P} & \mathbf{P} \cdot \hat{\mathbf{z}}^{(1)} & \mathbf{P} & -\mathbf{P} \cdot \hat{\mathbf{z}}^{(2)} \end{bmatrix} \begin{bmatrix} \Delta\mathbf{r}^{(1)} \\ \Delta\boldsymbol{\theta}^{(1)} \\ \Delta\mathbf{r}^{(2)} \\ \Delta\boldsymbol{\theta}^{(2)} \end{bmatrix} , \tag{7.9.19}$$

whereas the linearization of the three possible projections yields

$$D\mathbf{P}\cdot\mathbf{g}=\mathbf{Q}\cdot\Delta\boldsymbol{\theta}^{(1)}\,, \tag{7.9.20}$$

where

$$\mathbf{Q}=\begin{cases}\mathbf{Q}_1 &= \mathbf{0}\\ \mathbf{Q}_2 &= \left[\left(\mathbf{n}^{(1)}\cdot\mathbf{g}\right)\mathbf{I}+\mathbf{n}^{(1)}\otimes\mathbf{g}\right]\cdot\hat{\mathbf{n}}^{(1)}\\ \mathbf{Q}_3 &= -\left[\left(\mathbf{n}^{(1)}\cdot\mathbf{g}\right)\mathbf{I}+\mathbf{n}^{(1)}\otimes\mathbf{g}\right]\cdot\hat{\mathbf{n}}^{(1)}\end{cases}\quad. \tag{7.9.21}$$

Therefore, in the expression for $D\mathbf{f}^{(1)}$ in (7.9.7), we have

$$\boxed{\begin{aligned}\mathbf{K}^{(1)}_{fr} &= -\varepsilon_c\mathbf{P}\\ \mathbf{K}^{(1)}_{f\theta} &= \varepsilon_c\left(\mathbf{P}\cdot\hat{\mathbf{z}}^{(1)}+\mathbf{Q}\right)\\ \mathbf{K}^{(2)}_{fr} &= \varepsilon_c\mathbf{P}\\ \mathbf{K}^{(2)}_{f\theta} &= -\varepsilon_c\mathbf{P}\cdot\hat{\mathbf{z}}^{(2)}\end{aligned}}\,. \tag{7.9.22}$$

7.9.4.2 Reaction Moments from Torsional Springs

The reaction moment $\mathbf{m}^{(1)}$ generated by a torsional spring acting on rigid body (1) is given by

$$\boxed{\mathbf{m}^{(1)}=\boldsymbol{\mu}+\varepsilon_r\boldsymbol{\gamma}} \tag{7.9.23}$$

where

$$\boxed{\boldsymbol{\gamma}=\frac{1}{2}\sum_{j=1}^{k}\mathbf{e}^{(1)}_j\times\mathbf{e}^{(2)}_j} \tag{7.9.24}$$

is the angular gap function between the bases of rigid bodies (1) and (2), $\boldsymbol{\mu}$ is the (optional) Lagrange multiplier used when invoking the augmented Lagrangian method, and ε_r is a penalty parameter representing the torsional spring stiffness. We consider three cases for the choice of $\boldsymbol{\gamma}$:

$$\boldsymbol{\gamma}=\begin{cases}k=3 & \text{constrain relative rotation along all directions}\\ k=1 & \text{maintain free relative rotation along } \mathbf{e}^{(i)}_1\\ k=0 & \text{maintain free relative rotation along all directions}\end{cases} \tag{7.9.25}$$

For example, $k=3$ is used to model the reaction moment in a prismatic joint, whereas $k=1$ is used with revolute, cylindrical and planar joints.

Now, the linearization produces

$$D\mathbf{m}^{(1)}=\varepsilon_r D\boldsymbol{\gamma}\,,$$

where

$$D\boldsymbol{\gamma}=\mathbf{W}\cdot\Delta\boldsymbol{\theta}^{(1)}-\mathbf{W}^T\cdot\Delta\boldsymbol{\theta}^{(2)}$$

and

$$\mathbf{W}=\frac{1}{2}\sum_{j=1}^{k}\hat{\mathbf{e}}^{(2)}_j\cdot\hat{\mathbf{e}}^{(1)}_j\quad.$$

Therefore, in the expression for $D\mathbf{m}^{(1)}$ in (7.9.8), we have

$$\boxed{\begin{aligned}\mathbf{K}_{mr}^{(1)} &= \mathbf{0}\\ \mathbf{K}_{m\theta}^{(1)} &= \varepsilon_r \mathbf{W}\\ \mathbf{K}_{mr}^{(2)} &= \mathbf{0}\\ \mathbf{K}_{m\theta}^{(2)} &= -\varepsilon_r \mathbf{W}^T\end{aligned}}. \tag{7.9.26}$$

7.9.4.3 Reaction Forces from Dampers

The reaction force $\mathbf{f}^{(1)}$ on a damper is

$$\boxed{\mathbf{f}^{(1)} = \chi_c \mathbf{P}\cdot\dot{\mathbf{g}}}, \tag{7.9.27}$$

where $\dot{\mathbf{g}}$ is the time rate of change of the gap function,

$$\boxed{\dot{\mathbf{g}} = \mathbf{v}^{(2)} - \mathbf{v}^{(1)}}, \tag{7.9.28}$$

and $\mathbf{P}$ represents a projection as described in Section 7.9.4.1. In particular, $\mathbf{P}_1$ is used with spherical and revolute joints; $\mathbf{P}_2$ is used with prismatic and cylindrical joints; and $\mathbf{P}_3$ is used with planar joints. The parameter χ_c represents the damping coefficient.

The velocities of the insertion points are given by $\mathbf{v}^{(i)} = \dot{\mathbf{r}}^{(i)} + \boldsymbol{\omega}^{(i)} \times \mathbf{z}^{(i)}$, where $\boldsymbol{\omega}^{(i)}$ is the rigid body angular velocity. The linearization of $\mathbf{f}^{(1)}$ is

$$D\mathbf{f}^{(1)} = \varepsilon_c \left(\mathbf{P}\cdot D\dot{\mathbf{g}} + D\mathbf{P}\cdot\dot{\mathbf{g}}\right), \tag{7.9.29}$$

where

$$\mathbf{P}\cdot D\dot{\mathbf{g}} = \begin{bmatrix} -\mathbf{A} & \mathbf{B}^{(1)} & \mathbf{A} & -\mathbf{B}^{(2)}\end{bmatrix}\begin{bmatrix}\Delta\mathbf{r}^{(1)}\\ \Delta\boldsymbol{\theta}^{(1)}\\ \Delta\mathbf{r}^{(2)}\\ \Delta\boldsymbol{\theta}^{(2)}\end{bmatrix}, \tag{7.9.30}$$

with

$$\begin{aligned}\mathbf{A} &= \frac{\gamma}{\beta\Delta t}\mathbf{P}\\ \mathbf{B}^{(i)} &= \mathbf{P}\cdot\left(\frac{\gamma}{\beta\Delta t}\hat{\mathbf{z}}^{(i)}\cdot\mathbf{T}^T\left(\boldsymbol{\theta}^{(i)}\right) + \hat{\boldsymbol{\omega}}\cdot\hat{\mathbf{z}}^{(i)}\right)\end{aligned}. \tag{7.9.31}$$

Recall that β and γ are the Newmark parameters, and $\mathbf{T}(\boldsymbol{\theta})$ is given in (6.3.35). Similarly,

$$D\mathbf{P}\cdot\dot{\mathbf{g}} = \mathbf{V}\cdot\Delta\boldsymbol{\theta}^{(1)}, \tag{7.9.32}$$

where

$$\mathbf{V} = \begin{cases}\mathbf{V}_1 &= \mathbf{0}\\ \mathbf{V}_2 &= \left[\left(\mathbf{n}^{(1)}\cdot\dot{\mathbf{g}}\right)\mathbf{I} + \mathbf{n}^{(1)}\otimes\dot{\mathbf{g}}\right]\cdot\hat{\mathbf{n}}^{(1)}\\ \mathbf{V}_3 &= -\left[\left(\mathbf{n}^{(1)}\cdot\dot{\mathbf{g}}\right)\mathbf{I} + \mathbf{n}^{(1)}\otimes\dot{\mathbf{g}}\right]\cdot\hat{\mathbf{n}}^{(1)}\end{cases}. \tag{7.9.33}$$

Combining these results produces

$$\boxed{\begin{aligned}\mathbf{K}_{fr}^{(1)} &= -\chi_c\mathbf{A}\\ \mathbf{K}_{f\theta}^{(1)} &= \chi_c\left(\mathbf{B}^{(1)} + \mathbf{V}\right)\\ \mathbf{K}_{fr}^{(2)} &= \chi_c\mathbf{A}\\ \mathbf{K}_{f\theta}^{(2)} &= -\chi_c\mathbf{B}^{(2)}\end{aligned}} \tag{7.9.34}$$

7.9.4.4 Reaction Moments from Torsional Dampers

The reaction moment $\mathbf{m}^{(1)}$ arising from a torsional damper is

$$\boxed{\mathbf{m}^{(1)} = \chi_r \mathbf{P} \cdot \boldsymbol{\omega}}, \tag{7.9.35}$$

where

$$\boldsymbol{\omega} = \boldsymbol{\omega}^{(2)} - \boldsymbol{\omega}^{(1)} \tag{7.9.36}$$

is the angular velocity of body (2) relative to body (1), and $\mathbf{P}$ is the projection used in Section 7.9.4.1. In particular, $\mathbf{P}_1$ is used for joints that cannot undergo relative rotations along any direction, such as prismatic joints; $\mathbf{P}_2$ is used for joints that can rotate freely along a single axis, such as revolute, cylindrical and planar joints; in addition, $\mathbf{P} = \mathbf{0}$ for spherical joints. The linearization of $\mathbf{m}^{(1)}$ is

$$D\mathbf{m}^{(1)} = \chi_r \left(\mathbf{P} \cdot D\boldsymbol{\omega} + D\mathbf{P} \cdot \boldsymbol{\omega} \right) , \tag{7.9.37}$$

where

$$\mathbf{P} \cdot D\boldsymbol{\omega} = \mathbf{C}^{(2)} \cdot \Delta\boldsymbol{\theta}^{(2)} - \mathbf{C}^{(1)} \cdot \Delta\boldsymbol{\theta}^{(1)} \tag{7.9.38}$$

with

$$\mathbf{C}^{(i)} = \frac{\gamma}{\beta \Delta t} \mathbf{P} \cdot \mathbf{T}^T \left(\boldsymbol{\theta}^{(i)} \right) , \tag{7.9.39}$$

and

$$D\mathbf{P} \cdot \boldsymbol{\omega} = \mathbf{W} \cdot \Delta\boldsymbol{\theta}^{(1)} , \tag{7.9.40}$$

where

$$\mathbf{W} = \begin{cases} \mathbf{W}_1 & = \mathbf{0} \\ \mathbf{W}_2 & = \left[\left(\mathbf{n}^{(1)} \cdot \boldsymbol{\omega} \right) \mathbf{I} + \mathbf{n}^{(1)} \otimes \boldsymbol{\omega} \right] \cdot \hat{\mathbf{n}}^{(1)} \\ \mathbf{W}_3 & = - \left[\left(\mathbf{n}^{(1)} \cdot \boldsymbol{\omega} \right) \mathbf{I} + \mathbf{n}^{(1)} \otimes \boldsymbol{\omega} \right] \cdot \hat{\mathbf{n}}^{(1)} \end{cases} . \tag{7.9.41}$$

Combining these results now produces

$$\boxed{\begin{aligned} \mathbf{K}^{(1)}_{mr} &= \mathbf{0} \\ \mathbf{K}^{(1)}_{m\theta} &= \chi_r \left(-\mathbf{C}^{(1)} + \mathbf{W} \right) \\ \mathbf{K}^{(2)}_{mr} &= \mathbf{0} \\ \mathbf{K}^{(2)}_{m\theta} &= \chi_r \mathbf{C}^{(2)} \end{aligned}} . \tag{7.9.42}$$

7.9.4.5 Summary of Reaction Forces and Moment in Joints

Joint	Spherical	Revolute	Prismatic	Cylindrical	Planar	Lock
linear spring	$\mathbf{P}_1, \mathbf{Q}_1$	$\mathbf{P}_1, \mathbf{Q}_1$	$\mathbf{P}_2, \mathbf{Q}_2$	$\mathbf{P}_2, \mathbf{Q}_2$	$\mathbf{P}_3, \mathbf{Q}_3$	$\mathbf{P}_1, \mathbf{Q}_1$
torsional spring	$k = 0$	$k = 1$	$k = 3$	$k = 1$	$k = 1$	$k = 3$
linear damper	$\mathbf{P}_1, \mathbf{V}_1$	$\mathbf{P}_1, \mathbf{V}_1$	$\mathbf{P}_2, \mathbf{V}_2$	$\mathbf{P}_2, \mathbf{V}_2$	$\mathbf{P}_3, \mathbf{V}_3$	$\mathbf{P}_1, \mathbf{V}_1$
torsional damper	$\mathbf{0}, \mathbf{0}$	$\mathbf{P}_2, \mathbf{W}_2$	$\mathbf{P}_1, \mathbf{W}_1$	$\mathbf{P}_2, \mathbf{W}_2$	$\mathbf{P}_2, \mathbf{W}_2$	$\mathbf{P}_1, \mathbf{W}_1$

7.9.5 Prescribed Joint Forces and Moments

7.9.5.1 Prescribed Force at Joint

When a joint has a translational degree of freedom along $\mathbf{n}^{(1)}$, there may be a need to prescribe the force f along that direction. This means that the reaction force $\mathbf{f}^{(1)}$ may be supplemented with the force $f\,\mathbf{n}^{(1)}$,

$$\mathbf{f}^{(1)} = f\mathbf{n}^{(1)}\,, \tag{7.9.43}$$

and the linearization produces

$$D\mathbf{f}^{(1)} = -f\,\hat{\mathbf{n}}^{(1)}\cdot\Delta\boldsymbol{\theta}^{(1)}\,. \tag{7.9.44}$$

Thus,

$$\boxed{\mathbf{K}^{(1)}_{f\theta} = -f\,\hat{\mathbf{n}}^{(1)}}\,, \tag{7.9.45}$$

and

$$\boxed{\mathbf{K}^{(1)}_{fr} = \mathbf{K}^{(2)}_{fr} = \mathbf{K}^{(2)}_{f\theta} = \mathbf{0}}\,. \tag{7.9.46}$$

7.9.5.2 Prescribed Moment at Joint

When a joint has a rotational degree of freedom along $\mathbf{n}^{(1)}$, there may be a need to prescribe the moment m along that direction. This means that the reaction moment $\mathbf{m}^{(1)}$ may be supplemented with the moment $m\,\mathbf{n}^{(1)}$,

$$\mathbf{m}^{(1)} = m\,\mathbf{n}^{(1)}\,, \tag{7.9.47}$$

and the linearization produces

$$D\mathbf{m}^{(1)} = -m\,\hat{\mathbf{n}}^{(1)}\cdot\Delta\boldsymbol{\theta}^{(1)}\,. \tag{7.9.48}$$

Thus,

$$\boxed{\mathbf{K}^{(1)}_{m\theta} = -m\,\hat{\mathbf{n}}^{(1)}}\,, \tag{7.9.49}$$

and

$$\boxed{\mathbf{K}^{(1)}_{mr} = \mathbf{K}^{(2)}_{mr} = \mathbf{K}^{(2)}_{m\theta} = \mathbf{0}}\,. \tag{7.9.50}$$

7.9.6 Prescribed Joint Motion

7.9.6.1 Prescribed Displacement at Joint

When a joint has a translational degree of freedom along $\mathbf{n}^{(1)}$, there may be a need to prescribe the relative displacement d along that direction. This can be achieved by supplementing the joint reaction force with a force that closes the gap between the current and desired translation,

$$\mathbf{f}^{(1)} = \varepsilon_c\left[\left(\mathbf{n}^{(1)}\otimes\mathbf{n}^{(1)}\right)\cdot\mathbf{g} - d\,\mathbf{n}^{(1)}\right] = \varepsilon_c\left(\mathbf{P}_3\cdot\mathbf{g} - d\,\mathbf{n}^{(1)}\right)\,, \tag{7.9.51}$$

where $\mathbf{P}_3$ is given in (7.9.17). Then,

$$D\mathbf{f}^{(1)} = D\mathbf{P}_3\cdot\mathbf{g} + \mathbf{P}_3\cdot D\mathbf{g} + d\,\hat{\mathbf{n}}^{(1)}\cdot\Delta\boldsymbol{\theta}^{(1)} \tag{7.9.52}$$

Using the results of Section 7.9.4.1, the stiffnesses are supplemented with

$$\boxed{\begin{aligned}\mathbf{K}^{(1)}_{fr} &= -\varepsilon_c \mathbf{P}_3 \\ \mathbf{K}^{(1)}_{f\theta} &= \varepsilon_c \left(\mathbf{P}_3 \cdot \hat{\mathbf{z}}^{(1)} + \mathbf{Q} + d\,\hat{\mathbf{n}}^{(1)}\right) \\ \mathbf{K}^{(2)}_{fr} &= \varepsilon_c \mathbf{P}_3 \\ \mathbf{K}^{(2)}_{f\theta} &= -\varepsilon_c \mathbf{P}_3 \cdot \hat{\mathbf{z}}^{(2)}\end{aligned}}\,. \tag{7.9.53}$$

7.9.6.2 Prescribed Rotation at Joint

The relative rotation between the rigid bodies is

$$\mathbf{Q} = \mathbf{\Lambda}^{(2)} \cdot \mathbf{\Lambda}^{(1)T} = \sum_j \mathbf{e}^{(2)}_j \otimes \mathbf{e}^{(1)}_j \,. \tag{7.9.54}$$

We want it to be equal to a rotation by $\boldsymbol{\chi}$ as expressed in the basis $\mathbf{e}^{(1)}_j$,

$$\mathbf{A} = \exp\left[\boldsymbol{\chi}\right] \,. \tag{7.9.55}$$

We enforce this constraint by requiring that

$$\mathbf{A} \cdot \mathbf{Q}^T = \mathbf{I} \,. \tag{7.9.56}$$

We may thus evaluate

$$\mathbf{R} = \mathbf{A} \cdot \mathbf{Q}^T \,, \tag{7.9.57}$$

and expect that $\mathbf{R} = \mathbf{I}$ when the constraint is enforced. Note that $\mathbf{R}^T \cdot \mathbf{R} = \mathbf{I}$ because of the orthogonality of $\mathbf{Q}$ and $\mathbf{A}$, i.e., $\mathbf{R}$ is always orthogonal, even when the constraint is not enforced. The axial vector of $\mathbf{R}$ may be denoted by $\boldsymbol{\xi}$, i.e., $\mathbf{R} = \exp\left[\boldsymbol{\xi}\right]$, and the constraint is enforced when $\boldsymbol{\xi} = \mathbf{0}$. Therefore, a moment $\varepsilon_r \boldsymbol{\xi}$ needs to be prescribed,

$$\mathbf{m}^{(1)} = \varepsilon_r \boldsymbol{\xi} \,. \tag{7.9.58}$$

Since $\mathbf{R}$ is orthogonal, we can linearize it along an increment $\Delta\boldsymbol{\xi}$, $D\mathbf{R}\left[\Delta\boldsymbol{\xi}\right] = \Delta\hat{\boldsymbol{\xi}} \cdot \mathbf{R}$, from which it follows that $\Delta\hat{\boldsymbol{\xi}} = D\mathbf{R} \cdot \mathbf{R}^T$ with

$$D\mathbf{R} = \mathbf{A} \cdot D\mathbf{Q}^T = \mathbf{A} \cdot \left(\Delta\hat{\boldsymbol{\theta}}^{(1)} \cdot \mathbf{Q}^T - \mathbf{Q}^T \cdot \Delta\hat{\boldsymbol{\theta}}^{(2)}\right) \,, \tag{7.9.59}$$

so that

$$\Delta\hat{\boldsymbol{\xi}} = \mathbf{A} \cdot \Delta\hat{\boldsymbol{\theta}}^{(1)} \cdot \mathbf{A}^T - \mathbf{R} \cdot \Delta\hat{\boldsymbol{\theta}}^{(2)} \cdot \mathbf{R}^T \,. \tag{7.9.60}$$

From this expression we get

$$\Delta\boldsymbol{\xi} = \mathbf{A} \cdot \Delta\boldsymbol{\theta}^{(1)} - \mathbf{R} \cdot \Delta\boldsymbol{\theta}^{(2)} \,. \tag{7.9.61}$$

Thus,

$$D\mathbf{m}^{(1)} = \varepsilon_r \left(\mathbf{A} \cdot \Delta\boldsymbol{\theta}^{(1)} - \mathbf{R} \cdot \Delta\boldsymbol{\theta}^{(2)}\right) \,. \tag{7.9.62}$$

It follows that

$$\boxed{\mathbf{K}^{(1)}_{mr} = \mathbf{K}^{(2)}_{mr} = \mathbf{0}}, \tag{7.9.63}$$

and

$$\boxed{\begin{aligned}\mathbf{K}^{(1)}_{m\theta} &= \varepsilon_r \mathbf{A} \\ \mathbf{K}^{(2)}_{m\theta} &= -\varepsilon_r \mathbf{R}\end{aligned}}\,. \tag{7.9.64}$$

7.9.7 Other Rigid Connectors

7.9.7.1 Spring Between Rigid Bodies

Consider a spring between points $\mathbf{x}^{(i)}$ on rigid bodies (1) and (2). The spring force is oriented along $\mathbf{n}$, where

$$\mathbf{n} = \frac{\mathbf{x}^{(2)} - \mathbf{x}^{(1)}}{\left|\mathbf{x}^{(2)} - \mathbf{x}^{(1)}\right|} \,. \tag{7.9.65}$$

We may write

$$L = \left|\mathbf{x}^{(2)} - \mathbf{x}^{(1)}\right| \,, \quad L_0 = \left|\mathbf{X}^{(2)} - \mathbf{X}^{(2)}\right| \,. \tag{7.9.66}$$

Then, the spring force acting on body (1) is

$$\mathbf{f}^{(1)} = k\,(L - L_0)\,\mathbf{n} = k\left(\mathbf{x}^{(2)} - \mathbf{x}^{(1)} - L_0\mathbf{n}\right) \,, \tag{7.9.67}$$

where k is the spring constant. It is understood that the special case $L_0 = 0$ produces $\mathbf{f}^{(1)} = k\left(\mathbf{x}^{(2)} - \mathbf{x}^{(1)}\right)$. We do not need to use the augmented Lagrangian method here, therefore $\mathbf{f}^{(1)} = k\mathbf{c}$, where

$$\mathbf{c} = \mathbf{x}^{(2)}_{n+\alpha} - \mathbf{x}^{(1)}_{n+\alpha} - L_0\frac{\mathbf{x}^{(2)}_{n+\alpha} - \mathbf{x}^{(1)}_{n+\alpha}}{\left|\mathbf{x}^{(2)}_{n+\alpha} - \mathbf{x}^{(1)}_{n+\alpha}\right|} \,. \tag{7.9.68}$$

Since the spring may freely pivot about its insertion point, we let $\mathbf{m}^{(1)} = \mathbf{0}$. Thus,

$$\boxed{\begin{aligned} &\mathbf{f}^{(1)} = k\left(\mathbf{x}^{(2)}_{n+\alpha} - \mathbf{x}^{(1)}_{n+\alpha} - L_0\frac{\mathbf{x}^{(2)}_{n+\alpha} - \mathbf{x}^{(1)}_{n+\alpha}}{\left|\mathbf{x}^{(2)}_{n+\alpha} - \mathbf{x}^{(1)}_{n+\alpha}\right|}\right) \\ &\mathbf{m}^{(1)} = \mathbf{0} \end{aligned}} \tag{7.9.69}$$

and the virtual work associated with this spring is

$$\delta G = \left[\begin{array}{cccc} \delta\mathbf{r}^{(1)} & \delta\boldsymbol{\omega}^{(1)} & \delta\mathbf{r}^{(2)} & \delta\boldsymbol{\omega}^{(2)} \end{array}\right] \left[\begin{array}{c} \mathbf{f}^{(1)} \\ \hat{\mathbf{z}}^{(1)}_{n+\alpha}\cdot\mathbf{f}^{(1)} \\ -\mathbf{f}^{(1)} \\ -\hat{\mathbf{z}}^{(2)}_{n+\alpha}\cdot\mathbf{f}^{(1)} \end{array}\right] \,. \tag{7.9.70}$$

The linearization of δG may be expressed as

$$-D\delta G = \left[\begin{array}{cccc} \delta\mathbf{r}^{(1)} & \delta\boldsymbol{\omega}^{(1)} & \delta\mathbf{r}^{(2)} & \delta\boldsymbol{\omega}^{(2)} \end{array}\right] [\mathbf{K}] \left[\begin{array}{c} \Delta\mathbf{r}^{(1)} \\ \Delta\boldsymbol{\theta}^{(1)} \\ \Delta\mathbf{r}^{(2)} \\ \Delta\boldsymbol{\theta}^{(2)} \end{array}\right] \,, \tag{7.9.71}$$

where the stiffness matrix is

$$[\mathbf{K}] = k\alpha \left[\begin{array}{cccc} \mathbf{P} & -\mathbf{P}\cdot\hat{\mathbf{z}}^{(1)}_{n+1} & -\mathbf{P} & \mathbf{P}\cdot\hat{\mathbf{z}}^{(2)}_{n+1} \\ \hat{\mathbf{z}}^{(1)}_{n+\alpha}\cdot\mathbf{P} & -\hat{\mathbf{z}}^{(1)}_{n+\alpha}\cdot\mathbf{P}\cdot\hat{\mathbf{z}}^{(1)}_{n+1} & -\hat{\mathbf{z}}^{(1)}_{n+\alpha}\cdot\mathbf{P} & \hat{\mathbf{z}}^{(1)}_{n+\alpha}\cdot\mathbf{P}\cdot\hat{\mathbf{z}}^{(2)}_{n+1} \\ -\mathbf{P} & \mathbf{P}\cdot\hat{\mathbf{z}}^{(1)}_{n+1} & \mathbf{P} & -\mathbf{P}\cdot\hat{\mathbf{z}}^{(2)}_{n+1} \\ -\hat{\mathbf{z}}^{(2)}_{n+\alpha}\cdot\mathbf{P} & \hat{\mathbf{z}}^{(2)}_{n+\alpha}\cdot\mathbf{P}\cdot\hat{\mathbf{z}}^{(1)}_{n+1} & \hat{\mathbf{z}}^{(2)}_{n+\alpha}\cdot\mathbf{P} & -\hat{\mathbf{z}}^{(2)}_{n+\alpha}\cdot\mathbf{P}\cdot\hat{\mathbf{z}}^{(2)}_{n+1} \end{array}\right] \,, \tag{7.9.72}$$

with

$$\mathbf{P} = \left(1 - \frac{L_0}{L_{n+\alpha}}\right)\mathbf{I} + \frac{L_0}{L_{n+\alpha}}\mathbf{n}_{n+\alpha}\otimes\mathbf{n}_{n+\alpha} \,. \tag{7.9.73}$$

7.9.7.2 Damper Between Rigid Bodies

Consider a damper (e.g., a dashpot) inserted between points on two rigid bodies. The force generated by this dashpot is

$$\mathbf{f}^{(1)} = \varepsilon_c \dot{\mathbf{c}} \,. \tag{7.9.74}$$

where $\dot{\mathbf{c}}$ is the relative velocity between insertion points,

$$\dot{\mathbf{c}} = \mathbf{v}^{(2)}_{n+\alpha} - \mathbf{v}^{(1)}_{n+\alpha} \,. \tag{7.9.75}$$

This relative velocity is related to the rigid body degrees of freedom by

$$\begin{aligned} \mathbf{x}^{(i)}_{n+\alpha} &= \mathbf{r}^{(i)}_{n+\alpha} + \mathbf{z}^{(i)}_{n+\alpha} \\ \mathbf{v}^{(i)}_{n} &= \dot{\mathbf{r}}^{(i)}_{n} + \boldsymbol{\omega}_n \times \mathbf{z}^{(i)}_{n} \\ \mathbf{v}^{(i)}_{n+1} &= \dot{\mathbf{r}}^{(i)}_{n+1} + \boldsymbol{\omega}_{n+1} \times \mathbf{z}^{(i)}_{n+1} \\ \mathbf{v}^{(i)}_{n+\alpha} &= \alpha \mathbf{v}^{(i)}_{n+1} + (1-\alpha)\, \mathbf{v}^{(i)}_{n} \end{aligned} \,. \tag{7.9.76}$$

Since the dashpot may freely rotate about its insertion points, we set $\mathbf{m}^{(1)} = \mathbf{0}$. It follows that

$$\boxed{\begin{aligned} \mathbf{f}^{(1)} &= \varepsilon_c \left(\mathbf{v}^{(2)}_{n+\alpha} - \mathbf{v}^{(1)}_{n+\alpha} \right) \\ \mathbf{m}^{(1)} &= \mathbf{0} \end{aligned}} \,, \tag{7.9.77}$$

and the virtual work resulting from the dashpot is

$$\delta G = \left[\begin{array}{cccc} \delta \mathbf{r}^{(1)} & \delta \boldsymbol{\omega}^{(1)} & \delta \mathbf{r}^{(2)} & \delta \boldsymbol{\omega}^{(2)} \end{array} \right] \left[\begin{array}{c} \mathbf{f}^{(1)} \\ \hat{\mathbf{z}}^{(1)}_{n+\alpha} \cdot \mathbf{f}^{(1)} \\ -\mathbf{f}^{(1)} \\ -\hat{\mathbf{z}}^{(2)}_{n+\alpha} \cdot \mathbf{f}^{(1)} \end{array} \right] . \tag{7.9.78}$$

The linearization of δG may be written as

$$-D\delta G = \left[\begin{array}{cccc} \delta \mathbf{r}^{(1)} & \delta \boldsymbol{\omega}^{(1)} & \delta \mathbf{r}^{(2)} & \delta \boldsymbol{\omega}^{(2)} \end{array} \right] \varepsilon_c \alpha \left[\begin{array}{cccc} \mathbf{A} & -\mathbf{B}^{(1)} & -\mathbf{A} & \mathbf{B}^{(2)} \\ \hat{\mathbf{z}}^{(1)}_{n+\alpha} \cdot \mathbf{A} & -\hat{\mathbf{z}}^{(1)}_{n+\alpha} \cdot \mathbf{B}^{(1)} & -\hat{\mathbf{z}}^{(1)}_{n+\alpha} \cdot \mathbf{A} & \hat{\mathbf{z}}^{(1)}_{n+\alpha} \cdot \mathbf{B}^{(2)} \\ -\mathbf{A} & \mathbf{B}^{(1)} & \mathbf{A} & -\mathbf{B}^{(2)} \\ -\hat{\mathbf{z}}^{(2)}_{n+\alpha} \cdot \mathbf{A} & \hat{\mathbf{z}}^{(2)}_{n+\alpha} \cdot \mathbf{B}^{(1)} & \hat{\mathbf{z}}^{(2)}_{n+\alpha} \cdot \mathbf{A} & -\hat{\mathbf{z}}^{(2)}_{n+\alpha} \cdot \mathbf{B}^{(2)} \end{array} \right] \left[\begin{array}{c} \Delta \mathbf{r}^{(1)} \\ \Delta \boldsymbol{\theta}^{(1)} \\ \Delta \mathbf{r}^{(2)} \\ \Delta \boldsymbol{\theta}^{(2)} \end{array} \right] \tag{7.9.79}$$

where

$$[\mathbf{K}] = \varepsilon_c \alpha \left[\begin{array}{cccc} \mathbf{A} & -\mathbf{B}^{(1)} & -\mathbf{A} & \mathbf{B}^{(2)} \\ \hat{\mathbf{z}}^{(1)}_{n+\alpha} \cdot \mathbf{A} & -\hat{\mathbf{z}}^{(1)}_{n+\alpha} \cdot \mathbf{B}^{(1)} & -\hat{\mathbf{z}}^{(1)}_{n+\alpha} \cdot \mathbf{A} & \hat{\mathbf{z}}^{(1)}_{n+\alpha} \cdot \mathbf{B}^{(2)} \\ -\mathbf{A} & \mathbf{B}^{(1)} & \mathbf{A} & -\mathbf{B}^{(2)} \\ -\hat{\mathbf{z}}^{(2)}_{n+\alpha} \cdot \mathbf{A} & \hat{\mathbf{z}}^{(2)}_{n+\alpha} \cdot \mathbf{B}^{(1)} & \hat{\mathbf{z}}^{(2)}_{n+\alpha} \cdot \mathbf{A} & -\hat{\mathbf{z}}^{(2)}_{n+\alpha} \cdot \mathbf{B}^{(2)} \end{array} \right] , \tag{7.9.80}$$

and

$$\begin{aligned} \mathbf{A} &= \frac{\gamma}{\beta \Delta t} \mathbf{I} \\ \mathbf{B}^{(i)} &= \frac{\gamma}{\beta \Delta t} \hat{\mathbf{z}}^{(i)}_{n+1} \cdot \mathbf{T}^T \left(\boldsymbol{\theta}^{(i)} \right) + \hat{\boldsymbol{\omega}}_{n+1} \cdot \hat{\mathbf{z}}^{(i)}_{n+1} \end{aligned} \,. \tag{7.9.81}$$

7.9.7.3 Contractile Force Between Rigid Bodies

Consider a contractile force between points $\mathbf{x}^{(i)}$ on rigid bodies (1) and (2). The force is oriented along $\mathbf{n}$, where

$$\mathbf{n} = \frac{\mathbf{x}^{(2)} - \mathbf{x}^{(1)}}{\left|\mathbf{x}^{(2)} - \mathbf{x}^{(1)}\right|} \,. \tag{7.9.82}$$

Let $L = \left|\mathbf{x}^{(2)} - \mathbf{x}^{(1)}\right|$ and $L_0 = \left|\mathbf{X}^{(2)} - \mathbf{X}^{(2)}\right|$, so that the contractile force acting on body (1) is given by

$$\mathbf{f}^{(1)} = f_0 \mathbf{n} = \frac{f_0}{L}\left(\mathbf{x}^{(2)} - \mathbf{x}^{(1)}\right) \,. \tag{7.9.83}$$

We do not need to use the augmented Lagrangian method here, thus

$$\boxed{\begin{aligned} \mathbf{f}^{(1)} &= f_0 \frac{\mathbf{x}^{(2)}_{n+\alpha} - \mathbf{x}^{(1)}_{n+\alpha}}{\left|\mathbf{x}^{(2)}_{n+\alpha} - \mathbf{x}^{(1)}_{n+\alpha}\right|} \\ \mathbf{m}^{(1)} &= \mathbf{0} \end{aligned}} \tag{7.9.84}$$

where we assume that the contractile force pivots freely at the rigid body insertiones. The virtual work resulting from this contractile force is thus

$$\delta G = \left[\begin{array}{cccc} \delta\mathbf{r}^{(1)} & \delta\boldsymbol{\omega}^{(1)} & \delta\mathbf{r}^{(2)} & \delta\boldsymbol{\omega}^{(2)} \end{array}\right] \left[\begin{array}{c} \mathbf{f}^{(1)} \\ \hat{\mathbf{z}}^{(1)}_{n+\alpha} \cdot \mathbf{f}^{(1)} \\ -\mathbf{f}^{(1)} \\ -\hat{\mathbf{z}}^{(2)}_{n+\alpha} \cdot \mathbf{f}^{(1)} \end{array}\right] \,, \tag{7.9.85}$$

and its linearization is

$$-D\delta G = \left[\begin{array}{cccc} \delta\mathbf{r}^{(1)} & \delta\boldsymbol{\omega}^{(1)} & \delta\mathbf{r}^{(2)} & \delta\boldsymbol{\omega}^{(2)} \end{array}\right] [\mathbf{K}] \left[\begin{array}{c} \Delta\mathbf{r}^{(1)} \\ \Delta\boldsymbol{\theta}^{(1)} \\ \Delta\mathbf{r}^{(2)} \\ \Delta\boldsymbol{\theta}^{(2)} \end{array}\right] \,. \tag{7.9.86}$$

Here, the stiffness matrix is given by

$$[\mathbf{K}] = \alpha \frac{f_0}{L_{n+\alpha}} \left[\begin{array}{cccc} \mathbf{P} & -\mathbf{P}\cdot\hat{\mathbf{z}}^{(1)}_{n+1} & -\mathbf{P} & \mathbf{P}\cdot\hat{\mathbf{z}}^{(2)}_{n+1} \\ \hat{\mathbf{z}}^{(1)}_{n+\alpha}\cdot\mathbf{P} & -\hat{\mathbf{z}}^{(1)}_{n+\alpha}\cdot\mathbf{P}\cdot\hat{\mathbf{z}}^{(1)}_{n+1} & -\hat{\mathbf{z}}^{(1)}_{n+\alpha}\cdot\mathbf{P} & \hat{\mathbf{z}}^{(1)}_{n+\alpha}\cdot\mathbf{P}\cdot\hat{\mathbf{z}}^{(2)}_{n+1} \\ -\mathbf{P} & \mathbf{P}\cdot\hat{\mathbf{z}}^{(1)}_{n+1} & \mathbf{P} & -\mathbf{P}\cdot\hat{\mathbf{z}}^{(2)}_{n+1} \\ -\hat{\mathbf{z}}^{(2)}_{n+\alpha}\cdot\mathbf{P} & \hat{\mathbf{z}}^{(2)}_{n+\alpha}\cdot\mathbf{P}\cdot\hat{\mathbf{z}}^{(1)}_{n+1} & \hat{\mathbf{z}}^{(2)}_{n+\alpha}\cdot\mathbf{P} & -\hat{\mathbf{z}}^{(2)}_{n+\alpha}\cdot\mathbf{P}\cdot\hat{\mathbf{z}}^{(2)}_{n+1} \end{array}\right] \,, \tag{7.9.87}$$

where

$$\mathbf{P} = \mathbf{I} - \mathbf{n}_{n+\alpha} \otimes \mathbf{n}_{n+\alpha} \,. \tag{7.9.88}$$

7.10 Rigid-Deformable Coupling

In FEBio deformable bodies can be coupled with rigid bodies [70]. At these rigid-deformable interfaces, the coupling of nodal degrees of freedom of deformable elements that attach to rigid bodies requires a modification of the global stiffness matrix and residual vector. This section describes the coupling between rigid and deformable bodies.

The position of a node shared by any number of deformable finite elements is denoted by $\mathbf{x}$ in the current configuration. If the node belongs to one or more deformable elements but is not connected to a rigid body, then $\mathbf{x}$ is given in terms of the nodal displacement $\mathbf{u}$ by (2.3.2); the corresponding nodal virtual velocity is $\delta\mathbf{v}$ and the linearization of $\mathbf{x}$ along an incremental displacement is denoted by $\Delta\mathbf{u}$.

The contribution to the virtual work of the nodal force $\mathbf{f}^a$ at node a is given by

$$\delta G = \delta\mathbf{v}^a \cdot \mathbf{f}^a_{n+\alpha}\,, \tag{7.10.1}$$

whera $\delta\mathbf{v}^a$ is the virtual velocity of node a and $\mathbf{f}^a_{n+\alpha}$ is the global nodal force, evaluated at the intermediate time $t_{n+\alpha}$ as $\mathbf{f}^a_{n+\alpha} = \alpha\mathbf{f}^a_{n+1} + (1-\alpha)\,\mathbf{f}^a_n$. The linearization of this virtual work along the incremental displacement $\Delta\mathbf{u}^b$ of node b is

$$D\delta G = -\alpha\delta\mathbf{v}^a \cdot \mathbf{K}^{ab} \cdot \Delta\mathbf{u}^b, \tag{7.10.2}$$

where $\mathbf{K}^{ab} = \left(\partial\mathbf{f}^a/\partial\mathbf{x}^b\right)_{n+1}$ is the contribution to the global stiffness matrix from the interactions of the degrees of freedom of nodes a and b.

Now we consider the cases when either node a, or node b, or both, are attached to a rigid body. Our objective is to determine how to modify the global residual vector and stiffness matrix to account for the coupling of deformable and rigid body degrees of freedom.

When node a is attached to rigid body a, its position is given in terms of that rigid body's degrees of freedom by the general relation (6.3.18). The corresponding virtual velocity is given in (7.9.4), reproduced here as

$$\delta\mathbf{v}^a = \delta\mathbf{r}^a - \hat{\mathbf{z}}^a_{n+\alpha} \cdot \delta\boldsymbol{\theta}^a\,, \tag{7.10.3}$$

where $\mathbf{z}^a_{n+\alpha} = \boldsymbol{\Lambda}^a_{n+\alpha} \cdot \mathbf{Z}^a$ is the position of node a relative to the center of mass of rigid body a, at the intermediate time $t_{n+\alpha}$. Now, the contribution of the global nodal force $\mathbf{f}^a_{n+\alpha}$ to δG must be modified from (7.10.1) according to

$$\delta G = \delta\mathbf{v}^a \cdot \mathbf{f}^a_{n+\alpha} = \begin{bmatrix} \delta\mathbf{r}^a & \delta\boldsymbol{\theta}^a \end{bmatrix} \begin{bmatrix} \mathbf{f}^a_{n+\alpha} \\ \hat{\mathbf{z}}^a_{n+\alpha} \cdot \mathbf{f}^a_{n+\alpha} \end{bmatrix}. \tag{7.10.4}$$

In other words, the displacement degrees of freedom of node a should be eliminated from the global system of equations and replaced with the translation and rotation degrees of freedom of rigid body a. The force vector $\mathbf{f}^a_{n+\alpha}$ should be made to contribute to the translation degrees of freedom of the center of mass of rigid body a, whereas the moment $\mathbf{z}^a_{n+\alpha} \times \mathbf{f}^a_{n+\alpha}$ should contribute to the rotation degrees of freedom of the rigid body.

When node b is connected to rigid body b, the incremental displacement $\Delta\mathbf{u}^b$ should be replaced with the rigid body incremental motions,

$$\Delta\mathbf{u}^b = \Delta\mathbf{r}^b - \hat{\mathbf{z}}^b_{n+1} \cdot \Delta\boldsymbol{\theta}^b\,. \tag{7.10.5}$$

Now, the contribution $\mathbf{K}^{ab}$ to the global stiffness matrix needs to be modified from (7.10.2) according to the three possible cases:

- Node a belongs to rigid body a, node b belongs to flexible elements only,

$$D\delta G = -\alpha \begin{bmatrix} \delta\mathbf{r}^a & \delta\boldsymbol{\theta}^a \end{bmatrix} \begin{bmatrix} \mathbf{K}^{ab} \\ \hat{\mathbf{z}}^a_{n+\alpha} \cdot \mathbf{K}^{ab} \end{bmatrix} \left[\Delta\mathbf{u}^b\right]. \tag{7.10.6}$$

- Node b belongs to rigid body b, node a belongs to flexible elements only,

$$D\delta G = -\alpha \left[\delta\mathbf{v}^a\right] \begin{bmatrix} \mathbf{K}^{ab} & -\mathbf{K}^{ab} \cdot \hat{\mathbf{z}}^b_{n+1} \end{bmatrix} \begin{bmatrix} \Delta\mathbf{r}^b \\ \Delta\boldsymbol{\theta}^b \end{bmatrix}. \tag{7.10.7}$$

- Node a belongs to rigid body a, node b belongs to rigid body b,

$$D\delta G = -\alpha \left[\begin{array}{cc} \delta \mathbf{r}^a & \delta \boldsymbol{\theta}^a \end{array} \right] \left[\begin{array}{cc} \mathbf{K}^{ab} & -\mathbf{K}^{ab} \cdot \hat{\mathbf{z}}^b_{n+1} \\ \hat{\mathbf{z}}^a_{n+\alpha} \cdot \mathbf{K}^{ab} & -\hat{\mathbf{z}}^a_{n+\alpha} \cdot \mathbf{K}^{ab} \cdot \hat{\mathbf{z}}^b_{n+1} \end{array} \right] \left[\begin{array}{c} \Delta \mathbf{r}^b \\ \Delta \boldsymbol{\theta}^b \end{array} \right] . \tag{7.10.8}$$

Chapter 8

Optimization

This chapter describes the theoretical framework of FEBio's optimization module. This module can be used to optimize model parameters (like material parameters, or load values) in order to achieve an objective. The objective is generally the minimization of the *objective function*, to be introduced below.

8.1 The Objective Function

The objective function, which is to be minimized, can be defined as follows,

$$\varphi(\mathbf{a}) = \sum_{i=1}^{n} [y_i - f(x_i; \mathbf{a})]^2 .$$

Here, the (x_i, y_i) are user-defined data pairs and $f(x; \mathbf{a})$ is the function that extracts the corresponding data from the model. The optimization module tries to find the model parameters **a** that minimize the function φ. It does this by repeatedly evaluating the function y, which will usually call FEBio to solve a forward FE problem.

8.2 The Levenberg-Marquardt Method

One of the methods that is currently implemented in FEBio's optimization method is the constrained Levenberg-Marquardt method via the *levmar* library. (see `http://users.ics.forth.gr/~lourakis/levmar/` for more information on this library.)

The Levenberg-Marquardt method is a numerical algorithm that minimizes a function that is defined as a sum of squares of nonlinear functions, i.e. the objective function as defined above. It combines the steepest-descent method with a Gauss-Newton method to find the parameters that minimize the objective function.

The LM method requires a set of measured values (x_i, y_i) and an initial guess for the **a** vector. It then tries to find a better estimate for **a** by replacing it with $\mathbf{a} + \delta$. The function $f(x_i; \mathbf{a} + \delta)$ is linearly approximated.

$$f(x_i; \mathbf{a} + \delta) \approx f(x_i; \mathbf{a}) + \mathbf{J}_i \delta$$

where $\mathbf{J}_i$is the Jacobian of f with respect to δ. Substituting this in the objective function and minimizing with respect to δ leads to,

$$(\mathbf{J}^{\mathrm{T}}\mathbf{J})\delta = \mathbf{J}^{\mathrm{T}}(\mathbf{y} - \mathbf{f}(\boldsymbol{a}))$$

where **y** is the vector of y_i,and **f** is the vector of $f(x_i; \boldsymbol{a})$.

The main idea of the LM method is to replace this linear equation with the following.

$$(\mathbf{J}^{\mathrm{T}}\mathbf{J} + \mu(\mathbf{J}^{\mathrm{T}}\mathbf{J})_{ii})\delta = \mathbf{J}^{\mathrm{T}}(\mathbf{y} - \mathbf{f}(\boldsymbol{a}))$$

Here, $\mu$is a damping parameter that is controlled by the algorithm. When $\mu$is small, the method approximates Gauss-Newton, when $\mu$is large it is closer to a steepdest-descent method. The algorithm will modify try to modify μsuch that an improvement to the parameter vector **a** can be found in each iteration. The method will terminate when the value of the objective function falls below a user-specified tolerance (the *obj_tol* parameter in FEBio).

The evaluation of the Jacobian requires evaluating the derivatives of f with respect to **a**. These derivatives are approximated via forward difference formulas. For example, the k-th component of the gradient is approximated as follows.

$$\frac{\partial f}{\partial a_k} \approx \frac{1}{\delta a_k}\left[f\left(a_1, \cdots, a_k + \delta a_k, \cdots, a_m\right) - f\left(a_1, \cdots, a_k, \cdots, a_m\right)\right]$$

The value for $\delta a_k$is determined from the following formula.

$$\delta a_k = \varepsilon\left(1 + a_k\right)$$

where, ε is the forward difference scale factor (the *fdiff_scale* option in FEBio). In FEBio, the initial value for the damping parameter μcan be set with the *tau* parameter.

Bibliography

[1] M. B. Albro, N. O. Chahine, R. Li, K. Yeager, C. T. Hung, and G. A. Ateshian. Dynamic loading of deformable porous media can induce active solute transport. *J Biomech*, 41(15):3152–7, 2008.

[2] M. B. Albro, R. Li, R. E. Banerjee, C. T. Hung, and G. A. Ateshian. Validation of theoretical framework explaining active solute uptake in dynamically loaded porous media. *J Biomech*, 43(12):2267–73, 2010.

[3] E.M. Arruda and M.C. Boyce. A three-dimensional constitutive model for the large stretch behavior of rubber elastic materials. *J. Mech. Phys. Solids*, 41(2):389–412, 1993.

[4] G. A. Ateshian. Anisotropy of fibrous tissues in relation to the distribution of tensed and buckled fibers. *J Biomech Eng*, 129(2):240–9, 2007.

[5] G. A. Ateshian. On the theory of reactive mixtures for modeling biological growth. *Biomech Model Mechanobiol*, 6(6):423–45, 2007.

[6] G. A. Ateshian, M. Likhitpanichkul, and C. T. Hung. A mixture theory analysis for passive transport in osmotic loading of cells. *J Biomech*, 39(3):464–75, 2006.

[7] G. A. Ateshian, V. Rajan, N. O. Chahine, C. E. Canal, and C. T. Hung. Modeling the matrix of articular cartilage using a continuous fiber angular distribution predicts many observed phenomena. *J Biomech Eng*, 131(6):061003, 2009.

[8] G. A. Ateshian and T. Ricken. Multigenerational interstitial growth of biological tissues. *Biomech Model Mechanobiol*, 9(6):689–702, 2010.

[9] G. A. Ateshian and J. A. Weiss. Anisotropic hydraulic permeability under finite deformation. *Journal of biomechanical engineering*, 132(11):111004, 2010.

[10] G.A. Ateshian, M. B. Albro, S.A. Maas, and J.A. Weiss. Finite element implementation of mechanochemical phenomena in neutral deformable porous media under finite deformation. *Journal of Biomechanical Engineering*, 133(8):1005–1017, 2011.

[11] GA Ateshian, SA Maas, and J.A. Weiss. Finite element algorithm for frictionless contact of porous permeable media under finite deformation and sliding. *J. Biomech. Engn.*, 132(6):1006–1019, 2010.

[12] Gerard A Ateshian. The role of interstitial fluid pressurization in articular cartilage lubrication. *J Biomech*, 42(9):1163–76, Jun 2009.

[13] Gerard A Ateshian. Viscoelasticity using reactive constrained solid mixtures. *J Biomech*, 48(6):941–7, Apr 2015.

[14] Gerard A Ateshian, Benjamin J Ellis, and Jeffrey A Weiss. Equivalence between short-time biphasic and incompressible elastic material responses. *J Biomech Eng*, 129(3):405–12, Jun 2007.

[15] Gerard A Ateshian, Steve Maas, and Jeffrey A Weiss. Solute transport across a contact interface in deformable porous media. *J Biomech*, 45(6):1023–7, Apr 2012.

[16] Gerard A Ateshian, Jay J Shim, Steve A Maas, and Jeffrey A Weiss. Finite element framework for computational fluid dynamics in febio. *J Biomech Eng*, 140(2), Feb 2018.

[17] Evren U Azeloglu, Michael B Albro, Vikrum A Thimmappa, Gerard A Ateshian, and Kevin D Costa. Heterogeneous transmural proteoglycan distribution provides a mechanism for regulating residual stresses in the aorta. *Am J Physiol Heart Circ Physiol*, 294(3):H1197–205, Mar 2008.

[18] Klaus-Jürgen Bathe. *Finite element procedures in engineering analysis*. Prentice-Hall, Englewood Cliffs, N.J., 1982.

[19] Klaus-Jürgen Bathe and Eduardo N Dvorkin. A formulation of general shell elements—the use of mixed interpolation of tensorial components. *International journal for numerical methods in engineering*, 22(3):697–722, 1986.

[20] Y Bazilevs, JR Gohean, TJR Hughes, RD Moser, and Y Zhang. Patient-specific isogeometric fluid–structure interaction analysis of thoracic aortic blood flow due to implantation of the Jarvik 2000 left ventricular assist device. *Comput. Methods Appl. Mech. Engrg.*, 198(45):3534–3550, 2009.

[21] Yuri Bazilevs, Victor M Calo, Thomas JR Hughes, and Yongjie Zhang. Isogeometric fluid-structure interaction: theory, algorithms, and computations. *Computational mechanics*, 43(1):3–37, 2008.

[22] Dimitri P Bertsekas. *Constrained optimization and Lagrange multiplier methods*. Academic Press, New York, 1982.

[23] P. Betsch, F. Gruttmann, and Stein E. A 4-node finite shell element for the implementation of general hyperelastic 3d-elasticity at finite strains. *Comput. Methods Appl. Mech. Engrg*, 130:57–79, 1996.

[24] P Betsch and E Stein. An assumed strain approach avoiding artificial thickness straining for a non-linear 4-node shell element. *Communications in Numerical Methods in Engineering*, 11(11):899–909, 1995.

[25] M Bischoff and E Ramm. Shear deformable shell elements for large strains and rotations. *International Journal for Numerical Methods in Engineering*, 40(23):4427–4449, 1997.

[26] Manfred Bischoff, E Ramm, and J Irslinger. Models and finite elements for thin-walled structures. *Encyclopedia of Computational Mechanics Second Edition*, pages 1–86, 2018.

[27] Javier Bonet and Richard D. Wood. *Nonlinear continuum mechanics for finite element analysis*. Cambridge University Press, 1997.

[28] Nicola Bonora. A nonlinear cdm model for ductile failure. *Engineering fracture mechanics*, 58(1-2):11–28, 1997.

[29] Ray M. Bowen. Incompressible porous media models by use of the theory of mixtures. *Int J Eng Sci*, 18(9):1129–1148, 1980.

[30] R.M. Bowen. Theory of mixtures. *Continuum physics*, 3(Pt I), 1976.

[31] Jean-Louis Chaboche. Continuous damage mechanics—a tool to describe phenomena before crack initiation. *Nuclear Engineering and Design*, 64(2):233–247, 1981.

[32] Y I Cho and K R Kensey. Effects of the non-Newtonian viscosity of blood on flows in a diseased arterial vessel. Part 1: Steady flows. *Biorheology*, 28(3-4):241–62, 1991.

[33] John C Criscione, Jay D Humphrey, Andrew S Douglas, and William C Hunter. An invariant basis for natural strain which yields orthogonal stress response terms in isotropic hyperelasticity. *J. Mech. Phys. Solids*, 48(12):2445–2465, 2000.

[34] A. Curnier, He Qi-Chang, and P. Zysset. Conewise linear elastic materials. *J Elasticity*, 37(1):1–38, 1994.

[35] Alain Curnier, Qi-Chang He, and Anders Klarbring. Continuum mechanics modelling of large deformation contact with friction. In *Contact mechanics*, pages 145–158. Springer, 1995.

[36] C Agelet de Saracibar. A new frictional time integration algorithm for large slip multi-body frictional contact problems. *Computer Methods in Applied Mechanics and Engineering*, 142(3-4):303–334, 1997.

[37] Daniel Charles Drucker. Relation of experiments to mathematical theories of plasticity. *Journal of Applied Mechanics*, 1949.

[38] A.C. Eringen and J.D. Ingram. Continuum theory of chemically reacting media – 1. *Int J Eng Sci*, 3:197 – 212, 1965.

[39] Mahdi Esmaily Moghadam, Yuri Bazilevs, Tain-Yen Hsia, Irene E Vignon-Clementel, and Alison L Marsden. A comparison of outlet boundary treatments for prevention of backflow divergence with relevance to blood flow simulations. *Comput. Mech.*, 48(3):277–291, 2011.

[40] James D Foley, Andries van Dam, Steven K Feiner, and John F Hughes. Computer graphics: Principles and pract edition, 1996.

[41] Y. C Fung. *Biomechanics: mechanical properties of living tissues*. Springer-Verlag, New York, 1981.

[42] Y. C. Fung. *Biomechanics : mechanical properties of living tissues*. Springer-Verlag, New York, 2nd edition, 1993.

[43] Y. C. Fung, K. Fronek, and P. Patitucci. Pseudoelasticity of arteries and the choice of its mathematical expression. *Am J Physiol*, 237(5):H620–31, 1979.

[44] Y. C Fung, Nicholas Perrone, and M Anliker. *Biomechanics, its foundations and objectives*. Prentice-Hall, Englewood Cliffs, N.J., 1972.

[45] AE Giannakopoulos. The return mapping method for the integration of friction constitutive relations. *Computers & structures*, 32(1):157–167, 1989.

[46] Oscar Gonzalez. Exact energy and momentum conserving algorithms for general models in nonlinear elasticity. *Computer Methods in Applied Mechanics and Engineering*, 190(13):1763–1783, 2000.

[47] J. M. Guccione, A. D. McCulloch, and L. K. Waldman. Passive material properties of intact ventricular myocardium determined from a cylindrical model. *J Biomech Eng*, 113(1):42–55., 1991.

[48] Osman Gültekin, Hüsnü Dal, and Gerhard A Holzapfel. On the quasi-incompressible finite element analysis of anisotropic hyperelastic materials. *Computational mechanics*, 63(3):443–453, 2019.

[49] J Helfenstein, M Jabareen, Edoardo Mazza, and S Govindjee. On non-physical response in models for fiber-reinforced hyperelastic materials. *International Journal of Solids and Structures*, 47(16):2056–2061, 2010.

[50] M. H. Holmes and V. C. Mow. The nonlinear characteristics of soft gels and hydrated connective tissues in ultrafiltration. *J Biomech*, 23(11):1145–56, 1990.

[51] Gerhard A Holzapfel. *Nonlinear solid mechanics: a continuum approach for engineering*. Wiley, Chichester, 2000.

[52] A. Horowitz, I. Sheinman, Y. Lanir, M. Perl, and S. Sideman. Nonlinear incompressilbe finite element for simulating loading of cardiac tissue- part i: two dimensional formulation for thin myocardial strips. *Journal of Biomechanical Engineering, Transactions of the ASME*, 110(1):57–61, 1988.

[53] J S Hou, M H Holmes, W M Lai, and V C Mow. Boundary conditions at the cartilage-synovial fluid interface for joint lubrication and theoretical verifications. *J Biomech Eng*, 111(1):78–87, Feb 1989.

[54] J.R. Hughes and Wing Kam Liu. Nonlinear finite element analysis of shells: Part i. three-dimensional shells. *Computer Methods in Applied Mechanics and Engineering*, 26:331–362, 1980.

[55] J. D. Humphrey, R. K. Strumpf, and F. C. P. Yin. Determination of a constitutive relation for passive myocardium. i. a new functional form. *Journal of Biomechanical Engineering, Transactions of the ASME*, 112(3):333–339, 1990.

[56] J. D. Humphrey and F. C. P. Yin. On constitutive relations and finite deformations of passive cardiac tissue: I. a pseudostrain-energy function. *Journal of Biomechanical Engineering, Transactions of the ASME*, 109(4):298–304, 1987.

[57] Kenneth E Jansen, Christian H Whiting, and Gregory M Hulbert. A generalized-α method for integrating the filtered Navier–Stokes equations with a stabilized finite element method. *Comput. Methods Appl. Mech. Engrg.*, 190(3):305–319, 2000.

[58] Lazar M Kachanov. Rupture time under creep conditions. *International Journal of Fracture*, 1958.

[59] Aharon Katzir-Katchalsky and Peter F. Curran. *Nonequilibrium thermodynamics in biophysics*. Harvard University Press, Cambridge„ 1965.

[60] S Klinkel, F Gruttmann, and W Wagner. A continuum based three-dimensional shell element for laminated structures. *Computers & Structures*, 71(1):43–62, 1999.

[61] W. Michael Lai, David Rubin, and Erhard Krempl. *Introduction to continuum mechanics*. Butterworth-Heinemann/Elsevier, Amsterdam, 4th ed edition, 2010.

[62] Y. Lanir. Constitutive equations for fibrous connective tissues. *J Biomech*, 16(1):1–12, 1983.

[63] Torvard C. Laurent and Johan Killander. A theory of gel filtration and its experimental verification. *J Chromatogr*, 14:317–330, 1963.

[64] T. A. Laursen and J. C. Simo. Continuum-based finite element formulation for the implicit solution of multibody, large deformation frictional contact problems. *International Journal for Numerical Methods in Engineering*, 36(20):3451–3485, 1993.

[65] Tod A. Laursen. *Computational Contact and Impact Mechanics*. Springer, 2002.

[66] Jean Lemaitre. How to use damage mechanics. *Nuclear engineering and design*, 80(2):233–245, 1984.

[67] Jean Lemaitre. A continuous damage mechanics model for ductile fracture. *J. Eng. Mater. Technol.*, 1985.

[68] Jean Lemaitre and Rodrigue Desmorat. *Engineering damage mechanics: ductile, creep, fatigue and brittle failures*. Springer Science & Business Media, 2005.

[69] Richard H MacNeal. A simple quadrilateral shell element. *Computers & Structures*, 8(2):175–183, 1978.

[70] B. N. Maker. Rigid bodies for metal forming analysis with nike3d. *University of California, Lawrence Livermore Lab Rept*, UCRL-JC-119862:1–8, 1995.

[71] A Ya Malkin. Continuous relaxation spectrum-its advantages and methods of calculation. *Applied Mechanics and Engineering*, 11(2):235, 2006.

[72] J. E. Marsden and T. J. Hughes. *Mathematical Foundations of Elasticity*. Dover Publications, 1994.

[73] H. Matthies and G. Strang. The solution of nonlinear finite element equations. *Intl J Num Meth Eng*, 14:1613–26, 1979.

[74] R. L. Mauck, C. T. Hung, and G. A. Ateshian. Modeling of neutral solute transport in a dynamically loaded porous permeable gel: implications for articular cartilage biosynthesis and tissue engineering. *J Biomech Eng*, 125(5):602–14, 2003.

[75] V.C. Mow, S.C. Kuei, W.M. Lai, and C.G. Armstrong. Biphasic creep and stress relaxation of articular cartilage in compression: Theory and experiments. *J. Biomech. Eng.*, 102:73–84, 1980.

[76] Robert J Nims and Gerard A Ateshian. Reactive constrained mixtures for modeling the solid matrix of biological tissues. *Journal of Elasticity*, 129(1-2):69–105, 2017.

[77] Robert J Nims, Krista M Durney, Alexander D Cigan, Antoine Dusséaux, Clark T Hung, and Gerard A Ateshian. Continuum theory of fibrous tissue damage mechanics using bond kinetics: application to cartilage tissue engineering. *Interface Focus*, 6(1):20150063, Feb 2016.

[78] A. G. Ogston and C. F. Phelps. The partition of solutes between buffer solutions and solutions containing hyaluronic acid. *Biochem J*, 78:827–33, 1961.

[79] Ronald L Panton. *Incompressible flow*. John Wiley & Sons, 2006.

[80] Konstantinos Poulios and Yves Renard. An unconstrained integral approximation of large sliding frictional contact between deformable solids. *Computers & Structures*, 153:75–90, 2015.

[81] M. A. Puso and J. A. Weiss. Finite element implementation of anisotropic quasi-linear viscoelasticity using a discrete spectrum approximation. *J Biomech Eng*, 120(1):62–70, 1998.

[82] Michael Anthony Puso. An energy and momentum conserving method for rigid–flexible body dynamics. *International Journal for numerical methods in engineering*, 53(6):1393–1414, 2002.

[83] K. M. Quapp and J. A. Weiss. Material characterization of human medial collateral ligament. *J Biomech Eng*, 120(6):757–63, 1998.

[84] Yu N Rabotnov. *Elements of hereditary solid mechanics*. MIT Publishers, Moscow, 1980.

[85] J. N. Reddy. *An introduction to continuum mechanics : with applications*. Cambridge University Press, New York, 2008.

[86] J. N. Reddy and David K. Gartling. *The finite element method in heat transfer and fluid dynamics*. CRC Press, Boca Raton, FL, 2nd edition, 2001.

[87] Carlo Sansour. On the physical assumptions underlying the volumetric-isochoric split and the case of anisotropy. *European Journal of Mechanics-A/Solids*, 27(1):28–39, 2008.

[88] Roger A Sauer and Laura De Lorenzis. An unbiased computational contact formulation for 3d friction. *International Journal for Numerical Methods in Engineering*, 101(4):251–280, 2015.

[89] Jay J Shim and Gerard A Ateshian. A hybrid biphasic mixture formulation for modeling dynamics in porous deformable biological tissues. *Archive of Applied Mechanics*, pages 1–21, 2021.

[90] Jay J Shim, Steve A Maas, Jeffrey A Weiss, and Gerard A Ateshian. A formulation for fluid structure-interactions in febio using mixture theory. *J Biomech Eng*, Mar 2019.

[91] J Ci Simo and TA Laursen. An augmented lagrangian treatment of contact problems involving friction. *Computers & Structures*, 42(1):97–116, 1992.

[92] JC Simo. On a fully three-dimensional finite-strain viscoelastic damage model: formulation and computational aspects. *Computer methods in applied mechanics and engineering*, 60(2):153–173, 1987.

[93] J.C. Simo and F. Armero. Geometrically non-linear enhanced strain mixed methods and the method of incompatible modes. *International Journal for Numerical Methods in Engineering*, 33:1413–1419, 1992.

[94] JC Simo, F Armero, and RL Taylor. Improved versions of assumed enhanced strain tri-linear elements for 3d finite deformation problems. *Computer methods in applied mechanics and engineering*, 110(3-4):359–386, 1993.

[95] JC Simo and Nils Tarnow. The discrete energy-momentum method. conserving algorithms for nonlinear elastodynamics. *Zeitschrift für angewandte Mathematik und Physik (ZAMP)*, 43(5):757–792, 1992.

[96] J.C. Simo and R.L. Taylor. Quasi-incompressible finite elasticity in principal stretches: Continuum basis and numerical algorithms. *Computer Methods in Applied Mechanics and Engineering*, 85:273–310, 1991.

[97] Juan C Simo and JW Ju. Strain-and stress-based continuum damage models—i. formulation. *International journal of solids and structures*, 23(7):821–840, 1987.

[98] Juan C Simo and MS10587420724 Rifai. A class of mixed assumed strain methods and the method of incompatible modes. *International journal for numerical methods in engineering*, 29(8):1595–1638, 1990.

[99] Anthony James Merril Spencer. *Continuum Theory of the Mechanics of Fibre-Reinforced Composites*. Springer-Verlag, New York, 1984.

[100] D. N. Sun, W. Y. Gu, X. E. Guo, W. M. Lai, and V. C. Mow. A mixed finite element formulation of triphasic mechano-electrochemical theory for charged, hydrated biological soft tissues. *Int J Numer Meth Eng*, 45(10):1375–402, 1999.

[101] I. Tinoco Jr., K. Sauer, and J. C. Wang. *Physical chemistry : principles and applications in biological sciences*. Prentice Hall, 1995.

[102] C. Truesdell and R. Toupin. *The classical field theories*, volume III/1 of *Handbuch der physik*. Springer, Heidelberg, 1960.

[103] M Tur, FJ Fuenmayor, and P Wriggers. A mortar-based frictional contact formulation for large deformations using lagrange multipliers. *Computer Methods in Applied Mechanics and Engineering*, 198(37):2860–2873, 2009.

[104] K. Un and R. L. Spilker. A penetration-based finite element method for hyperelastic 3d biphasic tissues in contact. part ii: finite element simulations. *J Biomech Eng*, 128(6):934–42, 2006.

[105] D.R. Veronda and R.A. Westmann. Mechanical characterization of skin - finite deformations. *J. Biomechanics*, Vol. 3:111–124, 1970.

[106] Irene E Vignon-Clementel, C Alberto Figueroa, Kenneth E Jansen, and Charles A Taylor. Outflow boundary conditions for three-dimensional finite element modeling of blood flow and pressure in arteries. *Comput. Methods Appl. Mech. Engrg.*, 195(29):3776–3796, 2006.

[107] L Vu-Quoc and XG Tan. Optimal solid shells for non-linear analyses of multilayer composites. i. statics. *Computer methods in applied mechanics and engineering*, 192(9-10):975–1016, 2003.

[108] J.A. Weiss, B.N. Maker, and S. Govindjee. Finite element implementation of incompressible, transversely isotropic hyperelasticity. *Computer Methods in Applications of Mechanics and Engineering*, 135:107–128, 1996.

[109] P Wriggers. *Computational contact mechanics*. Springer, Berlin, 2nd ed edition, 2006.

[110] P Wriggers and Tod A Laursen. *Computational contact mechanics*, volume no. 498 of *CISM courses and lectures*. Springer, Wien, 2007.

[111] Peter Wriggers, T Vu Van, and Erwin Stein. Finite element formulation of large deformation impact-contact problems with friction. *Computers & Structures*, 37(3):319–331, 1990.

[112] Giorgio Zavarise and Laura De Lorenzis. The node-to-segment algorithm for 2d frictionless contact: classical formulation and special cases. *Computer Methods in Applied Mechanics and Engineering*, 198(41):3428–3451, 2009.

[113] Brandon Zimmerman, Steve A Maas, Jeffrey A Weiss, and Gerard A Ateshian. A finite element algorithm for large deformation biphasic frictional contact between porous-permeable hydrated soft tissues. *J Biomech Eng*, Aug 2021.

[114] Brandon K Zimmerman and Gerard A Ateshian. A surface-to-surface finite element algorithm for large deformation frictional contact in febio. *J Biomech Eng*, 140(8), 08 2018.

[115] Brandon K. Zimmerman, David Jiang, Jeffrey A. Weiss, Lucas H. Timmins, and Gerard A. Ateshian. On the use of constrained reactive mixtures of solids to model finite deformation isothermal elastoplasticity and elastoplastic damage mechanics. *Journal of the Mechanics and Physics of Solids*, page 104534, 2021.